



HAL
open science

Spectrométrie de mobilité ionique pour la lipidomique du plasma humain : vers la mesure standardisée de sections efficaces de collision

Anais George

► **To cite this version:**

Anais George. Spectrométrie de mobilité ionique pour la lipidomique du plasma humain : vers la mesure standardisée de sections efficaces de collision. Chimie analytique. Normandie Université, 2023. Français. NNT : 2023NORMR060 . tel-04580954

HAL Id: tel-04580954

<https://theses.hal.science/tel-04580954>

Submitted on 21 May 2024

HAL is a multi-disciplinary open access archive for the deposit and dissemination of scientific research documents, whether they are published or not. The documents may come from teaching and research institutions in France or abroad, or from public or private research centers.

L'archive ouverte pluridisciplinaire **HAL**, est destinée au dépôt et à la diffusion de documents scientifiques de niveau recherche, publiés ou non, émanant des établissements d'enseignement et de recherche français ou étrangers, des laboratoires publics ou privés.



Normandie Université



THÈSE

Pour obtenir le diplôme de doctorat

Spécialité **CHIMIE**

Préparée au sein de l'**Université de Rouen Normandie**

**Ion mobility spectrometry for human plasma lipidomics:
towards standardized collision cross sections**

Présentée et soutenue par
ANAI GEORGE

Thèse soutenue le 13/11/2023
devant le jury composé de :

M. BRUNO LE BIZEC	Professeur des Universités - Centre régional de l'INRAE Angers-Nantes Pays de la Loire	Rapporteur du jury
M. KEVIN PAGEL	Professeur des Universités - Université Freie de Berlin (ALL.)	Rapporteur du jury
MME JUSTINE BERTRAND-MICHEL	Ingénieur de Recherche - INRA de TOULOUSE	Membre du jury
MME CHRISTINE ENJALBAL	Professeur des Universités - UNIVERSITE MONTPELLIER 2 SCIENCES ET TECH DU LANGUEDOC	Membre du jury
MME ISABELLE SCHMITZ	INGENIEUR DE RECHERCHE (RECHERCHE CNRS) - Université de Rouen Normandie	Membre du jury
M. VINCENT LEVACHER	Directeur de Recherche - INSA de Rouen Normandie	Président du jury
MME CORINNE BOURHIS-LOUTELIER	Maître de Conférences - Université de Rouen Normandie	Directeur de thèse
M. FRANCOIS FENAILLE	Directeur de Recherche - Commissariat à l'Energie Atomique	Co-directeur de thèse

Thèse dirigée par **CORINNE BOURHIS-LOUTELIER** (CHIMIE ORGANIQUE, BIOORGANIQUE, REACTIVITE, ANALYSE) et **FRANCOIS FENAILLE** (Commissariat à l'Energie Atomique)

THÈSE

Pour obtenir le diplôme de doctorat

Spécialité Chimie

Préparée au sein de l'Université de Rouen Normandie

Ion mobility spectrometry for human plasma lipidomics: towards standardized collision cross sections

Présentée et soutenue par
Anaïs GEORGE

Thèse soutenue le 13 novembre 2023
devant le jury composé de

M. Bruno LE BIZEC	Professeur des Universités, Centre régional de l'INRAE Angers-Nantes, Pays de la Loire	Rapporteur
M. Kevin PAGEL	Professeur, Université Freie de Berlin	Rapporteur
Mme Justine BERTRAND-MICHEL	Ingénieure de recherche, Plateforme Metatoul - I2MC, Toulouse	Examinatrice
Mme Christine ENJALBAL	Professeure des universités, Université Montpellier 2 Sciences et Tech du Languedoc	Examinatrice
M. Vincent LEVACHER	Directeur de recherche CNRS, Laboratoire COBRA, Mont-Saint-Aignan	Président du jury
Mme Corinne LOUTELIER-BOURHIS	Maître de conférences de l'Université de Rouen Normandie, Laboratoire COBRA, Mont-Saint-Aignan	Directrice de thèse
M. François FENAILLE	Directeur de recherche, CEA Saclay	Co-directeur de thèse
Mme Isabelle SCHMITZ	Ingénieure de recherche CNRS, Laboratoire COBRA, Mont-Saint-Aignan	Co-encadrante

Thèse dirigée par le Dr. Corinne LOUTELIER-BOURHIS, laboratoire COBRA
Codirigée par François FENAILLE, CEA Saclay

A ma grand-mère,
Ma Mamie Nou

Acknowledgments/ Remerciements

I am extremely grateful to have had the opportunity to do this PhD thesis. It was a unique opportunity for me to discover different techniques, in different teams. I hope this work will be able to contribute to the development of ion mobility spectrometry in metabolomics. As a PhD is far from a single work person, I would like to thank every person who contributed, supported, and helped to realize the present work and fulfill the missions required to achieve the present dissertation.

I would like to express my deepest gratitude to the members of my thesis committee for accepting to judge my thesis work, and giving their precious time to read this dissertation and generate various discussions. I would like to express my sincere gratitude to Pr. Bruno Le Bizec and Pr. Kevin Pagel, for agreeing to review my manuscript. I would like to acknowledge Dr. Justine Bertrand-Michel and Pr. Chritine Enjalbal who graciously agreed to evaluate the present thesis. I would like to thank Dr. Vincent Levacher for agreeing to take part in my thesis defense. I sincerely thank you for agreeing to take part in the thesis jury and to attend the defense, where I hope many scientific discussions will take place.

This work was performed at COBRA laboratory, in collaboration with the CEA Saclay. First, I would like to express my deepest thanks to my thesis director Corinne Loutelier-Bourhis, and my co-director François Fenaille, for their exceptional guidance, strong support throughout my doctoral journey. I also acknowledge Isabelle Schmitz for her support and help during all these months and Benoit Colsch for his help in lipidomics. I also express my thanks to Carlos Afonso for his supervision and his various ideas on ion mobility and metabolomics.

I would like to express my gratitude to the International Society of ion mobility spectrometry for the Dave Atkinson Student Travel Awards 2022 which allowed me to travel to USA for the first time. Thank you Maggie for your kindness and your warm welcome to the society.

Thank you also for the second award which allowed me to join you in the 2023 edition of the annual meeting in Maastricht during my writing period, to share my thesis results. It was for me the occasion to meet a lot of people and share scientific knowledge but also various discussions. It was also the first time for me as a judge during the poster session, it was a great experience, shared with Brian, Alexander, Sandro and Richard. I would like to particularly thank Maxime, Lucia, Juliane, Patricia and Darya for our discussions and the great time spent with you in Maastricht. Thank you very much for your support during this emotional week.

“Le doute est une force. Une vraie et belle force. Veille simplement qu'elle te pousse toujours en avant”

Pierre Bottero

La thèse est un voyage, un chemin, un parcours dans une vie, semée de joie, de doutes, mais aussi semée d'embûches, de changements de chemin, de détours. Ce parcours a été parsemé de rires, de pleurs mais surtout de découvertes, de recherche scientifique mais aussi de soi, tel un chemin initiatique.

Je tiens à remercier de nouveau Corinne, sans toi cette thèse n'aurait pas vu le jour, tu m'as aidé, conseillé, soutenu, même dans mes pires moments de doute, même quand j'ai voulu tout abandonner, tu as toujours été disponible. Ces derniers mois ont été rudes, mais tu as toujours su être présente, active pour m'aider, jusqu'à même rêver de ma thèse. Je me sentais moins seule face à cette montagne de choses à faire, car je savais que tu m'aiderais à la franchir. Alors merci infiniment Corinne ! Sans toi, je n'aurais jamais réussi à franchir ce chemin semé d'embûches.

Merci à toi François, nous ne nous sommes rencontrés en réel que peu souvent, et la première fois en congrès mais tu as su te montrer à l'écoute, bienveillant et disponible pour me guider dans ce chemin.

Merci aussi à Isabelle de m'avoir formée, aidée à utiliser les instruments quand je suis arrivée au laboratoire et de m'avoir accompagnée à Lyon et Paris pour utiliser ces nouveaux instruments.

Merci Benoit pour ton aide avec les lipides, cela n'a pas été si facile à comprendre pour moi mais tu as su m'expliquer et corriger ces parties. Merci aussi à toi et Vincent pour les différents extraits de plasma que vous avez pu me fournir pour ce travail.

Merci aussi Carlos, pour vos idées, votre connaissance scientifique mais aussi votre bonne humeur et vos encouragements.

Je remercie tous mes encadrants d'avoir su m'accompagner durant ces trois années, cela n'a pas toujours été simple de concilier les avis de toutes les personnes intervenant dans les différents projets, mais nous avons su traverser ce chemin ensemble pour mener cette thèse.

Je tiens aussi à remercier Sandra, qui m'a ouvert les portes de son laboratoire pour que je puisse utiliser son TIMS-TOF. Merci pour ta formation et tes conseils sur ce nouvel instrument.

Je remercie Sabine et Florent qui m'ont accueillis au laboratoire ISA à Lyon pendant trois sessions qui m'ont permis de découvrir et expérimenter le DTIMS et ses spécificités. Merci à toutes les personnes du laboratoire ISA de m'avoir accueillie, conseillée et soutenue. Merci à Sophie pour sa gentillesse et son aide. Merci à Valentina de m'avoir accueillie pendant un week-end lors de ma dernière session. Merci aussi à Thomas de m'avoir inclus dans leurs pauses.

Merci à tous ces collaborateurs qui ont fait partie de ce chemin de thèse

Je remercie Julie pour son accompagnement en tant qu'enseignante référente pendant ces trois années. Merci de m'avoir soutenu et d'avoir su m'aider quand j'en avais besoin, tu es d'une écoute remarquable, je suis ressortie de nos rendez-vous boosté à chaque fois et prête à continuer ce chemin.

Je tiens aussi à remercier toutes les personnes qui ont pu m'accompagner dans la prise en main ou la gestion des petits soucis techniques sur les différents instruments que j'ai pu utiliser durant ces travaux de thèse. Je pense particulièrement à Laure, qui a installé, désinstallé et ré-installé le TIMS. J'aurais vraiment voulu que l'on laisse *Chouchou 2*, ça lui allait mieux comme nom ! Merci pour tes conseils, ton soutien, mais surtout ta bonne humeur durant tes nombreuses visites à Rouen.

Je tiens aussi à remercier toutes les personnes qui m'ont permises de faire une année en mission enseignement, notamment Corinne, Hélène et Laure pour leur aide pour la préparation des TPs mais aussi Françoise pour son soutien et son aide dans la salle de TP. Ta bonne humeur m'a aidée à gérer ces nombreux groupes, parfois dissipés.

Merci aussi à toi Gérald pour ton soutien, ta bonne humeur et ton aide face à tous mes problèmes administratifs pour les congrès (grâce à toi je n'ai jamais dormi sous les ponts !). Merci aussi pour le fauteuil, qui m'a épargné quelques douleurs.

La thèse n'est pas qu'un travail sur un sujet, mais c'est aussi participer à la vie du laboratoire. Je tiens à remercier tous mes collègues, tous ceux qui ont traversé mon chemin durant ces trois belles années à Rouen. L'arrivée dans cette ville n'aura pas été facile, avec la vie post-covid, mais vous avez su m'intégrer à cette petite équipe Analyse. Merci à toi Marie d'être toujours présente quand il y a un problème au laboratoire, de ton soutien face aux instruments capricieux. Merci Mathilde pour ta bonne humeur, ton aide précieuse et surtout ton soutien dans les moments difficiles, tu as toujours su m'écouter et me conseiller (Et encore félicitations !).

Je tiens particulièrement à remercier Delphine, tu as été mon rayon de soleil dans le bureau, ma bouffée d'air quand j'en avais besoin. Tu as su m'aider, me donner de la force dans ces derniers mois et nos discussions ont toujours été super enrichissantes, merci à toi ! Nos moments de craquage mental resteront dans ma mémoire ! Je te souhaite que ta dernière année se passe bien, je suis sûre que tu vas très bien gérer. Tu vas beaucoup me manquer...

Merci à Charlotte pour sa bonne humeur, son rire à faire trembler les murs, je m'en souviendrai longtemps mais aussi nos discussions profondes. Pleins de courage pour les quelques mois restants, je suis sûre que les étoiles vont s'aligner pour toi ! Merci Maxime pour ta gentillesse et ton aide, tu m'as fait gagner beaucoup de temps avec tes petits codes sur DataAnalysis. Je me souviendrai de notre trio à Los Angeles, pleins de souvenirs et de beaux moments de rigolades !

Merci à toi Aurélien pour ta bienveillance et ta si grande gentillesse, tu as su me donner le sourire quand j'en avais besoin !

Un immense merci à tous les étudiants, doctorants et post-doctorants, que ce soit les anciens ou ceux qui sont encore au laboratoire et notamment Olivier pour ton aide, tes courgettes (on s'en souviendra tous je pense) mais je ne peux pas te remercier d'avoir contribué (avec moi je te l'accorde) aux multiples problèmes sur le TIMS, j'espère que cette fois-ci tu vas enfin pouvoir finir tes images ! Merci à Jason, j'espère que tu sauras me remplacer pour les flash discussions (et non ça ne s'appelle pas encore flash point). Merci aussi à Julien, pour ton accueil dans le bureau. Je remercie aussi Estelle, Clément, Nathaniel, Oscar, Johann, Leïla, Marie, Hend, Matthieu, Gautier, Sébastien mais aussi le nouvel arrivant Théo ou encore le futur doctorant, Guillaume, vous amenez de la vie dans le bureau qui a parfois été un peu vide. J'espère que vous prendrez soin de mon bouquet de fleurs séchées, il a quand même survécu deux ans dans ce bureau. Merci aussi aux stagiaires et étudiants de passage, je pense particulièrement à l'humour de Solweig, mais aussi à Anaïs et Estelle. Je me souviendrai des soirées bar ou karaoké, de nos discussions, rigolades ou encore des jeux le midi !

Merci aussi Chloé pour nos discussions devant le HCT ou le TIMS colère. Pleins de soutiens et de courage pour la fin de thèse !

Olive, si tu passes par-là, je te souhaite de réussir les JO2024, vu tes progrès en quelques mois en natation, je suis sûre que c'est possible !

Je remercie aussi tous les stagiaires ou étudiants en projet tuteuré qui ont passés quelques semaines ou mois au laboratoire pour travailler sur divers projets en lien avec mon sujet de thèse. Merci à Nihel, Priscillia, Bastien, Katia, Stacy, Max, Gauthier, Cassandre, Louis-François et particulièrement à Yaël pour son investissement et de m'avoir permise de finir une publication scientifique.

Je tiens à remercier cette équipe, tous les étudiants de l'équipe Masse, et plus généralement de l'équipe Analyse de m'avoir aidée et soutenue. Je n'oublierai pas tous ses moments et particulièrement les congrès et évènements que nous avons passés ensemble.


J'ai eu la chance durant ce doctorat de participer à de nombreuses journées, congrès ou cours. Je tiens donc à remercier le Réseau Français de Métabolomique et Fluxomique qui m'a permis de présenter mes résultats de thèse pour la première fois à Aussois, et surtout qui m'a permis de rencontrer mon co-directeur de thèse pour la première fois en personne. J'ai pu découvrir le concept de bonne bouffe, bonne science.

Je remercie aussi le Club Jeune de Société Française de Spectrométrie de Masse de m'avoir permise de présenter à trois reprises mes travaux durant les trois années de thèse, les rencontres en visio, à Lyon et Marseille ont toujours été très enrichissantes et m'ont permises de découvrir autant de sciences que de personnes très sympathiques. Je remercie la SFSM de m'avoir donné cette bourse de voyage qui m'a permis de faire mon premier congrès international Metabolomics en Espagne. J'ai pu y faire mon premier oral en anglais, et découvrir de nombreuses personnes, merci à Thomas, Jessica, Hikmat, Christian ainsi que Arianna, Manon, Matthieu, les belges du groupe, merci de m'avoir fait vivre cette expérience enrichissante avec vous. Merci aussi à François et Anne-Laure pour les bons moments passés avec vous pendant cette semaine riche.

Je me souviens aussi d'Analytics, qui m'a permis de présenter mes travaux de thèse sous forme de flash présentation et du poster n°1 et ainsi des nombreux échanges qui en découlent.

Je tiens aussi à remercier de nouveau le RFMF, qui m'a accordé une bourse de voyage qui m'a permis de voyager aux Etats-Unis pour aller pour la première fois à l'ASMS, afin de présenter un poster sur mes résultats de thèse, ceci a été une expérience enrichissante.

Je remercie ma famille Totoro qui me permet d'avoir toujours un lien avec l'ECPM, école qui m'a vu grandir et évoluer. Pleins de soutiens à Tristan et Gaby, j'espère que je pourrais vous revoir bientôt, et rencontrer toute la famille Totoro !

Je tiens sincèrement à remercier le discord PhD Student, qui m'a soutenu, aidé. Faire partie de cette communauté, pouvoir échanger avec d'autres doctorants sur ces doutes, questionnements, coups de blues mais aussi victoires. Cela a été ma petite escale, mais aussi ma motivation en rejoignant plusieurs autres doctorants pour se motiver ensemble à avancer malgré les difficultés de la thèse, vive les Work Together ! Je pense aussi à l'IRL à Lyon, qui m'a permis de découvrir certains d'entre vous, je ne vais pas risquer de citer certains mais je suis sûre que vous vous reconnaîtrez. Merci tout simplement ! 

Merci aussi à toute l'équipe du rush, qui aura suivie mes nombreux doutes, questionnements et tous les rebondissements pendant la phase de rédaction assez compliquée. Merci à tous.tes de m'avoir soutenue, encouragée, sans vous cette phase aurait été bien plus difficile. Je sais que nous sommes beaucoup à soutenir en cette fin d'année, je vous donne beaucoup de force, vous allez tous.tes faire une magnifique soutenance ! 😊

Merci aussi à la petite équipe de chimie analytique que j'ai pu rencontrer à Analytics, ça m'a fait plaisir de vous voir ! Merci pour vos conseils et votre soutien dans le chan *Chimie*.

Merci aussi aux quelques personnes qui contribuent à 28% dans l'Horloge Parlante et aux chers boullieristes avec des ambitions toujours plus élevées, on pourrait nous prendre pour une secte peut-être, mais vous m'avez fait beaucoup de bien 🍷

Merci à toute l'équipe de modération ! Partager les réunions, et tous ces moments avec vous afin de modérer cet espace est toujours très enrichissant. Cela me permet d'apprendre beaucoup et notamment sur la communication avec de nombreuses personnes. Vous m'avez apporté beaucoup et vive les emojis ! Vous êtes une équipe au top ! Merci beaucoup les modératrices ! 🌈

Je remercie aussi cette thèse, qui m'aura permis de grandir, d'affronter de grandes difficultés. Ces 3 ans ont été très riches en émotions, en doutes, en pleurs, en remise en question mais je me sens grandie, changée.

Pour une petite touche d'humour, je ne remercie pas le covid qui aura su se montrer particulièrement féroce et tenace, et surtout dans les pires moments. Mon corps aura été soumis à de rudes épreuves pendant cette thèse, mais il est maintenant prêt à braver toutes les épreuves.

Je tiens aussi à remercier mes ami.es de m'avoir soutenue. Je pense particulièrement à Valentina, tu as su être présente, attentive, tu m'as soutenu dans les bons comme les mauvais moments. Merci pour tous ces moments partagés, que ce soit les rigolades et discussions dans le bureau, ou même ton mariage ! Je te souhaite tout le meilleur du monde, et une très belle vie, tu le mérites ma belle ! ❤️

Je remercie aussi Lisa, je ne te connaissais que très peu mais nous avons appris à nous découvrir en Sicile et j'ai adoré nos discussions et nos délires. Merci à toi pour ton soutien, je suis sûre que ta soutenance se passera très bien.

Je remercie Jérôme, tu es et resteras une personne géniale ! Merci de m'avoir encouragé et soutenu ! Merci pour tes mêmes quand j'ai un coup de blues, ton ouverture d'esprit et tes rires à mes blagues nulles !

Merci à tous ceux qui ont fait escale dans ma vie, avec un message, une attention, certains échanges intéressants, je pense particulièrement à Pascal, Julien, mais surtout Lucas, merci à toi. Je remercie Arnaud pour sa gentillesse, son écoute qui m'a permis de changer, grandir, de prendre confiance en moi et d'oser, ce qui a été d'une aide précieuse pendant cette thèse.

Merci aussi à ce petit ange, je sais que tu te reconnaîtras, qui m'aura permis de passer ces derniers mois plus sereinement. Nous avons échangé beaucoup de moments ensemble, de joie, de doutes, de pleurs parfois mais tu m'auras toujours permis de voir le bon côté de la vie. Merci de m'avoir sauvée, sans toi cette thèse ne serait pas ce qu'elle est !

Je tiens à remercier ma famille et particulièrement mes parents, d'avoir toujours su me donner confiance en moi, me pousser à l'action, depuis toujours et surtout pendant ces huit années d'études, au départ en déménageant à Strasbourg, puis en me suivant dans tous mes déplacements. Même si je sais que pour vous tout cela est un peu obscur, vous avez toujours su me soutenir.

Merci à mon petit frère, d'être celui qu'il est, de me soutenir et de me faire rire, de toujours être présent, dans les bons et moins bons moments. Merci beaucoup à toi ! Merci aussi à Fanny. ❤️

Je remercie aussi mes grands-parents d'avoir su se montrer présents, et aimants ! Merci Mamie pour tes petits plats, tes appels, ton soutien et surtout ta sauce tomate ! Merci Papi pour ta joie, tes sourires, et même si tu ne l'utilises pas beaucoup, je sais que je peux t'appeler si j'ai besoin (surtout si j'ai besoin de légumes, je pourrais même venir si les magasins ferment, on ne pourrait pas mourir de faim).

Merci à mes tantes, oncles, cousins, cousines, d'être présents et à l'écoute, même à l'autre bout du monde, j'espère vous revoir bientôt les Réunionnais.es !

Je remercie particulièrement ma grand-mère, ma Mamie Nou qui a toujours cru en moi, même depuis les étoiles et qui j'espère est fière de moi ! Je t'aime au-delà des étoiles ❤️

Je remercie une dernière fois toutes les personnes qui ont contribué de près ou de loin à l'élaboration de cette thèse, que ce soit d'un point de vue scientifique mais surtout pour le soutien moral. J'ai certainement oublié quelques personnes, ne m'en voulez pas, je pense aussi à vous et je vous remercie sincèrement d'avoir fait un passage dans ma vie pendant ces trois années de thèse!

Je finirais simplement par un **MERCI** !

« On s'adapte,
On improvise,
On domine »
Mon papa,

Adapté du film *Le Maître de guerre*

Table of Contents

Acknowledgments/ Remerciements.....	- 5 -
Table of Contents	- 12 -
List of figures.....	- 15 -
List of Tables.....	- 19 -
Abbreviations.....	- 20 -
General introduction	- 21 -
Chapter I. Metabolomics by mass spectrometry	- 23 -
I.1. Introduction to metabolomics	- 23 -
I.1.1. Definitions.....	- 23 -
I.1.2. Lipidomics introduction	- 25 -
I.1.3. Applications of metabolomics and lipidomics	- 27 -
I.1.1. Classification of metabolites	- 28 -
I.1.2. Approaches in metabolomics.....	- 30 -
I.1.3. The Metabolomics workflow	- 31 -
I.2. Sample preparation: from collection to analysis	- 32 -
I.2.1. Collection of the samples, quenching and deproteinization.....	- 33 -
I.2.2. Extraction technique	- 34 -
I.3. Mass spectrometry-based metabolomics	- 37 -
I.3.1. Overview of metabolomics analysis	- 37 -
I.3.2. Mass spectrometry instrumentation	- 38 -
I.3.3. Direct introduction mass spectrometry.....	- 42 -
I.3.4. Coupling with separation based techniques.....	- 42 -
I.3.5. Imaging metabolomics.....	- 45 -
I.3.6. Complementarity with NMR analysis	- 46 -
I.4. Data treatment	- 47 -
I.4.1. Data processing.....	- 47 -
I.4.2. Data analysis by statistical tools	- 47 -
I.5. Metabolites annotation	- 49 -
I.5.1. Descriptors and matching with libraries	- 49 -
I.5.2. Standardization of metabolite identification.....	- 52 -
I.5.3. Standardization in lipid identification	- 52 -
I.5.4. Other tools for annotation	- 54 -
I.6. Conclusion of chapter I	- 55 -
Chapter II. Ion mobility for metabolomics.....	- 56 -
2.1. Ion mobility spectrometry	- 56 -
2.1.1. Introduction to ion mobility spectrometry	- 56 -
2.1.2. Applications of ion mobility	- 57 -
2.2. Ion mobility instrumentation	- 58 -
2.2.1. Drift tube ion mobility spectrometry	- 58 -
2.2.2. Travelling wave ion mobility spectrometry	- 60 -
2.2.3. New high-resolution techniques.....	- 61 -
2.2.4. Other techniques	- 64 -
2.2.5. Resolving power, resolution, selectivity, sensitivity and duty cycle	- 65 -

2.3.	Ion mobility-mass spectrometry (IM-MS)	- 67 -
2.3.1.	Ionization source for IMS	- 67 -
2.3.2.	Mass analysers	- 67 -
2.3.3.	Complementarity of IMS and MS	- 68 -
2.4.	IM-MS approaches used in metabolomics	- 68 -
2.4.1.	Direct introduction	- 69 -
2.4.2.	Chromatographic separation	- 70 -
2.4.3.	Tandem ion mobility spectrometry (IMS/IMS)	- 70 -
2.5.	Data treatment and annotation using IMS	- 71 -
2.5.1.	Data processing of LC-IMS-MS/MS data	- 71 -
2.5.2.	Structural elucidation of compounds using IMS	- 72 -
2.6.	IMS as an additional separation dimension	- 75 -
2.6.1.	Isomer separation by IM-MS	- 76 -
2.6.2.	Parameters influencing the IMS separation	- 77 -
2.6.3.	Mobility-mass correlation	- 79 -
2.7.	Collision Cross Section as an additional descriptor	- 80 -
2.7.1.	Definition of the CCS	- 80 -
2.7.2.	Experimental CCS values	- 81 -
2.7.3.	Computational calculations of CCS values	- 84 -
2.7.4.	Machine learning CCS prediction	- 85 -
2.7.5.	CCS databases	- 86 -
2.7.6.	CCS contribution in metabolites annotation	- 90 -
2.8.	Challenges to include IMS in Metabolomics workflows	- 92 -
2.8.1.	CCS determination : calibration issues	- 92 -
2.8.2.	Evaluation of the experimental CCS values	- 96 -
2.9.	Conclusions of chapter II	- 97 -
Chapter III.	Influence of experimental parameters on CCS determination	- 98 -
3.1.	Introduction	- 98 -
3.2.	Influence of experimental conditions on TIMS measurements	- 99 -
3.2.1.	Influence of LC and source parameters on ^{TIMS} CCS determination (Article)	- 99 -
3.2.2.	Influence of the TIMS conditions	- 117 -
3.3.	Influence of source and multiplexing conditions on ^{DT} CCS values	- 118 -
3.3.1.	Source parameters	- 118 -
3.3.2.	Influence of multiplexed acquisition on the CCS determination	- 119 -
3.4.	Influence of experimental parameters on TWIMS instrument	- 120 -
3.4.1.	Influence of the source parameters on ^{TW} CCS	- 120 -
3.4.2.	Influence of the IMS conditions	- 120 -
3.5.	Conclusion and perspectives	- 121 -
Chapter IV.	Study of the TWIMS calibration procedure towards the reduction of the CCS deviations	- 122 -
4.1.	Introduction	- 122 -
4.2.	Study of calibrants	- 122 -
4.3.	Study of calibrants to standardize lipid ^{TW} CCS values (Article)	- 123 -
4.3.1.	Abstract	- 124 -
4.3.2.	Introduction	- 124 -
4.3.3.	Experimental section	- 126 -
4.3.4.	Results and discussion	- 128 -

4.3.5. Conclusions.....	- 134 -
4.3.6. References.....	- 135 -
4.3.7. Supplementary information.....	- 139 -
4.4. Conclusion and perspectives.....	- 166 -
Chapter V. Influence of the instruments on the measurement of collision cross sections-	167 -
5.1. Introduction.....	- 167 -
5.2. Comparison of lipid CCS values from three instruments (Article).....	- 167 -
5.2.1. Abstract.....	- 168 -
5.2.2. Introduction.....	- 169 -
5.2.3. Experimental section.....	- 171 -
5.2.4. Results and discussion.....	- 173 -
5.2.5. Conclusion.....	- 179 -
5.2.6. Supporting information.....	- 184 -
5.3. Discussion on stepped-field CCS values.....	- 203 -
5.4. Conclusion.....	- 205 -
Conclusions and perspectives.....	- 207 -
Résumé en Français (Summary in French).....	- 210 -
Introduction.....	- 210 -
Matériel et méthodes.....	- 211 -
Résultats.....	- 211 -
Influence des paramètres expérimentaux sur la détermination des CCS.....	- 212 -
Etude lipidomique d'échantillon de plasma par TWIMS-MS : mise en place d'une procédure de réétalonnage pour obtenir des CCS interoperables.....	- 213 -
Etude inter-plateformes de trois techniques de mobilité ionique pour la détermination des CCS de lipides plasmatiques.....	- 215 -
Conclusion et perspectives.....	- 216 -
Communications and formations.....	- 220 -
Bibliography.....	- 222 -

List of figures

Figure I-1: Representation of the "omics" sciences (adapted from (Steuer, Brockbals, et Kraemer 2019))	- 23 -
Figure I-2: Representation of the metabolomic human network, showing the different pathways between metabolites (adapted from http://pathways2.embl.de/iPath1/ (Letunic et al. 2008)).....	- 24 -
Figure I-3: Lipid classification, example of one representative lipid per class (from (Eoin Fahy et al. 2011)).....	- 25 -
Figure I-4: Chemical structures of phospholipid classes by distinguishing both hydrophobic and hydrophilic parts (Red: phosphate group, green: glycerol, pink: sphingosine, blue green: fatty acid chains). PA: phosphatidic acid, PS: phosphatidylserine, PE: phosphatidylethanolamine, PC: phosphatidylcholine, PI: phosphatidylinositol, PG: phosphatidylglycerol, from (Boldyreva et al. 2021)).....	- 26 -
Figure I-5: Concentrations of lipid species reported for the NIST SRM 1950 reference plasma, according to the different classes (from (Burla et al. 2018))	- 28 -
Figure I-6: Metabolites classification: primary, secondary metabolites and xenobiotics; from (Junot et al. 2014))	- 29 -
Figure I-7: HMDB classification for the identified metabolites of the study. The HMDB superclasses and classes were represented in part A and B respectively, from (Z. Du et al. 2022)).....	- 29 -
Figure I-8: Plant secondary metabolism classification, from (Sharma et al. 2022)).....	- 30 -
Figure I-9: Two main types of metabolomics analyses: untargeted vs targeted, from (San-Martin et al. 2020))	- 31 -
Figure I-10: Metabolomics workflow (from (Delvaux, Rathahao-Paris, et Alves 2021))	- 32 -
Figure I-11: Example of the steps of sample preparation according to the different matrices before LC/MS analysis; from (Roca et al. 2021).	- 34 -
Figure I-12: Solvents or solvents mixtures used in the extraction procedure in metabolomics and lipidomics according to the polarity or X logP of the different compound classes, from (Cajka et Fiehn 2016)).....	- 35 -
Figure I-13: Different lipid extraction methods for lipidomics studies and the lipid classes associated, from (Tumanov et Kamphorst 2017))	- 36 -
Figure I-14: Venn diagram representing the specificity and the overlap of metabolites detected by four analytical method: FIA-MS (blue), GC-MS (green), LC-MS (black), NMR (red) in skeletal muscle metabolomics (Bruno et al. 2018))	- 38 -
Figure I-15: Schematic representation of a mass spectrometer with some possibilities for each part of the instrument.....	- 38 -
Figure I-16: Complementarity of the ionization source for metabolomics; from (Y. Wang et al. 2015)).....	- 40 -

Figure I-17: Different acquisition modes useful for metabolomics study, in the left from (Courant et al. 2014) and in the right, from (Krasny et Huang 2021).....	- 41 -
Figure I-18: Comparison of three LC phases according to the analyte polarity and the sensitivity in ESI-MS, from (Kahsay et al. 2014).....	- 44 -
Figure I-19: Comparative study of HILIC and RPLC in LC-MS analyses of human urine and plasma in positive and negative ESI modes. Metabolome coverage of human urine and plasma by Venn diagrams representing the proportion and quantity of metabolic features detected in HILIC or RPLC (Hypersil Gold and Zorbax SB), adapted from (Contrepolis, Jiang, et Snyder 2015).	- 44 -
Figure I-20: a) Growth of NMR, MS and combined metabolomics study (review on pubmed done in 2020). b) Representation of both advantages and drawbacks of RMN and MS and reasons to combine both techniques. Reprinted from (Letertre, Dervilly, et Giraudeau 2021). -	46 -
Figure I-21: Schematic representation of the different steps of metabolomics data analysis, from (Anwardeen et al. 2023)	- 48 -
Figure I-22: Number of possible structures depending of the different levels of mass accuracy regarding PubChem compounds database, adapted from (May et McLean 2016).....	- 49 -
Figure I-23: Analysis of the human metabolome coverage and the percentage that can be detected by LC-MS analysis, from (Roca et al. 2021).	- 51 -
Figure I-24: Confidence levels for metabolite annotation, from (Schrimpe-Rutledge et al. 2016) . -	52 -
Figure I-25: Structure of the lipid PC(18:0/18:1(9Z))	- 53 -
Figure I-26: Annotation of a specific lipid according to the annotation level of the species (adapted from (Liebisch et al. 2020))	- 54 -
Figure II-1: Description of the developments in IMS instrumentations from 1896 to 2014, from (May et McLean 2015).....	- 56 -
Figure II-2: Different types of IMS technology with key points describing the technique, reprinted from (Dodds et Baker 2019)	- 58 -
Figure II-3: Schematic representation of a DTIMS instrumentation	- 59 -
Figure II-4: (A) Schematic representation of a DTIMS instrument with an enlargement on the trapping ion funnel where the multiplexing is implemented. (B) Conventional single pulse method. (C) Multiplexing method: series of ion pulses with a setting interval time, from (May et al. 2020). Based on a Agilent 6560 instrument	- 60 -
Figure II-5 : Schematic representation of a TWIMS instrumentation	- 61 -
Figure II-6: Cyclic IMS (Waters Select Series Cyclic IMS) instrumentation and an example of a separation of three compounds after 1 and 5 passes onto the cIMS; adapted from (Ujma et al. 2019).....	- 61 -
Figure II-7: IMS separation of different compounds according to the IMS instrumentation used (DTIMS, 44cm SLIM, 13m SLIM) ; adapted from (Deng et al. 2016)Trapped Ion mobility spectrometry.....	- 62 -

Figure II-8: Schematic representation of a TIMS instrumentation.....	- 63 -
Figure II-9: Description of the three steps occurring on the TIMS cell during each cycle time (adapted from (Ridgeway et al. 2018))	- 63 -
Figure II-10: Schematic representation of different approaches of PASEF. Unknown ions are shown in blue, analyte ions in red, yellow, and green, corresponding to the fragmentation experiment; from (Rudt et al. 2023).....	- 74 -
Figure II-11: Coverage of the Mass Spectrometry Metabolite Library of Standards (MSMLS) depending on the different analysis strategies employed; from (Nichols et al. 2018).	- 75 -
Figure II-12: TIMS spectra of isomer lipid species with cis in blue, trans in red and mixture in black according to the scan rate (Sr) used, adapted from (Jeanne Dit Fouque et al. 2019) ..	- 76 -
Figure II-13: IMS spectra of different isomer lipid species according to the IMS resolving power, adapted from (Tu et al. 2019)	- 77 -
Figure II-14: Separation of some ions depending on the drift gas used (R.A.: relative abundance) and the peak-to-peak resolution Rpp representing for three couple of ions according to the gas, from (Morris et al. 2019).....	- 78 -
Figure II-15: Examples of mobility-mass correlation curves of various classes of metabolites from blood sample, in the left, adapted from (Dwivedi, Schultz, et Jr 2010) and different lipid classes, adapted from (Tu et al. 2019).....	- 79 -
Figure II-16: Mobility-mass correlation curves showing four different compound classes of contaminants and their metabolites which can be present in biological fluids, adapted from (Belova et al. 2021).	- 80 -
Figure II-17: Illustrations of four approaches used to determine theoretical CCS values. a: projection approximation, b: projection superposition approximation; c: Exact hard sphere scattering and d: trajectory method; adapted from (Sarah Markley Stow 2015).	- 85 -
Figure II-18: Construction of CCS databases using A: machine learning prediction; B: experimental measurements; C: Theoretical calculations to obtain the advantages for component identification (D); from (X. Li et al. 2023)	- 87 -
Figure II-19: Schematic representation of the workflow used for annotation of untargeted analysis by IMS-MS using scoring levels for each of the descriptor; from (Dodds et Baker 2019)	- 90 -
Figure II-20: Improvement of metabolite annotation using the CCS values. a: Example of rank improvement for 6-hydroxycoumarin, b: Reduction of the number of possible candidates according to the CCS tolerance applied, c: Average candidates using different samples and using different descriptors, adapted from (Zhiwei Zhou et al. 2020).....	- 91 -
Figure III-1 : LC-IM-MS workflows implemented for lipid analyses involving three different IMS strategies: from sample preparation to acquisitions and data processing	- 98 -
Figure S3: Influence of the nebulizer pressure (0.5-5 bar) for PE 10:0/10:0 [M+Na] ⁺ at 0.4 mL/min, T _{DGop} =250 °C, F _{DGop} =8 L/min (triplicates analysis have been performed)	- 115 -
Figure III-2: Drift times in function of the source conditions for LPC 16:0 and PC 16:0/16:0....	- 118 -

Figure III-3: Schematic representation of the Synapt instrument (Waters Corporation).. - 120 -

Figure IV-1 : Schematic representation of the objective of the chapter 4 - 122 -

Figure V-1: Schematic representation of the workflow used in this Chapter..... - 167 -

Figure 1: Evaluation of the method and intra-instrument performance, for the three different technologies. For DTIMS, the conditions (c1-c5) have been described in Table SA2 and for TIMS (c1-c3) in Table SA3, details have been previously reported for TWIMS [29] - 175 -

Figure V-2: Comparison of the ^{DT}CCS values, obtained with different calibrants with literature CCS values ((Hines et al. 2016) (Tsugawa et al. 2020b) (Vasilopoulou et al. 2020) (Leaprot et al. 2019) (Zheng, Aly, et al. 2017)) and stepped-field CCS values - 205 -

Figure V-3: Resume of the experiments made on the three instruments showing the repeatability and reproducibility of the CCS measurement using Tune Mix as calibrant. - 206 -

List of Tables

Table I-1: Comparison of some characteristics of different analysers, adapted from (J. Wang, Wang, et Han 2019)	- 40 -
Table I-2: LIPID MAPS indentifiers (LM_ID) format, adapted from (Sud et al. 2007)	- 53 -
Table II-1: Characteristics of some ion mobility technologies.....	- 66 -
Table II-2: Some major experimental CCS databases of metabolites, lipid or other compounds.....	- 88 -
Table II-3: Information on some calibrants: m/z and CCS values in Å ² in both positive and negative mode, the reference publication, and the application areas.....	- 94 -
Table S4: Lipid species detected in this study, in positive and negative mode respectively	- 114 -
Table III-1: TIMS parameters tested through three sets of conditions (c1, c2 and c3)....	- 117 -
Table III-2: ^{TIMS} CCS values obtained for seven plasma lipids in positive mode, according to the various sets of conditions tested, (mean CCS values with at least triplicates of analysis) .	- 117 -
Table III-3: Source parameters of the different tested conditions (Low values, basic set-up, and high values)	- 118 -
Table III-4: Ion mobility conditions for the experiments performed on the Agilent DTIMS system.....	- 119 -
Table III-5: ^{DT} CCS values of seven plasma lipids determined for five different IMS conditions (among which c4 and c5 correspond to multiplexing parameters).....	- 119 -
Table SA2 : Ion mobility conditions for the experiments performed on the Agilent DTIMS system.....	- 187 -
Table V-1: DTIMS parameters for stepped-field experiments	- 203 -
Table V-2: Comparison of CCS values of Tune Mix calibrant obtained using different conditions and the reference CCS values (Sarah M. Stow et al. 2017)	- 203 -
Table V-3: Comparison of the CCS values of Tune Mix calibrant obtained at different time intervals over one year and the reference CCS values (Sarah M. Stow et al. 2017)	- 204 -
Table V-4: Stepped-field CCS values of lipid standards and comparison with literature CCS values.....	- 204 -

Abbreviations

AIMS: Aspiration IMS
APCI: Atmospheric Pressure Chemical Ionisation
CCS: Collision cross sections
CID: Collision Induced Dissociation
cIM: cyclic IMS
DMA: differential mobility analyser
DMS: Differential ion mobility
DTIMS: Drift tube ion mobility spectrometry
ESI: Electrospray Ionisation
FAIMS: Field asymmetric ion mobility spectrometer
FT-ICR: Fourier Transform Ion Cyclotron Resonance
FWHM: Full Width at Half Maximum
GC: Gas Chromatography
HILIC: Hydrophilic Interaction Liquid Chromatography
HPLC: High Performance Liquid Chromatography
HRMS: High Resolution Mass Spectrometry
IMS: ion mobility spectrometry
m/z: mass to charge ratio
MALDI: Matrix Assisted Laser Desorption Ionisation
MS/MS: tandem mass spectrometry
MS: Mass Spectrometry
MSI: MS imaging
NMR: Nuclear Magnetic Resonance
OLIMS: Open loop IMS
PCA: Principal Component Analysis
PLS-DA: Partial Least Square Discriminant Analysis
QC: Quality Control
RPLC: Reversed Phase liquid chromatography
Rt: retention time
S/N: Signal to Noise Ratio
SFC: Supercritical Fluid Chromatography
SLIM: Structures for Lossless Ion Manipulation
TIMS: Trapped ion mobility spectrometry
TM-IMS: transversal modulation IMS
TOF: Time of Flight
TWIMS: travelling wave ion mobility spectrometry
UPLC: Ultra Performance Liquid Chromatography

General introduction

Let's imagine being able to explore the "heart" of each cell, each drop of blood and understand the chemical processes that drive life, revealing every unknown secret and solve the mysteries. Such an exciting opportunity is provided to some extent by the rapid expansion of metabolomics. Since, 20 years, metabolomics has paved the way to a greater understanding of biology, human health, and our environment by examining metabolites, molecules reflecting the different metabolism and metabolic pathways. Lipids and metabolites are vital and extremely diverse in both their structural and functional nature. The human metabolome has been studied using a variety of techniques, including nuclear magnetic resonance (NMR) and mass spectrometry (MS). Every metabolomics study advances our knowledge of biochemical processes and how living systems work, even though we still do not fully understand all the metabolic pathways and know all the metabolites making the metabolome (Ryan et Robards 2006). Confidently identifying metabolites still represents a huge analytical challenge. Up to now, it is estimated that only a few percentages of the human metabolome has been identified (Wishart, Guo, et al. 2022). Although the exact number of metabolites is not yet known, the metabolome is known to be extremely large, including numerous isobaric and isomeric metabolites (Courant et al. 2014).

High-resolution mass spectrometry (MS) has been widely implemented in metabolomics and lipidomics studies, generally hyphenated to liquid chromatography (LC). Thus, different analytical and structural information, such as retention time (RT), accurate mass measurement and fragmentation pattern from MS/MS data are provided by LC-MS/MS to annotate metabolites according to well-described levels of confidence. However, unambiguous assignment is still common as numerous isomers (diastereoisomers, enantiomers, regioisomers, cis/trans isomers,...) or isobars are present in biological samples and remain difficult to be definitely identified (Ben Faleh et al. 2023). Coupling ion mobility spectrometry (IMS) to liquid chromatography-high-resolution mass spectrometry in metabolomics workflows provides several benefits. Indeed, it brings an additional dimension of separation, increases peak capacity and affords a new molecular physico-chemical descriptor, the collision cross-section (CCS). IMS permits a gas-phase separation of ions according to their respective mobilities, in a cell filled with a buffer gas (He or N₂) and under the influence of an electrical field. The measurement of the ion mobility provides access to the collision cross-section (CCS) which reflects the three-dimensional structure of the ion. This additional descriptor enables more reliable identification of compounds, since it is added to RT, accurate *m/z*, MS/MS fragmentation data and isotopic pattern, already widely used for compound annotation in traditional LC-MS analyses. CCS derives from ion mobility using either a primary method (without calibration) or a secondary method which requires a calibration procedure (Gabelica et al. 2019). Currently, several IMS technologies that can be coupled to MS permit experimental CCS determination. The most widely employed are the drift tube ion mobility spectrometry (DTIMS) which satisfies primary method definition (Ibrahim et al. 2015), the travelling wave ion mobility spectrometry (TWIMS) (Giles et al. 2004; Richardson, Langridge, et Giles 2018) and the trapped ion mobility spectrometry (TIMS) (Fernandez-Lima et al. 2011; Michelmann et al. 2015) which implies secondary methods requiring calibrant. The CCS is a promising descriptor to support metabolite and lipid annotation in untargeted analysis, in particular through library search in CCS databases (Paglia et al. 2015; Paglia et Astarita 2017; Delvaux, Rathahao-Paris, et Alves 2021). High repeatability and robustness within 2% or even 1% of CCS values have been demonstrated (Hernández-Mesa et al. 2020). Moreover, reproducibility between CCS determined with DTIMS and those from

TWIMS or TIMS has been reported for a majority of compounds, and systematic comparisons revealed excellent interlaboratory performance (M. L. Feuerstein, Hernández-Mesa, Kiehne, et al. 2022). However, exceptions with CCS deviations up to 6% or 7% remained (Hinnenkamp et al. 2018; M. L. Feuerstein, Hernández-Mesa, Kiehne, et al. 2022). These CCS discrepancies (for a defined buffer gas) mainly come from unharmonized calibration procedures, available standards (calibrants) and the lack of consensus on reference CCS values. May et al highlighted the need of measurement standardization, agreement on reference CCS values and unified reference databases (May et McLean 2022). Moreover, Gabelica et al also warned on the urgency and importance to agree on values for a set of primary standards (Gabelica et al. 2019). Defining a set of reference and standardized procedures is therefore necessary for the further use of CCS as an annotation descriptor.

The aim of this research project is to study and develop standardization tools for CCS measurements to enable CCS alignment, to integrate this descriptor into metabolomics analyses, and to improve the reliability of metabolite annotation. For that purpose, various possible causes of deviations on CCS measurements have been evaluated for three different IMS commercial technologies coupled to mass spectrometry, DTIMS, TIMS and TWIMS. First, the experimental parameters related to sample introduction and electrospray ionization source, in particular for TIMS MS instrument design. In this instrument in which the IMS cell is located right after the ESI source, the influence of the ionization/desorption conditions have been studied to evaluate their influence on the ion mobility and also on CCS determination. Then, the IMS parameters of each of three technologies have been studied to determine their contribution on CCS deviations. The calibration procedure has also been examined, in particular through the study of eleven distinct commercial calibrants. Then, interplatform evaluation was performed comparing the three different ion mobility technologies with a standardized procedure implying a unique calibration standard.

The first chapter presents the bibliographic introduction on metabolomics analyses by mass spectrometry introducing the relevance to use ion mobility spectrometry. The second chapter exposes the IMS principle, the different technologies, the CCS definition, applications and contribution in metabolomics, CCS determination with related issues.

The three other chapters present the results of this research project. The chapter 3 reports the study of the influence of experimental parameters, such as ESI source and IMS cell parameters, on the CCS determination, for each of the three different IMS technologies. Thus, electrospray source parameters have been studied on the three instruments, with a focus on the TIMS instrument. IMS cell parameters have also been evaluated to estimate their contribution to the uncertainties on CCS determination.

The chapter 4 is dedicated to the study of ion mobility calibration procedure using the TWIMS cell and, in particular the evaluation of eleven commercial calibrants currently utilized in metabolomics and lipidomics. For that purpose, lipids of human plasma have been used as analytes model. A CCS realignment strategy allowing to reduce the CCS deviations due to calibrating substance has been proposed.

The chapter 5 exposes an interplatform and interlaboratory study through the comparison of 130 CCS determined by the three technologies DTIMS, TWIMS and TIMS for various lipids present in human plasma. Intra-instrument repeatability and interplatforms reproducibility were evaluated. These results constitute a complement to recent studies (M. L. Feuerstein, Hernández-Mesa, Kiehne, et al. 2022) and afford additional information on interplatform and interlaboratory evaluation, in particular in the lipidomics field.

Chapter I. Metabolomics by mass spectrometry

I.1. Introduction to metabolomics

I.1.1. Definitions

Metabolomics is the global analysis of metabolome which corresponds to the whole set of metabolites, usually small molecules (< 1500 Da) present in a biological system, organisms, cells or tissues. Metabolome and metabolomics were firstly defined in 1990's (Oliver et al. 1998), including peptides, lipids, amino acids, nucleic acids, vitamins, food compounds, drugs, pollutants, pesticides, and numerous other chemical classes (Wishart et al. 2013). Both "metabonomics" (Nicholson et al. 2002) and "metabolomics" (Fiehn 2002) terms appeared in 2002, but, in practice, they are often used for the same purpose (Nicholson et Lindon 2008). In details, metabolomics refers to the study of the metabolome whereas metabonomics refers to the study of the multiparametric metabolic responses of a particular living organism to pathogenic stimuli or genetic modification (Ramsden 2009) Both concepts have the same objective, the study of the metabolome (Ryan et Robards 2006). Metabolomics constitutes one of the "omics" science, such as exposomics, microbiomics, genomics, transcriptomics and proteomics. Genomics refers to the study of genetic information and DNA in a biological cell, transcriptomics is the study of gene expression, corresponding to all the RNA transcripts present in a cell, proteomics deals with the study of proteins, as illustrated with Figure I-1 (Steuer, Brockbals, et Kraemer 2019). Metabolomics is the final step of these omics sciences, and unlike the genome or proteome, the metabolome reflects the molecular phenotype of a human being (Fiehn 2002).

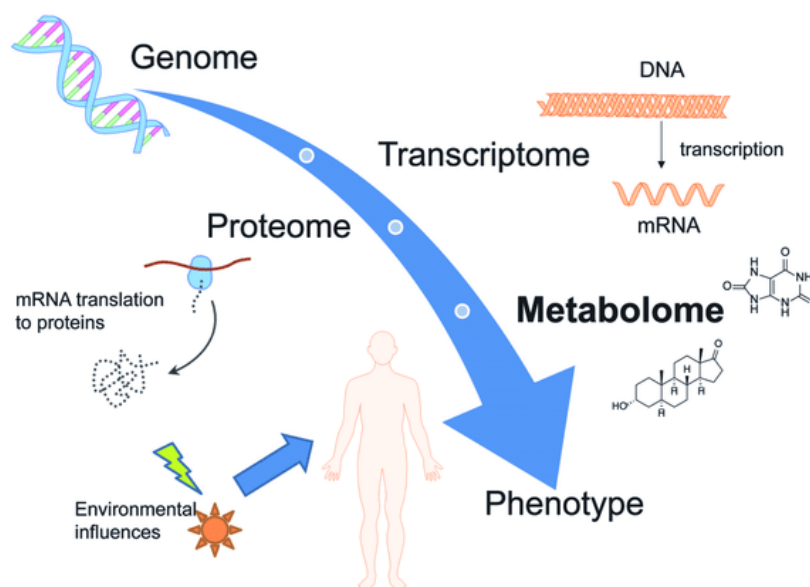


Figure I-1: Representation of the "omics" sciences (adapted from (Steuer, Brockbals, et Kraemer 2019))

The metabolome is thought to be the closest representation of phenotype and for this reason shows huge potential in a health context for the understanding of cellular processes in both healthy and diseased persons, also for biomarker discovery and personalized medicine (Guijas et al. 2018).

The phenotype changes could not always be explained by the genome, transcriptome or proteome, this is why the metabolome was extensively studied in the past 20 years. Metabolome analysis is complicated due to the huge number of compounds, the high diversity of their chemical classes, but also the dynamic ranges of concentrations which can be between pmol.L^{-1} and mmol.L^{-1} (Dunn et Ellis 2005; Psychogios et al. 2011). Although a complete understanding of all the metabolic pathways and all the metabolites involved in the metabolome are not yet fully known, every metabolomics study allows a better understanding of the biochemical processes and the functioning of the living systems (Ryan et Robards 2006). In each cell, at a given time, many substrates are transformed by enzymes, various biosynthesis processes occur, and many other molecules are biodegraded, all these reactions constituting the metabolism. The Figure I-2 depicts a visualization of the molecular pathways evolving in the human metabolism. It is highly complex but also highly organised and well-ordered (Fani 2012).

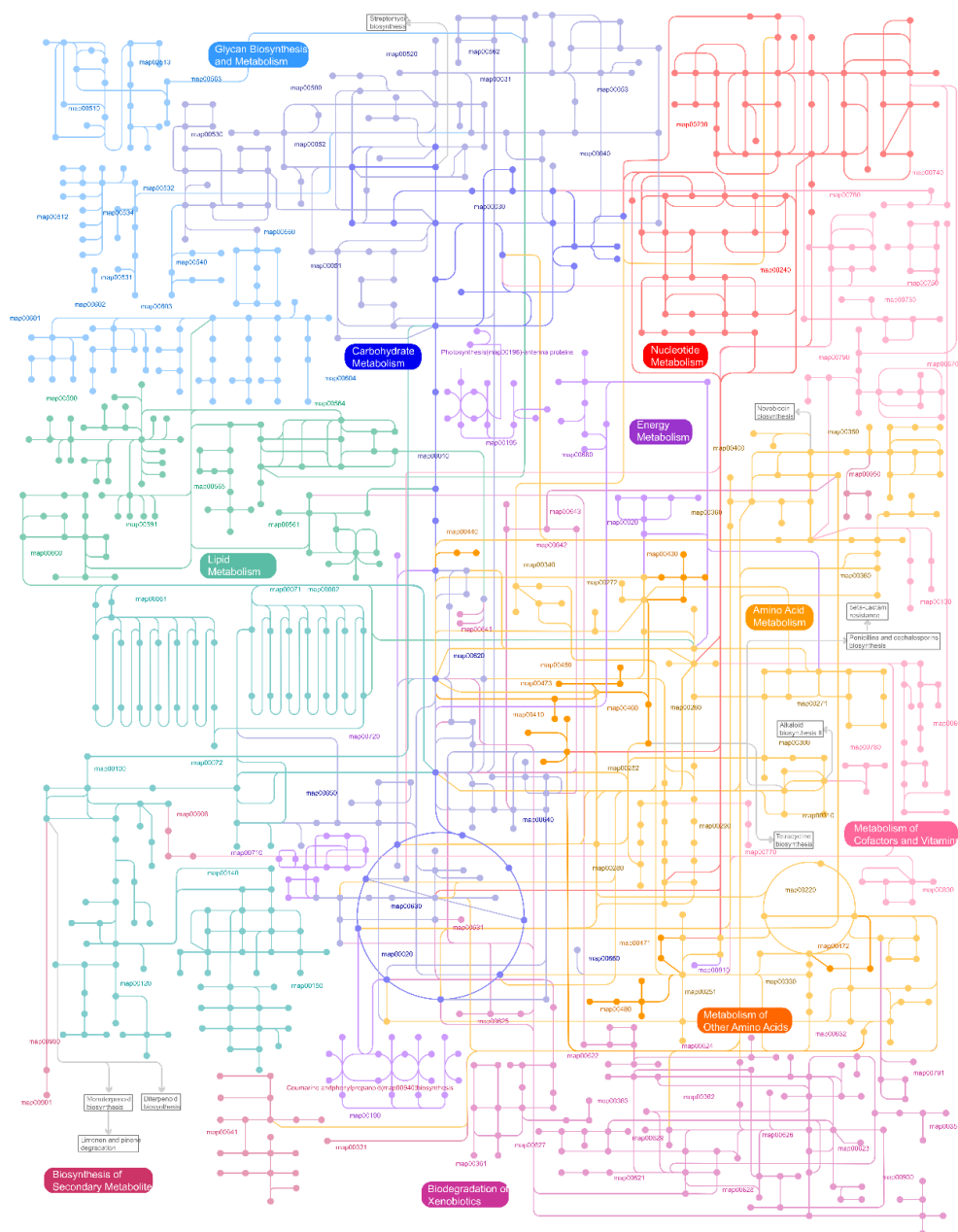


Figure I-2: Representation of the metabolomic human network, showing the different pathways between metabolites (adapted from <http://pathways2.embl.de/iPath1/> (Letunic et al. 2008))

I.1.2. Lipidomics introduction

I.1.2.1. Lipidomics definition and nomenclature

Few years after the beginning of metabolism study, a subpart of metabolomics, lipidomics, became the subject of more and more research. It aims to characterize organism's lipids to understand their influence on biological systems such as membrane architecture, cell signalling, lipid-lipid or lipid-protein interactions ... Lipids constitute an important class of biomolecules involved in the biological membranes, and many other biological functions. Lipids can be defined as hydrophobic molecules, and the constituents of the fatty matter of living organisms. A large diversity of compounds and chemical classes can be put into the lipid class, which can be divided into 8 categories: fatty acyls, glycerolipids, glycerophospholipids, sphingolipids, sterol lipids, prenol lipids, saccharolipids, and polyketides (Eoin Fahy et al. 2005). Examples of structures from each lipid class are reported Figure I-3. Each of these categories contains classes and subclasses, defined thanks to the head groups (Eoin Fahy et al. 2005). A coherent framework to represent lipid structures has been proposed by the LIPID MAPS consortium, as lipid structure of a same lipid could appear quite different from one publication to another, or from one database to another. LIPID MAPS® Structure Database (LMSD) contains 47,981 unique lipid structures, including 25,934 from experimental data and 22,047 computationally-generated (July 2023) which can be downloaded or used online on the LIPID MAPS® website (<http://www.lipidmaps.org>)(E. Fahy et al. 2007).

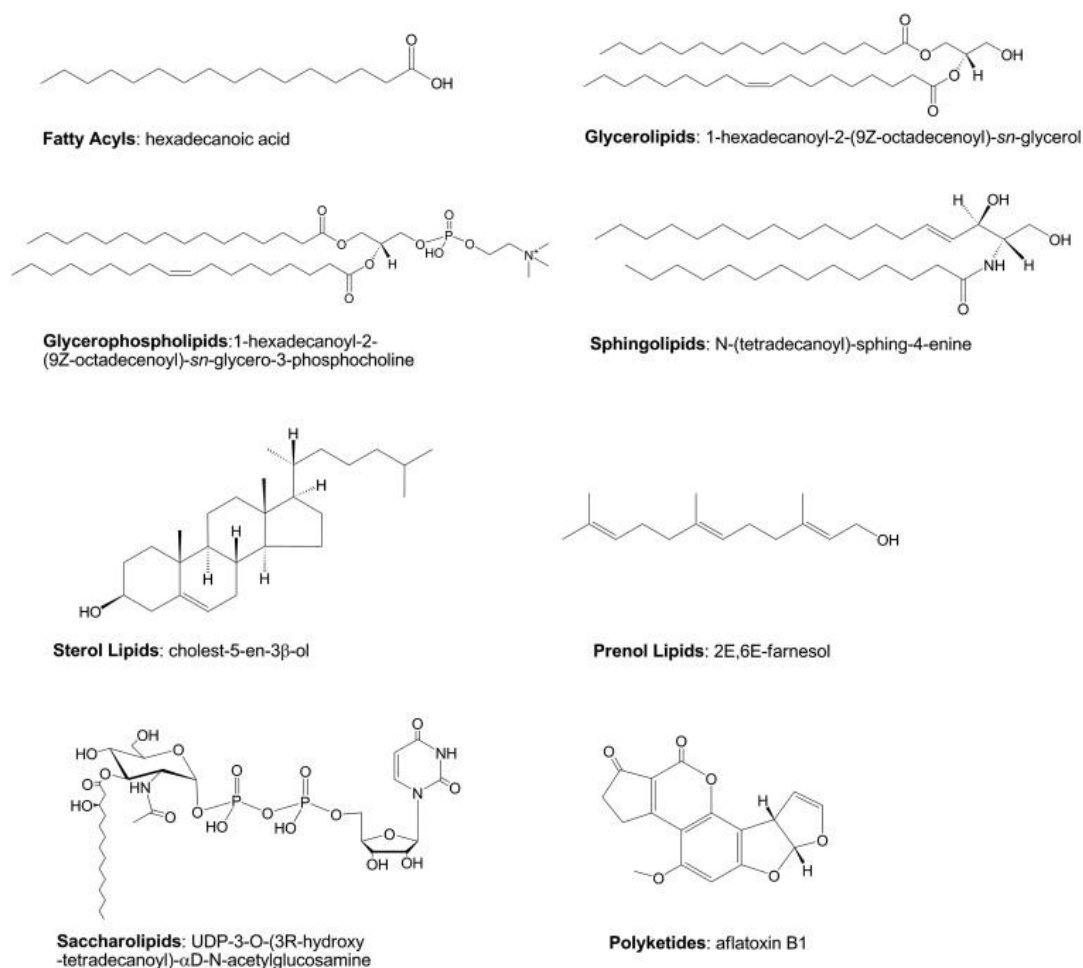


Figure I-3: Lipid classification, example of one representative lipid per class (from (Eoin Fahy et al. 2011))

I.1.2.2. Lipid classification

Lipid categories are separated into three groups, the non-polar lipids, containing the cholesterol, cholesterol esters and triglycerides; polar lipids including glycerophospholipids and sphingolipids; and lipid metabolites (Han et Gross 2005).

❖ Non-polar lipids

They are mainly constituted with cholesterol (Chol) and their esters (CE), and acylglycerol: Monoacylglycerols (MG), Diacylglycerols (DG), Triacylglycerols (TG). These lipids have a large hydrophobic part and are found in the plasma membrane for cholesterol, or cellular oil droplets and lipoproteins for CE and TG (Han et Gross 2005). The fraction of sterols depends on the matrices and can reach 50% in plasma membranes.

❖ Polar lipids

Glycerophospholipids (or phosphoglycerides) represent the most important class of phospholipids, which consist of a polar head group attached to a glycerol backbone and up to two fatty acyl chains. Those are a significant portion of membranes lipids, in bacteria, plants or mammals. They contain two parts, one hydrophobic, the other hydrophilic, which gives them amphibious properties. Due to this, phospholipids can be arranged into sheets by hydrophobic interactions between phospholipid molecules and hydrophilic interactions between phospholipids and water (Figure I-4). They are present in the spinal cord, brain, liver or heart. The hydrophilic part determines the class of the lipid, as shown at the top left of the Figure I-4.

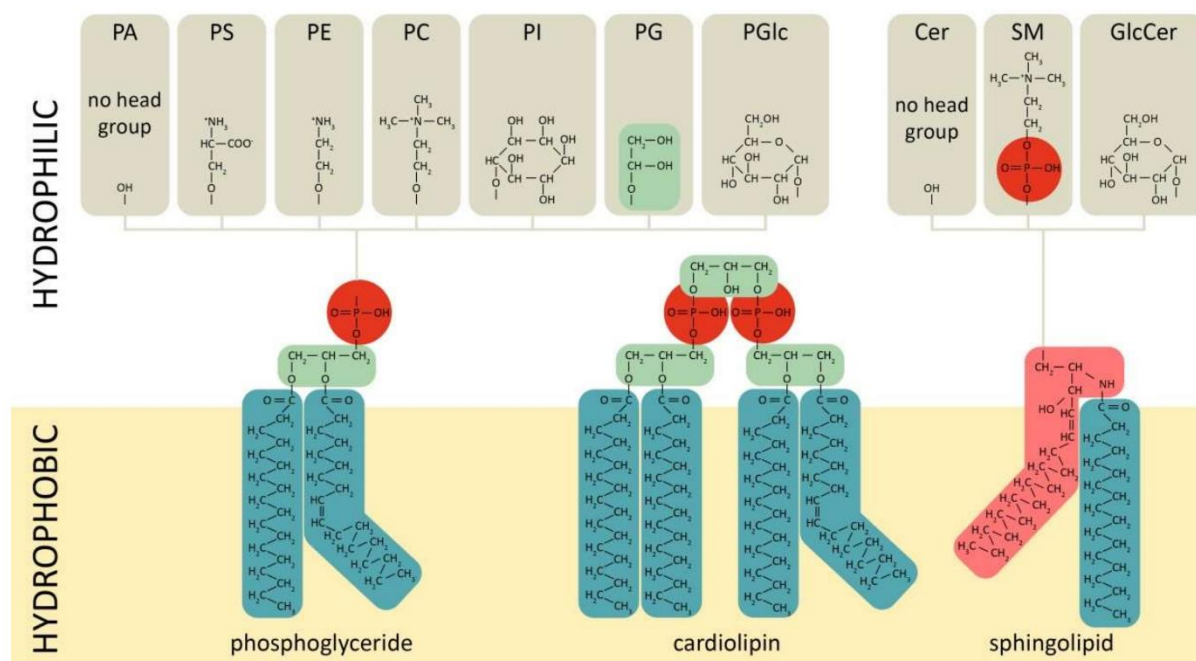


Figure I-4: Chemical structures of phospholipid classes by distinguishing both hydrophobic and hydrophilic parts (Red: phosphate group, green: glycerol, pink: sphingosine, blue green: fatty acid chains). PA: phosphatidic acid, PS: phosphatidylserine, PE: phosphatidylethanolamine, PC: phosphatidylcholine, PI: phosphatidylinositol, PG: phosphatidylglycerol, from (Boldyreva et al. 2021)

The second category of polar lipids are the sphingolipids, their fraction is less important than glycerophospholipids. They differ from the glycerophospholipids because they contain a sphingosine group and not a glycerol (as shown in Figure I-4). Different hydrophilic parts can compose a sphingolipid, providing different classes of lipids, as Ceramides (Cer), sphingomyelin (SM) or

Glucosylceramide (GlcCer). They play an important role in the membrane, cell function regulation and human diseases, as inflammation, cancer, neurologic and psychiatric disorders (Futerman 2021).

The third group of polar lipids are the glycolipids, which include glycosphingolipids and glyceroglycolipids. Both these classes contain a main difference, the hydrophobic part. The structure consists of a monosaccharide or oligosaccharide group fixed to a sphingolipid or a glycerol group with one or two fatty acids.

❖ Lipid metabolites

This last group associated to lipid species refers to their metabolites, products of enzymatic reactions or precursors, such as nonesterified fatty acids, fatty acid esters, acylCoAs, lysolipids, and ceramides. Lipid metabolites are biologically active and can be involved in some pathological conditions.

I.1.3. Applications of metabolomics and lipidomics

I.1.3.1. Applications of metabolomics

Metabolomics has been used for a wide scope of applications, as in medicine, pharmaceutical sciences, food and nutrition sciences, toxicology, agriculture or environment. For medicine application, metabolomics has been used for biomarker discovery, helping the early diagnosis of diseases; or for the comprehension of pathological mechanisms (Johnson, Ivanisevic, et Siuzdak 2016), such as diabetes (Morze et al. 2022). Metabolomics can also be used in pharmacology, to evaluate the effects of drugs, to identify potential new drugs and their interactions (Wishart 2016; Alarcon-Barrera et al. 2022). Metabolite profiling helps the development of precision and personalized medicine and treatment strategies (Pang et Hu 2023; Jacob et al. 2019). Food metabolomics has emerged in different aspects, as an indicator of food quality and safety or nutrition (Adebo et al. 2017; S. Li et al. 2021). Foodomics allows the control of food quality and food authentication, for instance to pinpoint frauds by determining the origin of products, for example for analysis of virgin olive oil (Gil-Solsona et al. 2016). Many matrices can be analysed with metabolomics workflows as milk, cereals, meat, fish, fruits or vegetables (Selamat, Rozani, et Murugesu 2021). Metabolomics in nutrition field, can be used to assess the impact of diet (Guasch-Ferré, Bhupathiraju, et Hu 2018). Metabolomics is also particularly useful in toxicology, or in environment or ecology studies, to identify biomarkers of exposure or environmental biomarkers, or apprehend the interactions between organisms and their ecosystems. Exposomics studies have grown with this objective, to understand environmental exposures, for example focusing on air pollution or water toxicants (Sun et al. 2022; Vineis et al. 2017).

I.1.3.2. Applications of lipidomics

The lipidome is part of the metabolome, thus variations with time, perturbations or environment can be experienced on lipid species too. As metabolites, the lipid concentrations are broad into a large range, according to their classes, as shown in Figure I-5. Lipidomics is crucial for diagnosing disorders and understand the mechanisms behind the development of some diseases. It was proven changes on the lipidome in diabetes, but also with other diseases as neurodegenerative disorders (Calvano, Palmisano, et Cataldi 2018; Shamim et al. 2018) as Alzheimer's and Parkinson's diseases (Chiurchiù et al. 2022) or cancer (J. Wang, Wang, et Han 2021).

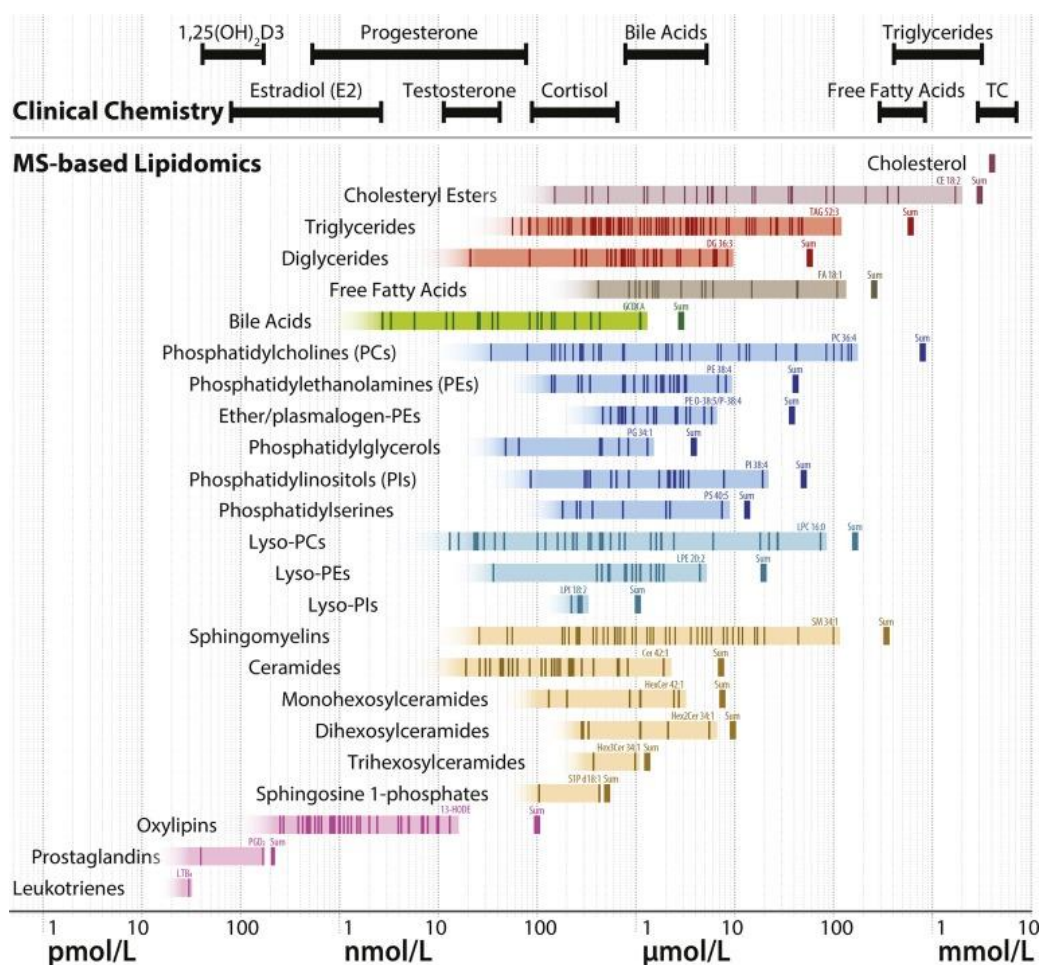


Figure I-5: Concentrations of lipid species reported for the NIST SRM 1950 reference plasma, according to the different classes (from (Burla et al. 2018))

Regarding the diversity of metabolites and lipids, numerous analytical methods could be useful to characterize the whole metabolome. In addition, metabolomics studies aim at different objectives as the differentiation of groups (for example, healthy individuals and diseased patients) to identify the metabolites that have changed or to determine differences in metabolite concentrations, and to understand the interactions with the biological system (genes, proteins...). These objectives cannot be achieved with a single method, this is why different approaches and techniques can be used together.

I.1.1. Classification of metabolites

The metabolome includes all small molecules that can be separated into three categories. First, the primary metabolites, which are ubiquitous, are produced by the vital metabolic pathways of the cells and have a direct role in the cell development, cell division, growth, respiration, photosynthesis or reproduction. This is the case for amino-acids, organic acids, nucleotides, sugars and lipids. The secondary metabolites are kingdom-specific and indirectly involved in the cell development. They are synthesized for a particular function for example, hormones or metabolites for defence purposes by plant organisms. The third category is the xenobiotics, compounds which are unexpectedly introduced in the organism and are not naturally produced, such as drugs, pesticides from food, pollutants from the environment (Junot et al. 2014). The xenometabolomics was defined as the profiling of xenobiotics, their products from biotransformation and their metabolites, present within an organism exposed to pollutants, food components or drugs (Holmes et al. 2007).

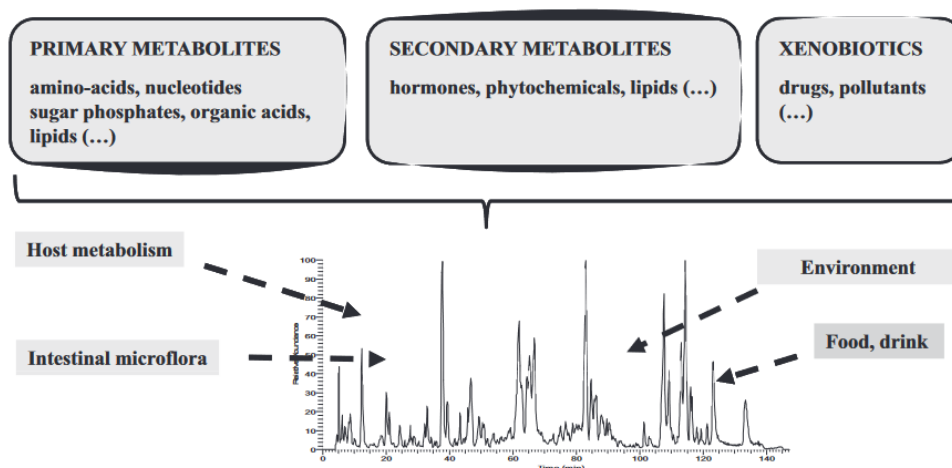


Figure I-6: Metabolites classification: primary, secondary metabolites and xenobiotics; from (Junot et al. 2014)

All these metabolites could be classified depending on their chemical classes. Thus, the classification used by the Human Metabolome DataBase (HMDB) for human metabolites is based on the various metabolite chemical classes (Wishart, Guo, et al. 2022). An example of this classification is displayed with the exploration of the metabolome from microbiota (Figure I-7). Tools and web applications such as ClassyFire have been developed to allow automated structural classification (Djombou Feunang et al. 2016).

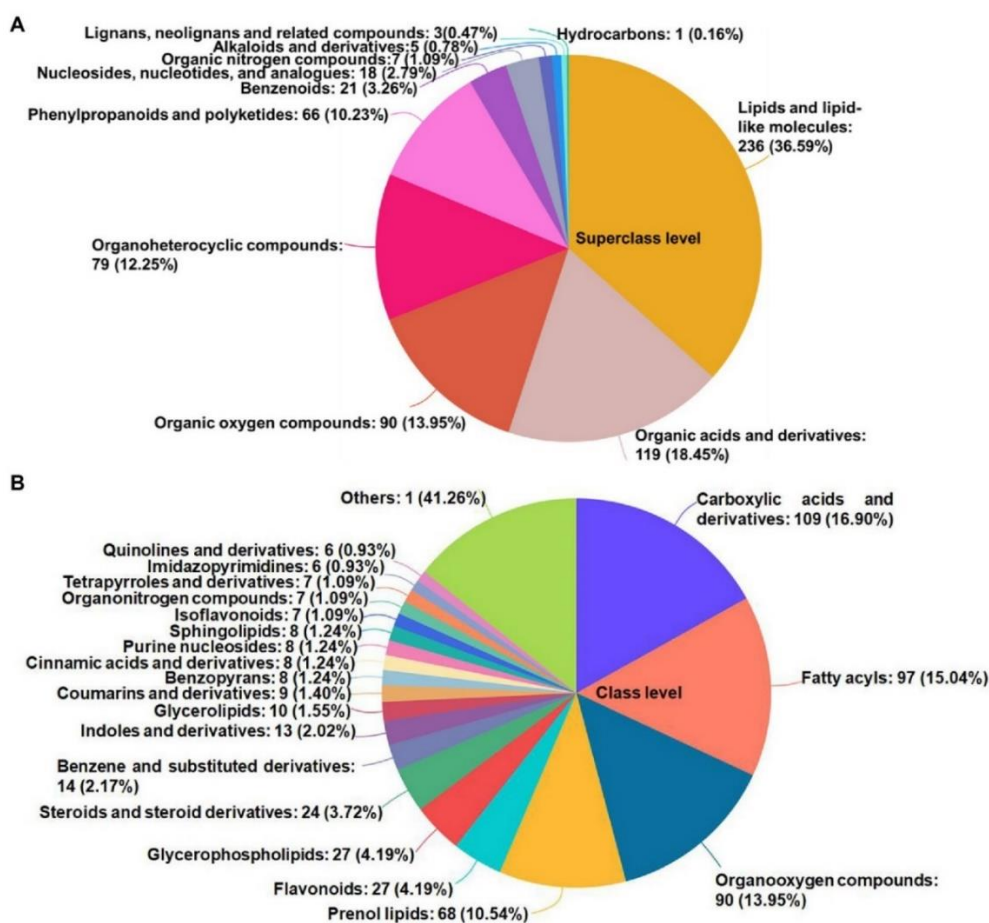


Figure I-7: HMDB classification for the identified metabolites of the study. The HMDB superclasses and classes were represented in part A and B respectively, from (Z. Du et al. 2022)

Concerning the plant kingdom, specific rules of taxonomy have been established to link the various species to their corresponding secondary metabolites. Plant secondary metabolites can be separated into four major categories as described in Figure I-8 (Sharma et al. 2022). Alkaloids, terpenoids, phenolics and sulphur containing compounds, which are specifically present in comparison to animal kingdom.

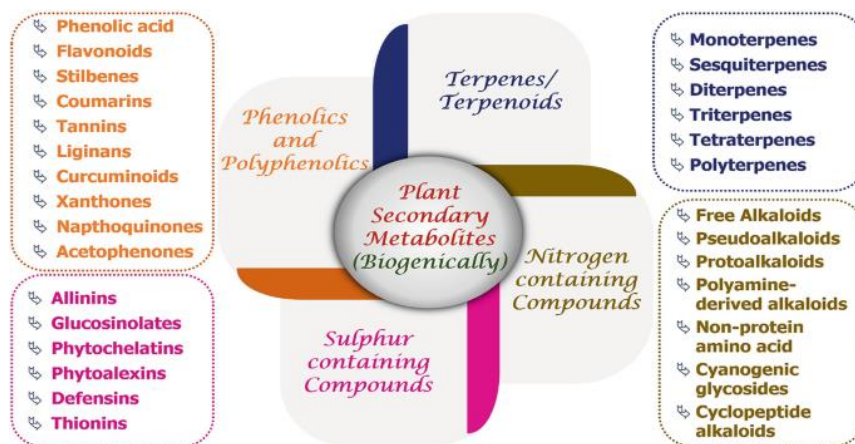


Figure I-8: Plant secondary metabolism classification, from (Sharma et al. 2022)

I.1.2. Approaches in metabolomics

Metabolomics can be divided into two main different types of analysis: targeted or untargeted approaches. The choice of one approach and / or the other depends on the biological question and the level of sensitivity required (Figure I-9) (Lelli et al. 2021).

Indeed, untargeted metabolomics is the systematic and comprehensive analysis of all the metabolites detectable in the samples. Those analyses are unbiased and without any *a priori*, and also called global metabolomics (San-Martin et al. 2020). They are used for the discovery of biomarkers by comparing healthy and non-healthy tissues from a cohort, for instance. This approach can also be called 'molecular fingerprinting' (Dunn et Ellis 2005).

Targeted analyses focus on quantitative study of some specific metabolites. For example, quantitation of some metabolites potentially found as biomarkers for a specific disease is implemented to confirm the results of the untargeted approach and go further in the disease understanding. The biomarkers are indicators of molecular or cellular changes that might occur during or after an exposure. Biomarkers can be divided into different types. The biomarkers of exposure correspond to the detection of the toxic compound at a concentration that reveals an external or internal exposure. The biomarkers of effect are related to the interactions between the toxicant and a biological target, including early and clinical effects. The biomarkers of susceptibility study the inter-individual differences in response to toxicants, knowing that individuals can present a difference of sensitivity of a compound (Aitio et al. 2007; Nordberg 2010). Targeted approach can also be divided into 'metabolite target analysis' which describes the analyses of some metabolite relative to a specific metabolic pathway, or 'metabolite profiling' which is the analysis of a pre-defined number of metabolites (Dunn et Ellis 2005). These approaches need a knowledge of the sample and metabolites searched, already driven by a hypothesis (Kell et Oliver 2004).

Depending on the research question, one approach can be favored over the other, and different analytical tools can be used. It is the combination of both approaches which can be useful for the discovery of metabolites biomarkers. Nowadays, new hybrid metabolomics approaches have been developed (Li Chen, Zhong, et Zhu 2020).

Currently, two main analytical tools allow targeted and untargeted approaches, nuclear magnetic resonance (NMR) spectroscopy and mass spectrometry (MS). The first is robust, non-destructive and provides quantitative information on multiple metabolites using internal reference compound. The second is a highly sensitive technique that requires very few amounts of sample and allows the analysis of complex mixtures *via* coupling with liquid or gas chromatography (LC-MS or GC-MS), capillary electrophoresis (CE) or even with ion mobility spectrometry (IMS) as it will be further detailed in the manuscript.

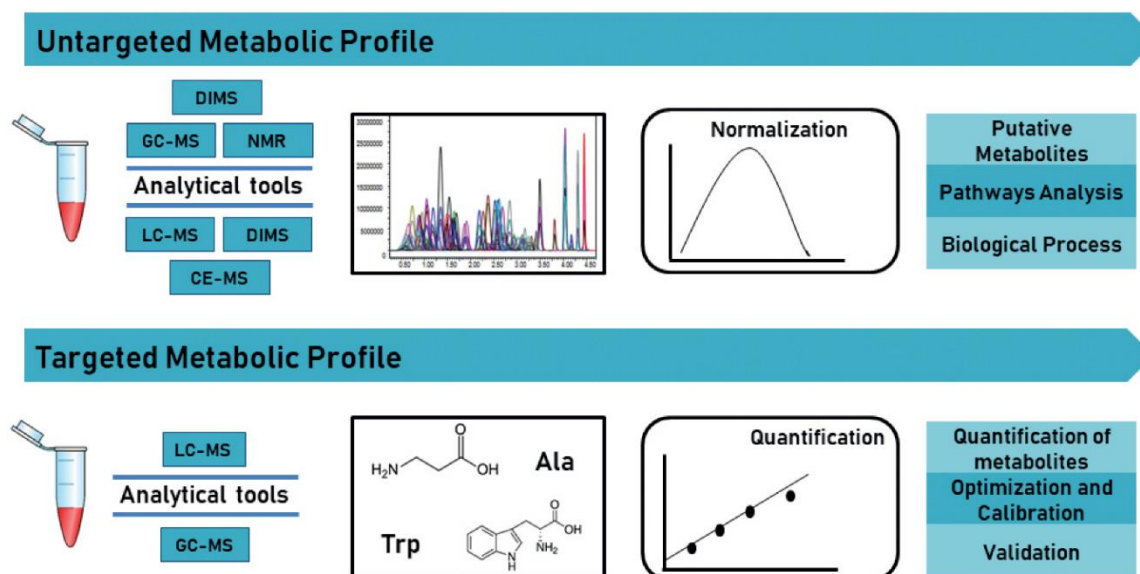


Figure I-9: Two main types of metabolomics analyses: untargeted vs targeted, from (San-Martin et al. 2020)

I.1.3. The Metabolomics workflow

Metabolomics analysis consists in different stages: from the sample collection, spectral acquisition to the data processing to answer the biological question. To characterise all the metabolome, and his complexity with untargeted approaches, it is necessary to extract the most information possible from the samples. For that, and to overcome the analytical variability, a huge number of samples has to be analysed. This is also a pre-requisite for the statistical analyses. To ensure reproducibility of the analyses, a strictly identical workflow has to be carried out for all samples (Figure I-10).

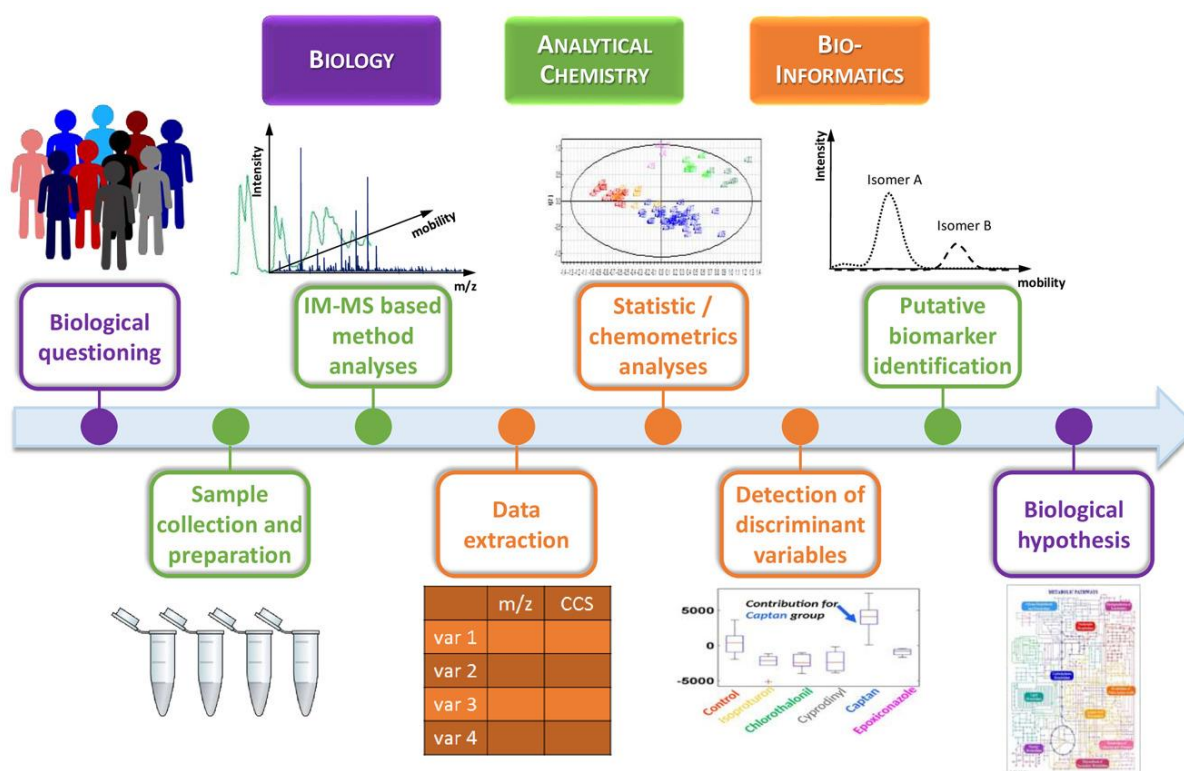


Figure I-10: Metabolomics workflow (from (Delvaux, Rathahao-Paris, et Alves 2021))

All the steps of this workflow must be developed on the basis of the biological question, to create a precise and adapted design of experiment. From the biological question, the objectives must also be clearly defined before conceiving the experimental design. There are many possible objectives, such as the discovery of new biomarkers, the validation of a biological hypothesis from a previous study, the understanding of a pathway, of the underlying biochemical mechanisms or the influence of the environment. From that, the type of metabolomics analyses must be chosen, from targeted to untargeted analyses. Then, the metabolomics workflow is adapted, and for each step of the workflow, some choices have to be carefully made. The experimental design must allow to highlight which differences we are looking for, as healthy/diseased patients, and to be careful with all the steps to avoid the bias and particularly the confounding factors. With untargeted workflows, all the difference between groups will be highlighted, all the factors must be known as precisely as possible. The confounding factors may be analytical or biological. For the analytical ones, the difference can occur during the analyses, and can be managed with some precautions, as the randomization of the samples order and signal intensity correction algorithms. Biological factors can be due to the sample selection, for example for studying the cardiovascular risks, the diets of the individuals must be considered. The number of samples involved in the study must be set carefully in order to get relevant statistical analyses, and to take into account the capabilities of the analytical laboratory.

I.2. Sample preparation: from collection to analysis

The goal of sample preparation step is to extract the maximum of relevant information from the sample to answer the biological question.

I.2.1. Collection of the samples, quenching and deproteinization

Sample collection is the first key point to define. The question “which type of samples will be used for the study?” must be carefully answered, taking into account the aims of the study, the biological question but also choosing the samples the most easily to collect, with relative short sample preparation and feasible analysis. Different types of samples can be analysed in metabolomics, such as urine or blood samples, cerebrospinal fluid, feces, and plants extract (Figure I-11). Another question is relative to the time of sampling. Indeed, metabolism changes over time, and physiological changes can cause variations in metabolites structure or concentrations, for example due to an exposition, or after a meal (Courant et al. 2014). Urine is for example widely influenced by physiological changes as diet, gender, age (J. Wu et Gao 2015). Modifications of the metabolites from urine samples were still observable after six hours of an intake of almonds (Llorach et al. 2010).

To study blood samples, a choice has to be made between plasma and serum (Burla et al. 2018). Both are part of the blood without the red cells. For serum samples, anti-coagulants are not needed but a delay of 30 minutes is required for the clot formation and fibrinogen is absent whereas for plasma, anti-coagulants are needed for purification, but it can be prepared just after collection and fibrinogen is present. Metabolites from serum and plasma samples have been studied and it was demonstrated that both are comparable for NMR study (Sotelo-Orozco et al. 2021) but another study showed higher metabolite concentrations in serum samples (Yu et al. 2011). A recent study demonstrated an undeniable impact of the blood collection tubes on metabolomic and lipoprotein profiles, by comparing serum with plasma using citrate or EDTA as anti-coagulant (Vignoli et al. 2022). These conclusions have been also demonstrated, with 46% of metabolites that have significant differences meaning that coagulation processes alter the metabolites levels (X. Liu et al. 2018).

After the choice of the samples and the sampling time, the collection must follow a strict procedure which must be reproducible, for all samples, to avoid unwanted deviations between control and patients, for example. Indeed, contaminants can be retrieved in all steps of the sample preparation and must be avoided, but above all must be reproducible between samples (Bowen et Remaley 2014; López-Bascón et al. 2016).

After sample collection, metabolism do not stop automatically, enzymatic reactions still occur to form or degrade metabolites. Thus, a step of quenching has been demonstrated necessary in order to stabilize the metabolism. The most common protocol for the quenching step is the snap-freezing in liquid nitrogen. This is even more important for some type of samples, as cells or tissues (González-Domínguez et al. 2020).

The aliquoting step must be done at the time of collection, before any freezing to avoid sample degradation by multiple freeze-thaw cycles. The number and quantity of the aliquots should be carefully thought during the experiment study. If any sample transport is needed, this must be done at cold temperature to avoid the defrosting and the possible degradation (González-Domínguez et al. 2020). The samples must be stored in an ultra-freezer, at -80°C. Short-term storage at lower temperature could be planned under consideration, and only if ultra-freezers are not available, at -20°C up to one week for blood samples (Zivkovic et al. 2009) and less than one month at -20°C and 5 days at 4°C for urine samples (Laparre et al. 2017).

Before analysis, an additional step of deproteinization is required because protein content can cause signal suppression, loss of sensitivity or damages to the chromatographic separation (Cajka et Fiehn 2016).

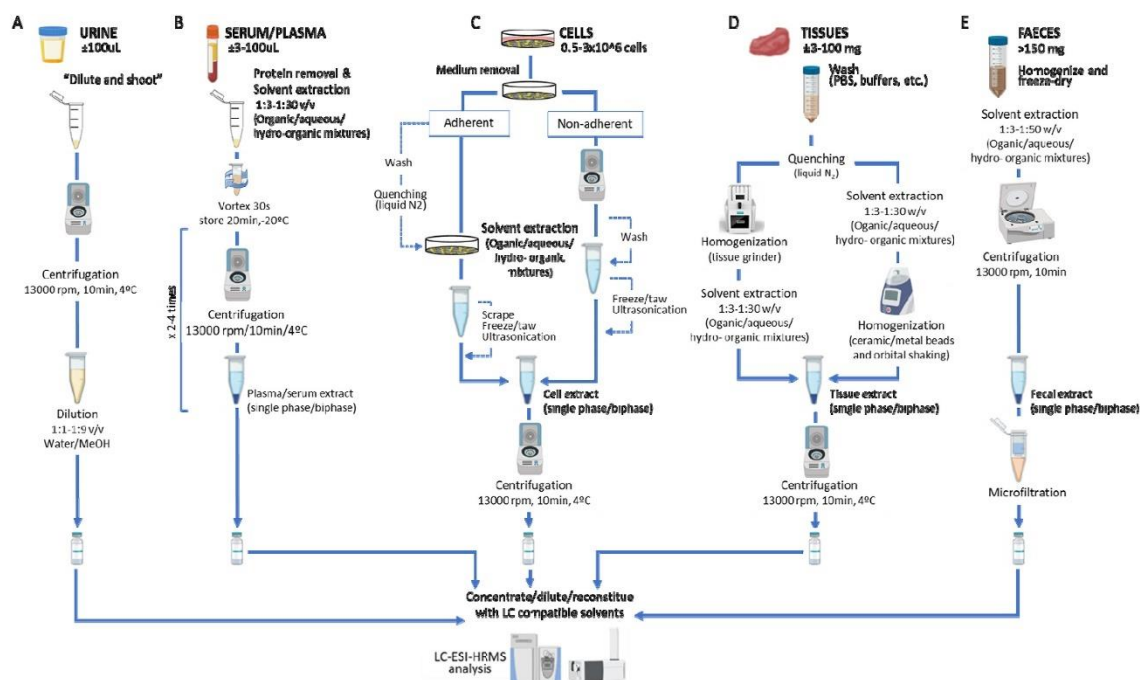


Figure I-11: Example of the steps of sample preparation according to the different matrices before LC/MS analysis; from (Roca et al. 2021).

I.2.2. Extraction technique

Measuring all the metabolites present in one sample is hardly attainable because of the huge diversity of metabolites in terms of chemical classes or concentrations. This is why there is no reference method for metabolomics sample preparation, but this depends on the study, the analytes or the approaches. For untargeted analyses, the goal of the sample preparation is to extract many metabolite classes for which the study experiment has been designed, without loss of compounds of interest. But more importantly, the method must be highly reproducible, because the changes of intensity observed in the data must be dependent on the analytes itself and not on the extraction procedure (Courant et al. 2014). To obtain a wide coverage of metabolites, a minimal sample pre-treatment should be preferred, as solvent-protein precipitation, for blood, for example or dilute-and-shoot method, for urine par example (Cajka et Fiehn 2016).

For hypothesis-driven targeted analyses, liquid-liquid extraction (LLE) or solid-phase extraction (SPE) can be added to enhance targeted metabolites intensities that help enhancing the signal-to-noise ratios and remove the unwanted species which can cause signal suppression. However, with the apparition of novels separation techniques, as ion mobility and high-resolution techniques, these extraction steps could be removed.

Due to the large range of chemical properties of metabolites and lipids, and particularly the diversity in polarity, their predicted octanol/water coefficient ($X \log P$) is about approximately 40 orders of magnitude. Multiple solvent or solvent mixtures as methanol, acetonitrile can be used for metabolites extraction but more apolar solvents have to be considered for lipid extraction (CH_2Cl_2 , CHCl_3 , MTBE, ...). The metabolites classes extracted with these solvents have been organized according to their polarity and their $X \log P$ (Figure I-12).

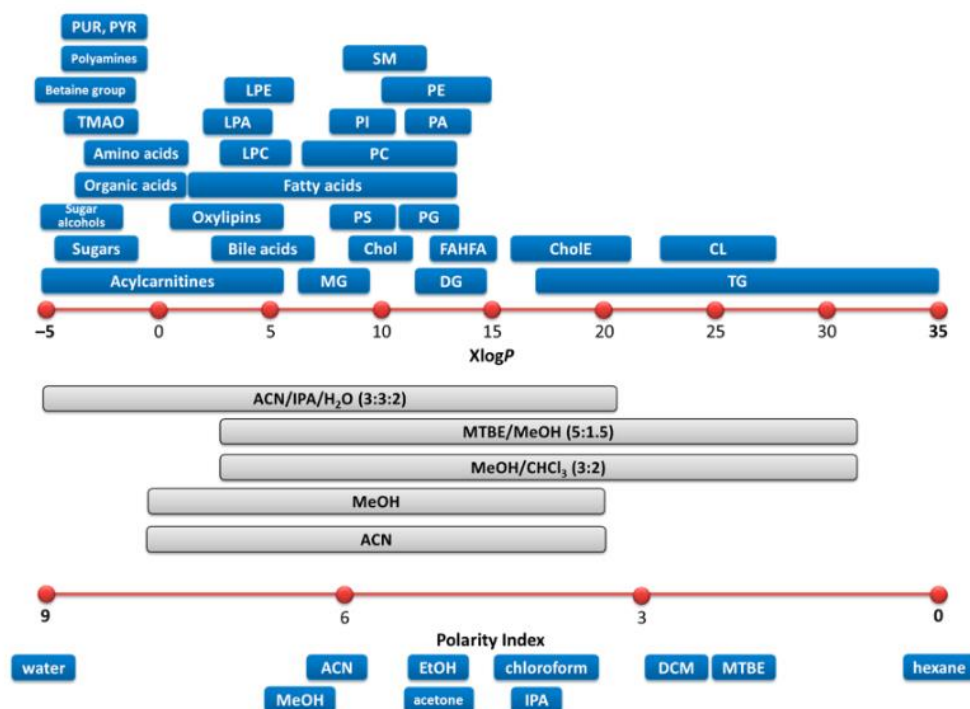


Figure I-12: Solvents or solvents mixtures used in the extraction procedure in metabolomics and lipidomics according to the polarity or $X \log P$ of the different compound classes, from (Cajka et Fiehn 2016)

The last step of sample preparation is the evaporation for sample conservation, analytes concentration and use of solvent compatible with the analysis to re-suspend the dry extract.

Different techniques for metabolites extraction could be used depending on the metabolites, the samples, or the analysis that will be done. The extraction based on liquid-liquid extraction (LLE) is often used to extract specific metabolites on a complex sample. This extraction is based on differences in compounds solubility between two non-miscible solvents (Sreekumar et al. 2009; Mushtaq et al. 2014; R. Liu et al. 2018; Schomakers et al. 2022). Another extraction protocol based on solid-phase extraction (SPE) or solid-phase microextraction (SPME) is used to purify or pre-concentrate some of the analytes present in the samples, particularly those in trace levels (Vuckovic et Pawliszyn 2011; Bojko et al. 2014; Sitnikov, Monnin, et Vuckovic 2016; Gong et al. 2022).

An automated procedure, called turbulent flow chromatography (TFC) has been developed for high-throughput analysis. The sample is injected into a column with high flow rate generating conditions of turbulent flow allowing to retain the small molecules and to wash the proteins. This step was followed by the elution of the metabolites into traditional separation chromatographic column (Couchman 2012; Michopoulos et al. 2010).

Extraction by protein precipitation is used to remove the proteins from the sample, allowing to reduce signal suppression and enhance the sensitivity of metabolites. The addition of organic solvents, high concentration salts solution, basic or acidic solutions induce alterations in protein structures and thus their precipitation. Different organic solvent based protein precipitations have been studied, resulting to a robust protocol for global serum analysis with 100% methanol, in comparison to acetonitrile, acetone, ethanol and combination of methanol and acetone or acetonitrile (Want et al. 2006). Whereas another study shows that optimal solvent compositions are methanol/ethanol (1:1, v/v) or methanol/acetonitrile/acetone (1:1:1, v/v/v) (Bruce et al. 2009). Improvements to this method have

been done, to limit the co-precipitation with hydrophobic metabolites with digestion with proteinase K (Wawrzyniak et al. 2018) or an automatization using 96-well-plate (Margaryan et al. 2020).

Ultrafiltration protocol may also be used for liquid samples. Semi-permeable membranes are used as filter, allowing the passage of specific molecular weight compounds (Daykin et al. 2002). A step of extraction of the membranes with chloroform can be added to desorb metabolites and avoid possible loss of hydrophobic compounds (Tiziani et al. 2008).

In lipidomics, the preferred sample preparation protocol is based on liquid-liquid extraction (LLE). Two extractions based on solvent mixtures of chloroform, methanol and water, Folch protocol (Folch, Lees, et Stanley 1957) and Bligh and Dyer protocol (Bligh et Dyer 1959) have been widely used. Folch extraction method was developed for brain tissues, using two steps, the homogeneization with 2:1 chloroform/methanol mixture and a washing step with water or saline solution. The lower phase obtained from the resulting mixture contains the lipid part of the sample (Folch, Lees, et Stanley 1957). This method was used or adapted in some lipidomics studies as for yeast and mouse samples (Knittelfelder et al. 2014) or for cell pellets of lysates (Nakayasu et al. 2016). Bligh and Dyer method is performed with a mixture of chloroform, methanol and water in different proportions, depending on the samples (Bligh et Dyer 1959). Some studies review this step of extraction and promotes the use of Folch or Bligh and Dyer methods because they induce the higher lipid coverage (Reis et al. 2013; Ulmer et al. 2018). However, the use of chloroform is controverted because it is highly toxic and due to his low density, the lipid phase is the lower one, thus contaminations with compounds from the other phase are probable. For this purpose, Matyash method, also called MTBE method has been developed, because the use of methyl tert-butyl ether is less toxic and his density is higher, the lipids will be retrieved in the upper phase. Lipids are extracted with a mixture of 10:3:2.5 of MTBE/Methanol/water (Matyash et al. 2008). Several lipid extraction methods have been developed and a single method cannot be sufficient to retrieve all lipid classed due to their huge diversity. To cover the whole lipidome from very lipophilic lipids as TG, CE to hydrophilic lipids as LPA, Acyl-CoA, multiple extractions must be required as shown in Figure I-13 (Tumanov et Kamphorst 2017).

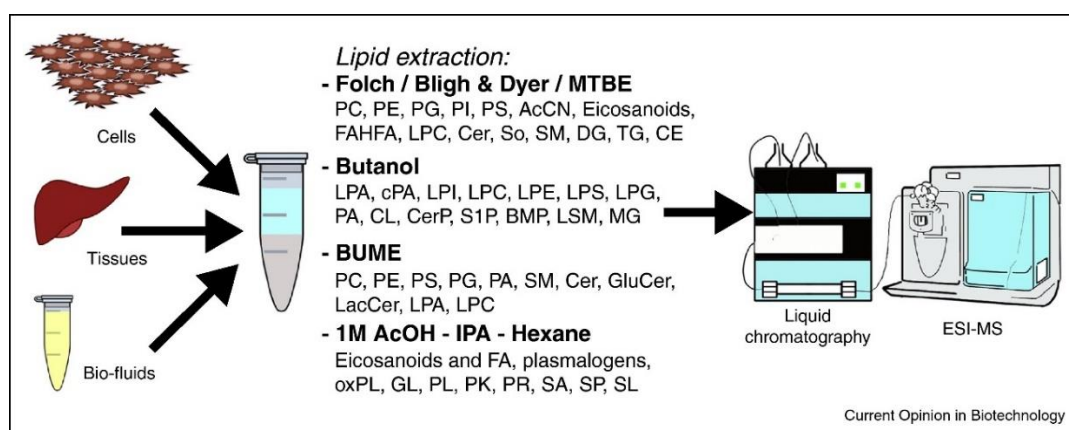


Figure I-13: Different lipid extraction methods for lipidomics studies and the lipid classes associated, from (Tumanov et Kamphorst 2017)

Other extraction techniques could be used for targeted analysis, to obtain only a specific or some lipid classes, principally based on liquid-liquid extraction (LLE) or solid-phase extraction (SPE) (Aldana, Romero-Otero, et Cala 2020). SPE is not a good choice for untargeted analysis but become a really

valuable method for the need to focus on a reduced number of lipid classes (Züllig, Trötz Müller, et Köfeler 2020).

Lipid extraction has been widely performed using two-phase extraction protocols using chloroform or MTBE based solvent mixtures. The two phases contain the lipids for the most unipolar part and the more polar metabolites in the other part. The combination of both parts could be analyzed to ensure a higher coverage, but particular attention must be paid to matrix effects (Cajka et Fiehn 2016). Plasma extraction could be performed directly on inserts on HPLC vials, and injection of the upper and lower phase has to be done by changing the needle position (Godzien et al. 2013; Whiley et al. 2012). The analysis of both polar metabolites and lipids parts could also be done by a single analysis, for example by mixing the lower and upper extraction phases, evaporate them and re-suspend before analysis (S. Chen et al. 2013). MPLEx (metabolites, protein and lipid extraction) is an extraction method that allows the study of the three omics using the same sample, to simplify the multi-omics measurements and to enable a better understanding for some biological questions, by decreasing the experimental variation (Nakayasu et al. 2016).

I.3. Mass spectrometry-based metabolomics

I.3.1. Overview of metabolomics analysis

As previously described, metabolites exhibit very diverse chemical classes and concentration ranges. For this purpose, many different technologies could be used to perform metabolomics analysis. The choice of the analytical platform depends on the sample, the biological question, knowing that the selected platform must detect a large number of metabolites, as much as possible, but also allow their confident identification even their quantification. The number of metabolites is still unknown but assumed to be very large, with possibly ten to hundred metabolites at a same molecular weight (Courant et al. 2014). For all these remarks, no universal analytical platform exists, and each has its advantages and drawbacks.

Numerous platforms have been employed for metabolomics, as infrared spectrometry, UV-visible absorption and fluorescence, thin layer chromatography, coulometry, electrochemistry techniques, capillary electrophoresis. However, the most used techniques are nuclear magnetic resonance (NMR) and mass spectrometry (MS), often coupled with gas chromatography (GC) or liquid chromatography (LC).

Mass spectrometry offers many advantages for metabolites analysis, as its sensitivity, the detection of a large number of metabolites classes at their physiological concentration without pre-concentration. It enables to annotate metabolites by measuring their molecular mass, which leads to their chemical formulas, depending on the precision of the analyser used. Fragmentation spectrum adds structural information and by comparison with databases helps the metabolite annotation.

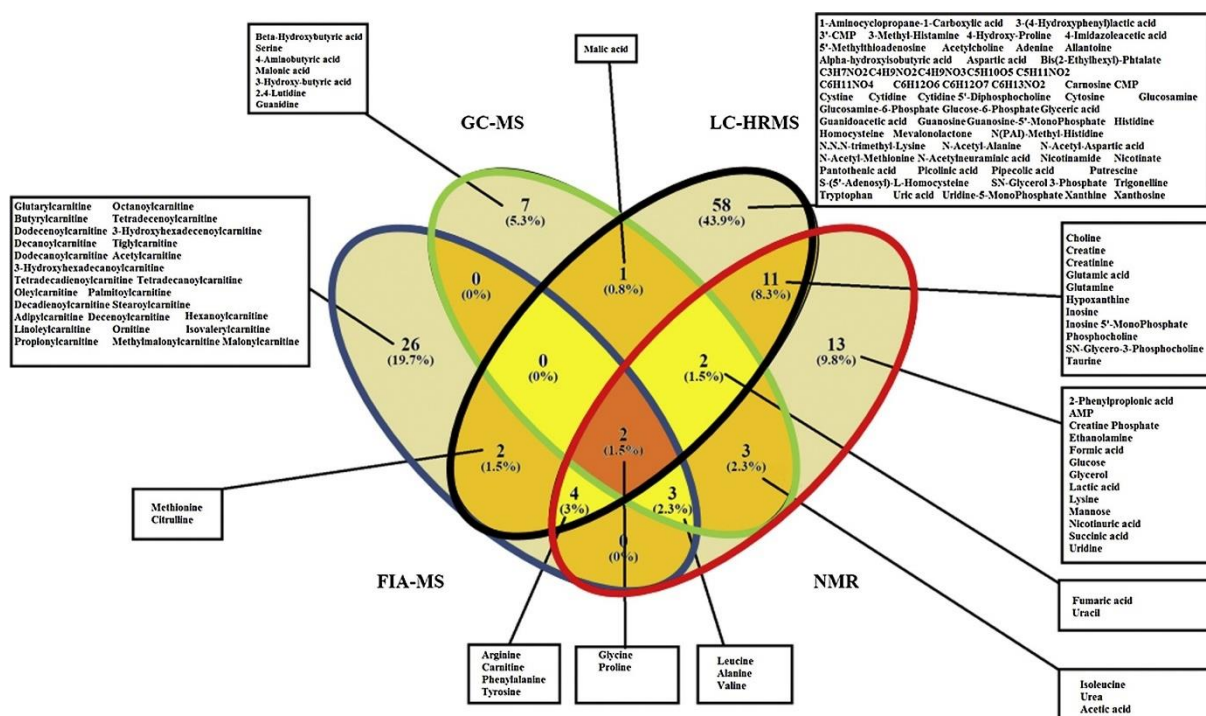


Figure I-14: Venn diagram representing the specificity and the overlap of metabolites detected by four analytical method: FIA-MS (blue), GC-MS (green), LC-MS (black), NMR (red) in skeletal muscle metabolomics (Bruno et al. 2018)

I.3.2. Mass spectrometry instrumentation

Mass spectrometry is an analytical technique widely used in the biomedical field. This technique separates species according to their mass over charge ratio (m/z). Technically, a mass spectrometer is composed of three different parts. After introducing the sample, a source allows to ionize the analytes, one or more analysers permit to separate the ions and the detector allows to count the ions. Finally, a system of data acquisition and treatment allows to visualize, record mass spectra, and control the parameters of the acquisition (Figure I-15). Analysers and detectors are maintained under vacuum to minimize the ion-molecule interactions such as reactions or collisions.

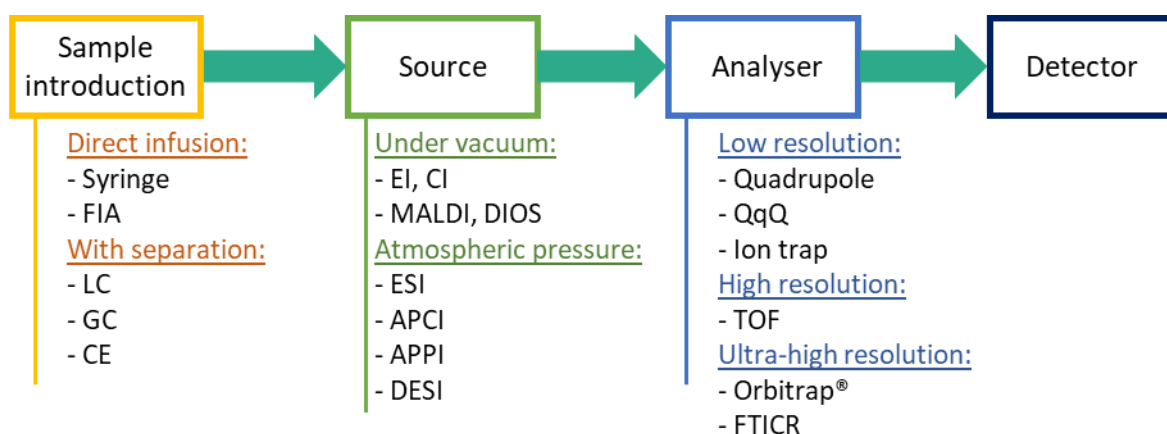


Figure I-15: Schematic representation of a mass spectrometer with some possibilities for each part of the instrument

I.3.2.1. Ionization source

The choice of the ion source depends on the sample analyzed, the matrix, the instrument used, and the technique used to introduce the sample into the mass spectrometer. The sources can be classified into atmospheric pressure and in vacuum sources. The different sources are complementary and can be classed according to the polarity of the analytes as described in Figure I-16. For small, thermostable and volatile molecules, GC-MS using electron ionization (EI), which operates under vacuum, is usually performed. When metabolites are too polar and insufficiently volatile, a derivatization step can be required before GC-MS. The ionizing electrons of 70 eV produce molecular ions which can exhibit high internal energy and fragment yielding highly reproducible fragmentation spectra (Courant et al. 2014). This led to the creation of universal mass spectral libraries such as the Institute of Standards and Technology (NIST). This database facilitates the identification of metabolites. Chemical ionisation (CI) source can also be used in GC-MS analyses and can complement EI as CI presents the advantage to yield intact molecular species (generally protonated or deprotonated molecules in positive or negative ion modes, respectively) with very few fragmentations. However, GC-CI-MS is less frequently reported in metabolomics.

Electrospray (ESI) is the most widely encountered ionisation technique for metabolomics studies, in particular when LC-MS coupling is required. ESI is an atmospheric pressure source which is adapted to a large range of polarity and can work in both positive and negative modes. It is a soft ionisation, which generates intact ion species, usually without fragmentation (De Hoffmann et Stroobant 2007). The main drawback of this source is the ion suppression that appears for concentrated samples, when many analytes arrive in the same time, a competition may occur which can cause losses and enhancements in signal intensity (Antignac et al. 2005).

Other sources can be used in metabolomics, as the atmospheric pressure chemical ionisation (APCI) or atmospheric pressure photoionization (APPI). In APPI, the analytes are either directly or indirectly (using a dopant) ionized using a UV lamp, while in APCI, a corona discharge needle produces metastable ions from nitrogen atmosphere and then from solvent at high energy that react with the analytes to ionize them. APCI is a soft ionisation source, useful for weakly polar or non-polar compounds (Figure I-16) (Commisso et al. 2017). APPI is not a soft ionisation source, but can be complementary to ESI and APCI for some compounds difficult to ionize. It has been used in an Alzheimer study (González-Domínguez, García-Barrera, et Gómez-Ariza 2015). The complementary of the three sources (ESI, APCI and APPI) was demonstrated for the global plasma metabolomics (Tian et al. 2013). Other sources have been reported for direct analysis in metabolomics as matrix assisted laser desorption ionisation (MALDI) (Salviati, Sommella, et Campiglia 2022; Calabrese et al. 2023), desorption ionization on silicon (DIOS) (Nordström et al. 2008), desorption electrospray ionization (DESI) (He et al. 2022; Qi et al. 2021) or secondary ion mass spectrometry (SIMS) (Fletcher et al. 2013; Pareek et al. 2020).

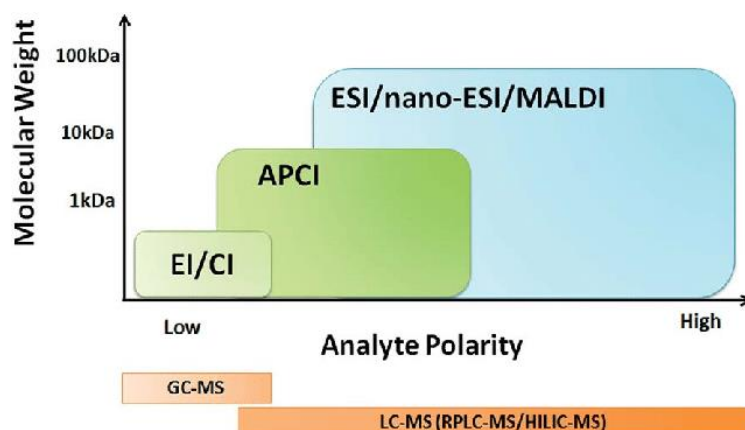


Figure I-16: Complementarity of the ionization source for metabolomics; from (Y. Wang et al. 2015)

I.3.2.2. Mass analysers

Several mass analysers can be used in metabolomics, depending on the study purpose. Combination of mass analysers is possible in a single instrument leading to hybrid instrument or triple quadrupole. Each has its own advantages and drawbacks due to its respective characteristics. An overview is displayed in Table I-1. In the analysers, the ions are separated by the m/z ratio, using electric or/and magnetic fields. The mass resolution is generally calculated by dividing the mass m by the full width at half maximum (FWHM) at a given m/z .

Table I-1: Comparison of some characteristics of different analysers, adapted from (J. Wang, Wang, et Han 2019)

Mass analyser	Mass resolution	Mass accuracy (ppm)	Sensitivity	Identification	Quantification
LTQ (QLIT)	2000	100-500	Good	++	+
QqQ	1000	100-1500	High	+	+++
TOF/Q-TOF	10,000-200,000	5-50	High	++	+++
Orbitrap	100,000-800,000	<5	Medium	+++	++
FTICR	>1,000,000	<1-2	Medium	+++	++

In general, low resolution mass spectrometer ($R < 10,000$) are not used nowadays for untargeted metabolomics, so quadrupole linear ion trap (QLIT or LTQ) is not used alone but combined with other analysers. The triple quadrupole (QqQ) is constituted of two quadrupoles separated by a collision cell and is mostly used for targeted analysis.

Time of flight (TOF) analysers have a high resolution ($R > 10,000$), high sensitivity, and high acquisition rate (up to 100 Hz). TOF analysers can be combined with a quadrupole (Q-TOF) allowing to perform MS/MS experiments. Some improvements have been made to obtain better resolution ($R > 100,000$), as with the multi-reflecting Time-of-Flight (MRT) commercialized by Waters recently (Millar et al. 2022). Exhibiting a better resolution than Q-TOF, Orbitrap and Fourier Transform Ion Cyclotron Resonance (FTICR) analysers are qualified as ultra-high resolution mass spectrometers ($R > 200,000$). Both have unique capabilities in terms of mass resolution and mass accuracy. However, the acquisition rate is relatively low in comparison to TOF, which can present limitations with the coupling of high-efficient separation techniques such as GC or CE.

I.3.2.3. Acquisition modes and MS/MS

A mass spectrometer can be used with different acquisition scan modes. The most common is the full-scan mode, particularly for untargeted metabolomics study. The analyser scans all the ions in a defined

m/z range. Another mode is the selected ion monitoring (SIM) when the mass analyser is not scanning but focused on specific m/z values. This mode can be used for targeted approaches, but is not widespread because insufficiently selective (Manini, 2000). Other modes can be applied when the instrument is composed of at least two analysers. These modes allow to perform tandem mass spectrometry (MS/MS) experiments (Figure I-17).

Untargeted metabolomics studies can resort to different MS/MS acquisition modes (I.-L. Wu et al. 2020). First, data dependent acquisition (DDA), where the first analyser scans all the m/z of precursor ions (survey scan, MS1) and selects the ions to be fragmented in the collision cell, yielding product ions that are then scanned in the second analyser, using some rules as a maximum number of ions by scan and an intensity threshold (Figure I-17.E) (Defossez et al. 2023). To enhance reproducibility and have more MS/MS spectra during one acquisition, a second mode that allows all precursor ions to simultaneously generate product ions (without any selection) in the collision cell can be implemented: such mode is either “All ion fragmentation” (AIF) for Orbitrap, “MS^E” or “All Ions MS/MS” for some Q-TOF. In this mode, it can be difficult to determine relationships between precursor and product ions in complex samples where co-elutions are probable. A third mode, intermediate strategy between AIF and DDA, is “data independent acquisition” (DIA) that implies a wide isolation window for filtering a group of precursor ions with the first analyser. These precursor ions are dissociated in the collision cell to produce MS² spectra (Figure I-17.F). However, an important step of data treatment and deconvolution is required to understand DIA or AIF experiments (Pezzatti et al. 2020). DDA and DIA have been compared for the identification and quantification of metabolites in human plasma (Barbier Saint Hilaire et al. 2020). Some improvements of this type of acquisition have been made, with for example SWATH experiments (Raetz, Bonner, et Hopfgartner 2020).

For more targeted analysis or metabolite profiling, different modes can be applied. One possibility is the precursor ion scanning, where the first analyser scans a range of precursor m/z while the second is focused on targeted product ions to be specific of the target class of compounds (Figure I-17.B). Neutral loss scanning implies scanning of the two analysers with a specific offset, the specified m/z shift corresponds to a specific loss which is characteristic of a compound class, such as the loss of the headgroup in lipidomics study (Figure I-17.C). Finally, multiple reaction monitoring (MRM) targets a specific precursor which produces a specific product ion (Figure I-17.D). This mode is particularly useful to monitor known metabolites or metabolites quantitation in targeted analyses (Courant et al. 2014).

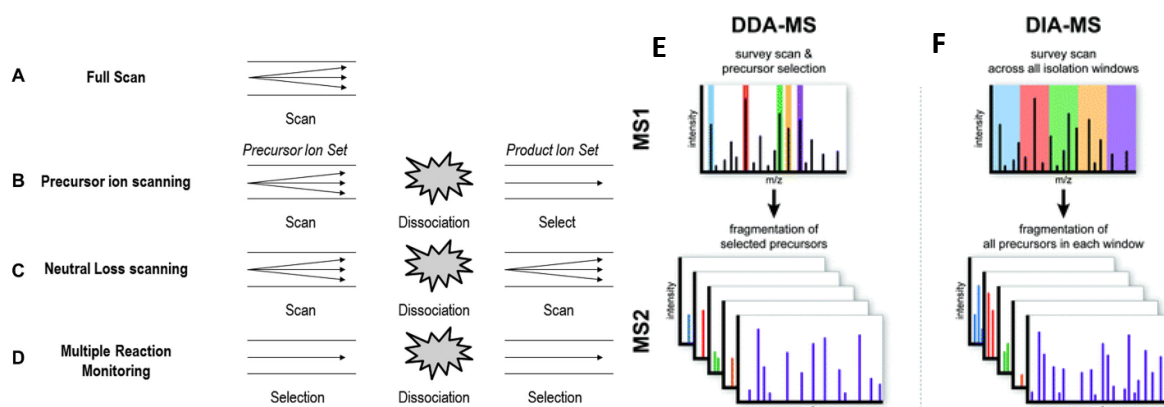


Figure I-17: Different acquisition modes useful for metabolomics study, in the left from (Courant et al. 2014) and in the right, from (Krasny et Huang 2021)

I.3.3. Direct introduction mass spectrometry

The sample can be introduced directly into the mass spectrometer by using infusion or flow injection analysis (FIA). This method is called Direct Injection Mass Spectrometry (DIMS). Such introduction is often used with ultra high resolution mass spectrometers in full scan mode (Rathahao-Paris, Alves, et Paris 2021). This method has been successfully applied in metabolomics, such as for human plasma samples, *Arabidopsis* extracts, heart tissue extracts (González-Domínguez, Sayago, et Fernández-Recamales 2017; Habchi et al. 2016). For lipidomics studies, the term shotgun lipidomics is used to refer to direct infusion coupled to electrospray mass spectrometry techniques (Züllig, Trötz Müller, et Köfeler 2020). It has been reported with QqQ instruments, as although they are low-resolution, it is possible to select the lipids from each class thanks to the neutral loss of their polar head (Han et Gross 2005). It is a powerful method in terms of high throughput, with 360-720 samples analysed per day and the data treatment can be facilitated. However, this method can cause strong matrix effects, with potential ion suppression (Courant et al. 2014). Another difficulty is due to the samples which can exhibit various isomeric or isobaric compounds. For example, for lipid species, to differentiate protonated molecule of PC 36:0 at m/z 790.631987 to the one of PE 40:7 at m/z 790.538087, a resolution of 20,000 is sufficient, whereas to differentiate those of PC 36:4 (m/z 782.569387) and of PC 34:1 (m/z 782.566981) a resolution of 600,000 is required (Züllig et Köfeler 2021). The resolution of the mass instrument is therefore a determinant factor to separate lipid species in DIMS without prior separation technique (Bielow et al. 2017).

To address these issues, the coupling of mass instruments with prior separation techniques is relevant.

I.3.4. Coupling with separation based techniques

Different types of coupling with mass spectrometry can be used depending on the sample and the biological question. The most described techniques are gas chromatography (GC) or liquid chromatography (LC) but CE can be implemented. Analytes can be separated according to their physico-chemical properties, owing to polarity, which allow reducing matrix effects and ion suppression. The identification of metabolites can be facilitated due to the separation information, as the retention time (rt) of the compound.

I.3.4.1. Gas chromatography-mass spectrometry

Gas chromatography coupled to mass spectrometry (GC-MS) is one of the oldest coupling. Samples are first vaporized, then separated in a capillary chromatographic column, under either isotherm condition or temperature gradient using an inert gas as eluent. The compounds are separated owing to their relative vapor pressure and their affinities with the stationary phase. This technique of high efficiency and high resolution provides sharp and reproducible peaks allowing the separation of numerous compounds from complex samples

As previously mentioned, GC-MS is appropriate for volatile or nonpolar compounds. GC-MS is mostly associated with EI source which provides structural information from in-source fragmentation. The highly reproducible EI mass spectra (using electrons of 70 eV) permit the construction of universal databases helpful for metabolites identification. However chemical derivatization could be performed to analyse non-volatile compounds, implying longer sample preparation. GC-MS have been used to identify and quantify up to 200 metabolites in human biofluid samples (Fiehn 2016). An interlaboratory study was performed on GC-MS metabolomics analysis of human plasma and indicated that standardized protocols were required to compare those data (Lin et al. 2020).

Several improvements in GC-MS have been made as the coupling with two-dimensional gas chromatography (GCxGC or 2D-GC) which allows to increase peak capacity and the capability of separation (Higgins Kepler et al. 2018; Beale et al. 2018). This technique was recently used in metabolomics for the analysis of fecal samples (Nam et al. 2022). 2D-GC can be also coupled with ultra-high resolution mass spectrometers as Orbitrap, for example for the study of biofilms, with the detection of more than 400 features (Weidt et al. 2016). More recently, 270 metabolites from human plasma samples were identified by GC-Orbitrap using EI and CI sources (Misra et Olivier 2020).

I.3.4.2. Liquid chromatography-mass spectrometry

Liquid chromatography (LC) is based on the separation of compounds carried by a liquid (mobile phase) through solid particles (stationary phase). High performance liquid chromatography (HPLC) allows the separation of the analytes thanks to their affinities to the stationary phase which is adapted to the samples and to the mobile phase which composition can change to perform elution gradient. Contrary to GC separation, non-volatile compounds can be analysed and separated in LC. To enhance the separation, Ultra-High Performance Liquid Chromatography (UHPLC) was developed by reducing the size of the particles of the stationary phase to sub-2 μ m. This has increased separation efficiency, resolution and peak capacity in shorter timeframe. UHPLC is now the standard for metabolomics analysis.

Several LC modes are used, categorised according to their stationary phases: the main are Normal-phase (NPLC), reversed-phase (RPLC), ion chromatography (IC), affinity (AC) or Hydrophilic Interaction Liquid Chromatography (HILIC). The most popular phase is reverse phase liquid chromatography (RPLC), which is frequently carried out in various research fields, using a hydrophobic stationary phase such as octadecyl carbon chain-bonded silica (C18). This phase allows the separation of polar, medium polar to non-polar metabolites. Elution gradient of organic solvent such as acetonitrile or methanol in an aqueous mobile phase is commonly used. RPLC is also used in lipidomics studies, but isopropanol is added to the mobile phase, usually at the end of the elution gradient to elute all lipid classes, up to the most hydrophobic as TG or cholesterol. Using isopropanol in UHPLC generates high backpressures. However, this issue can be prevented by a temperature increase, within the limits allowed by the column specifications, so as not to damage the column. Different buffers or modifiers can be added to the mobile phase, as ammonium formate or formic acid to enhance the detection of some lipid classes (Cajka et Fiehn 2016).

Hydrophilic Interaction Liquid Chromatography (HILIC) best separates the very polar metabolites and can be complementary to RPLC in term of the analyte polarity (Figure I-18). The stationary phase is polar as for NPLC but the mobile phases are mainly similar to those of RPLC: bonded silica with polar groups such as amino, amide or diol (Kahsay et al. 2014). Similarly to RPLC, and contrary to normal phase, HILIC mobile phases are mostly composed of water and organic solvents as acetonitrile and methanol.

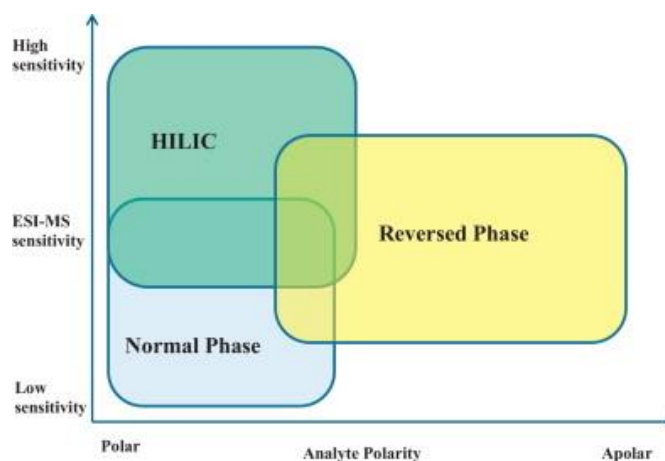


Figure I-18: Comparison of three LC phases according to the analyte polarity and the sensitivity in ESI-MS, from (Kahsay et al. 2014)

A comparative study in LCMS analyses of urine and plasma showed that the combination of both RP and HILIC modes allows to expand the metabolome coverage and to detect more metabolites as HILIC and RPLC are complementary in terms of analytes polarity (Figure I-19) (Contrepolis, Jiang, et Snyder 2015). This combination can lead to a better understanding of metabolome pathways and the discovery of new biomarkers as in liver cancers (J. Chen et al. 2009).

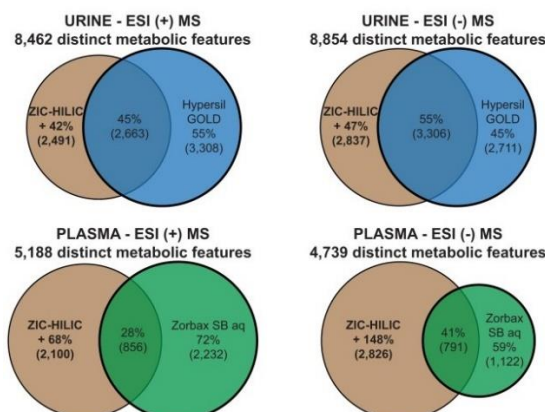


Figure I-19: Comparative study of HILIC and RPLC in LC-MS analyses of human urine and plasma in positive and negative ESI modes. Metabolome coverage of human urine and plasma by Venn diagrams representing the proportion and quantity of metabolic features detected in HILIC or RPLC (Hypersil Gold and Zorbax SB), adapted from (Contrepolis, Jiang, et Snyder 2015).

Normal phase and HILIC can also be used in lipidomics study, allowing a separation of the lipids according to their headgroups classes, which facilitates the annotation (Sokol et al. 2013; Hines, Herron, et Xu 2017; Amy Li, Hines, et Xu 2020).

Due to the possibility to combine a large diversity of chromatographic modes, liquid chromatography covers a large range of polarity allowing the analysis of the whole metabolome. Minimal sample preparation can be carried out for LC analysis. Access to the intact ion species in LC-MS using API sources is a great advantage compared to GC-MS analysis. However, particular attention must be paid to the ion suppression phenomenon. To access structural information, supplementary analyses using MS/MS are required (Courant et al. 2014).

I.3.4.3. Other separation techniques

Due to the metabolome great complexity and the significant variations in physico-chemical characteristics across different metabolites and lipid classes, none of the methods described above can provide a complete and thorough investigation of the metabolome. In this context, other separation techniques have been investigated, to achieve better metabolome coverage by combining different techniques.

For example, supercritical fluid chromatography (SFC) has been investigated in metabolomics. In SFC, the mobile phase is mainly composed of supercritical carbon dioxide (CO₂), and co-solvents as methanol or acetonitrile can be added. SFC can be used for polar and non-polar analytes, such as polar metabolites or lipid species. SFC could improve the metabolome coverage and reduce time analysis and environmental impact (van de Velde, Guillarme, et Kohler 2020; Shulaev et Isaac 2018; Gordillo 2021). Improvements have been made such as Ultra-high performance SFC (UPHSFC) which identifies 3.4 times more lipids than UHPLC method, in a run time 40% shorter (Lísa et al. 2017).

Capillary-electrophoresis (CE) coupled with MS can also be used for metabolomics. The separation of the compounds is performed according to their ability to migrate within an electrolyte-filled capillary under the influence of an electric field. Thus, metabolites are separated based on their charge and size according to their electrophoretic mobility (μ_e). Their apparent migration is the sum of μ_e and the electroosmotic flux EOF (Ramautar, Demirci, et Jong 2006; Sugimoto 2021). The main advantages are the very high efficiency (millions of theoretical plates) and resolution due to the very narrow capillary diameter and the flat flow, compared to the pumped parabolic flow of the HPLC. This technique has known various improvements including the developments of novel CE-MS approaches that showed a strong potential to increase the sensitivity, metabolic coverage and sample throughput in metabolomics (W. Zhang, Hankemeier, et Ramautar 2017).

Ion mobility spectrometry (IMS) that will be fully described in Chapter 2 is also a technique which has been successfully coupled with mass spectrometry (IMS-MS) in metabolomics.

I.3.5. Imaging metabolomics

Mass spectrometry imaging (MSI) is one of the major techniques allowing the study of spatially resolved metabolomics. MSI provides two-dimension images of metabolites in a tissue section. It is particularly important for cancer research, for the localization of the tumor and healthy tissues (Ma et Fernández 2022; He et al. 2022).

To visualize the spatial distribution of metabolites, different techniques can be employed, as MALDI, DESI, SIMS, LAESI (laser ablation electrospray ionization) and AP-MALDI (Atmospheric pressure MALDI). They all have their own characteristics, and the choice of the technique is made according to the sample, the sample preparation, the spatial resolution required (Gao et al. 2023). For MALDI imaging, a sample pretreatment with a matrix deposition is required and must be optimized according to the sample and the metabolites which can be desorbed differently depending on the matrix used. Whereas, for DESI imaging, no sample preparation is required, but the spatial resolution is lower (100-200 μm) than with MALDI which can reach resolution of 5 μm under certain conditions (J. Wang, Wang, et Han 2019).

I.3.6. Complementarity with NMR analysis

Nuclear Magnetic Resonance (NMR) is typically used for the structural elucidation of compounds in purified samples but could also be used for complex mixtures, as biological samples. NMR has the advantage of being a robust, reproducible, non-destructive and quantitative method, requiring minimal sample preparation, which is particularly well suited to the analysis of complex samples. Thus NMR can address different challenges in addition to the structural elucidation, such as the quantitation, comparative metabolomics study, metabolite-proteins interactions or isotope-tracing metabolites (Moco 2022). Its main limit is its lack of sensitivity. However, NMR based Metabolomics is growing in the community and is complementary to mass spectrometry as shown in Figure I-20.a (Wishart, Cheng, et al. 2022; Letertre, Dervilly, et Giraudeau 2021). MS allows a large metabolite coverage with its high sensitivity whereas NMR is more robust and allows the quantitation more easily. It has been shown that combination of both NMR and MS techniques could lead to high sensitivity, robustness, metabolite coverage allowing in particular a larger and easier identification of metabolites (Letertre, Dervilly, et Giraudeau 2021). A statistical approach allowing the co-analysis of data from both NMR and MS (SHY) was used to annotate unknown compounds, linked to drug taking, in urine samples (Crockford et al. 2005; Bingol et al. 2015; Boiteau et al. 2018). To enable faster annotation, two integrated approaches, SUMMIT MS/NMR and NMR/MS Translator, combining 2D NMR and high-resolution mass spectrometry (HRMS) have been developed (Bingol et al. 2015). These approaches compare predicted spectra from HRMS (accurate m/z) and NMR (2D HSQC ^{13}C - ^1H) data respectively, with experimental spectra: molecular structures are identified when the information obtained by MS and NMR correspond. A third ISEL NMR/MS approach, which uses the SUMMIT principle but adds an additional dimension by integrating MS/MS, has also been proposed (Boiteau et al. 2018).

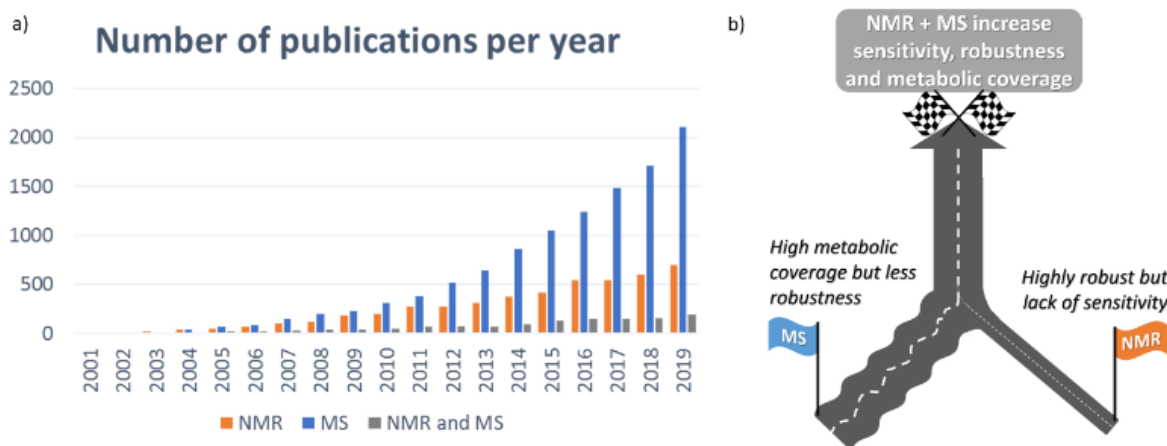


Figure I-20: a) Growth of NMR, MS and combined metabolomics study (review on pubmed done in 2020). b) Representation of both advantages and drawbacks of RMN and MS and reasons to combine both techniques. Reprinted from (Letertre, Dervilly, et Giraudeau 2021)

The combination of the two techniques has been applied in different fields such as clinical applications as personalized medicine (Letertre, Giraudeau, et de Tullio 2021), environmental exposure (Labine et Simpson 2020) or identification of unknown metabolites by combining a large range of information (Leggett et al. 2019).

I.4. Data treatment

I.4.1. Data processing

After data acquisition, a critical step of data processing is required in metabolomics workflow, and it depends on the analysis performed and of the initial biological question. The objective is to convert the raw data obtained with the instrument to peak tables useful for statistical analysis (Courant et al. 2014).

For direct introduction analysis, the pre-processing step is faster because there is no need to search or align chromatographic peaks. In DIA, the only issue is the small shifts that can occur in mass measurements leading to incorrect assignment. The use of internal calibration can minimize this issue (Courant et al. 2014). In addition, a metabolite can be assigned to multiple features according to the sample due to the presence of many isomers. In LC-MS or GC-MS data, multiple steps are required in data processing, such as filtering, detection of the features by peak picking algorithms, peak alignment to correct the shifts in retention times, or data normalization (Cajka et Fiehn 2016; Züllig, Trötz Müller, et Köfeler 2020). The aim is to obtain a data table or matrix in which each row represents a feature and each column, a characteristic such as m/z , retention time, intensity. Many types of software allow to perform these pre-processing steps such as vendor softwares, for example, Unifi, Progenesis QI, from Waters, MassHunter from Agilent Technologies, or Metaboscape from Bruker Daltonics. Open-source tools have been also developed such as MZmine (Schmid et al. 2023), XCMS (C. A. Smith et al. 2006), MetaboAnalyst (J. Xia et al. 2009), MS-Dial (Tsugawa et al. 2020a), Workflow4Metabolomics (W4M) (Giacomoni et al. 2015), ... For open-source softwares, an additional step of data conversion is eventually required to convert raw data to an open format, such as mzXML, mzML, cdf. Many tools and resources are available for metabolomics studies, about 80 in 2020 (Misra 2021). Even though, the data processing step is crucial, and all these tools may induce deviations in the resulting data table, if not properly used and can influence the conclusions of the study. Few comparative studies have been performed to compare the software tools (Cajka et Fiehn 2016; Hemmer et al. 2020). For example, a single LC-MS dataset can lead to different biomarkers depending on the data processing software, with only two of the 14 potential biomarkers in common over the three software tools compared for a cancer study (Yanhua Chen et al. 2013).

I.4.2. Data analysis by statistical tools

After obtaining the relevant data table with all the features and their properties, a step of data analysis is needed to understand the data. This data table is complicated and difficult to understand without powerful statistical tools. The goal of data analysis is to understand the relation between the groups of samples and find the answer to the biological question. Different steps can be useful as described in (Figure I-21).

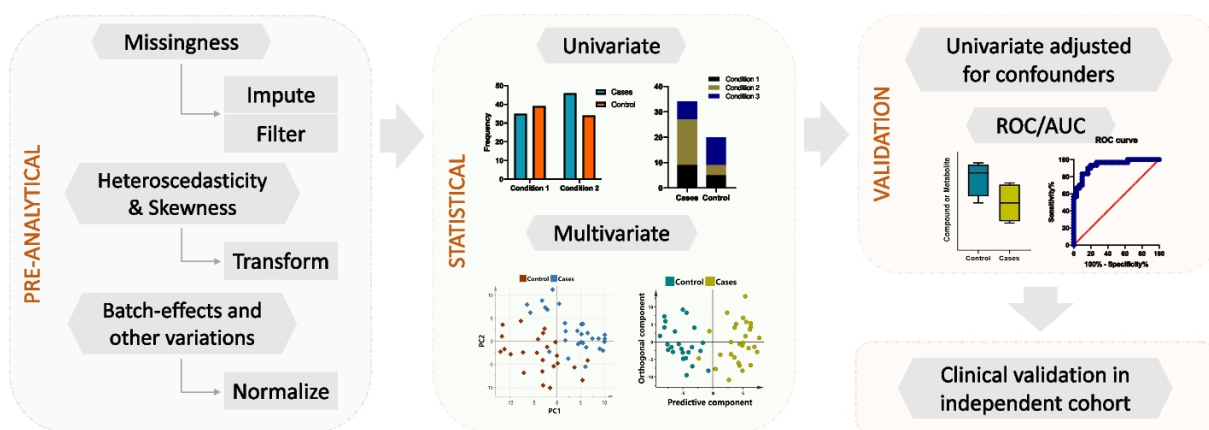


Figure I-21: Schematic representation of the different steps of metabolomics data analysis, from (Anwardeen et al. 2023)

Some data pre-treatments are required before statistical approaches. Indeed, several metabolites missingness can be retrieved in the data matrix due to the detection level of the analytical technique or an incorrect peak alignment. The variations as the skewness of the data or batch-effects can cause errors in statistical methods. Therefore, some transformations or normalizations can be required prior to statistical analysis (Courant et al. 2014; Anwardeen et al. 2023).

Different statistical approaches exist, such as univariate or multivariate methods. Commonly, the combination of both approaches is used in metabolomics. Univariate methods may reveal potential compounds which differs between the different sample groups in terms of intensity differences, as for example the Student's t-test. However, these methods do not consider the correlation between variables, thus, multivariate analysis are particularly useful for biomarkers discovery or compound changes in metabolomics studies. Multivariate methods allow to reduce the complexity of the data matrix and highlight the relevant information from the whole dataset. These methods can be supervised or not. The most popular unsupervised method is the principal component analysis (PCA), which allows a projection with only a few variables (called principal component PC), reducing the large number of variables present in the dataset. The first principal component contains the main variance in the dataset, the second PC explains most of the remaining variance, etc. The most significant sources of variability are expected to be revealed through PCA analysis. However, the most important factor of variability is often not the most relevant factors to explain the biological differences (Antonelli et al. 2019). PCA is for example used as a data quality tool, to control the outliers analysis and the quality control (QC) (Yang Chen, Li, et Xu 2022). Thus, supervised methods can be valuable to detect biological relevant differences, such as Partial least squares-discriminant analysis (PLS-DA) or orthogonal PLS-DA (OPLS-DA) (López-Hernández et al. 2021; Tonoyan et al. 2021).

A last step of validation of the potential biomarkers can be done, with for example a receiver operating characteristics (ROC) curve analysis to assess the specificity and sensitivity of a potential biomarker (Anwardeen et al. 2023).

Data analysis tools can also be used to integrate multi-omics data, as proteomics, transcriptomics and other omics approaches. The combination of proteomics and metabolomics were used to investigate the genetic differences of autistic children (Shen et al. 2022).

I.5. Metabolites annotation

The metabolite annotation is a crucial step in the metabolomics workflow. The aim is to annotate or identify the metabolites and particularly the potential biomarkers revealed in the previous statistical step. That implies to transform potentially relevant features into identified compounds which could be interpretable biologically. This step is an important bottleneck for the metabolomics community and a major challenge that has not been fully overcome yet.

I.5.1. Descriptors and matching with libraries

Metabolite identification is based on different descriptors obtained thanks to MS analyses hyphenated to chromatographic separation: the accurate mass measure m/z , the retention time and the fragmentation spectrum are the most common descriptors measured. At first, matching with libraries can be done based on accurate mass measurements. It will be particularly sensitive on the precision of the method, e.g. within a ppm range for example. As the accuracy of the mass measurements vary depending on the instrument employed, the mass tolerance entered for database searches differ accordingly. Consequently, the number of possible structures differ in function of the tolerance specified. For example, using database such as PubChem, more than 10,000 structures are proposed even with a tolerance of 1 ppm (Figure I-22) (May et McLean 2016). Ultra high resolution mass spectrometry can significantly limit the number of possibilities with accurate mass measurements within 100 ppb, (May et McLean 2016; Schrimpe-Rutledge et al. 2016).

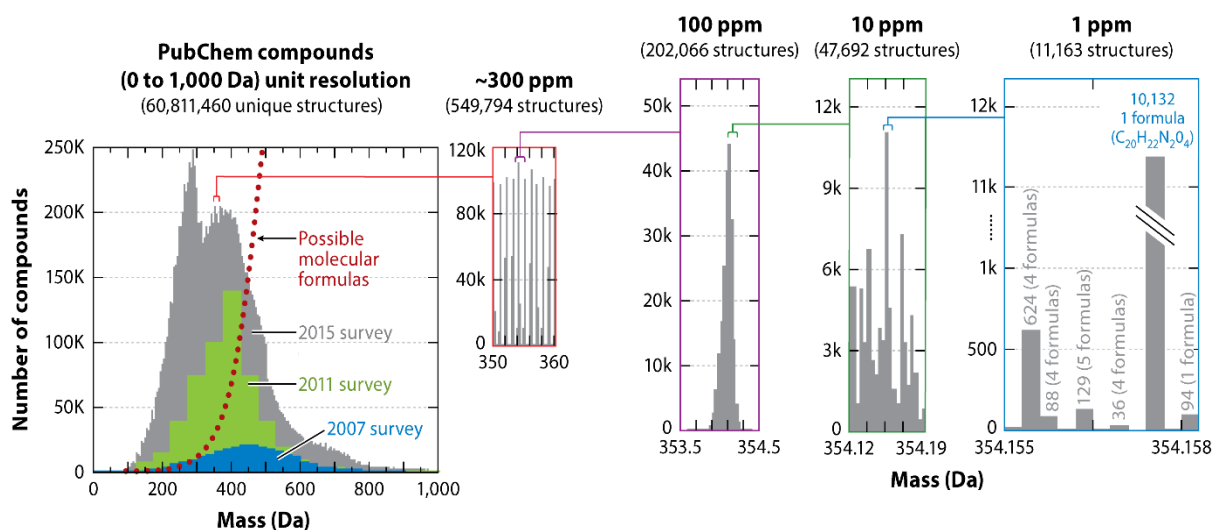


Figure I-22: Number of possible structures depending of the different levels of mass accuracy regarding PubChem compounds database, adapted from (May et McLean 2016)

Other descriptors are required such as the retention time (for LC-MS data) that could be a clue to deduce some physico-chemical properties. Retention times prediction can also be useful to reduce the possible candidates, up to 68% reduction on mouse blood plasma analysis with Retip (Bonini et al. 2020; Witting et Böcker 2020). With metabolite imaging experiments, the spatial distribution could help the annotation.

Another valuable descriptor is the MS/MS spectrum which provides structural information about the compound and can be compared with many spectra in libraries. Several publicly available libraries or databases have been developed, containing MS/MS data as ChempSpider, METLIN (C. A. Smith et al. 2005), Human Metabolome Database (HMDB) (Wishart, Guo, et al. 2022), MassBank (Horai et al. 2010),

NIST mass spectral library, mzCloud, or GNPS (Leao et al. 2021). Some are specialized in lipidomics studies as LipidBlast (Kind et al. 2013), Lipidmaps (E. Fahy et al. 2007) or Lipidweb (former LipidHome) (Hartler 2015). Numerous software tools have integrated some of these libraries to facilitate the metabolite annotation.

Figure I-23 shows that 118,000 compounds are expected in the human metabolome by compiling all the different databases. However, the total number of metabolites in human metabolome is estimated at around 5,000,000 and only a few of those compounds can be analyzed in LC-MS and retrieved in the databases or comparison with experimental data (Roca et al. 2021). This is why some efforts must be made to characterize unknown metabolites.

Optical spectroscopy or NMR experiments could also be used in complement for metabolite annotation.

As it will be discussed in the ion mobility chapter, collision cross sections measurements when coupling LC-MS with ion mobility could also be used as a descriptor to enhance the confidence of metabolites annotation.

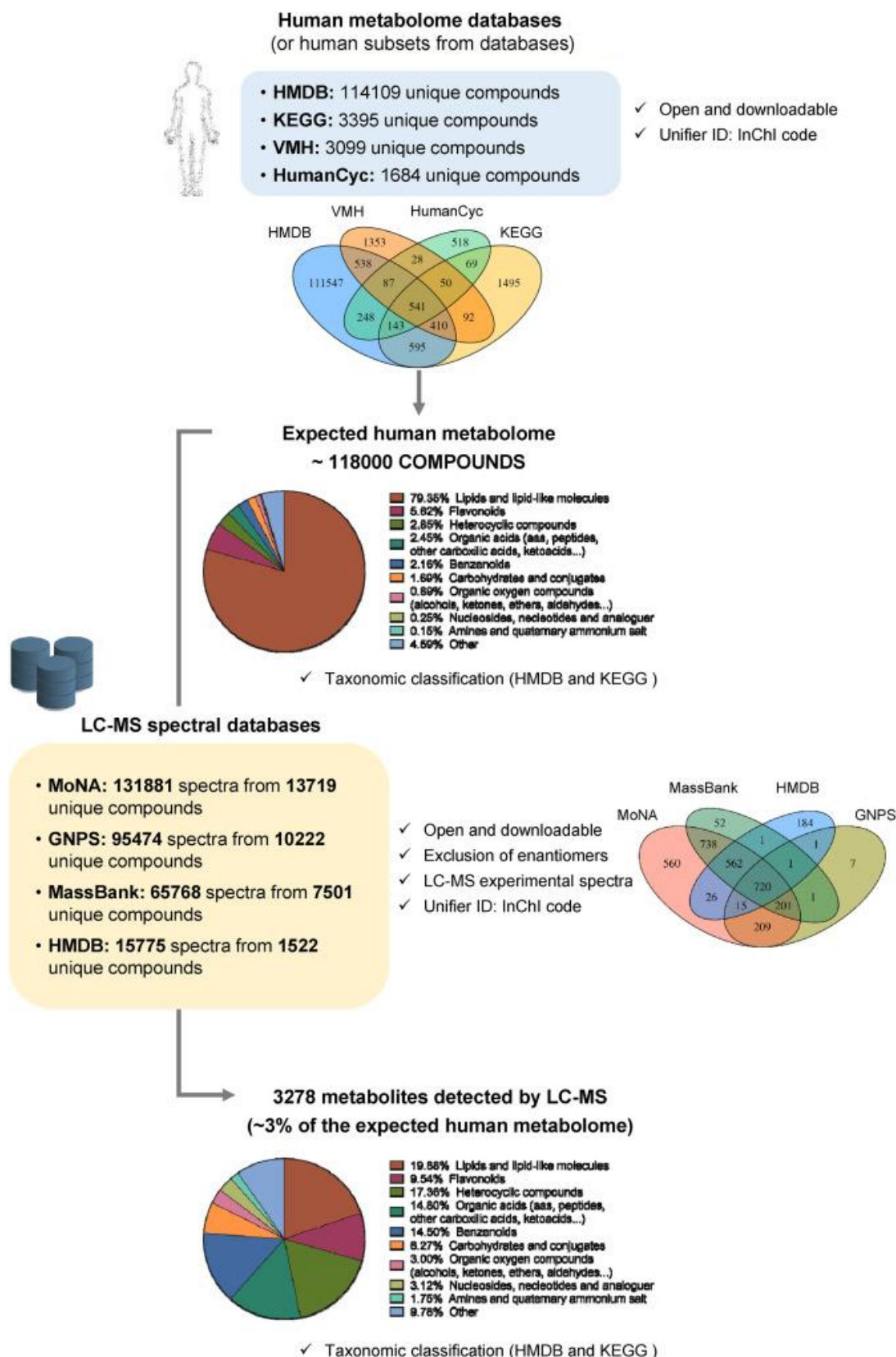


Figure I-23: Analysis of the human metabolome coverage and the percentage that can be detected by LC-MS analysis, from (Roca et al. 2021).

I.5.2. Standardization of metabolite identification

To standardize this crucial identification step, different confidence levels have been developed based on these descriptors. The first, proposed by the Metabolomics Standards initiative, contained four levels (Fiehn et al. 2007) including identified metabolites (level 1), presumed annotated compounds (level 2), presumed characterized compound classes (level 3), and unknown compounds (level 4) (Salek et al. 2013; Yang Chen, Li, et Xu 2022). Other scales were further developed, to precise the levels according to the improvement of the analysis, as the resolution and mass precision of the instrument. A scale with five levels has been proposed in Figure I-24 by various metabolomics teams (May et McLean 2016; Schrimpe-Rutledge et al. 2016). The level 1 which is the highest level of confidence, corresponds to identification of a metabolite which chemical structure is confirmed with at least two independent characteristics identical to those of the authentic chemical standard analyzed in identical conditions. If the chemical standard is not available, the metabolite can be annotated (putative identification, level 2) using the MS/MS spectra, a match with MS/MS library and all the information retrieved by the analysis (retention time, accurate m/z). Thus, database search cannot lead by itself to level 1 of identification (Kodra et al. 2022; Theodoridis et al. 2023). For level 3, tentative structure is proposed on the basis of accurate m/z and other orthogonal information but without any matching with a MS/MS spectrum. For level 4 and 5, only the m/z is used to characterize the compound. Level 4 corresponds to unique molecular formula, retrieved only using ultra high-resolution instruments and thanks to accurate mass measurements, isotope abundance distribution, charge state, etc. The level 5 proposes from 10,000 molecules (filter of 1 ppm using ultra high-resolution mass spectrometer) to 200,000 molecules (unit resolution) on the basis of m/z measurement and a library search (ex : PubChem).

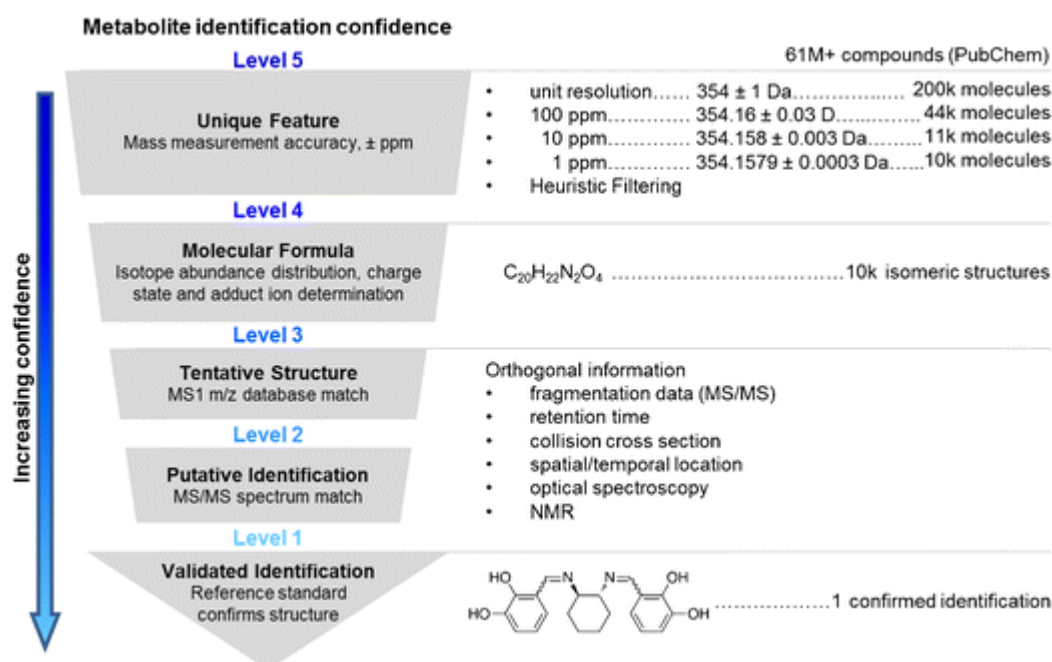


Figure I-24: Confidence levels for metabolite annotation, from (Schrimpe-Rutledge et al. 2016)

I.5.3. Standardization in lipid identification

An initiative of standardization of the lipid categories by LipidMaps can allow a better comprehension between the different studies. To promote the use of lipidomics, a standardized nomenclature and shorthand annotation have to be used as a common language (Liebisch et al. 2020). For that a unique

LIPID MAPS identifier (LM_ID) was created for each lipid structure based on the categorisation, containing 12 characters according to the Table I-2.

Table I-2: LIPID MAPS indentifiers (LM_ID) format, adapted from (Sud et al. 2007)

Characters	Character position	Description
LMFA01030001	1–2	Database designation
LMFA01030001	3–4	Two-letter category code
LMFA01030001	5–6	Two-digit class code
LMFA01030001	7–8	Two-digit subclass code
LMFA01030001	9–12	Unique four character identified with in a subclass

Note that a same lipid can be named using different ways, depending on the nomenclature or the precision of the analysis used. For example, the phosphatidylcholine PC(18:0/18:1(9Z)) shown in Figure I-25, which LM_ID is LMGP01010761, has several names as:

- 1-octadecanoyl-2-(9Z-octadecenoyl)-sn-glycero-3-phosphocholine
- Choline phosphate, 3-ester with L-2-oleo-1-stearin
- 1-Stearoyl-2-oleoyl-sn-glycero-3-phosphocholine
- L-alpha-1-Stearoyl-2-oleoyl lecithin
- L-alpha-1-Stearoyl-2-oleoylphosphatidylcholine
- SOPC
- PC(18:0/18:1) or PC 18:0/18:1
- PC(36:1) or PC 36:1
- PC(18:0_18:1) or PC 18:0_18:1

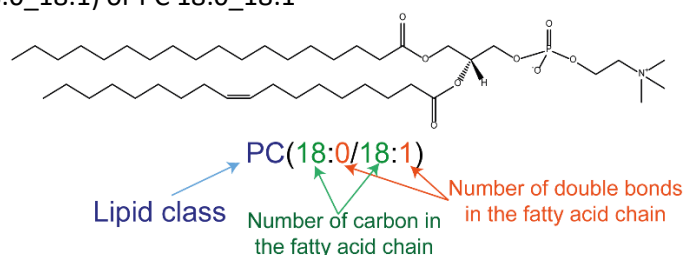


Figure I-25: Structure of the lipid PC(18:0/18:1(9Z))

In short notation, the numbers represent the number of carbons in the fatty acid chain: the number of double bounds in fatty acid chain (Figure I-25). Different notations can be used depending on the analysis performed and the level of annotation as described in Figure I-26. The symbols “/” and “_” are respectively used when the *sn*-positions of the constitutive fatty acyl groups are known or not. (Liebisch et al. 2020). The *sn*-position correspond to the stereospecific numbering, to differentiate with another convention, where the steric information was not taking into account. This numbering is used to number the carbon atoms of glycerol, the carbon atom on top in Fisher projection is designated as carbon number 1. The *sn*-position of the fatty acid chains has an important influence on the cell function, and for diagnostics (Beermann et al. 2005). Rather than the total amount of fatty acids in the triglyceride, fatty acids at the *sn*-2 position appear to affect cholesterol levels (Soek Sin 2016). According to the lipid classes, the notation can be changed, based on the same pattern as described by the LIPID MAPS® initiative (Liebisch et al. 2020).

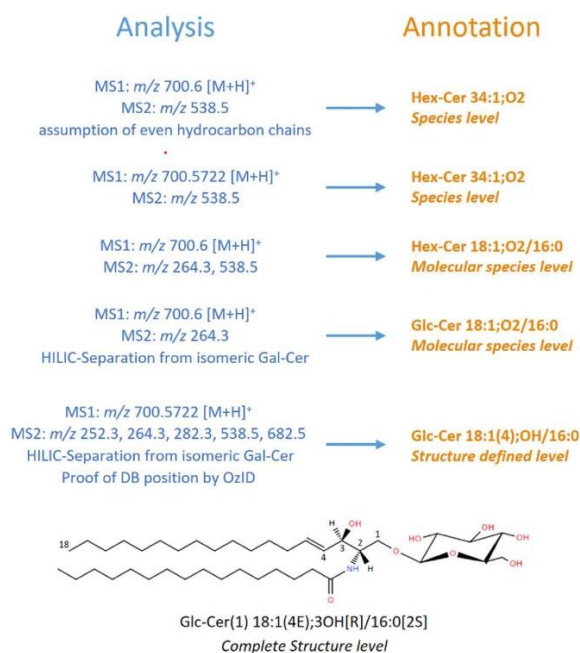


Figure I-26: Annotation of a specific lipid according to the annotation level of the species (adapted from (Liebisch et al. 2020))

I.5.4. Other tools for annotation

As lipid can be separated into classes and into a class, the structure differs only by the length of the fatty acid chains, for most of the classes, the fragmentation follows a pattern and typical fragments can be retrieved and help the annotation process (Colsch et al. 2017).

Molecular network is a recent bioinformatic tool used for data visualization, treatment, or MS/MS spectra interpretation. This method is based on the idea that similar compounds or compounds belonging to the same chemical family have similar fragmentation patterns. Thus, regrouping compounds is achieved on the basis that their fragmentation spectra exhibit the same fragments or fragmentation systematics. This method facilitates compound annotation and data interpretation (Perez De Souza et al. 2020). Two major tools can be used, Global Natural Products Social molecular networking (GNPS) platform (Schmid et al. 2021) or Metgem software (Elie, Santerre, et Touboul 2019).

Some other tools can help the annotation as Kendrick mass defect analysis or Van Krevelen diagram (Rathahao-Paris et al. 2015; Sueur et al. 2022).

In metabolomics, all features detected are not completely identified with the libraries and many compounds remain unknowns. To solve this issue, many experiments must be performed, to obtain as much information as possible on the compound, as MS/MS experiments with different settings as the collision energy. Multiple NMR experiments can give also precious structural information. A fractionation of the complex samples could help the annotation by reducing the complexity of the sample (Kind et Fiehn 2010). The SUMMIT MS/NMR approach provides a significant improvement in structural elucidation by combining high-resolution MS, NMR experiments and cheminformatics (Leggett et al. 2019).

I.6. Conclusion of chapter I

Analytical approaches and data analysis have known improvements making metabolomics a powerful tool for biomarkers discovery, cancer research and many fields. Thanks to these evolutions, the scientific community is very hopeful for the future even if many challenges must be overcome. As we have mentioned in chapter I, all difficulties have not been addressed yet, the LC-MS/MS approach is not fully satisfactory. Indeed, the chromatographic dimension cannot separate all species in such complex samples and MS analyzer cannot separate isomeric species. Moreover, one of the most important bottlenecks in metabolomics approaches is the annotation step.

This is why, new strategies have been proposed as, for example, the addition of ion mobility spectrometry (IMS) in the metabolomics workflow which seems to address some of the challenges. IMS provides an additional dimension of separation which may overcome the issue of isomeric separation. Furthermore, it affords an additional descriptor, the collision cross section (CCS) that may help metabolite annotation. Hence, the following chapter II describes ion mobility spectrometry and its use in metabolomics.

Chapter II. Ion mobility for metabolomics

2.1. Ion mobility spectrometry

2.1.1. Introduction to ion mobility spectrometry

Ion mobility spectrometry (IMS) is a gas-phase ion separation technique. The ions are separated under an electric field into a chamber filled with a buffer or drift gas.

First research regarding mobility of ions in gas phase at atmospheric pressure was developed in 1890s and the theory of mobility was initiated before 1910 (Rutherford 1897; Franck et Pohl 1908; Borsdorf et Eiceman 2006). The first commercial ion mobility instrument was introduced in 1970, as the Plasma Chromatography™ (Cohen et Karasek 1970). The principle of this instrument is quite similar as modern technology which has undergone significant improvements in engineering and technologies (Borsdorf et Eiceman 2006). The developments of IMS over the years have known a widespread growth and have been well-described (May et McLean 2015, Figure II-1).

Then, many reviews have covered the basic concepts and application of ion mobility in metabolomics and lipidomics fields.

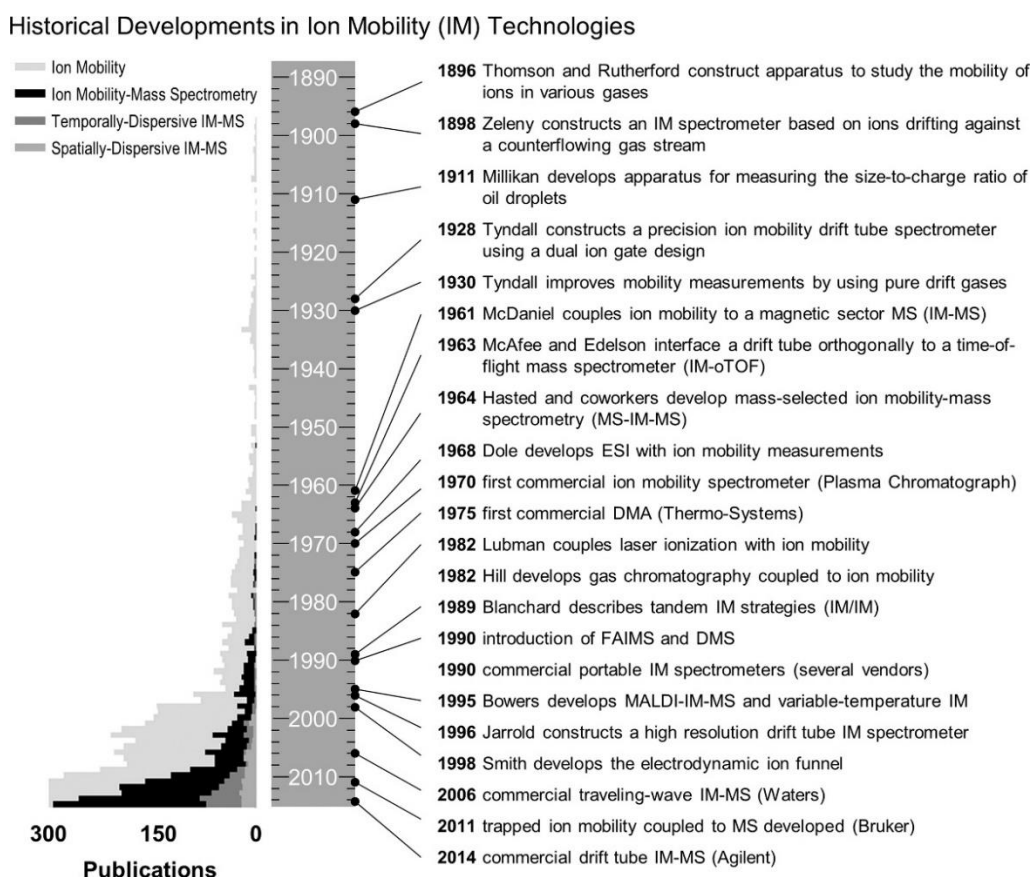


Figure II-1: Description of the developments in IMS instrumentations from 1896 to 2014, from (May et McLean 2015)

In IMS technique, the mobility (K) of the ions is directly related to the shape, size and charge of the ions and the nature of the buffer gas used. The mobility is related to the velocity (v) of the ions divided by the electric field (E) (Equation [1]). Knowing the length (l) of the IMS tube, the velocity of the ions

can be derived using the drift time (t_D) (Equation [1]) (Gabelica et Marklund 2018; May et McLean 2015).

$$K = \frac{v}{E} = \frac{l}{t_D E} \quad [1]$$

The mobility provides information on the interactions between the ions and the buffer gas and depends on the collision frequency of the ions with the gas molecule. This frequency depends on the number of gas molecule per unit volume (N), so the pressure (p) and the temperature (T). The reduced mobility K_0 , normalized to standard pressure (760 mmHg) and temperature (273.15 K) conditions is generally used to permit comparison of results (Equation [2]) (Clemmer et Jarrold 1997).

$$K_0 = K \frac{N}{N_0} = K \frac{p}{p_0} \frac{T_0}{T} \quad [2]$$

The mobility of the ions can be used to determine their collision cross section (CCS) in the buffer gas thanks to the Mason-Schamp equation (Equation [3]) (Revercomb et Mason 1975). This equation can be used only at low electric field and when the ion velocity is small compared to ion thermal velocity (Gabelica et Marklund 2018; Clemmer et Jarrold 1997).

$$CCS = \frac{3ze}{16N_0} \frac{1}{K_0} \sqrt{\frac{2\pi}{\mu k_B T}} \quad \text{with } \mu = \frac{M_{ion} \times M_{gas}}{M_{ion} + M_{gas}} = \frac{1}{\frac{1}{M_{gas}} + \frac{1}{M_{ion}}} \quad [3]$$

where μ is the reduced mass, M_{ion} the mass of the ion and M_{gas} the mass of the buffer gas used, z the ion charge, e the electron charge, N_0 the gas number density, k_B the Boltzmann's constant. (Mason 1958; Gabelica et al. 2019)

2.1.2. Applications of ion mobility

Ion mobility spectrometry has many applications, in various fields of chemistry, biochemistry and physics. Hand-held ion mobility spectrometers are used for explosives and narcotics detection (Turner et Brokenshire 1994). AirSense Analytics society produces ion mobility spectrometers for military use to detect chemical warfare agents, or explosives. Nuctech society has been developed on ion mobility spectrometry with 2 IMS cells to be used in checkpoint airport. Small instruments can also be used for medical purposes, as the detection of bacteria, or other compounds from human exhaled air (Steppert et al. 2021; Westhoff, Friedrich, et Baumbach 2022). Olfactomics uses differential mobility spectrometry (DMS) technology implemented on a small instrument to detect breast cancer when the surgeon cuts the tissue during the surgery (Kontunen et al. 2021).

Ion mobility spectrometry was coupled to mass spectrometry to extend the use of IMS to other applications, from large biomolecules to small analytes. Nowadays, there are various commercial IM-MS instruments which differ in their technologies (Figure II-2). The different instruments can be classified according to three main categories (Hernandez-Mesa, M., et al. 2019, Paglia, Smith, et Astarita 2021):

- the time-dispersive instruments as DTIMS (drift tube ion mobility spectrometry), TWIMS (travelling wave ion mobility spectrometry), SLIM (Structures for Lossless Ion Manipulation) and DMA (Differential mobility analyzers),
- the trapping and selective release as TIMS (trapped ion mobility spectrometry), cIMS (cyclic ion mobility spectrometry)

- and the space-dispersive as FAIMS (High-field asymmetric waveform ion mobility spectrometry), DIMS or DMS (differential ion mobility spectrometry) (Paglia, Smith, et Astarita 2021; Hernández-Mesa, Ropartz, et al. 2019).

Another classification can be made based on the measurement principles. Methods can be linear or dependent on the electric field. In linear methods, the K_0 values are considered independent of the electric field, it is the case for DTIMS, TWIMS, TIMS and DMA (Gabelica et al. 2019). For nonlinear methods, as DIMS or FAIMS, the separation of ions is based on the dependence to the electric field.

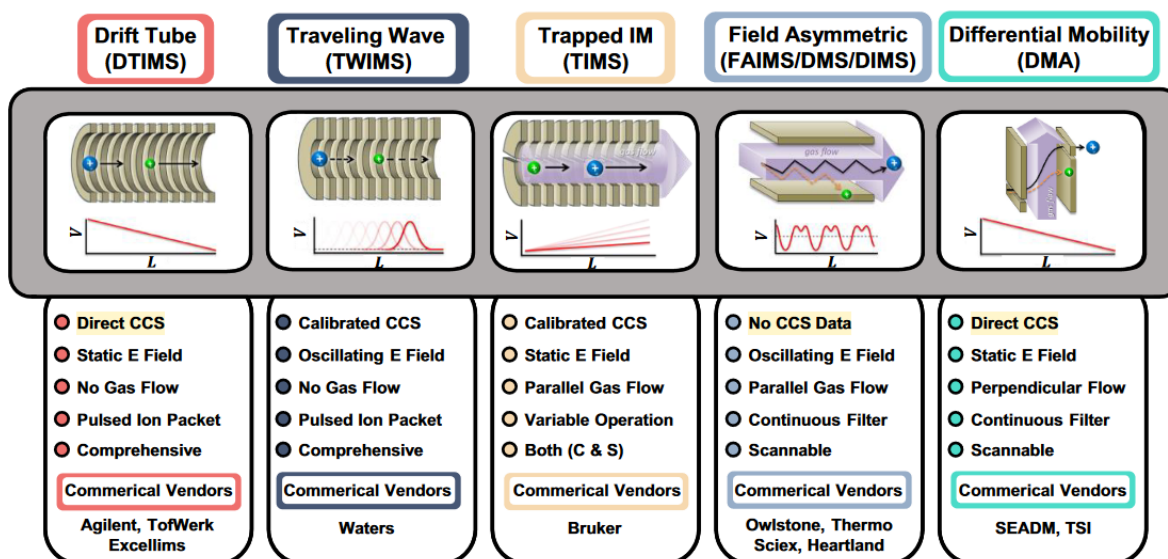


Figure II-2: Different types of IMS technology with key points describing the technique, reprinted from (Dodds et Baker 2019)

2.2. Ion mobility instrumentation

2.2.1. Drift tube ion mobility spectrometry

2.2.1.1. Principle of the technique

The drift tube ion mobility spectrometer (DTIMS) is often described as the classic configuration of current IMS instrumentation. The ions formed in the ion source move through a continuous electric field in a drift tube filled with a buffer gas (Figure II-3). This cell consists of a series of stacked-ring electrodes in which the electric field is created. The buffer gas also called drift gas is mostly nitrogen, but helium, argon or other neutral gas can also be used. The pressure is maintained constant around 1-15 mbar. The gas is an important component for ion separation, it must be controlled, particularly the percentage of water into the cell. The ions are formed in the source region and are transferred to the drift tube with an electronic ion gate. When the ion gate is closed, the ions move under the influence of a uniformly applied weak electric field, at a constant velocity proportional to the electric field and the mobility of the ion (deduced from Equation [1]) but are more or less slowed down by collisions with the buffer gas, depending on their collision cross section. The smaller CCS corresponds to higher ion mobilities, and shorter drift times used for the ions to pass through the drift tube. As a uniform field is applied, K can be measured using Equation [1] and the CCS can be determined from the Mason-Schamp equation. Obtaining CCS from this principle, described as the primary method, constitutes a significant advantage of DTIMS. It is noteworthy that the first approximation made in drift

tube ion mobility system, is the measure of the reduced mobility K_0 instead of the mobility K , using a normalization of the pressure and the temperature.

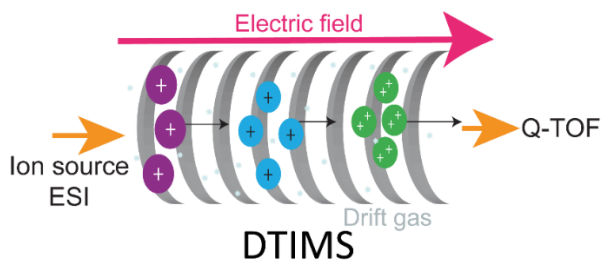


Figure II-3: Schematic representation of a DTIMS instrumentation

Different vendors have commercialized this IMS technology, as Agilent, TofWerk or Excellims. Various laboratories have built their own drift tube which has integrated into a mass spectrometer. Various designs were developed, some of the most recent ones involve a printed circuit board (Chantipmanee et Hauser 2021) or composite material (Ahrens et al. 2020).

2.2.1.2. Multiplexing strategies

An advantage of the DTIMS technique is the comprehensive ion collection, which collects all mobilities in a single experiment. The analyte ions are separated in a single pulsed experiment and thus all the mobilities of ions are separated in an IMS scan. However, since the DTIMS works with ion pulses, the duty cycle is lower than for continuous methods, and can be less than 1%. An ion trap is often used before the IMS cell to increase the duty cycle, typically to 5-30% (Dodds et Baker 2019; May et al. 2020). For this purpose, multiplexing strategies have been developed to allow better sensitivity and duty cycle. Several ion pulses are introduced into the cell during a cycle, at a define interval time while the first pulse is separated (Figure II-4). Different IMS ion multiplexing have been developed since 1985, where the IMS spectrum is reconstructed by a Fourier Transform (FT) (Knorr et al. 1985). Hadamard Transformation (HT) was also used to reconstruct the spectrum to obtain the drift times. This type of ion multiplexing strategy allowed an increase in duty cycle up to 50% and an improvement in sensitivity (Belov et al. 2007; Morrison, Siems, et Clowers 2016). Extended Hadamard demultiplexing and deconvolution have been combined into a single step to create a new post-processing demultiplexing tool called High resolution demultiplexing (HRdm) to improve the resolution in the ion mobility dimension. This method provides an 8-fold gain in ion signal, and an improvement of the IMS resolving power, between 180 and 250, in comparison to approximately 60 in conventional DTIMS. It has been demonstrated that the CCS values are identical using either standard DTIMS or HRdm processed data sets. Moreover, HRdm timeframe is compatible with the chromatographic dimension (May et al. 2020).

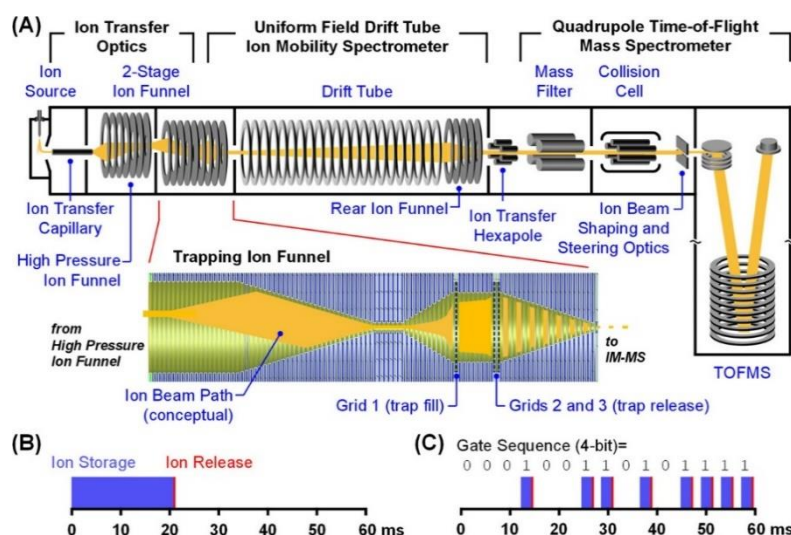


Figure II-4: (A) Schematic representation of a DTIMS instrument with an enlargement on the trapping ion funnel where the multiplexing is implemented. (B) Conventional single pulse method. (C) Multiplexing method: series of ion pulses with a setting interval time, from (May et al. 2020). Based on a Agilent 6560 instrument

2.2.2. Travelling wave ion mobility spectrometry

Another IMS technique which has induced the widespread use of IMS in analytical science, in particular with the commercial IM-MS instrument from Waters Corporation, is the travelling wave ion mobility spectrometry (TWIMS). Contrary to DTIMS technique, the electric field is variable in TWIMS, and can be described as waves of potentials (Figure II-5). The TWIMS consists of a series of electrodes which form a stacked ring ion guide (SRIG) (Giles et al. 2004). Radio frequency (RF) voltages in opposite phases are applied to adjacent ring electrodes to permit radial ion confinement and high transmission efficiency (Pringle et al. 2007; Javahery et Thomson 1997). A pulsed DC voltage is superimposed on the RF voltages to push the ions axially through the cell in a wave motion. Then, a succession of these waves of potential drives the ions towards the end of the SRIG, but collisions with the buffer gas slow down the ions that roll over the waves, depending on their CCS. Ions of higher CCS roll over the wave more frequently than smaller ions which more likely “surf” the waves. The ion separation can be optimized by adjusting the voltage (height) and velocity of the waves as well as the pressure of the buffer gas. The number of roll overs undergone by ions differs according to the size, shape and charge of the ions allowing their separation. As the electric field is not constant and uniform, the relationship between the CCS and t_d is more complex (Equation [4]), and a calibration with ions of known CCS is required to determine A and B coefficients for CCS determination (D. P. Smith et al. 2009).

$$CCS = \frac{3ze}{16N} \times \sqrt{\left(\frac{1}{m} + \frac{1}{M}\right)} \times \sqrt{\frac{2\pi}{kT}} \times \frac{760}{P} \times \frac{T}{273,15} \times At_d^B \quad [4]$$

However, this method of separation does not allow to access to K values. Ion motions in TWIMS have been studied by simulations, allowing to determine three different steps: the ions surfing, a region of transition and a steady state ion roll-over (May et McLean 2013). The wave velocity has an important role on the ion motion, especially for nitrogen and argon drift gases. The resolving power of current commercial TWIM instrument is about 50. Influence of different buffer gas has been investigated. It has been shown that, at low wave velocity, the resolving power is higher in argon than in nitrogen and an inversion occurs at high wave velocity. A loss in resolving power can be observed at higher wave velocity, which could be explained by higher ion-gas diffusion when the ions stay longer in the TWIM cell (May et McLean 2013).

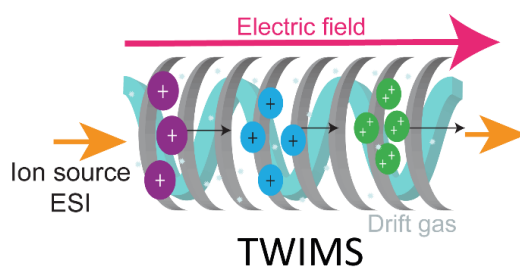


Figure II-5 : Schematic representation of a TWIMS instrumentation

2.2.3. New high-resolution techniques

2.2.3.1. Cyclic-IMS

The first cyclic IMS device was developed in 2009, with a series of four DTIMS devices put into a circle (Merenbloom et al. 2009). The first commercialized cyclic IMS was the cIMS by Waters in 2019 which relies on TWIMS technology (Giles et al. 2019). Ions move around this cyclic device and undergo multiple passes (Figure II-6). This allows to extend the overall path length (one path length is about 98 cm) and therefore increases the IMS resolution when several passes are achieved. The cyclic instrument is a multi-functions instrument, because various types of experiments can be performed as the mobility selection (IMS^n Isolation), activation, storage and IMS^n as well as a combination of these experiments. The major advantages of this technique are the very high ion mobility resolving power (60 to 80 for a single pass) and the capabilities to perform IMS^n (Paglia, Smith, et Astarita 2021; Delafield et al. 2022). The resolution increases with the square root of the number of passes. A resolution of 750 has been achieved using 100 passes for a peptide analysis (Giles et al. 2019). The separation of a mixture of three pentasaccharides (cellopentaose, maltopentaose, and branched mannopentaose) has also been achieved with only 5 passes in the device, as shown in Figure II-6 (Ujma et al. 2019).

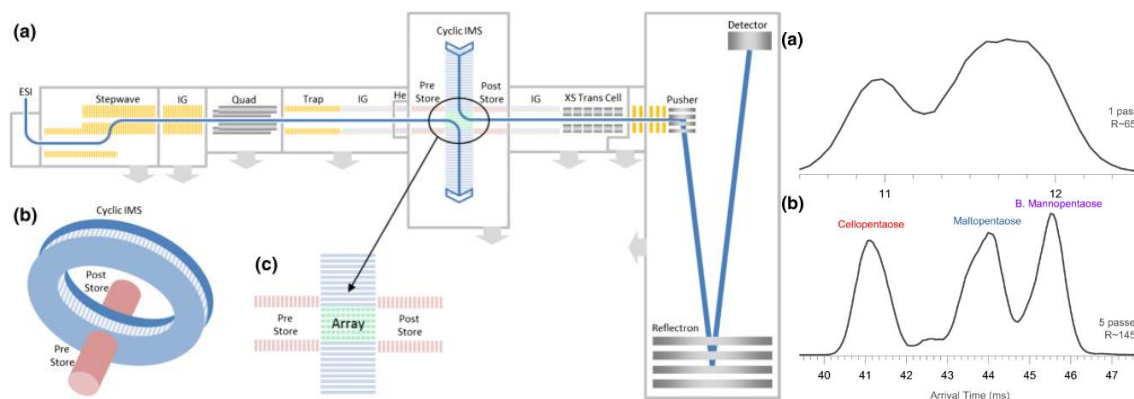


Figure II-6: Cyclic IMS (Waters Select Series Cyclic IMS) instrumentation and an example of a separation of three compounds after 1 and 5 passes onto the cIMS; adapted from (Ujma et al. 2019)

An important limitation of the cIMS is the loss of sensitivity when multiple passes are used. Thus, Chi et al. showed that two ions which were observed after 11 passes were hardly detected after 25 passes. Thus, it was no longer possible to detect the lowest intensity peaks (Chi, Wang, et Ng 2022). cIMS has been used in various applications, for example, for proteins (Harrison et al. 2022; Snyder et al. 2021), peptides, glycans and carbohydrates (Ollivier et al. 2021; Ropartz et al. 2022) or metabolites (Naznin et al. 2023) and particularly for the separation of isomers (de Bruin et al. 2022; Gibson et al. 2022) or enantiomers (Cooper-Shepherd et al. 2022).

2.2.3.2. SLIM

Structures for Lossless Ion Manipulation (SLIM) devices, developed by R. D. Smith and coworkers in 2014, are other high-resolution ion mobility technologies. They consist in printed circuit boards where electric fields (RF and DC potentials) can be applied onto electrodes at the surfaces of the board to trap and guide ions with negligible losses (Tolmachev et al. 2014). As ions can be separated over a much longer path length than in traditional DTIMS, significantly higher resolutions and separation capacity can be attained with SLIM (Webb et al. 2014). The path length can also be adapted depending on the applications and the resolution required. For example, a 13 m SLIM IMS allowed the separation of peptide, amino-acid or lipid isomers that could not be achieved in neither 90 cm DTIMS nor 44 cm SLIM IMS (Figure II-7) (Deng et al. 2016). Ultra-long paths (SLIM-SUPER) allowed to achieve ultra-high-resolution separations. In these devices, ions underwent over 81 passes through a 13.5 m serpentine path resulting in a total path length of 1.1km (Deng et al. 2017).

To benefit of both the ultrahigh-resolution and the extended mobility range, a multilevel SLIM has been developed, involving multiple stacked serpentine paths. Ions moved between the levels thanks to ion escalators (Hollerbach et al. 2020). To enhance the sensitivity and the high-throughput of the measurements, a new SLIM arrangement has been investigated by performing the ion accumulation and separation on the same time (Ailin Li, Nagy, et al. 2020).

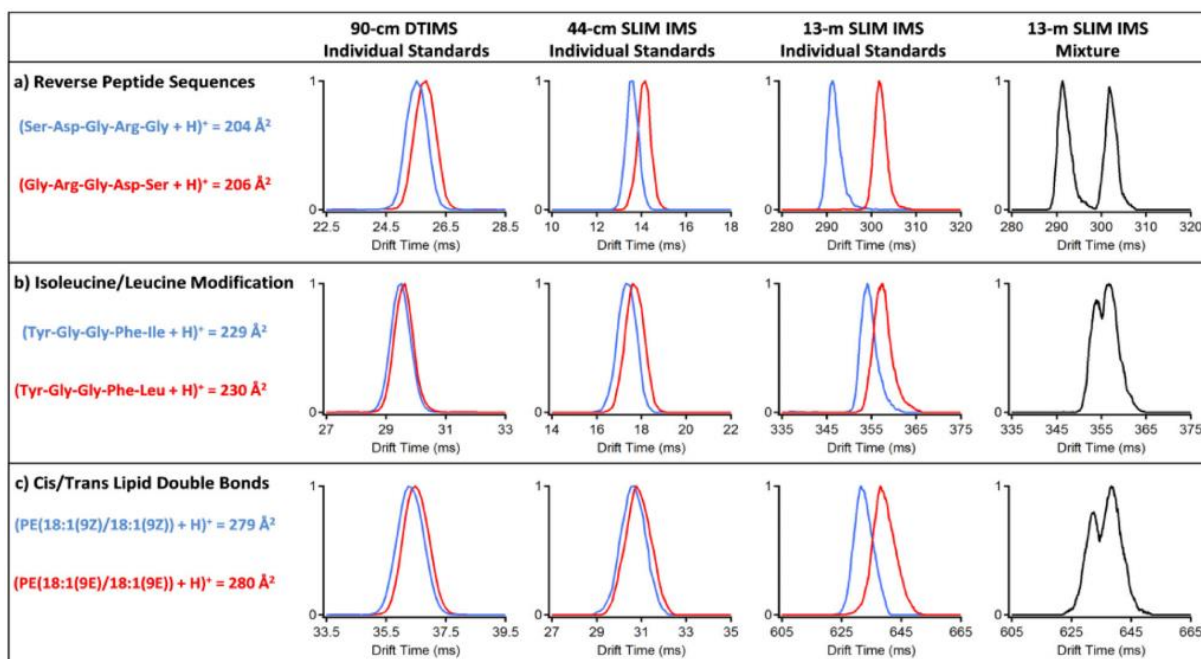


Figure II-7: IMS separation of different compounds according to the IMS instrumentation used (DTIMS, 44cm SLIM, 13m SLIM) ; adapted from (Deng et al. 2016) Trapped Ion mobility spectrometry

Recently developed, the trapped ion mobility spectrometry (TIMS) operates differently than DTIMS and TWIMS and uses electrical field to push the ions in a static buffer gas. TIMS is an ion funnel based device. It involves electric field to hold the ions against a gas flow that moves towards the exit of the cell (Michelmann et al. 2015) (Figure II-8). Different gases or gas mixtures may be used depending on the analytical problem, the most widely used being nitrogen. TIMS-TOF instrument was commercialized by Bruker Daltonics in 2017.

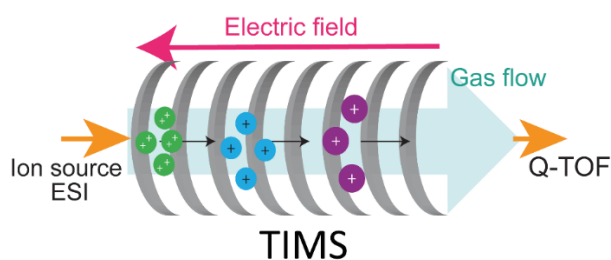


Figure II-8: Schematic representation of a TIMS instrumentation

Ion separation assumes three steps:

The first and second steps are ion accumulation and trapping, respectively. The ions are introduced into the ion mobility cell and then trapped by applying an electric field between the ion funnel and the cell output electrode. In the second step, the ions are blocked by the electrical field which direction is opposite to that of the buffer gas flow.

Then, in the final step, elution and separation of ions occur by gradually decreasing the potential ramp. That permits to expel the ions from the mobility cell by the second ion funnel according to their respective mobilities. The larger ions or those exhibiting a more unfolded conformation leave the tube faster than the smaller or more compact ions, unlike in TWIMS or DTIMS (Figure II-9). The fundamentals and theory of the TIMS have been investigated and detailed (Michelmann et al. 2015; Silveira et al. 2016; Ridgeway et al. 2019). Due to its functioning, TIMS allows high resolution ($R > 200$ for singly charged ions) within a small cell (about 5-10 cm). The resolving power of TIMS can be increased by using longer trap times, without decreasing the duty cycle, and therefore without ion loss. The high sensitivity of this cell can be achieved because the diffusion of ions is reduced thanks to the use of the ion funnel (Clowers et al. 2008). Various types of analyses can be performed, as the “sequential analysis” TIMS, the selective accumulation TIMS, the parallel accumulation TIMS, and the “parallel accumulation serial fragmentation” (PASEF) method (Ridgeway et al. 2019) which increases the analytical capabilities of this instrument.

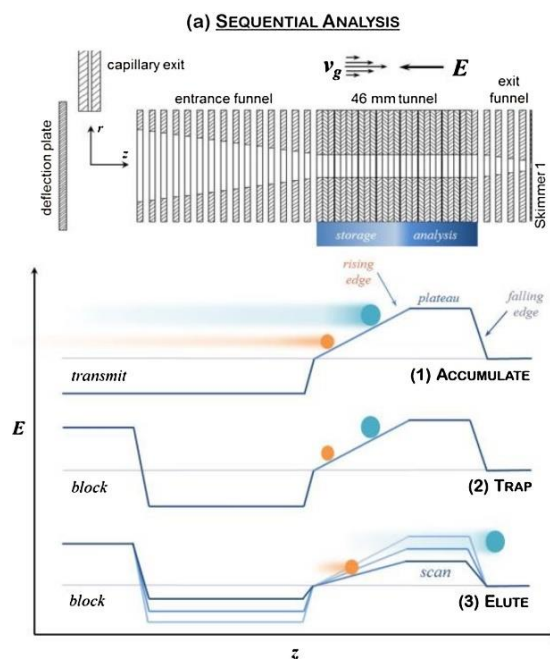


Figure II-9: Description of the three steps occurring on the TIMS cell during each cycle time (adapted from (Ridgeway et al. 2018))

2.2.4. Other techniques

Differential mobility analyzers (DMA) were comparable to DTIMS devices, because both use a constant electric field (Dodds et Baker 2019). However, DMA differs from DTIMS because the gas flow is perpendicular to the electric field and the DMA device operates at ambient pressure. The challenge is to keep a laminar sheath gas flow in the cell. This technique is principally used as an ion filter or to detect large analytes such as macromolecules, (Hogan et al. 2011) virus or even aerosol particles (Reischl 1991). Some investigations were carried out to separate isomers of metabolites with three IMS techniques including DMA (Werres et al. 2019). The mobility can be measured directly as with DTIMS, which remains the reference in ion mobility measurement (Masike, Stander, et de Villiers 2021). For DMA, the applied voltage is linearly proportional to the inverse mobility of the ions. Furthermore, it has been proposed to determine CCS by resorting to a single point calibration using tetraheptylammonium ion. Calibration was performed with other tetraalkylammonium ions and the difference in CCS values using the different one-point calibration were less than 2% in CCS (Ouyang et al. 2013).

The transversal modulation IMS (TM-IMS) is a new approach to directly measure the mobility by using resonant peaks. This technique can be considered as a subtype of the DMA technique (Vidal-de-Miguel et al. 2015) but it operates using an oscillating electric field instead of a high field used in DMA and it does not require a precise constant gas flow as in DMA (Cumeras et al. 2015a). The ion trajectory could be quite complicated. This technique can be coupled in tandem to perform IMS-IMS experiments and is compatible with MS but there are mechanical challenges (Rawat, Vidal-de-Miguel, et Hogan 2015; Vidal-de-Miguel, Macía, et Cuevas 2012).

Differential ion mobility (DMS) or field asymmetric ion mobility spectrometry (FAIMS) are other techniques for gas-phase ion separation. Their principles are common, but they differ in their configurations: DMS corresponds to planar FAIMS involving two flat parallel electrodes while cylindrical electrodes are involved in FAIMS (coaxial or c-FAIMS) (Guevremont 2004; Krylov 2003). An electric field is applied on two parallel electrodes perpendicular to the ion motion through a buffer gas. The ions move up and down according to the asymmetric electric field between the two electrodes, and a compensation voltage (CV) is applied to allow ions to retrieve a straight line, to exit the cell. The ions are thus separated according to their CV values. As a high electric field is applied, the ion velocity into the drift cell is no longer proportional to the electric field, this is why CCS values are not available with FAIMS/DMS (Purves et Guevremont 1999; Delvaux, Rathahao-Paris, et Alves 2021). . This technique has been used for various applications for the separation of different analyte classes, as chemical weapons, pharmaceuticals or pollutants (M. Kolakowski et Mester 2007).

Aspiration IMS (AIMS) or Open loop IMS (OLIMS) are other techniques where ions are carried in a buffer gas flow through an electric field generated by several electrodes (often 8 electrodes). The polarity of electric field is inverted on the electrodes to allow the ion motion and separation. The ions will be detected by collision with the electrodes, ion with higher mobility will collide with the first electrode, whereas ion with smaller mobility will traverse through the cell to collide the last electrode (Ratiu et al. 2017; Cumeras et al. 2015a).

2.2.5. Resolving power, resolution, selectivity, sensitivity and duty cycle

The resolving power and resolution of IMS are used to compare instrument performances. The resolving power R_p is defined with Equation [5] where x is the direct measurement using t_d for DTIMS and TWIMS, CV for FAIMS and DMS or V for DMA and Δx is the FWHM. The resolving power is calculated using a single peak of the ion mobility spectrum and using the domains where the measurements are performed without conversion (Cumeras et al. 2015b).

$$R_p = \frac{x}{\Delta x} \quad [5]$$

Sometimes the resolving power is reported directly on the CCS values, which can induce higher resolving power than with the direct measurements (Dodds, May, et McLean 2017).

The resolution R is used to describe the ability to separate two peaks (the measurement of peak-to-peak separation) and the associated equation is similar to that used in chromatography (Equation [6]).

$$R = 2 \frac{|x_2 - x_1|}{\Delta x} \quad [6]$$

where x_2 and x_1 correspond to the previously defined variables. The IMS resolution is limited by the broadening of peaks which can be caused by different factors such as the diffusion of ions, coulombic repulsion, the uniformity of gradient electric field, temperature or pressure fluctuations and/or ion-ion and ion-molecule reactions into the drift cell (with the gas or other ions) (Cumeras et al. 2015b).

The sensitivity and the selectivity constitute other important criteria to compare the IMS instruments (Table II-1). The selectivity represents the ability to transmit ions in a specific mobility range. The sensitivity is related to the ability to conduct ions through the different parts of the instrument. For that, the duty cycle can be used to compare instrumentation, because it represents the part (percentage) of the ions actually analyzed and correlates with the sensitivity. The DTIMS and TWIMS instrumentation use pulsed ion injection, which leads to low duty cycle, and consequently low sensitivity. However, in the case of DTIMS, some multiplexing strategies have been developed to counteract this phenomenon. TIMS instrumentation operates with accumulation and trapping steps as well as ion funnels which allow to have a high duty cycle up to 100% and thus a high sensitivity.

Table II-1: Characteristics of some ion mobility technologies

IMS technology	Commercial vendors	Resolving power	Duty cycle	CCS measurements	Additional tool for annotation	Advantages	Drawbacks
DTIMS	Agilent, TofWerk Excellims	60-80	1-50%	Without or with calibration	-	Direct measurement of CCS values	Low duty cycle
TWIMS	Waters	40-50	15-90%	Calibration required	CCS of fragment ions	Large mobility range, structural analysis	Possible changes in ion conformation
cIMS	Waters	80-750	Depends on the number of passes	Calibration required	Available IMS ⁿ	Super high IM resolving power (isomer separation)	Low duty cycle with multiple passes
SLIM	MOBILion	200-300	up to 100%	Calibration required	-	High resolving power, high duty cycle	
TIMS	Bruker	200-400	up to 100%	Calibration required	PASEF mode	High duty cycle, different modes allowing increasing the resolving power, PASEF mode	Necessity to have powerful software tools
FAIMS	Thermo, Sciex, Owistone, Heartland	30-40	up to 100%	Not available	-	Adaptable to many mass analyzers, increased S/N ratio	Impossible to obtain CCS, optimization of parameters required for ion transmission

2.3. Ion mobility-mass spectrometry (IM-MS)

For metabolomics purpose, the ion mobility spectrometry is often coupled with mass spectrometry and hyphenated techniques such as liquid or gas chromatography, supercritical chromatography and capillary electrophoresis in a lesser extent.

2.3.1. Ionization source for IMS

As IMS is a post-ionization separation technique, the formation of ions from neutral sample molecules constitutes a key step and the choice of the ion source which depends on the physicochemical properties of the sample analytes has to be correctly handled. For gas phase samples, three common sources can be used, radioactive, corona discharge or photoionization. The radioactive source is the most commonly used for IMS spectrometer, because it is a stable and reliable ionization which is simple and does not need power, which is a crucial advantage for mobile spectrometers. For safety reason, the spectrometer must be controlled and have proper ventilation (St. Louis, Hill, et Eiceman 1990). For volatile, apolar and thermostable compounds in solution (organic solvent), EI and CI sources are appropriate but ASAP or APGC can be used.

Electrospray (ESI) is the most relevant ionization technique for polar or semi polar compounds in solution, such as metabolites and other biomolecules in aqueous solutions such as biological fluids. It is the most common and appropriate method for a wide range of compounds and samples. Other ambient sources such as APCI (Singh et al. 2023), APPI (Zheng et al. 2018), ASAP (Mendes Siqueira et al. 2018) have been utilized but in a lesser extent, as well as DESI (Parrot et al. 2018), DART (Fowble et al. 2017), LAESI or LADESI (Stopka et Vertes 2020) and MALDI (Neumann et al. 2020) after sample deposit onto a surface permitted IM-MS analyses. These sources can also be used for solid samples such as tissues, plant cells, ... (Eiceman, Karpas, et Jr 2013). Imaging mass spectrometry can be carried out on tissues using MALDI and provide spatial information in metabolomics or proteomics studies (Eberlin et al. 2011; Cordeiro et al. 2020).

2.3.2. Mass analysers

IM-MS coupling was developed, with different mass spectrometers such as quadrupole (Q), triple quadrupole (Kozole et al. 2011), ion trap (Clowers et Hill 2005) and time of flight (TOF) analyzers thanks to the compatibility of scanning rates of IMS devices and mass analyzers. Indeed, the IMS devices operate in the millisecond scale while MS analyzers exhibit microsecond acquisition scan rates. This allows multiple MS acquisitions for each ion mobility spectrum (Paglia, Smith, et Astarita 2021). The state of the art IM-MS coupling for metabolomics usually involves, in addition to IM device, hybrid quadrupole - time of flight (Q-TOF) which offers high-resolution, accurate mass measurements and tandem mass spectrometry, necessary for metabolite annotation (Baker et al. 2007). Many of them are commercial IM-MS instruments (Agilent, Waters or Bruker).

IM-MS coupling incorporating ultra-high-resolution mass spectrometers such as Orbitrap or FTICR are more challenging because technological adjustments regarding the time scale are required. Indeed, Orbitrap and FTICR exhibit slow acquisition rates (up to 1s for FTICR experiments) which can compromise combination with IMS. Thus, various strategies have been developed such as the dual gate for the coupling of DTIMS with Orbitrap, which allowed various applications in proteomics and for petroleum samples (Ibrahim et al. 2016). Orbitrap instrument was also coupled to atmospheric

pressure DTIMS to characterize isomeric composition of samples (Keelor et al. 2017; Kaszycki et al. 2019) and to the SLIM resulting of an average CCS resolving power of 218 (Hollerbach et al. 2023).

As the TIMS device allows a trapping of ions, it can be coupled with FTICR instrument, which exhibits relatively low acquisition rate compared to other analyzers, allowing to combine both high-resolution ion mobility spectrometry and ultra-high-resolution mass spectrometry (Ridgeway et al. 2018; J. F. Maillard et al. 2021). FAIMS instrumentation has also been successfully coupled with Orbitrap (Saba et al. 2009; Bekker-Jensen et al. 2020) and FTICR instruments (Robinson et al. 2006; Kailemia et al. 2014).

2.3.3. Complementarity of IMS and MS

The addition of ion mobility spectrometry to mass spectrometry provides several benefits such as the possibility to separate different charge states, compound classes and isomers, to improve the sensitivity and dynamic range thanks to the partitioning of chemical noise, to increase the feature detection and annotation confidence via the resort to CCS. Moreover, the use of IMS in databases can reduce false-positive annotation. Other information could be provided by coupling IMS with fragmentation techniques.

The selection of the most suitable analytical technique for each specific application requires an evaluation of different criteria. The more important criteria is to clearly state the scientific question to set up the experiments knowing that each instrument has its own capabilities, advantages and limitations. Some characteristics and criteria have to be evaluated to choose an IM-MS instrument:

- IMS resolving power required to separate the compounds
- Need of the CCS values to help compound annotation
- The capability of the instrument in term of fragmentation and structural information (pseudo IMS³ or IMSⁿ)
- Choice of ionization source and sample introduction (coupling with chromatography) required for the analysis
- Choice of the mass analyzer which can be coupled to perform IM-MS analysis, its mass resolution and its capability in term of ion fragmentation and structural information

To get insight of the advantages and limitations to incorporate IMS in metabolomics and lipidomics workflows, it is a prerequisite to study how IMS can be integrated as an additional separation dimension and the challenges to resolve.

2.4. IM-MS approaches used in metabolomics

IMS has the ability to be easily combined with MS instruments currently used in metabolomics workflows. Thus, the approaches already used in MS-based metabolomics can be transposed with IMS as direct introduction IM-MS or front-end separation techniques coupled to IM-MS instruments. Thus, different protocols or procedures have been developed to integrate DTIMS, TWIMS or FAIMS in metabolomics or lipidomics workflows (Paglia et Astarita 2017; Amy Li, Hines, et Xu 2020).

2.4.1. Direct introduction

Direct introduction mass spectrometry (DI-MS) has been increasingly reported for metabolomics studies to enhance high-throughput analyses, supposing thousands of samples per day, compared to a maximum of one hundred for LC-MS workflows (Fuhrer et Zamboni 2015). In consequence, ultra-high resolution is generally necessary to avoid misinterpretation of ions. The main advantage is that DI permits direct analysis with minor sample preparation. It can also be performed using different ionization techniques, as previously mentioned in 2.3.1 section, ESI (Wen et al. 2022) and MALDI (Calabrese et al. 2023) being the mostly used. However, ion suppression effects can occur, mostly for ESI, which can induce low signal to noise ratio. Indeed, other drawbacks as strong matrix effects, and the fact that isobaric (in the case of low-resolution mass analyzer) or isomeric species cannot be distinguished in DI-MS have not been resolved. Thus, incorporating IMS dimension could address these issues because it allows the separation of metabolite ions according to their m/z and their mobility (Jackson et al. 2005; Leng et al. 2015; Delvaux et al. 2021). Flow injection analysis (FIA) approaches which imply injection of the sample into a mobile phase flowing (Artati et al. 2022) constitute a specific case of DI-MS which was associated with IM-MS configuration for the characterization of human milk oligosaccharides using TIMS (Delvaux et al. 2021), opioid profiling using DTIMS (Butler et Baker 2022) or analysis of Faba bean seeds by FIA-FAIMS-MS (H. Zhang et al. 2023). The direct infusion of lipid species, called 'shotgun lipidomics', widely used in various applications (Nikolaichuk et al. 2022; Foged, Maeda, et Bilgin 2023) was associated with DTIMS (Rose et al. 2021) or even SLIM technique (Wormwood Moser et al. 2021). Solid phase extraction (SPE) has also been coupled in line to IM-MS providing a methodology for the rapid screening of opioids in urine samples (Butler et Baker 2022) and for the quantitation of metabolites in biological fluids (X. Zhang et al. 2016).

An advantage of DI-IM-MS compared to DI-MS is the improvement of peak capacity which has been demonstrated by several studies. For example, a six-fold improvement has been reported for human blood analysis (Dwivedi, Schultz, et Jr 2010) or a five-fold increase in peak detection for lipid fingerprints by TWIMS-MS (Paglia et al. 2015). Another benefit of IMS is the possibility to correlate the ion mobility dimension with the m/z dimension, leading to ion mobility-mass correlation curves. These curves allow a separation of compounds classes. Lipids have been successfully separated from other compound classes such as peptides, oligosaccharides or carbohydrates (May et al. 2014). Metabolites from blood samples could be separated into different classes: amino acids, organic acids, fatty acids, prostaglandins, carbohydrates, purines, pyrimidines, etc (Dwivedi, Schultz, et Jr 2010). Sphingolipids and phospholipids could also be separated by plotting the CCS against m/z (Leaptrot et al. 2019). A combination of the CCS and the m/z values using different tolerance criteria have been performed for a shotgun lipidomic study of brain sample. Tolerances of 10 ppm for m/z and 2% for CCS values permitted the annotation of 34 lipid species in brain extracts. Applying a tolerance of 10 ppm without resorting to CCS values led in 21 false negative annotations. Even using a tolerance of 5 ppm for m/z , still without CCS values, 9 mismatches and 13 false negative annotation were found (Paglia et al. 2015). The CCS values allow to reduce the false-negative and false-positive in lipid annotation.

MALDI analyses or imaging, can also be considered. However, the matrix ions can be hard to distinguish from the analytes ones. Thus, ion mobility can help to separate the signals from analytes to the ones of background (Dwivedi et al. 2010; Jackson et al. 2005). Imaging has been increasingly used with the coupling of ion mobility particularly with the MALDI-TIMS technique (Neumann et al. 2020; B. Li et al. 2021; J. Chen et al. 2023). DESI source allows the direct metabolite analyses by imaging mass spectrometry without addition of any matrix (Ellis et al. 2019; Holm et al. 2022). Ion mobility is a

precious help for biological tissue imaging with the additional separation dimension allowing to improve the signal to noise ratio or specificity (Rivera et al. 2020).

Due to the complexity of the biological samples, and the strong matrix effects, the chromatographic dimension may still be required prior to the MS or IM-MS technique.

2.4.2. Chromatographic separation

Traditional workflows used in metabolomics involve chromatographic separation prior to mass spectrometry. Different front-end separation techniques can be coupled to IMS-MS, as liquid chromatography, gas chromatography, but also capillary electrophoresis or even microfluidics (Pičmanová et al. 2022; Tebani et al. 2016; Wellmann et al. 2022; Zheng, Wojcik, et al. 2017). As mentioned in the chapter I, liquid chromatography using either RPLC or HILIC phases is the mostly used method for metabolites and lipids separations.

Then, some studies showed that IMS provides experimental CCS values which are highly reproducible and do not suffer from matrix effects contrary to retention times (RT) (Paglia et al. 2014). Thus, CCS measurements are more reliable than RT and can add confidence in the metabolite annotation in LC-IM-MS analyses. Moreover, the CCS values may help the retention time alignment (C. A. Smith et al. 2006). For example, pigments have been identified using LC-UV-TWIMS-MS, and the authors showed that the addition of ion mobility allowed to increase the peak capacity to 15% and to resolve 5 co-eluting isobaric species (Pacini et al. 2015).

Multidimensional chromatographic separation could also be used in metabolomics. The comparison of LC×LC-MS and LC-IM-MS for the analysis of human plasma lipids has shown the advantages of both approaches. A higher number of features were detected using LC×LC-MS, but the LC-TIMS-MS approach offered a higher separation potential considering the analysis time, a better sensitivity (the 2D LC separation generates sample dilution), a high throughput investigation, structural information *via* the CCS values as additional molecular descriptors (Baglai et al. 2017).

Other separation techniques have been coupled to IM-MS and tend to be developed in the future. Gas chromatography (GC) has been recently coupled to IM-MS to analyze Pacific oyster (Lipin Chen et al. 2023) or to determine the botanical origin of honey samples (Arroyo-Manzanares et al. 2022). An orthogonal partial least squares-discriminant analysis (OPLS-DA) permitted to discriminate five different origins of honey samples. Capillary zone electrophoresis (CZE) principle is close to that of mobility spectrometry, regarding the separation of ionic species under the influence of an electric field. However, CZE is performed in a silica-fused capillary filled with an electrolyte solution whereas IMS operates in gas phase. CZE-IM-MS coupling permitted to analyze approximately 600 metabolites. The addition of IMS was particularly interesting for poorly ionized or neutral compounds as carbohydrate isomers (Drouin et al. 2021). Another coupling involved supercritical fluid chromatography (SFC) prior to IM-MS and was tested in 1987 (Rokushika, Hatano, et Hill 1987). The coupling SFC×IMS has been recently reported for the investigation of red chili pepper (Donato et al. 2018), lipid analysis of HepG2 cells (Meckelmann et al. 2022), structural annotation of glycerolipids (T. Xia et al. 2021) or for the study of radix curcumae (Ye, Dong, et Cao 2023).

2.4.3. Tandem ion mobility spectrometry (IMS/IMS)

Multiple ion mobility cells can be coupled before MS to enhance the separation. For example, FAIMS-DTIMS-MS was utilized for protein analysis and revealed high orthogonality of the two techniques

(Tang et al. 2005). As FAIMS acts as a filter, the sensitivity can be reduced, and ions losses can occur in the interface between FAIMS and DTIMS. Consequently, a μ FAIMS device was developed to enhance the sensitivity (Wilks et al. 2012). The evaluation of the coupling of μ FAIMS and DTIMS seemed promising (X. Zhang et al. 2015) even if technological improvements of the FAIMS device were required to get higher sensitivity and resolution (Zheng, Wojcik, et al. 2017).

The tandem ion mobility spectrometry as DTIMS-DTIMS or TIMS-TIMS (Koeniger et al. 2006; Merenbloom et al. 2008) were applied for bradykinin and tryptic peptides from human hemoglobin. The traditional LC-MS/MS workflow has been compared to an IMS-IMS-MS approach for protein analyses in human plasma samples. The IMS-IMS-MS workflow allowed high-throughput analyses, 70 sample acquisitions per day and 60-70 proteins per sample from a 4 min experiment (Valentine et al. 2009).

Tandem ion mobility spectrometry can be helpful for structural analysis, using a combination of IMS-IMS and MS/MS experiments (Ollivier et al. 2021) using pre or post-IMS fragmentation. IMS-IMS experiments were also conducted in a Cyclic-IMS device (Ujma et al. 2019; Ollivier et al. 2022). Tandem TIMS (tTIMS) or TIMS-TIMS was recently developed and constitutes a promising tool for various analyses, as protein analysis (F. C. Liu et al. 2018; F. C. Liu, Ridgeway, et al. 2022; F. C. Liu, Kirk, et al. 2022). The development of tandem ion mobility experiments experienced a growth of interest, with the availability of new instruments. New fragmentation techniques are expected to be associated with IMS instruments and new software tools need to be developed for easier multi-dimensional data analysis (Eldrid et Thalassinos 2020).

2.5. Data treatment and annotation using IMS

2.5.1. Data processing of LC-IMS-MS/MS data

Experimental data must be processed to extract the required and relevant information for metabolite annotation and sample analysis. Data processing contains different steps as the data alignment, peak picking and filtering commonly used for LC-MS data. Incorporating IMS to the traditional data processing workflow adds an orthogonal descriptor to the classical (m/z , RT and MS/MS) descriptors which leads to four-dimensional structural information. This additional dimension makes data processing more challenging.

Most of the data are processed using constructor softwares as Unifi (Waters Corporation) (Calabrese et al. 2022; Regueiro, Negreira, et Berntssen 2016) or Progenesis QI (Waters Corporation) (Paglia et Astarita 2017; Jariyasopit et al. 2022), or Metaboscape from Bruker Daltonics (Schroeder et al. 2020; Vasilopoulou et al. 2020; Rudt et al. 2023). Public tools have been developed, to handle IM-MS/MS data and LC-IM-MS/MS data. The first one was LC-IMS-MS Feature Finder which has been used in proteomics and metabolomics studies (Crowell et al. 2013; Delvaux, Rathahao-Paris, et Alves 2021). Different software tools have been reviewed recently for lipidomics studies (Ross et al. 2023). Skyline (MacLean et al. 2018; Kirkwood et al. 2022), MS-DIAL (Tsugawa et al. 2020a; 2020b), MZmine3 (Schmid et al. 2023) and DEIMos (Colby et al. 2022) are various tools which may cover the whole data processing workflow, from the feature extraction to compound annotation, depending on the tool. (Colby et al. 2022; Schmid et al. 2023) PNNL-PreProcessor allows to perform correction of the data before feature extraction (Bilbao et al. 2021). Some tools are specialized for one compound class, as for lipid analysis,

as LiPydomics (Ross et al. 2020), LipidIMMS (Lipid4DAnalyzer) (Z. Zhou et al. 2019; X. Chen, Zhou, et Zhu 2020).

Concerning the CCS calibration, AllCCS (Zhiwei Zhou et al. 2020) and DEIMos are able to perform CCS calibration whereas MS-DIAL and MZmine3 can only treat already calibrated data (Ross et al. 2023). A comparison of Skyline and MS-DIAL has been carried out and showed similar performances for DTIMS and TIMS published dataset (Ross et al. 2023). A significant influence of the variables from experimental measurements has been detected. Furthermore, the data treatment is dependent on the user because careful attention must be done to check the annotation manually, which is a time-consuming step but also essential.

2.5.2. Structural elucidation of compounds using IMS

As previously mentioned, ion mobility spectrometry can help the annotation in different ways, by providing CCS as a new descriptor and adding another dimension of separation which could help to eliminate the contaminants and visualize the low concentrated analytes. Moreover, IMS combined with MS/MS fragmentation proved to aid compound annotation, in particular for unknown metabolites or lipids which are not referenced in databases and for which no commercial or synthetic standard are available.

2.5.2.1. Post-IMS fragmentation

With IM-MS instruments, MS/MS experiments can be performed by collision induced dissociation (CID) in a collision cell (generally quadrupole or hexapole cell located between the IMS part and the mass analyser). Combining IMS and MS/MS experiments, the CID spectra can be improved *via* a clean-up of the data. Thus, clean MS/MS spectra can be obtained by removing background or contaminants signals. Then, as IMS can separate isobars or isomers species, specific MS/MS spectra are obtained for each isomeric compound which help the annotation of all the isomeric species (Harvey et al. 2015; Paglia et Astarita 2017).

MS/MS is essential and often decisive for metabolite annotation. Data-dependent acquisition (DDA) is widely used in metabolomics untargeted LC-MS workflows. However, DDA approach can present bottlenecks such as difficulties to sensitively detect and catch MS/MS spectra for all the metabolites in large samples and sometimes, MS/MS data is missing. This bottleneck can be explained by the fact that MS/MS is performed on selected most intense precursor ions and low abundant ions are not fragmented. Thus, data-independent acquisition (DIA) strategy has been proposed to obtain all fragment ions for all precursors simultaneously. The advantages are increased coverage of observable metabolites and reduction of false negatives. This also eliminates the need to accumulate additional DDA acquisitions to fragment all ions. However, DIA experiments could be complicated to interpret due to the high complexity of the data because each MS/MS spectrum comes from the fragmentation of many co-eluting compounds. To solve this issue, the DIA experiments can be performed after the IMS separation which allows the differentiation of each MS/MS spectrum, and thus obtaining cleaner MS/MS spectra. This can facilitate the identification of compounds and reduce the false positives (Pacini et al. 2015; Paglia et Astarita 2017). Depending on the manufacturers, DIA is also called all-ion fragmentation (AIF), MS^E or HDMS^E. Recent developments concerning DDA and DIA have been recently reported for lipidomics analyses (Valmori et al. 2023).

2.5.2.2. Pre-IMS fragmentation

Some IM-MS instruments present the possibility to fragment ions before the IMS separation. This approach has been used for lipid analyses, using concerted tandem and traveling wave ion mobility mass spectrometry (CTS analysis) (Hankin et al. 2016). CTS approach provides a 4D dataset which includes nominal precursor ion mass, product ion mobility, accurate mass of product ion, and ion abundance. The combination of diagnostic fragment ions with their CCS values is a powerful tool to help the annotation of lipids in a biological sample (Berry et al. 2017). Another similar approach has been used for annotation of saccharides, the shotgun ion mobility mass spectrometry sequencing SIMMS² where intact saccharides were analysed by IM-MS and CCS values of fragment ions were determined to help the identification (Miller et al. 2020). CCS values of fragment ion as fingerprint have been used also for carbohydrates (Hofmann et al. 2017) and particularly for glycan analyses (Hofmann et al. 2017; Harvey et al. 2018).

2.5.2.3. Pre + Post-IMS fragmentation

The combination of fragmentation before and after the IMS separation has been developed to enhance the structural information level to help the annotation. Time-aligned parallel (TAP) fragmentation has been used to improve the annotation of lipid species, particularly to identify constitutive fatty acyl chains of phosphatidylcholines and determine double bond position in unsaturated acyl chains (Castro-Perez et al. 2011). This approach allows to perform pseudo MS³ acquisitions, by fragmenting precursor ions in the first collision cell (before IMS cell), separating the resulting fragment ions in the IMS cell, allowing to align second generation fragment ions obtained in the second collision cell after IMS (Einarsdottir et al. 2017; Paglia et al. 2017). To improve chemical structure elucidation, a protocol combining experimental and computational workflows to acquire and use MS³ data was proposed. The database-assisted structure elucidation of metabolites in biofluids was achieved using MolFind² software (Samaraweera, Hill, et al. 2020).

2.5.2.4. PASEF

TIMS instrument has a particular configuration to perform MS/MS experiments combined and synchronized with IMS separation, called parallel accumulation - serial fragmentation (PASEF). In PASEF acquisition mode (Figure II-10.a), the first step is the acquisition of a full scan TIMS-MS experiment (MS¹) to determine m/z value and mobility of each precursor ion creating a precursor target list. Then, in a second step, all precursor ions are accumulated in parallel (ions of different mobility are trapped at different positions) and released sequentially in function of their ion mobility. The quadrupole is synchronized and is mass positioned on each precursor m/z switching from one to another (sub-millisecond switching time) allowing serial selection and fragmentation of multiple precursors in single 50 ms acquisition (3 ms for each precursor selected). Note that MS/MS spectra are acquired in the usual way: the precursor ions are fragmented in the collision cell with a collision gas and fragment ions are then analyzed by the TOF analyzer. The number of PASEF scans can be adapted to the sample and method (In Figure II-10.a, presenting 3 PASEF scans per cycle). The fragment ions are aligned with the precursor thanks to the IMS dimension, allowing to perform PASEF heat map. This procedure is repeated throughout the entire acquisition (Meier et al. 2015; Rudt et al. 2023). The PASEF mode allows to increase the sensitivity and selectivity, and the number of MS/MS per analysis. All these benefits help the annotation of more compounds into complex samples. The PASEF mode was used in a lipidomics study showing an improvement of human lipidome coverage of three to four-fold in

comparison to the traditional workflow with more than 180,000 MS/MS spectra in 30 minutes analysis (Vasilopoulou et al. 2020).

Other PASEF approaches have been developed recently to enhance the compound annotation step, as dia-PASEF or prm-PASEF. dia-PASEF does not use a MS¹ scan before fragmentation, but a low isolation window on the quadrupole using the mobility-*m/z* correlation. Mass-mobility windows have been scanned during a PASEF-cycle, thus each PASEF scan can provide several MS/MS spectra (Figure II-10.b). dia-PASEF compared to dda-PASEF leads to a higher fragmentation rate and precursor ions of low concentrated analytes could also be fragmented (Meier et al. 2020; Rudt et al. 2023). This method was already used in proteomics studies (Demichev et al. 2022; Skowronek et Meier 2022; Oliynyk et Meier 2023). In comparison, prm-PASEF can be used for targeted analysis by using a list of precursor ions, defined from previous dda-PASEF acquisition (Figure II-10.c). prm-PASEF provides higher selectivity and reproducibility and has been used in quantitation study (Lesur et Dittmar 2021; Brzhozovskiy et al. 2022). A peptides library from cerebrospinal fluid has been proposed to improve dia- and prm-PASEF studies (Mun et al. 2022).

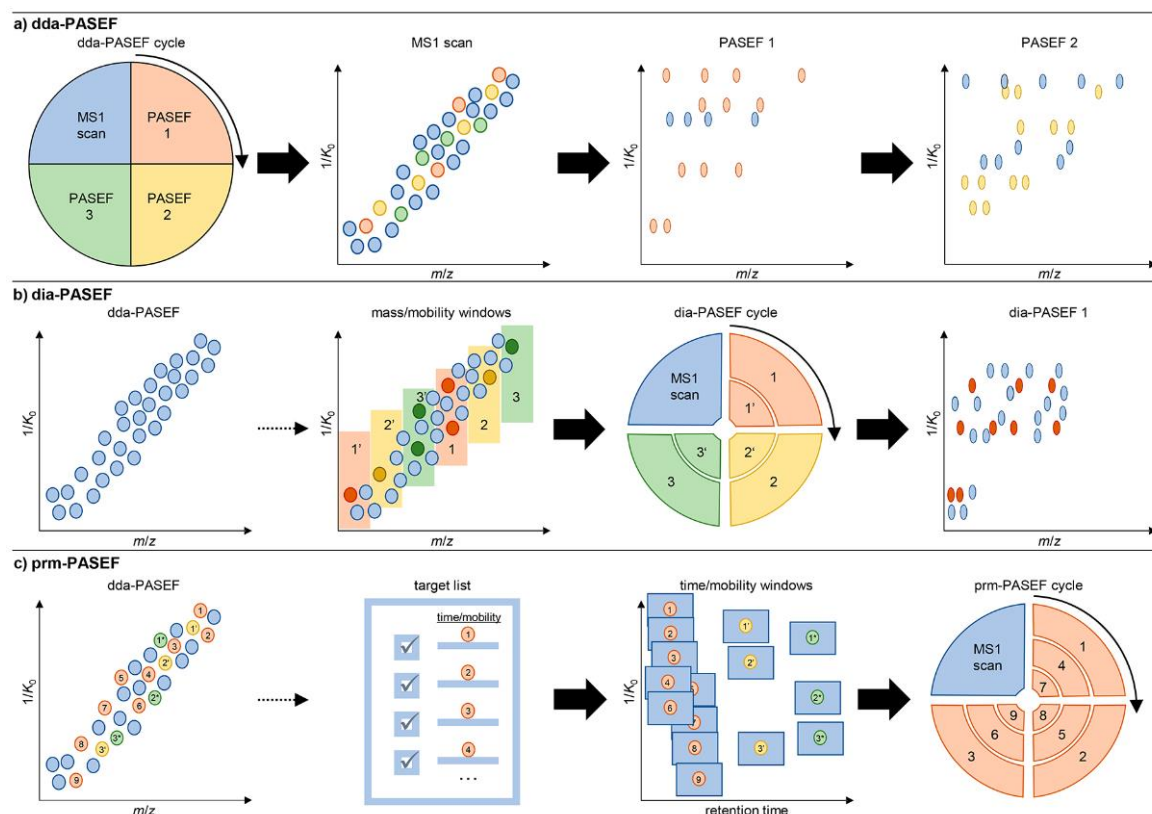


Figure II-10: Schematic representation of different approaches of PASEF. Unknown ions are shown in blue, analyte ions in red, yellow, and green, corresponding to the fragmentation experiment; from (Rudt et al. 2023).

All these three approaches proved to be helpful for lipidomics studies. The dda-PASEF seems to be better for lipid annotation for unknown compounds, than the dia-PASEF, which does not provide fragment-to-precursor assignment and presents a data treatment step complex and time-consuming. For known samples, the rm-PASEF is appropriate and provides better MS/MS spectra for low concentrated lipid species (Rudt et al. 2023).

Recently, other improvements of the PASEF approaches have been developed, as midiaPASEF with a integrating algorithm Snakemake-based MIDIAID (Distler et al. 2023) or speedy-PASEF, as a combination of DIA analysis with data analysis using DIA-NN tool (Szyrwiel et al. 2023).

2.5.2.5. Other acquisition strategies

A new acquisition strategy combining DIA with DTIMS, called drift tube ion mobility directed quadrupole all ions (IM-QRAI) has been developed (M. Feuerstein et al. 2021). This method allows the precursor ion isolation thanks to the drift time which minimizes spectral interferences in the complex DIA dataset.

Ozonolysis can also be used with ion mobility, to help lipid annotation by identifying the number and the position of the double bond(s) in the lipid structure. This was implemented in FAIMS instrument (Pham et al. 2013) for PC analyses and in DTIM-MS (B. L. J. Poed et al. 2018) as well as LC-DTIM-MS (Harris et al., 2018).

2.6. IMS as an additional separation dimension

Metabolites and lipids are spread into numerous classes with a consequent part of isobaric and isomeric species. As mass spectrometry alone cannot separate the isomeric species and not always the isobaric species, depending on the mass resolution, IMS offers an additional separation dimension in metabolomics or lipidomics workflow that can help isomer or isobar differentiation. This can concern regioisomers, cis/trans isomers, double bonds positions isomers or stereoisomers.

Mass Spectrometry Metabolite Library of Standards (MSMLS) was used to evaluate the usefulness of ion mobility as a separation method for isomeric species. 64% of the MSMLS metabolites could be annotated using a 40,000-mass resolving power TOF analyzer (Figure II-11). Enhancing mass resolving power using FTICR increased the percentage of covered metabolites up to 67%, but 33% remained impossible to differentiate, because they were isomeric species. Using low resolving power IMS instrument (70 CCS/ Δ CCS), additional 10% of metabolites can be resolved and with high-resolution IMS device this percentage may be much higher (Nichols et al. 2018).

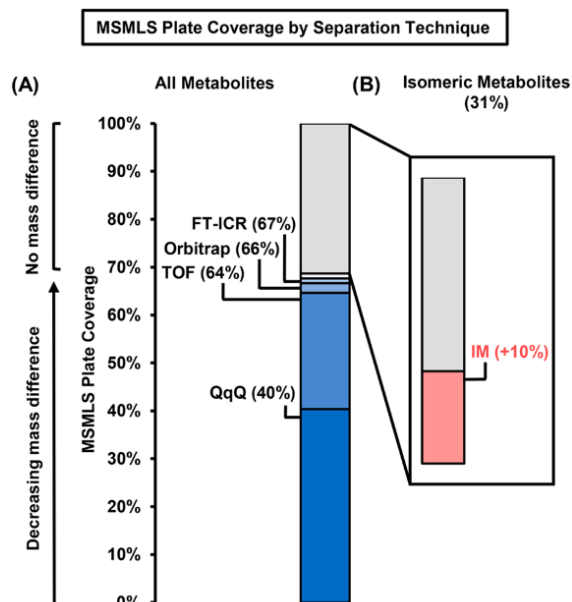


Figure II-11: Coverage of the Mass Spectrometry Metabolite Library of Standards (MSMLS) depending on the different analysis strategies employed; from (Nichols et al. 2018).

As shown *via* this example, IMS can provide an orthogonal separation dimension to MS which can help resolving the complexity of the metabolome.

2.6.1. Isomer separation by IM-MS

The differentiation of isomeric species in metabolomics and lipidomics is particularly important as differences in structure may lead to differences in physical, chemical or biological properties (Q. Wu et al. 2020). IM-MS-based separation has various applications for glycans (Manz et Pagel 2018; Johanna Hofmann et Pagel 2017), peptides, proteins, lipids or amino-acid isomeric species (Q. Wu et al. 2020). The separation of isomer species by IM-MS can require high IMS resolving power, if the differences of structures are particularly small. The ability to separate isomers depends on the category of isomers and on the instrument resolving power. With TWIMS instrument, α - and β -anomers have been successfully separated because they differ in the stereochemistry of the terminal glycosidic linkage ($\Delta\text{CCS} \approx 17 \text{ \AA}^2$) whereas trisaccharides which differ from the orientation of a hydroxyl group ($\Delta\text{CCS} \approx 1 \text{ \AA}^2$) were not separated (J. Hofmann et al. 2015). Some cis/trans isomer lipids have been successfully resolved by TWIMS and DTIMS, at least partially. But high-resolution IMS techniques allow a better separation, as with high resolution FAIMS or SLIM (Zheng, Smith, et Baker 2018). TIMS instrument allows also the separation of cis/trans and $\Delta 6$ - $\Delta 9$ phosphatidylcholine (PC), as shown by Figure II-12 (Jeanne Dit Fouque et al. 2019). Moreover, regioisomers of phosphatidylcholine have been separated with cyclic IMS experiments, after 30 passes (B. Poada et al. 2023). Another strategy involved cationisation with copper(II) and multimer formation with D-proline (Pro) as a chiral reference compound to separate enantiomers of aromatic amino acids which could be therefore differentiated by TWIM-MS (Domalain et al. 2014).

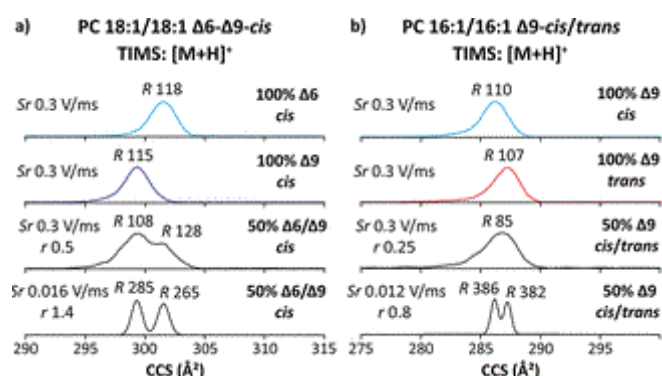


Figure II-12: TIMS spectra of isomer lipid species with cis in blue, trans in red and mixture in black according to the scan rate (Sr) used, adapted from (Jeanne Dit Fouque et al. 2019)

The Figure II-13 shows that acyl-chain isomers, regio-isomers, double-bond isomers and cis/trans isomers of PC are separated at high IMS resolving power. A very small shift can be observed between two isomer peaks for a resolving power of 50 corresponding to the TWIMS/DTIMS instruments whereas with a resolving power of 500, mostly all of the lipid isomers are fully separated except in the case of *sn*-position isomers that are only partially resolved (Tu et al. 2019). Even for MALDI imaging, lipid isomers can be partially separated using TIMS instrument showing the spatial distribution of both isomers (J. Chen et al. 2023).

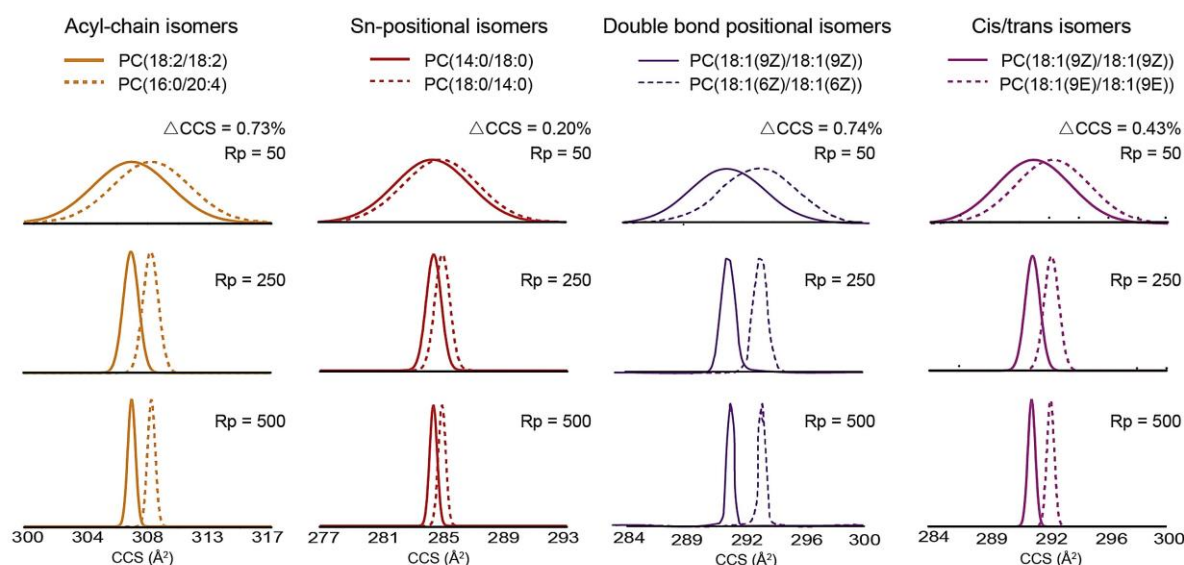


Figure II-13: IMS spectra of different isomer lipid species according to the IMS resolving power, adapted from (Tu et al. 2019)

As described in this part, some metabolite or lipid isomers can be separated by IM-MS. A tutorial has been made (Song et al. 2023) but improvement is needed to increase the resolving power and thus obtain a better separation of isomeric species. For that, different approaches could be used, as the optimization of experimental parameters, the use of different buffer gas, the derivatization or metal adduct formation (Paglia, Smith, et Astarita 2021).

2.6.2. Parameters influencing the IMS separation

2.6.2.1. Instrumental parameters

Instrumental parameters adjustments can increase the resolving power of the ion mobility technique leading to a better separation of compound isomers. For example, the voltage of the DTIMS cell or the length can be increased to enhance the resolving power (Odenkirk et Baker 2020). However, an increase of length can induce higher ion diffusion resulting in peak broadening, ion losses and reduction of sensitivity. Furthermore, an increase of the electric field could prevent the use of DTIMS in stepped-field mode because the low field limit is no more respected (Dodds et Baker 2019). In TWIMS instrument, buffer gas pressure, the voltage (height) and velocity of the waves can also be adjusted to enhance the ion separation (Campuzano et Giles 2019). The cyclic IMS and SLIM devices are based on the TWIMS principle and can allow a better ion separation due to the increase of the path length. However, ion losses can occur because of too high ion path. In TIMS instrument, the elution scan rate can be reduced and the ramp time extended to enhance the resolving power, however, the mobility detection range is reduced (Ridgeway et al. 2018; 2019).

2.6.2.2. Buffer gas adjustments

Nitrogen and helium, in a lesser extent, are common buffer gas in IMS studies. However, other buffer gas or some gas modifiers can be introduced into the IMS cell to enhance ion separations.

The influence of different buffer gas, such as helium (He), nitrogen (N₂), argon (Ar), carbon dioxide (CO₂), sulfur hexafluoride, or gas mixtures on the ion separation has been widely investigated (Asbury et Hill 2000; Bleiholder et al. 2015; Kurulugama et al. 2015; Morris et al. 2019). Changes on ion separation may depend on the buffer gas (Figure II-14, (Morris et al. 2019)), and on compound classes

(Delvaux, Rathahao-Paris, et Alves 2021). Depending on the buffer gas used in the IMS cell, separation evolves and even some inversions can occur (for maltohexaose and HFAP m/z 922, Figure II-14). Nitrogen and argon permit a better peak-to-peak resolution for low mass compounds, whereas higher resolution is observed in carbon dioxide for some pairs of ions as with maltose and HFAP m/z 322 (Figure II-14A and B). Nitrogen demonstrates high resolving power and peak capacity for a large range of compounds (Morris et al. 2019).

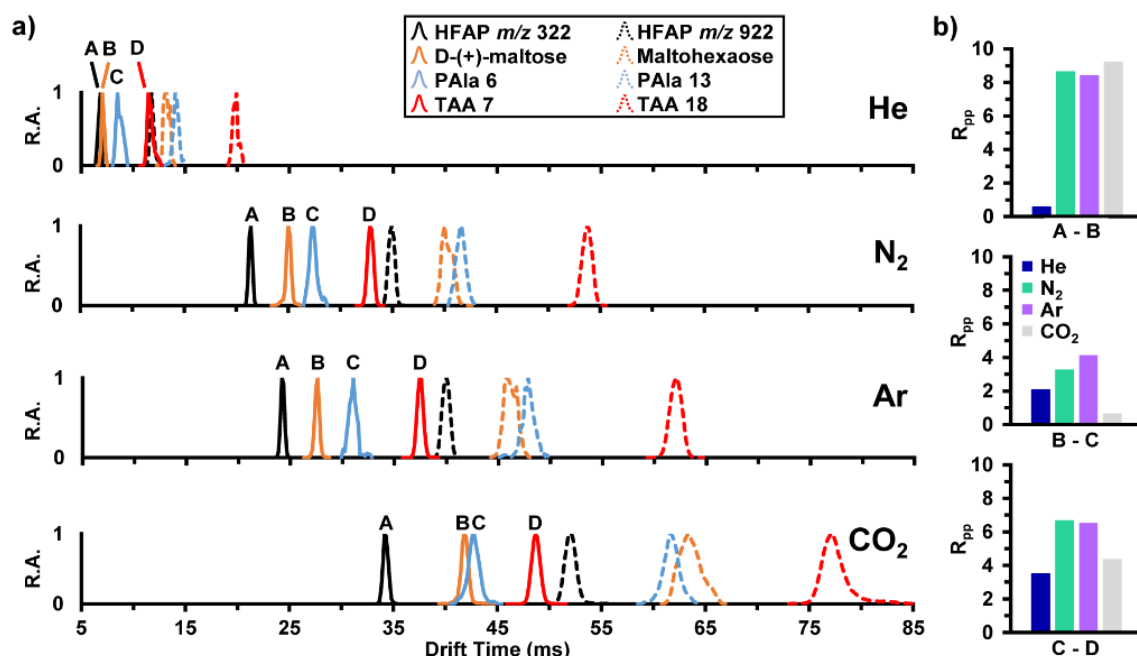


Figure II-14: Separation of some ions depending on the drift gas used (R.A.: relative abundance) and the peak-to-peak resolution R_{pp} representing for three couple of ions according to the gas, from (Morris et al. 2019).

Different gas modifiers or dopants can also be added in order to enhance the IMS separation. Chemical modifiers are often solvents, as methanol, ethanol, isopropanol, 1-butanol, acetonitrile or other, added into the IMS cell in small proportion (Waraksa et al. 2016; Šala et al. 2016; Fernández-Maestre, Wu, et Hill Jr. 2012; Fernandez-Maestre 2018; Kemperman, Chouinard, et Yost 2023). In addition to these clustering modifiers, some non-clustering modifiers (cyclohexane, hexane, or octane) can be used to form binary mixture to improve selectivity and resolution, as previously reported for DMS-MS study (Ruskic, Klont, et Hopfgartner 2021). Xylene isomers have been separated adding chemical modifiers in helium buffer gas in the FAIMS device (X. Du et al. 2022). Even chiral modifiers were investigated to allow a separation of enantiomers with IMS, as with S-(+)-2-butanol and R-(-)-2-butanol (Dwivedi et al. 2006).

2.6.2.3. Adducts formation and ion conformation

The addition of specific cations can influence the conformation of ions in the gas phase. The difference of CCS values depends on the ions and so of the cation which plays a role on the Δ CCS. That may help the isomer separation in IMS (Kemperman, Chouinard, et Yost 2023). The influence of various metal adducts (sodium, potassium, and silver) on flavonoid isomers separation has been studied. Depending on the metal cation, changes in CCS were observed and were explained by conformation evolutions. Silver adducts lead to more compact ions than sodium and potassium adducts, which allow the flavonoid isomers separation (Clowers et Hill Jr 2006). Metal cation addition has also been used to enhance the separation of glycans (Zheng, Zhang, et al. 2017), carbohydrates (Huang et Dodds 2015),

steroids (Rister, Martin, et Dodds 2019) or drugs (Zietek et al. 2018) isomers. Changes of the conformation of heparin-protein interaction have been studied thanks to the addition of sodium ion (Seo, Schenauer, et Leary 2011). The addition of alkali metal (lithium, potassium, rubidium and cesium) and alkaline earth metal (magnesium, calcium, strontium and barium) was studied to separate conformers of both 25-hydroxyvitamin D3 and its epimer. The ratio of open/closed conformers increased with the size of the cation (Chouinard et al. 2018).

Furthermore, measuring dimer ions instead of monomer species helps the separation of isomers in the IMS cell due to significant differences of their structures into the gas-phase. This phenomenon has been used for bile acids (Kemperman, Chouinard, et Yost 2023) and steroids (Rister et Dodds 2020).

Derivatization reagents have been used to enhance the separation and the characterization of compounds and particularly isomers. The use of derivatization of hydroxyl stereoisomers as testosterone/epitestosterone by 1,1-carbonyldiimidazole showed an increase of the IMS resolution which allows the separation of the steroid isomers (Velosa et al. 2022). Chiral amino acids have also been successfully separated thanks to an on-tissue derivatization followed by direct analysis of the tissue by MALDI-TIMS mass spectrometry imaging (Xie et al. 2022).

2.6.3. Mobility-mass correlation

The coupling of IMS and MS provides two descriptors, m/z and CCS values which can help the annotation of compounds. Furthermore, m/z and CCS (or CCS versus m/z) correlation curves can also help to differentiate compound classes. Peptides, carbohydrates, lipids exhibit three distinct curves in the 2D IM-MS space which allow their easy separation and provide help for annotation (Woods et al. 2004). Various classes of metabolites show also different correlation curves by plotting the arrival times versus m/z , as shown in Figure II-15.A (Dwivedi, Schultz, et Jr 2010). Separations of lipid categories, lipid classes or lipids in function of their acyl chain lengths were obtained by plotting predicted CCS values against m/z values (Figure II-15.B). For example, sphingolipids have CCS values higher than glycerophospholipids (Hines, Herron, et Xu 2017; Tu et al. 2019). The classes of glycerophospholipids can also be separated into sub-classes (Paglia et al. 2015).

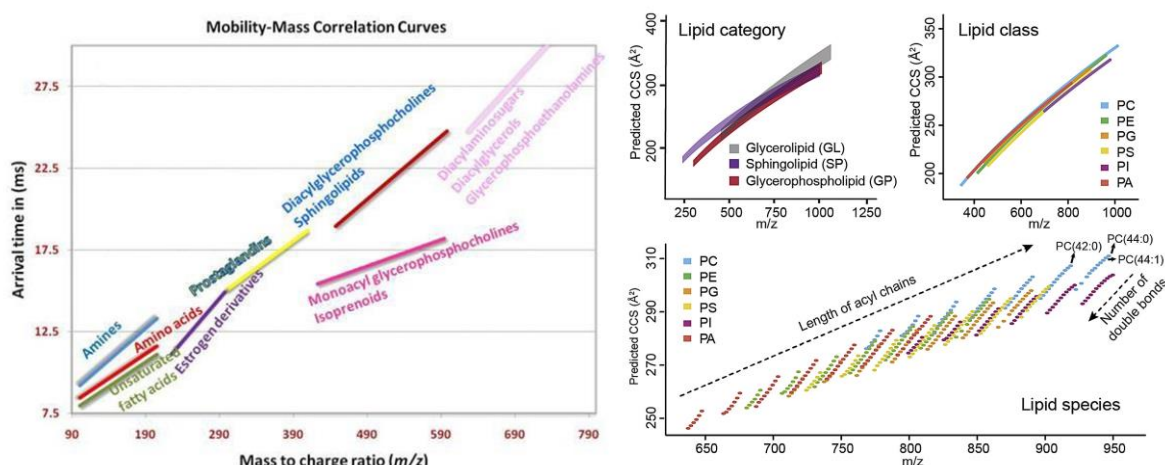


Figure II-15: Examples of mobility-mass correlation curves of various classes of metabolites from blood sample, in the left, adapted from (Dwivedi, Schultz, et Jr 2010) and different lipid classes, adapted from (Tu et al. 2019)

The differentiation of compound classes can go further, by separating contaminant classes, as shown in Figure II-16. These contaminants are classed into compounds of emerging concerns (CEC) and their detection is crucial in environmental and human matrices. The separation of these contaminants and their metabolites into the mobility-mass correlation curves enable a rapid annotation and could help the screening of different samples (Belova et al. 2021).

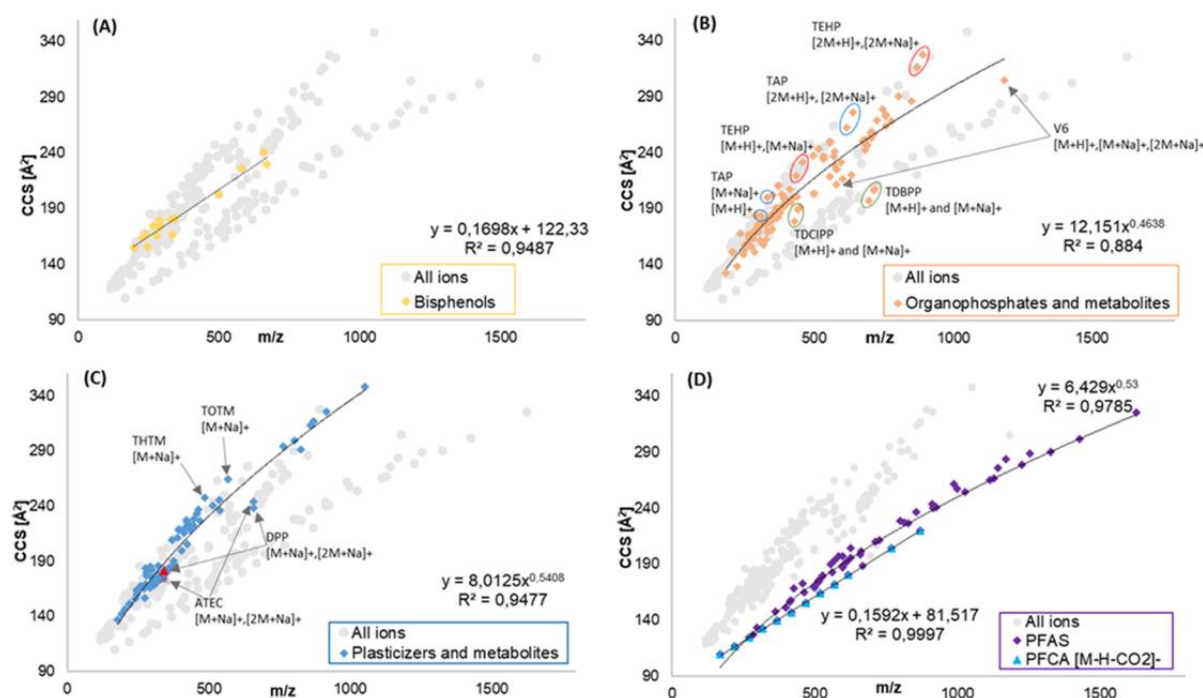


Figure II-16: Mobility-mass correlation curves showing four different compound classes of contaminants and their metabolites which can be present in biological fluids, adapted from (Belova et al. 2021).

Mobility-mass correlation curves allow also to separate ions according to their charge states, thus monomer, dimer, trimer or tetramer peptide ions could be distinctly differentiated (Gabelica 2021).

The correlation can be extended with other parameters, such as the retention time (RT), to perform 3D correlation plots (RT- m/z -CCS), allowing a better separation of compound classes and particularly lipid classes (Vasilopoulou et al. 2020).

2.7. Collision Cross Section as an additional descriptor

2.7.1. Definition of the CCS

The collision cross section is described as a measure of the size and shape (i.e. 3D structure) of an ion in a definite buffer gas (Gabelica 2021). Thus, CCS is a measure of the ion-gas pair, and it depends on the buffer gas which is ideally smaller than the ion. The first approximation that was made to understand the physics of the CCS values, was that the CCS reflected a hard-sphere, but this approximation could cause deviations and some theoretical works have been conducted to find a better understanding of the collision cross sections (Gabelica et Marklund 2018; Simón-Manso 2023). As real molecules are not perfect sphere, collisions can occur from all directions and the CCS is a measurement of the momentum transfer over all possible collisions. The CCS depends on the ion-neutral interaction potential but also on the temperature (Equation [3]). The CCS values decrease with

the temperature. Indeed, simulations have shown a relative CCS change of 0.13% per Kelvin, in nitrogen around 300 K, for fullerene ion C_{60}^+ (which presents with a unique conformation) (Gabelica et Marklund 2018). Thus, the CCS is more than just a “size” and physical considerations have to be taken into account. CCS is not an intrinsic property of an ion as it depends on the buffer gas and on the temperature (May, Morris, et McLean 2017)..

The collision cross sections can be determined experimentally using various IMS instrumentation, as DTIMS, TWIMS, c-IMS, SLIM, TIMS. However, CCS can also be computationally calculated from theoretical structures obtained either by molecular dynamics or by quantum chemistry and they can also be deduced from machine learning prediction leading to numerous available CCS databases, as it will be further described in detail.

2.7.2. Experimental CCS values

Experimental collision cross sections can be determined by two different methods. The primary method which is defined as “**a method having the highest metrological qualities, whose operation can be completely described and understood, for which a complete uncertainty statement can be written in terms of the SI, and whose results are, therefore, accepted without reference to a standard of the quantity being measured**” (BIPM, 1995; Quinn, 1997; Milton & Quinn, 2001; Taylor, Kipphardt, & De Bievre, 2001) corresponds to DTIMS stepped field method and do not require calibration step. The secondary methods cannot permit direct access to CCS with the first principles resorting to kinetic theory because the equations involved in secondary methods are more complex. The determination of CCS in these cases needs a calibration step using reference ions of known CCS (previously determined by the primary method). TWIMS, c-IMS, SLIM IMS, TIMS permit access to CCS as secondary methods.

Then, it is recommended to use the nomenclature of the compendium of collision cross section values which requires that the notation of CCS specify the instrument (superscript) and the buffer gas (subscript) used for CCS measurements. For instance, CCS values determined using DTIMS in helium are noted $^{DT}CCS_{He}$ while those determined in TWIMS with nitrogen are $^{TW}CCS_{N_2}$. The first are primary values obtained without calibration while the second are secondary values obtained after calibration.

2.3.2.1. DTIMS stepped field vs single-field CCS

DTIMS stepped-field method satisfies the primary method definition and CCS values can be directly deduced from measured ion mobility K using the Mason-Schamp equation (Equation [3]) which is a fundamental IM relationship derived from first principles of the kinetic theory of gases (Mason & Schamp, 1958 (Dodds et Baker 2019). In practical, ion mobility experiments are performed using different electric fields (usually five axial potentials). A linear regression (Equation [7]) derived from Equation [1] is obtained and allows the access to K from drift times t_d for each potential and then the determination of the CCS values. The stepped-field CCS values are primary values considered as the “gold reference” which constitute a major advantage of the DTIMS technology (Sarah M. Stow et al. 2017; Kartowikromo, Olajide, et Hamid 2023).

$$t_A = t_d + t_0 = \left(\frac{L^2}{K_0} \cdot \frac{T_0 p}{T p_0} \right) \cdot \frac{1}{\Delta V} + t_0 \quad [7]$$

where t_A is the arrival time, which is the sum of t_d plus a time t_0 spent outside the drift region.

However, accurate determination of the different instrumental or experimental parameters such as the effective length, the pressure, the temperature inside the tube remains difficult. Then, even if it is a prerequisite that these parameters do not change and stay strictly identical throughout the whole experiment, in practice, it remains difficult to implement. The electric field must be constant in all points of the cell but small fluctuations due to electronics functioning remain difficult to avoid. Furthermore, the stepped-field experiments may take a long time which is not compatible with chromatographic separations prior to IM-MS experiments, precluding the use of stepped-field method in LC-MS workflows (Sarah M. Stow et al. 2017; Kartowikromo, Olajide, et Hamid 2023). The determination of K or CCS values using this primary method requires ideal conditions (Gabelica et Marklund 2018).

Thus, to overcome these issues, an additional step of calibration with ions of known K_0 can be carried out (Gabelica 2021). Using DTIMS, calibrated CCS are obtained by the single-field method which includes a calibration step and measurements performed using a unique value of the electric field. The time-scale compatibility of the single-field method with chromatographic separation is another advantage of this approach (Dodds et Baker 2019).

The resulting calibrated CCS values, also called single-field CCS values, are determined using Equation [8] which derives from Equation [7] where β and t_{fix} are respectively the slope of the linear curve and the intercept (Kartowikromo, Olajide, et Hamid 2023)

$$t_A = t_{fix} + \beta_1 \cdot \gamma CCS + \beta_2 \cdot \gamma CCS = t_{fix} + \beta \cdot \gamma CCS \quad [8]$$

where $\gamma = [m_i / (m_i + m_{gas})]^{1/2} / z$ (to be calculated for each calibrant and analyte ion), and β_1 is a constant depending on the buffer gas and the ion transfer settings outside of the drift region, ($\beta_2 \cdot \gamma CCS$) is the true drift time (t_d), β_2 is a coefficient dependent on the experimental gas pressure, temperature, electric field, and geometry of the drift tube. The term β thus involves experimental conditions experienced by the ion (i.e., temperature, pressure, field strength).

The calibration needs to be performed using calibrants with well-known K_0 , measured by the primary (stepped-field) method. Calibrants and analytes have to be analyzed in identical IM-MS conditions to obtain the linear calibration curve (Equation [8]) (Kartowikromo, Olajide, et Hamid 2023).

2.3.2.2. TWIMS CCS determination

In TWIMS, the electric field is no more constant but variable and can be described by successive waves of potentials. Due to non-uniform electric field, the Mason-Schamp equation is no more applicable as in DTIMS, and the TWIMS device must be calibrated (Cumeras et al. 2015a). As previously described (Gabelica et al. 2019), different calibration curves can be used, as the power law (Paglia et Astarita 2017), the linearized version (Ruotolo et al. 2008), the polynomial curve (Bush, Campuzano, et Robinson 2012). The equation currently used is a modified version of the power law (Equation [4]), including the t_0 parameter to force the curve through zero (Equation [9]):

$$CCS' = A' (t_d' - t_0)^B \quad [9]$$

with CCS' and t_d' respectively, the corrected value of CCS by the charge and the reduced mass (Equation [10]) and corrected drift time by the m/z of the ion and the EDC delay (C) which depends on the instrument used (Equations [10] and [11]).

$$CCS' = \frac{CCS \sqrt{\mu}}{z} \quad \text{with} \quad \mu = \frac{M_{ion} \times M_{gas}}{M_{ion} + M_{gas}} = \frac{1}{\frac{1}{M_{gas}} + \frac{1}{M_{ion}}} \quad [10]$$

$$t_d' = t_d - \frac{c\sqrt{m/z}}{1000} \quad [11]$$

This equation is used by Waters in the Unifi software (Calabrese et al. 2020). Historically, the calibrant firstly used for TWIMS experiments was a mixture of alanine oligomers (polyalanine). Then, other calibrants have been employed including Major Mix, dextran, glycans, TAA,...

Besides, methods have been developed to determine the CCS values directly from the TWIMS drift times, modelled on the primary method concept. For that purpose, the theory of the TWIMS ion motion has been studied (Shvartsburg et Smith 2008; Richardson, Langridge, et Giles 2018). A computational tool was thus proposed to calculate the CCS values from TWIMS drift times without calibration, by using low wave velocities which could mimic similar behaviors than in DTIMS cell (Mortensen, Susa, et Williams 2017). A semi-empirical framework has been developed to understand the width of IMS peaks of some peptide ions according to different TWIMS parameters (Dixit et Ruotolo 2019). A new calibration function has been developed to enhance the traditional power law function, by solving ion motion equations in TWIMS cell and taking into account the velocity relaxation of ions (Richardson et al. 2021). A new software package IMScal has been also developed for this new calibration procedure. However, this calibration procedure is not yet currently used in metabolomics applications.

The calibration step, required for CCS determination using TWIMS, adds uncertainty on the resulting CCS values. Uncertainties on the CCS experimental determination has been evaluated for four proteins. The use of error propagation through the calibration could help to provide more robust CCS measurements (Edwards, Tran, et Gallagher 2021).

CCS can also be derived from cIMS measurements with one pass, as for linear TWIMS (Giles et al. 2019). The CCS determined for leucine encephalin, after polyalanine calibration, was in good agreement with ^{DT}CCS value (0.7% difference) (Giles et al. 2019). Different studies used the cIMS, to discover new perfluoroalkyl substances (MacNeil et al. 2022) or evaluate the enantiomeric composition (Cooper-Shepherd et al. 2022), both used the Major Mix as calibrant. Further improvements have to be brought to obtain more precise CCS values using HR cIMS through multiple passes experiments (Giles et al. 2019).

The CCS calibration is also possible with SLIM instrumentation. Three different calibrants, ESI-Low concentration Tuning mix, polyalanine and a SLIM calibrant based on eight compounds were tested to calibrate lipid and bile acid standards. The resulting ^{SLIM}CCS values are similar to ^{DT}CCS obtained with the stepped-field method within an accuracy of 1-2% (Ailin Li, Conant, et al. 2020). Another study evaluated the lipid calibration on SLIM device by comparing ESI-Low concentration Tuning Mix calibrant with lipid-based calibrants. The Tune Mix calibration resulted in systematic bias of 2-3%, whereas with lipid calibrant, the bias has been reduced to 0.5%. A correction strategy has been proposed based on the Tune Mix calibration, implementing a specific linear correction using a differentiation of the lipid subclasses, resulting on low bias (< 0.4%) (Rose et al. 2022).

2.3.2.3. TIMS CCS determination

The ^{TIMS}CCS values were determined from the $1/K_0$ values obtained from TIMS experiments, using the Mason-Schamp equation (Equation [3]). The K_0 values are calibrated using a linear fit. An empirical calibration function has been used, with a and b the constants and V_m the voltage measured when the ion exits the TIMS cell (Equation [12]).

$$K_0 = a + \frac{b}{V_m} \quad [12]$$

The constants depend on the TIMS parameters, due to the empirical nature of the calibration equation. Therefore, a calibration is required when a TIMS parameter is changed. Another calibration strategy has been described based on a Taylor expansion of instrument properties (Chai et al. 2018).

The ESI-Low concentration Tuning Mix (Tune Mix) is the mostly used calibrant for ^{TIMS}CCS determination (Schroeder et al. 2020; Di Poto et al. 2021).

2.7.3. Computational calculations of CCS values

Besides experimental CCS, calculated values can provide additional structural information. They are an alternative to access CCS of metabolites for which no experimental CCS is available because of the lack of authentic chemical standards. They can also permit to confirm annotation when calculated and experimental CCS are in agreement. The theoretical CCS values have been calculated by using simulations of the collision and interaction between gas molecule and the ion of known structure. While experimental CCS are derived from measurement of drift time or reduced mobility, calculated CCS values are derived from tridimensional theoretical structures of the gas phase ion (Sarah Markley Stow 2015).

These theoretical, or computationally modeled, structures, are obtained by molecular modelling achieved using either molecular dynamics or quantum chemistry (DFT). Then the cartesian coordinates of these modeled structures permit to calculate their collision cross sections using programs, such as MOBCAL or IMoS developed by Jarrold (Mesleh et al. 1996) and Larriba (Larriba et Hogan 2013), respectively. This Fortran program includes three different computational approaches, the projection approximation (PA), the exact hard sphere scattering (EHSS) and the trajectory method (TM). The simplest method is the projection approximation where the gas phase molecule is projected on a 2D surface (Figure II-17.a) thanks to a computer algorithm. The projection is repeated multiple times by changing the orientation of the molecule and the CCS value is obtained by averaging all the projections obtained (Paizs 2015). In this approach, the ion is considered as a superposition of atomic hard spheres. This method does not take into account the charge, long range interactions or the multiple collisions with the buffer gas. Even if this method is considered approximate, the CCS values obtained are almost similar to those obtained by experimental measurements using helium as buffer gas, and for large molecules. This can be explained by the totally elastic collisions between the gas phase ion in the drift tube and helium, an inert monoatomic gas. Molecular drift gases, like nitrogen, collide with the gas phase ion in a totally elastic manner, prolonging the drift time and increasing the experimental CCS values. As a result, in order to properly offer agreement with experimental observations, the drift gas must be taken into account while theoretically calculating CCS values (Sarah Markley Stow 2015; Paizs 2015; Turzo et al. 2023). Another method called projected superposition approximation (PSA) was derived from PA by adding the size and shape effects, using a shape factor, to predict protein CCS values (Figure II-17.b) (Bleiholder, Wyttenbach, et Bowers 2011; Bleiholder, Contreras, et Bowers 2013). The exact hard sphere scattering (Figure II-17.c) and the trajectory method (Figure II-17.d) use the measurements of scattering angles to determine the CCS. EHSS approach represents the atoms as

hard spheres whereas in TM approach, the atoms are represented by Lennard-Jones potentials (Campuzano et al. 2012). TM approach takes into account ion-molecule interactions, buffer gas polarizability and the charge of the ion. The last modified version of the trajectory method permits the CCS calculations with nitrogen as drift gas, by adjusting the Lennard-Jones parameters and constitutes the most complete version for CCS calculations. This method is adapted to CCS calculation of small molecules as metabolites but presents limitations for CCS calculations of larger molecules because of excessive time of calculation due to computational complexity.

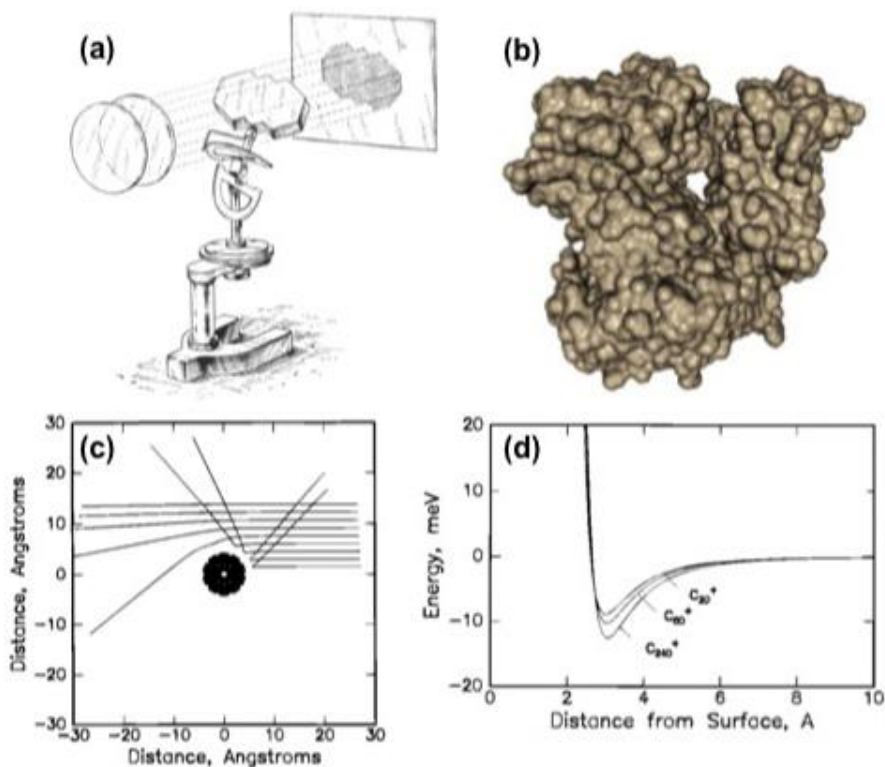


Figure II-17: Illustrations of four approaches used to determine theoretical CCS values. a: projection approximation, b: projection superposition approximation; c: Exact hard sphere scattering and d: trajectory method; adapted from (Sarah Markley Stow 2015).

Different calculation tools have been developed, historically, the first was MOBCAL. but other computational tools as IMoS (Larriba-Andaluz et al. 2015), collidoscope (Ewing et al. 2017) or ROSIE-PARS (Turzo et al. 2023) were then developed using different calculations methods and providing more user-friendly interfaces (Kartowikromo, Olajide, et Hamid 2023).

2.7.4. Machine learning CCS prediction

Machine learning (ML) based prediction models are recent approaches allowing the determination of predicted CCS values using different prediction algorithms. Typically, the model is constructed from an experimental training dataset, a set of molecular descriptors obtained from chemical structures using various programs, and a validation dataset. Two distinct methods have been used: regression models or support vector regression (SVR) models, which are selective and relatively accurate for specific class of compounds and artificial neural network (Kartowikromo, Olajide, et Hamid 2023). Various tools have been developed to predict the CCS values of metabolites and lipids, as MetCCS (Zhiwei Zhou, Xiong, et Zhu 2017), LipidCCS (Zhiwei Zhou et al. 2017), AllCCS (Zhiwei Zhou et al. 2020), CCSbase (Ross, Cho, et Xu 2020), dmCCS (Ross et al. 2022), Lipydomics (Ross et al. 2020), CCSondemand (Broeckling et al. 2021), CCSP2.0, DeepCCS (Plante et al. 2019), DarkChem (Colby et al. 2020), CCS Predictor 2.0 (Rainey

et al. 2022). Very recently, highly accurate machine learning algorithm (CCSP 2.0) enables CCS predictions which are better aligned with FAIR (Findable, Accessible, Interoperable, and Reusable) data principles.

Various comparative studies have been performed to evaluate *in silico* predicted CCS values against calculated and experimental values. For example, CCS prediction accuracy was tested comparing predicted values from ML CCSP2.0 with CCS values in the McLean CCS Compendium. Median relative errors of 1.25, 1.73, and 1.87% were respectively obtained for 170 [M – H]⁻, 155 [M + H]⁺, and 138 [M + Na]⁺ adducts. A comparison of a modified MOBCAL algorithm with three different machine learning (ML) algorithms showed that the three ML prediction models provide lower average errors (2.7-3.4% according to the model) against 4.6% using MOBCAL. The main advantages of ML models is the low computational cost with a result in few minutes (around 10 min) which is not achievable with theoretical calculations (Gonzales et al. 2016).

Some studies combined the prediction of the CCS values with prediction of retention times (Ross et al. 2020; Celma et al. 2022; Akhlaqi et al. 2023) which allowed to have more confidence in the annotation.

The prediction models are based on experimental dataset, essentially obtained with low resolving power instruments (principally DTIMS and TWIMS instruments) which in general do not allow to distinguish isomer species. Thus, the distinction between isomers or compounds exhibiting close CCS values is still difficult or even unachievable using ML predicted CCS (Kartowikromo, Olajide, et Hamid 2023). The standardization of the experimental CCS determination procedure may also help to increase the relevance and accuracy of *in silico* predicted CCS values (Paglia, Smith, et Astarita 2021).

Experimental, theoretically calculated and ML-based predicted CCS values can be gathered to construct CCS databases which know an important development since few years.

2.7.5. CCS databases

The CCS databases have been constructed using different sources of CCS data including experimental CCS values, but also computationally calculated or machine learning predicted CCS values (Figure II-18).

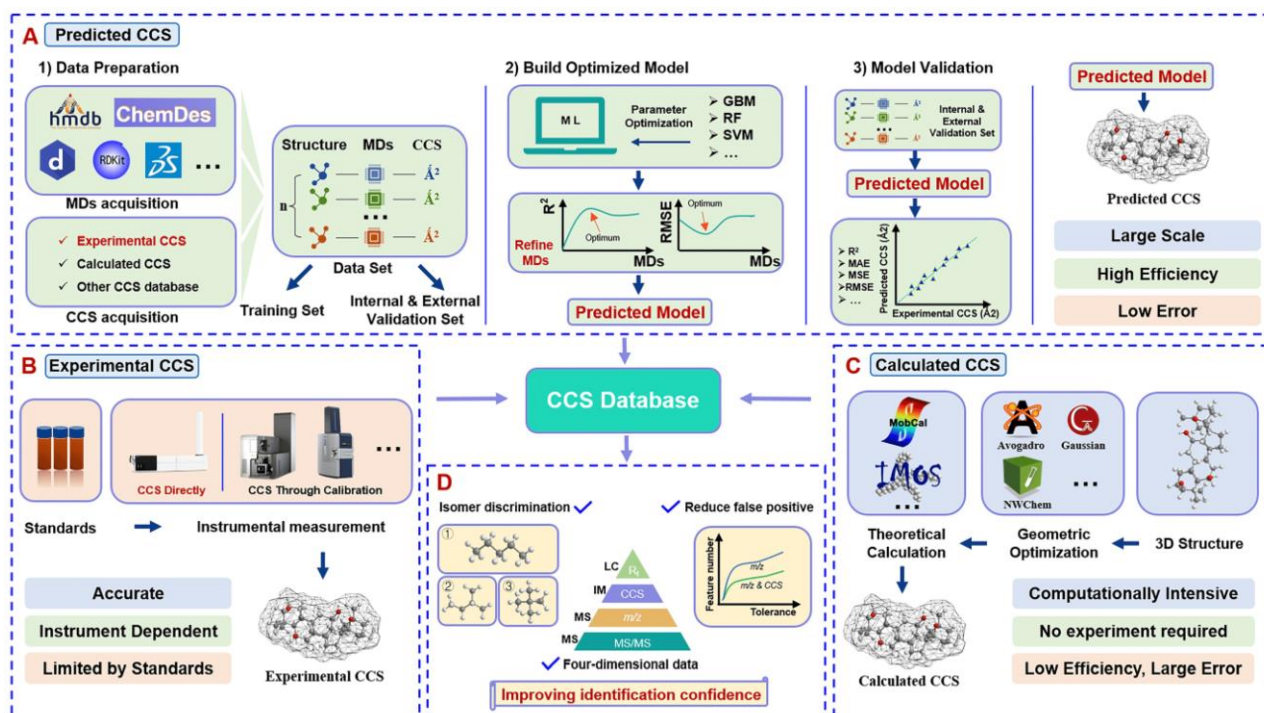


Figure II-18: Construction of CCS databases using A: machine learning prediction; B: experimental measurements; C: Theoretical calculations to obtain the advantages for component identification (D); from (X. Li et al. 2023)

In the last decade, numerous CCS databases compiling experimentally derived CCS of peptides, glycans, metabolites, lipids, drugs, xenobiotics and other small molecules have been reported and are available in web resources. Most of them concern metabolomics and lipidomics applications, gathering experimental CCS values from different technologies, mostly DTIMS and TWIMS, and more recently TIMS. A list of 33 experimental CCS databases is displayed in Table II-2. The CCS databases can be integrated in the data processing workflow to improve the confidence of the annotation adding an orthogonal molecular descriptor allowing the differentiation of isobars or isomers species and reducing the false positive.

Paglia et al showed that fixing cut-offs of 10 ppm for mass precision and of $\pm 2\%$ in CCS precision for database search criteria, allowed high confident identification of 34 brain-lipid species, with elimination of 21 mismatched lipid identifications (false positives). (Paglia, 2015)

Recently, more than a dozen databases of *in silico* predicted CCS have been reported and are also available as interactive resources and can be downloaded. The AllCCS database, referred as a CCS atlas, compile more than 5000 experimental CCS and about 12 million predicted CCS for more than 1.6 million of compounds. (Zhou et al 2020)

Gabelica et al mentioned that the evaluation of uncertainties concerning the CCS values published in databases is still not reported and constitutes an issue for CCS database use (Gabelica et al. 2019).

Table II-2: Some major experimental CCS databases of metabolites, lipid or other compounds

Compound type	Number of compounds	Number of CCS values	Instrument	IMS method (calibrant)	References
Metabolites	125	209 CCS: 96+/113-	TWIMS: Synapt G2 HDMS from 3 independent laboratories	Polyalanine	Paglia et al. (2014)
Metabolites and lipids	76	87	TWIMS: Synapt G2-S	polyalanine	Zhang (2015)
Metabolites	400	396+/400-	DTIMS: Agilent 6560	Tune Mix	Zhou et al. (2016)
Metabolites and xenobiotics	> 500	826	DTIMS: Agilent 6560 using nanoESI, APCI and APPI sources	Stepped-field method (length of tube=78.24cm)	Zheng, Aly, et al. (2017)
Metabolites, lipids, peptides and proteins	65	-	DTIMS: 4 different Agilent 6560	Stepped field and single field (Tune Mix)	Stow et al. (2017)
Metabolites	417	1246 CCS: 701+/545-	DTIMS: Agilent 6560	Stepped field and single field (Tune Mix)	Nichols et al. (2018)
Metabolites	510	942 CCS: 463+/479-	TWIMS: two Synapt G2 S and Synapt G2 Si versions	Major Mix	Nye et al. (2019)
Metabolites	1142	3833 (1216 single-field)	DTIMS	Stepped field and single field (13 reference standards)	Unified CCS compendium Picache et al. (2019)
Metabolites	2193	5119	DTIMS + TWIMS + In-silico prediction	14 datasets, 4 independent labs, and 2 instrument platforms	Zhou et al. (2020)
Peptides, carbohydrates, lipids, TAA	594	594 CCS+	DTIMS: Agilent 6560	Stepped-field method (TAA as internal mobility calibration)	May et al. (2014)
Lipids	130	-	DTIMS: Tofwerk IMS-TOF	Hadamard-type multiplexing method	Groessl et al. (2015)
13 lipid classes	244	244 CCS: 101+/143-	TWIMS: different Synapt G2 HDMS	Polyalanine	Paglia et al. (2015)
12 lipid classes	-	250 CCS: 165+/93-	UPLC-TWIMS: Synapt G2-Si	PE and PC lipids	Hines, Herron, et al. (2017)
Lipids	380	458 CCS: 329+/129-	DTIMS: Agilent 6560	Tune Mix	Zhou et al. (2017)
4 lipid classes	429	-	UPLC DTIMS analysis of bovine milk samples: Agilent 6560	Tune Mix	Blaženović et al. (2018)

Chapter II. Ion mobility for metabolomics

7 lipid classes	217	456 CCS	DTIMS: Agilent 6560	Tune Mix/TAA	Leaptrot et al. (2019)
Lipids	1856	1856	TIMS	Tune Mix	Vasilopoulou et al. (2020)
Lipids	87	142	4 TWIMS instruments: Synapt G2-S, G2-Si + 2 Vion	Major Mix	Hernández-Mesa et al. (2020)
Lipids	112	207	TWIMS: Synapt G2-Si	Major Mix	Jariyasopit et al. (2022)
Drugs	10	-	Modified Synapt HDMS Synapt G2 HDMS	Stepped-field method Drugs	Campuzano et al. (2012)
Glycans and oligosaccharides + fragments	-	900	DTIMS and TWIMS	-	Struwe, et al (2016)
N-glycans	500	500	Modified Synapt G1 HDMS Synapt G2-S HDMS	Stepped-field method Dextran	Hoffman et al. (2014)
pesticides	275	-	DTIMS: Agilent 6560	Tune Mix	Kurulugama et al. (2015)
Drug-like compounds and pesticides	~500	~500	DTIMS: Agilent 6560	Tune Mix	Stephan, Hippler, et al. (2016)
Drug or drug-like molecules	2000	1425 CCS+	TWIMS: Synapt G2-Si HDMS	Polyalanine and drugs	Hines, Ross, et al. (2017)
Xenobiotics	124	124	DTIMS: Agilent 6560 TWIMS: Vion IM-Q-TOF-MS	Stepped-field method Major Mix	Hinnenkamp et al. (2018)
Mycotoxins	37	~100	TWIMS: Synapt G2 HDMS	Polyalanine	Righetti (2018)
Steroids	300	1080 CCS	TWIMS: Synapt G2-S HDMS	Major Mix	Hernández-Mesa et al. (2018)
xenobiotics, pharmaceuticals	364	357 CCS+	UHPLC/TWIMS: VION IMS QTOF	Major Mix	Mollerup et al. (2018)
plant natural products	146	343 CCS –	UHPLC-TIMS-QTOF-MS TimsTOF Pro	Tune Mix	Schroeder et al. (2019)
Bile acid	47	400	DTIMS: Agilent 6560	Tune Mix	Poland et al. (2020)
Mycotoxins	53	225	TWIMS: 3 instruments (2 Vion + 1 Synapt G2-Si)	Major Mix	Righetti et al. (2020)
Doping agents	192	192	TWIMS: Vion	Major Mix	Plachka et al. (2021)

2.7.6. CCS contribution in metabolites annotation

To integrate the CCS values as molecular descriptors in metabolite annotation, and permit searches in databases, the values compiled in these databases must be reference CCS. As previously mentioned, CCS databases are constructed from experimental data, calculated CCS and *in silico* predictions. All these CCS values must be reliable to be used as reference. For this purpose, Zhou et al propose to assign confidence levels to the CCS values which compose their database that they called unified CCS values (Zhiwei Zhou et al. 2020). For each unified CCS value which is an average of experimental CCS values from different instrument platforms, and is specific to a compound and its ion, confidence level was assigned according to the following guidelines:

- **Level 1:** the unified CCS is calculated using experimental CCS records from ≥ 2 independent datasets in DTIM-MS instruments, and the maximum CCS difference is $\leq 1\%$
- **Level 2:** the unified CCS is calculated using experimental CCS records from ≥ 2 independent datasets in different commercial instruments (DTIM-MS, TWIM-MS, or TIMS-MS), and the maximum CCS difference is $\leq 3\%$
- **Level 3:** when unified CCS is only reported in one dataset from commercial instruments (DTIM-MS, TWIM-MS, or TIMS-MS)
- **Conflict:** when unified CCS is calculated using experimental CCS records from ≥ 2 independent datasets in different commercial instruments, but the maximum CCS difference is $>3\%$
- **Level 4:** predicted CCS values

This scoring method is provided on the AllCCS database on the website (<http://allccs.zhulab.cn/>). This allows to have a better idea of the confidence of the CCS value. However, only the AllCCS database uses this method. Moreover, computationally calculated CCS values have not been integrated in level definitions yet.

Integrating CCS values in the process of metabolite identification can increase the level of annotation described in metabolomics (see section I.5.1 for standardized identification levels) as CCS constitutes a third orthogonal information to retention time and accurate m/z (Delvaux et al. 2021). In this idea, a proposition of a scoring system has been developed including CCS, in addition to the traditional descriptors used in metabolomics, i.e. accurate m/z , isotopic ratio, MS/MS spectra (Figure II-19).

Untargeted Annotations by IMS-MS

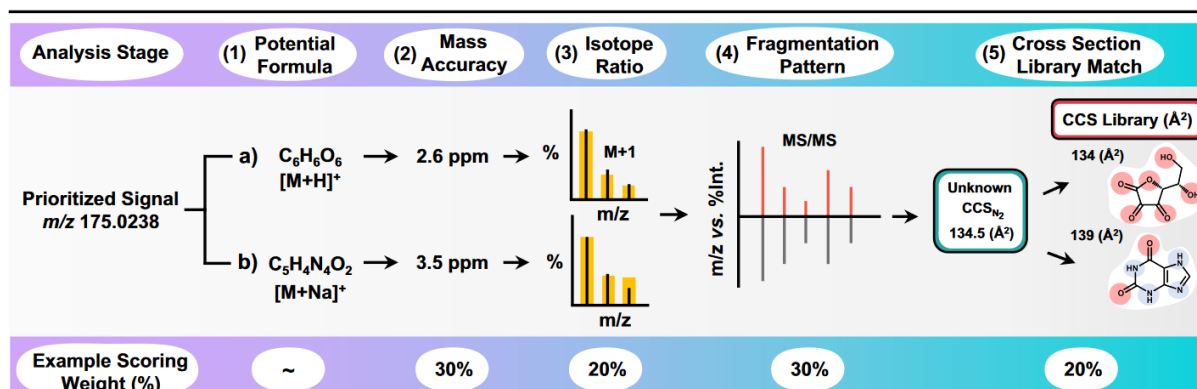


Figure II-19: Schematic representation of the workflow used for annotation of untargeted analysis by IMS-MS using scoring levels for each of the descriptor; from (Dodds et Baker 2019)

In this system, a 20% of scoring weight is attributed to the CCS library matching. Then, Hernández-Mesa et al proposed to refine and modulate this scoring weight taking into account the precision of

the library matching (associated to bias between CCS of unknown/candidate and CCS in library) (Hernández-Mesa et al. 2020). Thus, the following scoring weights were described:

- 20% for bias of $\pm 1\%$
- 10-15% if the bias is between 1 and 1.5%
- 5-10% if the bias is between 1.5 and 2%
- 0% if the candidate has a bias higher than 2%

This adjustment was proposed to address the problem of biases exceeding 2%, which could lead to false annotation (Hernández-Mesa et al. 2020). Thus, this first approach has to be improved and a consensus of the ion mobility community has to be reached concerning these scoring weights and the whole method.

Meanwhile, various studies have shown that CCS can constitute valuable additional descriptors which have demonstrated their potential to refine the number of possible candidates and reduce the number of false-positive annotations. The Figure II-20 shows three examples of metabolite annotation improvements using the CCS values (Zhiwei Zhou et al. 2020). Figure 45.a shows a rank improvement, *via* the example of 6-Hydroxycoumarin, with addition of CCS in multi-dimensional match approach (m/z + MS/MS + CCS). Figure II-20.b depicts candidates' reduction from 9 to 2 with the reduction of CCS match tolerance, using both CCS and m/z descriptors. This reduction tends to 1 when three descriptors (m/z , MS/MS and CCS) are considered. The candidate number decreases with the increase of descriptors (in particular when including CCS), as demonstrated in different biological samples (Figure II-20.c).

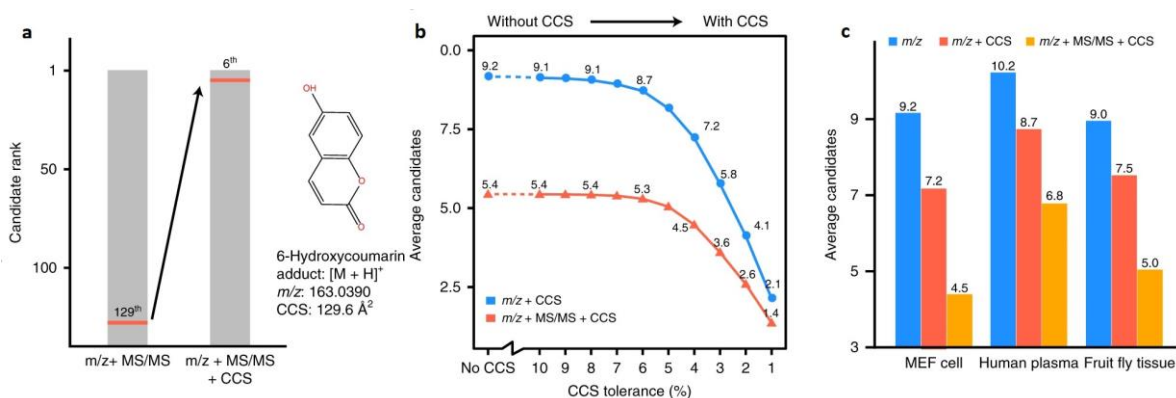


Figure II-20: Improvement of metabolite annotation using the CCS values. a: Example of rank improvement for 6-hydroxycoumarin, b: Reduction of the number of possible candidates according to the CCS tolerance applied, c: Average candidates using different samples and using different descriptors, adapted from (Zhiwei Zhou et al. 2020)

So, the addition of CCS values as a new descriptor for metabolomics annotation has proved to reduce the number of possible candidates. However, the resort of CCS values in annotation process, in particular for library searches, requires that they must be robust, reproducible and reliable. Furthermore, the CCS match tolerance has to be as low as possible to reduce the number of candidates (as shown in Figure II-20.b). Thus, uncertainties associated with experimental CCS values need to be carefully evaluated and the errors relative to the CCS determination reduced. Gabelica et al have reviewed and detailed uncertainties to consider for CCS determination (Gabelica et al. 2019).

2.8. Challenges to include IMS in Metabolomics workflows

Different challenges have to be solved to evaluate and reduce the different biases and errors that could occur in CCS determination. Two major points and their related issues have to be addressed, the mobility calibration and the evaluation of the precision (in repeatability and reproducibility conditions) of the CCS values.

2.8.1. CCS determination : calibration issues

To determine experimental CCS values, a step of calibration is required in almost all metabolomics studies as secondary methods are used, which is not a prerequisite for stepped-field CCS values. This step of the CCS determination process is crucial to obtain reliable CCS values. Some points have to be addressed such as the choice of the calibrant, evaluation of CCS deviations associated with the calibrant and the calibration mode, external or internal, for correct CCS estimation.

2.8.1.1. Evolution of the ion mobility calibration and related calibrants

At the early stage, ion mobility spectrometry was not coupled to mass spectrometry, and the applications were predominantly military or security. IMS calibrants or reference standards, containing either one, or several compounds (such as tetraalkylammonium halides), were used to detect positive or negative ions. However, the extend of applications, with for example bioanalytical science, highlighted the need of a consensus regarding the choice of reference calibrants to evaluate the IMS spectrometers performance (Kaur-Atwal et al. 2009). Tetraalkylammonium salts (TAA) have been re-used as IMS calibrants (Campuzano et al. 2012; J. Maillard et al. 2020) and as internal standards (Leaptrot et al. 2019).

Afterwards, IM-MS analyses were carried out on proteins and peptides using a peptide, the poly-*DL*-alanine to calibrate the TWIMS cell (Bush, Campuzano, et Robinson 2012). Using ESI source, appropriate for peptides and proteins, polyalanine presents the advantages to provide numerous and abundant ions in both positive and negative mode due to its polymeric nature and to the different possible charge states. In addition, poly-*DL*-alanine is commercially available and inexpensive. All these benefits are important properties for being a calibrant (Bush, Campuzano, et Robinson 2012). This calibrant has been massively used for calibration of TWIMS instrument for multiple applications, even in metabolomics and lipidomics (Paglia et al. 2014; 2015; Righetti et al. 2020). Polyalanine was also used as mass calibrant for MALDI technique because this peptide provides good signal in both positive and negative modes using classical matrices, as DHB and HCCA (Gruendling et al. 2016). Another polypeptide, polyglycine has been described as IMS calibrant (Knapman et al. 2010). Other calibrants have been developed, and commercial solutions, even in kits, were proposed. Mixtures of various compounds were also developed by instrument manufacturers for IMS calibration. Thus, the Major Mix IMS calibration kit contains polyalanine oligomers, small molecules (drugs) and ultramark[®] components and is provided by Waters corporation. This calibrant has been widely used in various applications, mostly in lipidomics and metabolomics (Nye et al. 2019; Hernández-Mesa et al. 2020). Drugs like compounds, present in the Major Mix IMS calibration kit, were described previously for IMS calibration (Campuzano et al. 2012). Another commercial mixture is the ESI low concentration Tuning Mix (Tune Mix, Agilent) solution which contains different hexakis(fluoroalkoxy)phosphazines and is commonly used for CCS calibration of DTIMS (single field mode). Tune Mix can also be used for mass calibration.

These two commercial mixtures allow CCS calibration in both positive and negative ions, Tune Mix solution offering a broader CCS range than the Major Mix kit.

To facilitate IMS calibration in proteomics studies, an artificial protein, which generates a collection of peptides under proteolysis, was designed to calibrate TWIMS cell using a single standard (Chawner et al. 2012). This standard, termed QCAL-IM, enables TMCCS determination of peptide ion, for charge states +1 to +3 and has also been used for glycopeptides CCS determination (Both et al. 2014). The same technology QconCAT has been used to provide a retention time standard, RePLiCal (Holman, McLean, et Eyers 2016).

N-glycans, from commercially available glycoproteins, have been measured using a modified Synapt HDMS instrument where the TWIM cell was replaced by an RF-confining drift tube allowing the determination of absolute CCS in helium and nitrogen. They were then used as calibrants for glycans and carbohydrates (Pagel et Harvey 2013; Gelb et al. 2014). Moreover, dextran, a carbohydrate polymer, was also evaluated and proved to be a good candidate for CCS calibration using TWIMS instrument. Dextran can be used as a reference substance in chromatography (for retention time) but also as mass and CCS calibrant (Johanna Hofmann et al. 2014). Dextran oligosaccharides could also be used as internal calibrant for LC-IM-MS analysis, which offers more flexibility than external calibration strategies, which can be a great advantage for modern IMS instruments as TIMS, cIMS or SLIM (Manz et al. 2022).

Lipids have also been suggested as calibrant for CCS determination in lipidomics (Hines et al. 2016).

A generalized calibration strategy using poly(ethylene) oxide has been proposed to reduce the CCS or K_0 errors due to calibration (Haler et al. 2017). Other polymers, polylactide and polyethylene glycol and dextran have also been suggested for calibration in positive ion mode (Duez et al. 2017). Polymers offer the opportunity to generate, in ESI, numerous ions covering a broad mass range and a large CCS window for different charge states, in a single sample.

Some particular efforts have been brought to find calibrants for the negative ionization mode. Forsythe et al. determined ^{DT}CCS of deprotonated molecules of polyalanine and polymalic acid, and then evaluated both polymers as TWIMS calibrants, in terms of accuracy and precision of the TMCCS values. They both showed similar results and appeared to be appropriate calibrants for TMCCS determination of negative ions. Absolute errors for TMCCS values were all less than $\pm 1.0\%$ in comparison to ^{DT}CCS values. (Forsythe et al. 2015)

Polymalic acid has been used for carbohydrate CCS determination (L. Li et al. 2018). Another calibrant using polyoxometalate has been proposed (Hupin et al. 2018).

Phosphoric acid cluster anions were used as reference compounds for TWIMS cell calibration in negative ion mode. This calibrant offers a wide CCS range as well as different charge states (from -1 to -3). Accuracy tests on ions derived from polyalanine, dextran, and the hexakis(fluoroalkoxy)phosphazine (m/z 622) evidenced a bias of 9–11 \AA^2 (between TMCCS_{N2} and previously published ^{DT}CCS_{N2}).

Some of the common calibrants employed for CCS determination are reported in Table II-3.

Table II-3: Information on some calibrants: m/z and CCS values in \AA^2 in both positive and negative mode, the reference publication, and the application areas

Calibrants	Positive mode		Negative mode		Reference publication	Application areas	Examples of used publications
	m/z	CCS (N_2)	m/z	CCS (N_2)			
Polyalanine (z=1)	232-1013	151-306	230-1011		Bush, Campuzano, et Robinson 2012	Lipidomics, Metabolomics	
Polyalanine (z=2)	400-933	296-470	398-931				
Polyalanine (z=3)	456-787	482-674	454-785				
Dextran (z=1)	365-1985	179-425	341-2004	174-430	Johanna Hofmann et al. 2014	Glycans, oligosaccharides, lipidomics	
Polyglycine	304-760	160-248	-	-	<u>Knapman et al. 2010</u>		
Tune Mix	118-2722	121-438	113-2834	109-432		Lipidomics, Metabolomics	
Major Mix	152-1921	130-373	150-1165	131-276		Metabolomics	
TAA	74-466	107-258	-	-		Lipidomics	
Drugs standards	122-609	125-254	-	-			
PEG	393-1537	116-325	-	-	(Duez et al. 2017)		
PEO	363-1111	175-343	-	-	(Haler et al. 2017)		
Polymalic acid	-	-	133-945	114-261	(Forsythe et al. 2015)		
Lipid standards	Depending of the reference publication					Lipidomics	
PE and PC	412-958	202-331	410-1016	199-331	(Hines et al. 2016)	Lipidomics	

2.8.1.2. Evaluation of the IMS calibrants

As the calibration step is critical for CCS determination, several studies have evaluated the different calibrants previously mentioned, in particular for TWIMS instruments. Phospholipids CCS have been determined using both phospholipids and peptides as calibrants, showing higher precision using phospholipids rather than peptides as the deviation was reduced from 7% (with peptide calibrants) to 0.5% (Ridenour et al. 2010). Carbohydrates and peptides calibrants have been evaluated for the CCS determination of both carbohydrates and peptides testing either the match of chemical class and charge state (Gelb et al. 2014). The use of peptides to calibrate carbohydrates or the inverse resulted in low bias of approximately 1%, which was within the inherent uncertainty of the TWIMS measurements. However, changing the charge state between calibrants and analytes resulted in larger errors, around 3.5%. The matching of the charge state is necessary whereas the matching of compound classes is not an absolute prerequisite in this example (Gelb et al. 2014).

Different calibrants have also been studied for phospholipid CCS determination. Polyalanine, TAA, Tune Mix and lipid standards composed of PE and PC have been compared by TWIMS-MS. Using the lipid calibrants, the majority of the ^{TW}CCS values of several classes of phospholipids were within 2% error of the CCS values measured by DTIM. The authors recommended the use of PCs for CCS calibration phospholipids in positive mode and the use of PEs for negative mode. Matched calibrants

present better results for the lipid CCS determination than polyalanine or other tested calibrants (Hines et al. 2016). Dextran calibration for lipid CCS led to a systematic shift with deviations up to 9% when comparing with literature CCS values. A correction has been proposed by plotting the literature ^{DT}CCS values against the experimental ^{TW}CCS values which allowed a reduction of the deviations to less than 2% and to determine new CCS values for cardiolipins (Deschamps et al. 2019). A comparison of polyalanine and major mix calibration to determine mycotoxins CCS values has shown an impact of the calibration on the CCS (Righetti et al. 2020).

A recent comparison of different calibration has been performed on three IMS instruments, using Agilent Tune Mix and Waters Major Mix as calibrants with new DTIMS CCS values and a new set of steroids calibrants to determine steroids CCS values. Major Mix calibrant shows the better results by comparing TWIMS CCS values with DTIMS and TIMS CCS values derived from a previous study with 95% of the CCS values within 1.29% of the DTIMS CCS and 1.12% of the TIMS CCS values. The Tune Mix shows a negative systematic bias of 1.8% compared to DTIMS and TIMS datasets. The steroids calibrant results in a positive bias of 0.5%, which is better than the Tune Mix calibrant, but class-specific calibrant do not demonstrate better results than commercial calibrant (M. L. Feuerstein, Hernández-Mesa, Valadbeigi, et al. 2022).

In these studies, the bias was calculated as the relative difference between new experimental data and reference values (CCS_{ref} , from literature for example) according to [Equation 13]:

$$\%CCS\ bias = \frac{CCS - CCS_{ref}}{CCS_{ref}} \times 100 [13]$$

Rose et al. specified that the CCS_{ref} should correspond to ^{DT}CCS values. Thus, the CCS bias defined as the relative difference between measured CCS (secondary methods) and reference ^{DT}CCS values (CCS_{ref}) could constitute a comparison metric which allows to evaluate the accuracy of the different calibration methods (Rose et al. 2022). The ^{DT}CCS values (CCS_{ref}) can be the standardized ^{DT}CCS values of the Unified CCS Compendium (Picache, 2019).

2.8.1.3. Importance of choosing the good calibrant

The calibrant must be chosen carefully using different criteria. The reference compounds must be primary standards which are not sensitive to sample manipulation and chemically stable to long-term storage with the possibility to be used with several solvents, ionization parameters and sources. They must be robust to the compound concentration, practical, inexpensive, easy to handle, with high purity and low toxicity (Kaur-Atwal et al. 2009; Gabelica et al. 2019). Since few years, the question of a unique primary standard compound has been stated.

Indeed, different calibrants have been proposed and utilized to determine the CCS values. To each calibrant corresponds a different reference system. That could induce some bias in the CCS determination. Thus, a consensus of the ion mobility community has to be obtained on a unique reference standard. (Gabelica et al. 2019; Paglia, Smith, et Astarita 2021).

Then, in 2019, Gabelica et al. reported that instead of the measurement principles or instrument design (as the use of different IMS technology), a large bias between approaches is directly attributed to the selection of the primary values for the calibrant ions. Thus, the importance of an agreement on the primary standards and calibrants to use the full potential of ion mobility spectrometry has been highlighted again (Gabelica et al. 2019)..

2.8.2. Evaluation of the experimental CCS values

Numerous publications reported the need to carefully evaluate experimental CCS in term of robustness, stability and consistency between laboratory and instruments. An accepted criteria for CCS database query of 2% has been accepted, as relative standard deviations for CCS values less than 2% have been reported (Paglia et al. 2015; Paglia et Astarita 2017).

2.8.2.1. Long-term robustness evaluation

It has been reported that CCS are reproducible in the long-term. The reproducibility of CCS values of steroids was evaluated and good inter-day repeatability was obtained with relative standard deviations lower than 0.9% for CCS measurements of 297 CCS across 4 months (Hernández-Mesa, Monteau, et al. 2019). Moreover, 95.7% of CCS values had a RSD within 1%, across 1.5 years (Hernández-Mesa et al. 2020).

2.8.2.2. Stability in different matrices and concentration

The stability of the CCS value has been evaluated in different biological matrices (plasma, urine, red blood cells and platelets) and at different analyte concentrations. These biological fluids or tissues have been tested on 94 different metabolites resulting in mean relative standard deviation less than 2% for 97% of the CCS values (Paglia et al. 2014).

Five food matrices (green tea powder, fresh garlic, leek, fresh herb chives and rye) have been chosen to evaluate the matrix effects on pesticides CCS values. Resulting TWIMS drift times and consequently the CCS values were not influenced by matrix and concentration (Gosciny et al. 2019). Similar conclusion was reported by comparing CCS determined using different lipid extracts, as from porcine brain, E. coli or yeast (Paglia et al. 2015).

2.8.2.3. Intra-laboratory and inter-laboratory evaluation

The intra-laboratory repeatability was evaluated by different studies. The measurements of CCS values have been demonstrated highly repeatable using TWIMS instruments, as reported in various studies (Hernández-Mesa et al. 2020; Paglia et al. 2015; Righetti et al. 2020). Paglia et al. analyzed lipid extracts from human brain using LC-TWIM-MS, and reported a mean intra-laboratory analytical precision RSD of about 0.2% for ^{TW}CCS values (Paglia et al. 2015). CCS measurements for 53 mycotoxins were compared using two Vion TWIMS Q-TOF MS (Waters) instruments and a Synapt G2-Si TWIMS Q-TOF MS (Waters) located in different laboratories: the average RDS on the ^{TW}CCS_{N₂} measurements, were 0.25% considering the two Vion instruments and 0.14% on the three instruments (Δ CCS < 2%) (Righetti et al. 2020). Interlaboratory repeatability of ^{TW}CCS measurements has also been reported for two versions of Synapt (G2-Si and G2-S) instruments in DI-IM-MS and LC-IM-MS approaches which provide comparable CCS values for 542 metabolites in rat urine within \pm 1% deviation for 270 (89.7%) of the metabolites (Nye et al. 2019). ^{TW}CCS_{N₂} of 87 steroids were cross-validated using four TWIMS instruments (two Vion TWIMS Q-TOF MS (Waters), a Synapt G2-S and a Synapt G2-Si) with RSD below 1.5% which permit to build a cross-laboratory ^{TW}CCS_{N₂} database (142 ions) (Righetti et al. 2020; Hernández-Mesa et al. 2020).

^{DT}CCS values of more than 120 ions has been reported and compared using four modified DTIM-MS Agilent instruments, demonstrating good interlaboratory reproducibility with RSD of 0.34% for stepped-field CCS values and of 0.54% for single-field CCS values (Stow et al. 2017).

2.8.2.4. Inter-instrumental evaluation

Inter-instrumental comparisons have also been reported by comparing DTIMS and TWIMS CCS values resulting in deviations lower than 2% for 56 contaminants of emerging concern (Belova et al. 2022) and lower than 1% for several classes of compounds (64 pesticides, 35 pharmaceuticals and 25 metabolites of pesticides) but deviations up to 6.2% have been observed (Hinnenkamp et al. 2018).

A comparison of three commercially available ion mobility techniques, DTIMS, TWIMS and TIMS have resulted in an excellent interlaboratory comparison for 95% of the steroids studied, with deviations of $\pm 1\%$ between ^{TIMS}CCS and ^{DT}CCS and of $\pm 2\%$ between ^{TW}CCS and ^{DT}CCS , but larger deviations up to 7% were reported for some compounds (M. L. Feuerstein, Hernández-Mesa, Kiehne, et al. 2022).

Harmonization of protocols to determine CCS values is crucial for the whole ion mobility community and particularly for metabolomics and lipidomics applications, because, for now, CCS databases are still dependent of the IMS technology used and the comparison of CCS measurements obtained from different technologies as DTIMS, TWIMS or TIMS remains an issue (Chai et al. 2018; Haler et al. 2017; Naylor et al. 2019)

2.9. Conclusions of chapter II

Ion mobility is becoming a new tool for metabolomics thanks to the development of new commercially available instruments combining IMS with MS-based instrumentation and software solutions. IMS provides a new dimension of separation which increases the peak capacity, improves the metabolites and lipid detection and annotation, and can help for isomers separations. Secondly, IMS can be used in complement with fragmentation techniques to improve the structural characterization of metabolites and lipids, with the potential to perform IMSⁿ, and to use the CCS of fragments as an information for annotation. Thirdly, IMS provides an additional descriptor for metabolomics annotation, the collision cross sections. With the high reproducibility of CCS values, CCS databases have been created to be used as a tool for metabolite annotation.

However, some improvements must be undertaken to benefit from the whole IM-MS possibilities in metabolomics workflows. The challenge is to have reproducible CCS values between instruments and techniques. For that purpose, harmonization of the procedures or protocols to determine CCS values has to be made, particularly, the choice of reference standards and calibrant for ion mobility. The sources of errors or deviations must be known and treated with careful attention.

Chapter III. Influence of experimental parameters on CCS determination

3.1. Introduction

Although it is well described that CCS is intrinsic to an ion in a defined buffer gas and does not depend on experimental parameters, unlike drift times and mobilities, it is worth checking the impact of these parameters on the determination of the CCS values, in particular for IMS devices positioned right after the ESI source. Indeed, it has been reported that FIA and ESI parameters had impact on the ion mobilities of small and aromatic compounds, a series of naphthalic anhydrides (Zhang et al. 2022). These parameters are related to LC flow-rate (for LC-MS or FIA-MS analyses), solvent composition, source conditions (nebulizer gas pressure, desolvation gas temperature and flow-rate), in particular in the case of ESI source which is generally employed in LC-MS metabolomics workflows, in addition to parameters associated to IMS conditions and designs. In this chapter, the influence of all these experimental parameters on the ion mobility and the consequence on the CCS determination using TIMS, DTIMS and TWIMS instruments are presented. Figure III-1 depicts the LC-IM-MS workflow we have implemented to evaluate experimental parameters using commercial standard of lipids prior to plasma lipids analyses. It independently involves the three IMS technologies, each coupled to a Q-TOF mass spectrometer. The purple surround highlights the focus of the chapter III.

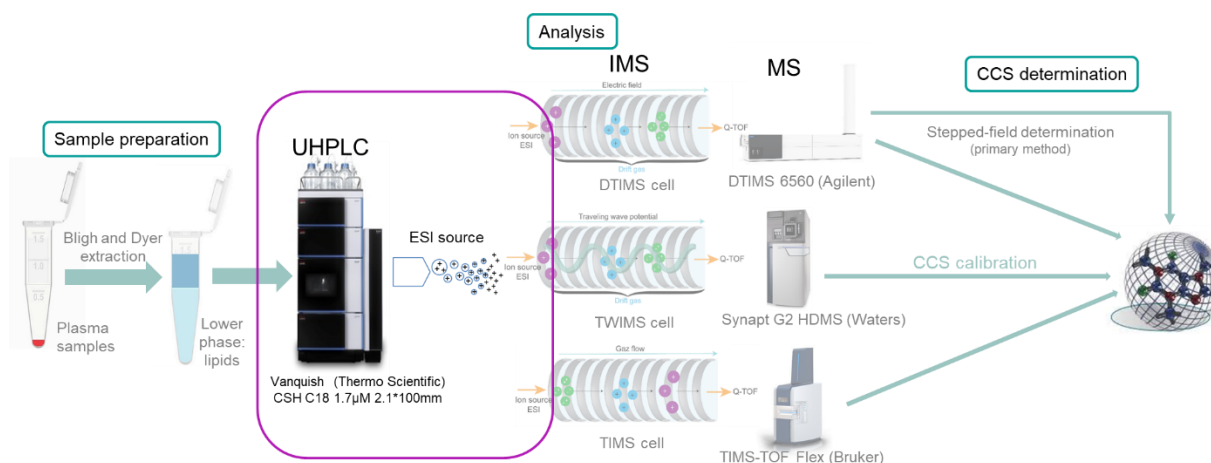


Figure III-1 : LC-IM-MS workflows implemented for lipid analyses involving three different IMS strategies: from sample preparation to acquisitions and data processing

First, ESI source parameters (flow-rate and temperature of the desolvation gas as well as nebulizer gas pressure) have been studied under infusion and LC conditions. We observed that, using ESI-TIMS-Q-TOF configuration, the source and infusion parameters have an influence on the reduced mobility of the ions, thus on the $1/K_0$ and, as a consequence, on the CCS determination. The influence of these source parameters has also been evaluated for DTIMS and TWIMS devices and is briefly discussed in this chapter. Then, the influence of the IMS conditions has also been investigated. In the case of TIMS instrument, three different sets of IM conditions have been compared. For DTIMS instrument, the

instrumental ion mobility parameters as well as multiplexing strategy have been evaluated. In the case of TWIMS instrument, comparison of wave height and velocity where some issues were highlighted.

3.2. Influence of experimental conditions on TIMS measurements

3.2.1. Influence of LC and source parameters on ^{TIMS}CCS determination (Article)

We first evaluated the influence of ESI source and flow injection analysis parameters on ion mobility measurements using a TIMS-TOF MS instrument and the consecutive impact on CCS determination. The results of this study are detailed in the article entitled “Impact of source conditions on collision cross sections determination by trapped ion mobility spectrometry”, submitted in the Journal of the American Society for Mass Spectrometry.

Impact of source conditions on collision cross section determination by trapped ion mobility spectrometry

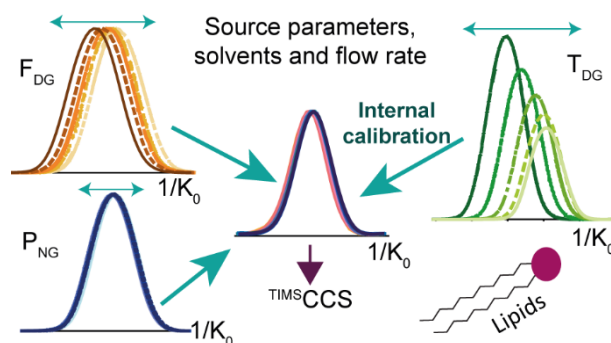
Anaïs C. George¹, Isabelle Schmitz¹, Benoit Colsch², Carlos Afonso¹, François Fenaille², Corinne Loutelier-Bourhis^{1*}

¹Univ Rouen Normandie, INSA Rouen Normandie, CNRS, Normandie Univ, COBRA UMR 6014, INC3M FR 3038, F-76000 Rouen, France

²Université Paris-Saclay, CEA, INRAE, Département Médicaments et Technologies pour la Santé (DMTS), MetaboHUB, F-91191 Gif sur Yvette, France.

3.2.1.1. Abstract

Collision cross section (CCS) values determined in ion mobility-mass spectrometry (IM-MS) are increasingly employed as additional descriptors in metabolomics studies. CCS values must therefore be reproducible, and the causes of deviations must be carefully known and controlled. Here, we analyzed lipid standards by trapped ion mobility spectrometry-mass spectrometry (TIMS-MS) to evaluate the effects of solvent and flow rate in flow injection analysis (FIA), as well as electrospray source parameters including nebulizer gas pressure, drying gas flow rate, and temperature, on the ion mobility and CCS values. The stability of ion mobility experiments was studied over ten hours, which established the need for a delay-time of twenty minutes to stabilize source parameters (mostly pressure and temperature). Modifications of electrospray source parameters induced shifts of ion mobility peaks, and even the occurrence of an additional peak in the ion mobility spectra. This behaviour could be essentially explained by ion-solvent cluster formation. Changes in source parameters were also found to impact CCS value measurements, inducing deviations up to 0.8%. However, internal calibration with the Tune Mix calibrant reduced CCS deviations to 0.1%. Thus, optimization of source parameters is essential to achieve a good desolvation of lipid ions and avoid misinterpretation of peaks in ion mobility spectra due to solvent effects. This work highlights the importance of internal calibration to ensure interoperable CCS values, usable in metabolomics annotation.

**Keywords:**

- Lipids
- Solvent-ion cluster
- Collision cross section
- Ion mobility - mass spectrometry
- Trapped ion mobility spectrometry

3.2.1.2. Introduction

In the last few decades, ion mobility spectrometry (IMS) has been increasingly adopted by the metabolomics community as a powerful tool that can be implemented in traditional liquid chromatography-mass spectrometry (LC-MS) workflows.^{1,2} IMS allows gas phase separation of ions thanks to an electric field in a tube filled with a buffer gas such as helium or nitrogen. The ions are separated according to their size, shape, and charge. IMS provides an additional separation dimension, which increases the peak capacity. IMS affords also information on the three-dimensional structure of ions through their collision cross sections (CCS), which constitutes a useful molecular descriptor for annotation in metabolomics and lipidomics studies.³ The CCS reduces false positive rate in metabolite annotation and yields high-confidence annotation for metabolites using CCS listed in databases.^{4,5} Publicly available CCS databases (e.g. AllCCS⁴ and MetCCS⁶ for metabolites, LipidCCS⁷ for lipids) compile both experimental and predicted values. In order to use CCS values as a descriptor, the measurement precisions should be better than 2% or even 1%, as determined by a consensus from several reported studies with a reproducibility precision within 1% and 2%.⁸⁻¹⁰ To reach this goal, the determination of CCS values needs to be well-controlled. Experimental CCS values can be determined with different instruments, such as drift tube IMS (DTIMS)^{11,12}, travelling wave IMS (TWIMS)^{13,14} or trapped IMS (TIMS)^{15,16}. Most of the IMS cells need to be calibrated, using reference compounds of known CCS values previously determined by DTIMS in stepped-field mode (primary method)¹⁷. This calibration step and the choice of the reference compounds are particularly important as deviations up to 20% can be observed depending on the calibrant used¹⁸. Such deviations can preclude the use of CCS as a descriptor for the annotation¹⁷.

CCS deviations may also be due to changes in solvents or in instrumental parameters.^{19,20} Zhang et al.¹⁹ studied isomers of naphthalic anhydride by electrospray ionization (ESI) coupled to TIMS-MS and showed that solvents, infusion flow-rate, nebulizer gas pressure and drying gas rate change the ion mobility measurements because of ion-solvent cluster formation that enlarges ion mobility peaks, increases CCS, or causes the appearance of other peaks. Solvent clusters can be both an advantage because they can help the mobility separation (separation of amino acids became possible with addition of alcohol modifiers)²¹ and a drawback because CCS determination remains uncertain if partially solvated ions are taken into account in the ion mobility measurement. Particular attention

should be paid to this point since the use of CCS as molecular descriptors for metabolite annotation requires CCS measurements on completely desolvated ions. For the TIMS-MS instrument, this mention is particularly justified as the trapped ion mobility cell is located just after the ESI ion source in metabolomics LC-MS workflows. Thus, in this study, we aimed to evaluate the impact of ESI parameters, such as nebulizer gas pressure, drying gas temperature and flow rate as well as LC parameters as solvents and infusion flow rate on the ion mobility measurement and CCS determination of a series of lipid ions. We aim to complete the previous study on naphthalic anhydride analogues¹⁶ which present small and rigid organic structures, differing from lipids, which exhibit apolar, long and flexible acyl chains. Therefore, the behavior of both classes of compounds can drastically differ in the ESI source and in the TIMS cell. This work also highlights the importance of internal calibration.

3.2.1.3. Experimental section

Chemical and reagents.

Methanol (MeOH), chloroform, acetonitrile (ACN), isopropanol and formic acid (FA) were purchased from Fischer Scientific (UK, Loughborough), and ammonium formate from Sigma-Aldrich (Saint Quentin Fallavier, France). Except for HPLC-grade chloroform, all solvents and buffers used were LC-MS grade. Seven standard lipids were purchased from Avanti Polar Lipids (AL, USA): phosphatidylethanolamine (PE), lysophosphatidylethanolamine (LPE), phosphatidylcholine (PC) and lysophosphatidylcholine (LPC): PE 6:0/6:0, PE 10:0/10:0, PE 15:0/15:0, PC 16:0/16:0, LPC 16:0, LPE 16:0, PE 18:1/18:1 Δ^9 cis, as well as standard lipids from the Differential Ion Mobility System Suitability LIPIDOMIX kit (DIMS kit) which contains ceramide (Cer), sphingomyelin (SM), triacylglycerols (TG): Cer 18:1;O2/18:1, SM 18:1;O2/18:1, TG 18:1/18:1/18:1. Tune Mix solution containing six hexakis(fluoroalkoxy)phosphazines (ESI-low concentration tuning mix, G1969-85000) was purchased from Agilent Technologies and was used as received.

Sample preparation.

Standard lipids were dissolved in chloroform/methanol (50/50, v/v) to yield 10 mM stock solutions which were then mixed to obtain a pooled solution at 1mM. This solution was mixed with the DIMS kit solution at 1 mg/mL (50/50, v/v) and diluted in MeOH/isopropanol/H₂O (65/35/5, v/v/v) to obtain a 20 μ M final solution for standard lipids and 20 μ g/mL for the DTIMS kit.

IMS-MS analyses: calibration and acquisition conditions.

The TIMS-MS experiments were performed using a TIMS TOF Flex (Bruker Daltonics, Bremen, Germany) equipped with an electrospray source (Apollo II) and a transfer cartridge SRIG MALDI 2. The samples were injected in flow injection analysis (FIA) using an UHPLC system (Vanquish, Thermo Scientific, San Jose, CA, USA), coupled to the mass spectrometer. The LC system was monitored by Bruker Compass Hystar 6.2.1.13 and the instrument by TIMSControl 4.1.8. FIA experiments were performed at a flow rate of 0.4 mL/min, using a 75 μ m \times 550mm nanocapillary (ThermoFischer Scientific) located in the oven compartment set a 25°C. The sampler was set at 10°C. The injected volumes were 1 μ L in positive mode and 2 μ L in negative mode (except for stability analyses where 1 μ L was injected). Mass spectra were recorded over m/z 50-1600 in positive mode and m/z 50-1650 in negative mode. The IMS parameters were adjusted to detect all lipid species, within a large ion mobility range corresponding to inverse of reduced mobilities ($1/K_0$) from 0.55 to 1.90 V.s/cm². The ramp time was 100 ms, and the ramp rate 9.42 Hz. Then, the method with the adjusted parameters was applied on the instrument at least 30 minutes before calibration and analysis. External mass calibration was performed with a sodium formate solution composed of 10% FA/0.1 M NaOH/ACN (1/1/8), in HPC

(High precision calibration) mode. External mobility calibration proceeded in two steps. First, in positive mode, the voltage of the m/z 622 ion of the tune mix was adjusted at 132 V by modifying the nitrogen pressure, to ensure that all ions were within the mobility range. Then, the calibration step was performed using all the ions of the calibrant (Tune mix) *via* a linear function. For all analyses, a push of Tune Mix at the end of the FIA run was carried out, using a 6-way valve, with a flow rate of 150 $\mu\text{L}/\text{min}$ in positive mode and 50 $\mu\text{L}\cdot\text{min}^{-1}$ in negative mode, to ensure internal mobility calibration in the acquisition.

Different ion source parameters were tested, in both positive and negative ion modes, such as nebulizer gas pressure (P_{NG} : 0.5-5 bar), drying gas temperature (T_{DG} :150-350 °C) and drying gas flow rate (F_{DG} : 4-12 L/min). One of these three parameters was tested independently while the two others were set at recommended values for a FIA flow rate of 0.4 mL/min. Optimal parameters, recommended for a FIA flow rate of 0.4 mL/min using this ESI source, were 2.7 bar for the nebulizer gas pressure (P_{NGop}), 250 °C for the drying gas temperature (T_{DGop}) and 8 L/min, for the flow rate (F_{DGop}). FIA analyses were performed in triplicate for each set of parameters and a twenty minute delay before each triplicate acquisition was set to wait for the instrument stabilization.

Four solvent mixtures were tested, A consisted of acetonitrile/aqueous ammonium formate (10 mM) (40/60, v/v); B of isopropanol/acetonitrile/aqueous ammonium formate (10 mM) (88/8/4, v/v/v); 0.1% formic acid (FA) was added to both A and B mixtures, acetonitrile/water (50/50, v/v) and isopropanol/water (90/10, v/v). In addition, using ACN/H₂O (50/50, v/v), different FIA flow rates were tested (0.1-0.5 mL/min), using either optimal source parameters ($P_{\text{NGop}} = 2.7$ bar, $T_{\text{DGop}} = 250$ °C and $F_{\text{DGop}} = 8$ L/min, defined for a FIA flow rate of 0.4 mL/min) or poor desolvation parameters ($P_{\text{NG}} = 0.5$ bar, $T_{\text{DG}} = 150$ °C and $F_{\text{DG}} = 4$ L/min).

Stability analyses were performed by injection of the solution of standard lipids, every three minutes during forty-five minute runs and then every hour for ten hours, in triplicate in both positive and negative modes, using the optimal source parameters previously mentioned for a FIA flow rate of 0.4 mL/min ($P_{\text{NGop}} = 2.7$ bar, $T_{\text{DGop}} = 250$ °C and $F_{\text{DGop}} = 8$ L/min). To study the instrument stability and observe the evolution of ion mobilities, we first set the source parameters under poor desolvation conditions (0.5 bar, 150 °C and 4 L/min) for 20 min (an analysis of 20 minutes using poor desolvation was first carried out) before each stability analytical sequence. Additional parameters have been described in the SI.

Data processing and CCS determination.

Raw data were first processed using Data Analysis 6.0 (Bruker Daltonics, Bremen, Germany) to visualise the base peak chromatograms (BPC) and mass spectra and to extract the K_0 values and ion mobility spectra. Origin 2018 64 bit (OriginLab Corporation, Northampton, MA, USA) was used to normalize and compare the ion mobility spectra. Then, MetaboScape 8.0.2 software (Bruker Daltonics, Bremen, Germany) was used to extract the ion parameters including m/z , $1/K_0$ and CCS values of each standard lipid ion. The CCS values were determined using Metaboscape either after a single step of external calibration or with an internal calibration performed by injecting the calibrant at the end of the acquisition.

3.2.1.4. Results and discussion

The experiments were conducted using a mix of ten commercial standard lipids (4 PE, 1 LPE, 1 PC, 1 LPC, 1 Cer, 1 SM and 1 TG) that gave 16 ions (9 $[\text{M}+\text{H}]^+$ and 7 $[\text{M}+\text{Na}]^+$) in positive mode and 8 ions (5 $[\text{M}-\text{H}]^-$ and 3 $[\text{M}+\text{HCOO}]^-$) in negative mode (Table S1). The figures and discussion presented in this article are illustrated with representative lipids, the LPC 16:0 $[\text{M}+\text{H}]^+$ at m/z 496.3371, in positive mode and PE 6:0/6:0 $[\text{M}-\text{H}]^-$ at m/z 410.1919 in negative mode, but similar results were obtained for all the

other standard lipids. Additional results are presented in the supporting information and discussed below.

Stability of the ion mobility measurements over 10 hours.

First, the stability of ion mobility experiments was studied. In that purpose, the 100 μM standard lipid solution was injected in triplicate in both positive and negative ion modes, every three minutes for the first 45-minutes and then every hour for the next 10 hours (Figure 1A and 1B), using recommended source parameters for ion desolvation at a FIA flow rate of 0.4 mL/min, i.e. $P_{\text{NGop}} = 2.7$ bar, $T_{\text{DGop}} = 250$ °C and $F_{\text{DGop}} = 8$ L/min. For the first experiments (from 0 to 20 minutes), important shifts in the extracted ion mobility spectra (EIM) were observed, resulting in significant $1/K_0$ changes up to 1% (for example, in the case of a representative example, the LPC 16:0, 1.114 V.s/cm² for initial experiment, 1.117 V.s/cm² after 3 minutes, 1.120 V.s/cm² after 6 minutes and 1.126 V.s/cm² after 21 minutes). After 20 minutes, the EIM perfectly overlapped for each studied ion, yielding constant $1/K_0$ values, meaning that stable instrumental conditions were reached. Thus, after an important evolution of the EIM during the first 20 minutes, a stabilization was noticed. These results were observed in both positive and negative ion modes. Consequently, for all the experiments conducted in this study, a 20 minute-delay was applied before starting acquisition following each parameter adjustment.

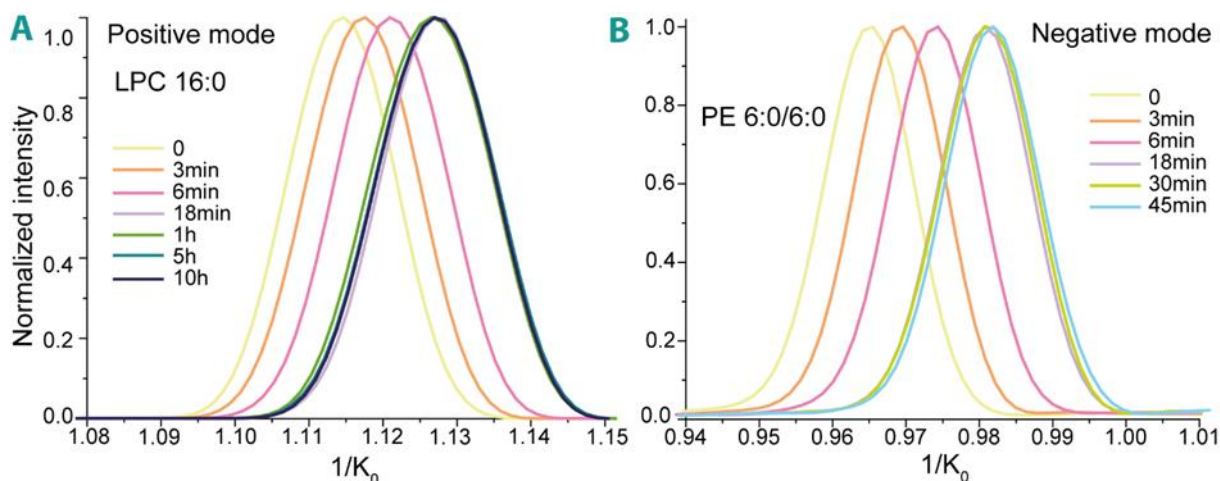


Figure 1: Stability of the ion mobility measurements for (A) LPC 16:0 $[M+H]^+$ and (B) PE 6:0/6:0 $[M-H]^-$. FIA flow-rate = 0.4 mL/min, $T_{\text{DGop}} = 250$ °C, $F_{\text{DGop}} = 8$ L/min, $P_{\text{NGop}} = 2.7$ bar, with experiments performed every three minutes for forty-five minutes and every hour for ten hours.

Influence of the FIA solvent and flow rate.

As previously mentioned, the standard lipid solution was injected in flow injection analysis (FIA). The influence of FIA solvents and flow rate on the ion desolvation and thus on ion mobility measurements was studied. The source parameters were $P_{\text{NGop}} = 2.7$ bar, $T_{\text{DGop}} = 250$ °C and $F_{\text{DGop}} = 8$ L/min corresponding to recommended parameters for a flow rate at 0.4 mL/min. Changing the FIA solvents does not change the ion mobility spectra of the studied lipid ions (Figure S1), meaning that the nature of solvent does not have a significant influence when optimal desolvation parameters are used. Thus, in these optimal ESI conditions, whatever the solvent, ion mobility of lipids is unaffected, unlike previous results regarding aromatic compounds for which changes in solvents induced changes in ion mobilities. This remark is of particular interest because LC gradient is most often used in LC-IMS-MS analyses in lipidomics or metabolomics. Then, we studied the influence of FIA flow rate. Using optimal

source parameters for a flow rate of 0.4 mL/min ($P_{\text{NGOP}} = 2.7$ bar, $T_{\text{DGOP}} = 250$ °C and $F_{\text{DGOP}} = 8$ L/min), variation of the FIA flow rate did not change ion mobility spectra. Thus, the $1/K_0$ values remained constant, meaning that the desolvation was sufficient (Figure A and 2.B). However, when we chose poor desolvation parameters by reducing the nebulizer gas pressure (0.5 bar), the drying gas temperature (150°C) and flow rate (4 L/min), important shifts of the ion mobility peaks and an increase of the $1/K_0$ values were observed when the FIA flow rate varied from 0.1 to 0.5 mL/min (Figure 2.B and 2.D). For instance, in positive ion mode, a 0.5% increase of $1/K_0$ values was observed for LPC 16:0 $[\text{M}+\text{H}]^+$, from 1.128 V.s/cm² for an FIA flow rate of 0.1 mL/min to 1.134 V.s/cm² for an FIA flow rate of 0.5 mL/min. In negative mode, the same trend was observed, and moreover, under poor desolvation conditions, a second peak at higher $1/K_0$ value appeared (Figure 2D). The relative intensity of this peak increased with the FIA flow rate. The presence of the peak at higher $1/K_0$ may be due to the formation of either adducts (for example $[\text{M}+\text{HCOO}]^-$) or solvated species in the TIMS cell which further desolvate when entering the low-pressure region of the instrument. These species are then detected as deprotonated species as both peaks correspond to identical m/z 410.1898 and only one structural isomer exists for this lipid.

Figure A second IM peak also appears for PE 10:0/10:0 (m/z 522.3187) in negative mode, but with a lower intensity. For PE 15:0/15:0 at m/z 662.4739, a peak enlargement is observed instead (Figure S2). In addition, for PE 18:1/18:1 at m/z 742.5362, the peak seems almost symmetric, with a normal full-width at half maximum (FWHM), compared to the same peak with good desolvation conditions (around 0.017 Vs/cm²). This phenomenon is not observed with the other lipid species, not even for LPE 16:0 at m/z 452.2767 (Figure S2) or for LPC 16:0. This might be explained by the length of the fatty acid chain. As PE 6:0/6:0 has smaller chains than the others PE lipids, the solvent represents a bigger part in the solvent-ion cluster. Further research is required to explain exactly this phenomenon.

This observation shows that optimal desolvation conditions are required to avoid this phenomenon which could lead to data misinterpretation, artefactually orienting the analyst towards the presence of an isomer. For that, parameters which have an influence on the desolvation, such as nebulizer pressure, drying gas temperature and flow rate, were studied.

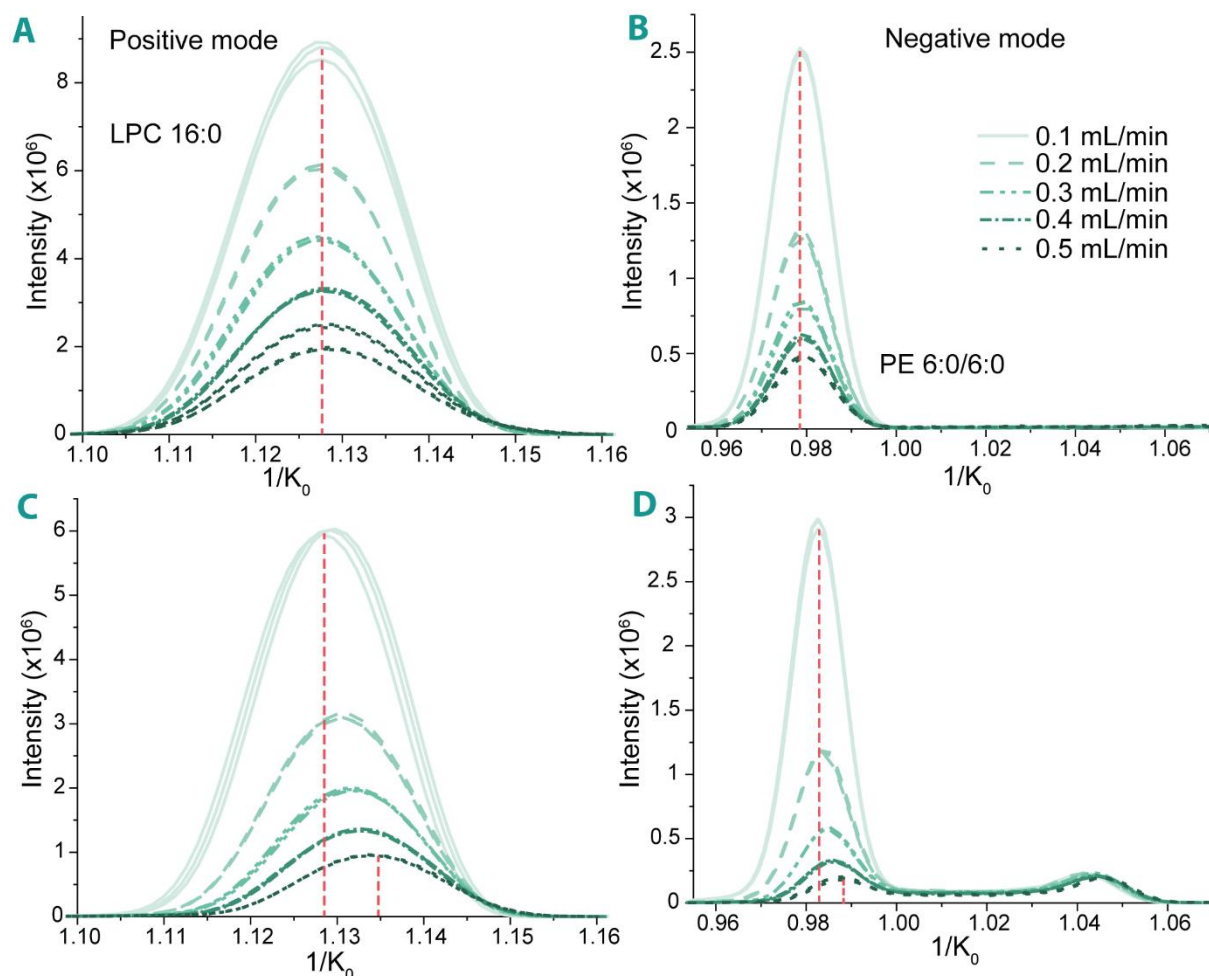


Figure 2: Influence of the FIA flow rate (0.1-0.5 mL/min) for (A,C) LPC 16:0 $[M+H]^+$ and (B,D) PE 6:0/6:0 $[M-H]^-$. (A,B) $T_{DGop}=250\text{ }^{\circ}\text{C}$, $F_{DGop}=8\text{ L/min}$, $P_{NGop}=2.7\text{ bar}$ and (C,D) $T_{DG}=150\text{ }^{\circ}\text{C}$, $F_{DG}=4\text{ L/min}$, $P_{NG}=0.5\text{ bar}$

Influence of source parameters on $1/K_0$ measurements.

As shown in the previous section and in literature,^{22,23} the source parameters can have a direct influence on ion formation, including conversion of ions in solution to ions in gas phase. Consequently, these parameters have an influence on solvent declustering that can further affect the ion mobility measurements, in particular if ion desolvation is not fully achieved when ions enter the TIMS cell. The influence of the three main source parameters, nebulizer pressure, drying gas flow rate and temperature, on ion mobility spectra was therefore studied independently using a FIA flow rate of 0.4 mL/min (classical flow rate reported for UHPLC MS metabolomics workflows).

First, the nebulizer pressure was varied from 0.5 bar to 5 bar, in 0.5 bar step from 0.5 to 1 bar then in 1 bar step from 1 bar to 5 bar. It is well-described that the nebulizer gas flow allows to create the spray of sample solution and thus the charged droplets. The solvent then evaporates allowing to concentrate the charges. Desolvated ions are formed in the gas phase and separated in the mass spectrometer. As displayed in Figure A, changing the nebulizer pressure has no significant effect, except eventually at 0.5 bar (very small shift of the EIM). The effect of the nebulizer pressure was more pronounced for other lipids studied in positive mode, as the PE 10:0/10:0 (Figure S3). In negative mode, a gradual shift of the ion mobility is revealed, as for instance, in Figure 3B, for PE 6:0/6:0 $[M-H]^-$ towards higher $1/K_0$, when the nebulizer gas pressure decreases meaning that desolvation is not complete. A deviation of 0.4%

for $1/K_0$ values (0.978 V.s/cm² at 5 bar to 0.982 V.s/cm² at 0.5 bar) was observed for the PE 6:0/6:0 [M-H]⁻. The nebulizer pressure is therefore a parameter to consider for desolvation. It needs to be adjusted to eliminate solvent clusters in TIMS instrument, as previously demonstrated for 1,8-naphthalic anhydride cations.¹⁹

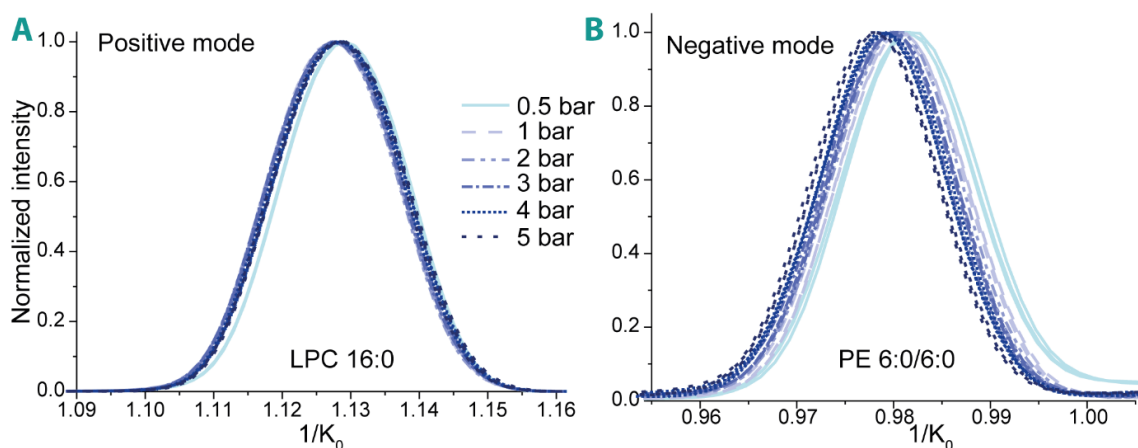


Figure 3: Influence of the nebulizer pressure (0.5-5 bar) for (A) LPC 16:0 [M+H]⁺ and (B) PE 6:0/6:0 [M-H]⁻ at FIA flow-rate= 0.4 mL/min, $T_{DGop}=250$ °C and $F_{DGop}=8$ L/min

The drying gas has to completely evaporate the solvent contained in the small droplets formed by electrospray. The drying gas is composed of pressurized nitrogen and flows in the opposite direction of the charged droplets in the gas chamber. Drying gas flow rate was varied from 4 L/min to 12 L/min to evaluate its effect on the ion mobility experiments (Figure). A significant influence of this parameter can be observed, as a decrease of the drying gas flow rate induce shifts of the EIM spectra towards higher $1/K_0$ values meaning weaker desolvation of the ions.

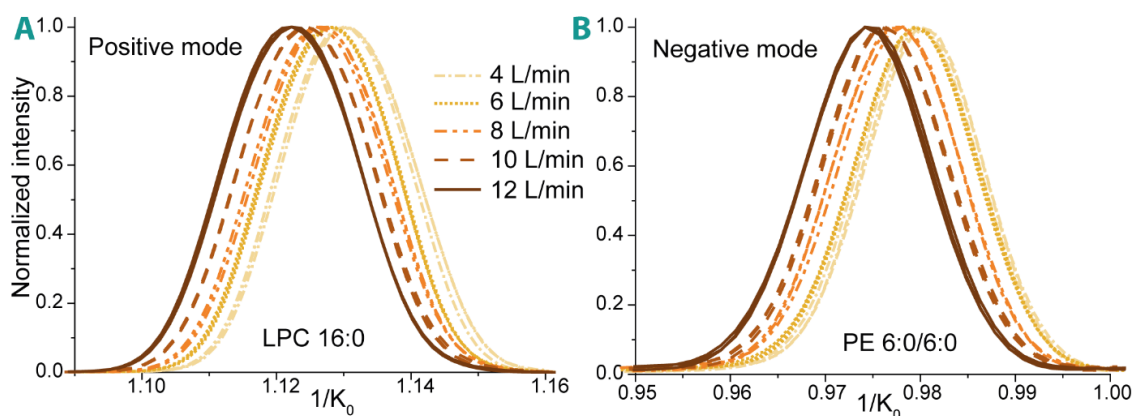


Figure 4: Influence of the drying gas flow rate (4-12 L/min) for (A) LPC 16:0 [M+H]⁺ and (B) PE 6:0/6:0 [M-H]⁻ at FIA Flow-rate= 0.4 mL/min, $T_{DGop}=250$ °C and $P_{NGop}=2.7$ bar

A heater is used to adjust the temperature of the drying gas, which helps to enhance the desolvation process in the electrospray source. The drying gas temperature is an important ESI source parameter which need to be adapted to each application.²⁴ To evaluate its influence, we varied this parameter from 150 °C to 350 °C (Figure). A decrease in drying gas temperature induces notable shifts in the ion mobility spectra towards higher $1/K_0$ values, meaning that the solvation of the ions is higher, and clusters of solvents can be formed. The $1/K_0$ values change up to 2% (from 0.980 V.s/cm² at 150 °C to 0.960 V.s/cm² at 350 °C for PE 6:0/6:0 [M-H]⁻). We also noticed that the intensity decreased with temperature, because the ionization and the desolvation are less efficient. This parameter seems to

have the most important influence on the desolvation process because the shifts in $1/K_0$ are higher with drying gas temperature than with drying gas flow rate or nebulizer pressure, with $1/K_0$ deviation of approximately 2% for drying gas temperature against 0.7% for the drying gas flow rate and less than 0.4% for the nebulizer pressure.

The shifts in the reduced mobility due to changes in source temperature can be due to multiple reasons, such as the change in desolvation or the addition of solvent in the IMS cell. Moreover, reduced mobility K_0 has been defined to allow comparison values between different laboratories as mobility is dependent of pressure and temperature.²⁵ However, even if reduced mobility K_0 mostly compensates for gas number density-caused effects, it still depends on ion and gas velocity and consequently on temperature.²⁵ Mobility also depends on the E/N ratio where E is the electrical field and N the gas number density, and it is assumed that in the low-field limit, the dependence becomes negligible.¹⁷ However, this limit is not yet precisely and clearly defined.²⁶ Then, even if investigations on the effective temperature inside the TIMS instrument have been conducted using "thermometer" ions,^{27,28} further experiments and investigations are still needed to understand the exact phenomena occurring inside the TIMS cell.

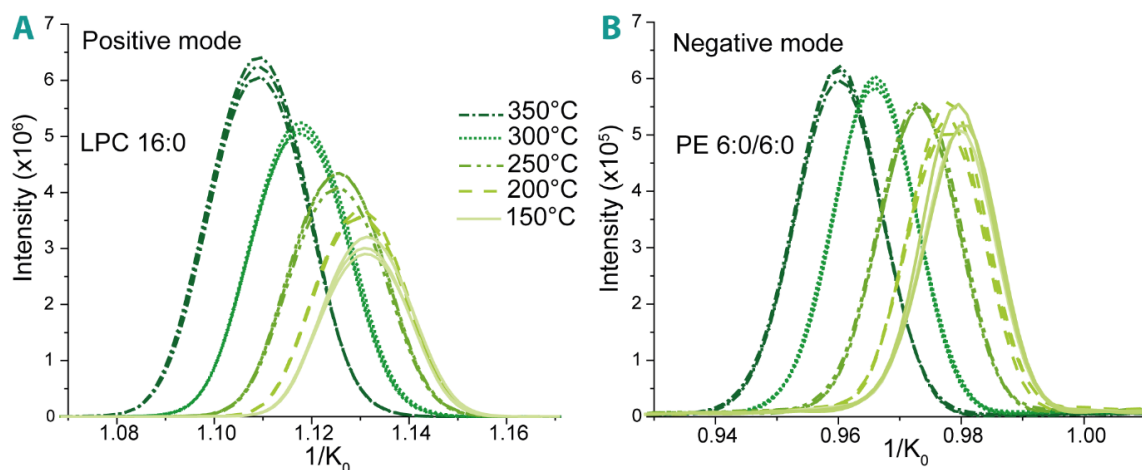


Figure 5: Influence of the drying gas temperature (150-350 °C) for (A) LPC 16:0 $[M+H]^+$ and (B) PE 6:0/6:0 $[M-H]^-$ at FIA flow-rate=0.4 mL/min, F_{DGop} =8 L/min, P_{NGop} =2.7 bar. The experiments were carried out as triplicates.

Different assumptions can be made to explain the shift of the TIMS mobility when parameters were changed. Indeed, when the three studied source parameters decreased or FIA flow rate increased, solvent could not evaporate and therefore ion-solvent clusters were transferred to the TIMS cell, resulting in higher $1/K_0$ values. This phenomenon was already described for 1,8-naphthalic anhydride.¹⁹ The presence of solvent in the ion mobility cell can also play the role of gas modifiers or dopants. Some chemical modifiers such as methanol, ethanol, isopropanol, 1-butanol, acetonitrile or others, in small proportion have been used to improve the IMS separation.²⁹⁻³³ The presence of water in the gas flowing through the IMS cell can also affect the ion mobility separation, as an increase of water content leads to an increase of drift time.³⁴

In addition, we could observe that ion mobility evolves with the pressure measured in the TIMS cell ("Tunnel In Vacuum") (Figure S3). As this pressure increases with increasing nebulizer pressure, drying gas flow rate and temperature, it can be assumed that the source parameters directly influence the pressure in the IMS cell and therefore ion mobility. That can be explained as the IMS cell is directly located after the source in the TIMS-TOF MS instrument.

Further experiments and theoretical calculations should be carried out to test and verify these hypotheses but are outside of the scope of this study.

Influence on the collision cross sections.

After studying the influence of source parameters and solvents on ion mobility, the impact of these parameters was evaluated on the determination of collision cross sections. As expected according to the Mason-Schamp equation, the changes in $1/K_0$ induced consistently changes in CCS, similar conclusions can be reached, i.e. influence of source parameters and solvents are identical on the CCS and $1/K_0$ values. For example, regarding the drying gas temperature experiments, the CCS values decreased when increasing the temperature (FigureC), more likely because the increase of temperature permits to eliminate solvent clusters to get better desolvation (desolvated ions exhibit smaller CCS than solvated species as previously reported by Zhang et al¹⁹). An internal calibration can be applied to the raw data, by injecting a calibrant solution during the acquisition. Here, we injected the Tune Mix calibrant at the end of each analysis. With this internal mobility calibration performed thanks to the Metaboscape software, the shifts were considerably reduced, and the CCS realigned (FigureB and 6D). The relative standard deviation was near 0.1 % over the fifteen CCS values, in comparison to 0.8% without internal calibration. The same conclusions were obtained for drying gas flow rate experiments (Figure S5). These results highlight the importance of an internal mobility calibration for CCS determination using TIMS-MS instrument to retrieve interoperable CCS values.

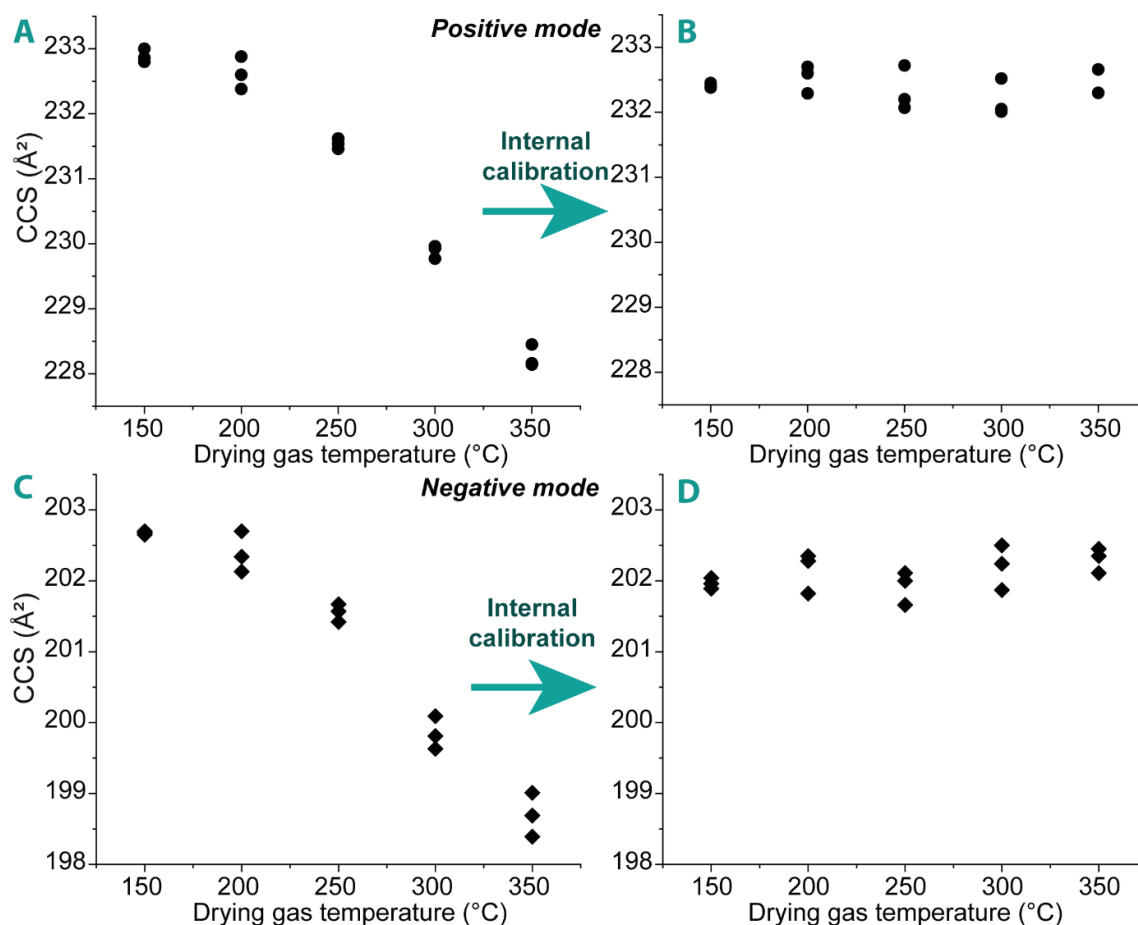


Figure 6: Influence of the drying gas temperature (150-350 °C) on the CCS values without (A,C) and with (B,D) internal calibration, in positive for LPC 16:0 (A,B) and negative, for PE 6:0/6:0 (C,D)

3.2.1.5. Conclusions

Solvents and FIA flow rates (0.1-0.5 mL/min) as well as different ion source parameters such as nebulizer gas pressure (0.5-5 bar), drying gas temperature (150-350 °C) and flow rate (4-12 L/min) were tested, using lipid standards in both positive and negative ion modes, to evaluate their influence on TIMS inverse mobility and CCS values. Using the recommended source conditions for a flow rate of 0.4 mL/min, the ion mobility spectra are constant whatever the solvent used for sample introduction. Under poor desolvation conditions, the reverse mobility shifts and second peak appears, which may be due to ion-solvent cluster, as reported in a previous study.¹⁹ Shifts on the ion mobility spectra are also observed by changing source parameters. They are even more noticeable for drying gas temperature and flow rate. A stabilization time of twenty minutes is essential for repeatable measurements. Therefore, particular attention must be paid to ensure good desolvation conditions, to avoid formation of ion-solvent cluster which could lead to misinterpretation of the ion mobility peaks. These results were consistent with a previous study¹⁹, and, in the case of lipids, the optimal desolvation conditions imply increase of the nebulizer gas pressure (at 2.7 bar), of the drying gas temperature (at 250°C) and of drying gas flow rate (at 8 L/min) for a FIA flow-rate of 0.4 mL/min currently used in lipidomics LC-MS workflows. The main differences between our study and that of Zhang *et al.* lie in the studied compounds and in the FIA flow rates. We chose to carry out this study with flow rates used in metabolomics LC-MS workflows, i.e. 0.1 to 0.4 mL/min, which were much higher than those studied by Zhang *et al.* Then, the lipid ion mobilities evolved in a slightly different way to that of naphthalic anhydrides, as no peak broadening was observed in the case of lipids.

The influence of the parameters on the CCS values was also studied, demonstrating that internal ion mobility calibration reduces shifts on the CCS values from 0.8% to 0.1%. Indeed, strictly identical parameters must be used for both analytes and calibrant in IMS measurements, including source parameters and solvent or flow rate of the sample introduction.

We have demonstrated that, using good desolvation conditions, the eventual small shifts that can occur in ion mobilities can be easily corrected using an internal mobility calibration. Consequently, the guarantee of good desolvation conditions can allow to obtain interoperable CCS values which may be used as descriptors for annotation in metabolomics and lipidomics.

3.2.1.6. References

- (1) Delvaux, A.; Rathahao-Paris, E.; Alves, S. Different Ion Mobility-Mass Spectrometry Coupling Techniques to Promote Metabolomics. *Mass Spectrometry Reviews* 2021. <https://doi.org/10.1002/mas.21685>.
- (2) Paglia, G.; Smith, A. J.; Astarita, G. Ion Mobility Mass Spectrometry in the Omics Era: Challenges and Opportunities for Metabolomics and Lipidomics. *Mass Spectrometry Reviews* 2021. <https://doi.org/10.1002/mas.21686>.
- (3) Zhang, X.; Kew, K.; Reisdorph, R.; Sartain, M.; Powell, R.; Armstrong, M.; Quinn, K.; Cruickshank-Quinn, C.; Walmsley, S.; Bokatzian, S.; Darland, E.; Rain, M.; Imatani, K.; Reisdorph, N. Performance of a High-Pressure Liquid Chromatography-Ion Mobility-Mass Spectrometry System for Metabolic Profiling. *Anal. Chem.* 2017, 89 (12), 6384–6391. <https://doi.org/10.1021/acs.analchem.6b04628>.
- (4) Zhou, Z.; Luo, M.; Chen, X.; Yin, Y.; Xiong, X.; Wang, R.; Zhu, Z.-J. Ion Mobility Collision Cross-Section Atlas for Known and Unknown Metabolite Annotation in Untargeted Metabolomics. *Nat Commun* 2020, 11 (1), 4334. <https://doi.org/10.1038/s41467-020-18171-8>.
- (5) Lenski, M.; Maallem, S.; Zarccone, G.; Garçon, G.; Lo-Guidice, J.-M.; Anthérieu, S.; Allorge, D. Prediction of a Large-Scale Database of Collision Cross-Section and Retention Time Using Machine Learning to Reduce False Positive Annotations in Untargeted Metabolomics. *Metabolites* 2023, 13 (2), 282. <https://doi.org/10.3390/metabo13020282>.

- (6) Zhou, Z.; Xiong, X.; Zhu, Z.-J. MetCCS Predictor: A Web Server for Predicting Collision Cross-Section Values of Metabolites in Ion Mobility-Mass Spectrometry Based Metabolomics. *Bioinformatics* 2017, 33 (14), 2235–2237. <https://doi.org/10.1093/bioinformatics/btx140>.
- (7) Zhou, Z.; Tu, J.; Xiong, X.; Shen, X.; Zhu, Z.-J. LipidCCS: Prediction of Collision Cross-Section Values for Lipids with High Precision To Support Ion Mobility–Mass Spectrometry-Based Lipidomics. *Anal. Chem.* 2017, 89 (17), 9559–9566. <https://doi.org/10.1021/acs.analchem.7b02625>.
- (8) Paglia, G.; Angel, P.; Williams, J. P.; Richardson, K.; Olivos, H. J.; Thompson, J. W.; Menikarachchi, L.; Lai, S.; Walsh, C.; Moseley, A.; Plumb, R. S.; Grant, D. F.; Palsson, B. O.; Langridge, J.; Geromanos, S.; Astarita, G. Ion Mobility-Derived Collision Cross Section As an Additional Measure for Lipid Fingerprinting and Identification. *Analytical Chemistry* 2015, 87 (2), 1137–1144. <https://doi.org/10.1021/ac503715v>.
- (9) Paglia, G.; Astarita, G. Metabolomics and Lipidomics Using Traveling-Wave Ion Mobility Mass Spectrometry. *Nat Protoc* 2017, 12 (4), 797–813. <https://doi.org/10.1038/nprot.2017.013>.
- (10) Nye, L. C.; Williams, J. P.; Munjoma, N. C.; Letertre, M. P. M.; Coen, M.; Bouwmeester, R.; Martens, L.; Swann, J. R.; Nicholson, J. K.; Plumb, R. S.; McCullagh, M.; Gethings, L. A.; Lai, S.; Langridge, J. I.; Vissers, J. P. C.; Wilson, I. D. A Comparison of Collision Cross Section Values Obtained via Travelling Wave Ion Mobility-Mass Spectrometry and Ultra High Performance Liquid Chromatography-Ion Mobility-Mass Spectrometry: Application to the Characterisation of Metabolites in Rat Urine. *Journal of Chromatography A* 2019, 1602, 386–396. <https://doi.org/10.1016/j.chroma.2019.06.056>.
- (11) Odenkirk, M. T.; Baker, E. S. Utilizing Drift Tube Ion Mobility Spectrometry for the Evaluation of Metabolites and Xenobiotics. *Methods Mol Biol* 2020, 2084, 35–54. https://doi.org/10.1007/978-1-0716-0030-6_2.
- (12) Nichols, C. M.; Dodds, J. N.; Rose, B. S.; Picache, J. A.; Morris, C. B.; Codreanu, S. G.; May, J. C.; Sherrod, S. D.; McLean, J. A. Untargeted Molecular Discovery in Primary Metabolism: Collision Cross Section as a Molecular Descriptor in Ion Mobility-Mass Spectrometry. *Anal. Chem.* 2018, 90 (24), 14484–14492. <https://doi.org/10.1021/acs.analchem.8b04322>.
- (13) Deschamps, E.; Schmitz-Afonso, I.; Schaumann, A.; Dé, E.; Loutelier-Bourhis, C.; Alexandre, S.; Afonso, C. Determination of the Collision Cross Sections of Cardiolipins and Phospholipids from *Pseudomonas Aeruginosa* by Traveling Wave Ion Mobility Spectrometry-Mass Spectrometry Using a Novel Correction Strategy. *Anal Bioanal Chem* 2019, 411 (30), 8123–8131. <https://doi.org/10.1007/s00216-019-02194-2>.
- (14) Paglia, G.; Astarita, G. Traveling Wave Ion Mobility Mass Spectrometry: Metabolomics Applications. In *High-Throughput Metabolomics*; D'Alessandro, A., Ed.; Methods in Molecular Biology; Springer New York: New York, NY, 2019; Vol. 1978, pp 39–53. https://doi.org/10.1007/978-1-4939-9236-2_4.
- (15) Schroeder, M.; Meyer, S. W.; Heyman, H. M.; Barsch, A.; Sumner, L. W. Generation of a Collision Cross Section Library for Multi-Dimensional Plant Metabolomics Using UHPLC-Trapped Ion Mobility-MS/MS. *Metabolites* 2020, 10 (1), 13. <https://doi.org/10.3390/metabo10010013>.
- (16) Rathahao-Paris, E.; Delvaux, A.; Li, M.; Guillon, B.; Venot, E.; Fenaille, F.; Adel-Patient, K.; Alves, S. Rapid Structural Characterization of Human Milk Oligosaccharides and Distinction of Their Isomers Using Trapped Ion Mobility Spectrometry Time-of-Flight Mass Spectrometry. *Journal of Mass Spectrometry* 2022, 57 (10), e4885. <https://doi.org/10.1002/jms.4885>.
- (17) Gabelica, V.; Afonso, C.; Barran, P.; Benesch, J. L. P.; Road, M.; Bush, M. F.; Campuzano, I. D. G.; Causon, T.; Clowers, B. H.; Creaser, C. S. Recommendations for Reporting Ion Mobility Mass Spectrometry Measurements. *Mass Spectrometry Reviews* 2019, 59. <https://doi.org/10.1002/mas.21585>.
- (18) George, A. C.; Schmitz-Afonso, I.; Marie, V.; Colsch, B.; Fenaille, F.; Afonso, C.; Loutelier-Bourhis, C. A Re-Calibration Procedure for Interoperable Lipid Collision Cross Section Values Measured by Traveling Wave Ion Mobility Spectrometry. *Analytica Chimica Acta* 2022, 340236. <https://doi.org/10.1016/j.aca.2022.340236>.
- (19) Zhang, L.; Wang, Y.; Zheng, F.; Zhu, D.; Liang, Y.; Shi, Q. Influence Exerted by the Solvent Effect on the Mobility Peak of 1,8-Naphthalic Anhydride in Ion Mobility Spectrometry. *J. Am. Soc. Mass Spectrom.* 2022. <https://doi.org/10.1021/jasms.1c00299>.
- (20) Boschmans, J.; Jacobs, S.; Williams, J. P.; Palmer, M.; Richardson, K.; Giles, K.; Laphorn, C.; Herrebout, W. A.; Lemièrre, F.; Sobott, F. Combining Density Functional Theory (DFT) and Collision Cross-Section (CCS) Calculations to Analyze the Gas-Phase Behaviour of Small Molecules and Their Protonation Site Isomers. *Analyst* 2016, 141 (13), 4044–4054. <https://doi.org/10.1039/C5AN02456K>.

- (21) Kwantwi-Barima, P.; Hogan, C. J.; Clowers, B. H. Probing Gas-Phase-Clustering Thermodynamics with Ion Mobility–Mass Spectrometry: Association Energies of Phenylalanine Ions with Gas-Phase Alcohols. *J. Am. Soc. Mass Spectrom.* 2020, 31 (9), 1803–1814. <https://doi.org/10.1021/jasms.0c00020>.
- (22) Kebarle, P.; Peschke, M. On the Mechanisms by Which the Charged Droplets Produced by Electrospray Lead to Gas Phase Ions. *Analytica Chimica Acta* 2000, 406 (1), 11–35. [https://doi.org/10.1016/S0003-2670\(99\)00598-X](https://doi.org/10.1016/S0003-2670(99)00598-X).
- (23) Kebarle, P.; Verkerk, U. H. Electrospray: From Ions in Solution to Ions in the Gas Phase, What We Know Now. *Mass Spectrometry Reviews* 2009, 28 (6), 898–917. <https://doi.org/10.1002/mas.20247>.
- (24) Moreiras, G.; Leão, J. M.; Gago-Martínez, A. Design of Experiments for the Optimization of Electrospray Ionization in the LC-MS/MS Analysis of Ciguatoxins. *Journal of Mass Spectrometry* 2018, 53 (11), 1059–1069. <https://doi.org/10.1002/jms.4281>.
- (25) Gabelica, V. Ion Mobility -Mass Spectrometry: An Overview. In *Ion Mobility-Mass Spectrometry:: Fundamentals and Applications*; Sobott, F., Ashcroft, A., Eds.; New Developments in Mass Spectrometry; Royal Society of Chemistry, 2021; pp 1–25. <https://doi.org/10.1039/9781839162886-00001>.
- (26) Hauck, B. C.; Siems, W. F.; Harden, C. S.; McHugh, V. M.; Hill, H. H. Jr. Determination of E/N Influence on K₀ Values within the Low Field Region of Ion Mobility Spectrometry. *J. Phys. Chem. A* 2017, 121 (11), 2274–2281. <https://doi.org/10.1021/acs.jpca.6b12331>.
- (27) Morsa, D.; Hanozin, E.; Eppe, G.; Quinton, L.; Gabelica, V.; Pauw, E. D. Effective Temperature and Structural Rearrangement in Trapped Ion Mobility Spectrometry. *Anal. Chem.* 2020, 92 (6), 4573–4582. <https://doi.org/10.1021/acs.analchem.9b05850>.
- (28) Morsa, D.; Hanozin, E.; Gabelica, V.; De Pauw, E. Response to Comment on Effective Temperature and Structural Rearrangement in Trapped Ion Mobility Spectrometry. *Anal. Chem.* 2020, 92 (24), 16334–16337. <https://doi.org/10.1021/acs.analchem.0c03937>.
- (29) Waraksa, E.; Perycz, U.; Namieśnik, J.; Sillanpää, M.; Dymerski, T.; Wójtowicz, M.; Puton, J. Dopants and Gas Modifiers in Ion Mobility Spectrometry. *TrAC Trends in Analytical Chemistry* 2016, 82, 237–249. <https://doi.org/10.1016/j.trac.2016.06.009>.
- (30) Šála, M.; Lída, M.; Campbell, J. L.; Holčápek, M. Determination of Triacylglycerol Regioisomers Using Differential Mobility Spectrometry. *Rapid Commun Mass Spectrom* 2016, 30 (2), 256–264. <https://doi.org/10.1002/rcm.7430>.
- (31) Fernández-Maestre, R.; Wu, C.; Hill Jr., H. H. Buffer Gas Modifiers Effect Resolution in Ion Mobility Spectrometry through Selective Ion-Molecule Clustering Reactions. *Rapid Communications in Mass Spectrometry* 2012, 26 (19), 2211–2223. <https://doi.org/10.1002/rcm.6335>.
- (32) Fernandez-Maestre, R. Buffer Gas Additives (Modifiers/Shift Reagents) in Ion Mobility Spectrometry: Applications, Predictions of Mobility Shifts, and Influence of Interaction Energy and Structure. *Journal of Mass Spectrometry* 2018, 53 (7), 598–613. <https://doi.org/10.1002/jms.4190>.
- (33) Kemperman, R. H. J.; Chouinard, C. D.; Yost, R. A. Characterization of Bile Acid Isomers and the Implementation of High-Resolution Demultiplexing with Ion Mobility-Mass Spectrometry. *J. Am. Soc. Mass Spectrom.* 2023. <https://doi.org/10.1021/jasms.3c00143>.
- (34) Wolańska, I.; Piwowarski, K.; Budzyńska, E.; Puton, J. Effect of Humidity on the Mobilities of Small Ions in Ion Mobility Spectrometry. *Anal. Chem.* 2023, 95 (22), 8505–8511. <https://doi.org/10.1021/acs.analchem.3c00435>.

3.2.1.7. Supplementary information

Figures

Figure S1: Influence of the FIA solvents using both mobile phase and mix of solvents for (A) LPC 16:0 [M+H]⁺ and (B) PE 6:0/6:0 [M-H]⁻ at TDGop=250 °C, FDGop=8 L/min, PNGop=2.7 bar

Figure S2: Influence of the FIA flow rate (0.1-0.5 mL/min) for (A) PE 10:0/10:0 [M-H]⁻, (B) PE 15:0/15:0 [M-H]⁻, (C) PE 18:1/18:1 [M-H]⁻ and (D) LPE 16:0 [M-H]⁻ at TDGop=150 °C, FDGop=4 L/min, PNGop=0.5 bar

Figure S3: Influence of the nebulizer pressure (0.5-5 bar) for PE 10:0/10:0 [M+Na]⁺ at 0.4 mL/min, TDGop=250 °C, FDGop=8 L/min (triplicates analysis have been performed)

Figure S4: Evolution of the pressure inside the IMS cell according to the drying gas temperature

Figure S5: Influence of the drying gas flow rate (4-12 L/min) on the CCS values (A,C) without and (B,D) with internal calibration, in (A,B) positive and (C,D) negative

Tables

Table S1: Experimental parameters used for the TIMS-TOF Flex system in both positive and negative modes.

Table S2: T-Rex 4D processing parameters in Metaboscape software.

Table S3: Compound detection parameters for IMS peaks in Data Analysis software.

Table S4: Lipid species detected in this study, in positive and negative mode respectively.

TIMS experiments

The IMS parameters were adjusted to detect all the lipid species, within a large ion mobility range corresponding to reduced mobilities ($1/K_0$) from 0.55 to 1.90 V.s.cm⁻².

Table S1: Experimental parameters used for the TIMS-TOF Flex system in both positive and negative modes

ESI source parameters			TIMS settings		
	Positive	Negative	Mode	Custom	
Nebulizer (bar)	0.5-5	0.5-5	1/K0 start (V.s/cm ²)	0.55	
Dry gas (L/min)	4-12	4-12	1/K0 end (V.s/cm ²)	1.9	
Dry temp (°C)	150-350	150-350	Ramp time (ms)	100	
Scan range	50-1600	50-1650	Accumulation time (ms)	100	
End plate Offset (V)	500	500	Duty cycle (%)	100	
Capillary (V)	4500	-3500	Ramp rate (Hz)	9.43	

Tune parameters			
Transfer parameters	Positive	Negative	
Deflection 1 Delta (V)	80	-80	
Funnel 1 RF (Vpp)	500	500	
isCID Energy (eV)	0	0	
Funnel 2 RF (Vpp)	250	250	
Multipole RF (Vpp)	250	200	
Collision Cell			
Collision Energy (eV)	10	10	
Collision RF (Vpp)	1100	1100	
Quadrupole			
Ion Energy (eV)	5	5	
Low mass (m/z)	150	150	
Focus Pre TOF			
Transfer time (μs)	65	65	
Pre Pulse Storage (μs)	5	5	

Tune parameters: TIMS			
Offsets	Positive	Negative	
Δt1 (V)	-20	20	
Δt2 (V)	-120	120	
Δt3 (V)	80	-80	
Δt4 (V)	100	-100	
Δt5 (V)	0	0	
Δt6 (V)	100	-100	
Collision Cell In (V)	220	-220	
Ion Charge Control (ICC)	Enable	Enable	
Target intensity (M)	7.5	7.5	

Data processing

The data processings were performed using *Metaboscape and Data Analysis* (Bruker) softwares

Metaboscape parameters

In Metaboscape software, different parameters have to be registered to perform the data analysis processing.

The feature table was created by first giving an explicit name containing at least the number (given in sample list) of the processed acquisition. The filtering parameters were set at around a third of the total number of analyses, in 'Minimum # features for extraction' and 'Presence of feature in minimum # of analyses'.

The processing parameters are indicated in the Table SA4. The primary ion was $[M+H]^+$ in positive mode and $[M-H]^-$ in negative mode. Seed ions were $[M+Na]^+$ and $[M-HCOO]^-$ and common ions were $[M+NH_4]^+$ and $[M-H-H_2O]^-$ or $[M-CH_3]^-$. The mobility calibration was performed by specifying the reference lists using Tune Mix calibrant information, and by using the default parameter in retention time range.

Table S2: T-Rex 4D processing parameters in Metaboscape software

T-Rex 4D Processing		
	Positive mode	Negative mode
Peak Detection		
Intensity threshold (counts)	1000	1000
Minimum 4D Peak Size (points)	100	100
Feature signal	Intensity	Intensity
Enable recursive feature extraction	Yes	Yes
Minimum 4D Peak Size (recursive) (points)	10	10
Ranges		
Retention time (min)	0-2	0-2
Mass (m/z)	50-1600	50-1650

Data Analysis

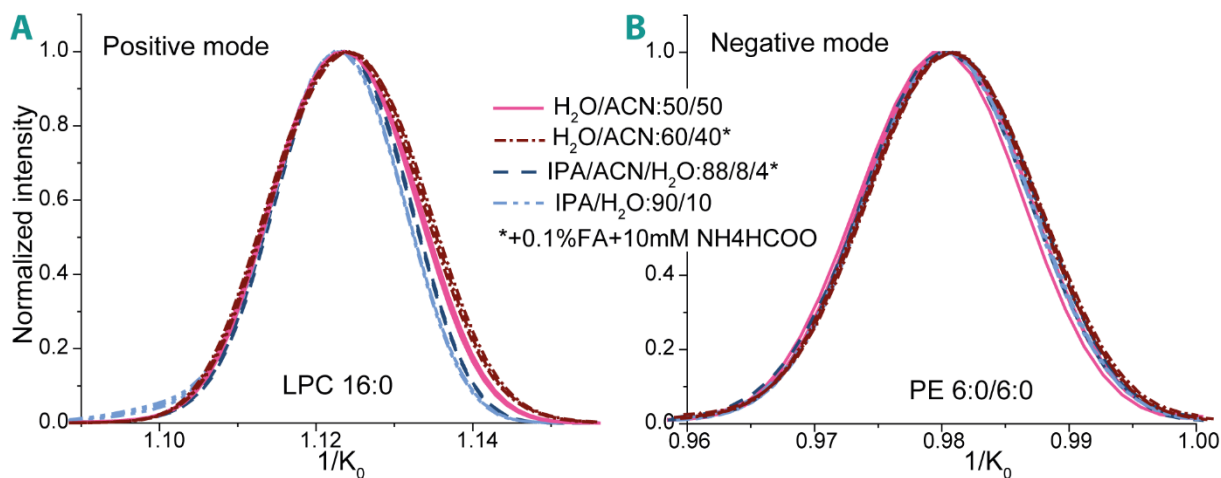
Using mass spectra, lipid ions were selected to extract the ion mobility spectrum for each ion .

Table S3: Compound detection parameters for IMS peaks in Data Analysis software

Compound detection in 'Find Mobilogram'	
Sensitivity	99
Area threshold (Relative %)	5
Intensity threshold (absolute)	50
Min. peak valley	Off
Peak resolution	250

Table S4: Lipid species detected in this study, in positive and negative mode respectively

Positive mode			Negative mode		
Lipids	Ions	m/z	Lipids	Ions	m/z
PE 6:0/6:0	[M+H] ⁺	412.2111	PE 6:0/6:0	[M-H] ⁻	410.2226
PE 6:0/6:0	[M+Na] ⁺	434.1923	LPE 16:0	[M-H] ⁻	452.3048
LPE 16:0	[M+H] ⁺	454.2962	PE 10:0/10:0	[M-H] ⁻	522.3591
LPE 16:0	[M+Na] ⁺	476.2784	LPC 16:0	[M+HCOO] ⁻	540.3629
LPC 16:0	[M+H] ⁺	496.3419	Cer 18:1;O2/18:1	[M+HCOO] ⁻	608.5697
LPC 16:0	[M+Na] ⁺	518.3231	PE 15:0/15:0	[M-H] ⁻	662.5139
PE 10:0/10:0	[M+H] ⁺	524.3378	PE 18:1(9Z)/18:1(9Z)	[M-H] ⁻	742.5914
PE 10:0/10:0	[M+Na] ⁺	546.3183	PC 16:0/16:0	[M+HCOO] ⁻	778.6152
Cer 18:1;O2/18:1	[M+H] ⁺	564.5372			
PE 15:0/15:0	[M+H] ⁺	664.4908			
SM 18:1;O2/18:1	[M+H] ⁺	729.5794			
PC 16:0/16:0	[M+H] ⁺	734.556			
PC 16:0/16:0	[M+Na] ⁺	756.5511			
PE 18:1(9Z)/18:1(9Z)	[M+H] ⁺	744.5472			
PE 18:1(9Z)/18:1(9Z)	[M+Na] ⁺	766.5337			
TG 18:1/18:1/18:1	[M+Na] ⁺	907.7721			

Figure S1: Influence of the FIA solvents using both mobile phase and mix of solvents for (A) LPC 16:0 [M+H]⁺ and (B) PE 6:0/6:0 [M-H]⁻ at TDGop=250 °C, FDGop=8 L/min, PNGop=2.7 bar

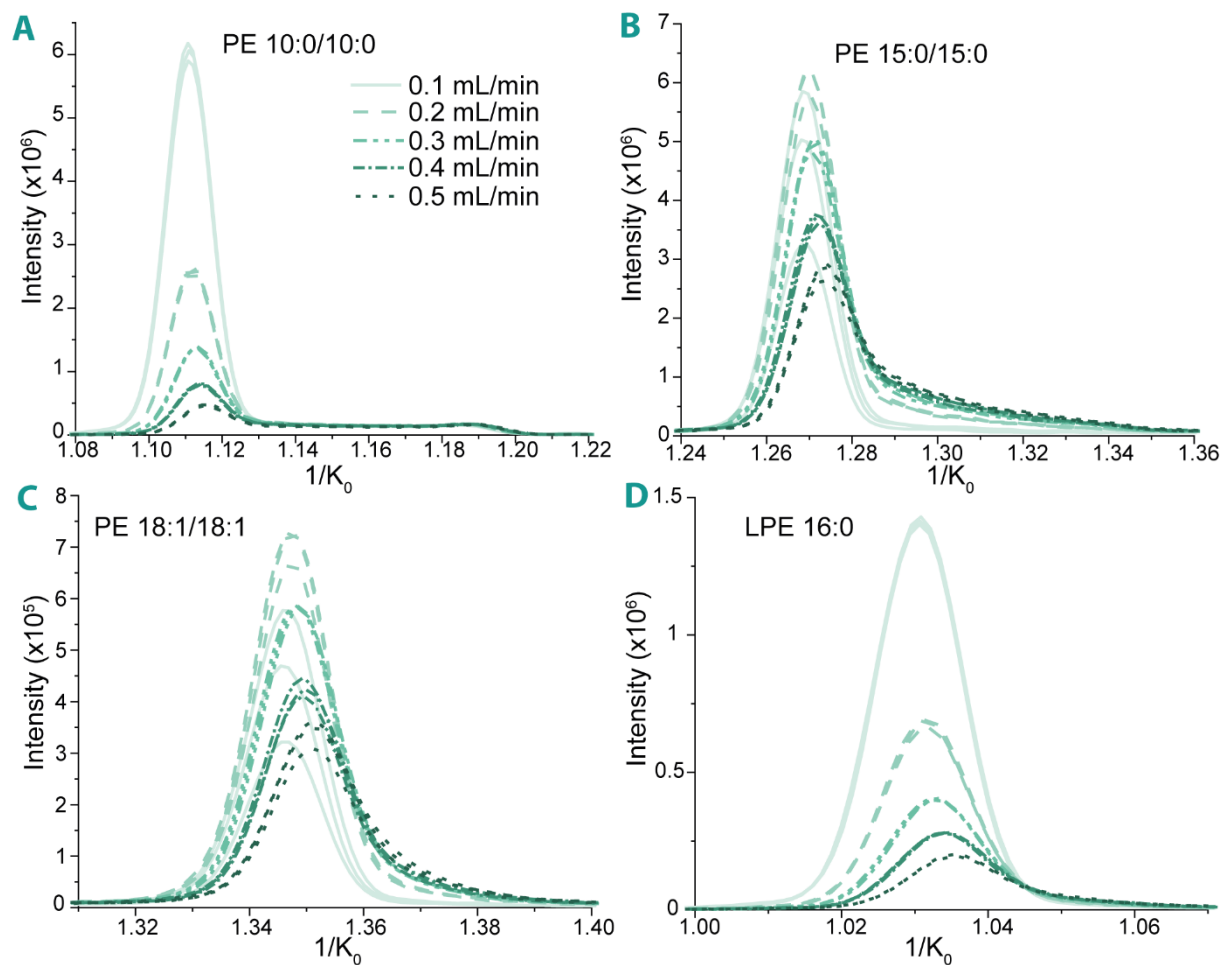


Figure S2: Influence of the FIA flow rate (0.1-0.5 mL/min) for (A) PE 10:0/10:0 [M-H]⁻, (B) PE 15:0/15:0 [M-H]⁻, (C) PE 18:1/18:1 [M-H]⁻ and (D) LPE 16:0 [M-H]⁻ at $T_{DGop}=150$ °C, $F_{DGop}=4$ L/min, $P_{NGop}=0.5$ bar

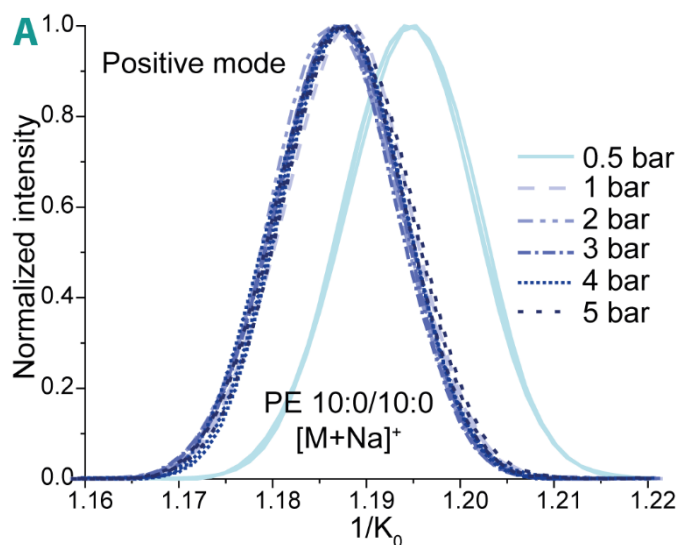


Figure S2: Influence of the nebulizer pressure (0.5-5 bar) for PE 10:0/10:0 [M+Na]⁺ at 0.4 mL/min, $T_{DGop}=250$ °C, $F_{DGop}=8$ L/min (triplicates analysis have been performed)

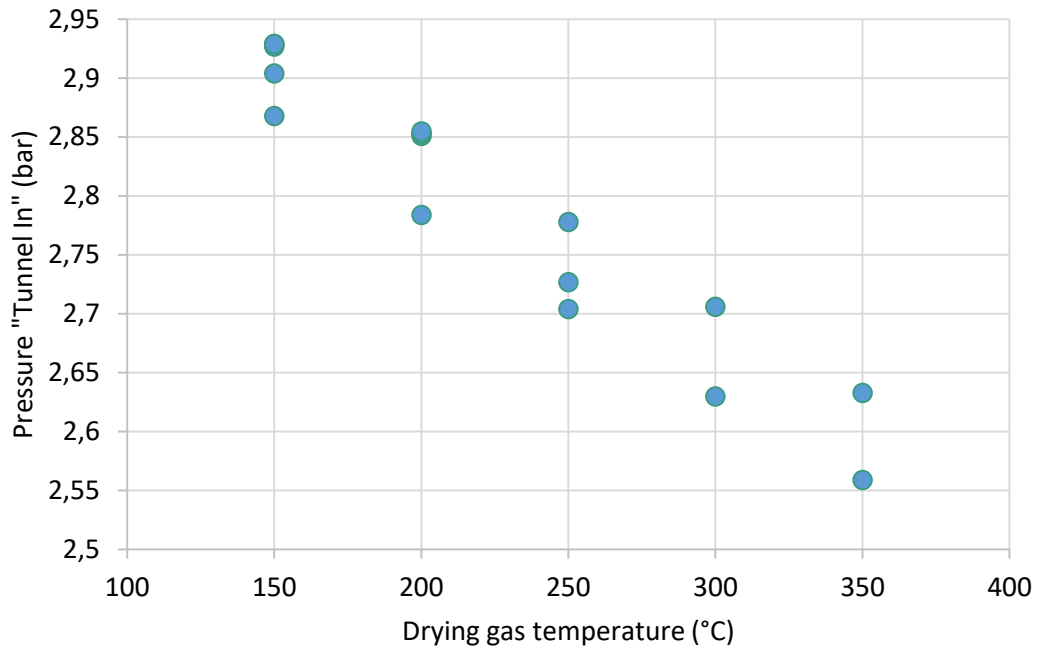


Figure S4: Evolution of the pressure inside the IMS cell according to the Drying gas temperature

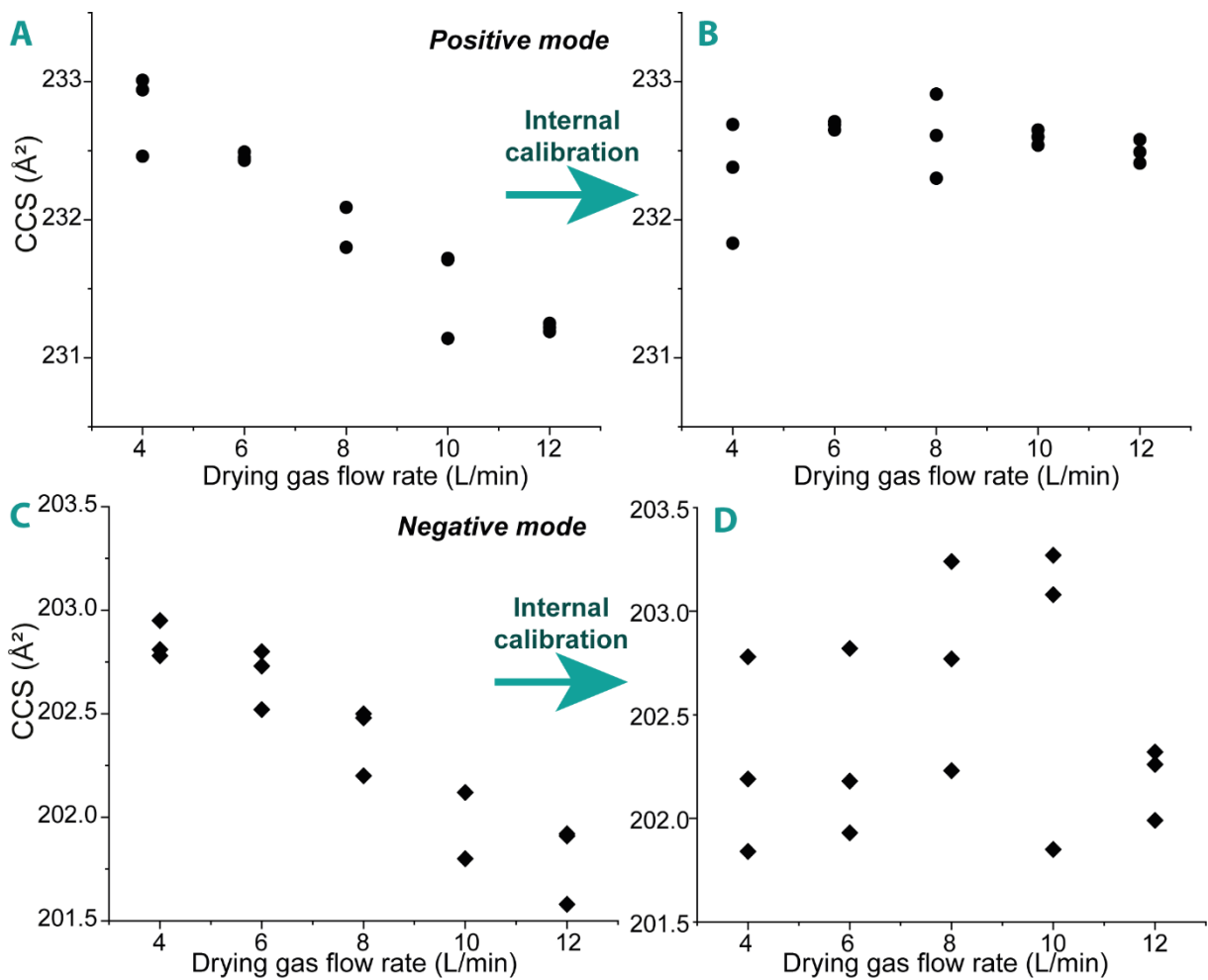


Figure S5: Influence of the drying gas flow rate (4-12 L/min) on the CCS values (A,C) without and (B,D) with internal calibration, in (A,B) positive and (C,D) negative

3.2.2. Influence of the TIMS conditions

After studying the influence of source conditions, we have evaluated the impact of ion mobility operating conditions on ion mobility measurements ($1/K_0$ and the consequence on ^{TIM}CCS). For this evaluation, the source parameters were set to ensure proper ion desolvation conditions. An internal mobility calibration was performed with Tune Mix calibrant for each IM condition. Three different ion mobility conditions, designed hereafter as c1, c2 and c3, were tested on the TIMS instrument (Table III-5).

Table III-5: TIMS parameters tested through three sets of conditions (c1, c2 and c3)

TIMS settings	c1	c2	c3
Mode	Custom	Custom	Custom
$1/K_0$ start (V.s/cm ²)	0.55	0.8	0.6
$1/K_0$ end (V.s/cm ²)	1.9	1.8	1.75
Ramp time (ms)	100	250	300
Accumulation time (ms)	100	100	100
Duty cycle (%)	100	100	100
Ramp rate (Hz)	9.43	3.91	3.27

Plasma samples were injected at least in triplicate for each set of conditions, and the ^{TIM}CCS values were determined independently. The resulting ^{TIM}CCS values of each lipid ion are similar for all sets of IMS conditions (for example, 295.04 Å², 295.40 Å² and 294.80 Å² for CE20:4), with an overall RSD of approximately 0.25% (Table III-6).

Table III-6: ^{TIM}CCS values obtained for seven plasma lipids in positive mode, according to the various sets of conditions tested, (mean CCS values with at least triplicates of analysis)

Lipids	Ions	m/z	rt (min)	CCS (Å ²)			Mean CCS (Å ²)	RSD (%)
				c1	c2	c3		
CE 20:4	[M+NH ₄] ⁺	690.6184	22.5	295.04	295.40	294.80	295.08	0.10
Cer 18:1;O2/12:0	[M+H-H ₂ O] ⁺	464.4455	13.0	243.70	243.43	243.67	243.60	0.06
LPC 16:0	[M+H] ⁺	496.3380	4.7	232.70	231.83	232.67	232.40	0.21
PC 16:0/16:0	[M+H] ⁺	734.5690	15.1	288.06	287.80	287.67	287.84	0.07
PC 18:1/18:1	[M+H] ⁺	786.6004	15.2	294.02	292.88	293.49	293.46	0.19
SM 18:2;O2/16:0	[M+H] ⁺	701.5317	18.6	281.70	284.00	284.05	283.25	0.47
TG 18:1_18:2_18:2	[M+NH ₄] ⁺	898.7799	22.2	324.26	326.10	322.47	324.28	0.56
Mean								0.25

These results showed that changing the ion mobility conditions do not significantly influence the determination of ^{TIM}CCS values in the TIMS instrument. Moreover, the PASEF mode has been tested and the same conclusion has been retrieved (data not shown).

3.3. Influence of source and multiplexing conditions on ^{DT}CCS values

3.3.1. Source parameters

The ESI source parameters of the DTIMS-MS instrument have also been tested to evaluate their possible effect on ^{DT}CCS determination. The evaluated parameters were sheath gas temperature, drying gas flow, nebulizer gas pressure and to a lesser extent, sheath gas flow and temperature, leading to three different sets of conditions (Table III-7). The first set, termed as “Low”, corresponded to the lower values of all parameters, i.e. gas flow-rate, pressure and temperature. The second set, termed as “basic” consisted in parameters we optimized for standard lipid study and the third set “High” corresponded to the higher values of drying gas flow, nebulizer gas pressure and sheath gas flow and temperature. Each condition has been tested in triplicate for both Tune Mix calibrants and lipid compounds.

Table III-7: Source parameters of the different tested conditions (Low values, basic set-up, and high values)

Source parameters	Low	Basic	High
drying gas temperature (°C)	150	300	350
sheath gas temperature (°C)	150	350	350
drying gas flow (L/min)	4	8	12
sheath gas flow (L/min)	4	12	12
nebulizer gas pressure (psi)	7	35	60
capillary voltage (kV)	3.5	3.5	3
nozzle voltage (V)	300	300	300
fragmentor voltage (V)	100	185	400
Oct 1 RF Vpp (V)	750	750	750

The results are presented in Figure III-3 for LPC 16:0 and PC 16:0/16:0 in positive ion mode. Source conditions have an influence on the drift time, up to 1% increase of the measured t_d is evidenced (Figure 1B). The drift time increased with the source parameters, i.e. for high gas flow-rate, pressure and temperature increased. Such trend cannot be explained by a desolvation issue and other assumptions have to be made, as for example, the possibility of sheath gas flow to “push” and accelerate the ions into the IMS cell inducing an initial velocity contribution and possibly impacting the ion mobility. This hypothesis must be studied more deeply, in order to understand the behavior of the ions into the IMS cell.

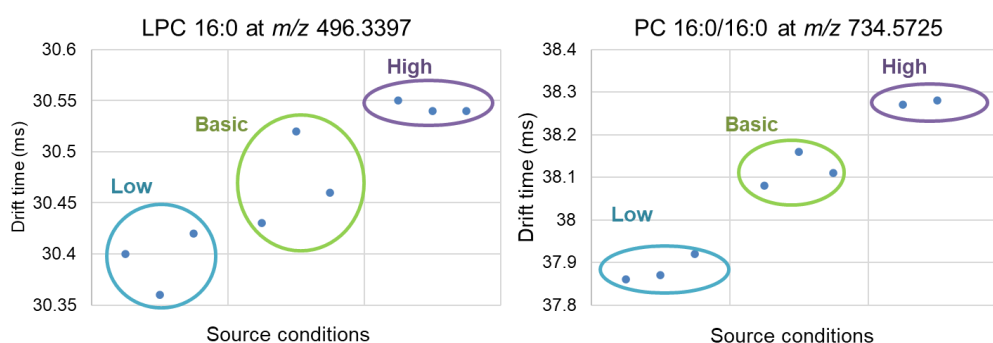


Figure III-3: Drift times in function of the source conditions for LPC 16:0 and PC 16:0/16:0

As source conditions have an influence on the drift times of ions, calibrant and analytes must be analyzed using strictly identical instrumental and operational parameters to determine the CCS values.

3.3.2. Influence of multiplexed acquisition on the CCS determination

To enhance the sensitivity in the DTIMS cell, multiplexing strategy could be carried out (Causon et al. 2019). Five different conditions have been tested on the DTIMS, including two conditions using multiplexing system, at 3-bit and 4-bit, (Table III-8).

Table III-8: Ion mobility conditions for the experiments performed on the Agilent DTIMS system

Conditions	c1	c2	c3	c4	c5
Drift-tube entrance (V)	1574	1474	1700	1574	1574
Drift-tube exit (V)	224	224	250	224	224
IM trap fill time (ms)	30	30	20	14.1	3.9
Trap release time (μ s)	300	300	150	100	200
IM transient rate	18	18	18	18	18
maximum DT (ms)	60	60	60	60	60
multiplexing	No	No	No	3-bit	4-bit

Multiplexing strategies allow to increase the sensitivity by reducing the trap fill and release times. An additional step for data treatment is required to reconstruct the IMS spectra using PNNL-Preprocessor tool (Bilbao et al. 2021). Except this additional processing step, all the five analyses have been processed using the same workflow. The resulting ^{DT}CCS values, determined for seven plasma lipids of different classes, are presented in Table III-9. The CCS values of the five different conditions are consistent, with RSD < 0.12%, reflecting a high repeatability of the CCS values with and without multiplexing implementation.

Table III-9: ^{DT}CCS values of seven plasma lipids determined for five different IMS conditions (among which c4 and c5 correspond to multiplexing parameters)

Lipids	Ions	m/z	rt (min)	CCS (\AA^2)					Mean CCS (\AA^2)	RSD (%)
				c1	c2	c3	c4	c5		
CE 18:2	$[M+NH_4]^+$	666.6189	22.2	289.95	289.83	289.95	290.22	290.52	290.02	0.10
Cer 18:1;O2/24:0	$[M+H-H_2O]^+$	632.6348	18.6	276.27	276.34	276.05	276.50	276.60	276.35	0.07
LPC 16:0	$[M+H]^+$	496.3401	4.0	229.94	229.66	230.03	230.23	230.47	230.05	0.12
PC 16:0/16:0	$[M+H]^+$	734.5708	14.5	283.47	283.56	283.45	283.81	283.71	283.63	0.05
PC 18:1/18:1	$[M+H]^+$	786.6022	14.7	290.62	290.26	290.27	290.82	290.53	290.47	0.07
SM 18:2;O2/16:0	$[M+H]^+$	701.5602	12.4	279.04	279.05	279.10	279.54	279.50	279.23	0.09
TG 18:1_18:2_18:2	$[M+NH_4]^+$	898.7876	21.6	321.37	321.19	320.39	321.31	321.34	321.09	0.11

These results demonstrated that neither multiplexing nor IMS conditions notably affect the CCS values determination of the studied lipids.

3.4. Influence of experimental parameters on TWIMS instrument

3.4.1. Influence of the source parameters on TMCCS

In the design of the Waters Synapt G2 HDMS instrument (Figure III-4), the ion mobility cell is located between the quadrupole and the time-of-flight mass analyzers, unlike Bruker TIMS-TOF MS and Agilent DTIMS-MS where the IMS cell is located immediately after the source. Thus, Synapt configuration permits to remove ion-solvent clustering as these species generally do not survive to the high vacuum region of the ion guide and the quadrupole. It has been previously shown, in the laboratory, that source parameters do not affect the ion mobility of the ions (Tebani et al. 2016). We have however checked that source parameters do not affect the drift times of the lipid ions, and consequently the CCS values. (data not shown).

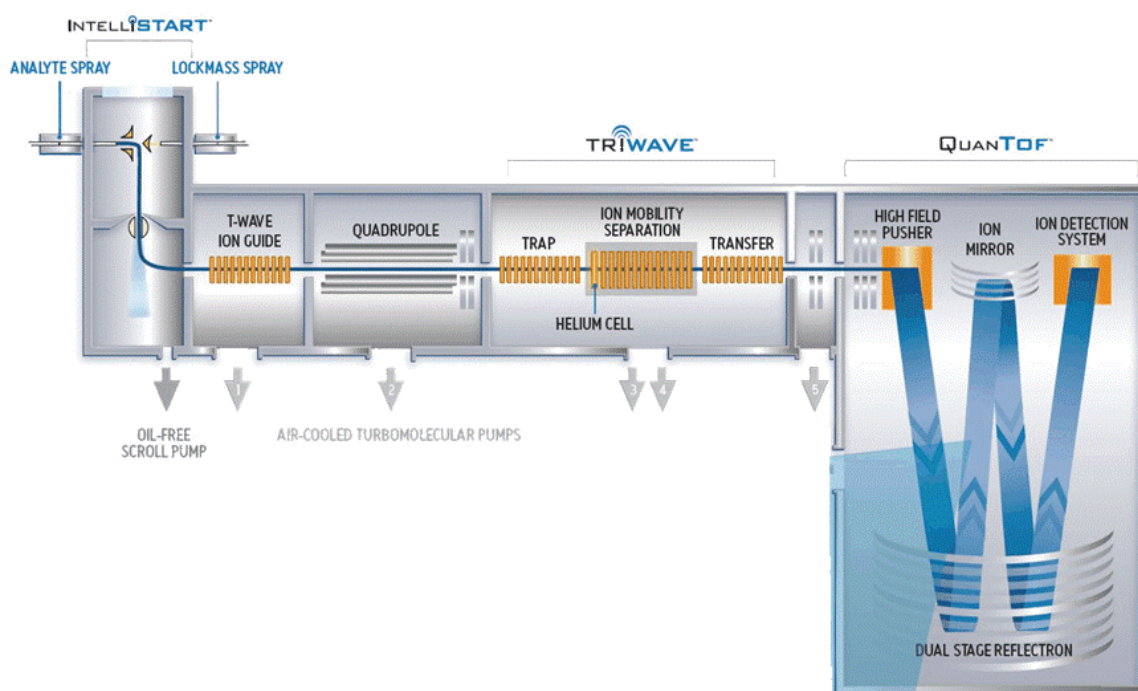


Figure III-4: Schematic representation of the Synapt instrument (Waters Corporation)

3.4.2. Influence of the IMS conditions

First, optimal IMS conditions were determined adjusting the IMS pressure, wave height and velocity, to enhance the ion mobility separation of lipid standard ions, by visualizing the drift time window and the distribution of lipid species.

A careful attention must be paid to the optimization of these parameters which are wave height and velocity to avoid some issues which can occur using too small or too high values. For example, the wrap around phenomenon can occur when slower ions are overtaken by faster ions.

After an optimization, three different conditions have been chosen and compared, using the same height of 40 V and different velocities of 500, 650 and 800 m/s. A high repeatability of the CCS values were retrieved with a very low mean RSD of 0.21%.

The TWIMS conditions represent an important factor to consider in order to obtain interoperable CCS values.

3.5. Conclusion and perspectives

The influence of ESI source as well as ion mobility parameters on the determination of lipid CCS values has been estimated for the three different IM devices. In the case of TIMS-TOF instrument, the results showed that infusion and source parameters (flow-rate and temperature of the desolvation gas as well as nebulizer gas pressure) have significant impact on ion mobilities measures and consecutively on the determination of CCS values, in agreement with previous results (L. Zhang et al. 2022). This can be explained by the location of the TIMS cell right after the ESI source. These results showed that source parameters need to be adjusted in order to ensure good desolvation of the ions. Then, internal ion mobility calibration permitted to retrieve comparable CCS values and provided a solution of CCS dependence upon source parameters. Thus, precise determination of the CCS values could be achieved for lipids from human plasma analyzed by LC-TIMS-MS. The study of source conditions in DTIMS instrument also allowed to show a small effect of the source parameters on the ^{DT}CCS values. This effect has not been proved in TWIMS instrument, due to the physical configuration of the instrument. Whatever the instrument, identical source conditions have to be applied for both calibrant and the samples analyses to avoid inaccurate CCS determination, in agreement with previous studies (Gabelica et al. 2019).

Then, the ion mobility parameters of each IMS cell have been studied, to evaluate their influence on the CCS determination. In the case of TIMS, the resulting CCS were highly similar values (RSD < 0.25%) showing high robustness even when changing IMS parameters and even using PASEF mode. For DTIMS, the RSD were lower than 0.5% even using multiplexing strategy. In TWIMS instrument, the wave height and velocity must be correctly adjusted to avoid some separation issues. Taking care of this particular point, the RSD was about 0.2% by comparing three IMS conditions.

After the evaluation of these experimental parameters, optimisation of the source and IMS parameters have been carried out for the three instruments, in order to evaluate the other potential sources of deviations, as the calibration and the use of different instruments.

Chapter IV. Study of the TWIMS calibration procedure towards the reduction of the CCS deviations

4.1. Introduction

In this chapter, the calibration procedure was studied as it is a crucial step for the determination of the CCS values using secondary methods. For that, eleven commercial calibrants were studied, in both positive and negative mode, on the TWIMS instrument. Lipids of human plasma were chosen as model analytes, to evaluate the ^{TW}CCS values obtained from the different calibrants. The purpose of this chapter is highlighted in the Figure IV-1 with the grey surround.

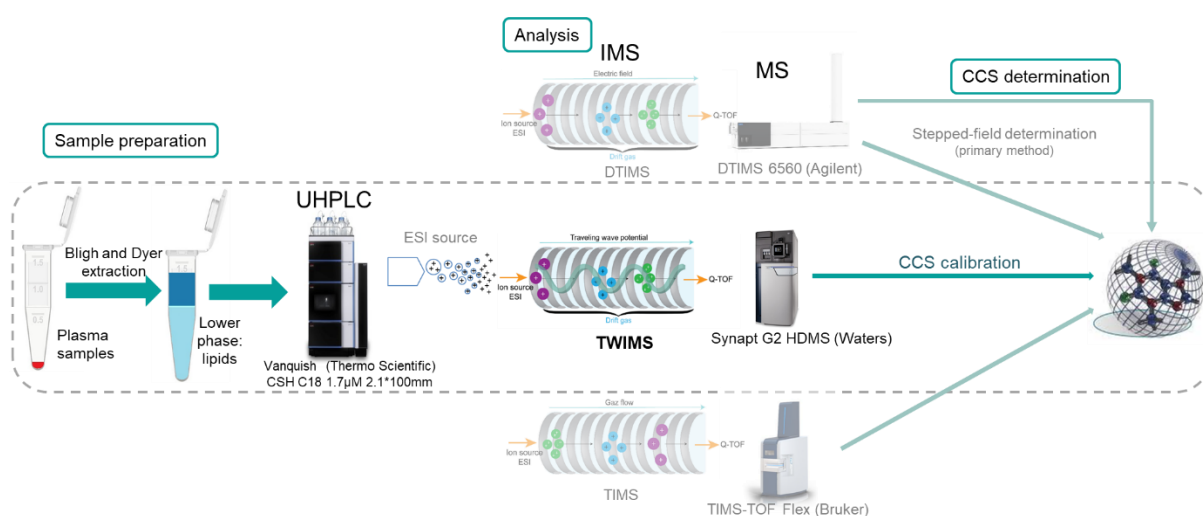


Figure IV-1 : Schematic representation of the objective of the chapter 4

After a careful evaluation of the calibrant, the human plasma lipid CCS values have been determined using the TWIMS instrument. A re-calibration strategy has been proposed to lower the deviations due to the use of different calibrants.

4.2. Study of calibrants

As previously described in the Chapter II, numerous calibrants commonly used in the literature (Table II-3) are commercially available. The use of a wide variety of calibrants can induce significant deviations in the determination of the CCS values.

To use a compound or a compound mixture as IMS calibrant, reference CCS values are required. Numerous reference CCS values have been published (see Chapter II) and are used in many studies. However, in the case of some calibrants, various CCS values are reported in the literature, differing from one article to another. Thus, the CCS values of polyalanine were compared among four different studies and the results proved to strongly diverge with deviations up to 3% (Richardson et al. 2021).

Besides, the Major Mix calibrant (provided by Waters Corporation) can incorporate different molecules depending on the study considered, which might have direct consequences on calibration accuracy.

As mentioned above, in the case of the widely used Tune Mix calibrant, different reference CCS values have been reported. Since the study by Stow et al. which compared the ^{DT}CCS values using four distinct instruments, (Stow et al. 2017), most publications reported that authors used their own intra-laboratory CCS values. Moreover, in the case of the Tune Mix calibrant, there are at least two distinct commercial solutions that surprisingly do not contain exactly the same compounds.

As the accuracy of the calibrant CCS values can vary significantly from one data resource to another, particular attention must be paid to the choice of a calibrant and its reference CCS values (Richardson et al. 2021)

A stability study of eleven calibrants have been performed, by keeping the calibrant solutions at different conservation temperature (-80°C, -20°C and ambient temperature) during six months. Another stability study relative to the addition of formic acid was also performed for all the calibrants, in both positive and negative mode, adjusting the content of formic acid in the solution to 1, 10 or 20%. As expected, calibrant solutions were more stable when stored at -80°C, thus the solutions were stored at -80°C for better stability or were freshly prepared, just before the analyses.

Therefore, we envisaged to perform the most comprehensive evaluation of available commercial calibrants for ^{TW}CCS measurements and aim the harmonisation of the CCS measurements proposing a strategy to realign CCS in a standardized approach. These results are presented in the article which was accepted in the journal *Analytica Chimica Acta*.

4.3. Study of calibrants to standardize lipid ^{TW}CCS values (Article)

A re-calibration procedure for interoperable lipid collision cross section values measured by traveling wave ion mobility spectrometry

Anaïs C. George¹, Isabelle Schmitz-Afonso¹, Vincent Marie², Benoit Colsch², François Fenaille², Carlos Afonso¹, Corinne Loutelier-Bourhis^{1*}

¹Normandie Université, UNIROUEN, INSA Rouen, CNRS, COBRA, 76000 Rouen (France)

²Université Paris-Saclay, CEA, INRAE, Département Médicaments et Technologies pour la Santé (DMTS), MetaboHUB, F-91191 Gif sur Yvette, France.

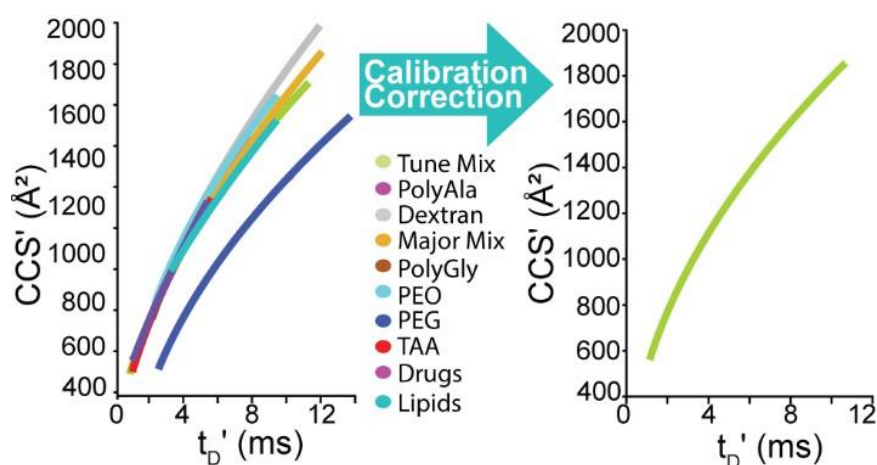
Keywords:

- Lipidomics
- Metabolomics
- Ion mobility calibration
- Collision cross section
- Ion mobility-mass spectrometry
- TWIMS

4.3.1. Abstract

Collision cross sections (CCS) have been described as relevant molecular descriptors in metabolomics and lipidomics analyses for ascertaining compound identity. Ion mobility spectrometry (IMS) allows to determine CCS with different techniques, such as drift tube ion mobility spectrometry (DTIMS), traveling wave ion mobility spectrometry (TWIMS) or trapped ion mobility spectrometry (TIMS). In contrast with DTIMS where CCS can be obtained directly with measured drift times and mathematical relationship, TWIMS and TIMS techniques require an additional step of calibration to obtain CCS values. However, literature reports significantly disparate CCS values depending on the calibrant used (often more than 10%), as no consensus has been reached to define a universal CCS reference standard or harmonized calibration procedure. Therefore, publicly available CCS databases cannot be regarded as readily interoperable and exchangeable.

Here, we performed a comprehensive evaluation of 11 distinct CCS calibrants in a traveling wave ion mobility spectrometry-mass spectrometry (TWIMS-MS) instrument. We showed that, using lipids from plasma as model compounds, CCS determination drastically fluctuates from one calibrant to the other with up to 25% differences, which precludes direct CCS comparison. Using the large panel of calibration curves generated, we showed that any CCS value can be efficiently re-calibrated relatively to the calibration curve made with the widely used Tune Mix solution whatever the calibration procedure originally used. The re-calibrated CCS values for each calibrant constitute a database which allows to correct any deviation on lipid CCS values whatever the calibrant originally used. Resulting corrected CCS values from plasma lipids were thus efficiently matched to those previously reported in the literature (with deviations <2%). Therefore, this work shows that unique and comparable CCS values can be obtained upon recalibration relatively to Tune Mix CCS values, while also paving the way for the establishment of a universal CCS database of various metabolite or lipid classes.



4.3.2. Introduction

Ion mobility spectrometry [1] (IMS) is a gas-phase separation technique of ions subjected to an electric field and migrating through a buffer gas, such as N_2 or He. The ions are separated in the ion mobility cell depending on their charge, size and shape. Measured drift times can then be converted into collision cross sections (CCS). Different ion mobility techniques have been described, for example, the drift tube ion mobility spectrometry (DTIMS), the trapped ion mobility spectrometry (TIMS) with a ramped static electric field, and the traveling wave ion mobility spectrometry (TWIMS) with a dynamic electric field, which could be schematized by successive potential waves. For the same length, the

TWIMS provides better resolution than a drift tube with a uniform electric field [2]. Experimental stepped-field CCS can be directly determined by DTIMS using the Mason-Schamp equation [3]. However, some parameters must be known for robust CCS determination including drift tube length, temperature and pressure, parameters that can be difficult to precisely measure. Due to these difficulties, CCS values determined by DTIMS in stepped-field mode may differ with significant deviations from one DTIMS instrument to another. With non-uniform field instruments such as TWIMS, despite some recent progress on the ion motion understanding [4], a calibration with standards of known CCS values is necessary to establish CCS from drift times. Commonly, a power-law calibration is used with ions of known CCS values obtained from DTIMS [5]. Another calibration approach based on fundamentals of ion motion has recently been proposed to obtain more robust CCS [4].

The reliable identification of metabolites and lipids in complex biological samples by liquid chromatography coupled to high resolution mass spectrometry (LC-HRMS) is still highly challenging due to the wide diversity of co-occurring chemical structures. It is now admitted that CCS values represent relevant descriptors, in addition to retention times, accurate mass measurements, isotope pattern as well as fragmentation spectra [6]. CCS values have been described to be a more reproducible descriptor than retention time values [6,7], and their use in metabolomics and lipidomics is therefore more and more widespread for improving confidence in metabolite/lipid annotation. In that context, several CCS databases have been created for compound annotation, such as the Bush [8] or Schroeder [9] databases or other online databases such as Unified CCS compendium [10] or AllCCS [11]. AllCCS database is particularly helpful for the annotation of small molecules and affords a collection of both experimental and predictive CCS values. Moreover, confidence levels have been associated to the CCS published in this database: level 1 corresponds to the most reliable ones, with at least two experimentally obtained CCS values within 1% difference from two independent datasets using DTIMS. If the difference between at least two CCS values is below 3% using DTIMS, TIMS or TWIMS, the attributed level is 2. The level 3 corresponds to a single CCS value. There is a particular level named "level conflict" which corresponds to a CCS difference larger than 3%. Finally, the level 4 corresponds to predicted values. The confidence in metabolite identification based on CCS measurements depends on the CCS tolerance [7, 12]. Even if an error of less than 2% [12] is generally considered acceptable, the use of CCS values in identification workflows often implies tolerance below 1% [13], in particular for isomers with very close CCS values. It was shown that CCS values obtained with instruments equipped with the same ion mobility technique and involving standardized calibration and acquisition procedures are highly reproducible, with interlaboratory reproducibility within 2% [6,7,14,15] or even 1% [16,17]. However, CCS values obtained with the same instrument but using different calibrants [18] as well as CCS values obtained with different instruments [19] can be substantially different. For example, drastically different CCS values have been reported for LPC (lysophosphatidylcholine) 16:0, *i.e.* 223.9 Å² [20], 229.8 Å² [21], and 233.3 Å² [22]. Deschamps et al. [23] observed a systematic shift (up to 9%) when comparing their phospholipids CCS measured by TWIMS to the literature values. Therefore, to use CCS as a reliable descriptor in metabolomics/lipidomics workflows and to obtain interoperable databases, it is necessary to minimize as much as possible the deviations between CCS values.

Polyalanine [24] has been historically used as CCS calibrant in various publications, even in lipidomic studies. [25] Currently, mixtures of various compounds developed by instrument manufacturers have also been used in lipidomics and metabolomics, as the ESI low concentration Tuning Mix (Tune Mix) [9, 16, 26-28] from Agilent which contains different hexakis(fluoroalkoxy)phosphazines and the Major

Mix IMS calibration kit [14, 15] from Waters which contains various small molecules, polyalanine and ultramark® components. Other calibrating substances have also been described such as dextran [29], polyglycine [30] or drugs [24]. Polymers can also be used including polyethylene glycol (PEG) [31], polylactic acid (PLA) or polyethylene oxide (PEO) [32]. The tetraalkylammonium salts (TAA) was proposed as a CCS calibrant [24, 33] or as internal standard [28]. Calibrants such as polymers, polyglycine, drugs and TAA are only used in the positive ion mode. Some calibrants are more specifically used for negative ion mode, such as polymalic acid [34]. Calibration should ideally be performed using calibrant molecules exhibiting similar physicochemical properties or from similar chemical classes and masses than analytes. Hines et al. [18] proposed the use of PC and PE to calibrate phospholipids CCS in positive and negative ion modes, respectively. Soft ion mobility conditions can also be used, which allow to eliminate the need of calibration [35] and use other calibrant species [36], however these soft conditions are not suited to large-scale analysis, such as lipidomics.

Nonetheless, the use of reference compounds still suffers from a lack of standardization due to disparities in CCS reported for each calibrating substance. The ion mobility community has recognized the need of a consensus, especially in the choice of reference materials and their CCS values [5].

In this work, we propose a re-calibration procedure to build an interoperable database of calibrant-corrected CCS values obtained on a TWIMS instrument. Such a database can be used by any user of the ion mobility community in order to tend towards unified corrected CCS values, obtained by plotting any correlation curve against Tune Mix. For this purpose, a comprehensive and comparative study of currently available calibrating substances was performed. Our study was focused on lipidomics, and more specifically on lipids present in human plasma used as model analytes. To our knowledge, this work represents the first proposition of corrected CCS database for IMS calibrants on a TWIMS instrument, thus allowing the drastic diminution of CCS deviations due to distinct calibrations.

4.3.3. Experimental section

Chemical and reagents.

Methanol (MeOH), chloroform, acetonitrile (ACN), isopropanol and formic acid (FA) were purchased from Fischer Scientific (UK, Loughborough), while ammonium formate was from Sigma-Aldrich (Saint Quentin Fallavier, France). Except chloroform which was HPLC grade, all solvents and buffers used were LC-MS grade. The IMS calibrants are prepared according to some reference publications, as detailed in supplementary information. Leucine enkephalin was purchased from Sigma-Aldrich (Saint Quentin Fallavier, France).

Sample preparation.

Plasma lipids were extracted according to a modified Bligh and Dyer method [37] as described by Seyer et al. [38] using human plasma CPD (Citrate-Phosphate-Dextrose) from three donors from BioPredic International (Rennes, France). 100 µL of human plasma CPD was added to 490 µL of chloroform/methanol 50:50 (v/v). Samples were vortexed for 60 seconds and then sonicated for 30 seconds using a sonication probe. Extraction was performed during 2 hours at 4°C with mixing. Then 75 µL of ultra-pure water was added, and samples were vortexed for 60 seconds before centrifugation at 12,000 g for 15 min at 4°C. The upper phase (aqueous phase), containing ganglioside species and several lysoglycerophospholipids, was transferred into a glass tube and then dried under a stream of nitrogen. The interphase, which consists in a protein disk, was discarded and the lower rich-lipid phase (organic phase) was pooled with the dried upper phase and also dried down. 400 µL of chloroform/methanol 50:50 (v/v) was added to eliminate the possible protein residue. After

centrifugation at 12,000g for 10 min at 4°C, samples were dried. Samples were then reconstituted with 100 µL of chloroform/methanol 50:50 (v/v), diluted 1/10 with a solution MeOH/isopropanol/H₂O 65:35:5 (v/v/v), vortexed for 30 seconds then centrifuged at 12,000 g for 10 min at 4°C before injection into the LC-HRMS system.

LC-IMS-MS analysis.

The LC-IMS-MS experiments were performed using an UHPLC system (Vanquish, Thermo Scientific, San Jose, CA, USA) coupled to an IMS Q-TOF mass spectrometer (SYNAPT G2 HDMS, Waters MS Technologies, Manchester, UK) equipped with an electrospray interface and a traveling wave ion mobility (TWIMS) cell.

Chromatographic separations were carried out using a 2.1 × 100 mm, Acquity UPLC CSH C18 1.7 µm column (Waters, Manchester, UK) equipped with a 0.2-µm prefilter. The sampler and column oven temperatures were set at 10 °C and 50 °C, respectively. The injection volumes were 2 µL and 10 µL, in positive and negative ion modes, respectively. The flow rate was 0.4 mL min⁻¹. Mobile phase A consisted of acetonitrile/aqueous ammonium formate (10 mM) (60:40) and mobile phase B of isopropanol/acetonitrile/ aqueous ammonium formate (10 mM) (88:8:4); 0.1 % formic acid (FA) was added to both mobile phases. The gradient was as follows: 0–2 min, 32% B; 2–14 min, 32–75% B; 14–26.5 min, 75–100% B; 26.5–30 min, 100% B; 30–30.5 min, 100–32% B; 30.5–35 min, 32% B.

Mass spectra were recorded over a *m/z* 50–2000 range in the sensitivity mode (resolution 10,000 FWHM at *m/z* 950). External mass calibration was performed with a sodium formate solution 10% FA/0.1M NaOH/ACN (1:1:8) before each analysis. Lockmass correction was performed by infusing leucine enkephalin (2 ng µL⁻¹ in water/isopropanol (1:1), 4 µL min⁻¹) *via* the LockSpray™ interface. Source and LockSpray™ parameters are given in the Table S1. MS/MS experiments were performed in both positive and negative ionization modes, under data dependent acquisition conditions (Waters Survey analysis) (Table S2). To confirm specific identifications of weak-abundant species in plasma samples, MS/MS acquisitions were performed in a targeted manner by selecting precursor ions in the quadrupole with a window of 1 *m/z* unit and using several retention time windows. Lipid identification was performed from *m/z* measurements, MS/MS spectra and using the MS-DIAL software [20]. All the annotations were manually verified with Masslynx 4.1 software (Waters).

The IMS parameters were: helium cell flow, 180 mL min⁻¹; IMS cell nitrogen flow, 80 mL min⁻¹ (2.9 mbar). For method validation, various traveling wave heights and velocities were applied, 30, 35, 40 V and 400, 500, 600 m s⁻¹ in positive mode and 500, 650, 800 m s⁻¹ in negative mode. Calibrant solutions were injected in the flow injection analysis (FIA) mode with a 50 µL min⁻¹ flow rate of ACN/H₂O (50:50) for all calibrants except lipid standards, where mobile phase A was used.

CCS measurements.

Raw data were processed with UNIFI 1.9.4 (Waters) to extract the corrected drift times, *t*_D' of both calibrants and samples. The drift times given by UNIFI software are corrected drift times *t*_D' which take into account a constant C representing the EDC Delay of the Synapt and the *m/z* of the ions according to the following equation [5]:

$$t'_D = t_D - \frac{C\sqrt{m/z}}{1000}$$

A calibration file was created for each calibrant giving t_D' values determined by the Unifi software and the corrected collision cross sections CCS' values calculated with the following equation:

$$CCS' = \frac{CCS \sqrt{\mu}}{z} \text{ with } \mu = \frac{m_{ion} m_{gaz}}{m_{ion} + m_{gaz}}$$

where CCS , z and μ correspond respectively to a reference CCS determined by DTIMS, the charge of the ion and the reduced mass of the ion in a definite buffer gas.

The CCS values of lipids from plasma samples and lipid standards using every calibration procedure were extracted from UNIFI software by adding the corresponding calibration file in the raw data. The calibration was made by UNIFI, which uses the equation [39]:

$$CCS' = A (t_D' - t_0)^N$$

where A , N and t_0 are fitting parameters, which demonstrated best results than the fitting without t_0 . In parallel, the CCS determination has been manually made using Masslynx 4.1 (Waters), Driftscope v2.9 (Waters) and Origin Pro 2018 b9.5.0.193 softwares to certify the UNIFI process (*i.e.* the calculation of the corrected drift time t_D' and the use of a calibration equation including the t_0 parameter to force the curve through zero). CCS values thus obtained were compared using Excel and a homemade Python script, which also allowed automated CCS comparison between different ion mobility conditions.

4.3.4. Results and discussion

Investigation of various ion mobility calibrants.

The first step of our study was to investigate most of the published and commonly used IMS calibrants. Thus, eleven different calibrants (Table SB1) have been analysed and used to build the corresponding calibration curves. Figures 1, SA1 and SA2 show the calibration curves obtained for the tested calibrants (equations are displayed in Tables SA3 and SA4) in both positive and negative ionisation modes. For each calibrant, different ion mobility parameters with different wave heights and velocities in both ionization modes were tested to evaluate the repeatability of CCS measurements (Figures SA3 SA10). Except PEG, all calibrants present similar calibration curves (Figure 1). Careful examination of the data demonstrates that the Tune Mix and lipid-based calibration curves are almost superimposed (Figure 1). Of note, calibration curves built from TAA, polyglycine and drug standards do not cover the entire lipid CCS range, which makes them inappropriate in the present context (Figure SA1).

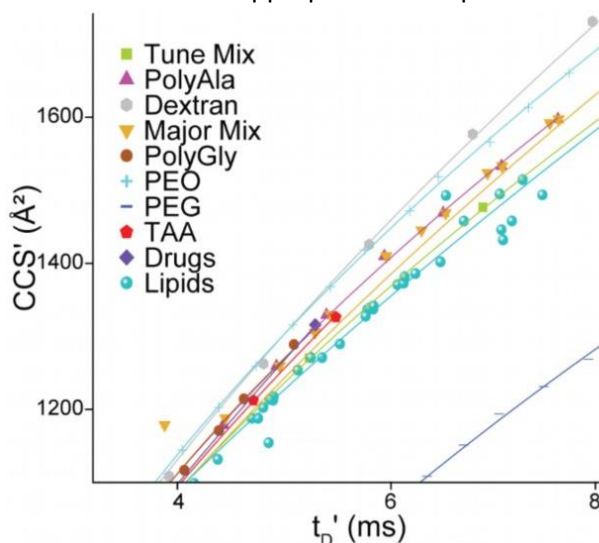


Figure 1: Calibration curves $CCS' = f(t_D')$ for different calibrants described for ion mobility in positive mode with an IMS pressure = 2.9 mbar, wave height=40 V and wave velocity=600 m/s.

Evaluation of different calibrants for plasma lipid CCS measurements.

The second step of this work was to evaluate the above tested calibrants for CCS measurements of lipids included in human plasma as model analytes. Therefore, LC-IMS-MS was carried out in positive and negative ionisation modes to detect the various lipid classes present in the plasma. Figure 2 illustrates the chromatographic separation of the lipid plasma extract analysed in the positive ionisation mode. Lipid annotation was first achieved thanks to accurate mass measurements and MS/MS spectra (Figures SA11-24 [40]). Thus, 59 and 51 lipids have been identified in positive and negative ionisation modes, respectively. The combination of IMS with the LC and MS dimensions allows to increase peak capacity by distinguishing overlapping signals that might originate from isomeric lipids. LC and IMS separations thus facilitate the acquisition of specific MS/MS spectra of isobaric and isomeric lipids. Under optimized LC-IMS-MS(/MS) conditions, up to 110 unique lipids can be identified in human plasma (Table SD1).

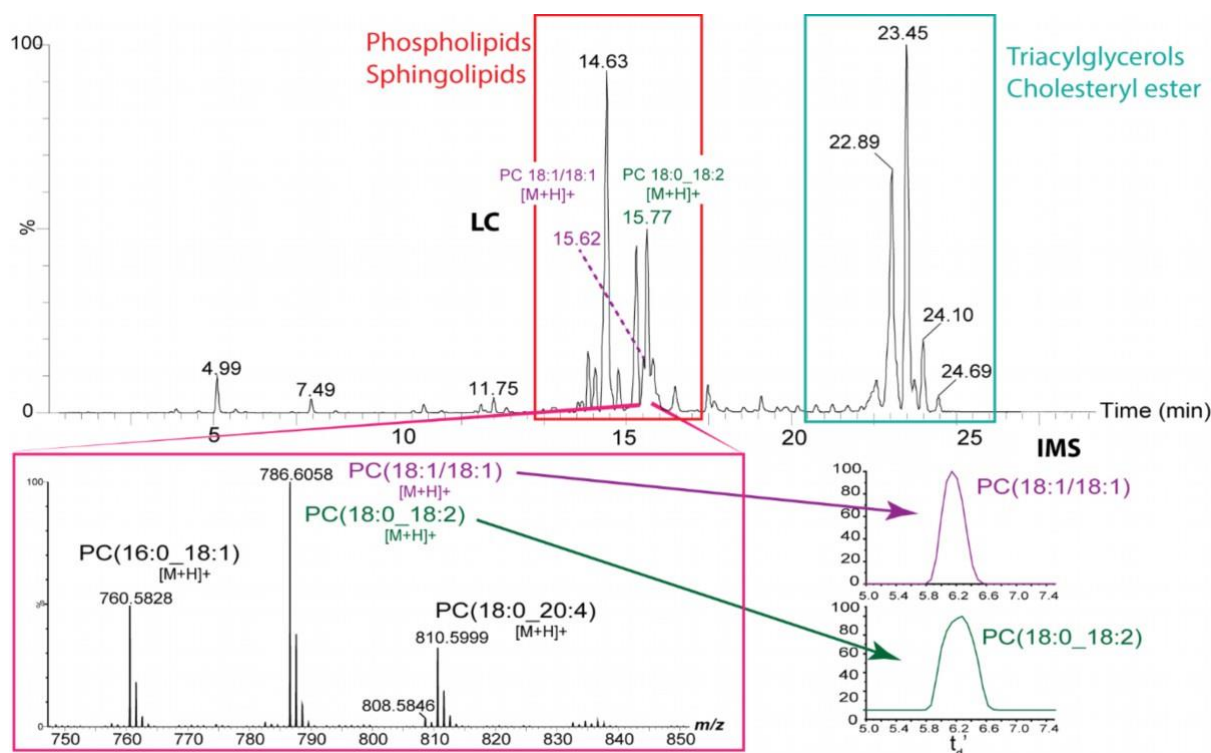


Figure 2: LC-IMS-MS of plasma samples in positive mode: chromatographic separation shows two main distinct time windows (phospholipids + sphingolipids, around 12-18 min and triacylglycerols + cholesteryl ester at 21-25 min). The MS spectrum corresponding to time window 15.50-15.80 min depicts three distinct protonated phosphatidylcholine (PC). Owing them, the m/z 786.6058 is an isomer mixture since different drift time and peak width (full width at half maximum, FWHM) were evidenced in the IM spectra. It is admitted that FWHM can be indicative of isomer heterogeneity when it is larger than expected considering the sole diffusion phenomenon [41]. Thus, the IM spectrum of the PC 18:0_18:2 which displays a larger peak than the one of the PC 18:1/18:1 means that PC 18:0_18:2 is probably a mixture of the two isomers PC 18:0/18:2 and PC 18:2/18:0. MS/MS spectra of both species are shown in Figures SA11-24.

After annotation, the CCS of the lipids present in the plasma sample have been determined in both positive and negative ionisation modes, using the different calibrants and the UNIFI software. Mean CCS values of plasma lipids and lipid standards were obtained from three technical replicates and under three different ion mobility conditions (see experimental part for wave heights and velocities

values) for having more representative values (corresponding drift times are displayed in Tables SC1 and SD1). Therefore, RSDs could be calculated with nine values. The results obtained for six representative lipid species are shown in Figure 3 for positive mode and Figure SA25 for negative mode. For each lipid, CCS values are of the same order of magnitude for almost all the calibrants, except for PEG calibrant, which led to highly underestimated CCS values. The disparities between CCS values (disparities are calculated by subtracting the most extreme CCS values before dividing by the mean) are up to 8% when excluding PEG and more than 27% when including PEG, in positive mode. In negative mode, the disparities are up to 3.5%. These values are far above the acceptable 1% limit, recommended by various publications [13]. Consistently with the calibration curves of Figure 1, we could notice that both the Tune Mix and the lipid calibrants led to very close CCS values for all the studied lipids while the other calibrants (except PEG) yielded higher CCS values. As a matter of fact, the mean relative deviations (mean relative deviation calculated by subtracting compared values by the mean of both values) between CCS calibrated with lipid standards and Tune Mix were within 0.7% in positive mode. All the lipid CCS values are reported in Tables SC2-3 for lipid standards and SD2-3 for plasma lipids. These results highlighted and confirmed the deleterious impact on CCS measurement accuracy of using different calibrants.

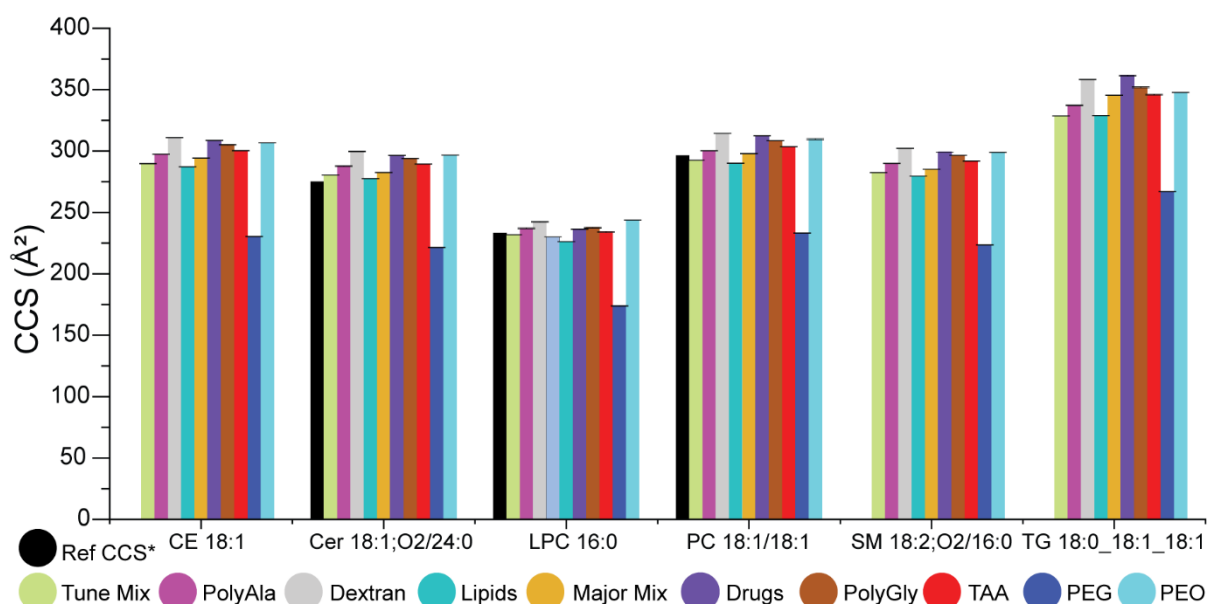


Figure 3: CCS values of representative lipids according to the calibrant used in positive ion mode. Ref CCS* are literature CCS determined by DTIMS in stepped field mode (if available). The error bars represent the RSD on nine values. The mean RSD are below 0.3% for all calibrants, thus error bars are not visible.

Then, CCS values determined with each studied calibrant were compared to lipid CCS reported in the literature or in public databases [27]. Several CCS values have been published for the same lipids, but using different IMS instruments, methodologies and calibrants, but unfortunately, only a few derived from DTIMS instruments. We decided to consider all the published CCS in the following order of relevance: i) the CCS obtained with DTIMS in stepped-field mode [28], ii) CCS determined with DTIMS in single field mode with an additional calibration step, [27] and iii) CCS derived from TIMS [20,42,43][20, 42, 43] or iv) TWIMS [18]. This comparison allows to check the general trend of the several calibrants for a maximum of lipid species. However, as previously mentioned, the literature CCS values can vary from one technique to another or from publication to another, we compared our CCS values with those from the literature determined by either DTIMS (stepped field or single-field),

TIMS or TWIMS. For that, we report the mean CCS values and RSD according to each technique (Figures S4, SA26-27 and Tables SC2.b, SD2.b, SC3.b and SD3.b). The comparison was then gathered in Table SD4. The CCS values depended highly from the reference publication, thus, all the publications used are also compared with our results in Tables SC2.c, SC3.c and SD2.c, SD3.c with the resumed comparison in Table SD5. The Figure4 and SA26-27 depict the mean relative deviations between literature CCS determined in stepped-field DTIMS mode and our plasma-derived lipid CCS values determined with each calibrant in both positive and negative modes. Thus, in positive mode, the largest deviations observed were near 20% with PEG as calibrant, as expected (see above). This polymer was used to calibrate saponin ions [44] but never in lipidomics analysis, thus potentially confirming its inappropriateness for lipids.

TAA, polyglycine and drug standards also led to large deviations, up to 3%, because their CCS range is not in agreement with the CCS range of plasma lipids. Therefore, it logically induces a bias in CCS determination. Although, PEO, dextran, polyalanine, Major Mix and polymalic acid cover the whole CCS range of plasma lipids, the mean relative deviations were still higher than 2% for these five calibrants in both acquisition modes. The deviations observed following polyalanine and polyglycine calibration could be potentially explained by co-occurring different conformations of these peptides that could induce ion mobility peak broadening, and consequently inaccurate or biased CCS measurements. This has already been reported for multicharged ions [45]. Our data are consistent with those from Hines et al. who demonstrated also the inherent errors of using polyalanine for calibration of lipids CCS [18]. In the case of the Major Mix IMS Calibration kit, some laboratories do not use the same ions from this mixture to build their calibration curves, thereby introducing additional CCS measurement variability (Table SA5) [19].

The smallest deviations observed between our CCS and those from the literature in stepped-field DTIMS mode were obtained with Tune Mix and lipid standards, yielding around 1% and less than 1% differences in positive and negative ionisation modes, respectively. Comparison with CCS values reported with TIMS or TWIMS leads to larger deviations, in most cases. In the case of published TWIMS CCS, the deviations are lowest using Major Mix (that calibrant mixture contains especially small molecule and polyalanine oligomers) in positive mode, which can be explained by the fact that most of the published CCS values are from the publication of Paglia et al, which used polyalanine as calibrant. In negative mode, the minimal deviations were observed with the calibrant lipid standard more probably because the published CCS are almost from the publication of Hines et al, 2017 which used PE and PC as calibrants. The deviation is about 1.68%, which can be explained because the lipid standards used contains several lipid classes, and not only PE and PC species. Comparing our re-calibrated CCS (by Tune Mix) with reported TIMS CCS values, the mean deviations are 0.41% [42], 0.33% [43] and 1.29% [20] according to the publication. For the two first ones, the Tune Mix was used as calibrant which explain the lowest deviation. For the third, the authors did not mention the calibrant used, which can be explained the higher deviation. Interestingly, CCS derived with different instrumental set-ups but with the same calibration procedure seem more similar than those obtained from the same instrument but using different calibrants. On the one hand, publications mentioned that CCS of lipids present in plasma samples seem correctly calibrated by lipid standards belonging to the same chemical class [18]. However, lipids can be of highly different structural classes exhibiting fatty acid chains of variable length and unsaturation degree [46]. Moreover, polyfunctional lipid species can present different ionized lipid species that can behave differently in the ion mobility cell.

Nevertheless, distinguishing all lipid classes, individual species and isomers to find the optimal standard to calibrate lipid species seems difficult in large-scale lipidomics analyses.

Tune Mix appear to be a good candidate as calibrant as it is largely used in the literature and commonly used for the measurement of drift tubes length. Moreover, it exhibits a wide range of CCS and narrow IM peaks. Many laboratories already use this mixture for either mass or ion mobility calibration [47]. Because of its extended m/z and CCS ranges (m/z 118-2722 and 113-2834, and 122-438 Å² and 109-432 Å² for positive and negative modes, respectively), Tune Mix can be successfully used in many fields of research and for many types of samples. An interlaboratory study was devised to obtain reliable CCS values for Tune Mix components using DTIMS [16] CCS values from the four involved laboratories were within 0.29% RSD (Table SA6). Since this publication, the ion mobility community appears to have reached a consensus on CCS values for Tune Mix ions [16]. One limitation of this calibrant is its inadequacy to calibrate multicharged ions since, it is recommended to calibrate species with ions of the same charge state [48]. Note that multicharged ions are more likely observed for proteins or peptides rather than for metabolites or lipids meaning that Tune Mix can be regarded as a possible reference calibrant in metabolomics or lipidomics analyses.

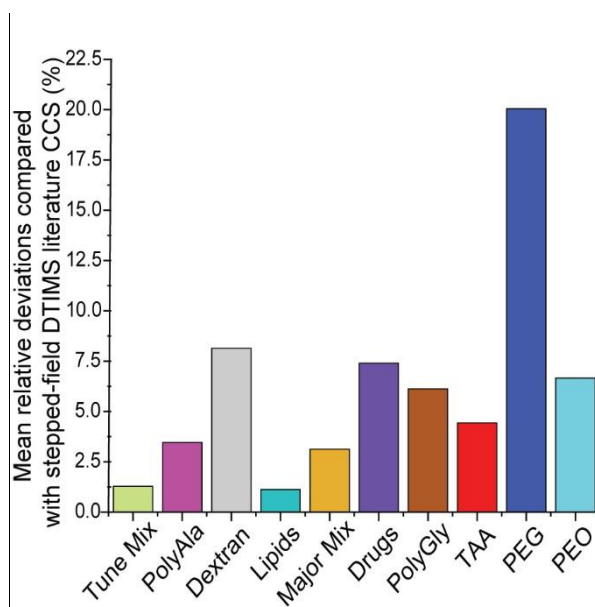


Figure 4: Comparison of deviations between lipid CCS from our calibrations and literature CCS determined with DTIMS in stepped-field mode according to the calibrant in positive mode

Toward a calibrant-corrected CCS database

As previously mentioned, and as shown by Figure1, S1 and S2, we propose to use Tune Mix as a reference calibrant. It demonstrated good repeatability in various ion mobility conditions, with a RSD on nine replicates below 0.3% in both ionisation modes. In addition, the deviations between our experimental CCS and literature CCS values are close to 1% and 2% in positive and negative ionisation modes, respectively.

In order to correct the significant deviations observed with the other calibrants, the CCS values of all the calibrants used were realigned to those obtained with the Tune Mix, by re-calibrating the calibrants with Tune Mix (Figure 5). The corresponding re-calibrated CCS values are presented in supplementary information (Table SB2). They constitute a calibrant-corrected CCS database that can be used to determine the CCS values of any sample whatever the calibrant that has been used. For example, we

used these calibrant-corrected CCS values to redefine the CCS of the lipids present in plasma, with the UNIFI software (Table 1 and Tables SC4-5 and SD6-7).

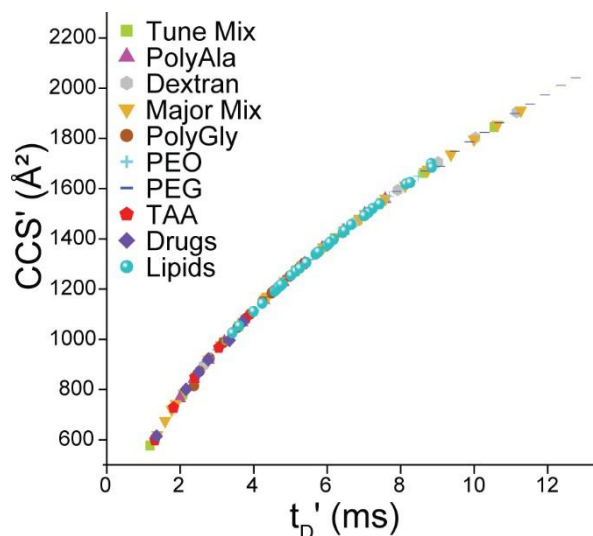


Figure 5: Tune Mix corrected calibration curves $CCS' = f(t_D')$ for different calibrants in positive mode with an IMS pressure=2.9 mbar, wave height=40 V and wave velocity=600 m/s. The CCS' represented are those re-calibrated by Tune Mix.

Table 1: CCS (\AA^2) of some plasma lipids in function of the calibrant, before and after re-calibration with Tune Mix. The ^{Corr}CCS columns correspond to lipid CCS determined using the calibrant-corrected CCS after Tune Mix realignment

Lipids on plasma	Ions	m/z	rt (min)	Stepped-field ΔT_{CCS}	Tune Mix			Lipid standards	
					CCS*	CCS*	$^{Corr}CCS^*$	CCS*	$^{Corr}CCS^*$
CE 18:1	$[M+NH_4]^+$	668.635	26.5		289.75	297.46	289.73	287.20	289.71
Cer 18:1;O2/24:0	$[M+H-H_2O]^+$	632.638	22.71	275.06 [28]	280.37	287.78	280.34	277.53	280.32
LPC 16:0	$[M+H]^+$	496.339	5.23	233.3 [22]	231.75	237.00	231.72	230.06	231.71
PC 18:1/18:1	$[M+H]^+$	786.599	18.2	296.42 [22]	293.31	301.11	293.28	290.95	293.27
SM 18:2;O2/16:0	$[M+H]^+$	701.557	15.44		282.47	289.95	282.44	279.69	282.42
TG 18:0_18:1_18:1	$[M+NH_4]^+$	904.834	26.75		328.61	337.24	328.61	328.88	328.66

*mean of 9 experiments

The recalibration performed with Tune Mix allows obtaining consistent CCS values for each lipid regardless of the calibrant, in both ionisation modes (Table 1 and Tables SC4-5 and SD6-7). The disparities between the CCS values obtained with the different corrected calibrants are within 0.2% in the positive mode and 0.07% in the negative mode, compared to 27% and 3.6% before correction, respectively.

This correction method allows to have a universal recalibration procedure and make comparable CCS values obtained with different calibration mixtures and within different facilities. Thus, this procedure can be further exploited to build an interoperable CCS database for lipids analysis as well as other species.

In order to demonstrate the relevance and value of our methodology, we used it to recalibrate a previously published dataset about the analysis of lipids from *Pseudomonas aeruginosa* [23]. This dataset was selected because the lipid CCS were determined using various calibrants, polyalanine,

dextran and lipids, using a TWIMS cell and all the experimental parameters, including the drift times of the calibrants as well as the corresponding calibration curves were provided. After recalibration, CCS values proved very similar to those of the Deschamps' publication [23]. For example, in the case of PC 36:2, Deschamps et al. [23] published a CCS value of 288.2 Å², while literature CCS was about 291.12 Å² [20]. By applying the Tune Mix re-calibration, we determined a ^{Corr}CCS value of 291.20 Å², exhibiting a deviation of 0.03% with previously published CCS [18], and therefore in almost perfect agreement. This re-calibration considerably reduces the deviations with literature CCS and can be applied to any CCS value provided if the calibration protocol and drift times values are known. The mean relative deviation with literature CCS values was below 1% for six lipids of *Pseudomonas aeruginosa*, using re-calibrated polyalanine and dextran calibrants (Table SB2). Moreover, the mean relative deviation observed between the corrected Deschamps' CCS [23] and our corrected CCS was below 0.5%, for the same six lipids (Table SB3), thus interoperable CCS databases could be successfully obtained by using the calibrant-corrected database presented in Table SB2.

Thus, using this procedure, CCS values were obtained for 130 plasma lipids (75 in positive mode and 45 in negative mode, Tables SD2-3) and 57 CCS from lipid standards (37 in positive mode and 20 in negative mode, Tables SC2-3). In addition, we also applied our approach to lipids present in a commercial mixture of pure lipid standards (Differential Ion Mobility System Suitability LIPIDOMIX kit) for which CCS had not been yet reported to our knowledge, in negative mode. Thus, we could determine the CCS values of 8 lipid standards including 6 unreported from the DIMS LIPIDOMIX kit in negative mode; PA 14:1/14:1, PI 14:1/14:1, PE 14:1/14:1, PG 14:1/14:1, PS 14:1/14:1 and PC 14:1/14:1 and two other commercial standards, PC 16:0/16:0 and PC 20:0/20:0 (Tables SA7 and SC6). Twenty one new lipid CCS from plasma in both ion modes have also been determined, such as Cer 18:1;O2/12:0, PC 13:0/13:0 or LPC 18:0 (Tables SA8, SA9 and SD8).

4.3.5. Conclusions

Whereas numerous calibrants are employed for ion mobility calibration, there are significant disparities between these CCS scales. Up to 25% deviation in CCS determination can be obtained depending on the calibrant used. In this work we used the Tune Mix to re-calibrate the CCS of several calibrants commonly used. These newly adjusted scales enabled the determination of plasma lipid CCS with very slight variations between experimentally determined CCS values, hence eliminating calibrant-induced deviations. For the investigated lipids, less than 0.2% deviations were consistently obtained across calibrants.

As a consequence, we believe that the obtained calibrant-corrected CCS values for each calibrant constitute a first step toward a universal calibration database relevant to the ion mobility community. This procedure was validated with a previously published lipid CCS dataset. We showed that our approach led to CCS deviations below 0.5%, thus demonstrating the possibility to realign any CCS by applying our calibration curves if the drift times of the samples and the calibrant are reported. This re-calibration approach can be a first step toward the elaboration of interoperable databases gathering consistent CCS values. This can be extended to various workflows, in lipidomics and more generally in metabolomics. As a proof-of-concept, a first list of 130 plasma lipid CCS is provided incorporating twenty-five previously unreported ones.

We believe that the use of such recalibrated CCS values can improve the use of CCS as a universal descriptor and would limit discrepancies between reported CCS values. This is particularly important for isomer differentiation that often present very close CCS values. With the use of high-resolution IMS

systems such as cIMS, SLIM and TIMS, the need of accurate CCS measurement will be also a particularly important improvement.

Acknowledgements

The authors gratefully acknowledge Estelle Deschamps, for her collaboration by giving the t_D values of the lipids relative to the CCS published in Deschamps et al. and Kevin Giles, for his help in understanding the CCS determination on UNIFI software and Waters for the use of UNIFI software.

This work was partially supported by University of Rouen Normandy, INSA Rouen Normandy, the Centre National de la Recherche Scientifique (CNRS), European Regional Development Fund (ERDF), Labex SynOrg (ANR-11-LABX-0029), Carnot Institute I2C, the graduate school for research XL-Chem (ANR-18-EURE-0020 XL CHEM) by Region Normandie and the MetaboHUB infrastructure (ANR-11-INBS-0010 grant).

Appendix A. supplementary data

Supplementary data can be found in Section 4.3.7. and online at <https://doi.org/10.1016/j.aca.2022.340236>.

4.3.6. References

- [1] W.S. Barnes, D.W. Martin, E.W. McDaniel, Mass Spectrographic Identification of the Ion Observed in Hydrogen Mobility Experiments, *Physical Review Letters*, 6 (1961) 110-111.
- [2] V. Gabelica, E. Marklund, Fundamentals of ion mobility spectrometry, *Current Opinion in Chemical Biology*, 42 (2018) 51-59.
- [3] E.A.S.J. Mason, H. W., Mobility of gaseous ions in weak electric fields, *Annals of physics*, 4, 233-270, (1958).
- [4] K. Richardson, D. Langridge, S.M. Dixit, B.T. Ruotolo, An Improved Calibration Approach for Traveling Wave Ion Mobility Spectrometry: Robust, High-Precision Collision Cross Sections, *Analytical Chemistry*, 93 (2021) 3542-3550.
- [5] V. Gabelica, A.A. Shvartsburg, C. Afonso, P. Barran, J.L.P. Benesch, C. Bleiholder, M.T. Bowers, A. Bilbao, M.F. Bush, J.L. Campbell, I.D.G. Campuzano, T. Causon, B.H. Clowers, C.S. Creaser, E. De Pauw, J. Far, F. Fernandez-Lima, J.C. Fjeldsted, K. Giles, M. Groessl, C.J. Hogan, S. Hann, H.I. Kim, R.T. Kurulugama, J.C. May, J.A. McLean, K. Pagel, K. Richardson, M.E. Ridgeway, F. Rosu, F. Sobott, K. Thalassinou, S.J. Valentine, T. Wyttenbach, Recommendations for reporting ion mobility Mass Spectrometry measurements, *Mass Spectrometry Reviews*, 38 (2019) 291-320.
- [6] G. Paglia, P. Angel, J.P. Williams, K. Richardson, H.J. Olivos, J.W. Thompson, L. Menikarachchi, S. Lai, C. Walsh, A. Moseley, R.S. Plumb, D.F. Grant, B.O. Palsson, J. Langridge, S. Geromanos, G. Astarita, Ion Mobility-Derived Collision Cross Section As an Additional Measure for Lipid Fingerprinting and Identification, *Analytical Chemistry*, 87 (2015) 1137-1144.
- [7] G. Paglia, J.P. Williams, L. Menikarachchi, J.W. Thompson, R. Tyldesley-Worster, S. Halldorsson, O. Rolfsson, A. Moseley, D. Grant, J. Langridge, B.O. Palsson, G. Astarita, Ion mobility derived collision cross sections to support metabolomics applications, *Anal Chem*, 86 (2014) 3985-3993.
- [8] M.F. Bush, I.D.G. Campuzano, C.V. Robinson, Ion Mobility Mass Spectrometry of Peptide Ions: Effects of Drift Gas and Calibration Strategies, *Analytical Chemistry*, 84 (2012) 7124-7130.

- [9] M. Schroeder, S.W. Meyer, H.M. Heyman, A. Barsch, L.W. Sumner, Generation of a Collision Cross Section Library for Multi-Dimensional Plant Metabolomics Using UHPLC-Trapped Ion Mobility-MS/MS, *Metabolites*, 10 (2019).
- [10] J.A. Picache, B.S. Rose, A. Balinski, K.L. Leaptrot, S.D. Sherrod, J.C. May, J.A. McLean, Collision cross section compendium to annotate and predict multi-omic compound identities, *Chem Sci*, 10 (2019) 983-993.
- [11] Z. Zhou, M. Luo, X. Chen, Y. Yin, X. Xiong, R. Wang, Z.J. Zhu, Ion mobility collision cross-section atlas for known and unknown metabolite annotation in untargeted metabolomics, *Nat Commun*, 11 (2020) 4334.
- [12] G. Paglia, G. Astarita, Metabolomics and lipidomics using traveling-wave ion mobility mass spectrometry, *Nature Protocols*, 12 (2017) 797-813.
- [13] A. Delvaux, E. Rathahao-Paris, S. Alves, An emerging powerful technique for distinguishing isomers: Trapped ion mobility spectrometry time-of-flight mass spectrometry for rapid characterization of estrogen isomers, *Rapid Communications in Mass Spectrometry*, 34 (2020).
- [14] L.C. Nye, J.P. Williams, N.C. Munjoma, M.P.M. Letertre, M. Coen, R. Bouwmeester, L. Martens, J.R. Swann, J.K. Nicholson, R.S. Plumb, M. McCullagh, L.A. Gethings, S. Lai, J.I. Langridge, J.P.C. Vissers, I.D. Wilson, A comparison of collision cross section values obtained via travelling wave ion mobility-mass spectrometry and ultra high performance liquid chromatography-ion mobility-mass spectrometry: Application to the characterisation of metabolites in rat urine, *J Chromatogr A*, 1602 (2019) 386-396.
- [15] M. Hernandez-Mesa, V. D'Atri, G. Barknowitz, M. Fanuel, J. Pezzatti, N. Dreolin, D. Ropartz, F. Monteau, E. Vigneau, S. Rudaz, S. Stead, H. Rogniaux, D. Guillarme, G. Dervilly, B. Le Bizec, Interlaboratory and Interplatform Study of Steroids Collision Cross Section by Traveling Wave Ion Mobility Spectrometry, *Anal Chem*, 92 (2020) 5013-5022.
- [16] S.M. Stow, T.J. Causon, X. Zheng, R.T. Kurulugama, T. Mairinger, J.C. May, E.E. Rennie, E.S. Baker, R.D. Smith, J.A. McLean, S. Hann, J.C. Fjeldsted, An Interlaboratory Evaluation of Drift Tube Ion Mobility-Mass Spectrometry Collision Cross Section Measurements, *Anal Chem*, 89 (2017) 9048-9055.
- [17] C.G. Vasilopoulou, K. Sulek, A.D. Brunner, N.S. Meitei, U. Schweiger-Hufnagel, S.W. Meyer, A. Barsch, M. Mann, F. Meier, Trapped ion mobility spectrometry and PASEF enable in-depth lipidomics from minimal sample amounts, *Nat Commun*, 11 (2020) 331.
- [18] K.M. Hines, J.C. May, J.A. McLean, L. Xu, Evaluation of Collision Cross Section Calibrants for Structural Analysis of Lipids by Traveling Wave Ion Mobility-Mass Spectrometry, *Anal Chem*, 88 (2016) 7329-7336.
- [19] V. Hinnenkamp, J. Klein, S.W. Meckelmann, P. Balsaa, T.C. Schmidt, O.J. Schmitz, Comparison of CCS Values Determined by Traveling Wave Ion Mobility Mass Spectrometry and Drift Tube Ion Mobility Mass Spectrometry, *Anal Chem*, 90 (2018) 12042-12050.
- [20] H. Tsugawa, K. Ikeda, M. Takahashi, A. Satoh, Y. Mori, H. Uchino, N. Okahashi, Y. Yamada, I. Tada, P. Bonini, Y. Higashi, Y. Okazaki, Z. Zhou, Z.J. Zhu, J. Koelmel, T. Cajka, O. Fiehn, K. Saito, M. Arita, M. Arita, A lipidome atlas in MS-DIAL 4, *Nat Biotechnol*, 38 (2020) 1159-1163.

- [21] Z. Zhou, J. Tu, X. Xiong, X. Shen, Z.-J. Zhu, LipidCCS: Prediction of Collision Cross-Section Values for Lipids with High Precision To Support Ion Mobility–Mass Spectrometry-Based Lipidomics, *Analytical Chemistry*, 89 (2017) 9559-9566.
- [22] X. Zheng, N.A. Aly, Y. Zhou, K.T. Dupuis, A. Bilbao, V.L. Paurus, D.J. Orton, R. Wilson, S.H. Payne, R.D. Smith, E.S. Baker, A structural examination and collision cross section database for over 500 metabolites and xenobiotics using drift tube ion mobility spectrometry, *Chem Sci*, 8 (2017) 7724-7736.
- [23] E. Deschamps, I. Schmitz-Afonso, A. Schaumann, E. De, C. Loutelier-Bourhis, S. Alexandre, C. Afonso, Determination of the collision cross sections of cardiolipins and phospholipids from *Pseudomonas aeruginosa* by traveling wave ion mobility spectrometry-mass spectrometry using a novel correction strategy, *Anal Bioanal Chem*, 411 (2019) 8123-8131.
- [24] I. Campuzano, M.F. Bush, C.V. Robinson, C. Beaumont, K. Richardson, H. Kim, H.I. Kim, Structural characterization of drug-like compounds by ion mobility mass spectrometry: comparison of theoretical and experimentally derived nitrogen collision cross sections, *Anal Chem*, 84 (2012) 1026-1033.
- [25] G. Paglia, M. Kliman, E. Claude, S. Geromanos, G. Astarita, Applications of ion-mobility mass spectrometry for lipid analysis, *Analytical and Bioanalytical Chemistry*, 407 (2015) 4995-5007.
- [26] A. Baglai, A.F.G. Gargano, J. Jordens, Y. Mengerink, M. Honing, S. van der Wal, P.J. Schoenmakers, Comprehensive lipidomic analysis of human plasma using multidimensional liquid- and gas-phase separations: Two-dimensional liquid chromatography-mass spectrometry vs. liquid chromatography-trapped-ion-mobility-mass spectrometry, *J Chromatogr A*, 1530 (2017) 90-103.
- [27] I. Blaženović, T. Shen, S.S. Mehta, T. Kind, J. Ji, M. Piparo, F. Cacciola, L. Mondello, O. Fiehn, Increasing Compound Identification Rates in Untargeted Lipidomics Research with Liquid Chromatography Drift Time–Ion Mobility Mass Spectrometry, *Analytical Chemistry*, 90 (2018) 10758-10764.
- [28] K.L. Leaptrot, J.C. May, J.N. Dodds, J.A. McLean, Ion mobility conformational lipid atlas for high confidence lipidomics, *Nature Communications*, 10 (2019).
- [29] J. Hofmann, W.B. Struwe, C.A. Scarff, J.H. Scrivens, D.J. Harvey, K. Pagel, Estimating Collision Cross Sections of Negatively Charged N-Glycans using Traveling Wave Ion Mobility-Mass Spectrometry, *Analytical Chemistry*, 86 (2014) 10789-10795.
- [30] T.W. Knapman, J.T. Berryman, I. Campuzano, S.A. Harris, A.E. Ashcroft, Considerations in experimental and theoretical collision cross-section measurements of small molecules using travelling wave ion mobility spectrometry-mass spectrometry, *International Journal of Mass Spectrometry*, 298 (2010) 17-23.
- [31] Q. Duez, F. Chirot, R. Lienard, T. Josse, C. Choi, O. Coulembier, P. Dugourd, J. Cornil, P. Gerbaux, J. De Winter, Polymers for Traveling Wave Ion Mobility Spectrometry Calibration, *J Am Soc Mass Spectrom*, 28 (2017) 2483-2491.
- [32] J.R.N. Haler, C. Kune, P. Massonnet, C. Comby-Zerbino, J. Jordens, M. Honing, Y. Mengerink, J. Far, E. De Pauw, Comprehensive Ion Mobility Calibration: Poly(ethylene oxide) Polymer Calibrants and General Strategies, *Anal Chem*, 89 (2017) 12076-12086.
- [33] J. Maillard, S. Hupin, N. Carrasco, I. Schmitz-Afonso, T. Gautier, C. Afonso, Structural elucidation of soluble organic matter: Application to Titan's haze, *Icarus*, 340 (2020) 113627.

- [34] J.G. Forsythe, A.S. Petrov, C.A. Walker, S.J. Allen, J.S. Pellissier, M.F. Bush, N.V. Hud, F.M. Fernandez, Collision cross section calibrants for negative ion mode traveling wave ion mobility-mass spectrometry, *Analyst*, 140 (2015) 6853-6861.
- [35] D.N. Mortensen, A.C. Susa, E.R. Williams, Collisional Cross-Sections with T-Wave Ion Mobility Spectrometry without Experimental Calibration, *J Am Soc Mass Spectrom*, 28 (2017) 1282-1292.
- [36] S. Hupin, H. Lavanant, S. Renaudineau, A. Proust, G. Izzet, M. Groessl, C. Afonso, A calibration framework for the determination of accurate collision cross sections of polyanions using polyoxometalate standards, *Rapid Commun Mass Spectrom*, 32 (2018) 1703-1710.
- [37] E.G.B.a.W.J. Dyer, A rapid method of total lipid extraction and purification. , *Canadian Journal of Biochemistry and Physiology*, 37 (8) (1959) 911-917.
- [38] A. Seyer, S. Boudah, S. Broudin, C. Junot, B. Colsch, Annotation of the human cerebrospinal fluid lipidome using high resolution mass spectrometry and a dedicated data processing workflow, *Metabolomics*, 12 (2016).
- [39] V. Calabrese, I. Schmitz-Afonso, C. Prevost, C. Afonso, A. Elomri, Molecular networking and collision cross section prediction for structural isomer and unknown compound identification in plant metabolomics: a case study applied to *Zanthoxylum heitzii* extracts, *Anal Bioanal Chem*, (2022).
- [40] B. Colsch, F. Fenaille, A. Warnet, C. Junot, J.C. Tabet, Mechanisms governing the fragmentation of glycerophospholipids containing choline and ethanolamine polar head groups, *Eur J Mass Spectrom (Chichester)*, 23 (2017) 427-444.
- [41] M. Farenc, B. Paupy, S. Marceau, E. Riches, C. Afonso, P. Giusti, Effective Ion Mobility Peak Width as a New Isomeric Descriptor for the Untargeted Analysis of Complex Mixtures Using Ion Mobility-Mass Spectrometry, *J Am Soc Mass Spectrom*, 28 (2017) 2476-2482.
- [42] X. Chen, Y. Yin, M. Luo, Z. Zhou, Y. Cai, Z.-J. Zhu, Trapped ion mobility spectrometry-mass spectrometry improves the coverage and accuracy of four-dimensional untargeted lipidomics, *Analytica Chimica Acta*, 1210 (2022).
- [43] F. Merciai, S. Musella, E. Sommella, A. Bertamino, A.M. D'Ursi, P. Campiglia, Development and application of a fast ultra-high performance liquid chromatography-trapped ion mobility mass spectrometry method for untargeted lipidomics, *Journal of Chromatography A*, 1673 (2022) 463124.
- [44] C. Decroo, E. Colson, V. Lemaure, G. Caulier, J. De Winter, G. Cabrera-Barjas, J. Cornil, P. Flammang, P. Gerbaux, Ion mobility mass spectrometry of saponin ions, *Rapid Communications in Mass Spectrometry*, 33 (2019) 22-33.
- [45] C.a. Clemmer, Large Anhydrous Polyalanine Ions: Evidence for Extended Helices and Onset of a More Compact State, *Journal of American Chemical Society*, 123 (2001) 1490-1498.
- [46] E. Fahy, M. Sud, D. Cotter, S. Subramaniam, LIPID MAPS online tools for lipid research, *Nucleic Acids Research*, 35 (2007) W606-W612.
- [47] M. Chai, M.N. Young, F.C. Liu, C. Bleiholder, A Transferable, Sample-Independent Calibration Procedure for Trapped Ion Mobility Spectrometry (TIMS), *Anal Chem*, 90 (2018) 9040-9047.
- [48] A.S. Gelb, R.E. Jarratt, Y. Huang, E.D. Dodds, A study of calibrant selection in measurement of carbohydrate and peptide ion-neutral collision cross sections by traveling wave ion mobility spectrometry, *Anal Chem*, 86 (2014) 11396-11402.

4.3.7. Supplementary information

Table of content:

Figure SA1: Calibration curves $CCS' = f(tD')$ for different calibrants described for ion mobility in positive mode with a IMS pressure = 2.9 mbar, wave height=40 V and wave velocity=600 m/s.

Figure SA2: Calibration curves $CCS' = f(tD')$ for different calibrants described for ion mobility in negative mode with a IMS pressure = 2.9 mbar, wave height=40 V and wave velocity=800 m/s.

Figure SA3: Calibration curve $CCS' = f(tD')$ for the ESI Low concentration Tuning Mix calibrant in both positive (on the left) and negative (on the right) modes with wave height=40, 35, 30V and wave velocity = 600, 500, 400m/s in positive mode and 800, 650 and 500 m/s in negative mode, respectively

Figure SA4: Calibration curve $CCS' = f(tD')$ for the lipid standards in both positive (on the left) and negative (on the right) modes with wave height=40, 35, 30V and wave velocity = 600, 500, 400m/s in positive mode and 800, 650 and 500 m/s in negative mode, respectively

Figure SA5: Calibration curve $CCS' = f(tD')$ for polyalanine in both positive (on the left) and negative (on the right) modes with wave height=40, 35, 30V and wave velocity = 600, 500, 400m/s in positive mode and 800, 650 and 500 m/s in negative mode, respectively

Figure SA6: Calibration curve $CCS' = f(tD')$ for dextran in both positive (on the left) and negative (on the right) modes with wave height=40, 35, 30V and wave velocity = 600, 500, 400m/s in positive mode and 800, 650 and 500 m/s in negative mode, respectively

Figure SA7: Calibration curve $CCS' = f(tD')$ for Major Mix in both positive (on the left) and negative (on the right) modes with wave height=40, 35, 30V and wave velocity = 600, 500, 400m/s in positive mode and 800, 650 and 500 m/s in negative mode, respectively

Figure SA8: Calibration curve $CCS' = f(tD')$ for Polyglycine (in the left) and TAA (in the right) in positive mode with wave height=40, 35, 30V and wave velocity = 600, 500, 400m/s

Figure SA9 : Calibration curve $CCS' = f(tD')$ for PEO (in the left) and PEG (in the right) in positive mode with wave height=40, 35, 30V and wave velocity = 600, 500, 400m/s

Figure SA10: Calibration curve $CCS' = f(tD')$ for the drug standards (in the left) in positive mode with wave height=40, 35, 30V and wave velocity = 600, 500, 400m/s and polymalic acid (in the right) in negative mode with wave height=40, 35, 30V and wave velocity = 800, 650 and 500 m/s

Figure SA11: MS/MS spectrum of LPC 16:0 with the adduct $[M+HCOO]^-$ in negative mode

Figure SA12: MS/MS spectrum of LPE 18:0 with the adduct $[M-H]^-$ in negative mode. Ion at m/z 78.9575 corresponds to PO_3^- ion from phosphate, ion at m/z 140.0186 corresponds to ethanolamine phosphate ion and ion at m/z 196.0432 to the neutral loss of C18:0 group.

Figure SA13: MS/MS spectrum of PI 16 :0_18 :1. The ion of m/z 152.9928 corresponds to the glycerol-3-phosphate with the loss of H₂O. The ions at m/z 241.0108 and 222.9983 correspond respectively to the inositol phosphate ion with the loss of H₂O and two H₂O. The ion at m/z 391.2205 corresponds to the neutral loss of C18:1 and inositol.

Figure SA14: MS/MS spectrum of PE 18:0_18:2 with the adduct $[M-H]^-$ in negative mode. Ion at m/z 140.0186 corresponds to ethanolamine phosphate ion and ion at m/z 196.0432 to the neutral loss of C18:0 group.

Figure SA15: MS/MS spectrum of PC 16:0_18:1 with the adduct $[M+H]^+$ in positive mode

Figure SA16: MS/MS spectrum of SM 18:1;O2_16:0 with the adduct $[M+HCOO]^-$ in negative mode

Figure SA17: MS/MS spectrum of SM 18:2;O2_16:0 with the adduct $[M+H]^+$ in positive mode

Figure SA18: MS/MS spectrum of CE 18:1 with the adduct $[M+NH_4]^+$ in positive mode

Figure SA19: MS/MS spectrum of TG 18:1_18:1_18:2 with the adduct $[M+NH_4]^+$ in positive mode

Figure SA20: MS/MS spectrum of Cer 18:1;O2/24:0 with the adduct $[M-H]^-$ in negative mode

Figure SA21: MS/MS spectrum of PC 18:1/18:1 with the adduct $[M+H]^+$ in positive mode

Figure SA22: MS/MS spectrum of PC 18 :0_18:2 with the adduct $[M+H]^+$ in positive mode

Figure SA23: MS/MS spectrum of PC 18:0_18:2 with the adduct $[M+HCOO]^-$ in negative mode

Figure SA24: MS/MS spectrum of PC 18:1/18:1 with the adduct $[M+HCOO]^-$ in negative mode

Figure SA25: CCS values of some lipids according to the calibrant used, in negative ion mode.

Figure SA26: Comparison of mean relative deviations between lipid CCS from our calibrations and reference CCS according to the calibrant in positive mode, by comparing with: a. all literature CCS values chosen in the order: DTIMS stepped-field, DTIMS single-field and TWIMS or TIMS. B. single-field DTIMS CCS values. C. TIMS CCS values. D. TWIMS CCS values

Figure SA27: Comparison of mean relative deviations between lipid CCS from our calibrations and reference CCS according to the calibrant in negative mode, by comparing with: A. stepped-field DTIMS, B. Single-field DTIMS, C. All literature CCS values chosen in the order: DTIMS stepped-field, DTIMS single-field and TWIMS or TIMS, D. TIMS, E. TWIMS.

Table SA1: Source parameters of LC-ESI-TOF-MS experiments in both positive and negative ion modes

Table SA2: Data dependent scan (survey scan, Waters) and additional MS/MS acquisition parameters of LC-IMS-MS experiments

Table SA3: Calibration curve equations for all calibrants in positive mode, with the equation: $CCS' = A(tD' - t_0)N$ using Origin software (Origin Pro 2018 b9.5.0.193)

Table SA4: Calibration curve equations for all calibrants in negative mode, with the equation: $CCS' = A(tD' - t_0)N$ using Origin software (Origin Pro 2018 b9.5.0.193)

Table SA5: Compounds used for different calibration with Major Mix (Waters) according to the publication

Table SA6: Reference CCS of Tune Mix in positive mode (in the left) and in negative mode (in the right) according to various publications

Table SA7: New published CCS values for lipid standards calibrated by the Tune Mix in negative ion mode

Table SA8: New published CCS values for plasma lipids calibrated by the Tune Mix in positive ion mode

Table SA9: New published CCS values for plasma lipids calibrated by the Tune Mix in negative ion mode

In the supplementary information B on calibrants (Excel file):

Table SB1.a: Information on calibrant used in positive ion mode: m/z, CCS, mean tD' determined with UNIFI software on the three ion mobility conditions (**See extract below**)

Table SB1.b: Information on calibrant used in negative ion mode: m/z, CCS, mean tD' determined with UNIFI software on the three ion mobility conditions

Table SB2: CCS database of calibrant re-calibrated by the Tune Mix in both positive and negative ionisation modes

Table SB3: Validation of corrected calibrants CCS values with the publication of Deschamps et al

In the supplementary information C on lipid standards (Excel file):

Table SC.1: Lipid standards drift times in positive and negative modes with the three different conditions. Three technical replicates were made for each condition.

Table SC2.a: Lipid standards CCS values in positive mode using each of the ten calibrants, RSD between our nine experimental CCS values is also reported

Table SC2.b: Lipid standards CCS values in positive mode using each of the ten calibrants with SD between our experimental CCS values and the reference CCS from literature according to the instrument and CCS method determination

Table SC2.c: Lipid standards CCS values in positive mode using each of the ten calibrants with SD between our experimental CCS values and the reference CCS from literature according to the publication

Table SC3.a: Lipid standards CCS values in negative mode using each of the six calibrants, RSD between our nine experimental CCS values is also reported

Table SC3.b: Lipid standards CCS values in negative mode using each of the six calibrants with SD between our experimental CCS values and the reference CCS from literature according to the instrument and CCS method determination

Table SC3.c: Lipid standards CCS values in negative mode using each of the six calibrants with SD between our experimental CCS values and the reference CCS from literature according to the publication

Table SC4: Lipid standards CCS determination in positive mode using each of the nine calibrants recalibrated by the Tune Mix, RSD between our nine experimental CCS is also reported

Table SC5: Lipid standards CCS determination in negative mode using each of the five calibrants recalibrated by the Tune Mix, RSD between our nine experimental CCS is also reported

Table SC6: New lipid CCS values from lipid standards that had not been published yet, to our knowledge

In the supplementary information D on plasma lipids (Excel file):

Table SD.1 : Plasma lipids drift times in positive and negative modes with the three different conditions. Three technical replicates were made for each condition.

Table SD2.a: Plasma lipids CCS values in positive mode using each of the ten calibrants, RSD between our nine experimental CCS values is also reported

Table SD2.b: Plasma lipids CCS values in positive mode using each of the ten calibrants with SD between our experimental CCS values and the reference CCS from literature according to the instrument and CCS method determination

Table SD2.c: Plasma lipids CCS values in positive mode using each of the ten calibrants with SD between our experimental CCS values and the reference CCS from literature according to the publication

Table SD3.a: Plasma lipids CCS values in negative mode using each of the six calibrants, RSD between our nine experimental CCS values is also reported

Table SD3.b: Plasma lipids CCS values in negative mode using each of the six calibrants with SD between our experimental CCS values and the reference CCS from literature according to the instrument and CCS method determination

Table SD3.c: Plasma lipids CCS values in negative mode using each of the six calibrants with SD between our experimental CCS values and the reference CCS from literature according to the publication

Table SD4: Comparison of our experimental CCS values according to the calibrant used with published CCS values from literature according to the instrument and the CCS determination method in both modes

Table SD5: Comparison of our experimental CCS values according to the calibrant used with published CCS values from literature according to the publication in both modes

Table SD6: Plasma lipids CCS determination in positive mode using each of the nine calibrants recalibrated by the Tune Mix, RSD between our nine experimental CCS is also reported

Table SD7: Plasma lipids CCS determination in negative mode using each of the five calibrants recalibrated by the Tune Mix, RSD between our nine experimental CCS is also reported

Table SD8: New plasma lipid CCS values that had not been published yet, to our knowledge

Supplemental Experimental Section

IMS calibrants preparation:

For the IMS calibration mixtures, Polyalanine (Sigma-Aldrich) and dextran (Fluka analytical) were first dissolved in H₂O at 1mM and then diluted to 10 μM in 1/1:ACN/H₂O for analysis. Lipids were purchased from Avanti Polar Lipids (AL, USA): PE 6:0/6:0, PE 10:0/10:0, PE 15:0/15:0, PC 20:0/20:0, PC 24:0/24:0, LPC 16:0, LPE 16:0, PE 18:1/18:1 Δ9 cis, PC 16:0/16:0 and lipids from the Differential Ion Mobility System Suitability LIPIDOMIX kit (DIMS kit). Lipids standards were dissolved in chloroform/methanol:50/50 (v/v) to yield 10mM stock solutions which were further diluted in methanol (MeOH)/isopropanol/H₂O:65/35/5 (v/v/v) to obtain a 100 μM final solution. Polyglycine (Sigma-Aldrich) was dissolved (1mg/mL) in formic acid, vortex stirred and sonicated until dissolution and diluted in ACN/H₂O 50:50 (v/v) to obtain a 10μg/mL solution. ESI Low-concentration Tuning Mix (Agilent) was injected directly in negative mode and with 10μg/mL of betaine added in the solution in positive mode. Major Mix IMS calibration kit was prepared by mixing 100 μL of the Major Mix Calibration Solution from Waters with 50 μL of the LCMS QC reference standard solution (Waters). The tetraalkylammonium (TAA) salts were purchased from Sigma-Aldrich, except tetrabutylammonium hydroxide solution and tetraoctylammonium bromide which were from Fluka analytical. The TAA salts were prepared in MeOH to 1 μM, except tetramethylammonium salt concentration which was 20 μM in MeOH. Poly(ethylene glycol) (PEG) and poly(ethylene oxide) monomethyl ether (PEO) solutions were purchased from Sigma-Aldrich. PEG were prepared from four products at 600, 1000, 2000, 3350 g/mol at a final concentration of 15 μM in ACN with 13 mM of NaI and PEO from two products at 700 and 2000 g/mol, at a final concentration of 5 μM in MeOH with 50 μM of NaCl, according to previously described protocols^{1,2} respectively.

The poly-L-malic acid was prepared from L-malic acid (Sigma-Aldrich) which was dissolved in H₂O to a 0.050 M concentration, the polymerisation was performed at 80°C for 24 hours in an open Eppendorf. The solution was reconstituted in the same amount of water and then diluted by 20 in ACN/H₂O:50/50 (v/v). A mixture of drug-like compounds³ was prepared at 1 μM in H₂O/MeOH:50/50 (v/v) from 1 mM stock solutions, for acetaminophen, alprenolol and colchicine in H₂O, for ondansetron, clozapine N-oxide and verapamil in MeOH and for reserpine in ACN/H₂O:50/50 +0.1% FA. All small molecules were purchased from Sigma-Aldrich apart for alprenolol, which was supplied by European Pharmacopoeia Reference Standard.

Table SA1: Source parameters of LC-ESI-TOF-MS experiments in both positive and negative ion modes

Ionization parameter	Positive ion mode	Negative ion mode
Capillary voltage	3 kV	-2.3 kV
Extraction cone voltage	6 V	5 V
Cone voltage	40 V	45 V
Cone gas flow	40 L.h ⁻¹	60 L.h ⁻¹
Desolvation gas flow	800 L.h ⁻¹	1000 L.h ⁻¹
Source temperature	120 °C	120 °C
Desolvation temperature	500 °C	500 °C
Reference scan frequency	15 s	15 s
Lockspray capillary voltage	2.8 kV	-2 kV
Lockspray cone voltage	25 V	25 V

Table SA2: Data dependent scan (survey scan, Waters) and additional MS/MS acquisition parameters of LC-IMS-MS experiments

Acquisition parameter	Values
Mass range acquisition	200-2000
Intensity threshold (positive mode)	800
Intensity threshold (negative mode)	600
Fragmented ion from each scan	3
Number of MS/MS scans for each ion	3
Exclusion time after MS/MS scan	10 s
Low mass Collision energy ramp	20-35 eV
High mass Collision energy ramp	35-50 eV
Additional MS/MS collision energy ramp	25-40 eV

UNIFI parameters:

The data processing with the UNIFI software were performed with an intensity threshold of 20 counts, a high background filter, the maximum number of peaks per channel is fixed at 200000. The lockmass settings were: the reference mass of 556.2766 and 554.2615 for both positive and negative ion mode, with a mass window of 0.1 m/z and a combine width on 3 scans. The targeted screen settings are not set for plasma analysis, but only for calibrant experiments: the target match tolerance was set at 10 ppm, adducts was changed in function of the calibrant species wanted.

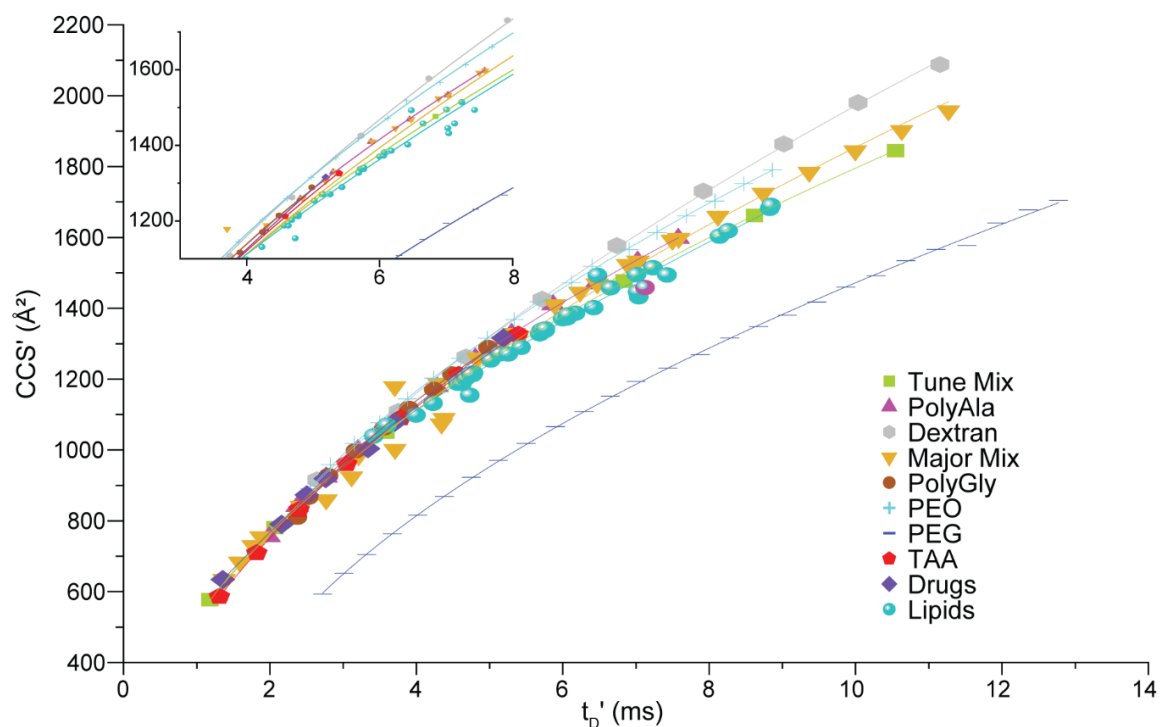


Figure SA1: Calibration curves $CCS' = f(t_D')$ for different calibrants described for ion mobility in positive mode with a IMS pressure = 2.9 mbar, wave height=40 V and wave velocity=600 m/s

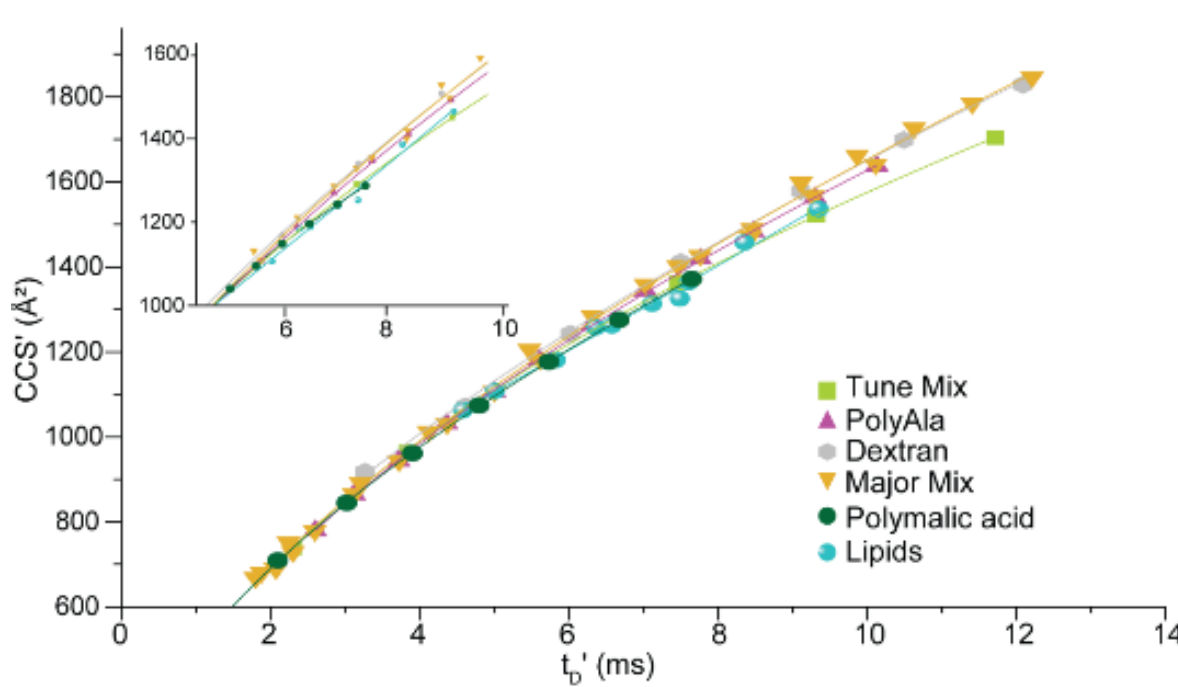


Figure SA2: Calibration curves $CCS' = f(t_D')$ for different calibrants described for ion mobility in negative mode with a IMS pressure = 2.9 mbar, wave height=40 V and wave velocity=800 m/s.

Calibrant	A	t_0	N
Tune Mix	554.24527 ± 5.40273	0.10455 ± 0.02594	0.51283 ± 0.00394
Polyalanine	625.62051 ± 15.34167	0.52026 ± 0.07321	0.48021 ± 0.01065
Dextran	535.33141 ± 32.11662	0.10717 ± 0.20756	0.56887 ± 0.02143
Major Mix	499.69694 ± 52.89797	-0.10613 ± 0.31544	0.56689 ± 0.04045
Polyglycine	719.36885 ± 70.37053	1.00541 ± 0.28307	0.41922 ± 0.05184
PEO	636.46654 ± 14.12044	0.54263 ± 0.07607	0.48801 ± 0.0088
PEG	470.55746 ± 10.30038	1.14877 ± 0.07297	0.52299 ± 0.00813
TAA	525.18383 ± 14.5804	0.09683 ± 0.06263	0.55682 ± 0.01351
Drug standards	399.664 ± 55.89147	-0.62126 ± 0.31638	0.67664 ± 0.06086
Lipid standards	410.10486 ± 141.3	-1.08571 ± 1.31725	0.61335 ± 0.11697

Table SA3: Calibration curve equations for all calibrants in positive mode, with the equation: $CCS' = A (t_D' - t_0)^N$ using Origin software (Origin Pro 2018 b9.5.0.193)

Calibrant	A	t_0	N
Tune Mix	503.9596 ± 11.34385	0.30893 ± 0.07709	0.4934 ± 0.00827
Polyalanine	431.19565 ± 11.99347	-0.05473 ± 0.09533	0.56747 ± 0.01011
Dextran	387.48115 ± 56.83304	-0.60605 ± 0.56996	0.60602 ± 0.04836
Major Mix	390.20107 ± 25.69704	-0.39651 ± 0.20474	0.6087 ± 0.02353
Polymalic acid	3.3217 ± 0.65083	1.93359 ± 0.20645	0.84883 ± 0.15015
Lipid standards	60.50266 ± 155.29345	-7.54213 ± 8.82223	1.13811 ± 0.69994

Table SA4: Calibration curve equations for all calibrants in negative mode, with the equation: $CCS' = A (t_D' - t_0)^N$ using Origin software (Origin Pro 2018 b9.5.0.193)

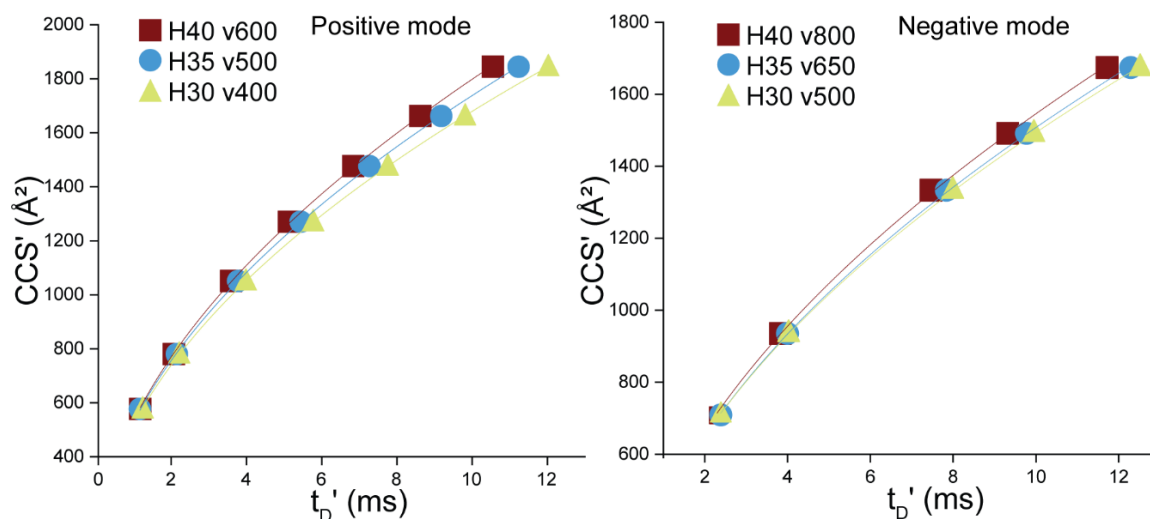


Figure SA3: Calibration curve $CCS'=f(t_D')$ for the ESI Low concentration Tuning Mix calibrant in both positive (on the left) and negative (on the right) modes with wave height=40, 35, 30V and wave velocity = 600, 500, 400m/s in positive mode and 800, 650 and 500 m/s in negative mode, respectively

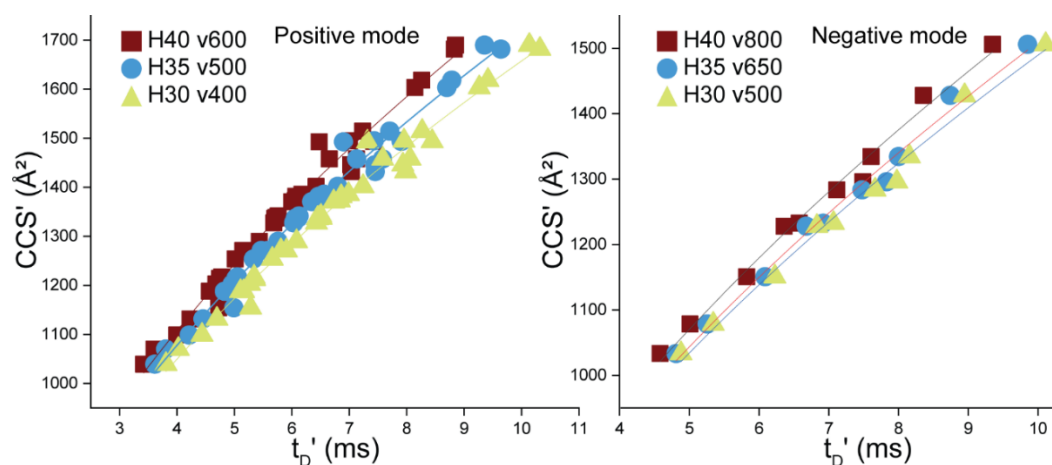


Figure SA4: Calibration curve $CCS'=f(t_D')$ for the lipid standards in both positive (on the left) and negative (on the right) modes with wave height=40, 35, 30V and wave velocity = 600, 500, 400m/s in positive mode and 800, 650 and 500 m/s in negative mode, respectively

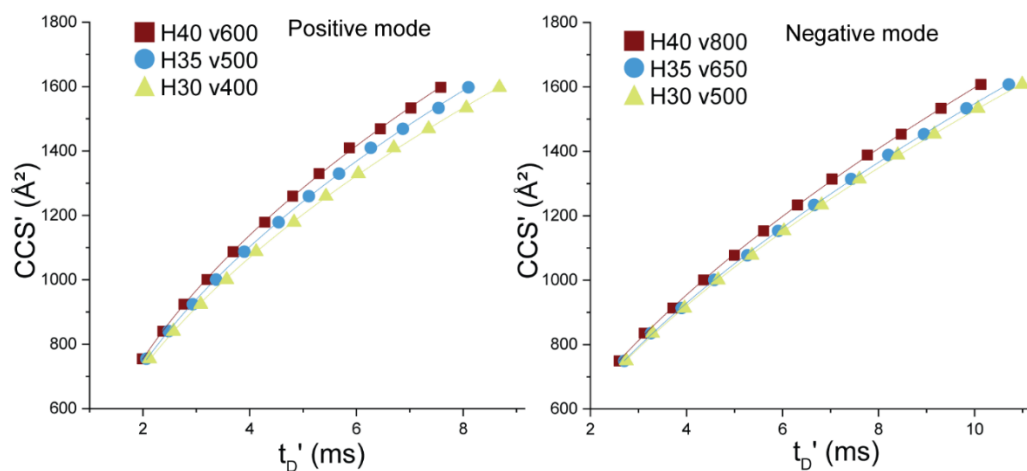


Figure SA5: Calibration curve $CCS'=f(t_D')$ for polyaniline in both positive (on the left) and negative (on the right) modes with wave height=40, 35, 30V and wave velocity = 600, 500, 400m/s in positive mode and 800, 650 and 500 m/s in negative mode, respectively

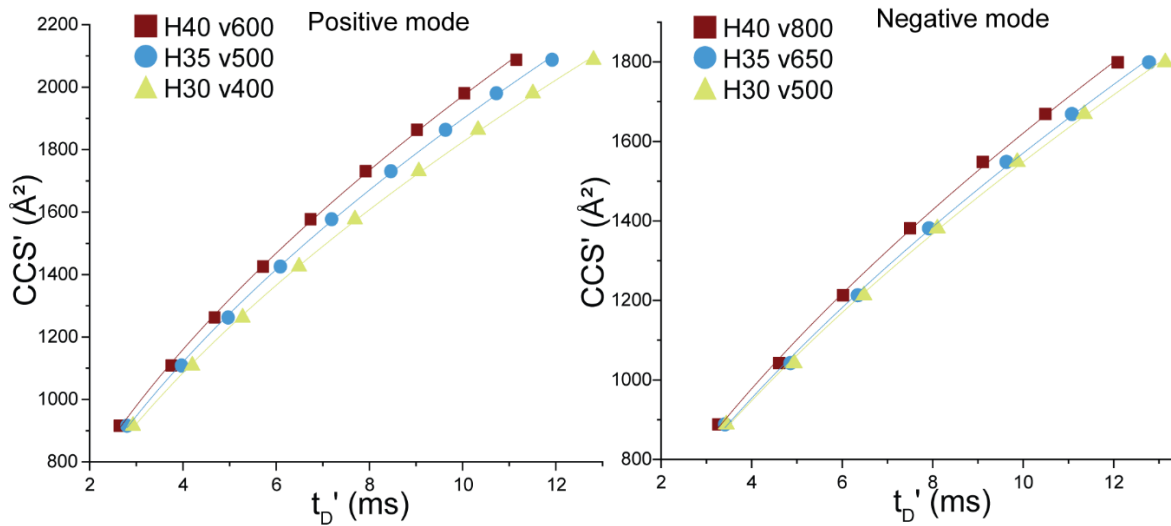


Figure SA6: Calibration curve $CCS'=f(t_D')$ for dextran in both positive (on the left) and negative (on the right) modes with wave height=40, 35, 30V and wave velocity = 600, 500, 400m/s in positive mode and 800, 650 and 500 m/s in negative mode, respectively

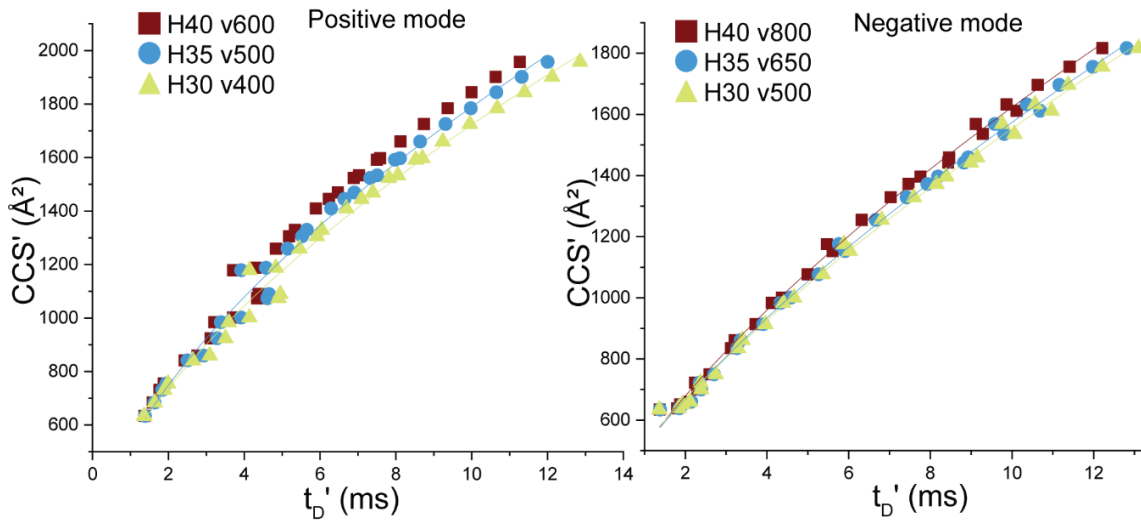


Figure SA7: Calibration curve $CCS'=f(t_D')$ for Major Mix in both positive (on the left) and negative (on the right) modes with wave height=40, 35, 30V and wave velocity = 600, 500, 400m/s in positive mode and 800, 650 and 500 m/s in negative mode, respectively

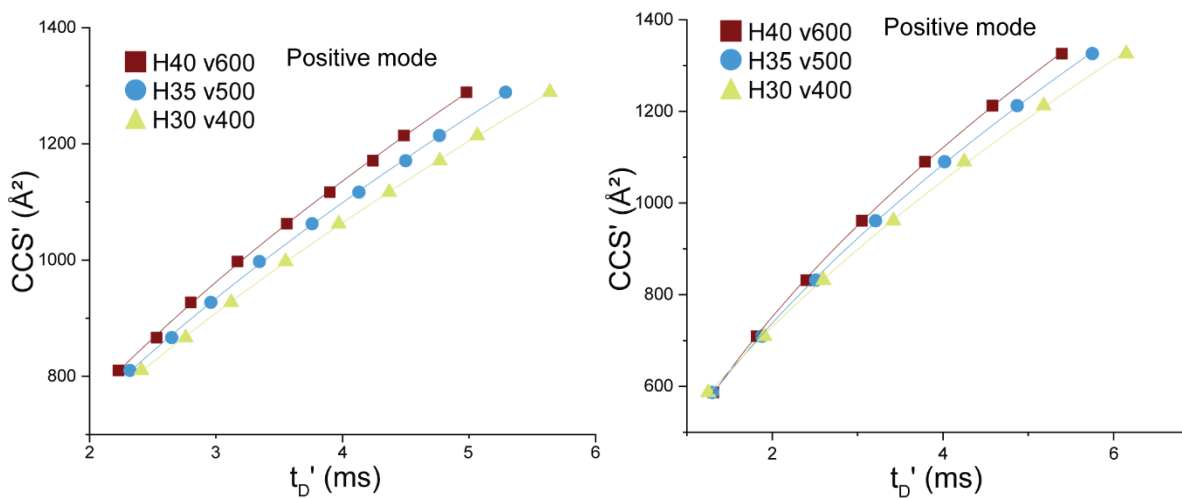


Figure SA8: Calibration curve $CCS'=f(t_D')$ for Polyglycine (in the left) and TAA (in the right) in positive mode with wave height=40, 35, 30V and wave velocity = 600, 500, 400m/s

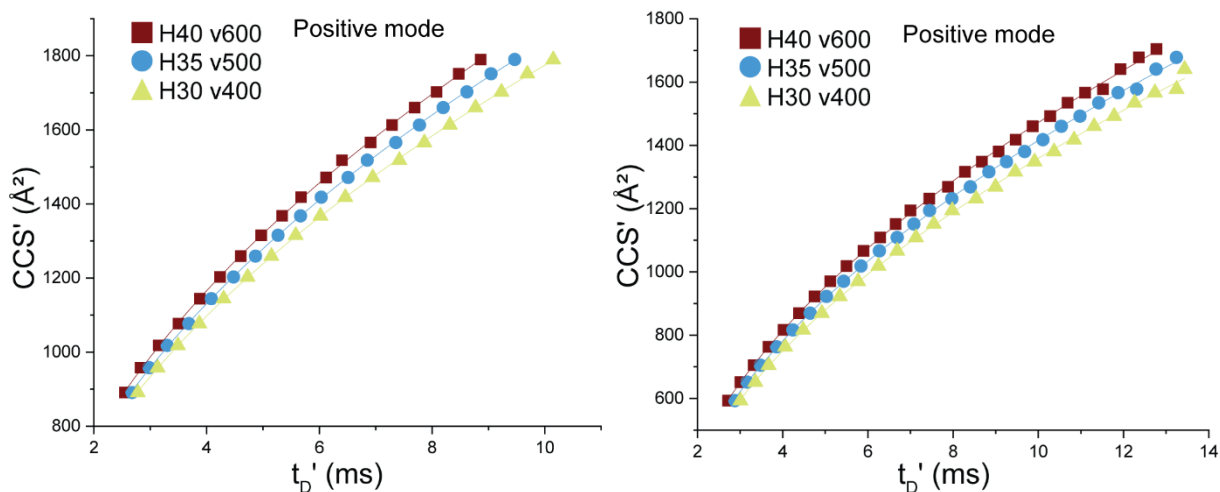


Figure SA9: Calibration curve $CCS'=f(t_D')$ for PEO (in the left) and PEG (in the right) in positive mode with wave height=40, 35, 30V and wave velocity = 600, 500, 400m/s

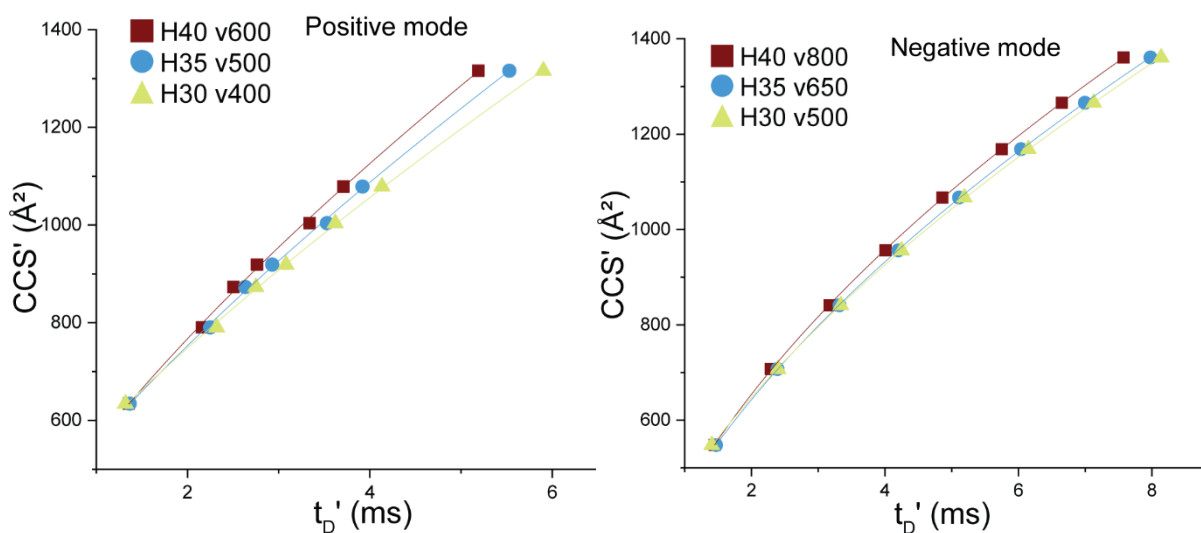


Figure SA10: Calibration curve $CCS'=f(t_D')$ for the drug standards (in the left) in positive mode with wave height=40, 35, 30V and wave velocity = 600, 500, 400m/s and polymalic acid (in the right) in negative mode with wave height=40, 35, 30V and wave velocity = 800, 650 and 500 m/s

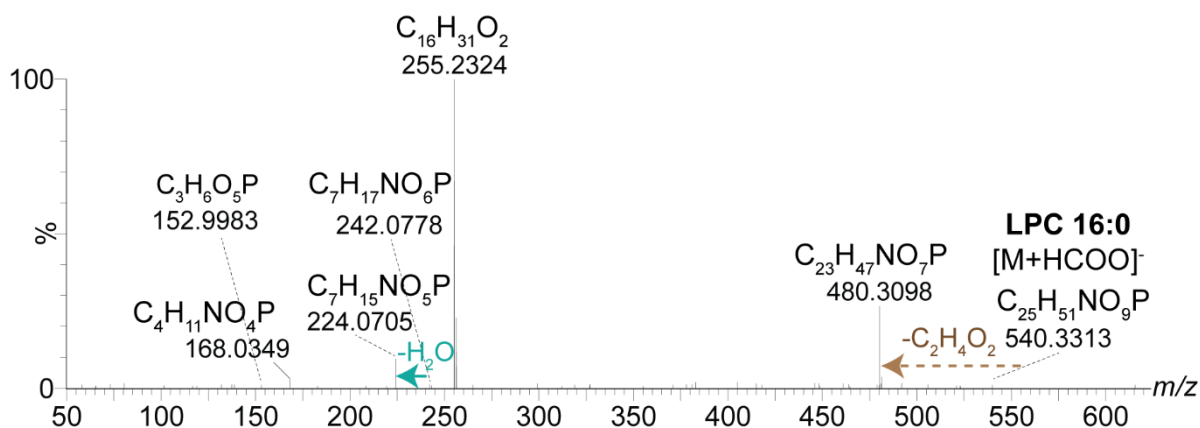


Figure SA11: MS/MS spectrum of LPC 16:0 with the adduct $[M+HCOO]^-$ in negative mode

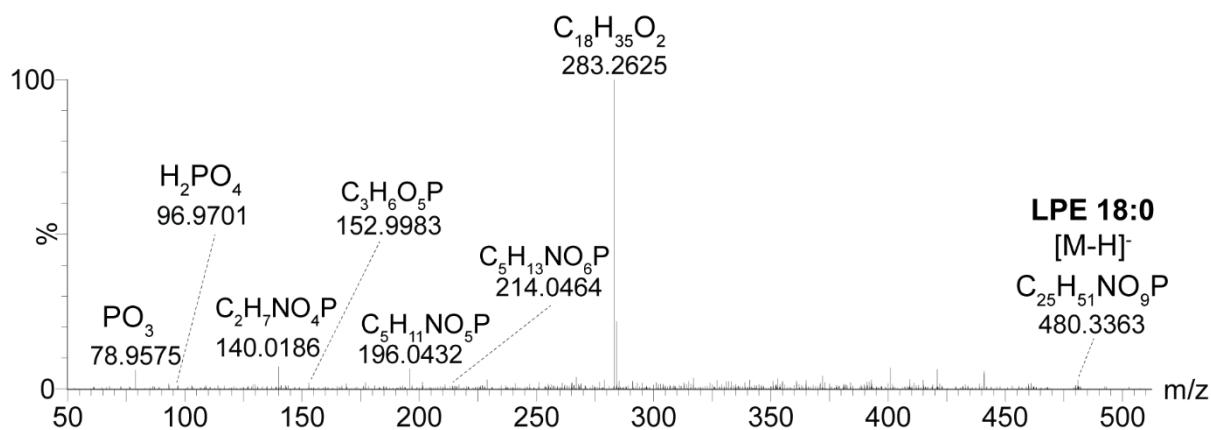


Figure SA12: MS/MS spectrum of LPE 18:0 with the adduct [M-H]⁻ in negative mode. Ion at m/z 78.9575 corresponds to PO₃⁻ ion from phosphate, ion at m/z 140.0186 corresponds to ethanolamine phosphate ion and ion at m/z 196.0432 to the neutral loss of C18:0 group.

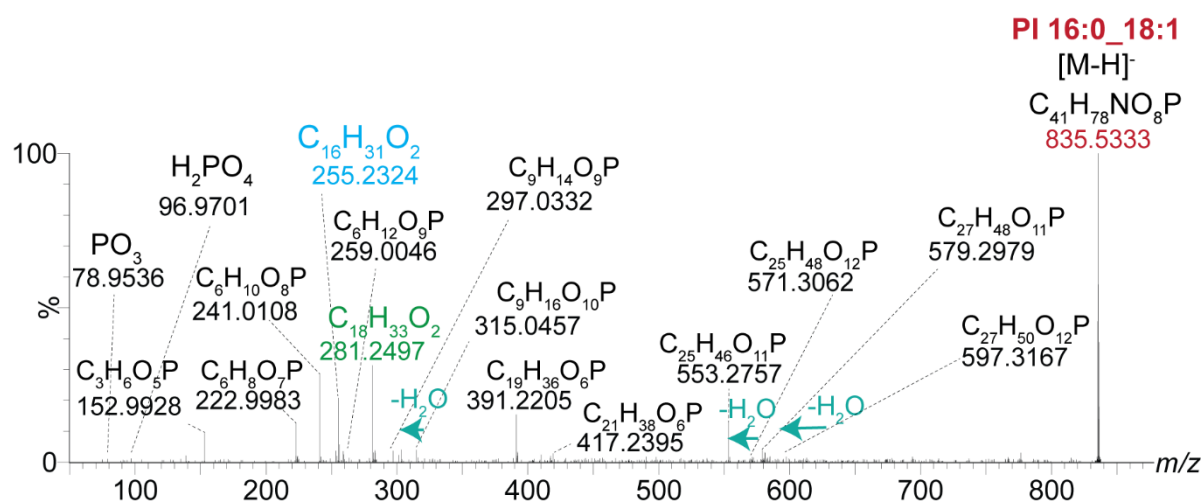


Figure SA13: MS/MS spectrum of PI 16:0_18:1. The ion of m/z 152.9928 corresponds to the glycerol-3-phosphate with the loss of H₂O. The ions at m/z 241.0108 and 222.9983 correspond respectively to the inositol phosphate ion with the loss of H₂O and two H₂O. The ion at m/z 391.2205 corresponds to the neutral loss of C18:1 and inositol.

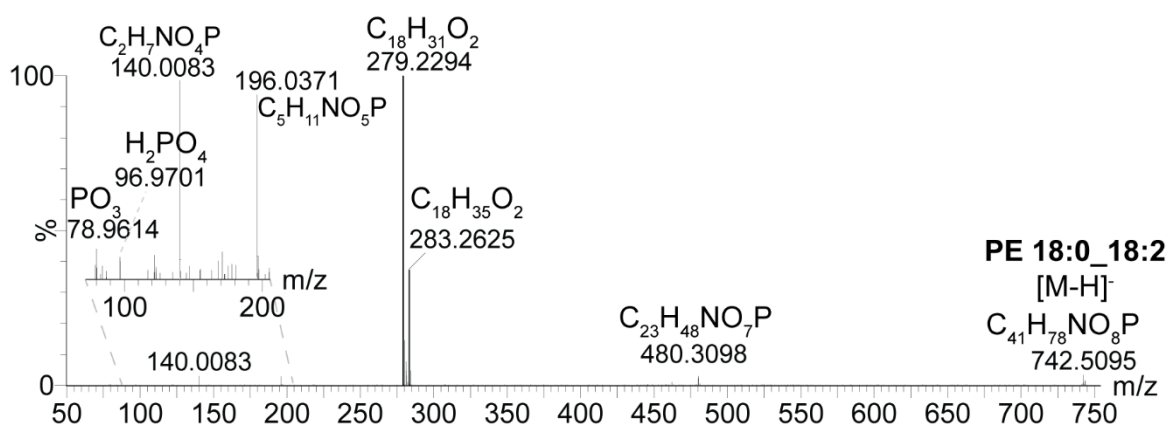


Figure SA14: MS/MS spectrum of PE 18:0_18:2 with the adduct [M-H]⁻ in negative mode. Ion at m/z 140.0186 corresponds to ethanolamine phosphate ion and ion at m/z 196.0432 to the neutral loss of C18:0 group.

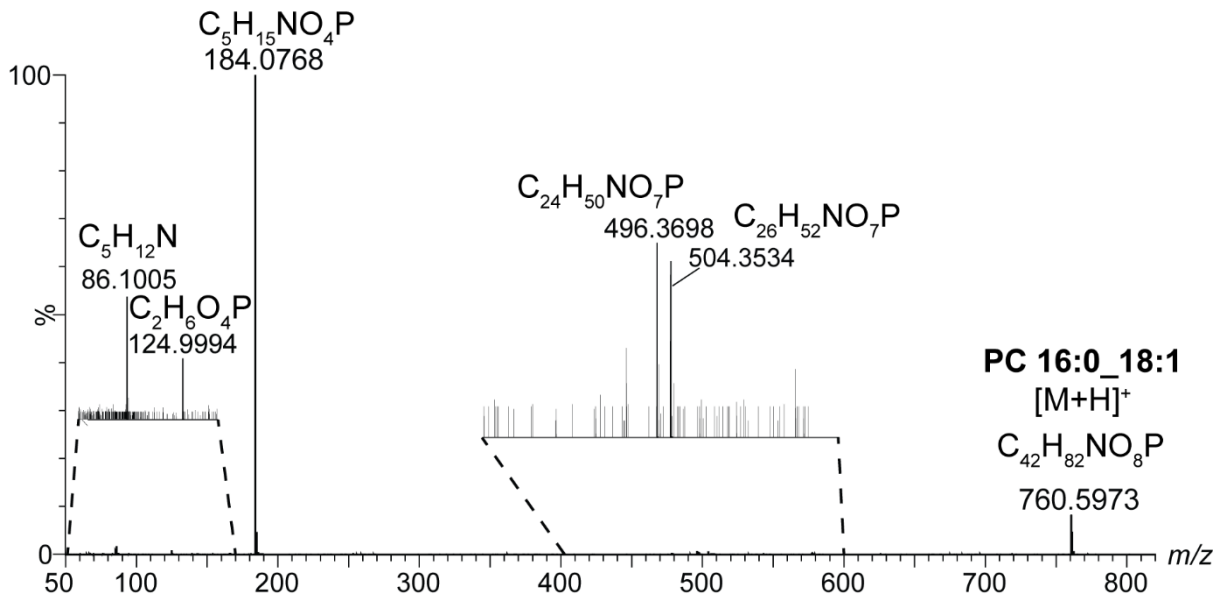


Figure SA15: MS/MS spectrum of PC 16:0_18:1 with the adduct [M+H]⁺ in positive mode

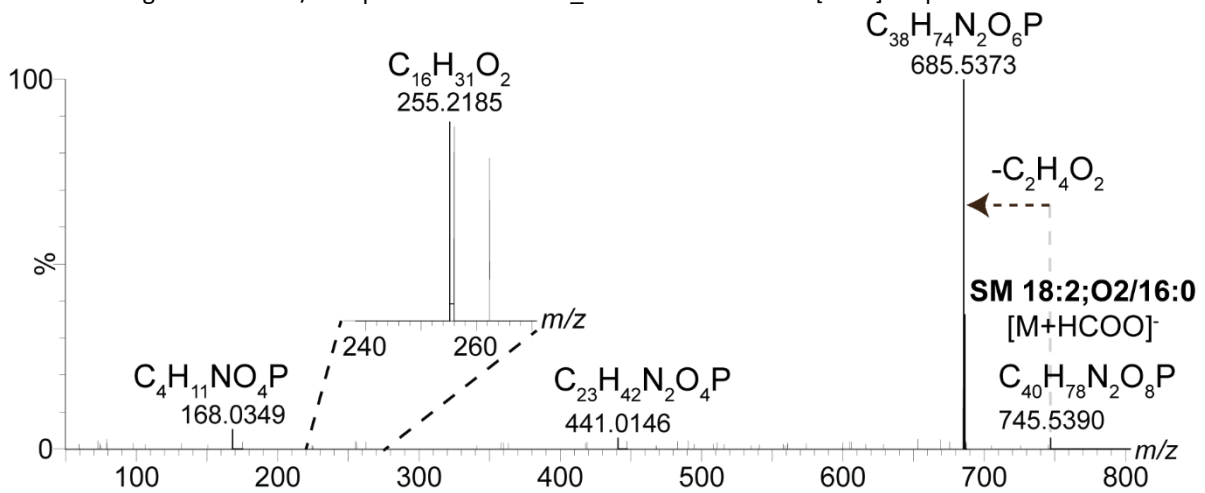


Figure SA16: MS/MS spectrum of SM 18:1;O2_16:0 with the adduct [M+HCOO]⁻ in negative mode

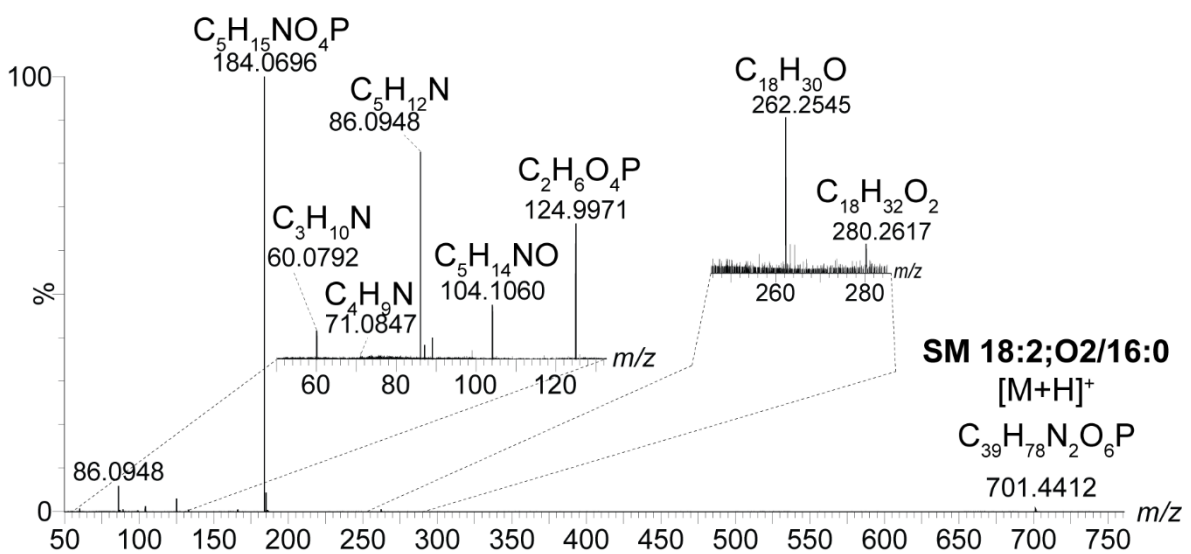


Figure SA17: MS/MS spectrum of SM 18:2;O2_16:0 with the adduct [M+H]⁺ in positive mode

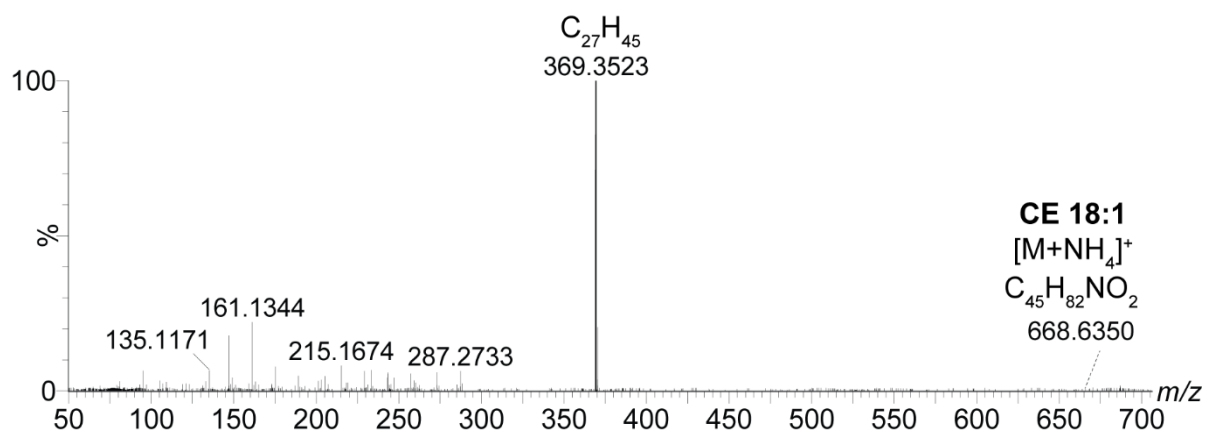


Figure SA18: MS/MS spectrum of CE 18:1 with the adduct $[M+NH_4]^+$ in positive mode

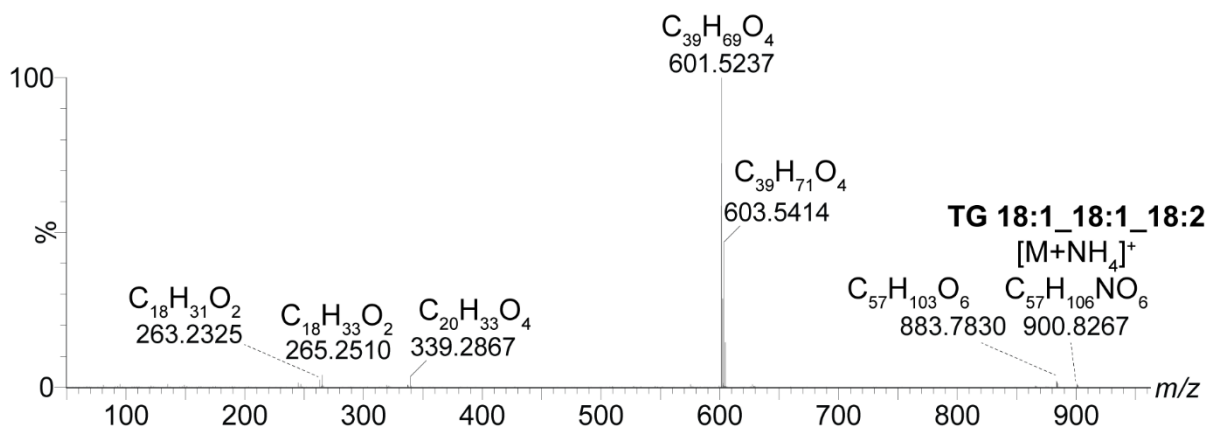


Figure SA19: MS/MS spectrum of TG 18:1_18:1_18:2 with the adduct $[M+NH_4]^+$ in positive mode

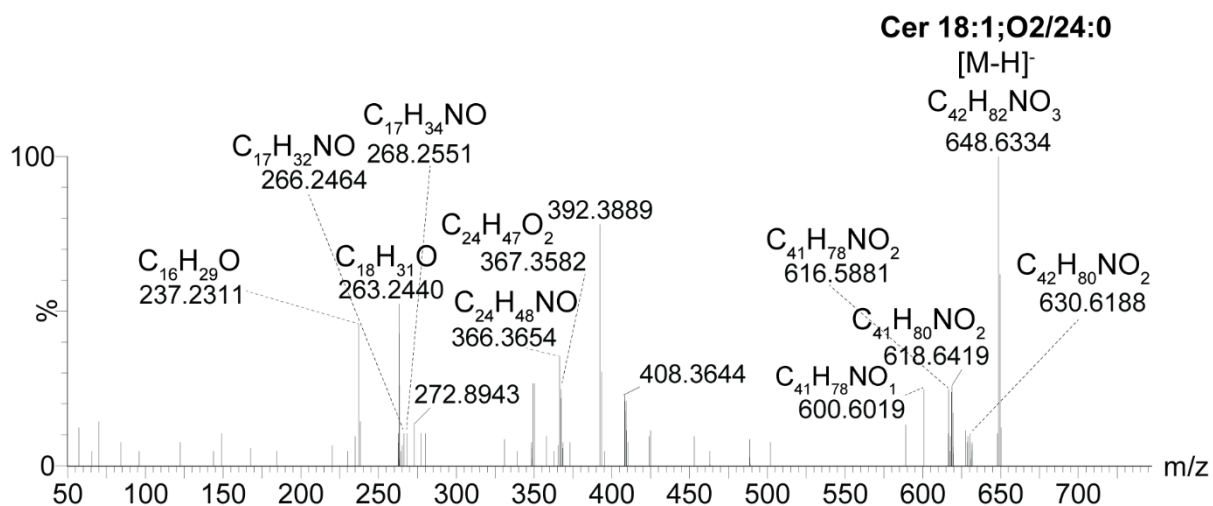


Figure SA20: MS/MS spectrum of Cer 18:1;O2/24:0 with the adduct $[M-H]^-$ in negative mode

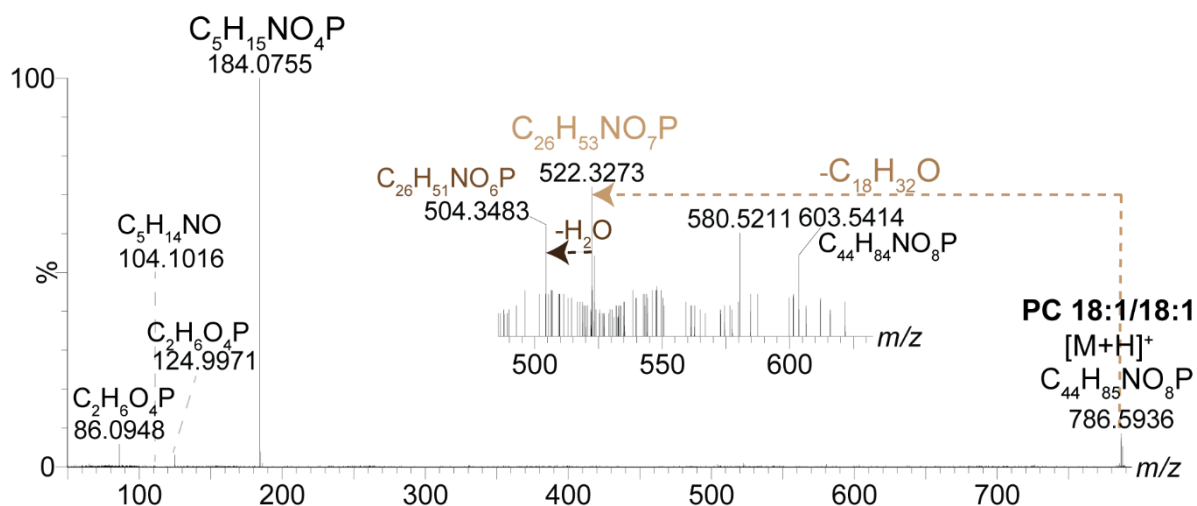


Figure SA21: MS/MS spectrum of PC 18:1/18:1 with the adduct $[M+H]^+$ in positive mode

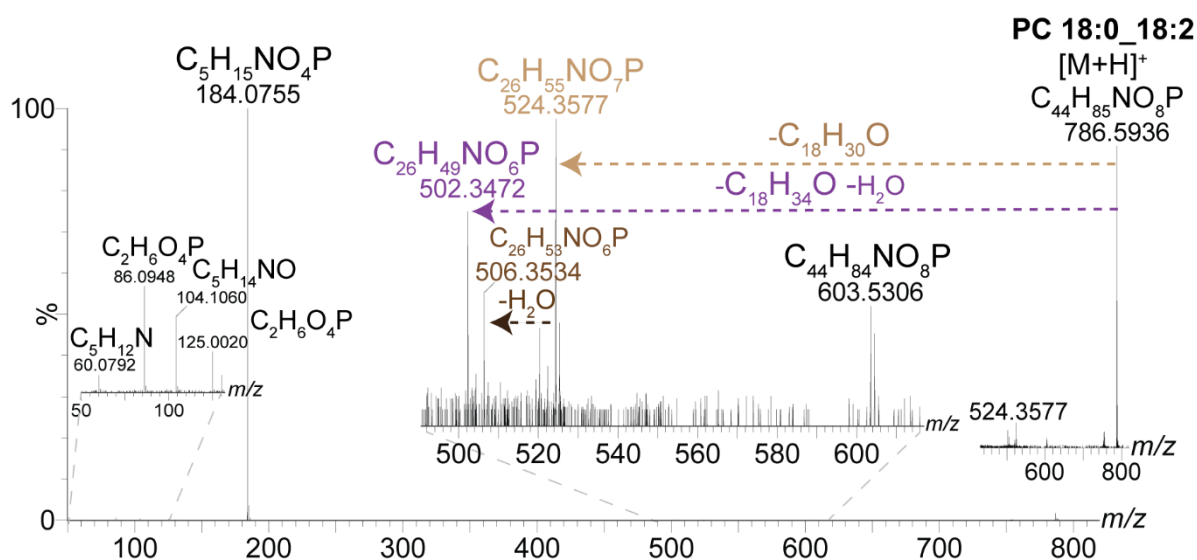


Figure SA22: MS/MS spectrum of PC 18:0_18:2 with the adduct $[M+H]^+$ in positive mode

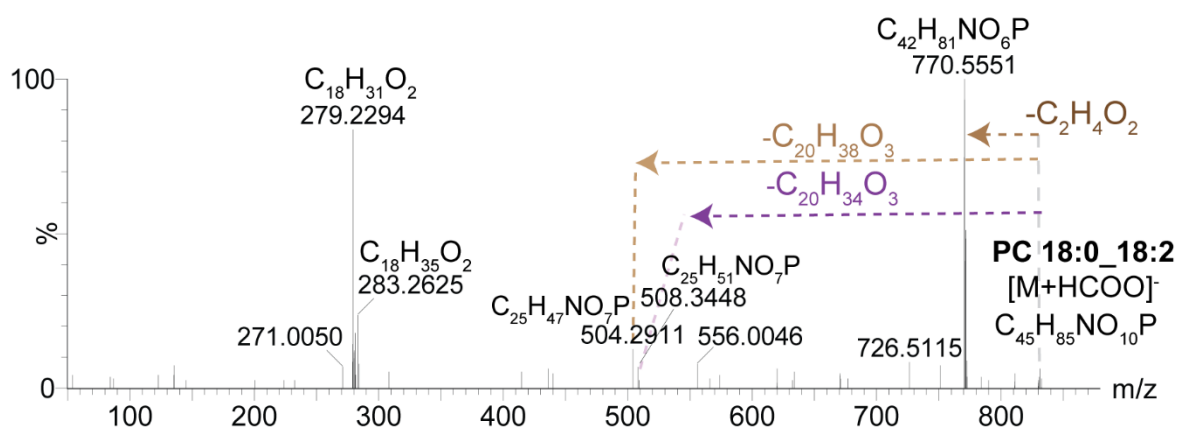


Figure SA23: MS/MS spectrum of PC 18:0_18:2 with the adduct $[M+HCOO]^-$ in negative mode

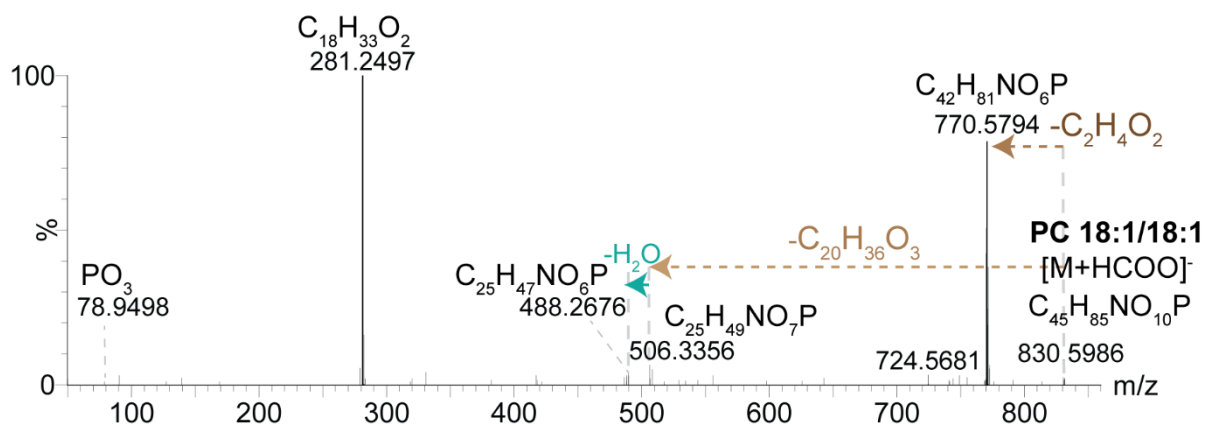


Figure SA24: MS/MS spectrum of PC 18:1/18:1 with the adduct $[M+HCOO]^-$ in negative mode

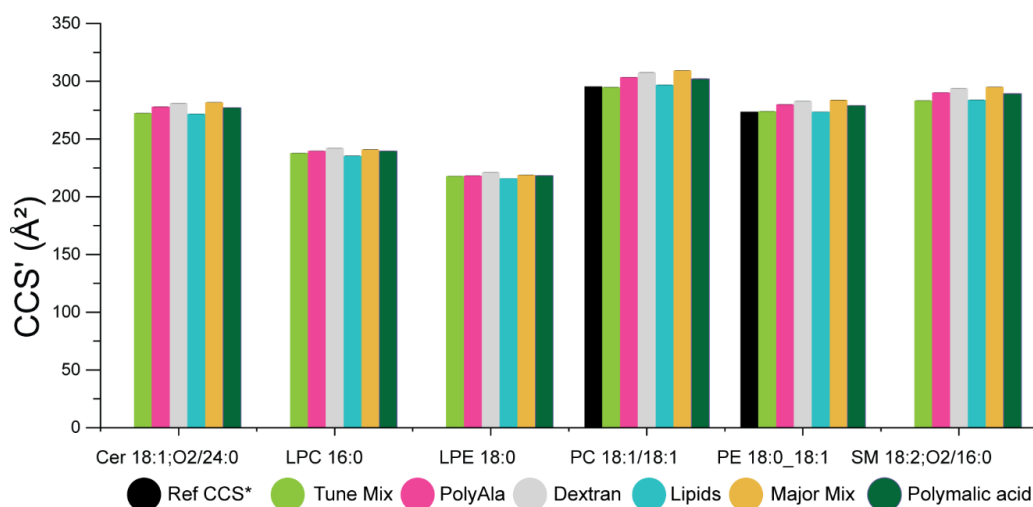


Figure SA25: CCS values of some lipids according to the calibrant used, in negative ion mode.

The error bars represent the RSD on nine values.

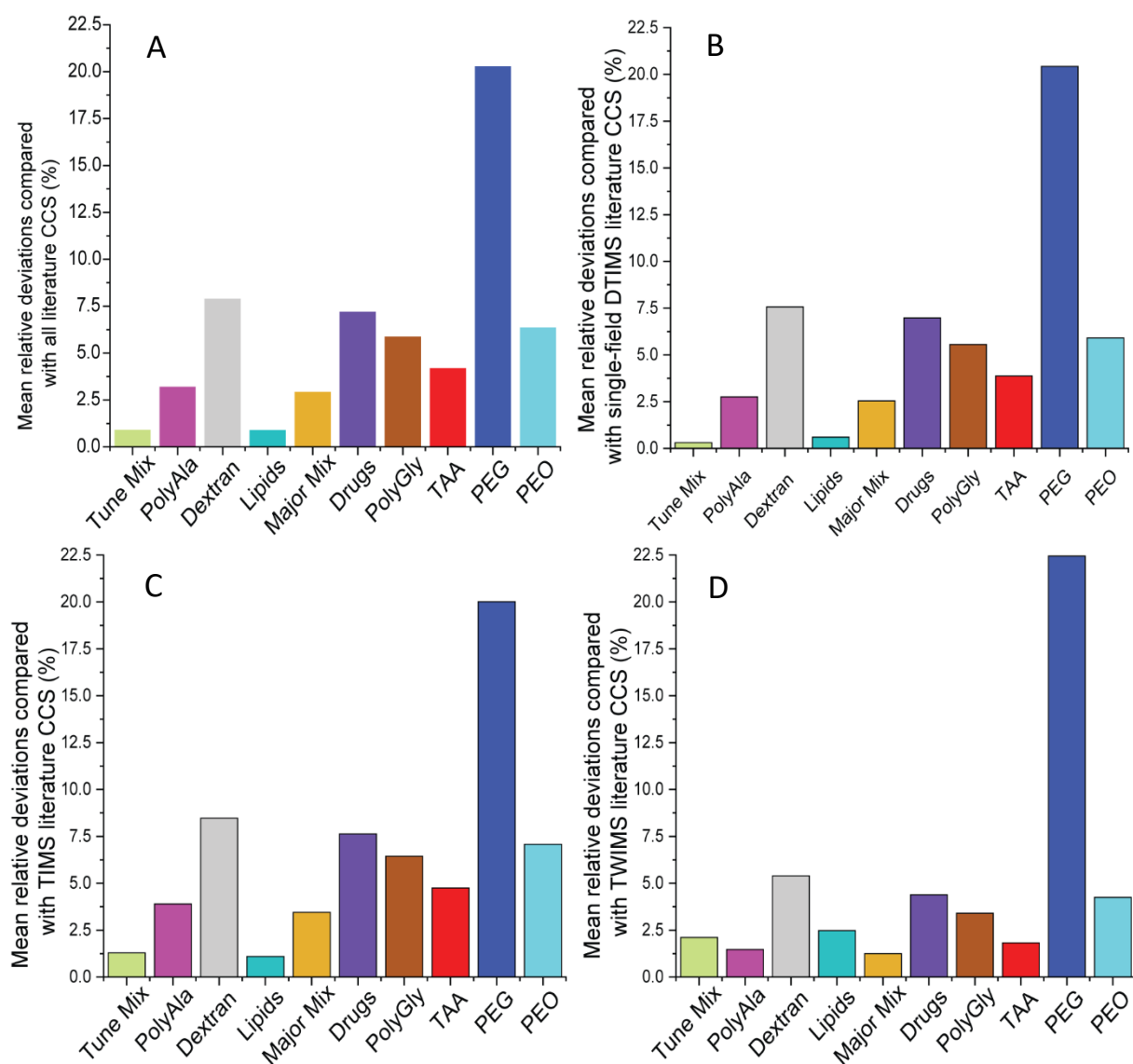


Figure SA26: Comparison of mean relative deviations between lipid CCS from our calibrations and reference CCS according to the calibrant in positive mode, by comparing with: a. all literature CCS values chosen in the order: DTIMS stepped-field, DTIMS single-field and TWIMS or TIMS. B. single-field DTIMS CCS values. C. TIMS CCS values. D. TWIMS CCS values

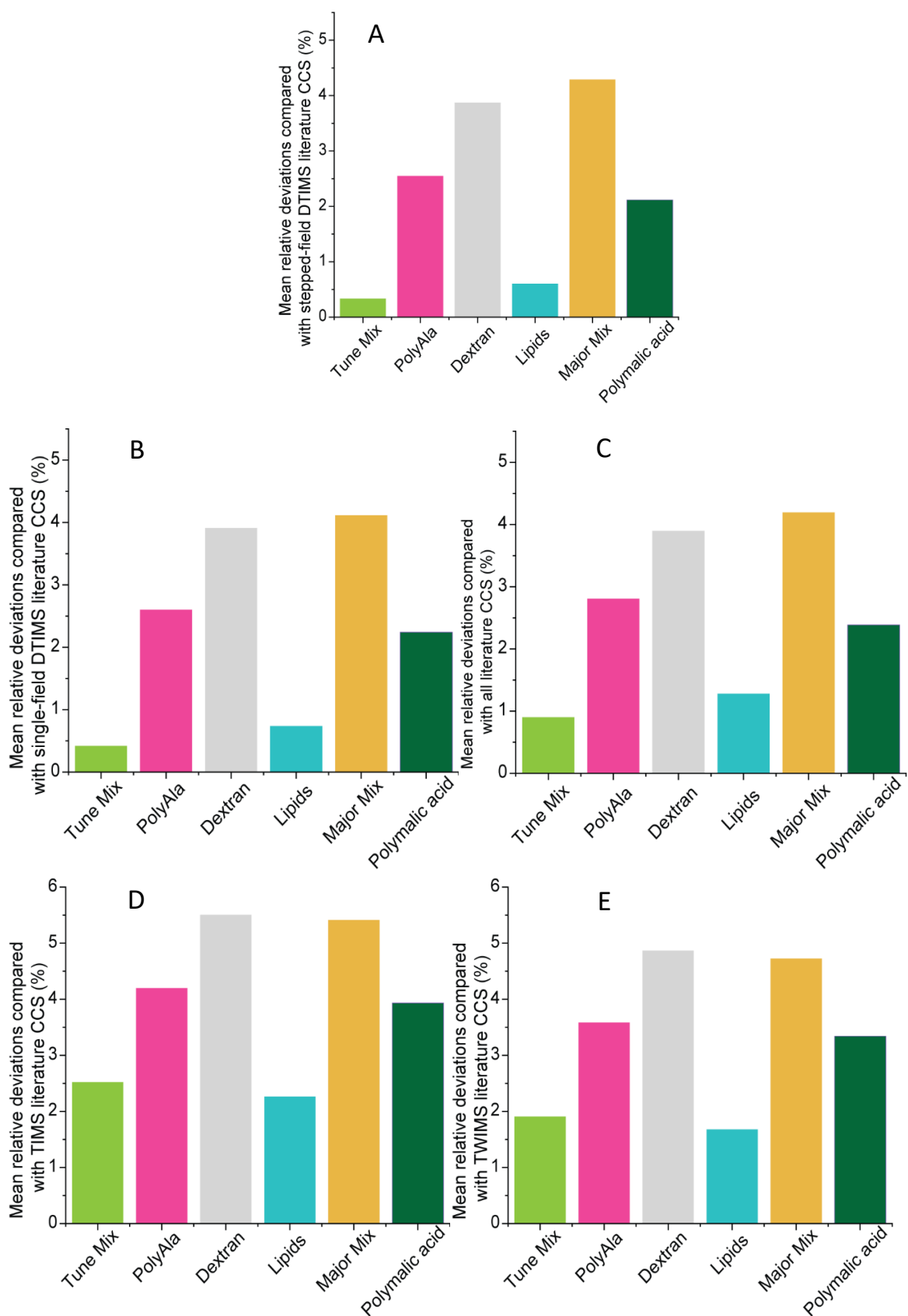


Figure SA27: Comparison of mean relative deviations between lipid CCS from our calibrations and reference CCS according to the calibrant in negative mode, by comparing with: A. stepped-field DTIMS, B. Single-field DTIMS, C. All literature CCS values chosen in the order: DTIMS stepped-field, DTIMS single-field and TWIMS or TIMS, D. TIMS, E. TWIMS.

Compounds	Theoretical m/z	CCS (N ₂) in Å ²	Hinnenkamp et al, 2018 ⁴	Gosciny et al, 2019 ⁵	Waters and Righetti et al, 2020 ⁶
acetaminophen	152.0712	130.4	x	x	x
caffeine	195.0882	138.2	x	x	x
sulfaguanidine	215.0603	146.8	x	x	x
polyalanine (n= 3)	232.1297	151		x	
polyalanine (n= 4)	303.1668	166		x	
sulfadimethoxine	311.0814	168.41	x	x	x
polyalanine (n= 5)	374.2039	181		x	
L-valyl-L-tyrosyl-L-valine	380.2185	191.7	x	x	x
polyalanine (n= 6)	445.2411	195		x	
verapamil	455.291	208.8	x	x	x
terfenadine	472.3216	228.7	x	x	x
polyalanine (n= 7)	516.2782	211	x	x	x
leucine-enkephaline	556.2771	229.8	x	x	x
polyalanine (n= 8)	587.3153	228	x	x	x
reserpine	609.2812	252.3	x	x	x
polyalanine (n= 9)	658.3524	243	x	x	x
polyalanine (n= 10)	729.3895	256	x	x	x
polyalanine (n= 11)	800.4266	271	x	x	x
polyalanine (n= 12)	871.4637	282	x	x	x
polyalanine (n= 13)	942.5009	294	x	x	x
polyalanine (n= 14)	1013.538	306		x	x
perfluoroalkylphosphazine 1	1022.004	263		x	x
polyalanine (n= 15)	1084.5751	321.5		x	x
perfluoroalkylphosphazine 2	1121.9976	276		x	x
polyalanine (n= 16)	1155.6122	333.6		x	x
Ultramark	1221.99119	291.2			x
	1321.98481	304			x
	1421.97842	316.7			x
	1521.97203	329			x
	1621.96564	340.1			x
	1721.95926	351.3			x
	1821.95287	362.1			x
	1921.94648	372.6			x

Table SA5: Compounds used for different calibration with Major Mix (Waters) according to the publication

Positive ion mode					Negative ion mode				
m/z	CCS (N ₂) in Å ²				m/z	CCS (N ₂) in Å ²			
	Stow et al, 2017 ⁷		Zhou et al, 2016 ⁸	Hernandez et al, 2014 ⁹		Stow et al, 2017 ⁷		Zhou et al, 2016 ⁸	Hernandez et al, 2014 ⁹
	Interlab	Intralab				Interlab	Intralab		
118	121.51	121.3	121.5	116.2	113	108.93	108.23		
322	153.67	153.73	153.4	151.9	302	140.66	140.04	136.6	109.6
622	202.67	202.96	202.4	202.4	602	180.94	180.77	178.4	172.8
922	243.05	243.64	242.7	243.8	1034	255.59	255.34	251.2	261.9
1222	281.25	282.2	280.9	274.1	1334	285.29	284.76	280.9	285.4
1522	315.79	316.96	315.7	317.2	1634	319.53	319.03	315.8	332.1
1822	350.43	351.25		342.5	1934	354.32	352.55		352.5
2122	381.4	383.03		388.3	2234	382.39	380.74		405.2
2422	410.28	412.96		429.5	2534	413.67	412.99		433.6
2722	437.94	441.21		447.4	2834	431.98	432.62		505.1

Table SA6: Reference CCS of Tune Mix in positive mode (in the left) and in negative mode (in the right) according to various publications

Lipid standards	Ions	m/z	CCS calibrated with Tune Mix	RSD (%) on nine values
PA 14:1/14 :1	[M-H] ⁻	587.373	239.45	0.20
PA 14:1/14 :1	[M+HCOO] ⁻	633.377	249.29	0.26
PE 14:1/14 :1	[M-H] ⁻	630.414	247.28	0.16
PE 14:1/14 :1	[M+HCOO] ⁻	676.418	260.06	0.24
PG 14:1/14 :1	[M-H] ⁻	661.408	254.90	0.24
PC 14:1/14:1	[M+HCOO] ⁻	718.466	272.66	0.33
PS 14:1/14 :1	[M-H] ⁻	674.403	258.28	0.30
PC 16:0/16:0	[M+HCOO] ⁻	778.560	286.58	0.27
PI 14:1/14 :1	[M-H] ⁻	749.424	269.81	0.26
PC 20:0/20:0	[M+HCOO] ⁻	890.687	308.75	0.28

Table SA7: New published CCS values for lipid standards calibrated by the Tune Mix in negative ion mode

Plasma lipids	Ions	m/z	rt	Tune Mix	
				Mean CCS (Å ²)	RSD (%)
Cer 18:1;O2/12:0	[M+H-H ₂ O] ⁺	464.451	13.38	242.58	0.12
Cholesterol	[M+H-H ₂ O] ⁺	369.369	19.68	204.37	0.23
HexCer 18:1;O2/12:0	[M+H-H ₂ O] ⁺	626.495	12.34	266.70	0.16
PC 13:0/13:0	[M+H] ⁺	650.479	11.87	268.64	0.16
PC 13:0/13:0	[M+Na] ⁺	672.462	11.87	272.46	0.16
PC 14:0_18:2	[M+H] ⁺	730.524	13.72	280.24	0.14
PC 16:0_18:1	[M+Na] ⁺	782.577	15.59	291.52	0.17
PC 16:0_20:4	[M+Na] ⁺	804.537	14.68	292.89	0.20
PC 18:0_18:1	[M+Na] ⁺	810.588	16.52	297.49	0.15
PC 18:0_20:4	[M+Na] ⁺	832.581	15.71	298.71	0.17
SM 18:2;O2/14:0	[M+H] ⁺	673.517	13.83	277.07	0.13

Table SA8: New published CCS values for plasma lipids calibrated by the Tune Mix in positive ion mode

Plasma lipids	Ions	m/z	rt	Tune Mix	
				Mean CCS (Å ²)	RSD (%)
Cer 18:1;O2/12:0	[M-H] ⁻	480.444	13.43	235.17	0.16
LPC 18:0	[M+HCOO] ⁻	568.363	7.65	244.57	0.20
LPC 18:2	[M+HCOO] ⁻	564.336	3.96	239.13	0.21
LPC 20:4	[M-H-CH ₃] ⁻	528.330	3.74	225.39	0.20
PC 18:0_18:2;O	[M+HCOO] ⁻	846.591	13.13	297.97	0.22
PC O-16:0_18:2	[M+HCOO] ⁻	788.538	14.32	288.72	0.18
PE 12:0_12:0	[M-H] ⁻	578.383	10.78	239.30	0.16
PE O-18:2_20:4	[M-H] ⁻	748.539	15.59	273.38	0.26
SM 18:1;O2/14:1	[M+HCOO] ⁻	717.523	12.08	277.57	0.27
SM 18:1;O2/15:0	[M+HCOO] ⁻	733.541	13.82	281.62	0.21

Table SA9: New published CCS values for plasma lipids calibrated by the Tune Mix in negative ion mode

References:

- (1) Duez, Q.; Chirot, F.; Lienard, R.; Josse, T.; Choi, C.; Coulembier, O.; Dugourd, P.; Cornil, J.; Gerbaux, P.; De Winter, J. *J Am Soc Mass Spectrom* 2017, 28, 2483-2491.
- (2) Haler, J. R. N.; Kune, C.; Massonnet, P.; Comby-Zerbino, C.; Jordens, J.; Honing, M.; Mengerink, Y.; Far, J.; De Pauw, E. *Anal Chem* 2017, 89, 12076-12086.
- (3) Campuzano, I.; Bush, M. F.; Robinson, C. V.; Beaumont, C.; Richardson, K.; Kim, H.; Kim, H. I. *Anal Chem* 2012, 84, 1026-1033.
- (4) Hinnenkamp, V.; Klein, J.; Meckelmann, S. W.; Balsaa, P.; Schmidt, T. C.; Schmitz, O. J. *Anal Chem* 2018, 90, 12042-12050.
- (5) Gosciny, S.; McCullagh, M.; Far, J.; De Pauw, E.; Eppe, G. *Rapid Commun Mass Spectrom* 2019, 33 Suppl 2, 34-48.
- (6) Righetti, L.; Dreolin, N.; Celma, A.; McCullagh, M.; Barknowitz, G.; Sancho, J. V.; Dall'Asta, C. *J Agric Food Chem* 2020, 68, 10937-10943.
- (7) Stow, S. M.; Causon, T. J.; Zheng, X.; Kurulugama, R. T.; Mairinger, T.; May, J. C.; Rennie, E. E.; Baker, E. S.; Smith, R. D.; McLean, J. A.; Hann, S.; Fjeldsted, J. C. *Anal Chem* 2017, 89, 9048-9055.
- (8) Zhou, Z.; Shen, X.; Tu, J.; Zhu, Z. *J. Anal Chem* 2016, 88, 11084-11091.
- (9) Hernandez, D. R.; Debord, J. D.; Ridgeway, M. E.; Kaplan, D. A.; Park, M. A.; Fernandez-Lima, F. *The Analyst* 2014, 139, 1913-1921.

Table SB1.a: Information on calibrant used in positive ion mode: m/z , CCS, mean tD' determined with UNIFI software on the three ion mobility conditions (extract)

Positive mode				Negative mode			
Lipids	Ions	m/z	RT	Lipids	Ions	m/z	RT
CE 18:1	[M+NH ₄] ⁺	668.635	26.5	Cer 18:1;O2/12:0	[M-H] ⁻	480.444	13.43
CE 18:2	[M+NH ₄] ⁺	666.624	25.95	Cer 18:1;O2/24:0	[M-H] ⁻	648.6334	19.78
CE 20:4	[M+NH ₄] ⁺	690.633	25.63	LPC 16:0	[M+HCOO] ⁻	540.3414	5.18
Cer 18:1;O2/12:0	[M+H-H ₂ O] ⁺	464.451	15.48	LPC 16:0	[M-H-CH ₃] ⁻	480.3098	5.18
Cer 18:1;O2/22:0	[M+H-H ₂ O] ⁺	604.605	21.76	LPC 18:0	[M-H-CH ₃] ⁻	508.3448	7.65
Cer 18:1;O2/23:0	[M+H-H ₂ O] ⁺	618.608	22.24	LPC 18:0	[M+HCOO] ⁻	568.3627	7.65
Cer 18:1;O2/24:0	[M+H-H ₂ O] ⁺	632.638	22.71	LPC 18:1	[M+HCOO] ⁻	566.3421	5.68
Cholesterol	[M+H-H ₂ O] ⁺	369.369	22.69	LPC 18:1	[M-H-CH ₃] ⁻	506.3257	5.68
HexCer 18:1;O2/12:0	[M+H-H ₂ O] ⁺	626.495	14.21	LPC 18:2	[M+HCOO] ⁻	564.3356	3.96
LPC 16:0	[M+Na] ⁺	518.338	5.23	LPC 18:2	[M-H-CH ₃] ⁻	504.3206	3.96
LPC 16:0	[M+H] ⁺	496.339	5.23	LPC 20:4	[M-H-CH ₃] ⁻	528.33	3.74
LPC 18:0	[M+H] ⁺	524.368	8.11	LPE 16:0	[M-H] ⁻	452.3	5.52
LPC 18:0	[M+Na] ⁺	546.36	8.11	LPE 17:0	[M-H] ⁻	494.34	6.44
LPC 18:1	[M+H] ⁺	522.357	5.78	LPE 18:0	[M-H] ⁻	480.34	7.94
LPC 18:1	[M+Na] ⁺	544.348	5.78	LPE 18:1	[M-H] ⁻	478.32	5.96
LPC 18:2	[M+H] ⁺	520.341	3.96	LPE 18:2	[M-H] ⁻	476.29	4.21
LPC 18:2	[M+Na] ⁺	542.32	3.96	PC 13:0_13:0	[M+HCOO] ⁻	694.4618	11.93
LPC 20:4	[M+H] ⁺	544.338	3.8	PC 14:0_18:2	[M+HCOO] ⁻	774.5294	13.76
LPC 20:4	[M+Na] ⁺	566.324	3.8	PC 15:0_18:2	[M+HCOO] ⁻	788.538	14.32
PC 13:0_13:0	[M+H] ⁺	650.479	13.64	PC 16:0/16:0	[M+HCOO] ⁻	778.5626	15.43
PC 13:0_13:0	[M+Na] ⁺	672.462	13.65	PC 16:0_18:0	[M+HCOO] ⁻	806.5667	15.57
PC 14:0_18:2	[M+H] ⁺	730.524	15.84	PC 16:0_18:1	[M+HCOO] ⁻	804.5811	15.57
PC 15:0_18:2	[M+H] ⁺	744.559	16.49	PC 16:0_18:2	[M+HCOO] ⁻	802.5606	14.85
PC 16:0/16:0	[M+H] ⁺	734.571	17.87	PC 16:0_20:4	[M+HCOO] ⁻	826.5583	14.75
PC 16:0_18:0	[M+H] ⁺	762.598	19.1	PC 16:0_20:5	[M+HCOO] ⁻	824.5482	14.09
PC 16:0_18:1	[M+H] ⁺	760.583	18.05	PC 16:1_18:2	[M+HCOO] ⁻	800.5304	14.01
PC 16:0_18:1	[M+Na] ⁺	782.577	18.05	PC 17:0_18:1	[M+HCOO] ⁻	818.6074	16.04
PC 16:0_20:4	[M+H] ⁺	782.577	17.03	PC 17:0_18:2	[M+HCOO] ⁻	816.5695	15.35
PC 16:0_20:4	[M+Na] ⁺	804.537	17.01	PC 18:0_18:1	[M+HCOO] ⁻	832.6035	16.54
PC 16:0_20:5	[M+H] ⁺	802.516	16.24	PC 18:0_18:2	[M+HCOO] ⁻	830.5356	15.8
PC 16:1_18:2	[M+H] ⁺	756.561	16.32	PC 18:0_18:2;O	[M+HCOO] ⁻	846.5911	13.13
PC 17:0_18:1	[M+H] ⁺	774.598	18.65	PC 18:0_20:3	[M+HCOO] ⁻	856.6206	16.1
PC 17:0_18:2	[M+H] ⁺	772.579	17.57	PC 18:0_20:4	[M+HCOO] ⁻	854.5998	15.72
PC 18:0_18:1	[M+H] ⁺	788.618	19.25	PC 18:0_22:0	[M+HCOO] ⁻	878.5798	15.51
PC 18:0_18:1	[M+Na] ⁺	810.588	19.25	PC 18:0_22:5	[M+HCOO] ⁻	880.6029	15.79
PC 18:0_18:2	[M+H] ⁺	786.606	18.4	PC 18:1/18:1	[M+HCOO] ⁻	830.586	15.83
PC 18:0_20:3	[M+H] ⁺	812.63	18.74	PC 18:2_20:4	[M+HCOO] ⁻	850.5652	14.55

PC 18:0_20:4	[M+H] ⁺	810.6	18.27	PC O-16:0_18:2	[M+HCOO] ⁻	788.538	14.32
PC 18:0_20:4	[M+Na] ⁺	832.581	18.27	PE 12:0_12:0	[M-H] ⁻	578.3827	10.78
PC 18:0_22:5	[M+H] ⁺	836.598	18.36	PE 16:0_20:4	[M-H] ⁻	738.5115	15.02
PC 18:0_22:6	[M+H] ⁺	834.601	18.01	PE 18:0_18:1	[M-H] ⁻	744.5484	16.81
PC 18:1/18:1	[M+H] ⁺	786.599	18.2	PE 18:0_18:2	[M-H] ⁻	742.5334	16.07
PC 16:0_18:2	[M+H] ⁺	758.571	17.13	PE 18:0_20:4	[M-H] ⁻	766.5427	15.98
PC 18:2_20:4	[M+H] ⁺	806.572	16.78	PE O-16:1_20:4	[M-H] ⁻	722.5098	15.5
PC 18:2_O-16:0	[M+H] ⁺	744.559	17.9	PE O-18:1_20:4	[M-H] ⁻	750.5499	16.47
SM 18:2;O2/14:0	[M+H] ⁺	673.517	13.83	PE O-18:2_20:4	[M-H] ⁻	748.5388	15.59
SM 18:1;O2/15:0	[M+H] ⁺	689.565	15.88	PI 16:0_18:1	[M-H] ⁻	835.508	14.6
SM 18:2;O2/16:0	[M+H] ⁺	701.557	15.44	PI 18:0_20:4	[M-H] ⁻	885.548	14.81
SM 34:1;O2	[M+H] ⁺	703.585	16.57	SM 18:2;O2/14:0	[M+HCOO] ⁻	717.5233	12.08
SM 34:1;O2	[M+Na] ⁺	725.557	16.57	SM 18:1;O2/15:0	[M+HCOO] ⁻	733.541	13.82
SM 36:1;O2	[M+H] ⁺	731.6	17.89	SM 18:2;O2/16:0	[M+HCOO] ⁻	745.551	13.42
SM 38:1;O2	[M+H] ⁺	759.643	19.17	SM 34:1;O2	[M+HCOO] ⁻	747.5581	14.37
SM 38:1;O2	[M+Na] ⁺	781.623	19.17	SM 40:1;O2	[M+HCOO] ⁻	831.6575	17.48
SM 40:1;O2	[M+H] ⁺	787.673	20.35	SM 42:1;O2	[M+HCOO] ⁻	859.6949	18.43
SM 40:1;O2	[M+Na] ⁺	809.667	20.35	SM 42:2;O2	[M+HCOO] ⁻	857.6703	17.42
SM 40:2;O2	[M+H] ⁺	785.662	19.38				
SM 41:1;O2	[M+H] ⁺	801.674	20.87				
SM 42:1;O2	[M+H] ⁺	815.712	21.38				
SM 42:1;O2	[M+Na] ⁺	837.673	21.38				
SM 42:2;O2	[M+H] ⁺	813.69	20.28				
SM 42:2;O2	[M+Na] ⁺	835.6622	20.25				
SM 42:3;O2	[M+H] ⁺	833.662	19.32				
SM 42:3;O2	[M+Na] ⁺	811.671	19.32				
SM 43:1;O2	[M+H] ⁺	829.7072	21.66				
SM 43:2;O2	[M+H] ⁺	827.706	20.6				
TG 12:0_14:0_16:0	[M+NH ₄] ⁺	740.663	24.35				
TG 14:0_16:0_18:0	[M+NH ₄] ⁺	824.778	26.19				
TG 16:0_18:0_18:0	[M+NH ₄] ⁺	880.848	27.17				
TG 16:0_18:0_18:1	[M+NH ₄] ⁺	878.825	26.73				
TG 16:0_18:0_20:0	[M+NH ₄] ⁺	908.876	27.6				
TG 16:0_18:1_18:1	[M+NH ₄] ⁺	876.804	26.26				
TG 16:0_18:2_20:4	[M+NH ₄] ⁺	896.776	24.91				
TG 18:0_18:1_18:1	[M+NH ₄] ⁺	904.834	26.75				
TG 18:1_18:1_18:2	[M+NH ₄] ⁺	900.814	25.67				
TG 18:1_18:2_18:2	[M+NH ₄] ⁺	898.781	25.4				

Table SB1.a: Information on calibrant used in positive ion mode: m/z , CCS, mean td' determined with UNIFI software on the three ion mobility conditions (extract)

							H40	H35	H30
Tune Mix	m/z	z	m	CCS (N_2) in \AA^2	$1/\mu$	CCS'	td'	td'	td'
TuneMix_118	118.0857	1	118.1	121.3	0.044	577.13	1.18	1.17	1.24
Tune Mix_322	322.048	1	322.0	153.73	0.039	780.33	2.07	2.15	2.21
TuneMix_622	622.0273	1	622.0	202.96	0.037	1050.69	3.59	3.78	3.98
TuneMix_922	922.0053	1	922.0	243.64	0.037	1270.21	5.13	5.44	5.77
TuneMix_1222	1221.9855	1	1222.0	282.2	0.037	1476.60	6.84	7.27	7.76
TuneMix_1522	1521.9696	1	1522.0	316.96	0.036	1662.15	8.62	9.18	9.81
TuneMix_1822	1821.9443	1	1821.9	351.25	0.036	1844.72	10.55	11.23	12.02

S.M. Stow, T.J. Causon, X. Zheng, R.T. Kurulugama, T. Mairinger, J.C. May, E.E. Rennie, E.S. Baker, R.D. Smith, J.A. McLean, S. Hann, J.C. Fjeldsted, An Interlaboratory Evaluation of Drift Tube Ion Mobility-Mass Spectrometry Collision Cross Section Measurements, *Anal Chem*, 89 (2017) 9048-9055.

							H40	H35	H30
Polyalanine	m/z	z	m	CCS (N_2) in \AA^2	$1/\mu$	CCS'	td'	td'	td'
Polyala_A3	232.1267	1	232.1	151.00	0.040	754.86	1.99	2.06	2.12
Polyala_A4	303.1657	1	303.2	166.00	0.039	840.52	2.37	2.48	2.57
Polyala_A5	374.2026	1	374.2	181.00	0.038	923.92	2.77	2.93	3.08
Polyala_A6	445.2398	1	445.2	195.00	0.038	1000.95	3.20	3.37	3.57
Polyala_A7	516.2769	1	516.3	211.00	0.038	1087.52	3.69	3.90	4.12
Polyala_A8	587.3121	1	587.3	228.00	0.037	1178.82	4.28	4.54	4.83
Polyala_A9	658.3467	1	658.3	243.00	0.037	1259.47	4.81	5.11	5.43
Polyala_A10	729.3831	1	729.4	256.00	0.037	1329.49	5.30	5.67	6.04
Polyala_A11	800.4205	1	800.4	271.00	0.037	1409.70	5.87	6.27	6.70
Polyala_A12	871.4576	1	871.5	282.00	0.037	1468.95	6.45	6.87	7.35
Polyala_A13	942.4941	1	942.5	294.00	0.037	1533.26	7.02	7.54	8.06
Polyala_A14	1013.5312	1	1013.5	306.00	0.037	1597.46	7.58	8.10	8.68

I. Campuzano, M.F. Bush, C.V. Robinson, C. Beaumont, K. Richardson, H. Kim, H.I. Kim, Structural characterization of drug-like compounds by ion mobility mass spectrometry: comparison of theoretical and experimentally derived nitrogen collision cross sections, *Anal Chem*, 84 (2012) 1026-1033.

							H40	H35	H30
Dextran	m/z	z	m	CCS (N_2) in \AA^2	$1/\mu$	CCS'	td'	td'	td'
dextran_2	365.1055	1	365.1	179.54	0.038	915.66	2.64	2.80	2.93
Dextran_3	527.1587	1	527.2	215.00	0.038	1108.74	3.75	3.97	4.20
Dextran_4	689.207	1	689.2	243.36	0.037	1262.51	4.68	4.97	5.28
Dextran_5	851.2588	1	851.3	273.81	0.037	1425.76	5.72	6.09	6.49
Dextran_6	1013.3099	1	1013.3	302.06	0.037	1576.88	6.74	7.19	7.69
Dextran_7	1175.3625	1	1175.4	330.94	0.037	1730.88	7.92	8.46	9.06
Dextran_8	1337.4144	1	1337.4	355.80	0.036	1863.53	9.02	9.63	10.33
Dextran_9	1499.4686	1	1499.5	377.70	0.036	1980.43	10.04	10.72	11.51
Dextran_10	1661.52	1	1661.5	397.83	0.036	2087.82	11.15	11.92	12.81

J. Hofmann, W.B. Struwe, C.A. Scarff, J.H. Scrivens, D.J. Harvey, K. Pagel, Estimating Collision Cross Sections of Negatively Charged N-Glycans using Traveling Wave Ion Mobility-Mass Spectrometry, *Analytical Chemistry*, 86 (2014) 10789-10795.

Major Mix	m/z	z	m	CCS (N_2) in \AA^2	$1/\mu$	CCS'	H40	H35	H30
							td'	td'	td'
Acetaminophen	152.0708	1	152.1	130.4	0.042	634.16	1.37	1.38	1.36
Caffeine	195.0868	1	195.1	138.2	0.041	683.92	1.59	1.63	1.64
sulfaguanidine	215.0585	1	215.1	146.8	0.040	730.75	1.77	1.84	1.89
Polyala_A3	232.107	1	232.1	151.00	0.040	754.86	1.88	1.95	1.99
sulfadimethoxine	311.0809	1	311.1	166.00	0.039	841.43	2.43	2.50	2.65
Polyala_A5	374.2015	1	374.2	168.4	0.038	859.60	2.77	2.93	3.09
L-valyl-L-tyrosyl-L-valine	380.218	1	380.2	181.00	0.038	924.43	3.12	3.29	3.51
Polyala_A6	445.2383	1	445.2	191.7	0.038	984.02	3.21	3.38	3.59
Verapamil	455.2911	1	455.3	195.00	0.038	1001.61	3.71	3.92	4.14
terfenadine	472.3221	1	472.3	208.8	0.038	1073.61	4.34	4.61	4.91
Polyala_A7	516.275	1	516.3	228.7	0.038	1178.75	3.71	3.92	4.14
leucine-enkephaline	556.2773	1	556.3	211	0.038	1089.54	4.38	4.65	4.95
Polyala_A8	587.3096	1	587.3	229.8	0.037	1188.12	4.30	4.57	4.84
Reserpine	609.2804	1	609.3	252.3	0.037	1305.52	5.19	5.53	5.91
Polyala_A9	658.3432	1	658.3	243	0.037	1259.47	4.84	5.15	5.46
Polyala_A10	729.3799	1	729.4	256	0.037	1329.49	5.34	5.65	6.04
Polyala_A11	800.4185	1	800.4	271	0.037	1409.70	5.89	6.29	6.69
Polyala_A12	871.4548	1	871.5	282	0.037	1468.95	6.47	6.91	7.39
Polyala_A13	942.4895	1	942.5	294	0.037	1533.26	7.03	7.51	8.05
Polyala_A14	1013.5278	1	1013.5	306	0.037	1597.46	7.59	8.11	8.70
perfluoroalkylphosphazine 2	1122.0684	1	1122.1	276.5	0.037	1445.33	6.24	6.64	7.09
MajorMix_1222	1221.9885	1	1222.0	291.2	0.037	1523.69	6.89	7.32	7.82
MajorMix_1322	1321.971	1	1322.0	304	0.036	1592.02	7.50	7.98	8.52
MajorMix_1422	1421.9671	1	1422.0	316.7	0.036	1659.74	8.12	8.64	9.24
MajorMix_1522	1521.9606	1	1522.0	329	0.036	1725.29	8.74	9.31	9.95
MAjorMix_1622	1621.9484	1	1621.9	340.1	0.036	1784.50	9.37	9.98	10.67
MajorMix_1722	1721.9416	1	1721.9	351.3	0.036	1844.17	10.00	10.65	11.39
MajorMix_1822	1821.9382	1	1821.9	362.1	0.036	1901.70	10.63	11.32	12.12
MajorMix_1922	1921.8912	1	1921.9	372.6	0.036	1957.62	11.27	12.00	12.86

CCS values from Waters

Polyglycine	m/z	z	m	CCS (N_2) in \AA^2	$1/\mu$	CCS'	H40	H35	H30
							td'	td'	td'
G6	304.1234	1	304.1	160.00	0.039	810.25	2.23	2.32	2.41
G7	361.1455	1	361.1	170.00	0.038	866.68	2.53	2.65	2.76
G8	418.1671	1	418.2	181.00	0.038	927.32	2.80	2.96	3.12
G9	475.1887	1	475.2	194.00	0.038	997.68	3.17	3.34	3.55
G10	532.2099	1	532.2	206.00	0.038	1062.57	3.56	3.76	3.97
G11	589.2292	1	589.2	216.00	0.037	1116.86	3.90	4.13	4.37
G12	646.2485	1	646.2	226.00	0.037	1170.91	4.24	4.50	4.77
G13	703.2679	1	703.3	234.00	0.037	1214.40	4.49	4.77	5.07
G14	760.2864	1	760.3	248.00	0.037	1288.91	4.98	5.29	5.64

T.W. Knapman, J.T. Berryman, I. Campuzano, S.A. Harris, A.E. Ashcroft, Considerations in experimental and theoretical collision cross-section measurements of small molecules using travelling wave ion mobility spectrometry-mass spectrometry, International Journal of Mass Spectrometry, 298 (2010) 17-23.

PEO	<i>m/z</i>	<i>z</i>	<i>m</i>	CCS (N ₂) in Å ²	1/ μ	CCS'	H40	H35	H30
							td'	td'	td'
PEO_7	363.1963	1	363.2	174.7	0.038	890.82	2.55	2.68	2.78
PEO_8	407.2253	1	407.2	187.2	0.038	958.27	2.83	2.98	3.13
PEO_9	451.2518	1	451.3	198.3	0.038	1018.30	3.15	3.30	3.49
PEO_10	495.2792	1	495.3	209.2	0.038	1077.07	3.50	3.68	3.87
PEO_11	539.3049	1	539.3	221.8	0.038	1144.44	3.88	4.08	4.30
PEO_12	583.3303	1	583.3	232.7	0.037	1202.93	4.24	4.48	4.73
PEO_13	627.3554	1	627.4	243.2	0.037	1259.23	4.61	4.87	5.15
PEO_14	671.3801	1	671.4	253.7	0.037	1315.44	4.97	5.27	5.58
PEO_15	715.406	1	715.4	263.5	0.037	1367.94	5.34	5.67	6.02
PEO_16	759.4326	1	759.4	272.9	0.037	1418.29	5.68	6.03	6.46
PEO_17	803.4585	1	803.5	282.9	0.037	1471.70	6.12	6.51	6.95
PEO_18	847.4849	1	847.5	291.6	0.037	1518.29	6.40	6.85	7.42
PEO_19	891.5106	1	891.5	300.5	0.037	1565.86	6.91	7.36	7.86
PEO_20	935.535	1	935.5	309.4	0.037	1613.40	7.29	7.78	8.32
PEO_21	979.5628	1	979.6	318.2	0.037	1660.37	7.69	8.20	8.77
PEO_22	1023.5889	1	1023.6	326.1	0.037	1702.61	8.08	8.62	9.23
PEO_23	1067.6158	1	1067.6	335.3	0.037	1751.61	8.47	9.05	9.69
PEO_24	1111.6149	1	1111.6	342.50	0.037	1790.13	8.86	9.47	10.15

J.R.N. Haler, C. Kune, P. Massonnet, C. Comby-Zerbino, J. Jordens, M. Honing, Y. Mengerink, J. Far, E. De Pauw, Comprehensive Ion Mobility Calibration: Poly(ethylene oxide) Polymer Calibrants and General Strategies, Anal Chem, 89 (2017) 12076-12086.

PEG	<i>m/z</i>	<i>z</i>	<i>m</i>	CCS (N ₂) in Å ²	1/ μ	CCS'	H40	H35	H30
							td'	td'	td'
PEG_8	393.2099	1	393.2	116	0.038	593.12	2.72	2.88	3.01
PEG_9	437.2364	1	437.2	127	0.038	651.55	3.01	3.17	3.36
PEG_10	481.2634	1	481.3	137	0.038	704.80	3.32	3.48	3.67
PEG_11	525.2898	1	525.3	148	0.038	763.15	3.67	3.86	4.06
PEG_12	569.3153	1	569.3	158	0.037	816.31	4.02	4.24	4.48
PEG_13	613.34	1	613.3	168	0.037	869.44	4.38	4.65	4.92
PEG_14	657.3653	1	657.4	178	0.037	922.54	4.75	5.03	5.34
PEG_15	701.3917	1	701.4	187	0.037	970.43	5.12	5.43	5.77
PEG_16	745.419	1	745.4	196	0.037	1018.29	5.50	5.84	6.25
PEG_17	789.4465	1	789.4	205	0.037	1066.13	5.90	6.27	6.69
PEG_18	833.4733	1	833.5	213	0.037	1108.74	6.29	6.69	7.13
PEG_19	877.5005	1	877.5	221	0.037	1151.32	6.65	7.08	7.55
PEG_20	921.5261	1	921.5	229	0.037	1193.88	7.00	7.45	7.98
PEG_21	965.5526	1	965.6	236	0.037	1231.20	7.44	7.97	8.54
PEG_22	1009.5794	1	1009.6	243	0.037	1268.50	7.88	8.41	9.00
PEG_23	1053.6073	1	1053.6	252	0.037	1316.23	8.28	8.84	9.46
PEG_24	1097.6334	1	1097.6	258	0.037	1348.26	8.68	9.25	9.91
PEG_25	1141.6276	1	1141.6	264	0.037	1380.28	9.07	9.68	10.37
PEG_26	1185.6851	1	1185.7	271	0.037	1417.51	9.47	10.11	10.84
PEG_27	1229.7093	1	1229.7	279	0.037	1459.96	9.87	10.54	11.31
PEG_28	1273.7337	1	1273.7	285	0.036	1491.93	10.28	10.98	11.78
PEG_29	1317.7602	1	1317.8	293	0.036	1534.36	10.69	11.42	12.26
PEG_30	1361.7841	1	1361.8	299	0.036	1566.31	11.10	11.87	12.74
PEG_31	1405.8074	1	1405.8	301	0.036	1577.28	11.52	12.31	13.25
PEG_32	1449.836	1	1449.8	313	0.036	1640.65	11.93	12.76	13.44
PEG_33	1493.862	1	1493.9	320	0.036	1677.81	12.36	13.24	
PEG_34	1537.8876	1	1537.9	325	0.036	1704.48	12.77		

Q. Duez, F. Chirot, R. Lienard, T. Josse, C. Choi, O. Coulembier, P. Dugourd, J. Cornil, P. Gerbaux, J. De Winter, *Polymers for Traveling Wave Ion Mobility Spectrometry Calibration*, *J Am Soc Mass Spectrom*, 28 (2017) 2483-2491.

TAA	<i>m/z</i>	<i>z</i>	<i>m</i>	CCS (N ₂) in Å ²	1/ μ	CCS'	H40	H35	H30
							td'	td'	td'
TAA_2	130.1586	1	130.2	122.2	0.043	586.65	1.31	1.30	1.25
TAA_3	186.2215	1	186.2	143.8	0.041	709.52	1.82	1.88	1.91
TAA_4	242.2836	1	242.3	166	0.040	831.73	2.40	2.51	2.60
TAA_5	298.3468	1	298.3	190	0.039	961.38	3.05	3.21	3.42
TAA_6	354.4093	1	354.4	214	0.039	1090.25	3.79	4.02	4.25
TAA_7	410.4716	1	410.5	236.8	0.038	1212.48	4.58	4.87	5.18
TAA_8	466.534	1	466.5	258	0.038	1326.13	5.39	5.75	6.15

I. Campuzano, M.F. Bush, C.V. Robinson, C. Beaumont, K. Richardson, H. Kim, H.I. Kim, *Structural characterization of drug-like compounds by ion mobility mass spectrometry: comparison of theoretical and experimentally derived nitrogen collision cross sections*, *Anal Chem*, 84 (2012) 1026-1033.

Drug standards	<i>m/z</i>	<i>z</i>	<i>m</i>	CCS (N ₂) in Å ²	1/ μ	CCS'	H40	H35	H30
							td'	td'	td'
Acetaminophen	152.0746	1	152.1	130.4	0.042	634.16	1.36	1.37	1.32
alprenolol	250.1796	1	250.2	157.5	0.040	790.43	2.16	2.25	2.32
Ondansetron	294.1601	1	294.2	172.7	0.039	873.31	2.50	2.63	2.75
Clozapine N-oxide	343.1313	1	343.1	180.6	0.039	918.98	2.76	2.93	3.08
Colchicine	400.1737	1	400.2	196.2	0.038	1003.78	3.34	3.53	3.62
Verapamil	455.2906	1	455.3	210.0	0.038	1078.66	3.71	3.92	4.13
Reserpine	609.2787	1	609.3	254.3	0.037	1315.87	5.19	5.53	5.90

I. Campuzano, M.F. Bush, C.V. Robinson, C. Beaumont, K. Richardson, H. Kim, H.I. Kim, *Structural characterization of drug-like compounds by ion mobility mass spectrometry: comparison of theoretical and experimentally derived nitrogen collision cross sections*, *Anal Chem*, 84 (2012) 1026-1033.

Lipids standards	<i>m/z</i>	<i>z</i>	<i>m</i>	CCS (N ₂) in Å ²	1/ μ	CCS'	H40	H35	H30
							td'	td'	td'
1,2-dihexanoyl-sn-glycero-3-phosphoethanolamine	412.2111	1	412.2	202.92a	0.038	1039.15	3.42	3.61	3.81
1,2-dihexanoyl-sn-glycero-3-phosphoethanolamine	434.192	1	434.2	208.63a	0.038	1070.11	3.60	3.80	4.02
1-hexadecanoyl-sn-glycero-3-phosphoethanolamine	454.2962	1	454.3	213.91a	0.038	1098.67	4.00	4.21	4.44
1-hexadecanoyl-sn-glycero-3-phosphoethanolamine	476.2727	1	476.3	220.01a	0.038	1131.52	4.23	4.45	4.70
1-hexadecanoyl-sn-glycero-3-phosphocholine	496.3419	1	496.3	230.74b	0.038	1188.04	4.57	4.83	5.11
1-hexadecanoyl-sn-glycero-3-phosphocholine	518.3232	1	518.3	223.94b	0.038	1154.33	4.73	4.99	5.28
1,2-di-(9Z-tetradecenoyl)-sn-glycerol	531.4037	1	531.4	230.30c	0.038	1187.84	4.63	4.89	5.16
1,2-di-(9Z-tetradecenoyl)-sn-glycerol	526.4477	1	526.4	235.12c	0.038	1212.45	4.77	5.05	5.35
1,2-di-(9Z-tetradecenoyl)-sn-glycerol	509.4217	1	509.4	235.67c	0.038	1214.25	4.74	5.03	5.35
1-(6Z-octadecenoyl)-sn-glycero-3-phosphocholine	522.3518	1	522.4	233.26c	0.038	1202.61	4.68	4.96	5.27
1-(6Z-octadecenoyl)-sn-glycero-3-phosphocholine	544.3423	1	544.3	235.87c	0.038	1217.32	4.78	5.05	5.34
1,2-didecanoyl-sn-glycero-3-phosphoethanolamine	524.3378	1	524.3	235.4a	0.038	1213.76	4.75	5.04	5.34
1,2-didecanoyl-sn-glycero-3-phosphoethanolamine	546.3189	1	546.3	242.92a	0.038	1253.82	5.02	5.33	5.66

N-(9Z-octadecenoyl)-sphing-4-enine	586.5186	1	586.5	258.54c	0.037	1336.67	5.70	6.06	6.45
N-(9Z-octadecenoyl)-sphing-4-enine	564.5354	1	564.5	258.90c	0.037	1337.33	5.76	6.11	6.51
1,2-di-(9Z-tetradecenoyl)-sn-glycero-3-phosphate	589.3878	1	589.4	245.83c	0.037	1271.12	5.15	5.47	5.81
1,2-di-(9Z-tetradecenoyl)-sn-glycero-3-phosphate	606.4136	1	606.4	245.61c	0.037	1270.78	5.26	5.57	5.91
1,2-di-(9Z-tetradecenoyl)-sn-glycero-3-phosphoethanolamine	632.4293	1	632.4	249.05c	0.037	1289.72	5.43	5.76	6.08
1,2-di-(9Z-tetradecenoyl)-sn-glycero-3-phosphoethanolamine	654.407	1	654.4	256.16c	0.037	1327.52	5.69	6.03	6.43
1,2-di-(9Z-tetradecenoyl)-sn-glycero-3-phospho-(1'-sn-glycerol)	663.4232	1	663.4	264.44c	0.037	1370.82	6.00	6.35	6.73
1,2-di-(9Z-tetradecenoyl)-sn-glycero-3-phospho-(1'-sn-glycerol)	680.4473	1	680.4	264.68c	0.037	1372.73	6.06	6.42	6.83
1,2-dipentadecanoyl-sn-glycero-3-phosphoethanolamine	664.4908	1	664.5	267.34a	0.037	1385.88	6.18	6.56	6.99
1,2-dipentadecanoyl-sn-glycero-3-phosphoethanolamine	686.4553	1	686.5	270.25a	0.037	1401.87	6.42	6.80	7.24
cholest-5-en-3beta-yl nonadecanoate	684.6612	1	684.7	291.96c	0.037	1514.40	7.23	7.71	8.27
1,2-di-(9E-tetradecenoyl)-sn-glycero-3-phosphocholine	674.4741	1	674.5	266.42c	0.037	1381.50	6.07	6.47	6.86
1,2-di-(9Z-tetradecenoyl)-sn-glycero-3-phosphoserine	676.4177	1	676.4	258.13c	0.037	1338.60	5.72	6.10	6.48
1,2-di-(9Z-tetradecenoyl)-sn-glycero-3-phosphoserine	698.4329	1	698.4	258.54c	0.037	1341.60	5.76	6.13	6.51
N-(9Z-octadecenoyl)-sphing-4-enine-1-phosphocholine	729.5872	1	729.6	287.60c	0.037	1493.60	7.43	7.91	8.44
N-(9Z-octadecenoyl)-sphing-4-enine-1-phosphocholine	751.5705	1	751.6	275.59c	0.037	1432.02	7.04	7.45	7.98
1,2-dihexadecanoyl-sn-glycero-3-phosphocholine	734.5669	1	734.6	278.4d	0.037	1446.01	7.02	7.45	7.94
1,2-dihexadecanoyl-sn-glycero-3-phosphocholine	756.5511	1	756.6	280.56d	0.037	1458.00	7.13	7.58	8.06
1,2-di-(9Z-octadecenoyl)-sn-glycero-3-phosphoethanolamine	744.5472	1	744.5	280.6e	0.037	1457.79	6.65	7.13	7.58
1,2-di-(9Z-octadecenoyl)-sn-glycero-3-phosphoethanolamine	766.5359	1	766.5	287.57e	0.037	1494.78	7.01	7.43	7.95
1,2-di-(9Z-tetradecenoyl)-sn-glycero-3-phospho-(1'-myo-inositol)	751.4347	1	751.4	287.29c	0.037	1492.82	6.48	6.90	7.32
1,2-dieicosanoyl-sn-glycero-3-phosphocholine	846.6911	1	846.7	307.97a	0.037	1603.50	8.14	8.70	9.27
1,2-dieicosanoyl-sn-glycero-3-phosphocholine	868.6773	1	868.7	310.72a	0.037	1618.47	8.26	8.79	9.42
1,2,3-tri-(9Z-octadecenoyl)-glycerol	902.8137	1	902.8	322.69c	0.037	1681.79	8.83	9.64	10.32
1,2,3-tri-(9Z-octadecenoyl)-glycerol	907.7721	1	907.8	324.23c	0.037	1690.00	8.85	9.36	10.14

a: Hines, K. M.; May, J. C.; McLean, J. A.; Xu, L. *Anal Chem* 2016, 88, 7329-7336.

b: Tsugawa, H.; Ikeda, K.; Takahashi, M.; Satoh, A.; Mori, Y.; Uchino, H.; Okahashi, N.; Yamada, Y.; Tada, I.; Bonini, P.; Higashi, Y.; Okazaki, Y.; Zhou, Z.; Zhu, Z.-J.; Koelmel, J.; Cajka, T.; Fiehn, O.; Saito, K.; Arita, M.; Arita, M.; Cold Spring Harbor Laboratory, 2020.

c: Vasilopoulou, C. G.; Sulek, K.; Brunner, A. D.; Meitei, N. S.; Schweiger-Hufnagel, U.; Meyer, S. W.; Barsch, A.; Mann, M.; Meier, F. *Nat Commun* 2020, 11, 331.

d: Leaptrot, K. L.; May, J. C.; Dodds, J. N.; McLean, J. A. *Nature Communications* 2019, 10.

e: Zheng, X.; Aly, N. A.; Zhou, Y.; Dupuis, K. T.; Bilbao, A.; Paurus, V. L.; Orton, D. J.; Wilson, R.; Payne, S. H.; Smith, R. D.; Baker, E. S. *Chem Sci* 2017, 8, 7724-7736.

4.4. Conclusion and perspectives

In this chapter, we have studied various commercial CCS calibrants and carried out their evaluation on lipid CCS measurements using the TWIMS-MS instrument in both positive and negative modes. Depending on the calibrant employed, CCS values can vary drastically with up to 25% deviation. To reduce these calibrant-induced deviations, we proposed to re-calibrate the ^{TW}CCS of ten of the commercial calibrants using the Tune Mix, as a reference calibrant to further re-align all the ^{TW}CCS we measured for lipids present in human plasma. These modified scales limit drastically calibrant-induced deviations and allow the access to comparable lipid CCS with very small deviations, less than 0.2% whatever the calibrant originally used. The re-calibrated CCS values for each calibrant constitute a database which allows to correct any deviation on lipid CCS values whatever the calibrant originally used. Resulting corrected CCS values from plasma lipids were thus efficiently matched to those previously reported in the literature (with deviations < 2%). Therefore, this work shows that unique and comparable CCS values can be obtained upon re-calibration relatively to Tune Mix CCS values.

We have also showed that this method could be used to any previously published study, if the drift times of the samples and the calibrant are reported. We think that by using these re-calibrated CCS values, the use of CCS as a universal descriptor can be achievable.

Chapter V. Influence of the instruments on the measurement of collision cross sections

5.1. Introduction

In the previous chapter, the importance of the calibration step and the choice of calibrant was addressed for the TWIMS instrument. In this chapter, the objective was to compare CCS values measured across three different IMS instruments: DTIMS, TWIMS and TIMS. Different potential causes of CCS deviations have been studied. First, the repeatability of the CCS values for each of the three IMS technologies, using four instruments, including two TIMS cells has been studied. A particular attention has been paid to understand how the CCS values were determined in the three instruments using commercial software tools. This is part of an article which has been submitted to *Analytica Chimica Acta*. The workflow used for this chapter is highlighted by Figure V-1.

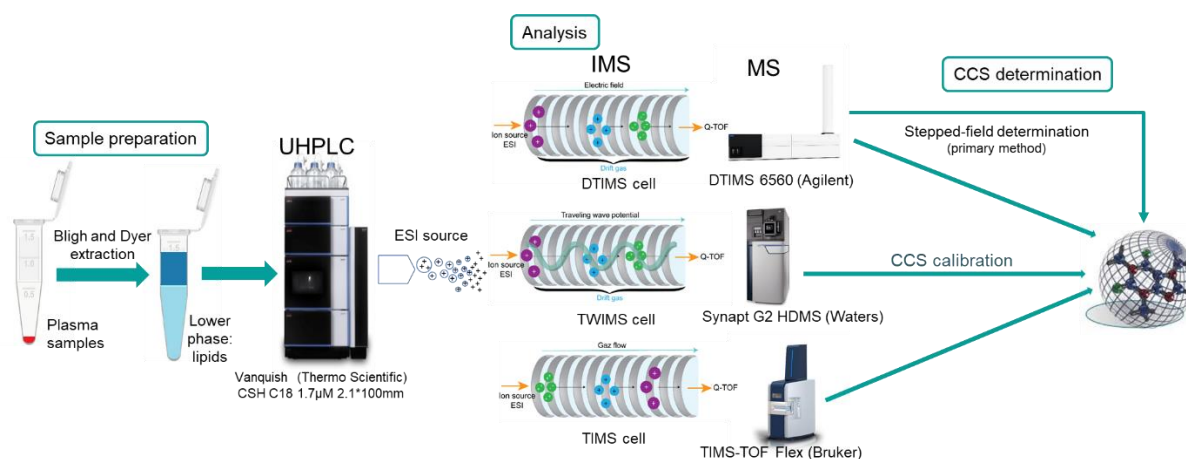


Figure V-1: Schematic representation of the workflow used in this Chapter

5.2. Comparison of lipid CCS values from three instruments (Article)

Interplatform comparison of three ion mobility techniques for human plasma lipid collision cross sections

Anaïs C. George¹, Isabelle Schmitz¹, Florent Rouvière², Sandra Alves³, Benoit Colsch⁴, Sabine Heinisch², Carlos Afonso¹, François Fenaille⁴, Corinne Loutelier-Bourhis^{1*}

¹Univ Rouen Normandie, INSA Rouen Normandie, CNRS, Normandie Univ, COBRA UMR 6014, INC3M FR 3038, F-76000 Rouen, France

²Université de Lyon, Institut des Sciences Analytiques, UMR 5280 CNRS, 5 rue de la Doua, 69100 Villeurbanne, France

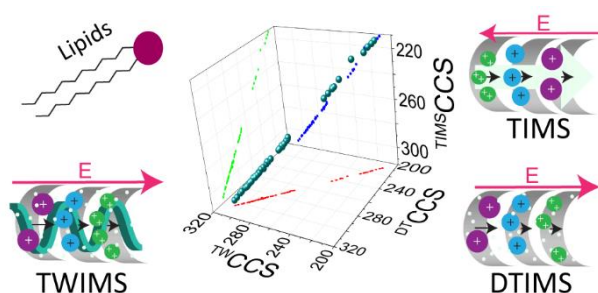
³Sorbonne Université, Faculté des Sciences et de l'Ingénierie, Institut Parisien de Chimie Moléculaire (IPCM), Paris, France

⁴Université Paris-Saclay, CEA, INRAE, Département Médicaments et Technologies pour la Santé (DMTS), MetaboHUB, F-91191 Gif sur Yvette, France.

5.2.1. Abstract

The implementation of ion mobility spectrometry (IMS) in liquid chromatography-high-resolution mass spectrometry (LC-HRMS) workflows has become a valuable tool for improving compound annotation in metabolomic analyses by increasing peak capacity and the addition of a molecular descriptor, the collision cross section (CCS). Although some studies reported high repeatability and reproducibility of CCS measurements and good interplatform agreement for small molecules, standardized protocols are still missing due to the lack of reference CCS values and reference materials.

Here, we present a comparison of CCS values of approximately one hundred lipid species commercially available and extracted from human plasma, determined using three different commercial ion mobility technologies from different laboratories, the drift tube IMS (DTIMS), the travelling wave IMS (TWIMS) and the trapped IMS (TIMS) to evaluate both instrument repeatability and interlaboratory reproducibility. We showed that CCS discrepancies of 0.3% (average) could occur depending on the data processing software tools. Moreover, eleven CCS calibrants were also evaluated yielding mean RSD below 2% for eight calibrants, ESI Low concentration tuning mix (Tune Mix) showing the lowest RSD (<0.5%) in both ion modes. Tune Mix calibrated CCS from the three different IMS instruments proved to be well correlated and highly reproducible ($R^2 > 0.995$ and mean RSD $\leq 1\%$). More than 90% of the lipid CCS had deviations of less than 1%, demonstrating high comparability between techniques, and the possibility to use the CCS as molecular descriptor. We also highlighted the need of standardized procedures for calibration, data acquisition, and data processing. This work demonstrates that using harmonized analytical conditions are required for interplatform reproducibility for CCS measurements of human plasma lipids.



Keywords:

- Lipidomics
- Inter-laboratory comparison
- Collision cross section
- Drift tube ion mobility spectrometry
- Travelling wave ion mobility spectrometry
- Trapped ion mobility spectrometry

Highlights:

- Comparison of three IMS platforms: TWIMS, TIMS, DTIMS
- Evaluation of CCS determination and calibration on each instrument
- Application to the measurement of CCS from ~110 human plasma lipids.

5.2.2. Introduction

Liquid chromatography coupled to high-resolution (tandem) mass spectrometry (LC-HRMS/MS) represents the most widely used approach for the analysis of organic compounds in many fields such as metabolomics and lipidomics. LC-HRMS/MS brings several complementary information for compound annotation such as retention time, accurate mass measurements and fragmentation patterns from MS/MS data. Due to the complexity and large diversity of molecules present in biological matrices, it is still necessary to improve compound annotation confidence. In that context, ion mobility - mass spectrometry (IM-MS) provides an additional separation dimension potentially useful to distinguish isomeric species, together with an additional molecular descriptor, the collision cross section (CCS) reflecting the 3D geometry of an ion in a particular buffer gas. Different ion mobility techniques are nowadays commercially available, such as drift tube IMS (DTIMS), travelling wave IMS (TWIMS), trapped IMS (TIMS) or high-field asymmetric IMS (FAIMS) often used upstream to HRMS. This last technology is a non-linear IMS technique [1], and is essentially used as a filter, and the determination of the CCS values can be more difficult. The DTIMS cell can be described as a tube filled with a buffer gas, in most cases nitrogen or helium at reduced pressure [2]. Ions move through the tube under an applied electric field, and they can be separated due to collisions with the buffer gas. Compact ions have less collisions with the drift gas, and thus exhibit higher drift velocities, higher mobilities and shorter drift times than more extended ions. Velocities of ions can be calculated from the experimentally measured drift times (t_D) by knowing the IMS tube length. Then, the experimental stepped-field CCS values can be directly determined using the Mason-Schamp equation [3]. However, some issues are still challenging for primary measurements, like measuring the pressure and temperature inside the tube and determining the tube length [4]. Thus, an additional calibration step is usually required before single-field CCS values can be determined [5].

Ions are similarly separated in the TWIMS cell [6], but the electric field is no more constant and uniform, allowing a better IMS resolution with a smaller tube [7]. However, in this case the relationship between t_D and the CCS is more complex. The principle of the TIMS cell is different, the ions are pushed by the gas and retained by the electric field. That involves a trapping step of the ions [8]. Then, the electric field is reduced according to a ramp, allowing the ions to leave gradually the tube, and to be separated. Thus, the extended ions will leave the tube before the smaller ions, in contrast to DTIMS and TWIMS. While the three IMS cells differ in their principles, they offer similar advantages. They allow an additional dimension of separation to the LC-MS methods, by increasing peak capacity and selectivity, and they also provide CCS values, structural molecular descriptors that reinforce compounds annotation. Another advantage consists in background filtering, allowing sensitivity enhancement, high quality MS² spectra [9], thus allowing the development of acquisition workflows such as PASEF mode [10].

It is now well admitted that CCS values facilitate compound identification. Several databases have been developed made publicly available by using single datasets[11,12] or by compiling different studies into online resources, such as the CCS compendium [13], AllCCS [14], LipidCCS [15], LIPID MAPS[®] Ion Mobility Database. In addition to experimental CCS data, CCS values either calculated from molecular dynamics or from quantum chemistry (density functional theory) or predicted by machine learning [14,15] have also been reported and constitute valuable inputs to existing databases. Nevertheless, all the CCS values reported and present in existing databases need to be comprehensively cross-validated to make them readily and confidently used for metabolite annotation. Interoperability of CCS databases is a prerequisite to full adoption by the metabolomics

community [16]. A few studies have already compared ion mobility technologies to establish the degree of polymerization [17] or conformers separation [18], while others reported that CCS measurements can be highly repeatable for low molecular weight compounds [5,19,20]. Stow et al, [5] studied the reproducibility of the ^{DT}CCS measurements for more than 120 unique ions from metabolites, peptides, lipids and proteins across three different laboratories equipped with the same commercially available uniform field DTIM-MS and a fourth laboratory equipped with a modified DTIM-MS used as reference instrument. For stepped-field measurements, a mean RSD of 0.29% was obtained over all the 120 ion species studied. For single-field CCS values, an overall average interlaboratory RSD of 0.38% was achieved for the three laboratories. Moreover, an average bias of 0.54% was obtained by comparing single-field CCS values with the corresponding reference stepped-field values [5]. Good inter- (over five days with three replicates per day) and intra-day (five replicates) repeatability (RSD < 1%) has been demonstrated for ^{TW}CCS values of 224 pesticide-derived ions [21]. Intra-laboratory reproducibility proved to be very stable for CCS of pesticides in food (e.g. tea powder, leek, garlic) [22]. High interlaboratory reproducibility (average RSD = 0.14%) and $\Delta CCS\% < 2\%$ were reported for ^{TW}CCS of 53 analytical standards of mycotoxins determined with three commercial TWIM-MS instruments (two Waters Vion and a Synapt G2-Si) [20]. Other inter-instrumental comparisons were carried out using TWIMS techniques, leading to RSD of $\pm 1\%$ for 87 steroids using four TWIMS instruments (2 Synapt and 2 Vion)[19] and 542 metabolites in rat urine, using 2 Synapt instruments [23]. Thus, these intra-technologies studies, involving identical IMS systems, demonstrated that CCS from either DTIMS or TWIMS devices are sufficiently repeatable to be robustly compared. Some research has also been conducted on the comparability of CCS measurements between TWIMS, DTIMS and/or TIMS platforms.²³ ^{TW}CCS and ^{DT}CCS have been compared for 124 commercial standards of pharmaceuticals, pesticides and their metabolites: 104 out of the 124 substances were detected with both instruments as $[M+H]^+$ and 97 as $[M+Na]^+$ ions leading to deviations < 1% for most substances. However some CCS showed larger deviations up to 6.2% [24]. Regarding lipidomics field, previous contributions comparing ^{SLIM}CCS and ^{TW}CCS , both against ^{DT}CCS , have been reported, which evidenced comparable CCS values [25,26]. Another recent study has demonstrated the comparability of three commercially available IMS techniques on 87 steroids compounds (a total of 142 CCS from $[M-H]^-$, $[M+H]^+$ or $[M+Na]^+$ ions), revealing excellent interlaboratory comparisons for 95% of ions with deviations of $\pm 1\%$ between ^{TIMS}CCS and ^{DT}CCS and of $\pm 2\%$ between ^{TW}CCS and ^{DT}CCS , but larger deviations up to 7% were reported.[27] The authors which also addressed the effect of external calibration on steroid CCS measurements using all three platforms, explained these discrepancies by the use of different calibrants for external calibration as both DTIM-MS and TIM-MS instruments were calibrated with the same set of calibrant ions (Tune Mix) and reference CCS values while the TWIM-MS systems were calibrated with different calibrants (Major Mix) and therefore using different reference CCS values [28]. As previously showed, the calibration step was crucial for CCS determination, particularly in lipidomics study [26,29,30], a comparison of lipid CCS values obtained from the three instruments using the same calibrant would be useful.

To tackle these issues, we measured and compared the CCS measurements of commercial lipid standards and plasma lipids using the three commercially available IMS technologies, DTIMS, TIMS and TWIMS coupled to Q-TOF mass spectrometers present in three distinct laboratories (four instruments were evaluated: a DTIM-MS, two TIM-MS and a TWIM-MS). Evaluation of the external calibration step was carried out by comparing eleven calibrants on the three IMS devices. Then, ^{TW}CCS , ^{TIMS}CCS and ^{DT}CCS were compared using the same set of calibrant ions (Tune Mix) and reference CCS values. In this

work, we thoroughly assessed all the potential sources of deviations that may occur during calibration, data acquisition, or processing.

5.2.3. Experimental section

Chemical and reagents.

Polyalanine, polyglycine, L-malic acid, poly(ethylene) glycol (PEG) and poly(ethylene oxide) monomethyl ether (PEO) were from Sigma-Aldrich (Saint Quentin Fallavier, France), and dextran from Fluka analytical (Steinheim, Germany). Lipids were purchased from Avanti Polar Lipids (AL, USA): PE 6:0/6:0, PE 10:0/10:0, PE 15:0/15:0, PC 20:0/20:0, PC 24:0/24:0, LPC 16:0, LPE 16:0, PE 18:1/18:1 Δ^9 cis, PC 16:0/16:0 and lipids from the Differential Ion Mobility System Suitability LIPIDOMIX kit (DIMS kit). Tune Mix solution containing six hexakis(fluoroalkoxy)phosphazines (ESI-low concentration tuning mix, G1969-85000) was purchased from Agilent Technologies. Major Mix IMS calibration kit was from Waters (Manchester, UK). The tetraalkylammonium (TAA) salts were purchased from Sigma-Aldrich, except tetrabutylammonium hydroxide solution and tetraoctylammonium bromide which were from Fluka analytical.

Drug-like compounds, i.e. acetaminophen, colchicine, ondansetron, clozapine N-oxide, verapamil, and reserpine were purchased from Sigma-Aldrich apart for alprenolol, which was supplied by European Pharmacopoeia Reference Standard.

For DTIMS experiments, acetonitrile (ACN), and methanol (MeOH) were LC-MS grade from Honeywell (Riedel-de Haen, Germany). Isopropanol was hypergrade for LC-MS from Supelco (Merck, Darmstadt, Germany). Water was obtained from an Elga Purelab Classic UV purification system (Veolia water STI, Le Plessis Robinson, France). Formic acid was obtained from Sigma-Aldrich (Steinheim, Germany). Ammonium formate was obtained from Acros Organics (Geel, Belgium).

For TIMS and TWIMS [29] experiment, methanol (MeOH), chloroform, acetonitrile (ACN), isopropanol and formic acid (FA) were purchased from Fischer Scientific (UK, Loughborough), while ammonium formate was from Sigma-Aldrich (Saint Quentin Fallavier, France). Except chloroform which was HPLC grade, all solvents and buffers used were LC-MS grade.

Sample preparation.

All the IMS calibrants were prepared according to previous reference publications [31–36] except ESI-low concentration tuning mix solution which was used as received. Details are provided in the supplementary information.

Plasma lipids were extracted according to a modified Bligh and Dyer method [37] as described in a previous work,[29] using human plasma purchased from three donors BioPredic International (Rennes, France). Lipid extracts were prepared from 50 μ L of plasma and were then reconstituted in 50 μ L of chloroform/methanol 50:50 (v/v) after extraction and evaporation. For DTIMS experiments, samples were then diluted 1/40 and 1/10, for positive and negative mode respectively; while for TIMS, they were diluted 1/1000 and 1/100 in positive mode and 1/100 and 1/10 in negative mode. The dilution series were made with a solution of MeOH/isopropanol/H₂O 65:35:5 (v/v/v), before injection into the LC-HRMS system. Lipid standards were prepared as previously described [29].

LC-IMS-MS analysis: calibration and acquisition conditions

Identical chromatographic set-ups were used for all the three IM-MS platforms, as previously described [29]. Chromatographic separations were performed using a 2.1 × 100 mm, Acquity UPLC CSH C18 1.7 μm column (Waters, Manchester, UK) equipped with a 0.2-μm prefilter. The sampler and column oven temperatures were set at 10 °C and 50 °C, respectively. The flow rate was 0.4 mL min⁻¹. Mobile phase A consisted of acetonitrile/aqueous ammonium formate (10mM) (60:40) and mobile phase B of isopropanol/acetonitrile/ aqueous ammonium formate (10mM) (88:8:4); 0.1 % formic acid (FA) was added to both mobile phases. The gradient was as follows: 0–2 min, 32% B; 2–14 min, 32–75% B; 14–26.5 min, 75–100% B; 26.5–30 min, 100% B; 30–30.5 min, 100–32% B; 30.5–35 min, 32% B.

TWIM-MS instrument. Instrumental conditions have been reported in a previous publication [29]. Briefly, an UHPLC system (Vanquish, Thermo Scientific, San Jose, CA, USA) coupled to a QTOF mass spectrometer (Synapt G2 HDMS, Waters MS Technologies, Manchester, UK) equipped with an electrospray source and a traveling wave ion mobility (TWIM) cell. Chromatographic system was monitored by Chromeleon 7.2.9 and the Synapt instrument by Masslynx V4.2 SCN991.

DTIM-MS instrument. The LC-DTIM-MS experiments were performed using an Infinite 1290 2D-LC chromatographic system (only the first dimension was used) coupled to a DTIM-QTOF mass spectrometer (Agilent 6560, Agilent Technologies, Waldbronn, Germany) equipped with a JetStream electrospray interface. Chromatographic system was monitored by Open lab CDS chemstation edition version C.01.09 [144] and DTIMS instrument by Agilent Masshunter version B.09.00. Details was done in the supplementary information as the IMS parameters are reported in Tables SA.1, SA.2.

TIM-MS instruments. Two TIMS instruments belonging to two different laboratories were evaluated.

TIMS-TOF Flex. A first series of LC-TIM-MS experiments were performed using an UHPLC system (Vanquish, Thermo Scientific, San Jose, CA, USA) hyphenated to a QTOF mass spectrometer (TIMS TOF Flex, Bruker Daltonics, Bremen, Germany) equipped with an electrospray source and a transfer cartridge SRIG MALDI 2. LC system was monitored by Bruker Compass Hystar 6.2.1.13 and the instrument by TIMScontrol 4.1.8. External calibration have been performed with sodium formate for mass, and with the chosen calibrant for ion mobility. An additional internal mobility calibration have been performed by injecting the calibrant at the beginning of the LC run with a 6-way valve. Details was done in the supplementary information as the IMS parameters are reported in Table SA.3.

TIMS-TOFTM. A second series of LC-TIM-MS experiments have also been performed with a second QTOF mass spectrometer (TIMS-TOFTM, Bruker Daltonics, Bremen, Germany) located in another laboratory at Sorbonne University, hyphenated with an Elute LC system (Bruker) monitored with HyStar 5.1.8.1. External calibration in *m/z* in quadratic mode and IMS in linear mode were performed with the Tune Mix solution. The instrument was monitored by otofControl 6.2 and data was visualized with Data Analysis.

Full details of all instrument parameters are reported in supplementary information (SI).

Data processing and CCS determination.

TWIMS experiments. Raw data were processed with UNIFI 1.9.4 and Masslynx 4.1 software (Waters) as previously described [29]. Driftscope v2.9 and Masslynx software were used to extract drift times to determine the CCS with Excel.

DTIMS experiments. Raw data were processed with MassHunter Qualitative Navigator B08.00 software (Agilent) to visualize the chromatographic and mass dimensions. Ion mobility results were processed using IM-MS Browser 10.0 by creating the feature list with the IMFE (IM-MS Feature Extraction) software tool for each analysis. Multiplexed data were first pre-processed with PNNL Preprocessor 3.14, to reconstruct the files [37]. A homemade python script was used to integrate LC, IMS and MS information of the identified lipids for all the analyses, i.e. m/z , rt , t_D and intensities. The CCS values were then determined from t_D using a calibration curve. The results were then manually examined to ensure the CCS values and inspected for potential missing values.

TIMS experiments. Raw data were processed using DataAnalysis 6.0 to visualize the results and extract the K_0 values and with MetaboScape 8.0.2 software (Bruker) to extract the ions parameters including m/z , rt , $1/K_0$ and CCS values of the identified lipid species. A homemade python script was used to group the CCS values of the identified lipid compounds for each analytical sequence. Each raw file has been internally calibrated using the ions from the IMS calibrants.

Full details of data processing are reported in SI.

5.2.4. Results and discussion

CCS determination.

Plasma samples and lipid standard solutions were analyzed using the four different instruments while keeping the same chromatographic conditions (i.e. column, mobile phases, gradient conditions, flow rate,...). Annotation of plasma lipids was performed on the basis of our previous study using 77 annotated plasma lipids and 19 lipid standards analyzed using the Synapt G2 instrument,[29] (Tables SB1-3). Although the electrospray ionization parameters were thoroughly optimized for each instrument, differences in the ionic species formed were observed depending on the ESI source. For example, LPC species analyzed in negative ion mode gave abundant $[M-CH_3]^-$ fragment ions compared to $[M+H]^-$ or $[M+HCOO]^-$ ions in ESI-TWIM-MS experiments, whereas the opposite trend was observed for ESI-DTIM-MS and the $[M-CH_3]^-$ fragment ion was almost undetectable using ESI-TIM-MS instrument. The Figure SA1 illustrates this issue with LPC 16:0 as a representative example. Consequently, we choose to report the CCS of lipid ions that we had previously detected and identified in TWIMS experiments [29]. Thus, 59 plasma lipids have been annotated in positive mode, with 75 distinct ions (40 $[M+H]^+$, 16 $[M+Na]^+$, 13 $[M+NH_4]^+$ and 6 $[M+H-H_2O]^+$). In negative mode, 55 ions from 51 lipids were annotated (33 $[M+HCOO]^-$, 16 $[M-H]^-$ and 6 $[M-CH_3]^-$, the latter ions being not detected in TIM-MS). Overall, a total of 130 CCS values over 77 unique lipid species were identified and monitored with each instrument. Thus, CCS values of human plasma lipids and lipid standards were independently determined with the four IM-MS instruments both in positive and negative ionization modes, taking care to systematically use the same IMS calibrant, i.e. the Tune Mix (see below) [29].

Software-associated deviations in determining CCS values from raw data.

We first evaluated the influence of data processing software tools on CCS determination. In the case of the commercial TWIMS instrument, three different software tools have been investigated and compared i) Masslynx in combination with Driftscope, ii) Progenesis Q1 and iii) Unifi (Figure SA2 and Table SB7). Rather unexpectedly, the CCS values determined using these three software packages differed to some extent, with 0.6% maximum deviation (0.3% on average), as a direct consequence of variability in peak picking and CCS calculation algorithms (see SI for details). As Unifi appears well

adapted to large batches processing (allowing batches processing, in contrary to Masslynx, that can only process individual raw files) and permits the monitoring of many processing parameters such as intensity thresholds as described in SI (in contrary to Progenesis QI), we decided to use Unifi to carry out all the data processing. In a similar manner, the Bruker software (Data Analysis and Metaboscape) have been compared for the determination of the TMCCS values (details in SI) and also showed mean deviation of 0.5%. Finally, Metaboscape was chosen for CCS determination because it allows simultaneous data processing for multiple raw data or lipidomic batches.

Moreover, one can note that the *Constant* value in the derived Mason-Schamp equation (Equation 1) used for ^{DT}CCS and TMCCS determination from the $1/K_0$ values extracted from IMS data slightly differs between publications or even between software, from 18500 [36,38] to 18510 (for Bruker software tools).

$$CCS = Constant \times \frac{z}{K_0} \sqrt{T \frac{Mm}{M+m}} \text{ with } Constant = \frac{3e}{16N_0} \sqrt{\frac{2\pi}{k_B C_{Da}}} \text{ Equation 1}$$

where z is the charge, T the temperature, K_0 the mobility of the ions, M and m , the mass of the analyte ion and the buffer gas, respectively and, e the electron charge, N_0 the gas number density, k_B the Boltzmann's constant and C_{Da} , the conversion of the m/z value in kg.

Details of the *Constant* calculation is provided in the SI. A global consensus on this value could be helpful to obtain more reproducible CCS values.

For the DTIMS data from Agilent instrument, data processing was performed using IM-MS Browser software, as it is the sole software available to process DTIMS data. There are then two possible procedures for calibration and CCS determination: the first proceeded entirely using IM-MS Browser software, the second used IM-MS Browser software to extract drift times (t_D) for both calibrants and samples. These t_D values were then imported into an Excel spreadsheet to determine the CCS values

according to Equation 2. $t_D = \beta \sqrt{\frac{m_i}{m_g + m_i}} CCS + t_{fix}$ where m_i is the mass of the ions and m_g is the mass of the drift gas, β and t_{fix} are, respectively, the slope and the intercept of the mobility calibration curve equation.

The parameters β and t_{fix} of the linear fitting, determined either by IM-MS Browser or using Excel were in good agreement. Both methods led to very similar CCS values with a mean relative deviation of 0.01% (details in SI). We chose the linear fitting with Excel because this method enabled faster data processing.

To conclude, deviations observed between CCS values calculated using different software processing tools, although slight ($\approx 0.3\%$) contribute to the whole uncertainty of the CCS measurement. Such software-dependent deviation needs to be minimized for a more robust use of CCS as molecular descriptor for annotation.

Method evaluation.

Different IMS parameters were tested for each of the three IMS technologies to evaluate the robustness of the methods for CCS measurements (Figure 2). For TWIMS experiments, three sets of wave heights and velocities have been tested, each in triplicates leading to nine experiments, [29] resulting in RSD of 0.21% for the CCS values (Table SB1.a). These values are in the same range as the

RSD of 0.14% previously reported for the mycotoxin study [20] and in the range of $\pm 1\%$ described for pesticides in food [22], steroids [19] and metabolites measured in rat urine [23]. For DTIMS experiments, CCS values assessed under five different conditions (changing the drift tube voltages and the multiplexing parameters [39,40] for two conditions, see Table SA2), a RSD of 0.21% was obtained (Table SB2.b). For TIMS experiments, the mobility ranges and the ramp time were changed to evaluate their influence on $1/K_0$ values. The mean RSD was 0.48% on $1/K_0$ values and 0.40% on CCS values (Table SB3.a). Altogether these data demonstrate excellent robustness in CCS measurement.

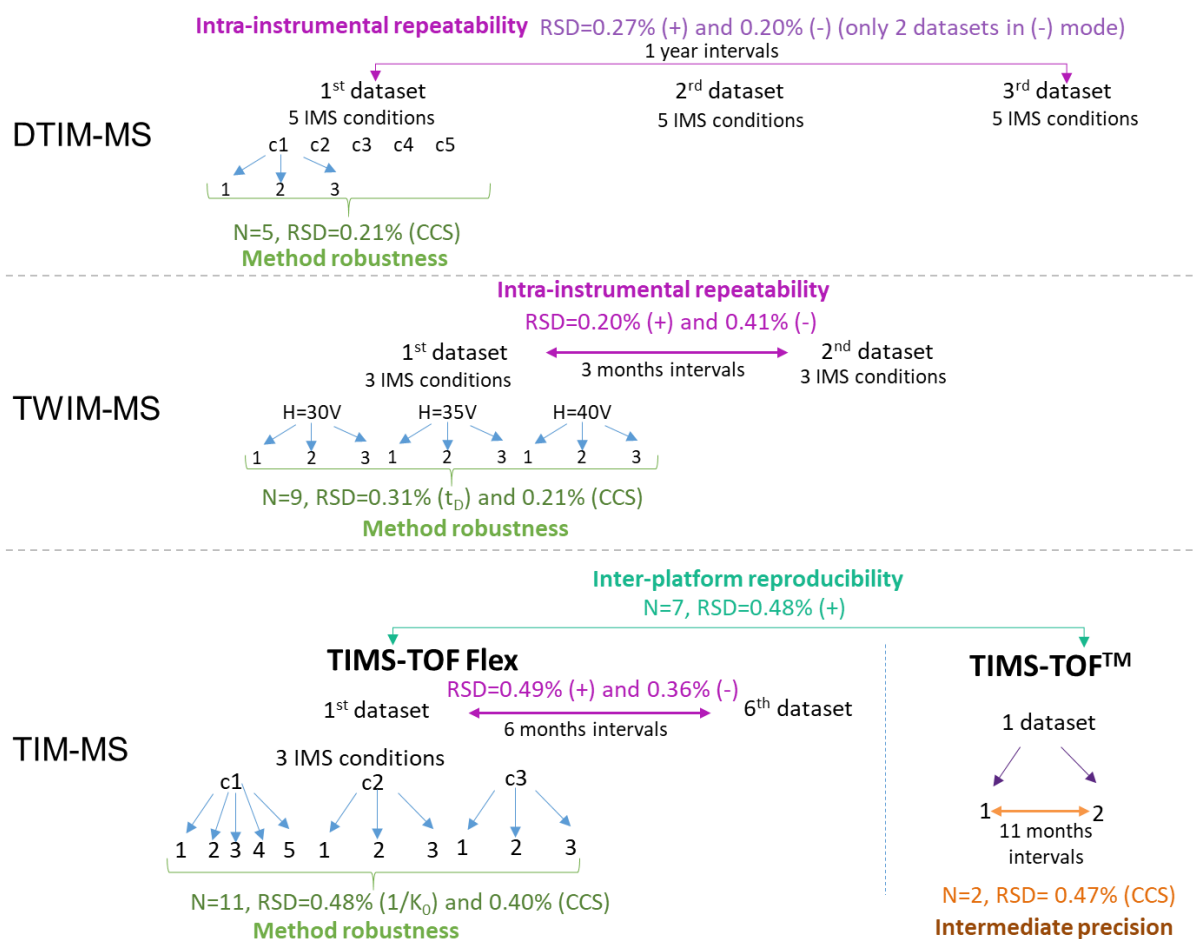


Figure 2: Evaluation of the method and intra-instrument performance, for the three different technologies. For DTIMS, the conditions (c1-c5) have been described in Table SA2 and for TIMS (c1-c3) in Table SA3, details have been previously reported for TWIMS [29]

Intra-instrument repeatability.

Long term intra-instrument repeatability was assessed for each of the three IMS techniques by repeating the CCS measurements at different time intervals (Figure 1). For TWIMS experiments, the comparison of two CCS data sets (nine replicates) at three months intervals gives a mean relative standard deviation of 0.20%, in positive mode and 0.41% in negative mode (Table SB1.b). RSD appears to be higher in the negative mode, because the intensities of lipid ions are in general slightly lower in this mode.

In the case of the DTIMS instrument, analytical sequences were performed at three different time intervals over one year (five experiments for each sequence, Figure 1). The resulting RSD on CCS values is 0.27% in positive mode and 0.20% in negative mode considering the whole data set. These results are similar to those published in an interlaboratory study, with RSD of 0.38% for single-field CCS values determined on three different DTIMS instruments [5].

For the TIMS instruments, two different platforms have been used. One dataset in positive mode was acquired (duplicate analyses at two different times interval) using the TIMS-TOF™ (Figure 1). Six analytical sequences in positive mode and five in negative mode were carried out using the TIMS-TOF Flex (Figure 1). The two data sets from TIMS-TOF™ acquired at an eleven months interval revealed a mean RSD of 0.47%, demonstrating a high intermediate precision over almost a year. The six datasets from TIMS-TOF Flex were acquired every month over 6 months, resulting in a RSD of 0.49%. The mean RSD of the CCS was 0.48% over the seven data sets, comparing the two instruments, resulting in an excellent inter-platform reproducibility. The RSD between the five data sets from TIMS-TOF™ in negative mode, was 0.36% (Table SB3.b). Table SA15 gathers the different RSD values obtained over all the measurements in both positive and negative ion modes.

Comparative study of different IMS calibrants to lower the CCS deviations between the three technologies.

All the CCS values, 75 in positive and 55 and negative ion modes, were determined with the three technologies using different sets of calibrants, which had been previously assessed for ^{TW}CCS of plasma lipids [29] (Tables SB5 and SB6). The Figure displays the RSD (%) between ^{DT}CCS , ^{TIM}CCS and ^{TW}CCS of the 75 values in positive ion mode and the 55 values in negative ion mode for each of the different calibrants.

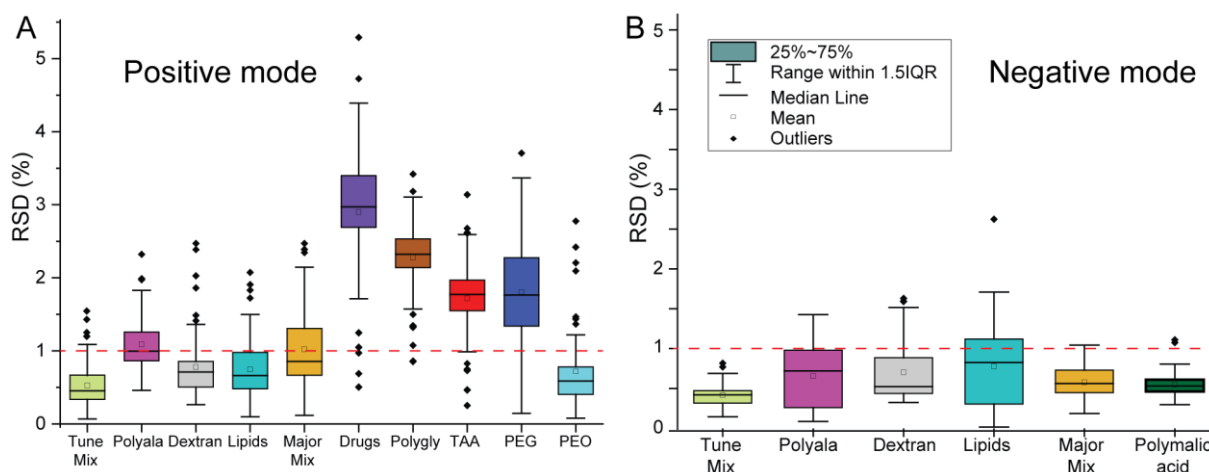


Figure 2: Boxplots representing the RSD (%) between $^{TW}CCS_{N_2}$, $^{TIM}CCS_{N_2}$ and $^{DT}CCS_{N_2}$ of plasma lipid in function of the calibrant used, in positive mode (A) on 75 values (see Table SB4a) and negative mode (B) on 55 values (see Table SB4b).

Mean RSD were below 2% for almost all calibrants, except the drugs and polyglycine calibrant sets because they do not cover the whole m/z and CCS ranges of all the plasma lipid ions. However, reproducible CCS values can be obtained with the other calibrants, when using identical set of calibrant with the different instruments. This confirms again the importance of the calibration step to ensure reproducible CCS values between instruments [16]. For PEG calibrant, the CCS range had to be adapted to get the most appropriate calibration curve and still remain to a RSD close to 2%. In the case of Major Mix calibrants, composed of polyalanine, drugs and Ultramark ions, the ions used for IM calibration

can differ according to the ion species detected on the three instruments, as already described in previous publications [20,22,24,29]. That can constitute another cause of CCS deviations. Comparing all the calibrants, one can note that the lowest mean relative standard deviations (around 0.5%) were obtained using Tune Mix as calibrant, both in positive and negative ion modes.

Comparison of the CCS determined with DTIMS, TWIMS and TIMS: the interplatform study.

The correlation between the CCS retrieved from the three techniques, calibrated with the Tune Mix, was evaluated in a pairwise manner (Tables SB4). The Tune Mix calibrant was used to evaluate the interplatform comparison, because it showed the lowest mean RSD between the ^{TW}CCS , ^{TIM}CCS and ^{DT}CCS (Figure 2). That was consistent with our previous study reporting that the lowest deviations between experimental ^{TW}CCS of plasma lipids and literature ^{DT}CCS (stepped-field mode) were obtained when Tune mix was used as calibrant [29]. Moreover, Tune Mix has been largely used in the literature for CCS determination of several types of analytes and commonly employed for the measurement of drift tube length. Then, a consensus on the CCS values of Tune Mix ions seemed to be reached since the interlaboratory evaluation of DTIM-MS has been performed for CCS measurements by Stow et al. [4]. Linear regressions were plotted to using plasma lipid ^{DT}CCS , ^{TW}CCS and ^{TIM}CCS data sets. The three datasets proved to be well correlated with coefficient of determination R^2 higher than 0.995 in both positive and negative ion modes (Figure). Furthermore, the slopes of the six linear regressions were close to 1. These observations are consistent with a previous study [27] where the slope was around 1 when plotting ^{TIM}CCS vs ^{DT}CCS but slightly higher than 1 when plotting either $^{TWIMS}CCS$ vs ^{DT}CCS or $^{TWIMS}CCS$ vs ^{TIM}CCS . The authors explained such positive slope shift by the use of different calibrants for TWIMS analysis (Major Mix) and for TIMS and DTIMS (Tune Mix). Further investigations were then carried out on calibration, which permitted to minimize the deviations between the three platforms using new reference CCS values [28].

Few outliers were observed, circled in red in Figure 2, which corresponded to low-abundant ions exhibiting poor IMS peak intensity and definition. Indeed, low signal-to-noise ratio can lead to erroneous or uncorrected peak picking and thus uncertainties on the CCS determination. This was particularly noticeable for ceramide lipid species that gave low abundant ions in the positive mode.

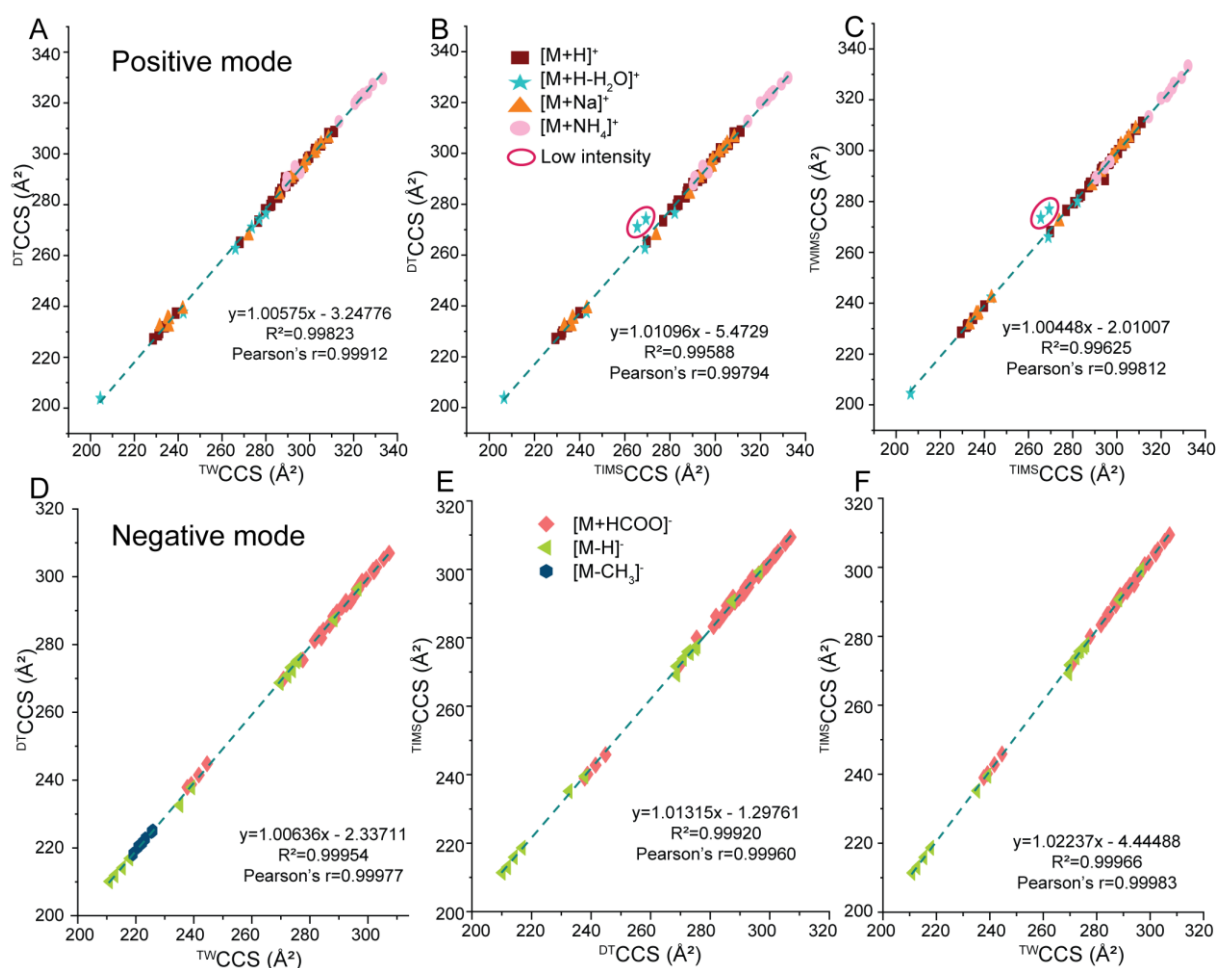


Figure 2: Linear regressions correlating CCS values retrieved from DTIMS, TWIMS and TIMS analyses in positive (A, B, C) and negative (D, E, F) ion modes using Tune Mix as calibrant, comparing $^{TW}CCS_{N2}$ and $^{DT}CCS_{N2}$ (A, D), $^{TIMS}CCS_{N2}$ and $^{DT}CCS_{N2}$ (B, E) and $^{TW}CCS_{N2}$ and $^{TIM}CCS_{N2}$ (E, F)..

To have a more global overview of the data collected, differences between all the CCS values retrieved from the three technologies were compared in a pairwise manner and depicted in Figure 3 as boxplots. For each of the three cases, the mean differences observed between CCS values from two instruments are below 1% in both positive and negative modes. The few outliers observed correspond to low-intensity signals, as previously discussed. Similar distributions of CCS differences were observed when comparing between ^{TIM}CCS and ^{TW}CCS (lowest mean deviation = 0.45% in positive mode and 0.61% in negative mode) and ^{TW}CCS and ^{DT}CCS (mean = 0.62% in positive mode and 0.28% in negative mode), while being slightly higher when studying ^{TIM}CCS and ^{DT}CCS (mean = 0.94% in positive mode and 0.83% in negative mode). From Figure 3 and Figure SA3, systematic differences can be observed by comparing the CCS values, and this comparison reveals that $^{TIM}CCS > ^{TW}CCS > ^{DT}CCS$. Each pairwise comparison shows a mean positive deviation of approximately +0.5% for ^{TW}CCS vs ^{DT}CCS and +0.8% for ^{TIM}CCS vs ^{DT}CCS , for positive and negative mode. A similar trend has been previously reported for CCS comparison of steroids [27].

More than 90% of the plasma lipid CCS values exhibit mean relative deviations between the three instruments below 1%, for both negative and positive modes. By comparing the three instruments in pairwise manner, as represented in Figure 2 and 3, three ions exhibit RSD higher than 2% with the maximum deviation obtained was about 3%, and can be explained by a low intensity signal for these ions. However, by eliminating these low signals, all RSD were below 2%. This indicates that CCS

matching between laboratories and IMS platforms is possible with deviations lower than 2% and a database search criteria of 2%, even 1% for most of the lipids, seems to be reachable, in agreement with previous studies [41,42].

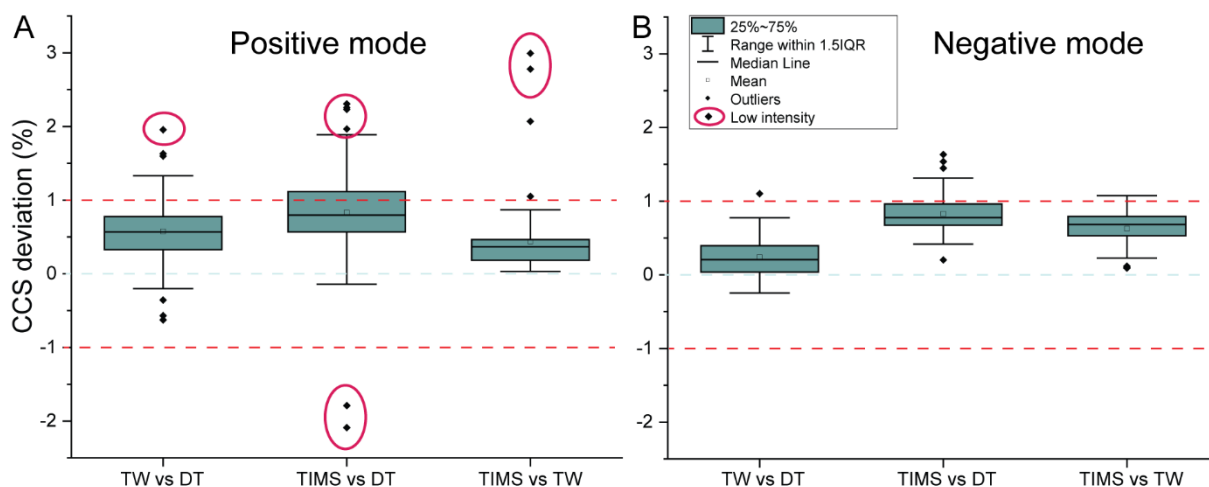


Figure 3: Boxplots representing the pairwise comparison of the different IMS technologies via CCS deviations, in positive mode on 75 CCS values (A) and negative (B) mode on 55 CCS values. To define the outliers, the range within 1.5IQR was calculated with: lower bound= $Q1-1.5 \times IQR$ and upper bound= $Q3+1.5 \times IQR$ where $Q1$ and $Q3$ represents respectively the first and third quartile of the data and IQR, the Inter-Quartile Range ($IQR=Q3-Q1$)

5.2.5. Conclusion

CCS are useful to improve confidence in compound annotation workflows by providing an additional descriptor to chemical libraries. This study compared three IMS technologies, DTIMS, TWIMS and TIMS for the determination of plasma lipid CCS. First, the intra-instrument long term repeatability was demonstrated as presenting with a high level of precision (average RSD $\leq 0.5\%$) for each of the three IMS technologies. We have also shown that deviations (average RSD $\approx 0.3\%$) can be introduced after data processing by the use of different algorithms or scripts for CCS determination. It appeared therefore essential to evaluate the deviations introduced by data processing software, as various commercial software tools are currently available. A solution to this issue could be the use of a unique software for all the IMS technologies, such as one of the recent open tools that have been developed to process LC-IM-MS/MS data [43–45].

One key point highlighted in this study is the importance of the calibration step. Several calibrants were investigated with each of the three IMS technologies (ten calibrants in positive mode and six in negative mode). It was shown that low deviations can be achieved when using the same calibrant with all three IMS technologies (mean deviation below 2% in positive ion mode considering almost all the studied calibrants except rugs and polyglycine which are out of lipid CCS and m/z ranges and below 1% in negative ion mode) demonstrating that the CCS values are highly comparable. The lowest deviations were obtained for Tune Mix calibrant with an average RSD value of $\approx 0.5\%$ in both positive and negative ion modes. To reduce the differences due to calibration, different strategies could be used, as for example internal calibration, by injecting the calibrant during the sample analysis, as it is the case for TIMS in this study, or by using stable isotope labelled internal standards [28].

Comparing the ^{TW}CCS , ^{TIMS}CCS and ^{DT}CCS , high interplatform and interlaboratory reproducibility was demonstrated with precision within 1% (average RSD) for CCS calibrated with Tune Mix, in both

positive and negative mode, considering all ionic species. More than 90 % of the CCS derived from lipid species exhibited deviations within 1% whatever the ionization mode. Thus, a CCS deviation of 1% can be reached for most of the studied lipids, and used for lipid annotation when analyzed under our standardized conditions. This study demonstrates that the constitution of interoperable CCS libraries is clearly feasible when working under well standardized conditions on both calibration, data acquisitions and data processing steps.

Acknowledgments

This work was partially supported by University of Rouen Normandy, INSA Rouen Normandy, the Centre National de la Recherche Scientifique (CNRS), European Regional Development Fund (ERDF), Labex SynOrg (ANR-11-LABX-0029), Carnot Institute I2C, the graduate school for research XL-Chem (ANR-18-EURE-0020 XL CHEM) by Region Normandie and the MetaboHUB infrastructure (ANR-11-INBS-0010 grant). The authors gratefully acknowledge all the people who contribute to this work and help for data acquisition and data treatment, particularly, Laure Maret, Aurélie Mème for their help with the TIMS-TOF Flex instrument and Alexandre Verdu for the help with Metaboscape software (Bruker Daltonics, France). We thank Hannah Florance and Jérémy Jeudy for their help with DTIMS technique and the data treatment process and Waters for the use of Unifi software.

Appendix A. supplementary data

More information on LC-IM-MS methodology, data processing and CCS measurements, comparison of lipid CCS from different types of commercial software, resume of repeatability and reproducibility testing, mass spectra showing ionization differences and comparison of deviations between instruments (PDF, File A)

Repeatability and reproducibility on CCS measurements with three instruments, comparison of plasma and standards CCS values with Tune Mix and with all calibrants in positive and negative modes, comparison of software on CCS values (Excel, File B).

REFERENCES

- [1] A.A. Shvartsburg, *Differential Ion Mobility Spectrometry: Nonlinear Ion Transport and Fundamentals of FAIMS*, CRC Press, 2008.
- [2] J.C. May, J.A. McLean, *Ion Mobility-Mass Spectrometry: Time-Dispersive Instrumentation*, *Anal. Chem.* 87 (2015) 1422–1436. <https://doi.org/10.1021/ac504720m>.
- [3] E.A.; S.J. Mason, *Mobility of gaseous ions in weak electric fields*, *Annals of Physics*, 4, 233-270. (1958).
- [4] V. Gabelica, *Ion Mobility -Mass Spectrometry: An Overview*, in: F. Sobott, A. Ashcroft (Eds.), *Ion Mobility-Mass Spectrometry: Fundamentals and Applications*, Royal Society of Chemistry, 2021: pp. 1–25. <https://doi.org/10.1039/9781839162886-00001>.
- [5] S.M. Stow, T.J. Causon, X. Zheng, R.T. Kurulugama, T. Mairinger, J.C. May, E.E. Rennie, E.S. Baker, R.D. Smith, J.A. McLean, S. Hann, J.C. Fjeldsted, *An Interlaboratory Evaluation of Drift Tube Ion Mobility–Mass Spectrometry Collision Cross Section Measurements*, *Anal. Chem.* 89 (2017) 9048–9055. <https://doi.org/10.1021/acs.analchem.7b01729>.
- [6] S.D. Pringle, K. Giles, J.L. Wildgoose, J.P. Williams, S.E. Slade, K. Thalassinou, R.H. Bateman, M.T. Bowers, J.H. Scrivens, *An investigation of the mobility separation of some peptide and protein ions using a new hybrid quadrupole/travelling wave IMS/oa-ToF instrument*,

- International Journal of Mass Spectrometry. 261 (2007) 1–12.
<https://doi.org/10.1016/j.ijms.2006.07.021>.
- [7] V. Gabelica, E. Marklund, Fundamentals of ion mobility spectrometry, *Current Opinion in Chemical Biology*. 42 (2018) 51–59. <https://doi.org/10.1016/j.cbpa.2017.10.022>.
- [8] K. Michelmann, J.A. Silveira, M.E. Ridgeway, M.A. Park, Fundamentals of Trapped Ion Mobility Spectrometry, *J. Am. Soc. Mass Spectrom.* 26 (2015) 14–24.
<https://doi.org/10.1007/s13361-014-0999-4>.
- [9] M. Hernandez-Mesa, F. Monteau, B. Le Bizec, G. Dervilly-Pinel, Potential of ion mobility-mass spectrometry for both targeted and non-targeted analysis of phase II steroid metabolites in urine, *Anal Chim Acta X*. 1 (2019) 100006. <https://doi.org/10.1016/j.acax.2019.100006>.
- [10] F. Meier, S. Beck, N. Grassl, M. Lubeck, M.A. Park, O. Raether, M. Mann, Parallel Accumulation–Serial Fragmentation (PASEF): Multiplying Sequencing Speed and Sensitivity by Synchronized Scans in a Trapped Ion Mobility Device, *J. Proteome Res.* 14 (2015) 5378–5387. <https://doi.org/10.1021/acs.jproteome.5b00932>.
- [11] M.F. Bush, I.D.G. Campuzano, C.V. Robinson, Ion Mobility Mass Spectrometry of Peptide Ions: Effects of Drift Gas and Calibration Strategies, *Anal. Chem.* 84 (2012) 7124–7130.
<https://doi.org/10.1021/ac3014498>.
- [12] M. Schroeder, S.W. Meyer, H.M. Heyman, A. Barsch, L.W. Sumner, Generation of a Collision Cross Section Library for Multi-Dimensional Plant Metabolomics Using UHPLC-Trapped Ion Mobility-MS/MS, *Metabolites*. 10 (2020) 13. <https://doi.org/10.3390/metabo10010013>.
- [13] J.C. May, C.B. Morris, J.A. McLean, Ion Mobility Collision Cross Section Compendium, *Anal. Chem.* 89 (2017) 1032–1044. <https://doi.org/10.1021/acs.analchem.6b04905>.
- [14] Z. Zhou, M. Luo, X. Chen, Y. Yin, X. Xiong, R. Wang, Z.-J. Zhu, Ion mobility collision cross-section atlas for known and unknown metabolite annotation in untargeted metabolomics, *Nat Commun.* 11 (2020) 4334. <https://doi.org/10.1038/s41467-020-18171-8>.
- [15] Z. Zhou, J. Tu, X. Xiong, X. Shen, Z.-J. Zhu, LipidCCS: Prediction of Collision Cross-Section Values for Lipids with High Precision To Support Ion Mobility–Mass Spectrometry-Based Lipidomics, *Anal. Chem.* 89 (2017) 9559–9566.
<https://doi.org/10.1021/acs.analchem.7b02625>.
- [16] V. Gabelica, C. Afonso, P. Barran, J.L.P. Benesch, M. Road, M.F. Bush, I.D.G. Campuzano, T. Causon, B.H. Clowers, C.S. Creaser, Recommendations for Reporting Ion Mobility Mass Spectrometry Measurements, *Mass Spectrometry Reviews*. (2019) 59.
<https://doi.org/10.1002/mas.21585>.
- [17] J.R.N. Haler, P. Massonnet, F. Chivot, C. Kune, C. Comby-Zerbino, J. Jordens, M. Honing, Y. Mengerink, J. Far, P. Dugourd, E. De Pauw, Comparison of Different Ion Mobility Setups Using Poly (Ethylene Oxide) PEO Polymers: Drift Tube, TIMS, and T-Wave, *J. Am. Soc. Mass Spectrom.* 29 (2018) 114–120. <https://doi.org/10.1007/s13361-017-1822-9>.
- [18] N.R. Oranzi, R.H.J. Kemperman, M.S. Wei, V.I. Petkovska, S.W. Granato, B. Rochon, J. Kaszycki, A. La Rotta, K. Jeanne Dit Fouque, F. Fernandez-Lima, R.A. Yost, Measuring the Integrity of Gas-Phase Conformers of Sodiated 25-Hydroxyvitamin D3 by Drift Tube, Traveling Wave, Trapped, and High-Field Asymmetric Ion Mobility, *Anal. Chem.* 91 (2019) 4092–4099.
<https://doi.org/10.1021/acs.analchem.8b05723>.
- [19] M. Hernandez-Mesa, V. D’Atri, G. Barknowitz, M. Fanuel, J. Pezzatti, N. Dreolin, D. Ropartz, F. Monteau, E. Vigneau, S. Rudaz, S. Stead, H. Rogniaux, D. Guillarme, G. Dervilly, B. Le Bizec, Interlaboratory and Interplatform Study of Steroids Collision Cross Section by Traveling Wave Ion Mobility Spectrometry, *Anal Chem.* 92 (2020) 5013–5022.
<https://doi.org/10.1021/acs.analchem.9b05247>.
- [20] L. Righetti, N. Dreolin, A. Celma, M. McCullagh, G. Barknowitz, J.V. Sancho, C. Dall’Asta, Travelling Wave Ion Mobility-Derived Collision Cross Section for Mycotoxins: Investigating Interlaboratory and Interplatform Reproducibility, *J. Agric. Food Chem.* 68 (2020) 10937–10943. <https://doi.org/10.1021/acs.jafc.0c04498>.

- [21] J. Regueiro, N. Negreira, M.H.G. Berntssen, Ion-Mobility-Derived Collision Cross Section as an Additional Identification Point for Multiresidue Screening of Pesticides in Fish Feed, *ACS Publications*. (2016). <https://doi.org/10.1021/acs.analchem.6b03381>.
- [22] S. Goscinny, M. McCullagh, J. Far, E. De Pauw, G. Eppe, Towards the use of ion mobility mass spectrometry derived collision cross section as a screening approach for unambiguous identification of targeted pesticides in food, *Rapid Commun Mass Spectrom*. 33 (2019) 34–48. <https://doi.org/10.1002/rcm.8395>.
- [23] L.C. Nye, J.P. Williams, N.C. Munjoma, M.P.M. Letertre, M. Coen, R. Bouwmeester, L. Martens, J.R. Swann, J.K. Nicholson, R.S. Plumb, M. McCullagh, L.A. Gethings, S. Lai, J.I. Langridge, J.P.C. Vissers, I.D. Wilson, A comparison of collision cross section values obtained via travelling wave ion mobility-mass spectrometry and ultra high performance liquid chromatography-ion mobility-mass spectrometry: Application to the characterisation of metabolites in rat urine, *Journal of Chromatography A*. 1602 (2019) 386–396. <https://doi.org/10.1016/j.chroma.2019.06.056>.
- [24] V. Hinnenkamp, J. Klein, S.W. Meckelmann, P. Balsaa, T.C. Schmidt, O.J. Schmitz, Comparison of CCS Values Determined by Traveling Wave Ion Mobility Mass Spectrometry and Drift Tube Ion Mobility Mass Spectrometry, *Anal. Chem*. 90 (2018) 12042–12050. <https://doi.org/10.1021/acs.analchem.8b02711>.
- [25] B.S. Rose, J.C. May, A.R. Reardon, J.A. McLean, Collision Cross-Section Calibration Strategy for Lipid Measurements in SLIM-Based High-Resolution Ion Mobility, *J. Am. Soc. Mass Spectrom*. (2022). <https://doi.org/10.1021/jasms.2c00067>.
- [26] K.M. Hines, J.C. May, J.A. McLean, L. Xu, Evaluation of Collision Cross Section Calibrants for Structural Analysis of Lipids by Traveling Wave Ion Mobility-Mass Spectrometry, *Anal. Chem*. 88 (2016) 7329–7336. <https://doi.org/10.1021/acs.analchem.6b01728>.
- [27] M.L. Feuerstein, M. Hernández-Mesa, A. Kiehne, B. Le Bizec, S. Hann, G. Dervilly, T. Causon, Comparability of Steroid Collision Cross Sections Using Three Different IM-HRMS Technologies: An Interplatform Study, *J. Am. Soc. Mass Spectrom*. (2022). <https://doi.org/10.1021/jasms.2c00196>.
- [28] M.L. Feuerstein, M. Hernández-Mesa, Y. Valadbeigi, B. Le Bizec, S. Hann, G. Dervilly, T. Causon, Critical evaluation of the role of external calibration strategies for IM-MS, *Anal Bioanal Chem*. (2022). <https://doi.org/10.1007/s00216-022-04263-5>.
- [29] A.C. George, I. Schmitz-Afonso, V. Marie, B. Colsch, F. Fenaille, C. Afonso, C. Loutelier-Bourhis, A re-calibration procedure for interoperable lipid collision cross section values measured by traveling wave ion mobility spectrometry, *Analytica Chimica Acta*. (2022) 340236. <https://doi.org/10.1016/j.aca.2022.340236>.
- [30] E. Deschamps, I. Schmitz-Afonso, A. Schaumann, E. Dé, C. Loutelier-Bourhis, S. Alexandre, C. Afonso, Determination of the collision cross sections of cardiolipins and phospholipids from *Pseudomonas aeruginosa* by traveling wave ion mobility spectrometry-mass spectrometry using a novel correction strategy, *Anal Bioanal Chem*. 411 (2019) 8123–8131. <https://doi.org/10.1007/s00216-019-02194-2>.
- [31] I. Campuzano, M.F. Bush, C.V. Robinson, C. Beaumont, K. Richardson, H. Kim, H.I. Kim, Structural Characterization of Drug-like Compounds by Ion Mobility Mass Spectrometry: Comparison of Theoretical and Experimentally Derived Nitrogen Collision Cross Sections, *Anal. Chem*. 84 (2012) 1026–1033. <https://doi.org/10.1021/ac202625t>.
- [32] Q. Duez, F. Chiro, R. Lienard, T. Josse, C. Choi, O. Coulembier, P. Dugourd, J. Cornil, P. Gerbaux, J. De Winter, Polymers for Traveling Wave Ion Mobility Spectrometry Calibration, *J Am Soc Mass Spectrom*. 28 (2017) 2483–2491. <https://doi.org/10.1007/s13361-017-1762-4>.
- [33] J. Hofmann, W.B. Struwe, C.A. Scarff, J.H. Scrivens, D.J. Harvey, K. Pagel, Estimating Collision Cross Sections of Negatively Charged *N*- Glycans using Traveling Wave Ion Mobility-Mass Spectrometry, *Anal. Chem*. 86 (2014) 10789–10795. <https://doi.org/10.1021/ac5028353>.
- [34] T.W. Knapman, J.T. Berryman, I. Campuzano, S.A. Harris, A.E. Ashcroft, Considerations in experimental and theoretical collision cross-section measurements of small molecules using

- travelling wave ion mobility spectrometry-mass spectrometry, *International Journal of Mass Spectrometry*. 298 (2010) 17–23. <https://doi.org/10.1016/j.ijms.2009.09.011>.
- [35] J.G. Forsythe, A.S. Petrov, C.A. Walker, S.J. Allen, J.S. Pellissier, M.F. Bush, N.V. Hud, F.M. Fernández, Collision cross section calibrants for negative ion mode traveling wave ion mobility-mass spectrometry, *Analyst*. 140 (2015) 6853–6861. <https://doi.org/10.1039/C5AN00946D>.
- [36] J.R.N. Haler, C. Kune, P. Massonnet, C. Comby-Zerbino, J. Jordens, M. Honing, Y. Mengerink, J. Far, E. De Pauw, Comprehensive Ion Mobility Calibration: Poly(ethylene oxide) Polymer Calibrants and General Strategies, *Anal. Chem.* 89 (2017) 12076–12086. <https://doi.org/10.1021/acs.analchem.7b02564>.
- [37] A. Bilbao, B.C. Gibbons, S.M. Stow, J.E. Kyle, K.J. Bloodsworth, S.H. Payne, R.D. Smith, Y.M. Ibrahim, E.S. Baker, J.C. Fjeldsted, A Preprocessing Tool for Enhanced Ion Mobility–Mass Spectrometry-Based Omics Workflows, *J. Proteome Res.* (2021). <https://doi.org/10.1021/acs.jproteome.1c00425>.
- [38] M.E. Ridgeway, M. Lubeck, J. Jordens, M. Mann, M.A. Park, Trapped ion mobility spectrometry: A short review, *International Journal of Mass Spectrometry*. 425 (2018) 22–35. <https://doi.org/10.1016/j.ijms.2018.01.006>.
- [39] T.J. Causon, L. Si-Hung, K. Newton, R.T. Kurulugama, J. Fjeldsted, S. Hann, Fundamental study of ion trapping and multiplexing using drift tube-ion mobility time-of-flight mass spectrometry for non-targeted metabolomics, *Anal Bioanal Chem.* 411 (2019) 6265–6274. <https://doi.org/10.1007/s00216-019-02021-8>.
- [40] J.C. May, R. Knochenmuss, J.C. Fjeldsted, J.A. McLean, Resolution of Isomeric Mixtures in Ion Mobility Using a Combined Demultiplexing and Peak Deconvolution Technique, *Anal. Chem.* 92 (2020) 9482–9492. <https://doi.org/10.1021/acs.analchem.9b05718>.
- [41] G. Paglia, A.J. Smith, G. Astarita, Ion mobility mass spectrometry in the omics era: Challenges and opportunities for metabolomics and lipidomics, *Mass Spectrometry Reviews*. (2021). <https://doi.org/10.1002/mas.21686>.
- [42] A. Delvaux, E. Rathahao-Paris, S. Alves, Different ion mobility-mass spectrometry coupling techniques to promote metabolomics, *Mass Spectrometry Reviews*. (2021). <https://doi.org/10.1002/mas.21685>.
- [43] H. Tsugawa, K. Ikeda, M. Takahashi, A. Satoh, Y. Mori, H. Uchino, N. Okahashi, Y. Yamada, I. Tada, P. Bonini, Y. Higashi, Y. Okazaki, Z. Zhou, Z.-J. Zhu, J. Koelmel, T. Cajka, O. Fiehn, K. Saito, M. Arita, M. Arita, A lipidome atlas in MS-DIAL 4, *Nat Biotechnol.* 38 (2020) 1159–1163. <https://doi.org/10.1038/s41587-020-0531-2>.
- [44] R. Schmid, S. Heuckeroth, A. Korf, A. Smirnov, O. Myers, T.S. Dyrland, R. Bushuiev, K.J. Murray, N. Hoffmann, M. Lu, A. Sarvepalli, Z. Zhang, M. Fleischauer, K. Dührkop, M. Wesner, S.J. Hoogstra, E. Rudt, O. Mokshyna, C. Brungs, K. Ponomarov, L. Mutabdžija, T. Damiani, C.J. Pudney, M. Earll, P.O. Helmer, T.R. Fallon, T. Schulze, A. Rivas-Ubach, A. Bilbao, H. Richter, L.-F. Nothias, M. Wang, M. Orešič, J.-K. Weng, S. Böcker, A. Jeibmann, H. Hayen, U. Karst, P.C. Dorrestein, D. Petras, X. Du, T. Pluskal, Integrative analysis of multimodal mass spectrometry data in MZmine 3, *Nat Biotechnol.* 41 (2023) 447–449. <https://doi.org/10.1038/s41587-023-01690-2>.
- [45] K.L. Crowell, G.W. Slysz, E.S. Baker, B.L. LaMarche, M.E. Monroe, Y.M. Ibrahim, S.H. Payne, G.A. Anderson, R.D. Smith, LC-IMS-MS Feature Finder: detecting multidimensional liquid chromatography, ion mobility and mass spectrometry features in complex datasets, *Bioinformatics*. 29 (2013) 2804–2805. <https://doi.org/10.1093/bioinformatics/btt465>.

5.2.6. Supporting information

Figures

Figure SA1: Mass spectra of the LPC 16:0, obtained on the different instruments in the negative ion mode

Figure SA2: Comparison of commercial software for 7 different lipid standards yielding different ion species.

Figure SA3: Comparison of the deviations between two instruments according to the CCS values of the ions, in positive (at the top) and negative (at the bottom) modes

Tables

Table SA1: Ionization parameters for the experiments performed on the Agilent DTIMS system in both positive and negative modes

Table SA2 : Ion mobility conditions for the experiments performed on the Agilent DTIMS system

Table SA3: Experimental parameters used for the TIMS-TOF Flex system in both positive and negative modes

Table SA4: T-Rex 4D processing parameters in Metaboscape software

Table SA5: Compound detection parameters for IMS peaks in Data Analysis software

Table SA6: Processing parameters in the Unifi software

Table SA7: Comparison of β and t_{fix} parameters determined using either IM-MS Browser or Excel software

Table SA8: Comparison of the drift times given by different types of Waters software

Table SA9: Comparison of the CCS values obtained with different types of software from Waters and the associated deviations

Table SA10: Constant of the Mason-Schamp equation

Table SA11: calibration characteristics as performed by Metaboscape using the Tune Mix calibrant

Table SA12: CCS determination of five selected lipids using either (Metaboscape + Excel) or Metaboscape software

Table SA13: 1/K0 raw of Tune Mix ions extracted using Data Analysis software and the corresponding 1/K0 ref

Table SA14: Parameters obtained with Data Analysis software for selected lipids

Table SA15: Intra-instrumental repeatability of the three instruments, RSD of the CCS values between different data sets in positive and negative modes and RSD on 1/K0 for TIMS and CCS values according to different IMS parameters (See Table SB1-3 for more details).

In the supplementary information B (Excel file):

Table SB1.a: Study of different ion mobility parameters on plasma lipids CCS values using Tune Mix as calibrants with TWIMS instrument

Table SB1.b: Repetability with different datasets of plasma lipids CCS values in TWIMS instrument using Tune Mix as calibrant

Table SB2.a: Study of different ion mobility parameters on plasma lipids CCS values using Tune Mix as calibrants with DTIMS instrument

Table SB2.b: Repetability with different datasets of plasma lipids CCS values in DTIMS instrument using Tune Mix as calibrant

Table SB3.a: Study of different ion mobility parameters on plasma lipids CCS values using Tune Mix as calibrants with TIMS instrument

Table SB3.b: Repetability with different datasets of plasma lipids CCS values in TIMS instruments using Tune Mix as calibrant

Table SB4.a: Plasma lipids CCS values in positive mode using Tune Mix as calibrants with all three instruments, deviations between CCS values and RSD between the three CCS values are also reported

Table SB4.b: Plasma lipids CCS values in negative mode using Tune Mix as calibrants with all three instruments, deviations between CCS values and RSD between the three CCS values are also reported

Table SB5.a: Plasma lipids CCS values in positive mode using all the ten calibrants tested with all three instruments, deviations between CCS values and RSD between the three CCS values are also reported

Table SB5.b: Plasma lipids CCS values in negative mode using all the six calibrants tested with all three instruments, deviations between CCS values and RSD between the three CCS values are also reported

Table SB6.a: Lipid standards CCS values in positive mode using all the ten calibrants tested with all three instruments, deviations between CCS values and RSD between the three CCS values are also reported

Table SB6.b: Lipid standards CCS values in negative mode using all the six calibrants tested with all three instruments, deviations between CCS values and RSD between the three CCS values are also reported

Table SB7: Lipid standard CCS values in positive mode determined using different software tools for a same raw data from each technology

LC-IMS-MS methodology

Identical chromatographic set-ups were used for the three IMS-MS platforms. Chromatographic separations were performed using a 2.1 × 100 mm, Acquity UPLC CSH C18 1.7 μm column (Waters, Manchester, UK) equipped with a 0.2-μm prefilter. The sampler and column oven temperatures were set at 10 °C and 50 °C, respectively. The flow rate was 0.4 mL min⁻¹. Mobile phase A consisted of acetonitrile/aqueous ammonium formate (10 mM) (40:60, v/v) and mobile phase B of isopropanol/acetonitrile/ aqueous ammonium formate (10 mM) (88:8:4, v/v/v); 0.1 % formic acid (FA) was added to both mobile phases. The gradient was as follows: 0–2 min, 32% B; 2–14 min, 32–75% B; 14–26.5 min, 75-100% B; 26.5–30 min, 100% B; 30–30.5 min, 100-32% B; 30.5–35 min, 32% B.

TWIMS experiments

An UHPLC system (Vanquish) coupled to an IMS QTOF mass spectrometer (SYNAPT G2 HDMS) equipped with a traveling wave ion mobility (TWIMS) cell was used. Mass spectra were recorded over a m/z 50–2000 range in the sensitivity mode (resolution 10,000 FWHM at m/z 950). External mass calibration was performed with a sodium formate solution (10% FA/0.1 M NaOH/ACN (1:1:8)) before each analysis. Lockmass correction was performed by infusing leucine enkephalin (2 ng μL⁻¹ in water/isopropanol (1:1), 4 μL min⁻¹) *via* the LockSpray™ interface. The source, IMS and MS/MS parameters were exactly those previously reported. [1]

DTIMS experiments

The LC-DTIMS-MS experiments were performed using an Infinite 1290 2D-LC chromatographic system (only the first dimension was used) coupled to a DTIMS Q-TOF mass spectrometer (Agilent 6560) equipped with a JetStream electrospray interface. Chromatographic system was monitored by Open lab CDS chemstation edition version C.01.09 [144] and DTIMS instrument by Agilent Masshunter version B.09.00.

Mobile phases were filtered for DTIMS experiments with ME24 mixed cellulose ester filters of 0.2 μm and 47mm diameter (Whatman). Plasma samples were diluted in 1/40 and 1/10 ratios and the injected volumes were 2 and 5 μL in positive and negative mode, respectively. Mass spectra were recorded over a m/z 50-1700 range. External mass calibration was performed with a Tune Mix solution. The IMS parameters are reported in the supplementary information (Table SA.1, SA.2). For method validation, various parameters were applied by varying the drift-tube entrance and exit voltages, and by testing the multiplexing capabilities (Table SA2)^{2,3}. Calibrant solutions were injected in the flow injection analysis (FIA) mode with the same flow rate of 0.4 mL.min⁻¹, before and after the LC sequence.

Table SA1: Ionization parameters for the experiments performed on the Agilent DTIMS system in both positive and negative modes

ESI source parameter	Positive mode	Negative mode
drying gas temperature (°C)	300	300
sheath gas temperature (°C)	350	350
drying gas flow (L/min)	8	8
sheath gas flow (L/min)	12	12
nebulizer gas pressure (psi)	35	35
capillary voltage (kV)	3.5	-3
nozzle voltage (V)	300	300
fragmentor voltage (V)	185	185
Oct. 1 RF Vpp (V)	750	750

Table SA10 : Ion mobility conditions for the experiments performed on the Agilent DTIMS system

Conditions	c1	c2	c3	c4	c5
Drift-tube entrance (V)	1574	1474	1700	1574	1574
Drift-tube exit (V)	224	224	250	224	224
IM trap fill time (ms)	30	30	20	14.1	3.9
Trap release time (μ s)	300	300	150	100	200
IM transient rate	18	18	18	18	18
maximum DT (ms)	60	60	60	60	60
multiplexing	No	No	No	3-bit	4-bit

TIMS experiments

The LC-TIMS-MS experiments were performed using an UHPLC system (Vanquish) hyphenated to a TIMS TOF Flex. The injected volumes were 2 or 3 μ L for the more diluted sample and 1 μ L for the other dilution. Mass spectra were recorded over the m/z 50-1600 and 50-1650 ranges in positive and negative mode, respectively. The IMS parameters were adjusted to detect all the lipid species, within a large ion mobility range corresponding to reduced mobilities ($1/K_0$) from 0.55 to 1.90 V.s.cm⁻². The ramp time was 100 ms, and the ramp rate 9.42 Hz. For method validation, various IMS parameters were evaluated, using the Tune Mix calibration kit (Table SA.3). Then, the method with the adjusted parameters was applied on the instrument at least 30 minutes before calibration and analysis. External mass calibration was performed with a sodium formate solution 10% FA/0.1 M NaOH/ACN (1:1:8), in HPC (High precision calibration) mode. External mobility calibration was performed in two steps. First, the voltage of the m/z 622 ion of the tune mix was adjusted at 132V by modifying the nitrogen pressure, to ensure that all ions were within the mobility range. Then, the second step consisting in the calibration step itself and could be proceeded using all the ions of the calibrant (for example, those of Tune mix) *via* a linear function. Eleven calibrants were tested for this IMS calibration step. The calibrations were performed before each LC-IMS-MS sequence. Additional internal mobility calibration have been performed by injecting the calibrant at the beginning of the LC run with a 6-way valve.

Table SA3: Experimental parameters used for the TIMS-TOF Flex system in both positive and negative modes

ESI source parameters	Positive	Negative
Scan range	50-1600	50-1650
End plate Offset (V)	500	500
Capillary (V)	4500	-3600
Nebulizer (bar)	2.7	2.7
Dry gas (L/min)	8	8
Dry temp ($^{\circ}$ C)	240	240

Tune parameters: TIMS		
Offsets	Positive	Negative
Δt_1 (V)	-20	20
Δt_2 (V)	-120	120
Δt_3 (V)	80	-80
Δt_4 (V)	100	-100
Δt_5 (V)	0	0
Δt_6 (V)	100	-100

Collision Cell In (V)	220	-220	TIMS settings		
Ion Charge Control (ICC)	Enable	Enable	c1	c2	c3
Target intensity (M)	7.5	7.5	Mode	Custom	Custom
Tune parameters			1/K0 start (V.s/cm ²)	0.55	0.8
Transfer parameters	<i>Positive</i>	<i>Negative</i>	1/K0 end (V.s/cm ²)	1.9	1.8
Defection 1 Delta (V)	80	-80	Ramp time (ms)	100	250
Funnel 1 RF (Vpp)	500	500	Accumulation time (ms)	100	300
isCID Energy (eV)	0	0	Duty cycle (%)	100	
Funnel 2 RF (Vpp)	250	250	Ramp rate (Hz)	9.43	3.91
Multipole RF (Vpp)	250	200			3.27
Collision Cell					
Collision Energy (eV)	10	10			
Collision RF (Vpp)	1100	1100			
Quadrupole					
Ion Energy (eV)	5	5			
Low mass (m/z)	150	150			
Focus Pre TOF					
Transfer time (μs)	65	65			
Pre Pulse Storage (μs)	5	5			

Calibrants used in this study [1]

The IMS calibration mixtures have been prepared according to the reference publication and the sensitivity of the instruments. The calibrants have been injected in Flow injection analysis (FIA) for TWIMS and DTIMS analysis and in infusion prior to each analysis sequence for TIMS instrument.

Polyalanine and dextran were first dissolved in H₂O at 1 mM and then diluted to 10 μM in 1/1:ACN/H₂O for analysis. Reference CCS values have been retrieved in Campuzano et al, [4] for polyalanine and in Hofmann et al, [5] for dextran.

Lipids were purchased as standards: PE 6:0/6:0, PE 10:0/10:0, PE 15:0/15:0, PC 20:0/20:0, PC 24:0/24:0, LPC 16:0, LPE 16:0, PE 18:1/18:1 Δ⁹ cis, PC 16:0/16:0 or from a kit: the Differential Ion Mobility System Suitability LIPIDOMIX kit (DIMS kit). Lipids standards were dissolved in chloroform/methanol:50/50 (v/v) to yield 10 mM stock solutions which were further diluted in methanol (MeOH)/isopropanol/H₂O:65/35/5 (v/v/v) to obtain a 100 μM final solution. Reference CCS have been retrieved in various publications [6–10], as mentioned in the supplementary information of a previous study [1].

Polyglycine was dissolved (1mg/mL) in formic acid, vortex stirred and sonicated until dissolution and diluted in ACN/H₂O 50:50 (v/v) to obtain a 10 μg.mL⁻¹ solution [11].

Tune Mix solution containing six hexakis(fluoroalkoxy)phosphazines (ESI-low concentration tuning mix, G1969-85000) was used as received. For TWIMS and DTIMS analyses, 10μg/mL of betaine added in the Tune Mix solution in positive mode. The CCS values used have been measured by Stow et al, [12].

Major Mix IMS calibration kit was prepared by mixing 100 μL of the Major Mix Calibration Solution from Waters with 50 μL of the LCMS QC reference standard solution (Waters). The reference CCS values used for this mix have been provided by Waters and has been discussed in previous articles [1,13]

The tetraalkylammonium (TAA) salts were prepared in MeOH to 1 μM , except tetramethylammonium salt concentration which was 20 μM in MeOH [4].

Poly(ethylene) glycol (PEG) were prepared from four products at 600, 1000, 2000, 3350 g/mol at a final concentration of 15 μM in ACN with 13 mM of NaI and poly(ethylene oxide) monomethyl ether (PEO) from two products at 700 and 2000 g/mol, at a final concentration of 5 μM in MeOH with 50 μM of NaCl, according to previously described protocols [14,15] respectively.

The poly-L-malic acid was prepared from L-malic acid which was dissolved in H_2O to a 0.050 M concentration, the polymerisation was performed at 80°C for 24 hours in an open Eppendorf [11]. The solution was reconstituted in the same amount of water and then diluted by 20 in ACN/ H_2O :50/50 (v/v).

A mixture of drug-like compounds [4] was prepared at 1 μM in H_2O /MeOH:50/50 (v/v) from 1 mM stock solutions, for acetaminophen, alprenolol and colchicine in H_2O , for ondansetron, clozapine N-oxide and verapamil in MeOH and for reserpine in ACN/ H_2O :50/50 +0.1% FA.

Data processing

Data processing using Agilent software

For processing the data from DTIMS experiments, only IM-MS Browser was used for the ion mobility dimension. However, MassHunter Qualitative Navigator software was used to visualize the data, in particular chromatograms and mass spectra.

In IM-MS Browser, the data processing was performed by creating feature table with the IMFE tool, in chromatographic dimension, the common organic molecule option was used for isotope model, the limit charge state was fixed to 1. The ion intensity was adapted to the data and the ions searched and the retention time was restricted to 0-28 minutes in positive mode and 0-24 minutes in negative mode.

Data processing using Bruker software

Metaboscape parameters

In Metaboscape software, different parameters have to be registered to do the data analysis processing. In each project, experiment have been created for each sequence analysis and one feature table was created for each analysis to retrieve more easily the CCS values of the annotated lipids at the end of the process and all the analysis for one given calibrant (triplicates) to check the CCS values at the end.

The feature table was created by first giving an explicit name with at least the number of the analysis processed. The filter parameters were set to one in 'Minimum # features for extraction' and 'Presence of feature in minimum # of analyses' in only one analysis was processed or two where triplicates were processed.

The processing parameters are indicated in the Table SA4. Ion deconvolution parameters were adapted, by removing the seed ions and common ions when one analysis was in the feature table. The

primary ion was $[M+H]^+$ in positive mode and $[M-H]^-$ in negative mode. Seed ions were $[M+Na]^+$ and $[M-HCOO]^-$ and common ions were $[M+NH_4]^+$ and $[M-H-H_2O]^-$ or $[M-CH_3]^-$.

To be consistent with all the calibrants, mass recalibration was not activated because with some calibrants, the mass range was not adapted to the lipid species. The mobility calibration was adapted for each calibrant, by changing the retention time range if needed, and the reference lists used for calibrating the instrument with m/z , CCS and charge of the ions of the calibrant.

The feature lists were then exported in csv files, while a python script to find the CCS values for all the files and group these values by mode and calibrant.

Table SA4: T-Rex 4D processing parameters in Metaboscape software

	T-Rex 4D Processing		
	Positive mode	Negative mode	Low intensity compounds
Peak Detection			
Intensity threshold (counts)	1000	1000	10
Minimum 4D Peak Size (points)	100	100	5
Feature signal	Intensity	Intensity	Intensity
Enable recursive feature extraction	Yes	Yes	Yes
Minimum 4D Peak Size (recursive) (points)	10	10	1
Ranges			
Retention time (min)	0.3-30	0.3-22	adapted
Mass (m/z)	300-950	400-900	adapted

Data Analysis

For some lipid species, the CCS values were also determined by the Data Analysis software. For that, the mobility calibration was completed by integrating the ion mobility spectrum of Tune mix calibrant with the parameters in Table SA5. Extracted ion chromatograms of lipids were obtained, based on the m/z values applying a width of ± 0.05 Da. In the mass spectra, lipid signals were selected to extract the ion mobility spectrum associated and the CCS value was obtained by giving the charge state of the ion.

Table SA5: Compound detection parameters for IMS peaks in Data Analysis software

Compound detection in 'Find Mobilogram'	
Sensitivity	99
Area threshold (Relative %)	5
Intensity threshold (absolute)	50
Min. peak valley	Off
Peak resolution	250

Data processing using Waters software

Unifi parameters

The data processing with the UNIFI software were performed with the parameters given in Table SA6. The targeted screen settings are not set for plasma analysis, but only for calibrant experiments: the target match tolerance was set at 10 ppm, adducts was adapted in function of the calibrant species.

Table SA6: Processing parameters in the Unifi software

Unifi parameters	
Experiment type	Chromatographic

Peak processing setting		
Automatic peak width		yes
Automatic peak detection threshold		yes
Peak integration		
Liftoff (%)		0
Touchdown (%)		0.5
Maximum allowed number of peaks per chromatogram		1000
Apply lock mass correction		yes
High energy intensity threshold		20 counts
Low energy intensity threshold		20 counts
Background filter		High
Maximum number of peaks to keep per channel		200000
Adducts/ions		+H, +Na, +NH ₄ or +HCOO, -H
Lock mass settings		
Combine width		3 scans
Mass window		0.1 m/z
Reference mass		556.2766 or 554.2615

Progenesis QI parameters

Some analyses were done with Progenesis software to compare the CCS values to those from Unifi. Basic settings were chosen for these analyses with a sensitivity of 3. The adducts or ions: [M+H]⁺, [M+Na]⁺, [M+NH₄]⁺ and [M+H-H₂O]⁺ were specified.

Masslynx and Driftscope parameters

Data treatment was also made with the combination of Masslynx and Driftscope, to compare the CCS obtained with Unifi and Progenesis. Driftscope was used to export the drift time values of the species. For that, the 2D representation of m/z over retention time was made and with the display range editor, a range around the retention time of the specific lipid was selected. The drift time are then exported for Masslynx. The extracted ion mobility spectrum of the specific ions was then performed in Masslynx and exported in csv file to fitting the IMS peak with Origin software. The CCS values were then obtained from these drift time values.

CCS determination

CCS determination using Agilent software

The single-field^{DTIMS} CCS values were determined by IM-MS Browser software and using Excel software. The mathematical relation between the drift time determined by the DTIMS experiments and the CCS

values is: $t_D = \beta \sqrt{\frac{m_i}{m_g + m_i}} CCS + t_{fix}$ where m_i is the mass of the ions and m_g is the mass of the drift gas, β and t_{fix} are the slope and the intercept of the mobility calibration curve equation, respectively.

Two types of software, IM-MS Browser and Excel (plotting the calibration curve), were then independently used to determine β and t_{fix} parameters. The two sets of β and t_{fix} parameters were then compared. The Table SA reports β and t_{fix} values and the deviation. Then, the lipid CCS values were determined using the two sets of parameters and compared: the mean deviation obtained is about

0.01%, which is negligible. Thus, we decided to determine the CCS values by plotting manually the calibration curve in Excel, which allow us a considerable time saving during the data analysis process.

Table SA7: Comparison of β and t_{fix} parameters determined using either IM-MS Browser or Excel software

	IM-MS browser	Excel	Deviation (%)
β	0.136672	0.136673	0.0007
t_{fix}	-0.068	-0.068418	0.6

We wish to mention here another cause of bias associated to the data processing software. We noticed that data extraction modes using IM-MS Browser can affect the drift time determination, resulting in a slight deviation of the CCS values; i.e., in the case of flow injection analysis (FIA) of a calibrant, extracting the scan at the apex of the FIA peak leads to β and t_{fix} parameters different than extracting an average of scans over the whole FIA peak (x scans, 1 minute of analysis), leading to deviation of almost 0.1% in the lipid CCS values.

CCS determination using Waters software

The ^{TW}CCS values were determined from the drift time obtained during the analysis. Different types of software tools have been used for Waters raw data: Masslynx + Driftscope, Unifi and Progenesis QI. In order to better understand the software functioning, the drift times and CCS values obtained with each software have been compared.

We have seen that the t_D from Masslynx and from Unifi or Progenesis was not exactly the same (Column 5 and 8 or 9 of Table SA8). We have seen that the fitting of IMS peak with Masslynx could lead to some errors, this is why the IMS peak was exported from Masslynx and Origin was used to do a Gaussian fitting of the peak, but this not resolve the deviations with Unifi or Progenesis.

Moreover, we know that for TWIMS experiments, a correction of the drift time can be made by taking into account a constant C representing the EDC Delay of the Synapt instrument and the m/z of the ions according to the following equation, where the t_D' represent the corrected drift time:

$$t_D' = t_D - \frac{C\sqrt{m/z}}{1000}$$

In order to understand if Unifi and Progenesis use this correction, both t_D and t_D' were determined, and the t_D' seems to fit very well with drift times obtained with Unifi (Table SA8). However, for Progenesis software, it is not understandable which of t_D or t_D' were calculated.

Table SA8: Comparison of the drift times given by different types of Waters software

Lipids	Ions	m/z	rt	Masslynx	Masslynx + fitting with Origin software		Unifi	Progenesis
				t_D	t_D	t_D'	t_D'	Drift time
PE 6:0/6:0	[M+H] ⁺	412.2111	1.03	2.90	2.92	2.89	2.89	2.90
PE 6:0/6:0	[M+Na] ⁺	434.1923	1.03	3.04	3.05	3.02	3.02	3.04
DG 14:1/14:1	[M+Na] ⁺	531.4037	15.64	3.93	3.93	3.89	3.89	4.00
PE 10:0/10:0	[M+H] ⁺	524.3378	7.52	4.00	4.02	3.99	3.99	3.93
PE 10:0/10:0	[M+Na] ⁺	546.3183	7.52	4.21	4.24	4.20	4.20	4.21
PG 14:1/14:1	[M+H] ⁺	663.4244	11.7	5.11	5.11	5.07	5.08	5.17
SM 18:1;O2/18:1	[M+H] ⁺	729.5794	15.99	6.28	6.29	6.24	6.24	5.73
SM 18:1;O2/18:1	[M+Na] ⁺	751.5705	15.99	6.14	6.12	6.07	6.06	5.93

PC 16:0/16:0	[M+H] ⁺	734.556	17.88	5.86	5.93	5.88	5.88	5.80
PC 16:0/16:0	[M+Na] ⁺	756.5511	17.88	6.07	6.07	6.03	6.00	6.21
TG 18:1/18:1/18:1	[M+NH ₄] ⁺	902.8053	26.24	7.52	7.57	7.53	7.48	7.80
TG 18:1/18:1/18:1	[M+Na] ⁺	907.7721	26.24	7.45	7.48	7.44	7.51	7.66

The same process was done to understand the CCS determination from t_D' . Thus, raw data were processed with Unifi to extract the corrected drift times, t_D' of both calibrants and samples. A calibration file was created for each calibrant giving t_D' values determined by the Unifi software and the corrected collision cross sections CCS' values calculated with the following equation:

$$CCS' = \frac{CCS \sqrt{\mu}}{z} \text{ with } \mu = \frac{m_{ion} m_{gaz}}{m_{ion} + m_{gaz}}$$

where CCS , z and μ correspond respectively to a reference CCS determined by DTIMS, the charge of the ion and the reduced mass of the ion in a definite buffer gas.

In parallel, CCS determination has been manually made using Masslynx 4.1, Driftscope v2.9 (Waters) and Origin Pro 2018 b9.5.0.193 software, with two different equations of fitting for the calibration curves: $CCS' = A t_D'^N$ and the fitting with t_0 : $CCS' = A (t_D' - t_0)^N$ where A , N and t_0 are fitting parameters, which demonstrated best results than the fitting without t_0 .

The CCS values were also determined with Progenesis Q1. All the CCS values were compared in the Table SA9.

Table SA9: Comparison of the CCS values obtained with different types of software from Waters and the associated deviations

Lipids	Ions	m/z	rt	CCS (Å ²)				Deviations between Unifi and Masslynx (fitting with t_0)	Deviations between Unifi and Progenesis
				Unifi	Masslynx + fitting	Masslynx + fitting with t_0	Progenesis		
PE 6:0/6:0	[M+H] ⁺	412.2111	1.03	200.74	200.52	200.80	200.88	0.03	0.07
PE 6:0/6:0	[M+Na] ⁺	434.1923	1.03	205.10	204.86	205.17	205.48	0.03	0.19
DG 14:1/14:1	[M+Na] ⁺	531.4037	15.6	232.89	232.43	232.83	231.50	0.03	0.60
PE 10:0/10:0	[M+H] ⁺	524.3378	7.52	234.74	235.62	236.02	233.70	0.54	0.44
PE 10:0/10:0	[M+Na] ⁺	546.3183	7.52	242.04	241.90	242.29	241.74	0.10	0.12
PG 14:1/14:1	[M+H] ⁺	663.4244	11.7	266.31	265.55	265.83	267.49	0.18	0.44
SM 18:1;O2/18:1	[M+H] ⁺	729.5794	16	295.33	295.57	295.59	296.17	0.09	0.28
SM 18:1;O2/18:1	[M+Na] ⁺	751.5705	16	290.90	291.13	291.19	289.42	0.10	0.51
PC 16:0/16:0	[M+H] ⁺	734.556	17.9	286.48	286.51	286.62	286.19	0.05	0.10
PC 16:0/16:0	[M+Na] ⁺	756.5511	17.9	289.35	289.92	290.00	289.39	0.22	0.01
TG 18:1/18:1/18:1	[M+NH ₄] ⁺	902.8053	26.2	323.30	324.67	324.32	321.50	0.31	0.56
TG 18:1/18:1/18:1	[M+Na] ⁺	907.7721	26.2	323.82	322.60	322.27	324.43	0.48	0.19
								0.18	0.29

The process with Masslynx was used to validate the Unifi process (*i.e.* the calculation of the corrected drift time t_D' and the use of a calibration equation including the t_0 parameter to force the curve through zero), this is why Unifi was used to determine both plasma lipids and lipid standards in this study.

CCS determination using Bruker software

The ^{TIMS}CCS values were determined from the $1/K_0$ values obtained from the TIMS experiments, using a derived Mason-schamp equation (equation 1), where z is the charge, T the temperature, M and m , the masses of the analyte ions and the drift gas, respectively. The Table SA10 depicts the values of the constants as well as the conversion of the m/z value in kg used for the calculation of the Constant, in the derived Mason-Schamp equation.

$$CCS = Constant \times \frac{z}{K_0} \sqrt{\frac{1}{T} \frac{M+m}{Mm}} \quad \text{with } Constant = \frac{3e}{16N_0} \sqrt{\frac{2\pi}{k_B C_{Da}}} \quad (1)$$

Table SA10: Constant of the Mason-Schamp equation

Constant	Value	Unity
gas number density (N_0)	$2.687 \cdot 10^{25}$	m^{-3}
Boltzmann's Constant (k_B)	$1,38 \cdot 10^{-23}$	J/K
π	3.141592654	
Electron charge (e)	$1.602 \cdot 10^{-19}$	C
Conversion of Da (C_{Da})	$1.66053904 \cdot 10^{-27}$	kg
Result for constant =	$1.85107 \cdot 10^{-20}$	

The result obtained for the Constant with these values, is $1.85107 \cdot 10^{-20}$ in SI units, which gives 18510.7 converting the unit of CCS (from m^2 into \AA^2) and the ion mobility unit (from $m^2 V^{-1} s^{-1}$ to $cm^2 V^{-1} s^{-1}$). However, this value can differ depending on the number of decimals used for the characteristic constants as electron charge or Boltzmann's constant. This value slightly differs from the value of 18500 mentioned by Ridgeway et al⁴, and from the value of 18509.863216340458 given by Bruker. The use of the rounded value of 18500 instead of the Bruker's value, can lead to a deviation of 0.05% in the CCS value, which could be considered negligible. However, as we attempted to minimise all the deviations for CCS determination, a deviation of 0 would be required on this Constant and a consensus should be reached concerning its value.

To understand how Metaboscape works, two data processing approaches were carried out: the first used Metaboscape only to collect the parameters of the ions, particularly the $1/K_{0 \text{ raw}}$ values and then Excel for mobility re-calibration and CCS determination. The second used the whole Metaboscape data processing, from the the $1/K_{0 \text{ raw}}$ determination to the mobility re-calibration process and CCS determination. (6th column Table SA12).

In both cases, the first step consisted in TIMS calibration using Tune Mix as calibrant.

Using the first data processing approach, the $1/K_{0 \text{ raw}}$ values of Tune Mix ions were extracted (using Metaboscape) and imported into an Excel file for plotting $1/K_{0 \text{ ref}}$ values (from Bruker values calculated in Metaboscape) in function of $1/K_{0 \text{ raw}}$ leading to equation 2:

$$\frac{1}{K_{0 \text{ ref}}} = 0.9945864 \times \frac{1}{K_{0 \text{ raw}}} - 0.0186896 \quad (2)$$

Table SA11: calibration characteristics as performed by Metaboscape using the Tune Mix calibrant

Calibration on Metaboscape with Tune Mix ions		
Ion (m/z)	1/K ₀ ref. ^a	1/K ₀ raw ^b
322.04812	0.736	0.753
622.028961	0.991	1.021
922.009799	1.199	1.228
1221.99064	1.393	1.42
1521.97148	1.568	1.591

a : Bruker values

b: extracted from the raw data using Metaboscape software

This equation 2 permits to determine the 1/K₀lipid values (noted as 1/K₀a, replacing 1/K₀ref by 1/K₀a in the equation 2) of the different lipids, from extracted 1/K₀raw values. Then, the equation (1), i.e. = $18500 \frac{z}{K_0} \sqrt{T \frac{Mm}{M+m}}$, was used to determine the CCS values of these lipids. The Table SA12 shows the results for five different lipids we chose as examples to illustrate our data processing approach.

In parallel, the second data processing using only Metaboscape software was carried out leading to another set of 1/K₀b and CCS values (Table SA12^b).

The deviations between the CCS values obtained from the first and the second data processing approaches are between 0.01 and 0.06% (Table SA12).

Table SA12: CCS determination of five selected lipids using either (Metaboscape + Excel) or Metaboscape software

Lipids	Ions	Measured m/z	RT [min]	1/K ₀ raw	Metaboscape +Excel ^{*a}		Metaboscape whole process ^b		Deviation (%)
					1/K ₀	CCS (Å ²)	1/K ₀	CCS (Å ²)	
PE 6:0/6:0	[M+H] ⁺	412.2096	1.53	0.998	0.974	201.542	0.974	201.5	0.02
PE 6:0/6:0	[M+Na] ⁺	434.1915	1.01	1.026	1.002	206.971	1.001	206.9	0.03
LPE 16:0	[M+H] ⁺	454.2928	6.43	1.073	1.049	216.338	1.048	216.2	0.06
LPC 16:0	[M+H] ⁺	496.3402	6.16	1.152	1.127	231.977	1.127	232	0.01
LPC 18:1	[M+H] ⁺	522.3559	6.64	1.169	1.144	235.144	1.143	235	0.06

A similar methodology was used to understand the data processing of Data Analysis software for CCS determination. Thus, two approaches were also tested, the first combining Data Analysis and Excel software, the second using only Data Analysis software.

For the first approach, 1/K₀raw of calibrants values were extracted using Data Analysis. Then, these 1/K₀raw values were imported in Excel for plotting 1/K₀ref (Table SA13) in function of 1/K₀raw (Table SA13) using Tune Mix reference ions. That led to equation 3 (using Excel).

$$\frac{1}{K_{0ref}} = 1.0107 \times \frac{1}{K_{0raw}} - 0.0413 \quad (3)$$

Table SA13: 1/K₀raw of Tune Mix ions extracted using Data Analysis software and the corresponding 1/K₀ref

Tune Mix Ion (m/z)	1/K ₀ ref. ^a	1/K ₀ raw ^b
622.029	0.9915	1.0209

922.0098	1.1986	1.2281
1221.9906	1.3934	1.4205
1521.9715	1.5685	1.5918

Then, the $1/K_{0c}$ of lipids were determined using the equation 3 (where $1/K_{0ref}$ was replaced by $1/K_{0c}$), and the CCS values were deduced using equation 1 with the Constant = 18500. The deviations between the CCS values determined by the combination of Data Analysis and Excel and by Data Analysis (Table SA14.d) are between 0.01 and 0.13%.

Table SA14: Parameters obtained with Data Analysis software for selected lipids

Lipids	Ions	Measured m/z	RT [min]	Data Analysis + Excel ^c			Data Analysis ^d		Deviation (%)
				$1/K_{0raw}$	$1/K_0$	CCS (\AA^2)	$1/K_0$	CCS (\AA^2)	
PE 6:0/6:0	[M+H] ⁺	412.2096	1.53	0.997	0.967	200.042	0.968	200.3	0.13
PE 6:0/6:0	[M+Na] ⁺	434.1915	1.01	1.025	0.995	205.581	0.996	205.7	0.06
LPE 16:0	[M+H] ⁺	454.2928	6.43	1.072	1.042	215.014	1.042	215.0	0.01
LPE 16:0	[M+Na] ⁺	476.3066	1.00	1.104	1.074	221.334	1.074	221.3	0.02
LPC 16:0	[M+H] ⁺	496.3402	6.16	1.153	1.124	231.418	1.124	231.3	0.05

The mean deviation obtained is about 0.5%, which is not negligible, if we intend to use CCS values as molecular descriptor. The difference between both software tools can be explained by the fact that they do not use the same processing script. As Metaboscape permits the automation of the data processing for huge metabolomics batches, we decided to work with this software.

Conclusion on data processing and CCS determination

All the software comparisons were evaluated together, for the three IMS technologies, leading to the Table SB7 and Figure SA1.

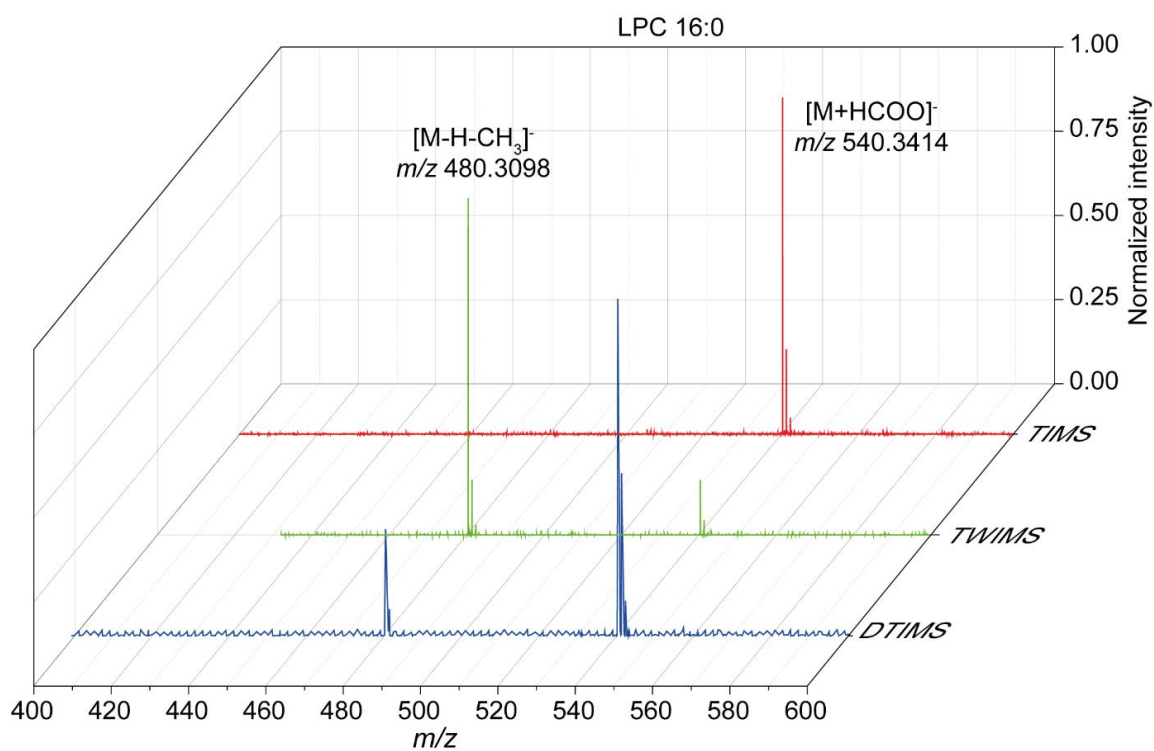
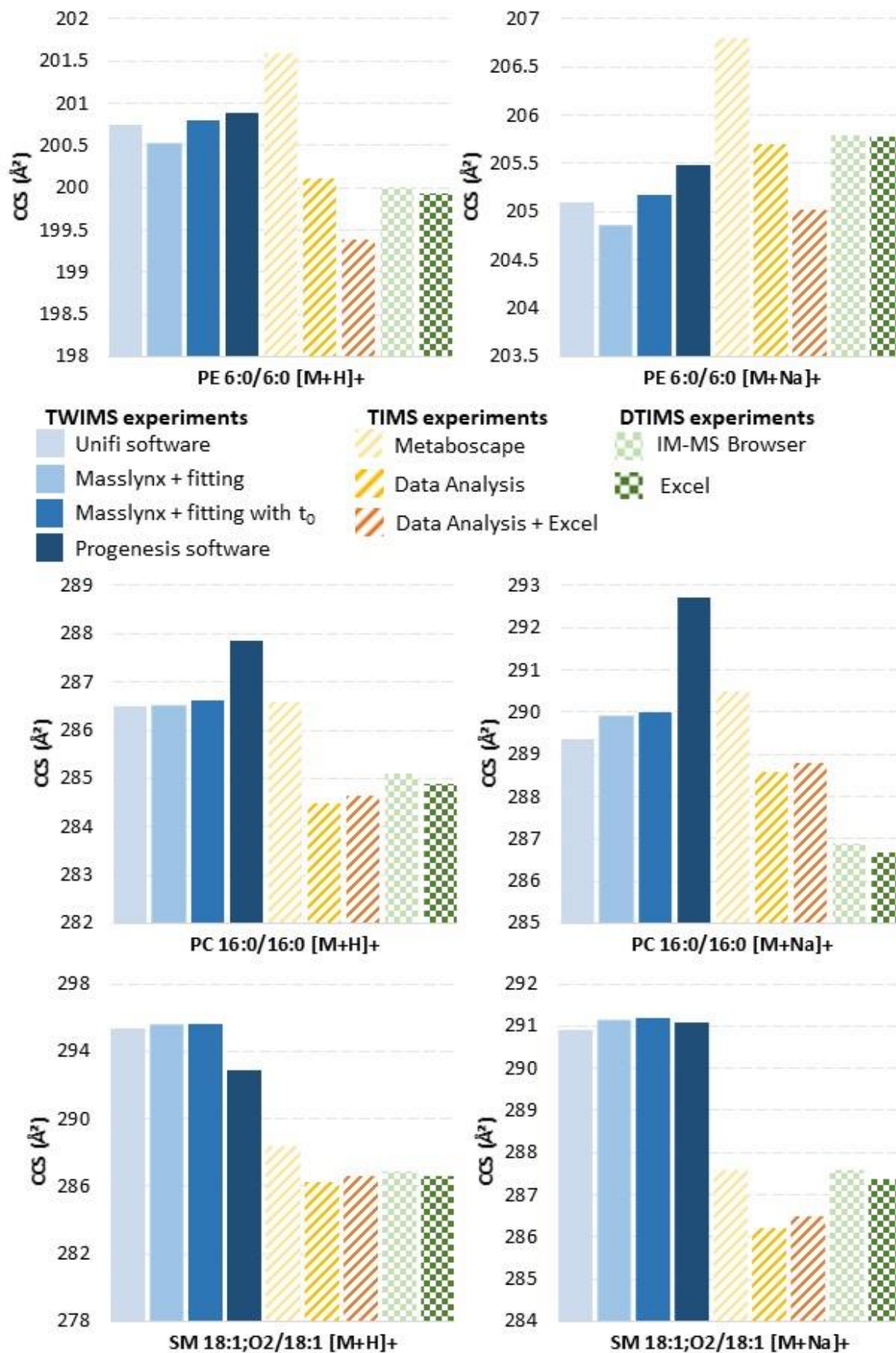


Figure SA1: Mass spectra of the LPC 16:0, obtained on the different instruments in the negative ion mode



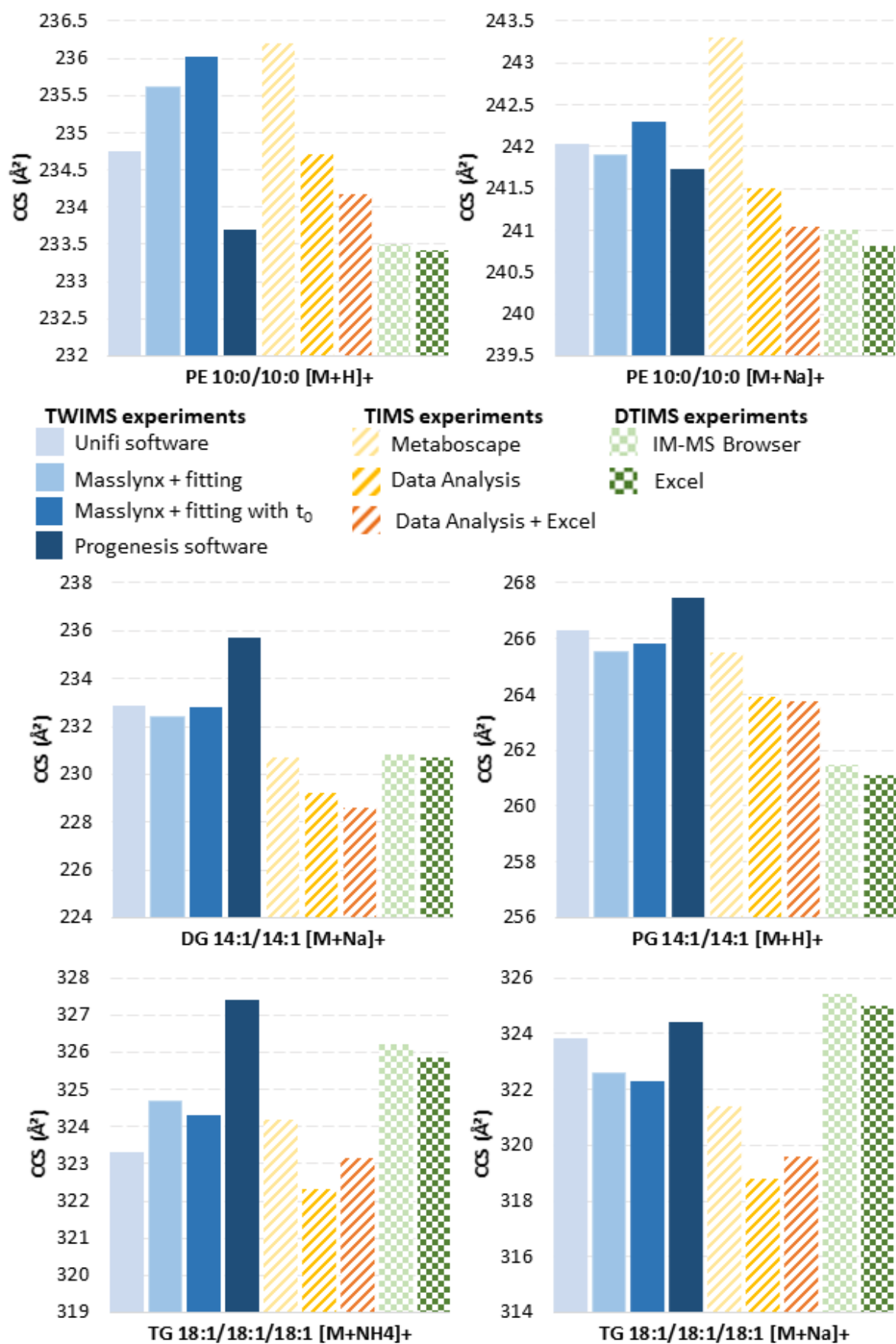


Figure SA2: Comparison of commercial software for 7 different lipid standards yielding different ion species.

Table SA15: Intra-instrumental repeatability of the three instruments, RSD of the CCS values between different data sets in positive and negative modes and RSD on $1/K_0$ for TIMS and CCS values according to different IMS parameters (See Table SB1-3 for more details)

Instrument	Different analytical sequences		Different IMS parameters	
	Positive	Negative	Positive	
	CCS		$1/K_0$	CCS
TWIMS	0.20	0.41	-	0.21
DTIMS	0.27	0.20	-	0.21
TIMS	0.48	0.36	0.48	0.40

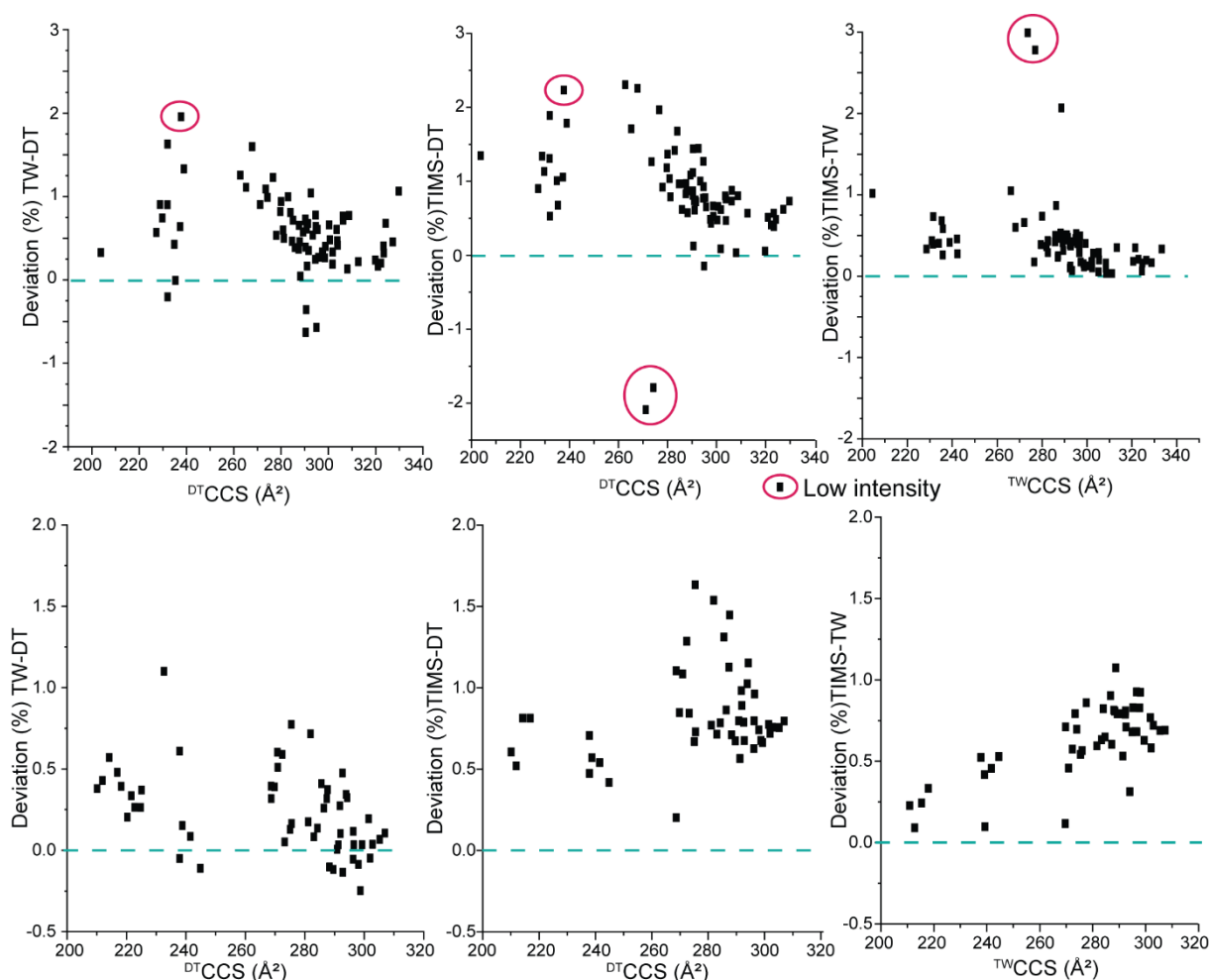


Figure SA3: Comparison of the deviations between two instruments according to the CCS values of the ions, in positive (at the top) and negative (at the bottom) modes

References

- [1] A.C. George, I. Schmitz-Afonso, V. Marie, B. Colsch, F. Fenaille, C. Afonso, C. Loutelier-Bourhis, A re-calibration procedure for interoperable lipid collision cross section values measured by traveling wave ion mobility spectrometry, *Analytica Chimica Acta*. (2022) 340236. <https://doi.org/10.1016/j.aca.2022.340236>.
- [2] T.J. Causon, L. Si-Hung, K. Newton, R.T. Kurulugama, J. Fjeldsted, S. Hann, Fundamental study of ion trapping and multiplexing using drift tube-ion mobility time-of-flight mass spectrometry for non-targeted metabolomics, *Anal Bioanal Chem*. 411 (2019) 6265–6274. <https://doi.org/10.1007/s00216-019-02021-8>.

- [3] J.C. May, R. Knochenmuss, J.C. Fjeldsted, J.A. McLean, Resolution of Isomeric Mixtures in Ion Mobility Using a Combined Demultiplexing and Peak Deconvolution Technique, *Anal. Chem.* 92 (2020) 9482–9492. <https://doi.org/10.1021/acs.analchem.9b05718>.
- [4] I. Campuzano, M.F. Bush, C.V. Robinson, C. Beaumont, K. Richardson, H. Kim, H.I. Kim, Structural Characterization of Drug-like Compounds by Ion Mobility Mass Spectrometry: Comparison of Theoretical and Experimentally Derived Nitrogen Collision Cross Sections, *Anal. Chem.* 84 (2012) 1026–1033. <https://doi.org/10.1021/ac202625t>.
- [5] J. Hofmann, W.B. Struwe, C.A. Scarff, J.H. Scrivens, D.J. Harvey, K. Pagel, Estimating Collision Cross Sections of Negatively Charged *N*- Glycans using Traveling Wave Ion Mobility-Mass Spectrometry, *Anal. Chem.* 86 (2014) 10789–10795. <https://doi.org/10.1021/ac5028353>.
- [6] K.M. Hines, J.C. May, J.A. McLean, L. Xu, Evaluation of Collision Cross Section Calibrants for Structural Analysis of Lipids by Traveling Wave Ion Mobility-Mass Spectrometry, *Anal. Chem.* 88 (2016) 7329–7336. <https://doi.org/10.1021/acs.analchem.6b01728>.
- [7] C.G. Vasilopoulou, K. Sulek, A.-D. Brunner, N.S. Meitei, U. Schweiger-Hufnagel, S.W. Meyer, A. Barsch, M. Mann, F. Meier, Trapped ion mobility spectrometry and PASEF enable in-depth lipidomics from minimal sample amounts, *Nature Communications.* 11 (2020) 331. <https://doi.org/10.1038/s41467-019-14044-x>.
- [8] H. Tsugawa, K. Ikeda, M. Takahashi, A. Satoh, Y. Mori, H. Uchino, N. Okahashi, Y. Yamada, I. Tada, P. Bonini, Y. Higashi, Y. Okazaki, Z. Zhou, Z.-J. Zhu, J. Koelmel, T. Cajka, O. Fiehn, K. Saito, M. Arita, M. Arita, A lipidome atlas in MS-DIAL 4, *Nat Biotechnol.* 38 (2020) 1159–1163. <https://doi.org/10.1038/s41587-020-0531-2>.
- [9] K.L. Leaptrot, J.C. May, J.N. Dodds, J.A. McLean, Ion mobility conformational lipid atlas for high confidence lipidomics, *Nature Communications.* 10 (2019) 985. <https://doi.org/10.1038/s41467-019-08897-5>.
- [10] X. Zheng, N.A. Aly, Y. Zhou, K.T. Dupuis, A. Bilbao, V.L. Paurus, D.J. Orton, R. Wilson, S.H. Payne, R.D. Smith, E.S. Baker, A structural examination and collision cross section database for over 500 metabolites and xenobiotics using drift tube ion mobility spectrometry, *Chem. Sci.* 8 (2017) 7724–7736. <https://doi.org/10.1039/C7SC03464D>.
- [11] T.W. Knapman, J.T. Berryman, I. Campuzano, S.A. Harris, A.E. Ashcroft, Considerations in experimental and theoretical collision cross-section measurements of small molecules using travelling wave ion mobility spectrometry-mass spectrometry, *International Journal of Mass Spectrometry.* 298 (2010) 17–23. <https://doi.org/10.1016/j.ijms.2009.09.011>.
- [12] S.M. Stow, T.J. Causon, X. Zheng, R.T. Kurulugama, T. Mairinger, J.C. May, E.E. Rennie, E.S. Baker, R.D. Smith, J.A. McLean, S. Hann, J.C. Fjeldsted, An Interlaboratory Evaluation of Drift Tube Ion Mobility–Mass Spectrometry Collision Cross Section Measurements, *Anal. Chem.* 89 (2017) 9048–9055. <https://doi.org/10.1021/acs.analchem.7b01729>.
- [13] V. Hinnenkamp, J. Klein, S.W. Meckelmann, P. Balsaa, T.C. Schmidt, O.J. Schmitz, Comparison of CCS Values Determined by Traveling Wave Ion Mobility Mass Spectrometry and Drift Tube Ion Mobility Mass Spectrometry, *Anal. Chem.* 90 (2018) 12042–12050. <https://doi.org/10.1021/acs.analchem.8b02711>.
- [14] Q. Duez, F. Chiro, R. Lienard, T. Josse, C. Choi, O. Coulembier, P. Dugourd, J. Cornil, P. Gerbaux, J. De Winter, Polymers for Traveling Wave Ion Mobility Spectrometry Calibration, *J Am Soc Mass Spectrom.* 28 (2017) 2483–2491. <https://doi.org/10.1007/s13361-017-1762-4>.
- [15] J.R.N. Haler, C. Kune, P. Massonnet, C. Comby-Zerbino, J. Jordens, M. Honing, Y. Mengerink, J. Far, E. De Pauw, Comprehensive Ion Mobility Calibration: Poly(ethylene oxide) Polymer Calibrants and General Strategies, *Anal. Chem.* 89 (2017) 12076–12086. <https://doi.org/10.1021/acs.analchem.7b02564>.
- [16] M.E. Ridgeway, M. Lubeck, J. Jordens, M. Mann, M.A. Park, Trapped ion mobility spectrometry: A short review, *International Journal of Mass Spectrometry.* 425 (2018) 22–35. <https://doi.org/10.1016/j.ijms.2018.01.006>.

Annexe 1: β and T_{fix} parameters used to determine the $^{\text{DT}}\text{CCS}$ values in both positive and negative ion modes

Calibrants	Parameters	Conditions DTIMS				
		c1	c2	c3	c4	c5
Tune Mix	β	0.13723246	0.14582383	0.12647986	0.13546965	0.13500537
	T_{Fix}	-0.13084821	-0.13372139	-0.03647021	0.31511907	0.39729837
Drugs	β	0.13051799	0.13861324	0.12060296	0.12925315	0.13011125
	T_{Fix}	1.12571453	1.20584562	1.04836502	1.50313144	1.29388906
Dextran	β	0.11594758	0.12264817	0.10851939	0.11441891	0.11394923
	T_{Fix}	3.56432871	3.93344434	3.02293666	4.01460747	4.11248341
Polygly	β	0.13081975	0.13916998	0.12099842	0.12916939	0.1282359
	T_{Fix}	1.125903	1.16449209	1.03397226	1.54684271	1.70494448
Lipids	β	0.15169031	0.15007158	0.13023703	0.13842996	0.13744379
	T_{Fix}	-3.4871837	-1.16076595	-0.95779947	-0.34624046	-0.18564809
Major Mix	β	0.12319551	0.13434303	0.11472735	0.12444877	0.12454467
	T_{Fix}	3.10895444	2.38881561	2.63476569	2.83854229	2.72397298
Polyala	β	0.13007706	0.13974601	0.12205344	0.13160816	0.13149563
	T_{Fix}	1.19924674	0.85310623	0.63734695	0.94821962	0.8911175
PEG	β	0.14047691	0.1513275	0.129333	0.14070645	0.14036577
	T_{Fix}	7.11235155	7.07194538	6.75603443	7.25826642	7.26248616
PEO	β	0.12571023	0.13399559	0.11782831	0.12507213	0.12461383
	T_{Fix}	1.1417703	1.04466999	0.66140603	1.38360127	1.4258658
TAA	β	0.13270318	0.14090146	0.12192686	0.13132022	0.13093297
	T_{Fix}	0.75292858	0.81470243	0.82787414	1.14302054	1.21039293

Calibrants	Parameters	Conditions DTIMS				
		c1	c2	c3	c4	c5
Tune Mix	β	0.138544	0.14721919	0.12781793	0.13683349	0.13589238
	T_{Fix}	-0.20560147	-0.23118914	-0.12190721	0.21249023	0.36363158
Dextran	β	0.12088759	0.12811101	0.11244131	0.12017811	0.10485021
	T_{Fix}	3.37785726	3.67016984	2.93127792	3.65692716	8.20575419
Lipids	β	0.13646049	0.14521103	0.12520477	0.13438938	0.13321402
	T_{Fix}	0.25851863	0.23708757	0.46882618	0.79784702	1.06383712
Major Mix	β	0.12527649	0.13157351	0.11470909	0.12316219	0.12242014
	T_{Fix}	2.07567047	2.49743267	2.17809196	2.69116824	2.80100004
Polyala	β	0.13033322	0.1393353	0.12048475	0.12843431	0.12737121
	T_{Fix}	1.60667718	1.21693467	1.26941547	1.82548049	2.05255819
Polymalic acid	β	0.1276456	0.1245264	0.11877	0.12686481	0.12743151
	T_{Fix}	2.07871851	4.77476359	1.77739559	2.34349639	2.22797718

5.3. Discussion on stepped-field CCS values

DTIMS instrument allows to determine single-field CCS values, as described in the previous article, but also stepped-field CCS values without any prior instrument ion mobility calibration.

Tune Mix solution and lipid standards have been analyzed to determine corresponding stepped-field CCS values. Samples were injected seven times every 30 seconds, and the drift tube entrance voltage has been changed every time, as shown in Table V-11.

Table V-11: DTIMS parameters for stepped-field experiments

Time Sequence	Time (min)	Drift tube entrance (V)	Drift tube Exit (V)
1	0-0.5	1074	
2	0.5-1	1174	
3	1-1.5	1274	
4	1.5-2	1374	224
5	2-2.5	1474	
6	2.5-3	1574	
7	3-3.5	1674	

The CCS values obtained for Tune Mix ions with this methodology, have been compared to the reference values obtained using a DTIMS instrument (Sarah M. Stow et al. 2017) and the results are shown in Table V-12 and Table V-13. Our CCS values were slightly lower than the reference values obtained by Stow et al (Table V-12), with a standard deviation (SD) up to 1.2%. Other experimental conditions have been tested to improve the accuracy of our measurements. The three conditions tested give the same CCS values with a mean RSD of 0.13%.

Table V-12: Comparison of CCS values of Tune Mix calibrant obtained using different conditions and the reference CCS values (Sarah M. Stow et al. 2017)

m/z	Reference CCS (\AA^2)	c1 (60ms)		c2 (90ms)		c3 (Source conditions)	
		CCS	SD (%)	CCS	SD (%)	CCS	SD (%)
118.0863	121.51	120.70	0.67	120.65	0.71	120.73	0.64
322.0482	153.67	152.37	0.85	152.30	0.90	152.27	0.92
622.0383	202.67	200.83	0.91	200.65	1.00	200.83	0.91
922.0190	243.05	241.33	0.71	240.70	0.97	240.90	0.89
1221.9982	281.25	279.33	0.68	278.60	0.95	278.63	0.93
1521.9758	315.79	312.03	1.20	314.50	0.41	312.87	0.93

The stability of CCS determination using stepped-field conditions has been studied over one year (Table V-13). The RSD obtained using the three CCS values obtained at three different time points was only 1.1%, which is slightly higher than the 0.3% reported by Stow et al (Sarah M. Stow et al. 2017).

Table V-13: Comparison of the CCS values of Tune Mix calibrant obtained at different time intervals over one year and the reference CCS values (Sarah M. Stow et al. 2017)

m/z	CCS (Å ²)			Mean CCS (Å ²)	RSD (%)	Reference CCS (Å ²)
	1 st	2 nd	3 rd			
118.0863		118.80	120.70	119.75	1.12	121.51
322.0482	151.20	150.60	152.37	151.39	0.59	153.67
622.0383	200.40	199.80	200.83	200.34	0.26	202.67
922.0190	241.60	240.40	241.33	241.11	0.26	243.05
1221.9982	280.35	278.80	279.33	279.49	0.28	281.25
1521.9758	311.80	310.80	312.03	311.54	0.21	315.79

For lipid standards, stepped-field CCS values have also been determined and compared with the literature CCS values. Deviations up to 2.8% and an acceptable mean deviation of 1.6% were observed (Table V-14).

Table V-14: Stepped-field CCS values of lipid standards and comparison with literature CCS values

Lipid standards	Ions	m/z	Published CCS (N ₂) in Å ²	Stepped-field ^{DT} CCS (Å ²)	SD (%)
PE 6:0/6:0	[M+H] ⁺	412.2111	202.92 ^a	197.40	2.76
PE 6:0/6:0	[M+Na] ⁺	434.1920	208.63 ^a	203.30	2.59
LPE 16:0	[M+H] ⁺	454.2962	213.91 ^a	209.30	2.18
LPC 16:0	[M+H] ⁺	496.3419	230.74 ^b	226.50	1.85
LPC 16:0	[M+Na] ⁺	518.3232	223.94 ^b	228.40	1.97
DG 14:1/14:1	[M+Na] ⁺	531.4037	230.30 ^c	227.40	1.27
DG 14:1/14:1	[M+NH ₄] ⁺	526.4477	235.12 ^c	231.50	1.55
LPC 18:1	[M+H] ⁺	522.3518	233.26 ^c	230.10	1.36
LPC 18:1	[M+Na] ⁺	544.3423	235.87 ^c	232.90	1.27
PE 10:0/10:0	[M+H] ⁺	524.3378	235.40 ^a	231.10	1.84
SM 18:1;O2/18:1	[M+H] ⁺	729.5872	287.60 ^c	283.60	1.40
PC 16:0/16:0	[M+H] ⁺	734.5669	278.40 ^d	281.20	1.00
PC 16:0/16:0	[M+Na] ⁺	756.5511	280.56 ^d	283.10	0.90
PE 18:1(9Z)/18:1(9Z)	[M+H] ⁺	744.5472	280.60 ^e	277.00	1.29
PI 14:1/14:1	[M+H] ⁺	751.4347	287.29 ^c	284.70	0.91
PC 20:0/20:0	[M+H] ⁺	846.6911	307.97 ^a	303.90	1.33
					1.59

a (Hines et al. 2016)
b (Tsugawa et al. 2020b)
c (Vasilopoulou et al. 2020)
d (Leaprot et al. 2019)
e (Zheng, Aly, et al. 2017)

Then, single-field CCS values of lipid standards have been determined using different calibrants and further compared to literature data (Figure V-3). The comparison of single-field CCS values with literature CCS values has also been represented. The results show that the deviation comparing the CCS values obtained with the same instrument, using both single-field and stepped-field CCS methods,

is higher than the deviation comparing single-field CCS values with literature values, which were determined using different types of instruments, whatever the calibrant used.

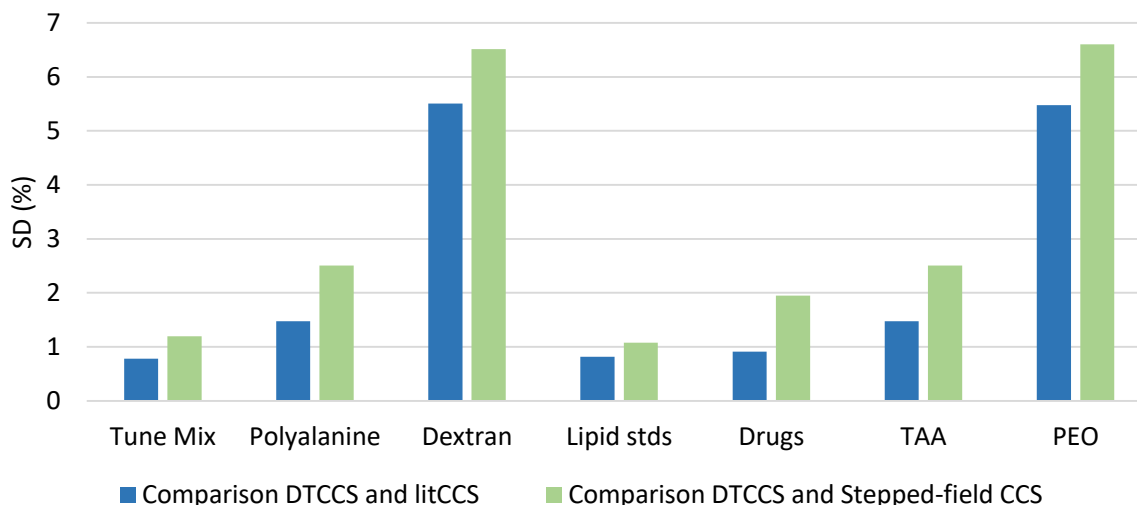


Figure V-3: Comparison of the ^{DT}CCS values, obtained with different calibrants with literature CCS values ((Hines et al. 2016) (Tsugawa et al. 2020b) (Vasilopoulou et al. 2020) (Leaprot et al. 2019) (Zheng, Aly, et al. 2017)) and stepped-field CCS values

These results demonstrated the need of improvements for stepped-field CCS values determination, because these values are used as reference in the primary method, in the ion mobility community. These values are thus crucial because they are used as reference for secondary methods such as TWIMS, TIMS and single-field calibration.

5.4. Conclusion

In this chapter, human plasma lipid CCS values were studied across three different IMS platforms using tune Mix as calibrant. The intra-instrument repeatability was shown to be very good with an average RSD of less than 0.5% for each of the three IMS technologies (Figure V-4). For the DTIMS instrument, two (in ion negative mode) and three (in positive ion mode) datasets (including five experiments for each dataset using different conditions) have been compared over one year resulting on a RSD of 0.20% and 0.27% in negative and positive ion modes respectively. Four datasets (two in positive and two in negative ion modes) using TWIMS instrument (with three experiments using three IMS conditions) have been compared, resulting on a RSD of 0.20% and 0.41% in positive and negative mode respectively. For TIMS, two instruments have been used, resulting on a global mean RSD of 0.48% for seven datasets using the two instruments. Six datasets have been compared using one TIMS-TOF Flex over six months, resulting on a RSD of 0.49% and 0.36%, in positive and negative mode respectively.

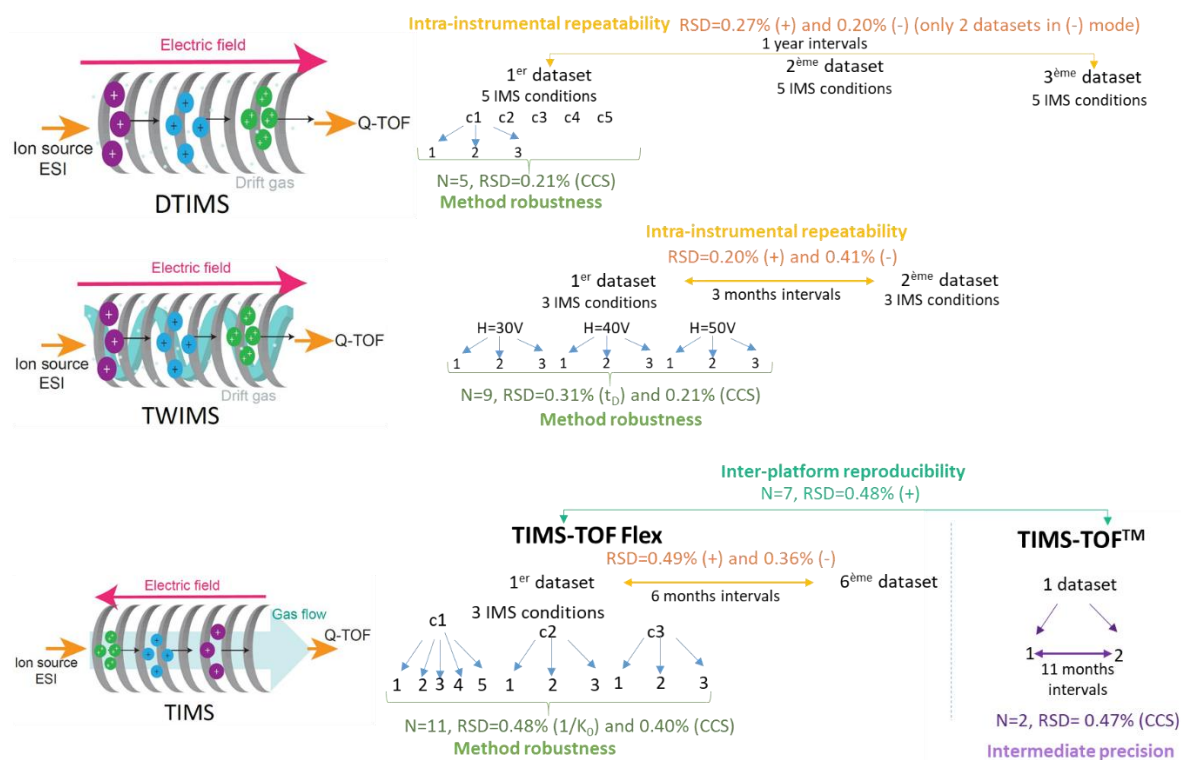


Figure V-4: Resume of the experiments made on the three instruments showing the repeatability and reproducibility of the CCS measurement using Tune Mix as calibrant

We showed that slight deviations of CCS (mean RSD of 0.5%) can be due to the algorithms or scripts of the different software tools utilized to determine the CCS. Estimation of these sources of deviations is essential as numerous commercial software tools are currently available. Utilizing a unique software for all IMS technologies, such as MS-DIAL or MZMine 3, could be a solution to this problem (Tsugawa et al. 2020a; Schmid et al. 2023; Crowell et al. 2013).

Overall, it has been shown that the CCS values of the studied lipids can be efficiently compared between the three instruments, with an average RSD lower than 2%, using almost all the calibrant tested, meaning that whatever the calibrant used, comparable CCS values have been obtained using different instruments.

Using the Tune Mix, a good agreement was found between the CCS values determined with DTIMS, TWIMS and TIMS, with a mean RSD within 1% in both positive and negative ion modes, for the 75 human plasma lipids. This is a good starting point to extend the use of the CCS in metabolomics and lower the tolerance used to compare experimental CCS with databases.

The stepped-field CCS values were compared with single-field CCS values, leading to slightly larger deviations than the deviations observed with the comparison of the three different instruments, meaning that progress must be performed to allow the comparison of all the CCS values, whatever the experimental determination method used.

Conclusions and perspectives

In order to integrate CCS as a molecular descriptor into metabolomics workflows and increase the reliability of metabolite annotation, the aim of this research project was to investigate and develop standardization of CCS measurements. For that purpose, the different potential causes of discrepancies on CCS measurements for three different IMS commercial mass spectrometry coupled technologies, DTIMS, TIMS, and TWIMS, have been explored.

First, the experimental parameters related to sample introduction and electrospray ionization source, have been studied to evaluate their influence on the ion mobility and also on CCS determination.

In the case of TIMS-TOF instrument, we showed that sample introduction modalities and source parameters (flow-rate and temperature of the desolvation gas as well as nebulizer gas pressure) had an impact, up to 2%, on ion mobilities and subsequently on the CCS values. The placement of the TIMS cell immediately following the ESI source could explain this issue associated to an insufficient desolvation process. These results demonstrated the necessity to adjust the source parameters to achieve efficient desolvation. Internal ion mobility calibration permitted to retrieve comparable CCS values and offered a solution to ensure the CCS reliability, whatever the source conditions. As a result, the ^{TIMS}CCS values of lipids from human plasma studied by LC-TIMS-MS could be determined precisely.

A minor impact of the source parameters on the ^{DT}CCS values determination has also been observed and estimated to less than 1%. Due to the design of the Q-TWIMS-qTOF instrument (Waters Synapt G2), where the TWIMS cell is positioned after the quadrupole preventing insufficient desolvation process, changes in ESI source parameters had no effect on CCS determination, as previously observed in the laboratory.

Then, the ion mobility parameters of each IMS technology have been studied to evaluate their influence on the CCS determination. In the three cases, high repeatability of CCS measurements has been demonstrated, with RSD < 0.5%, changing ion mobility parameters (1/K₀ range and ramp time for TIMS instrument, drift-tube entrance and exit voltages, trap fill and release times as well as multiplexing parameters for DTIMS instrument, wave height and wave velocity for TWIMS instrument).

To prevent inaccurate CCS determination, same source conditions must be used for both calibrant and sample analyses, regardless of the IMS device. A perspective could be the resort to internal mobility calibration for all ion mobility instruments allowing to limit or overcome the issues of potential deviations.

In a second part, the calibration procedure has been examined, in particular for the TWIMS instrument through the study of eleven distinct commercial calibrants. For that, lipids from human plasma samples have been used as model analytes. The CCS measurements could vary significantly, up to 25%, depending on the calibrant used. The ^{TW}CCS values determined with each of the eleven calibrants have been compared to lipid CCS reported in the literature or in public databases. The smallest deviations between our ^{TW}CCS and those from the literature were obtained with two calibrants, Tune Mix and

lipid standards, with around 1% and 2% difference in positive and negative ionisation modes, respectively. However, higher differences were observed for other calibrants. This showed that CCS measurement has to be standardized and CCS databases must be harmonized for successful comparison with experimental CCS values. That may imply the choice of a reference or primary standard as mentioned by Gabelica et al. (Gabelica et al. 2019). Tune Mix appears to be a good candidate as it is largely used in the literature and it is commonly used for the measurement of drift tubes length (Stow et al. 2017). Moreover, it has the advantages to offer a wide range of CCS and narrow IM peaks. Tune mix has been successfully used in many fields of research and for many types of samples.

Therefore, we proposed to use the Tune Mix as a reference calibrant to re-calibrate the CCS of the ten other calibrants. These newly adjusted scales reduced calibrant-induced deviations and enabled the determination of plasma lipid ^{TW}CCS with very weak discrepancies between experimental CCS values, regardless of the calibrants. For the investigated lipids, less than 0.2% deviation was consistently attained across calibrants. We have also shown that this method could be applied to any previously published study, if the drift times of both samples and calibrant ions are reported, as we validated our procedure with a previously published lipid CCS dataset. We think that this approach can yield standardized CCS values that can improve their use as physicochemical descriptor for lipid annotation.

Then, interplatform evaluation was performed comparing the three available ion mobility technologies using the same calibrant and sample, a lipid extract from human plasma. The intra-instrument repeatability appeared to be very good with an average RSD of less than 0.5% for each of the three IMS technologies.

We have also noted that slight but significant deviations can be due to the algorithms or scripts used to determine the CCS values. Therefore, it is important to assess these discrepancies produced by individual data processing software tools as there are currently many commercial software options, which are different for each instrument. Utilizing a unique software for all ion mobility technologies, such as MS-DIAL or MZMine 3 or another, could be a solution to this problem (Tsugawa et al. 2020a; Schmid et al. 2023; Crowell et al. 2013).

A key point highlighted in this interplatform study is the importance of the calibration step, in particular the use of common calibrant. The previously mentioned eleven calibrants were investigated with each of the three IMS technologies. It was shown that small CCS deviations could be obtained when the same calibrant was used with all three IMS technologies (mean deviation below 2% in positive ion mode considering almost all the studied calibrants except two of them which are outside the lipid CCS and m/z ranges and less than 1% in negative ion mode). Thus, the CCS values determined with different IMS technologies are highly comparable, if the same calibrant is used. These results are in agreement with those published by Feuerstein et al. during this thesis, which showed, *via* an interplatform study, the comparability of steroid collision cross sections using DTIMS, TWIMS and TIMS technologies (Feuerstein et al. 2022).

Comparing the ^{TW}CCS, ^{TIMS}CCS and ^{DT}CCS, using the Tune Mix as calibrant, a good agreement was observed with a mean RSD within 1%, in both positive and negative ion modes, considering all ionic species. Then, more than 90 % of lipid CCS showed deviations within 1% whatever the ionization mode. This study demonstrates that the constitution of interoperable CCS databases is clearly achievable

when standardized procedures and experimental conditions are implemented throughout the entire workflow, from acquisition to data processing.

Thus, this research project has demonstrated the importance of using standardized conditions to determine experimental CCS and showed that the choice of calibrant could have a significant impact on the CCS values determination. As mentioned by Gabelica et al., the ion mobility community has to urgently agree on a unique primary standard or a reference to use the full potential of ion mobility in metabolomics and lipidomics areas (Gabelica et al. 2019). Moreover, using stepped-field CCS values as reference could be an issue, because the resolving power of DTIMS technology is almost low, while new ion mobility technologies, such as TIMS, cIM and SLIM, exhibit higher ion mobility resolutions. Indeed, in most cases, current DTIMS instruments did not permit the separation of isomers leading to a unique CCS value while high-resolution techniques allow such separation, resulting in distinct CCS values. However, for now, the reference CCS arise from stepped field method using DTIMS instrument. The use of a unique reference, in a similar principle than the use of ^{12}C isotope as the mass reference to calculate all the masses of compounds and consequently the m/z values of the ions, can be a solution to many issues in ion mobility to determine experimental CCS values but also predicted CCS. We have also shown that a re-calibration strategy is possible. Thus, if a primary standard or a reference calibrant is chosen by the ion mobility community, this strategy can be applied to re-calibrate CCS values from previous or current studies (that report CCS with other standard than the reference) and re-align the CCS values of databases already available. Using a common reference calibrant and common CCS values for this reference material in every study, resulting experimental CCS can be a powerful descriptor to add in metabolomics and lipidomics studies.

Other perspectives to this work can be to extend this work to metabolites and perform large-scale metabolomics studies, but also to other compounds classes, as glycans or peptides. In the case of proteins, which give multiple charged ions in ESI, additional studies have to be performed to determine an appropriate reference compound for this compound class, as Tune Mix can only provide singly charged ions in both positive and negative ion modes. Another perspective can be the coupling of ultra-high resolution ion mobility instrument with ultra-high resolution mass spectrometer as the TIMS-FTICR MS, the evaluation of the performance of this instrument and its capability to determine CCS of very close structural compounds (isomers). Evaluation of its ability to perform DI-TIMS-FTICR experiments, i.e. without prior chromatographic separation, and comparison with LC-IMS-TOF MS approaches can also be envisaged.

Résumé en Français (Summary in French)

Introduction

Depuis 20 ans, la métabolomique ouvre la voie à une meilleure compréhension de la biologie, de la santé humaine et de notre environnement en étudiant les métabolites, des molécules qui reflètent les différentes voies métaboliques. Les lipides et les métabolites sont vitaux et extrêmement diversifiés, tant sur le plan structurel que fonctionnel. Le métabolome humain a été étudié à l'aide de diverses techniques, notamment la résonance magnétique nucléaire (RMN) et la spectrométrie de masse (MS). Chaque étude métabolomique fait progresser notre connaissance des processus biochimiques et du fonctionnement des systèmes vivants, même si nous ne comprenons pas encore parfaitement toutes les voies métaboliques et tous les métabolites impliqués dans le métabolome (Ryan et Robards 2006). Il a été rapporté que l'identification de plus de 1 % du métabolome humain connu reste un défi, même dans le cadre d'études métabolomiques de grande envergure (Wishart et al. 2022). Bien que le nombre exact de métabolites ne soit pas encore connu, on pense qu'il est extrêmement important, et comprend de nombreux métabolites ayant le même poids moléculaire (Courant et al. 2014).

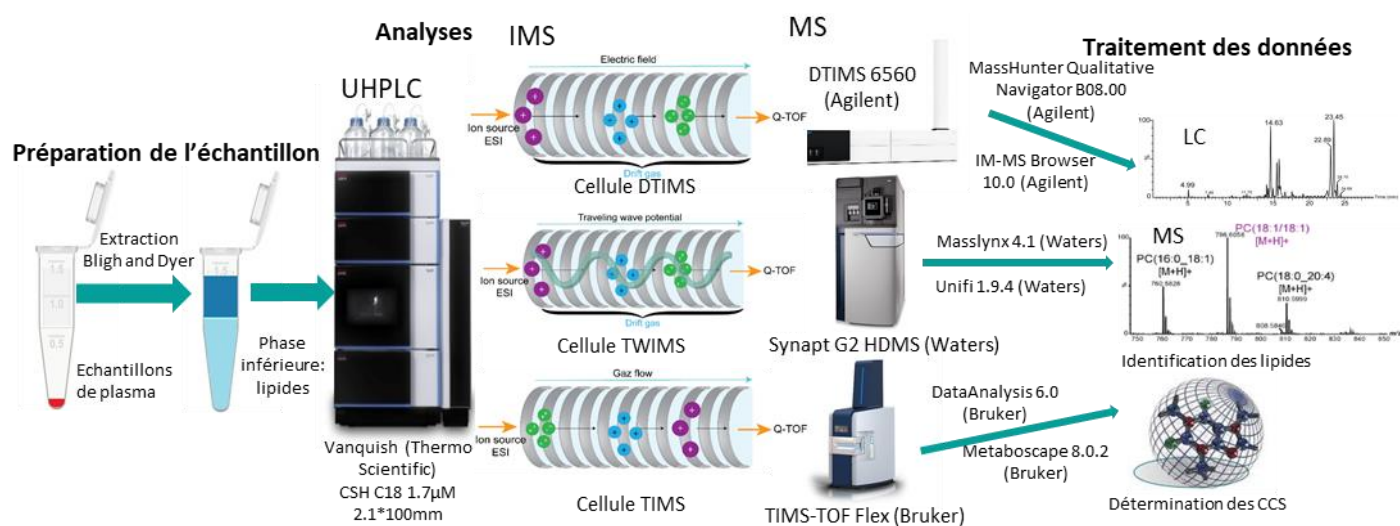
Les approches métabolomiques utilisant la spectrométrie de masse (MS) à haute résolution sont largement utilisées pour la caractérisation des échantillons biologiques, souvent en couplage avec des techniques de chromatographie, comme la chromatographie liquide (LC). Ainsi, différents descripteurs, tels que le temps de rétention (RT), la mesure de masse précise (m/z) et les spectres MS/MS sont fournis par la LC-MS/MS pour effectuer l'annotation des métabolites en fonction d'un niveau de confiance bien décrit. Cependant, l'identification des composés reste un challenge, notamment dû à la présence de nombreux isobares ou isomères. Ainsi, le couplage de la spectrométrie de mobilité ionique (IMS) à la spectrométrie de masse apporte une dimension de séparation supplémentaire ainsi qu'un nouveau descripteur physico-chimique, la section efficace de collision (CCS) qui reflète la structure tridimensionnelle d'un ion en phase gazeuse. La CCS peut être ajoutée aux autres descripteurs utilisés en métabolomique pour une identification plus sûre des composés. Actuellement, plusieurs technologies de spectrométrie de mobilité ionique pouvant être couplées à la spectrométrie de masse permettent la détermination expérimentale de la CCS. Les plus utilisées sont la spectrométrie de mobilité ionique à tube de dérive (DTIMS), qui est considérée comme la méthode primaire (Ibrahim et al., 2015), la spectrométrie de mobilité ionique à ondes progressives (TWIMS) (Giles, 2013 ; Giles et al., 2004 ; Richardson et al., 2018) et la spectrométrie de mobilité ionique piégée (TIMS) (Fernandez-Lima et al., 2011 ; Michelmann et al., 2015), qui sont des méthodes secondaires nécessitant un étalonnage. La CCS est un descripteur prometteur pour l'annotation des métabolites et des lipides dans les analyses non ciblées, en particulier par la recherche dans les bases de données de CCS. (Paglia & Astarita, 2017 ; Paglia et al., 2015). Toutefois, la littérature fait état de valeurs de CCS très disparates (jusqu'à 10 % d'écart) selon l'instrument ou l'étalon utilisé. Ces écarts de CCS sont principalement liés aux procédures d'étalonnage, aux étalons disponibles et à l'absence de consensus sur les valeurs de CCS de référence. Certaines études ont souligné la nécessité d'une normalisation des mesures et des bases de données de référence.

L'objectif de ce projet de recherche est d'étudier et de développer la standardisation des mesures de CCS afin de permettre l'alignement des CCS pour intégrer ce descripteur dans les analyses

métabolomiques et améliorer la fiabilité de l'annotation des métabolites. Pour ce faire, différentes causes possibles de déviations des mesures de CCS ont été évaluées pour trois technologies commerciales différentes couplées à la spectrométrie de masse, DTIMS, TIMS et TWIMS. Tout d'abord, les paramètres expérimentaux liés à l'introduction de l'échantillon et à la source d'ionisation par *electrospray* (ESI), en particulier pour les instruments TIMS-MS ont été étudiés afin d'évaluer leur influence sur la mobilité des ions et sur la détermination des CCS. Ensuite, les paramètres de l'IMS ont été étudiés pour les trois technologies IMS afin de déterminer leur contribution aux écarts de CCS. La procédure d'étalonnage a également été examinée, en particulier à travers l'étude de onze étalons différents. Ensuite, une évaluation inter-plateforme a été réalisée en comparant les trois différentes technologies de mobilité ionique lorsqu'une procédure standardisée impliquant un étalonnage unique a été mise en œuvre.

Matériel et méthodes

Les lipides ont été extraits du plasma humain à l'aide de la méthode Bligh et Dyer et ont été analysés par UHPLC-ESI-IMS-Q-TOF en utilisant un workflow de lipidomique standard impliquant une chromatographie liquide en phase inverse (colonne C18) pour la séparation. Trois instruments différents ont été comparés : Synapt G2 (Waters) équipé de la cellule TWIMS, DTIMS 6560 (Agilent) et TIMS-TOF Flex (Bruker). Différents paramètres de mobilité ionique ont également été évalués : la vitesse et la hauteur d'onde dans la cellule TWIMS, la tension appliquée et la capacité de multiplexing dans la cellule DTIMS et les paramètres de rampe dans la cellule TIMS. Les valeurs de CCS ont été déterminées par les logiciels Unifi (Waters), IM-MS Browser (Agilent) et Metaboscape (Bruker).



Workflow utilisé pour obtenir les CCS des lipides de plasma sur les trois instruments IMS: de la préparation de l'échantillon à l'analyse, puis le traitement des données (George et al. 2022)

Résultats

Les résultats sont présentés dans le manuscrit sous forme de trois chapitres. Le chapitre 3 présente l'étude de l'influence des paramètres expérimentaux, tels que les paramètres de la source *electrospray* et de la cellule IMS, sur la détermination des CCS, en utilisant chacune des trois technologies de

mobilité ionique. Le chapitre 4 est consacré à l'étude de l'étape d'étalonnage de la mobilité ionique à l'aide de l'instrument TWIMS. Pour cela, les lipides du plasma humain ont été utilisés comme modèle d'analyse. Une stratégie de réaligement des CCS permettant de réduire les déviations des CCS dues à l'étalonnage a été proposée. Le chapitre 5 permet la comparaison inter-plateforme des valeurs de CCS déterminées à l'aide de trois cellules de mobilité ionique différentes : DTIMS, TWIMS et TIMS.

Influence des paramètres expérimentaux sur la détermination des CCS

De nombreux paramètres peuvent influencer la mobilité des ions et donc la détermination des valeurs de CCS. Ces paramètres sont liés aux instruments IMS, aux étalons mais aussi à d'autres paramètres tels que le débit de la chromatographie, la composition du solvant, et les paramètres de la source, et aussi les paramètres influençant la séparation en mobilité ionique.

Premièrement, l'influence des paramètres d'introduction de l'échantillon et ceux impliqués dans le phénomène de désorption/ionisation de la source *electrospray* a été étudié sur des standards de lipides sur les trois instruments, avec tout d'abord un focus sur l'instrument TIMS où la cellule IMS est directement derrière la source. La stabilité des expériences de mobilité ionique a été étudiée pendant dix heures, ce qui a permis de déterminer un temps de stabilisation de vingt minutes pour que les paramètres de la source (principalement la pression et la température) se stabilisent. Les mélanges de solvant et les débits ont été étudiés ainsi que trois paramètres de la source *electrospray* : la pression de nébulisation, la température et le débit du drying gas. Les modifications de ces paramètres ont induit des déplacements et des élargissements des pics de mobilité ionique. L'apparition d'un pic supplémentaire dans les spectres de mobilité ionique a même été remarqué quand de mauvaises conditions de désolvatation sont utilisées. Cela pourrait s'expliquer par la formation de clusters ion-solvant ou par d'autres effets tels que des changements dans la pression de la cellule IMS. Comme la CCS est déterminée à partir de la mobilité des ions, les écarts de mobilité ont un impact sur les valeurs de CCS. Cependant, grâce à un étalonnage interne avec l'étalon Tune Mix (ESI Low concentration Tuning Mix, Agilent), les écarts ont pu être réduits de 0,79% à 0,10%. L'optimisation des paramètres de la source est donc essentielle pour obtenir une bonne désolvatation des ions de lipides et éviter une mauvaise interprétation des doubles pics dans les spectres de mobilité ionique. Ce travail a mis en évidence l'importance de l'étalonnage interne sur le TIMS pour garantir des valeurs de CCS interopérables, utilisables dans l'annotation métabolomique.

Trois conditions source différentes ont aussi été étudiées sur le DTIMS, utilisant les paramètres recommandés puis en mimant une faible désolvatation ou une très grande désolvatation (en diminuant ou augmentant les valeurs de certains paramètres). Un écart sur les temps de dérive des standards de lipides étudiés a été remarqué, induite par les trois conditions. Ainsi, comme les conditions de la source ont une influence sur les temps de dérive des ions, l'étalon et les échantillons doivent être analysés en utilisant des paramètres instrumentaux et opérationnels strictement identiques pour déterminer les valeurs de CCS.

Pour l'instrument TWIMS, la cellule IMS est séparée de la source par un quadripôle, ce qui permet de s'affranchir des problèmes de mauvaise désolvatation car les molécules de solvant ont le temps nécessaire pour s'évaporer avant que les ions n'arrivent dans la cellule IMS.

Deuxièmement, les paramètres influençant la séparation en mobilité ionique ont été étudiés sur les trois techniques de mobilité ionique. Dans le cas du TIMS, les valeurs de CCS obtenues étaient très

similaires (RSD < 0,25 %), ce qui montre une grande robustesse, même en cas de modification des paramètres de rampe dans la cellule IMS et même en utilisant le mode PASEF. Pour le DTIMS, les RSD étaient inférieurs à 0,5 % même en utilisant la stratégie de multiplexage. Dans l'instrument TWIMS, il a été démontré que la hauteur et la vitesse des vagues doivent être correctement ajustées pour éviter certains problèmes de séparation. En tenant compte de ce point particulier, le RSD en comparant trois conditions IMS avec des hauteurs et vitesses de vagues différentes était d'environ 0,2 %.

Etude lipidomique d'échantillon de plasma par TWIMS-MS : mise en place d'une procédure de réétalonnage pour obtenir des CCS interopérables

La deuxième étude est basée sur l'étude de l'étalonnage en CCS de l'instrument Q-TWIMS-qTOF (Synapt G2 Waters) équipé de la cellule TWIMS appliqué à un échantillon de plasma humain.

La première étape de notre étude a consisté à examiner les onze étalons publiés et actuellement majoritairement utilisés pour des expériences d'IMS et à construire les courbes d'étalonnage correspondantes. Pour chaque étalon, différents paramètres de mobilité ionique dans les deux modes d'ionisation ont été testés afin d'évaluer la répétabilité des mesures de CCS. À l'exception du PEG, tous les étalons présentent des courbes d'étalonnage montrant la même tendance. Un examen attentif des données montre que les courbes d'étalonnage établies à partir du Tune Mix et des lipides sont presque superposées. Il est à noter que les courbes d'étalonnage construites à partir de TAA, de polyglycine et de standards de médicaments ne couvrent pas toute la gamme de CCS des lipides, ce qui les rend inappropriées dans le présent contexte. Cette recherche préliminaire permet d'étudier les premiers avantages et inconvénients des étalons étudiés.

La deuxième étape de ce travail a permis d'évaluer ces différents étalons pour les mesures de CCS, en utilisant les lipides du plasma humain comme analytes modèles. Les lipides plasmatiques ont été identifiés avec les temps de rétention chromatographique, les masses précises et les spectres de fragmentation MS/MS avec l'aide des bases de données publiques. Les CCS de tous ces lipides identifiés avec certitude ont ensuite été déterminées en utilisant chaque étalon, en utilisant le logiciel UNIFI (Waters) et les valeurs obtenues ont été comparées entre elles. Pour chaque lipide, les valeurs de CCS sont du même ordre de grandeur pour tous les étalons, sauf pour un étalon, le PEG. Les disparités entre les valeurs de CCS (les disparités sont calculées en soustrayant les valeurs extrêmes de CCS avant de les diviser par les valeurs moyennes) atteignent 8 % lorsque le PEG est exclu et plus de 27 % lorsque le PEG est inclus, en mode positif. En mode négatif, les disparités atteignent 3,5%. Ces disparités sont bien plus élevées que la limite de 1% recommandée dans diverses publications pour la détermination des CCS. Ainsi, nous avons pu constater que le Tune Mix et les standards de lipides ont conduit à des valeurs de CCS très proches pour tous les lipides étudiés, tandis que les autres étalons (à l'exception du PEG) ont donné des valeurs de CCS plus élevées. Ces résultats ont mis en évidence et confirmé les inconvénients et l'impact de l'utilisation de différents étalons sur la précision des mesures de CCS.

Ensuite, les valeurs de CCS déterminées avec chaque étalon étudié ont été comparées aux CCS des lipides rapportées dans la littérature ou dans les bases de données publiques. Il arrive que différentes valeurs de CCS soient publiées dans la littérature pour les mêmes lipides, en fonction des instruments IMS, des méthodologies et des étalons choisis par les auteurs. En outre, seule une partie des valeurs de CCS a été publiée en utilisant le DTIMS en mode « stepped-field », c'est-à-dire sans étalonnage, mode reconnu dans la littérature comme nécessaire pour l'obtention de CCS de référence. Par conséquent, nous avons décidé de sélectionner pour notre comparaison les CCS publiées comme suit: tout d'abord, la CCS obtenue avec le DTIMS en mode « stepped-field », ensuite la CCS déterminée avec

le DTIMS en mode « single-field » avec une étape d'étalonnage supplémentaire et enfin avec le TIMS ou le TWIMS, qui nécessite un étalonnage. Ainsi, en mode positif, les écarts les plus importants ont été observés avec le PEG comme étalon, environ 20 %. Ce polymère a précédemment été utilisé pour étalonner les ions de saponine mais jamais dans l'analyse lipidomique, ce qui confirme son inadéquation pour les lipides.

Le TAA, la polyglycine et les standards de médicaments ont également conduit à des écarts importants, jusqu'à 8 %, car leur gamme de CCS ne correspond pas à celle des lipides plasmatiques. Par conséquent, cela induit logiquement un biais dans la détermination des CCS. Bien que le PEO, le dextran, la polyalanine, le Major Mix (Waters) et l'acide polymalique couvrent toute la gamme de CCS des lipides plasmatiques, les déviations relatives moyennes étaient encore supérieures à 3%, pour ces cinq étalons dans les deux modes d'ionisation. Dans le cas du kit d'étalonnage Major Mix, certains laboratoires n'utilisent pas les mêmes ions présents dans ce kit pour construire leurs courbes d'étalonnage, ce qui peut conduire à une déviation supplémentaire pour la détermination des CCS.

Les plus petits écarts observés entre nos CCS et ceux de la littérature ont été obtenus avec seulement deux étalons, le Tune Mix et les standards de lipides, avec environ 1% et 2% de différences dans les modes d'ionisation positif et négatif, respectivement. D'une part, des publications mentionnent que les CCS des lipides présents dans les échantillons de plasma semblent correctement étalonnées par des étalons lipides parce qu'ils appartiennent à la même classe chimique. Cependant, les lipides peuvent être de classes très différentes avec des structures constituées d'acides gras qui peuvent présenter différents types et longueurs de chaînes acyles saturées ou insaturées. Une telle diversité de structures induit des diversités de formes donnant des espèces lipidiques ionisées variées qui peuvent se comporter différemment dans la cellule de mobilité ionique. Par exemple, Hines et al. ont expliqué que les phosphatidylcholines (PC) peuvent être utilisés pour étalonner les espèces phosphatidyléthalamines (PE), en mode positif (Hines et al. 2016). Néanmoins, il semble difficile de distinguer toutes les classes de lipides, les espèces individuelles et les isomères afin de trouver le standard optimal pour étalonner les espèces lipidiques dans les analyses lipidomiques à grande échelle.

D'autre part, le Tune Mix, largement utilisé dans la littérature et couramment utilisé pour l'étalonnage de la longueur des tubes de dérive, présente une large gamme de CCS et des pics fins en mobilité ionique en raison de conformation moléculaire unique pour chaque phosphazine. De nombreux laboratoires utilisent déjà ce mélange pour l'étalonnage en masse ou en mobilité ionique. En raison de sa gamme étendue de m/z de 118-2722 et 113-2834, et de sa gamme de CCS, de 122-438 Å² et 109-432 Å² respectivement pour les modes d'ionisation positif et négatif, il peut être étendu à de nombreux domaines de recherche et d'échantillons. Une étude interlaboratoire impliquant quatre laboratoires différents a été réalisée à l'aide du DTIMS pour la détermination et la comparaison des CCS obtenues sans et avec étalonnage avec le Tune Mix : les valeurs de CCS étaient très proches avec un RSD < 0,29% en mode « stepped-field » (Sarah M. Stow et al. 2017). Depuis cette publication, la communauté semble avoir atteint un consensus sur les valeurs de CCS pour les ions du Tune Mix. Ces écarts particulièrement faibles entre nos valeurs de CCS étalonnées avec le Tune Mix et celles de la littérature peuvent s'expliquer par le fait que ces dernières ont été déterminées avec un DTIMS après étalonnage avec le Tune Mix.

Nous proposons d'utiliser le Tune Mix comme étalon de référence. Il présente une bonne répétabilité dans diverses conditions de mobilité ionique, avec un RSD sur les 9 analyses inférieur à 0,3% dans les deux modes d'ionisation. De plus, les déviations entre nos CCS expérimentales et les valeurs de CCS de la littérature sont proches de 1% et 2% dans les modes d'ionisation positif et négatif, respectivement. Afin de corriger les déviations significatives observées avec les autres étalons, les valeurs de CCS de

tous les étalons utilisés ont été réalignés sur celles du Tune Mix. Pour cela, tous les étalons ont été ré-étalonnés par le Tune Mix par la même procédure d'étalonnage que celle utilisée pour étalonner les lipides du plasma. Les courbes d'étalonnage obtenues après correction montrent un ajustement parfait entre toutes les courbes des étalons ré-étalonnés et celle du Tune Mix. Les valeurs de CCS des étalons corrigées constituent une base de données de CCS corrigées qui peut être utilisée pour déterminer les valeurs CCS de n'importe quel échantillon. La correction effectuée avec le Tune Mix permet d'obtenir des valeurs de CCS cohérentes pour chaque lipide quel que soit l'étalon utilisé, dans les deux modes d'ionisation. La disparité entre les valeurs de CCS corrigées obtenues avec les différents étalons est de 0,2% en mode positif et de 0,1% en mode négatif contre 27.0% et 3,6% avant correction.

Cette méthode de correction permet d'avoir une courbe d'étalonnage universelle et de pouvoir comparer les valeurs de CCS obtenues avec différents étalonnages, si les valeurs de CCS corrigées sont utilisées. Les CCS corrigées proposées pour les étalons peuvent être exploitées pour construire une base de données de CCS universelle pour l'analyse lipidomique ou pour d'autres domaines.

Afin de valider notre méthodologie et de démontrer davantage l'utilisation universelle de la base de données résultante, nous utilisons nos CCS d'étalons corrigées pour ré-étalonner un ensemble de données publié précédemment, concernant les lipides de *Pseudomonas aeruginosa*. L'écart relatif moyen avec les valeurs de CCS de la littérature était inférieur à 1 % pour six lipides de *Pseudomonas aeruginosa*, en utilisant les étalons polyalanine et dextran réalignés. De plus, l'écart relatif moyen observé entre les CCS corrigées de Deschamps et al. et nos CCS corrigées était inférieur à 0,5 %, pour les mêmes six lipides, de sorte que des bases de données de CCS interoperables ont pu être obtenues avec succès en utilisant la correction des étalons.

Cette étude montre l'importance de l'étalonnage pour utiliser la CCS comme descripteur pour l'identification des métabolites.

Etude inter-plateformes de trois techniques de mobilité ionique pour la détermination des CCS de lipides plasmatiques

Dans la partie précédente, l'importance de l'étalonnage a été soulignée pour l'instrument TWIMS. Dans cette partie, l'objectif était de comparer les valeurs de CCS mesurées par trois instruments IM différents : DTIMS, TWIMS et TIMS. Différentes sources potentielles d'écarts de CCS ont été étudiées. Tout d'abord, la répétabilité des valeurs de CCS pour chacune des trois techniques IMS, en utilisant quatre instruments, dont deux cellules TIMS, a été étudiée. Une attention particulière a été accordée à la compréhension de la manière dont les valeurs de CCS ont été déterminées dans les trois instruments à l'aide d'outils logiciels commerciaux.

L'influence significative des logiciels de traitement des données sur la détermination des CCS a été soulevée. Dans le cas de l'instrument commercial TWIMS, trois logiciels différents ont été étudiés et comparés : i) Masslynx en combinaison avec Driftscope, ii) Progenesis Q1 et iii) Unifi. De manière assez inattendue, les valeurs de CCS déterminées à l'aide de ces trois logiciels différaient dans une certaine mesure, avec un écart maximal de 0,9 % (0,5 % en moyenne), conséquence directe de la variabilité des algorithmes de sélection des pics et de calcul des CCS. De la même manière, les logiciels Bruker (Data Analysis et Metaboscape) ont été comparés pour la détermination des valeurs ^{TIMS}CCS et ont également montré des déviations de 0,5% en moyenne.

La répétabilité intra-instrument a été évaluée pour les trois techniques IMS en répétant les mesures de CCS à différents intervalles de temps. Les résultats montrent une très bonne répétabilité des mesures de CCS sur les trois techniques, avec des RSD largement inférieurs à 1%.

Les valeurs de CCS ont été déterminées avec les trois technologies à l'aide de différents calibrants, qui ont été évalués précédemment à l'aide de la cellule TWIMS. Les RSD moyens étaient inférieurs à 2 % pour presque tous les étalons, à l'exception des médicaments et de la polyglycine, car ils ne couvrent pas l'ensemble des gammes de masse et de CCS des espèces lipidiques. Cependant, des valeurs de CCS reproductibles peuvent être obtenues avec les autres étalons, si le même étalon est utilisé avec les différents instruments. Cela confirme à nouveau l'importance de l'étape d'étalonnage en CCS pour garantir des valeurs CCS reproductibles entre les instruments.

La corrélation entre les valeurs de CCS obtenues par les trois techniques, étalonnées avec le Tune Mix, a ensuite été évaluée. En représentant les CCS d'un instrument en fonction des CCS d'un deuxième, de bonnes corrélations sont retrouvées avec des coefficients de détermination R^2 supérieurs à 0,995 en mode d'ionisation positif et négatif. Quelques valeurs aberrantes ont été observées, et correspondaient à des ions peu abondants présentant une intensité et une définition de pic IMS médiocres. En effet, un faible rapport signal/bruit peut conduire à une sélection erronée des pics et donc à des variations des valeurs de CCS. Pour avoir une vue d'ensemble des données collectées, les différences entre toutes les valeurs de CCS obtenues à partir des trois techniques ont été comparées par paire. Pour chacun des trois cas, les différences moyennes observées entre les valeurs de CCS de deux instruments sont inférieures à 1 % dans les modes positif et négatif. Plus de 90% des valeurs de CCS des lipides plasmatiques présentent des écarts relatifs moyens entre les trois instruments inférieurs à 1%, tant pour le mode d'ionisation négatif que positif, tandis que tous les RSD sont inférieurs à 2%. Cela indique que la comparaison des CCS entre les laboratoires et les plates-formes IMS est possible avec une faible tolérance.

Ce travail montre que des conditions analytiques harmonisées peuvent donner une excellente reproductibilité inter-plateforme en termes de mesures de CCS.

Conclusion et perspectives

Afin d'intégrer la CCS en tant que descripteur moléculaire dans les workflows de métabolomique et d'augmenter la fiabilité de l'annotation des métabolites, l'objectif de ce projet de recherche était d'étudier et de développer la normalisation des mesures de CCS. Pour cela, les différentes causes potentielles de divergences dans les mesures de CCS pour trois technologies commerciales couplées de spectrométrie de masse et de spectrométrie de mobilité ionique différentes, DTIMS, TIMS et TWIMS, ont été explorées.

Tout d'abord, les paramètres expérimentaux liés à l'introduction de l'échantillon et à la source d'ionisation *electrospray* ont été étudiés afin d'évaluer leur influence sur la mobilité des ions et sur la détermination des CCS.

Dans le cas de l'instrument TIMS-TOF, nous avons montré que les modalités d'introduction des échantillons et les paramètres de la source (débit et température du gaz de désolvatation ainsi que

pression du gaz de nébulisation) avaient un impact, jusqu'à 2 %, sur les mobilités ioniques et, par la suite, sur les valeurs de CCS. Le placement de la cellule TIMS immédiatement après la source ESI pourrait expliquer ce problème lié à un processus de désolvatation insuffisant. Ces résultats ont démontré la nécessité d'ajuster les paramètres de la source pour obtenir une désolvatation efficace. L'étalonnage interne de la mobilité ionique a permis de récupérer des valeurs de CCS comparables et a offert une solution pour garantir la fiabilité des CCS, quelles que soient les conditions de la source. En conséquence, les valeurs ^{TIMS}CCS des lipides du plasma humain étudiés par LC-TIMS-MS ont pu être déterminées avec précision.

Un impact mineur des paramètres de la source sur la détermination des valeurs ^{DT}CCS, a également été observé. Cette influence n'a pas été remarquée sur l'instrument Q-TWIMS-qTOF (Waters Synapt G2) certainement en raison de la conception de l'instrument où la cellule TWIMS est positionnée après le quadripôle.

Ensuite, les paramètres de mobilité ionique de chaque technologie IMS ont été étudiés pour évaluer leur influence sur la détermination des CCS. Dans les trois cas, une répétabilité élevée des mesures de CCS a été démontrée, avec un RSD < 0,5 %, en modifiant les paramètres de mobilité ionique (plage de $1/K_0$ et temps de rampe pour l'instrument TIMS, tensions d'entrée et de sortie du tube à dérive, temps de remplissage et de libération du piège ainsi que les paramètres de multiplexing pour l'instrument DTIMS, et les hauteurs et vitesses de vague pour l'instrument TWIMS).

Pour éviter une détermination inexacte des CCS, les mêmes conditions de source doivent être utilisées pour les analyses de l'étalon et de l'échantillon, quel que soit la technologie de mobilité ionique. Une perspective pourrait être le recours systématique à l'étalonnage interne de la mobilité pour tous les instruments de mobilité ionique, comme ce qui a été utilisé sur le TIMS-TOF ce qui permettrait de limiter ou de surmonter les problèmes de déviations potentielles.

Dans une deuxième partie, la procédure d'étalonnage a été examinée, en particulier pour l'instrument TWIMS, à travers l'étude de onze étalons commerciaux distincts. Pour cela, des lipides provenant d'échantillons de plasma humain ont été utilisés comme analytes modèles. Les mesures de CCS peuvent varier de manière significative, jusqu'à 25 %, en fonction de l'étalon utilisé. Les valeurs de ^{TW}CCS que nous avons déterminées avec chacun des onze étalons ont été comparées aux CCS des lipides rapportés dans la littérature ou dans les bases de données publiques. Les écarts les plus faibles entre nos ^{TW}CCS et ceux de la littérature ont été obtenus avec deux calibrants, Tune Mix et les standards lipidiques, avec environ 1% et 2% de différence dans les modes d'ionisation positive et négative, respectivement. Cependant, des différences plus importantes ont été observées pour d'autres étalons. Cela montre que la mesure des CCS doit être normalisée et que les bases de données de CCS doivent être harmonisées pour une comparaison réussie avec les valeurs expérimentales des CCS. Cela peut impliquer le recours à une référence ou à un étalon primaire comme mentionné par Gabelica et al. (Gabelica et al. 2019).

Nous avons proposé d'utiliser le Tune Mix comme étalon de référence pour ré-étalonner les CCS des dix autres étalons. Ces échelles nouvellement ajustées ont réduit les écarts induits par les étalons et ont permis la détermination des ^{TW}CCS des lipides plasmatiques avec de très faibles écarts entre les valeurs de CCS expérimentales, quels que soit l'étalon utilisé. Pour les lipides étudiés, une déviation inférieure à 0,2 % a été obtenue en comparant tous les étalons. Nous avons également montré que cette méthode pouvait être utilisée pour toute étude publiée précédemment, si les temps de dérive

des échantillons et des étalons sont indiqués. Nous pensons que cette approche peut produire des valeurs de CCS standardisées qui peuvent améliorer leur utilisation en tant que descripteur physico-chimique pour l'annotation des lipides.

Ensuite, une évaluation interplateforme a été réalisée pour comparer les trois technologies de mobilité ionique disponibles en utilisant le même étalon et le même échantillon, un extrait lipidique de plasma humain. La répétabilité intra-instrument s'est avérée très bonne avec un RSD moyen inférieur à 0,5 % pour chacune des trois technologies IMS.

Nous avons également noté des écarts légers mais significatifs dus aux algorithmes ou aux scripts employés pour déterminer les valeurs de CCS. Par conséquent, il est important d'évaluer ces divergences produites par les outils logiciels de traitement des données, car il existe actuellement de nombreuses options logicielles commerciales, qui sont différentes pour chaque instrument. L'utilisation d'un logiciel unique pour toutes les technologies de mobilité ionique, comme MS-DIAL ou MZMine 3 ou autre, pourrait être une solution à ce problème (Tsugawa et al. 2020a ; Schmid et al. 2023 ; Crowell et al. 2013).

L'importance de l'étape d'étalonnage en CCS, en particulier l'utilisation d'un étalon commun, est un point clé mis en évidence dans cette étude interplateforme. Les onze étalons mentionnés précédemment ont été étudiés avec chacune des trois technologies IMS. Il a été démontré que de faibles écarts de CCS pouvaient être obtenus lorsque le même étalon était utilisé avec les trois technologies IMS (écart moyen inférieur à 2 % en mode d'ionisation positive en considérant presque tous les étalons étudiés, sauf deux d'entre eux qui sont en dehors des plages de CCS et de m/z des lipides, et inférieur à 1 % en mode d'ionisation négative). Ainsi, les valeurs de CCS déterminées avec différentes technologies IMS sont très comparables, si le même étalon est utilisé. Ces résultats sont en accord avec ceux publiés par Feuerstein et al. au cours de cette thèse, qui ont montré, *via* une étude interplateforme, la comparabilité des sections efficaces de collision des stéroïdes en utilisant les technologies DTIMS, TWIMS et TIMS (Feuerstein et al. 2022).

En comparant les ^{TW}CCS, les ^{TIM}CCS et les ^{DT}CCS, en utilisant le Tune Mix comme étalon, un bon accord a été observé avec un RSD moyen inférieur à 1 %, à la fois dans les modes positifs et négatifs, en tenant compte de toutes les espèces ioniques. Plus de 90 % des CCS lipidiques présentaient des écarts inférieurs à 1 %, quel que soit le mode d'ionisation. Cette étude démontre que la constitution de bases de données CCS interopérables est clairement réalisable lorsque des procédures et des conditions expérimentales standardisées sont mises en œuvre tout au long du flux de travail, de l'acquisition au traitement des données.

Ainsi, ce projet de recherche a démontré l'importance d'utiliser des conditions normalisées pour déterminer les CCS expérimentales et a montré que le choix de l'étalon pouvait avoir un impact significatif sur la détermination des valeurs de CCS. Comme le mentionne Gabelica et al, la communauté de mobilité ionique doit convenir de toute urgence d'un standard primaire unique ou une référence afin d'utiliser tout le potentiel de la mobilité ionique dans les domaines de la métabolomique et de la lipidomique. En outre, l'utilisation des valeurs CCS 'stepped-field' comme référence pourrait poser problème, car le pouvoir de résolution de la technologie DTIMS est plus faible que les nouvelles technologies de mobilité ionique, telles que TIMS, CIM et SLIM. En effet, dans la plupart des cas, les instruments DTIMS actuels n'ont pas permis la séparation des isomères conduisant

à une valeur de CCS unique, alors que les techniques à haute résolution permettent une telle séparation, conduisant à des valeurs de CCS distinctes. Cependant, pour l'instant, la CCS de référence provient de la méthode 'stepped-field' utilisant l'instrument DTIMS. L'utilisation d'une référence unique, selon un principe similaire à l'utilisation de l'isotope ^{12}C comme référence de masse pour calculer toutes les masses des composés et, par conséquent, les valeurs m/z des ions, peut constituer une solution à de nombreux problèmes liés à la mobilité des ions pour déterminer les valeurs de CCS expérimentales, mais aussi les valeurs de CCS prédites. Nous avons également montré qu'une stratégie de ré-étalonnage est possible. Ainsi, si un étalon primaire ou de référence est choisi par la communauté de mobilité ionique, cette stratégie peut être appliquée pour ré-étalonner les valeurs de CCS d'études précédemment publiées ou actuelles (qui rapportent les CCS avec un autre étalon que celui de référence) et ré-aligner les valeurs de CCS des bases de données déjà disponibles. En utilisant un étalon de référence commun et des valeurs de CCS communes pour ce matériau de référence dans toutes les études, les CCS expérimentales résultantes peuvent constituer un descripteur puissant à ajouter dans les études de métabolomique et de lipidomique.

D'autres perspectives à ce travail peuvent être d'étendre ce travail aux métabolites et de réaliser des études métabolomiques à grande échelle, mais aussi à d'autres classes de composés, comme les glycanes et les peptides. Dans le cas des protéines, qui donnent des ions chargés multiples en ESI, des études supplémentaires doivent être réalisées pour déterminer un composé de référence approprié pour cette classe de composés, car le Tune Mix ne peut fournir que des ions monochargés. Une autre perspective peut être le couplage d'un instrument de mobilité ionique à ultra-haute résolution avec un spectromètre de masse à ultra-haute résolution comme le spectromètre de masse à résonance cyclotronique ionique (TIMS-FTICR MS). Ce couplage permettra l'évaluation de la performance de cet instrument et sa capacité à déterminer la CCS de composés structuraux très proches (isomères) ainsi que l'évaluation de sa capacité à réaliser des expériences en infusion directe, c'est-à-dire sans séparation chromatographique préalable, et la comparaison avec les approches LC-IMS-TOF MS peuvent également être envisagées.

.

Communications and formations

Publications

- *A re-calibration procedure for interoperable lipid collision cross section values as measured by traveling wave ion mobility spectrometry.* Anaïs C. George, Isabelle Schmitz-Afonso, Vincent Marie, Benoit Colsch, François Fenaille, Carlos Afonso, Corinne Loutelier-Bourhis, *Analytica Chimica Acta*, 2022, 1226, 340236.
- *Impact of source conditions on collision cross sections determination by trapped ion mobility spectrometry.* Anaïs C. George, Isabelle Schmitz, Benoit Colsch, François Fenaille, Carlos Afonso, Corinne Loutelier-Bourhis, submitted to *Journal of the American Society for Mass Spectrometry*.
- *Interplatform comparison of three ion mobility techniques for human plasma lipidomics: from calibration to determination of collision cross sections.* Anaïs C. George, Isabelle Schmitz, Vincent Marie, Benoit Colsch, Florent Rouvière, Sandra Alves, Sabine Heinisch, François Fenaille, Carlos Afonso, Corinne Loutelier-Bourhis, to be submitted.

Oral and poster presentations

- Meeting of the International Society for Ion mobility Spectrometry (ISIMS2023) • August 2023 • Maastricht • «Lipid CCS determination using TIMS instrument: desolvation issues and comparison with TWIMS and DTIMS instruments»
- *Rencontres du Club Jeune de Spectrométrie de Masse (RCJSM) à Marseille, Oral presentation (March 2023)* : « Comparison of three ion mobility platforms to determine lipid collision cross sections.»
- Analytics Meeting, *Nantes, France. Flash communication and poster (September 2022)*: «Calibrant-corrected database for uniformized and comparable lipid collision cross sections values by traveling wave ion mobility spectrometry.»
- Meeting of the International Society for Ion mobility Spectrometry (ISIMS2022) • July 2022 • Memphis, USA • **Oral presentation** : . «A re-calibration procedure for interoperable lipid collision cross section values measured by traveling wave ion mobility spectrometry.»
- Meeting of the Metabolomics society 2022 • June 2022 • Valence, Spain • **Oral presentation** : «A universal ion mobility calibration for interoperable collision cross sections databases. »
- XXVIrd Young mass spectrometry club meetings • March 2022 • La neyrière, Pomeys (France) • **Oral presentation** : « A universal ion mobility calibration for interoperable collision cross sections databases »
- XXVrd Young mass spectrometry club meetings • March 2021 (Visio-conférence) • **Oral presentation** : « Metabolomics by high-resolution mass spectrometry coupled with ion mobility spectrometry. »

- JEDNC • 24-25 juin 2021 (visio-conference) • **Poster**
- Congress of the French metabolomics and fluxomics network (RFMF) • November 2021 • Aussois (France) • **Poster and flash communications** : « Lipidomics analysis of human plasma by liquid chromatography coupled with ion mobility and high-resolution mass spectrometry »

Liste des cours et formations suivis

1. Formations transversales : 124.5h
 - ✓ Intégrité scientifique (MOOC) : 15h
 - ✓ Open access et dépôt dans HAL (le 16 février 2021 en visio) : 2.5h
 - ✓ Rédiger un article scientifique (MOOC) : 20h
 - ✓ Entrepreneuriat XL Chem (29 juin 2021 en visio) : 4h
 - ✓ Protéger, valoriser et diffuser les résultats et produits de la recherche en sciences technologiques et santé (le 30 novembre 2021 en visio) : 3h
 - ✓ Participation à la journée PhDTalent : 6h
 - ✓ Formation à obsidian : 3h
 - ✓ Formations à l'enseignement (INSPE Mont Saint Aignan : d'octobre 2021 à avril 2022) : 30h
 - ✓ Enseignement (64h) : 12h
 - ✓ Encadrement de stagiaires : 35h
 - ✓ Activités de vulgarisation scientifique :
 - Participation au FENO (à Rouen le 11 septembre 2021) : 3h
 - Participation à la journée du patrimoine : 3h
 - Participation à l'opération DECLICS : 3h
2. Formations spécifiques : 393h
 - ✓ Formation Prévention, risque incendie, biologique, chimique (application NEO) : 2h
 - ✓ Hygiène et sécurité (les 2 et 12 février 2021 en visio) : 9h
 - ✓ Congrès CJSM (les 30 et 31 mars 2021 en visio) : 14+2h
 - ✓ Lipidmaps spring school (du 12 au 16 avril 2021 en visio) : 38h
 - ✓ Chromatographie (ED en visio le 2 juin 2021) : 3h
 - ✓ Congrès JFSM (du 14 au 24 juin 2021 en visio) : 24h
 - ✓ Congrès RFMF (du 23 au 26 novembre 2021 à Aussois, France) : 22h+1h
 - ✓ Select science virtual (le 15 février en visio) : 8h
 - ✓ Congrès CJSM (du 7 au 11 mars 2022 à Pomeys, France) : 30h+2h
 - ✓ Congrès p2M Symposium à Rouen les 24 et 25 mars 2022 : 10h
 - ✓ Congrès CJSM 2023 : 20 + 2h
 - ✓ Congrès ISIMS : 25h + 4h
 - ✓ Virtual analytical summit 2023 (visio) : 8h
 - ✓ Labex Synorg : 12h + 2h
 - ✓ Metabolomics : 40h + 4h
 - ✓ Analytics : 36+2h+1h
 - ✓ Formation TIMS-TOF Flex (4 formations) : 62h
 - ✓ Rédaction de la publication : 10h

Bibliography

- Adebo, Oluwafemi Ayodeji, Patrick Berka Njobeh, Janet AdeyinkaAdebiyi, Sefater Gbashi, Eugenie Kayitesi, Oluwafemi Ayodeji Adebo, Patrick Berka Njobeh, Janet AdeyinkaAdebiyi, Sefater Gbashi, et Eugenie Kayitesi. 2017. « Food Metabolomics: A New Frontier in Food Analysis and Its Application to Understanding Fermented Foods ». In *Functional Food - Improve Health through Adequate Food*. IntechOpen. <https://doi.org/10.5772/intechopen.69171>.
- Ahrens, André, Janina Möhle, Moritz Hitzemann, et Stefan Zimmermann. 2020. « Novel Ion Drift Tube for High-Performance Ion Mobility Spectrometers Based on a Composite Material ». *International Journal for Ion Mobility Spectrometry* 23 (2): 75-81. <https://doi.org/10.1007/s12127-020-00265-0>.
- Aitio, Antero, Alfred Bernard, Bruce A Fowler, et Gunnar F Nordberg. 2007. « Biological Monitoring and Biomarkers ». *Handbook on the Toxicology of Metals* 3rd ed. Academic Press/Elsevier (Chapter 4): 65-78.
- Akhlaqi, Masoumeh, Wei-Chieh Wang, Claudia Möckel, et Anneli Krueve. 2023. « Complementary Methods for Structural Assignment of Isomeric Candidate Structures in Non-Target Liquid Chromatography Ion Mobility High-Resolution Mass Spectrometric Analysis ». *Analytical and Bioanalytical Chemistry* 415 (21): 5247-59. <https://doi.org/10.1007/s00216-023-04852-y>.
- Alarcon-Barrera, Juan Carlos, Sarantos Kostidis, Alejandro Ondo-Mendez, et Martin Giera. 2022. « Recent Advances in Metabolomics Analysis for Early Drug Development ». *Drug Discovery Today* 27 (6): 1763-73. <https://doi.org/10.1016/j.drudis.2022.02.018>.
- Aldana, Julian, Adriana Romero-Otero, et Mónica P. Cala. 2020. « Exploring the Lipidome: Current Lipid Extraction Techniques for Mass Spectrometry Analysis ». *Metabolites* 10 (6). <https://doi.org/10.3390/metabo10060231>.
- Antignac, Jean-Philippe, Katia de Wasch, Fabrice Monteau, Hubert De Brabander, François Andre, et Bruno Le Bizec. 2005. « The Ion Suppression Phenomenon in Liquid Chromatography–Mass Spectrometry and Its Consequences in the Field of Residue Analysis ». *Analytica Chimica Acta*, EURORESIDUE V, Noordwijkerhout, The Netherlands, 10-12 May 2004., 529 (1): 129-36. <https://doi.org/10.1016/j.aca.2004.08.055>.
- Antonelli, Joseph, Brian L. Claggett, Mir Henglin, Andy Kim, Gavin Ovsak, Nicole Kim, Katherine Deng, et al. 2019. « Statistical Workflow for Feature Selection in Human Metabolomics Data ». *Metabolites* 9 (7): 143. <https://doi.org/10.3390/metabo9070143>.
- Anwardeen, Najeha R., Ilhame Diboun, Younes Mokrab, Asma A. Althani, et Mohamed A. Elrayess. 2023. « Statistical methods and resources for biomarker discovery using metabolomics ». *BMC Bioinformatics* 24 (1): 250. <https://doi.org/10.1186/s12859-023-05383-0>.
- Arroyo-Manzanares, Natalia, María García-Nicolás, Francisco Zafra-Navarro, Natalia Campillo, et Pilar Viñas. 2022. « A Non-Targeted Metabolomic Strategy for Characterization of the Botanical Origin of Honey Samples Using Headspace Gas Chromatography—Ion Mobility Spectrometry ». *Analytical Methods* 14 (48): 5047-55. <https://doi.org/10.1039/D2AY01479C>.
- Artati, Anna, Cornelia Prehn, Dominik Lutter, et Kenneth Allen Dyar. 2022. « Untargeted and Targeted Circadian Metabolomics Using Liquid Chromatography-Tandem Mass Spectrometry (LC-MS/MS) and Flow Injection-Electrospray Ionization-Tandem Mass Spectrometry (FIA-ESI-MS/MS) ». In *Circadian Regulation: Methods and Protocols*, édité par Guiomar Solanas et Patrick -Simon Welz, 311-27. Methods in Molecular Biology. New York, NY: Springer US. https://doi.org/10.1007/978-1-0716-2249-0_21.
- Asbury, G. Reid, et Herbert H Hill. 2000. « Using Different Drift Gases To Change Separation Factors (α) in Ion Mobility Spectrometry | Analytical Chemistry ». 2000. <https://pubs.acs.org/doi/10.1021/ac9908952>.
- Baglai, Anna, Andrea F.G. Gargano, Jan Jordens, Ynze Mengerink, Maarten Honing, Sjoerd van der Wal, et Peter J. Schoenmakers. 2017. « Comprehensive Lipidomic Analysis of Human

- Plasma Using Multidimensional Liquid- and Gas-Phase Separations: Two-Dimensional Liquid Chromatography–Mass Spectrometry vs. Liquid Chromatography–Trapped-Ion-Mobility–Mass Spectrometry ». *Journal of Chromatography A* 1530 (décembre): 90-103.
<https://doi.org/10.1016/j.chroma.2017.11.014>.
- Baker, Erin Shammel, Brian H. Clowers, Fumin Li, Keqi Tang, Aleksey V. Tolmachev, David C. Prior, Mikhail E. Belov, et Richard D. Smith. 2007. « Ion Mobility Spectrometry–Mass Spectrometry Performance Using Electrodynamical Ion Funnel and Elevated Drift Gas Pressures ». *Journal of the American Society for Mass Spectrometry* 18 (7): 1176-87.
<https://doi.org/10.1016/j.jasms.2007.03.031>.
- Barbier Saint Hilaire, Pierre, Kathleen Rousseau, Alexandre Seyer, Sylvain Dechaumet, Annelaure Damont, Christophe Junot, et François Fenaille. 2020. « Comparative Evaluation of Data Dependent and Data Independent Acquisition Workflows Implemented on an Orbitrap Fusion for Untargeted Metabolomics ». *Metabolites* 10 (4): 158.
<https://doi.org/10.3390/metabo10040158>.
- Beale, David J., Farhana R. Pinu, Konstantinos A. Kouremenos, Mahesha M. Poojary, Vinod K. Narayana, Berin A. Boughton, Komal Kanojia, Saravanan Dayalan, Oliver A. H. Jones, et Daniel A. Dias. 2018. « Review of Recent Developments in GC–MS Approaches to Metabolomics-Based Research ». *Metabolomics* 14 (11): 152. <https://doi.org/10.1007/s11306-018-1449-2>.
- Beermann, Christopher, Michael Möbius, Nadine Winterling, Joachim J. Schmitt, et Günther Boehm. 2005. « Sn-Position Determination of Phospholipid-Linked Fatty Acids Derived from Erythrocytes by Liquid Chromatography Electrospray Ionization Ion-Trap Mass Spectrometry ». *Lipids* 40 (2): 211-18. <https://doi.org/10.1007/s11745-005-1377-1>.
- Bekker-Jensen, Dorte B., Ana Martínez-Val, Sophia Steigerwald, Patrick Rütger, Kyle L. Fort, Tabiwang N. Arrey, Alexander Harder, Alexander Makarov, et Jesper V. Olsen. 2020. « A Compact Quadrupole-Orbitrap Mass Spectrometer with FAIMS Interface Improves Proteome Coverage in Short LC Gradients * ». *Molecular & Cellular Proteomics* 19 (4): 716-29.
<https://doi.org/10.1074/mcp.TIR119.001906>.
- Belov, Mikhail E., Michael A. Buschbach, David C. Prior, Keqi Tang, et Richard D. Smith. 2007. « Multiplexed Ion Mobility Spectrometry-Orthogonal Time-of-Flight Mass Spectrometry ». *Analytical Chemistry* 79 (6): 2451-62. <https://doi.org/10.1021/ac0617316>.
- Belova, Lidia, Noelia Caballero-Casero, Alexander L. N. van Nuijs, et Adrian Covaci. 2021. « Ion Mobility-High-Resolution Mass Spectrometry (IM-HRMS) for the Analysis of Contaminants of Emerging Concern (CECs): Database Compilation and Application to Urine Samples ». *Analytical Chemistry* 93 (16): 6428-36. <https://doi.org/10.1021/acs.analchem.1c00142>.
- Belova, Lidia, Alberto Celma, Glenn Van Haesendonck, Filip Lemièrre, Juan Vicente Sancho, Adrian Covaci, Alexander L. N. van Nuijs, et Lubertus Bijlsma. 2022. « Revealing the Differences in Collision Cross Section Values of Small Organic Molecules Acquired by Different Instrumental Designs and Prediction Models ». *Analytica Chimica Acta* 1229 (octobre): 340361.
<https://doi.org/10.1016/j.aca.2022.340361>.
- Ben Faleh, Ahmed, Stephan Warnke, Teun Van Wieringen, Ali H. Abikhodr, et Thomas R. Rizzo. 2023. « New Approach for the Identification of Isobaric and Isomeric Metabolites ». *Analytical Chemistry* 95 (18): 7118-26. <https://doi.org/10.1021/acs.analchem.2c04962>.
- Berry, Karin A. Zemski, Robert M. Barkley, Joseph J. Berry, Joseph A. Hankin, Emmy Hoyes, Jeffery M. Brown, et Robert C. Murphy. 2017. « Tandem Mass Spectrometry in Combination with Product Ion Mobility for the Identification of Phospholipids ». *Analytical Chemistry* 89 (1): 916-21. <https://doi.org/10.1021/acs.analchem.6b04047>.
- Bielow, Chris, Guido Mastrobuoni, Marica Orioli, et Stefan Kempa. 2017. « On Mass Ambiguities in High-Resolution Shotgun Lipidomics ». *Analytical Chemistry* 89 (5): 2986-94.
<https://doi.org/10.1021/acs.analchem.6b04456>.
- Bilbao, Aivett, Bryson C. Gibbons, Sarah M. Stow, Jennifer E. Kyle, Kent J. Bloodsworth, Samuel H. Payne, Richard D. Smith, Yehia M. Ibrahim, Erin S. Baker, et John C. Fjeldsted. 2021. « A

- Preprocessing Tool for Enhanced Ion Mobility–Mass Spectrometry-Based Omics Workflows ». *Journal of Proteome Research*, août. <https://doi.org/10.1021/acs.jproteome.1c00425>.
- Bingol, Kerem, Lei Bruschweiler-Li, Cao Yu, Arpad Somogyi, Fengli Zhang, et Rafael Bruschweiler. 2015. « Metabolomics Beyond Spectroscopic Databases: A Combined MS/NMR Strategy for the Rapid Identification of New Metabolites in Complex Mixtures ». *Analytical Chemistry* 87 (7): 3864-70. <https://doi.org/10.1021/ac504633z>.
- Bleiholder, Christian, Stephanie Contreras, et Michael T. Bowers. 2013. « A Novel Projection Approximation Algorithm for the Fast and Accurate Computation of Molecular Collision Cross Sections (IV). Application to Polypeptides ». *International Journal of Mass Spectrometry Complete* (354-355): 275-80. <https://doi.org/10.1016/j.ijms.2013.06.011>.
- Bleiholder, Christian, Nicholas R. Johnson, Stephanie Contreras, Thomas Wytenbach, et Michael T. Bowers. 2015. « Molecular Structures and Ion Mobility Cross Sections: Analysis of the Effects of He and N₂ Buffer Gas ». *Analytical Chemistry* 87 (14): 7196-7203. <https://doi.org/10.1021/acs.analchem.5b01429>.
- Bleiholder, Christian, Thomas Wytenbach, et Michael T. Bowers. 2011. « A novel projection approximation algorithm for the fast and accurate computation of molecular collision cross sections (I). Method ». *International Journal of Mass Spectrometry* 308 (1): 1-10. <https://doi.org/10.1016/j.ijms.2011.06.014>.
- Bligh, E G, et W J Dyer. 1959. « A RAPID METHOD OF TOTAL LIPID EXTRACTION AND PURIFICATION ». *Can. J. Biochem. Physiol.*, 7.
- Boiteau, Rene, David Hoyt, Carrie Nicora, Hannah Kinmonth-Schultz, Joy Ward, et Kerem Bingol. 2018. « Structure Elucidation of Unknown Metabolites in Metabolomics by Combined NMR and MS/MS Prediction ». *Metabolites* 8 (1): 8. <https://doi.org/10.3390/metabo8010008>.
- Bojko, Barbara, Nathaly Reyes-Garcés, Vincent Bessonneau, Krzysztof Goryński, Fatemeh Mousavi, Erica A. Souza Silva, et Janusz Pawliszyn. 2014. « Solid-Phase Microextraction in Metabolomics ». *TrAC Trends in Analytical Chemistry* 61 (octobre): 168-80. <https://doi.org/10.1016/j.trac.2014.07.005>.
- Boldyreva, Lidiya V., Maryana V. Morozova, Snezhanna S. Saydakova, et Elena N. Kozhevnikova. 2021. « Fat of the Gut: Epithelial Phospholipids in Inflammatory Bowel Diseases ». *International Journal of Molecular Sciences* 22 (21): 11682. <https://doi.org/10.3390/ijms222111682>.
- Bonini, Paolo, Tobias Kind, Hiroshi Tsugawa, Dinesh Kumar Barupal, et Oliver Fiehn. 2020. « Retip: Retention Time Prediction for Compound Annotation in Untargeted Metabolomics ». *Analytical Chemistry* 92 (11): 7515-22. <https://doi.org/10.1021/acs.analchem.9b05765>.
- Borsdorf, Helko, et Gary A. Eiceman. 2006. « Ion Mobility Spectrometry: Principles and Applications ». *Applied Spectroscopy Reviews* 41 (4): 323-75. <https://doi.org/10.1080/05704920600663469>.
- Both, P., A. P. Green, C. J. Gray, R. Šardžik, J. Voglmeir, C. Fontana, M. Austeri, et al. 2014. « Discrimination of Epimeric Glycans and Glycopeptides Using IM-MS and Its Potential for Carbohydrate Sequencing ». *Nature Chemistry* 6 (1): 65-74. <https://doi.org/10.1038/nchem.1817>.
- Bowen, Raffick A. R., et Alan T. Remaley. 2014. « Interferences from Blood Collection Tube Components on Clinical Chemistry Assays ». *Biochimica Medica* 24 (1): 31-44. <https://doi.org/10.11613/BM.2014.006>.
- Broeckling, Corey D., Linxing Yao, Giorgis Isaac, Marisa Gioioso, Valentin Ianchis, et Johannes P.C. Vissers. 2021. « Application of Predicted Collisional Cross Section to Metabolome Databases to Probabilistically Describe the Current and Future Ion Mobility Mass Spectrometry ». *Journal of the American Society for Mass Spectrometry* 32 (3): 661-69. <https://doi.org/10.1021/jasms.0c00375>.
- Bruce, Stephen J., Isabelle Tavazzi, Véronique Parisod, Serge Rezzi, Sunil Kochhar, et Philippe A. Guy. 2009. « Investigation of Human Blood Plasma Sample Preparation for Performing Metabolomics Using Ultrahigh Performance Liquid Chromatography/Mass Spectrometry ». *Analytical Chemistry* 81 (9): 3285-96. <https://doi.org/10.1021/ac8024569>.

- Bruin, Carlo Roberto de, Marie Hennebelle, Jean-Paul Vincken, et Wouter J. C. de Bruijn. 2022. « Separation of Flavonoid Isomers by Cyclic Ion Mobility Mass Spectrometry ». *Analytica Chimica Acta*, décembre, 340774. <https://doi.org/10.1016/j.aca.2022.340774>.
- Bruno, C., F. Patin, C. Bocca, L. Nadal-Desbarats, F. Bonnier, P. Reynier, P. Emond, et al. 2018. « The Combination of Four Analytical Methods to Explore Skeletal Muscle Metabolomics: Better Coverage of Metabolic Pathways or a Marketing Argument? » *Journal of Pharmaceutical and Biomedical Analysis* 148 (janvier): 273-79. <https://doi.org/10.1016/j.jpba.2017.10.013>.
- Brzhozovskiy, Alexander, Alexey Kononikhin, Anna E. Bugrova, Grigoriy I. Kovalev, Pierre-Olivier Schmit, Gary Kruppa, Evgeny N. Nikolaev, et Christoph H. Borchers. 2022. « The Parallel Reaction Monitoring-Parallel Accumulation-Serial Fragmentation (prm-PASEF) Approach for Multiplexed Absolute Quantitation of Proteins in Human Plasma ». *Analytical Chemistry* 94 (4): 2016-22. <https://doi.org/10.1021/acs.analchem.1c03782>.
- Burla, Bo, Makoto Arita, Masanori Arita, Anne K. Bendt, Amaury Cazenave-Gassiot, Edward A. Dennis, Kim Ekroos, et al. 2018. « MS-Based Lipidomics of Human Blood Plasma: A Community-Initiated Position Paper to Develop Accepted Guidelines1 ». *Journal of Lipid Research* 59 (10): 2001-17. <https://doi.org/10.1194/jlr.S087163>.
- Bush, Matthew F., Iain D. G. Campuzano, et Carol V. Robinson. 2012. « Ion Mobility Mass Spectrometry of Peptide Ions: Effects of Drift Gas and Calibration Strategies ». *Analytical Chemistry* 84 (16): 7124-30. <https://doi.org/10.1021/ac3014498>.
- Butler, Karen E., et Erin S. Baker. 2022. « A High-Throughput Ion Mobility Spectrometry-Mass Spectrometry Screening Method for Opioid Profiling ». *Journal of the American Society for Mass Spectrometry*, septembre. <https://doi.org/10.1021/jasms.2c00186>.
- Cajka, Tomas, et Oliver Fiehn. 2016. « Toward Merging Untargeted and Targeted Methods in Mass Spectrometry-Based Metabolomics and Lipidomics ». *Analytical Chemistry* 88 (1): 524-45. <https://doi.org/10.1021/acs.analchem.5b04491>.
- Calabrese, Valentina, Hélène Lavanant, Frédéric Rosu, Valérie Gabelica, et Carlos Afonso. 2020. « Collision Cross Sections of Phosphoric Acid Cluster Anions in Helium Measured by Drift Tube Ion Mobility Mass Spectrometry ». *Journal of the American Society for Mass Spectrometry* 31 (4): 969-81. <https://doi.org/10.1021/jasms.0c00034>.
- Calabrese, Valentina, Isabelle Schmitz-Afonso, Candice Prevost, Carlos Afonso, et Abdelhakim Elomri. 2022. « Molecular Networking and Collision Cross Section Prediction for Structural Isomer and Unknown Compound Identification in Plant Metabolomics: A Case Study Applied to *Zanthoxylum Heitzii* Extracts ». *Analytical and Bioanalytical Chemistry* 414 (14): 4103-18. <https://doi.org/10.1007/s00216-022-04059-7>.
- Calabrese, Valentina, Isabelle Schmitz-Afonso, Wassila Riah-Anglet, Isabelle Trinsoutrot-Gattin, Barbara Pawlak, et Carlos Afonso. 2023. « Direct introduction MALDI FTICR MS based on dried droplet deposition applied to non-targeted metabolomics on *Pisum Sativum* root exudates ». *Talanta* 253 (février): 123901. <https://doi.org/10.1016/j.talanta.2022.123901>.
- Calvano, Cosima D, Francesco Palmisano, et Tommaso RI Cataldi. 2018. « Understanding neurodegenerative disorders by MS-based lipidomics ». *Bioanalysis* 10 (11): 787-90. <https://doi.org/10.4155/bio-2018-0023>.
- Campuzano, et Kevin Giles. 2019. « Historical, Current and Future Developments of Travelling Wave Ion Mobility Mass Spectrometry: A Personal Perspective ». *TrAC Trends in Analytical Chemistry* 120 (novembre): 115620. <https://doi.org/10.1016/j.trac.2019.115620>.
- Campuzano, Iain, Matthew F. Bush, Carol V. Robinson, Claire Beaumont, Keith Richardson, Hyungjun Kim, et Hugh I. Kim. 2012. « Structural Characterization of Drug-like Compounds by Ion Mobility Mass Spectrometry: Comparison of Theoretical and Experimentally Derived Nitrogen Collision Cross Sections ». *Analytical Chemistry* 84 (2): 1026-33. <https://doi.org/10.1021/ac202625t>.
- Castro-Perez, Jose, Thomas P. Roddy, Nico M. M. Nibbering, Vinit Shah, David G. McLaren, Stephen Previs, Athula B. Attygalle, et al. 2011. « Localization of Fatty Acyl and Double Bond Positions in Phosphatidylcholines Using a Dual Stage CID Fragmentation Coupled with Ion Mobility

- Mass Spectrometry ». *Journal of the American Society for Mass Spectrometry* 22 (9): 1552-67. <https://doi.org/10.1007/s13361-011-0172-2>.
- Causon, Tim J., Le Si-Hung, Kenneth Newton, Ruwan T. Kurulugama, John Fjeldsted, et Stephan Hann. 2019. « Fundamental Study of Ion Trapping and Multiplexing Using Drift Tube-Ion Mobility Time-of-Flight Mass Spectrometry for Non-Targeted Metabolomics ». *Analytical and Bioanalytical Chemistry* 411 (24): 6265-74. <https://doi.org/10.1007/s00216-019-02021-8>.
- Celma, Alberto, Richard Bade, Juan Vicente Sancho, Félix Hernandez, Melissa Humphries, et Lubertus Bijlsma. 2022. « Prediction of Retention Time and Collision Cross Section (CCSH+, CCSH-, and CCSNa+) of Emerging Contaminants Using Multiple Adaptive Regression Splines ». *Journal of Chemical Information and Modeling* 62 (22): 5425-34. <https://doi.org/10.1021/acs.jcim.2c00847>.
- Chai, Mengqi, Meggie N. Young, Fanny C. Liu, et Christian Bleiholder. 2018. « A Transferable, Sample-Independent Calibration Procedure for Trapped Ion Mobility Spectrometry (TIMS) ». *Analytical Chemistry* 90 (15): 9040-47. <https://doi.org/10.1021/acs.analchem.8b01326>.
- Chantipmanee, Nattapong, et Peter C. Hauser. 2021. « Development of simple drift tube design for ion mobility spectrometry based on flexible printed circuit board material ». *Analytica Chimica Acta* 1170 (juillet): 338626. <https://doi.org/10.1016/j.aca.2021.338626>.
- Chawner, Ross, Bryan McCullough, Kevin Giles, Perdita E. Barran, Simon J. Gaskell, et Claire E. Eyers. 2012. « QconCAT Standard for Calibration of Ion Mobility-Mass Spectrometry Systems ». *Journal of Proteome Research* 11 (11): 5564-72. <https://doi.org/10.1021/pr3005327>.
- Chen, Jing, Wenzhao Wang, Shen Lv, Peiyuan Yin, Xinjie Zhao, Xin Lu, Fengxia Zhang, et Guowang Xu. 2009. « Metabonomics Study of Liver Cancer Based on Ultra Performance Liquid Chromatography Coupled to Mass Spectrometry with HILIC and RPLC Separations ». *Analytica Chimica Acta, Young Analytical Chemists in China*, 650 (1): 3-9. <https://doi.org/10.1016/j.aca.2009.03.039>.
- Chen, Jing, Peisi Xie, Qingyuan Dai, Pengfei Wu, Yu He, Zian Lin, et Zongwei Cai. 2023. « Spatial lipidomics and metabolomics of multicellular tumor spheroids using MALDI-2 and trapped ion mobility imaging ». *Talanta* 265 (décembre): 124795. <https://doi.org/10.1016/j.talanta.2023.124795>.
- Chen, Li, Fanyi Zhong, et Jiangjiang Zhu. 2020. « Bridging Targeted and Untargeted Mass Spectrometry-Based Metabolomics via Hybrid Approaches ». *Metabolites* 10 (9): 348. <https://doi.org/10.3390/metabo10090348>.
- Chen, Lipin, Xiaoyu Teng, Yu Liu, Haohao Shi, Zhaojie Li, et Changhu Xue. 2023. « The dynamic change of flavor characteristics in Pacific oyster (*Crassostrea gigas*) during depuration uncovered by mass spectrometry-based metabolomics combined with gas chromatography-ion mobility spectrometry (GC-IMS) ». *Food Chemistry*, août, 137277. <https://doi.org/10.1016/j.foodchem.2023.137277>.
- Chen, Shili, Miriam Hoene, Jia Li, Yanjie Li, Xinjie Zhao, Hans-Ulrich Häring, Erwin D. Schleicher, Cora Weigert, Guowang Xu, et Rainer Lehmann. 2013. « Simultaneous Extraction of Metabolome and Lipidome with Methyl Tert-Butyl Ether from a Single Small Tissue Sample for Ultra-High Performance Liquid Chromatography/Mass Spectrometry ». *Journal of Chromatography A* 1298 (juillet): 9-16. <https://doi.org/10.1016/j.chroma.2013.05.019>.
- Chen, Xi, Zhiwei Zhou, et Zheng-Jiang Zhu. 2020. « The Use of LipidIMMS Analyzer for Lipid Identification in Ion Mobility-Mass Spectrometry-Based Untargeted Lipidomics ». In *Ion Mobility-Mass Spectrometry*, édité par Giuseppe Paglia et Giuseppe Astarita, 2084:269-82. Methods in Molecular Biology. New York, NY: Springer US. https://doi.org/10.1007/978-1-0716-0030-6_17.
- Chen, Yang, En-Min Li, et Li-Yan Xu. 2022. « Guide to Metabolomics Analysis: A Bioinformatics Workflow ». *Metabolites* 12 (4): 357. <https://doi.org/10.3390/metabo12040357>.
- Chen, Yanhua, Jing Xu, Ruiping Zhang, Guoqing Shen, Yongmei Song, Jianghao Sun, Jiuming He, Qimin Zhan, et Zeper Abliz. 2013. « Assessment of Data Pre-Processing Methods for LC-MS/MS-

- Based Metabolomics of Uterine Cervix Cancer ». *Analyst* 138 (9): 2669-77.
<https://doi.org/10.1039/C3AN36818A>.
- Chi, Chia-Hsin, Yi-Sheng Wang, et Lean-Teik Ng. 2022. « Structural Characterization of Mushroom Polysaccharides by Cyclic Ion Mobility-Mass Spectrometry ». *Journal of Chromatography A* 1680 (septembre): 463445. <https://doi.org/10.1016/j.chroma.2022.463445>.
- Chiurchiù, Valerio, Marta Tiberi, Alessandro Matteocci, Federico Fazio, Hasibullah Siffeti, Stefano Saracini, Nicola Biagio Mercuri, et Giuseppe Sancesario. 2022. « Lipidomics of Bioactive Lipids in Alzheimer's and Parkinson's Diseases: Where Are We? » *International Journal of Molecular Sciences* 23 (11): 6235. <https://doi.org/10.3390/ijms23116235>.
- Chouinard, Christopher D., Vinícius Wilian D. Cruzeiro, Robin H. J. Kemperman, Nicholas R. Oranzi, Adrian E. Roitberg, et Richard A. Yost. 2018. « Cation-dependent conformations in 25-hydroxyvitamin D3-cation adducts measured by ion mobility-mass spectrometry and theoretical modeling ». *International Journal of Mass Spectrometry* 432 (septembre): 1-8. <https://doi.org/10.1016/j.ijms.2018.05.013>.
- Clemmer, David E., et Martin F. Jarrold. 1997. « Ion Mobility Measurements and Their Applications to Clusters and Biomolecules ». *Journal of Mass Spectrometry* 32 (6): 577-92. [https://doi.org/10.1002/\(SICI\)1096-9888\(199706\)32:6<577::AID-JMS530>3.0.CO;2-4](https://doi.org/10.1002/(SICI)1096-9888(199706)32:6<577::AID-JMS530>3.0.CO;2-4).
- Clowers, Brian H., et Herbert H. Hill. 2005. « Mass Analysis of Mobility-Selected Ion Populations Using Dual Gate, Ion Mobility, Quadrupole Ion Trap Mass Spectrometry ». *Analytical Chemistry* 77 (18): 5877-85. <https://doi.org/10.1021/ac050700s>.
- Clowers, Brian H., et Herbert H. Hill Jr. 2006. « Influence of Cation Adduction on the Separation Characteristics of Flavonoid Diglycoside Isomers Using Dual Gate-Ion Mobility-Quadrupole Ion Trap Mass Spectrometry ». *Journal of Mass Spectrometry* 41 (3): 339-51. <https://doi.org/10.1002/jms.994>.
- Clowers, Brian H., Yehia M. Ibrahim, David C. Prior, William F. Danielson, Mikhail E. Belov, et Richard D. Smith. 2008. « Enhanced Ion Utilization Efficiency Using an Electrodynamic Ion Funnel Trap as an Injection Mechanism for Ion Mobility Spectrometry ». *Analytical Chemistry* 80 (3): 612-23. <https://doi.org/10.1021/ac701648p>.
- Cohen, Martin J., et F. W. Karasek. 1970. « Plasma ChromatographyTM—A New Dimension for Gas Chromatography and Mass Spectrometry ». *Journal of Chromatographic Science* 8 (6): 330-37. <https://doi.org/10.1093/chromsci/8.6.330>.
- Colby, Sean M., Christine H. Chang, Jessica L. Bade, Jamie R. Nunez, Madison R. Blumer, Daniel J. Orton, Kent J. Bloodsworth, et al. 2022. « DEIMoS: An Open-Source Tool for Processing High-Dimensional Mass Spectrometry Data ». *Analytical Chemistry* 94 (16): 6130-38. <https://doi.org/10.1021/acs.analchem.1c05017>.
- Colby, Sean M., Jamie R. Nuñez, Nathan O. Hodas, Courtney D. Corley, et Ryan R. Renslow. 2020. « Deep Learning to Generate in Silico Chemical Property Libraries and Candidate Molecules for Small Molecule Identification in Complex Samples ». *Analytical Chemistry* 92 (2): 1720-29. <https://doi.org/10.1021/acs.analchem.9b02348>.
- Colsch, Benoit, François Fenaille, Anna Warnet, Christophe Junot, et Jean-Claude Tabet. 2017. « Mechanisms Governing the Fragmentation of Glycerophospholipids Containing Choline and Ethanolamine Polar Head Groups ». *European Journal of Mass Spectrometry* 23 (6): 427-44. <https://doi.org/10.1177/1469066717731668>.
- Commisso, Mauro, Andrea Anesi, Silvia Dal Santo, et Flavia Guzzo. 2017. « Performance Comparison of Electrospray Ionization and Atmospheric Pressure Chemical Ionization in Untargeted and Targeted Liquid Chromatography/Mass Spectrometry Based Metabolomics Analysis of Grapeberry Metabolites ». *Rapid Communications in Mass Spectrometry: RCM* 31 (3): 292-300. <https://doi.org/10.1002/rcm.7789>.
- Contrepois, Kévin, Lihua Jiang, et Michael Snyder. 2015. « Optimized Analytical Procedures for the Untargeted Metabolomic Profiling of Human Urine and Plasma by Combining Hydrophilic Interaction (HILIC) and Reverse-Phase Liquid Chromatography (RPLC)—Mass Spectrometry ».

- Molecular & Cellular Proteomics* 14 (6): 1684-95.
<https://doi.org/10.1074/mcp.M114.046508>.
- Cooper-Shepherd, Dale A., Hernando J. Olivos, Zhaoxiang Wu, et Martin E. Palmer. 2022. « Exploiting Self-Association to Evaluate Enantiomeric Composition by Cyclic Ion Mobility–Mass Spectrometry ». *Analytical Chemistry* 94 (23): 8441-48.
<https://doi.org/10.1021/acs.analchem.2c01212>.
- Cordeiro, Fernanda Bertuccez, Alan K. Jarmusch, Marisol León, Christina Ramires Ferreira, Valentina Pirro, Livia S. Eberlin, Judy Hallett, Maria Angelica Miglino, et Robert Graham Cooks. 2020. « Mammalian Ovarian Lipid Distributions by Desorption Electrospray Ionization–Mass Spectrometry (DESI-MS) Imaging ». *Analytical and Bioanalytical Chemistry* 412 (6): 1251-62.
<https://doi.org/10.1007/s00216-019-02352-6>.
- Couchman, Lewis. 2012. « Turbulent Flow Chromatography in Bioanalysis: A Review ». *Biomedical Chromatography* 26 (8): 892-905. <https://doi.org/10.1002/bmc.2769>.
- Courant, Frédérique, Jean-Philippe Antignac, Gaud Dervilly-Pinel, et Bruno Le Bizec. 2014. « Basics of Mass Spectrometry Based Metabolomics ». *PROTEOMICS* 14 (21-22): 2369-88.
<https://doi.org/10.1002/pmic.201400255>.
- Crockford, D. J., H. C. Keun, L. M. Smith, E. Holmes, et J. K. Nicholson. 2005. « Curve-Fitting Method for Direct Quantitation of Compounds in Complex Biological Mixtures Using ¹H NMR: Application in Metabonomic Toxicology Studies ». *Analytical Chemistry* 77 (14): 4556-62.
<https://doi.org/10.1021/ac0503456>.
- Crowell, Kevin L., Gordon W. Slys, Erin S. Baker, Brian L. LaMarche, Matthew E. Monroe, Yehia M. Ibrahim, Samuel H. Payne, Gordon A. Anderson, et Richard D. Smith. 2013. « LC-IMS-MS Feature Finder: detecting multidimensional liquid chromatography, ion mobility and mass spectrometry features in complex datasets ». *Bioinformatics* 29 (21): 2804-5.
<https://doi.org/10.1093/bioinformatics/btt465>.
- Cumeras, R., E. Figueras, C. E. Davis, J. I. Baumbach, et I. Gràcia. 2015a. « Review on Ion Mobility Spectrometry. Part 1: Current Instrumentation ». *The Analyst* 140 (5): 1376-90.
<https://doi.org/10.1039/C4AN01100G>.
- . 2015b. « Review on Ion Mobility Spectrometry. Part 2: Hyphenated Methods and Effects of Experimental Parameters ». *Analyst* 140 (5): 1391-1410.
<https://doi.org/10.1039/C4AN01101E>.
- Daykin, Clare A., Peta J. D. Foxall, Susan C. Connor, John C. Lindon, et Jeremy K. Nicholson. 2002. « The Comparison of Plasma Deproteinization Methods for the Detection of Low-Molecular-Weight Metabolites by ¹H Nuclear Magnetic Resonance Spectroscopy ». *Analytical Biochemistry* 304 (2): 220-30. <https://doi.org/10.1006/abio.2002.5637>.
- De Hoffmann, Edmond, et Vincent Stroobant. 2007. *Mass Spectrometry: Principles and Applications, 3rd Edition* | Wiley. <https://www.wiley.com/en-us/Mass+Spectrometry%3A+Principles+and+Applications%2C+3rd+Edition-p-9780470033104>.
- Defossez, Emmanuel, Julien Bourquin, Stephan von Reuss, Sergio Rasmann, et Gaétan Glauser. 2023. « Eight Key Rules for Successful Data-Dependent Acquisition in Mass Spectrometry-Based Metabolomics ». *Mass Spectrometry Reviews* 42 (1): 131-43.
<https://doi.org/10.1002/mas.21715>.
- Delafield, Daniel G., Gaoyuan Lu, Cameron J. Kaminsky, et Lingjun Li. 2022. « High-End Ion Mobility Mass Spectrometry: A Current Review of Analytical Capacity in Omics Applications and Structural Investigations ». *TrAC Trends in Analytical Chemistry* 157 (décembre): 116761.
<https://doi.org/10.1016/j.trac.2022.116761>.
- Delvaux, Aurélie, Estelle Rathahao-Paris, et Sandra Alves. 2021. « Different Ion Mobility-Mass Spectrometry Coupling Techniques to Promote Metabolomics ». *Mass Spectrometry Reviews*.
<https://doi.org/10.1002/mas.21685>.
- Delvaux, Aurélie, Estelle Rathahao-Paris, Blanche Guillon, Sophie Cholet, Karine Adel-Patient, François Fenaille, Christophe Junot, et Sandra Alves. 2021. « Trapped ion mobility

- spectrometry time-of-flight mass spectrometry for high throughput and high resolution characterization of human milk oligosaccharide isomers ». *Analytica Chimica Acta* 1180 (octobre): 338878. <https://doi.org/10.1016/j.aca.2021.338878>.
- Demichev, Vadim, Lukasz Szyrwił, Fengchao Yu, Guo Ci Teo, George Rosenberger, Agathe Niewianda, Daniela Ludwig, et al. 2022. « Dia-PASEF Data Analysis Using FragPipe and DIA-NN for Deep Proteomics of Low Sample Amounts ». *Nature Communications* 13 (1): 3944. <https://doi.org/10.1038/s41467-022-31492-0>.
- Deng, Liulin, Yehia M. Ibrahim, Erin S. Baker, Noor A. Aly, Ahmed M. Hamid, Xing Zhang, Xueyun Zheng, et al. 2016. « Ion Mobility Separations of Isomers Based upon Long Path Length Structures for Lossless Ion Manipulations Combined with Mass Spectrometry ». *ChemistrySelect* 1 (10): 2396-99. <https://doi.org/10.1002/slct.201600460>.
- Deng, Liulin, Ian K. Webb, Sandilya V. B. Garimella, Ahmed M. Hamid, Xueyun Zheng, Randolph V. Norheim, Spencer A. Prost, et al. 2017. « Serpentine Ultralong Path with Extended Routing (SUPER) High Resolution Traveling Wave Ion Mobility-MS using Structures for Lossless Ion Manipulations ». *Analytical Chemistry* 89 (8): 4628-34. <https://doi.org/10.1021/acs.analchem.7b00185>.
- Deschamps, Estelle, Isabelle Schmitz-Afonso, Annick Schaumann, Emmanuelle Dé, Corinne Loutelier-Bourhis, Stéphane Alexandre, et Carlos Afonso. 2019. « Determination of the Collision Cross Sections of Cardiolipins and Phospholipids from *Pseudomonas Aeruginosa* by Traveling Wave Ion Mobility Spectrometry-Mass Spectrometry Using a Novel Correction Strategy ». *Analytical and Bioanalytical Chemistry* 411 (30): 8123-31. <https://doi.org/10.1007/s00216-019-02194-2>.
- Di Poto, Cristina, Xiang Tian, Xuejun Peng, Heino M. Heyman, Matthias Szesny, Sonja Hess, et Lisa H. Cazares. 2021. « Metabolomic Profiling of Human Urine Samples Using LC-TIMS-QTOF Mass Spectrometry ». *Journal of the American Society for Mass Spectrometry* 32 (8): 2072-80. <https://doi.org/10.1021/jasms.0c00467>.
- Distler, Ute, Mateusz Krzysztof Łacki, Michał Piotr Startek, David Teschner, Sven Brehmer, Jens Decker, Thilo Schild, et al. 2023. « midiaPASEF Maximizes Information Content in Data-Independent Acquisition Proteomics ». Preprint. Bioinformatics. <https://doi.org/10.1101/2023.01.30.526204>.
- Dixit, Sugyan M., et Brandon T. Ruotolo. 2019. « A Semi-Empirical Framework for Interpreting Traveling Wave Ion Mobility Arrival Time Distributions ». *Journal of the American Society for Mass Spectrometry* 30 (6): 956-66. <https://doi.org/10.1007/s13361-019-02133-6>.
- Djombou Feunang, Yannick, Roman Eisner, Craig Knox, Leonid Chepelev, Janna Hastings, Gareth Owen, Eoin Fahy, et al. 2016. « ClassyFire: automated chemical classification with a comprehensive, computable taxonomy ». *Journal of Cheminformatics* 8 (1): 61. <https://doi.org/10.1186/s13321-016-0174-y>.
- Dodds, James N., et Erin S. Baker. 2019. « Ion Mobility Spectrometry: Fundamental Concepts, Instrumentation, Applications, and the Road Ahead ». *Journal of The American Society for Mass Spectrometry* 30 (11): 2185-95. <https://doi.org/10.1007/s13361-019-02288-2>.
- Dodds, James N., Jody C. May, et John A. McLean. 2017. « Correlating Resolving Power, Resolution, and Collision Cross Section: Unifying Cross-Platform Assessment of Separation Efficiency in Ion Mobility Spectrometry ». *Analytical Chemistry* 89 (22): 12176-84. <https://doi.org/10.1021/acs.analchem.7b02827>.
- Domalain, Virginie, Marie Hubert-Roux, Vincent Tognetti, Laurent Joubert, Catherine M. Lange, Jacques Rouden, et Carlos Afonso. 2014. « Enantiomeric Differentiation of Aromatic Amino Acids Using Traveling Wave Ion Mobility-Mass Spectrometry ». *Chemical Science* 5 (8): 3234-39. <https://doi.org/10.1039/C4SC00443D>.
- Donato, Paola, Daniele Giuffrida, Marianna Oteri, Veronica Inferrera, Paola Dugo, et Luigi Mondello. 2018. « Supercritical Fluid Chromatography × Ultra-High Pressure Liquid Chromatography for Red Chill Pepper Fingerprinting by Photodiode Array, Quadrupole-Time-of-Flight and Ion

- Mobility Mass Spectrometry (SFC × RP-UHPLC-PDA-Q-ToF MS-IMS) ». *Food Analytical Methods* 11 (12): 3331-41. <https://doi.org/10.1007/s12161-018-1307-x>.
- Drouin, Nicolas, Andreas Mielcarek, Christian Wenz, et Serge Rudaz. 2021. « Evaluation of Ion Mobility in Capillary Electrophoresis Coupled to Mass Spectrometry for the Identification in Metabolomics ». *ELECTROPHORESIS* 42 (4): 342-49. <https://doi.org/10.1002/elps.202000120>.
- Du, Xiaoxia, Yifei Wang, Hongda Zeng, Hao Zeng, Zhencheng Chen, et Hua Li. 2022. « High-Field Asymmetric Waveform Ion Mobility Spectrometry for Xylene Isomer Separation Assisted by Helium-Chemical Modifiers ». *Analytical Methods* 14 (45): 4649-58. <https://doi.org/10.1039/D2AY01098D>.
- Du, Zhumei, Lin Sun, Yanli Lin, Fuyu Yang, et Yimin Cai. 2022. « Using PacBio SMRT Sequencing Technology and Metabolomics to Explore the Microbiota-Metabolome Interaction Related to Silage Fermentation of Woody Plant ». *Frontiers in Microbiology* 13. <https://www.frontiersin.org/articles/10.3389/fmicb.2022.857431>.
- Duez, Q., F. Chirot, R. Lienard, T. Josse, C. Choi, O. Coulembier, P. Dugourd, J. Cornil, P. Gerbaux, et J. De Winter. 2017. « Polymers for Traveling Wave Ion Mobility Spectrometry Calibration ». *J Am Soc Mass Spectrom* 28 (11): 2483-91. <https://doi.org/10.1007/s13361-017-1762-4>.
- Dunn, Warwick B., et David. I. Ellis. 2005. « Metabolomics: Current Analytical Platforms and Methodologies ». *TrAC Trends in Analytical Chemistry* 24 (4): 285-94. <https://doi.org/10.1016/j.trac.2004.11.021>.
- Dwivedi, Prabha, Geoffery Puzon, Maggie Tam, Denis Langlais, Shelley Jackson, Kimberly Kaplan, William F. Siems, et al. 2010. « Metabolic Profiling of Escherichia Coli by Ion Mobility-Mass Spectrometry with MALDI Ion Source ». *Journal of Mass Spectrometry: JMS* 45 (12): 1383-93. <https://doi.org/10.1002/jms.1850>.
- Dwivedi, Prabha, Albert J. Schultz, et Herbert H. Hill Jr. 2010. « Metabolic Profiling of Human Blood by High-Resolution Ion Mobility Mass Spectrometry (IM-MS) ». *International Journal of Mass Spectrometry* 298 (1-3): 78-90. <https://doi.org/10.1016/j.ijms.2010.02.007>.
- Dwivedi, Prabha, Ching Wu, Laura M. Matz, Brian H. Clowers, William F. Siems, et Herbert H. Hill. 2006. « Gas-Phase Chiral Separations by Ion Mobility Spectrometry ». *Analytical Chemistry* 78 (24): 8200-8206. <https://doi.org/10.1021/ac0608772>.
- Eberlin, Livia S., Xiaohui Liu, Christina R. Ferreira, Sandro Santagata, Nathalie Y.R. Agar, et R. Graham Cooks. 2011. « Desorption Electrospray Ionization Then MALDI Mass Spectrometry Imaging of Lipid and Protein Distributions in Single Tissue Sections ». *Analytical Chemistry* 83 (22): 8366-71. <https://doi.org/10.1021/ac202016x>.
- Edwards, Alexis N., Hien M. Tran, et Elyssia S. Gallagher. 2021. « Propagating Error through Traveling-Wave Ion Mobility Calibration ». *Journal of the American Society for Mass Spectrometry* 32 (11): 2621-30. <https://doi.org/10.1021/jasms.1c00144>.
- Eiceman, G A, Z Karpas, et Herbert H Hill Jr. 2013. « Ion Mobility Spectrometry ».
- Einarsdottir, Eydis, Manuela Magnúsdóttir, Giuseppe Astarita, Matthias Köck, Helga M. Ögmundsdóttir, Margret Thorsteinsdóttir, Hans Tore Rapp, Sesselja Omarsdóttir, et Giuseppe Paglia. 2017. « Metabolic Profiling as a Screening Tool for Cytotoxic Compounds: Identification of 3-Alkyl Pyridine Alkaloids from Sponges Collected at a Shallow Water Hydrothermal Vent Site North of Iceland ». *Marine Drugs* 15 (2): 52. <https://doi.org/10.3390/md15020052>.
- Eldrid, Charles, et Konstantinos Thalassinou. 2020. « Developments in tandem ion mobility mass spectrometry ». *Biochemical Society Transactions* 48 (6): 2457-66. <https://doi.org/10.1042/BST20190788>.
- Elie, Nicolas, Cyrille Santerre, et David Touboul. 2019. « Generation of a Molecular Network from Electron Ionization Mass Spectrometry Data by Combining MZmine2 and MetGem Software ». *Analytical Chemistry* 91 (18): 11489-92. <https://doi.org/10.1021/acs.analchem.9b02802>.
- Ellis, Berkley M., Caleb N. Fischer, Leroy B. Martin, Brian O. Bachmann, et John A. McLean. 2019. « Spatiochemically Profiling Microbial Interactions with Membrane Scaffolded Desorption

- Electrospray Ionization-Ion Mobility-Imaging Mass Spectrometry and Unsupervised Segmentation ». *Analytical Chemistry* 91 (21): 13703-11. <https://doi.org/10.1021/acs.analchem.9b02992>.
- Ewing, Simon A., Micah T. Donor, Jesse W. Wilson, et James S. Prell. 2017. « Collidoscope: An Improved Tool for Computing Collisional Cross-Sections with the Trajectory Method ». *Journal of the American Society for Mass Spectrometry* 28 (4): 587-96. <https://doi.org/10.1007/s13361-017-1594-2>.
- Fahy, E., M. Sud, D. Cotter, et S. Subramaniam. 2007. « LIPID MAPS online tools for lipid research ». *Nucleic Acids Research* 35 (Web Server): W606-12. <https://doi.org/10.1093/nar/gkm324>.
- Fahy, Eoin, Dawn Cotter, Manish Sud, et Shankar Subramaniam. 2011. « Lipid Classification, Structures and Tools ». *Biochimica et Biophysica Acta (BBA) - Molecular and Cell Biology of Lipids, Lipidomics and Imaging Mass Spectrometry*, 1811 (11): 637-47. <https://doi.org/10.1016/j.bbalip.2011.06.009>.
- Fahy, Eoin, Shankar Subramaniam, H. Alex Brown, Christopher K. Glass, Alfred H. Merrill, Robert C. Murphy, Christian R. H. Raetz, et al. 2005. « A Comprehensive Classification System for Lipids1 ». *Journal of Lipid Research* 46 (5): 839-61. <https://doi.org/10.1194/jlr.E400004-JLR200>.
- Fani, Renato. 2012. « The Origin and Evolution of Metabolic Pathways: Why and How Did Primordial Cells Construct Metabolic Routes? ». *Evolution: Education and Outreach* 5 (3): 367-81. <https://doi.org/10.1007/s12052-012-0439-5>.
- Fernandez-Lima, Francisco, Desmond A. Kaplan, J. Suetering, et Melvin A. Park. 2011. « Gas-Phase Separation Using a Trapped Ion Mobility Spectrometer ». *International Journal for Ion Mobility Spectrometry* 14 (2): 93-98. <https://doi.org/10.1007/s12127-011-0067-8>.
- Fernandez-Maestre, Roberto. 2018. « Buffer Gas Additives (Modifiers/Shift Reagents) in Ion Mobility Spectrometry: Applications, Predictions of Mobility Shifts, and Influence of Interaction Energy and Structure ». *Journal of Mass Spectrometry* 53 (7): 598-613. <https://doi.org/10.1002/jms.4190>.
- Fernández-Maestre, Roberto, Ching Wu, et Herbert H. Hill Jr. 2012. « Buffer Gas Modifiers Effect Resolution in Ion Mobility Spectrometry through Selective Ion-Molecule Clustering Reactions ». *Rapid Communications in Mass Spectrometry* 26 (19): 2211-23. <https://doi.org/10.1002/rcm.6335>.
- Feuerstein, Max, Ruwan Kurulugama, Stephan Hann, et Tim Causon. 2021. « Novel acquisition strategies for metabolomics using drift tube ion mobility-quadrupole resolved all ions time-of-flight mass spectrometry (IM-QRAI-TOFMS) ». *Analytica Chimica Acta* 1163 (avril): 338508. <https://doi.org/10.1016/j.aca.2021.338508>.
- Feuerstein, Max L., Maykel Hernández-Mesa, Andrea Kiehne, Bruno Le Bizec, Stephan Hann, Gaud Dervilly, et Tim Causon. 2022. « Comparability of Steroid Collision Cross Sections Using Three Different IM-HRMS Technologies: An Interplatform Study ». *Journal of the American Society for Mass Spectrometry*, septembre. <https://doi.org/10.1021/jasms.2c00196>.
- Feuerstein, Max L., Maykel Hernández-Mesa, Younes Valadbeigi, Bruno Le Bizec, Stephan Hann, Gaud Dervilly, et Tim Causon. 2022. « Critical Evaluation of the Role of External Calibration Strategies for IM-MS ». *Analytical and Bioanalytical Chemistry*, août. <https://doi.org/10.1007/s00216-022-04263-5>.
- Fiehn, Oliver. 2002. « Metabolomics – the Link between Genotypes and Phenotypes ». *Plant Molecular Biology* 48 (1): 155-71. <https://doi.org/10.1023/A:1013713905833>.
- . 2016. « Metabolomics by Gas Chromatography-Mass Spectrometry: the combination of targeted and untargeted profiling ». *Current protocols in molecular biology / edited by Frederick M. Ausubel ... [et al.]* 114 (avril): 30.4.1-30.4.32. <https://doi.org/10.1002/0471142727.mb3004s114>.
- Fiehn, Oliver, Don Robertson, Jules Griffin, Mariet van der Werf, Basil Nikolau, Norman Morrison, Lloyd W. Sumner, et al. 2007. « The Metabolomics Standards Initiative (MSI) ». *Metabolomics* 3 (3): 175-78. <https://doi.org/10.1007/s11306-007-0070-6>.

- Fletcher, John S., Helen L. Kotze, Emily G. Armitage, Nicholas P. Lockyer, et John C. Vickerman. 2013. « Evaluating the Challenges Associated with Time-of-Fight Secondary Ion Mass Spectrometry for Metabolomics Using Pure and Mixed Metabolites ». *Metabolomics* 9 (3): 535-44. <https://doi.org/10.1007/s11306-012-0487-4>.
- Foged, Mads Møller, Kenji Maeda, et Mesut Bilgin. 2023. « Profiling the Mammalian Lipidome by Quantitative Shotgun Lipidomics ». In *Lipidomics: Methods and Protocols*, édité par Sanjoy K. Bhattacharya, 89-102. Methods in Molecular Biology. New York, NY: Springer US. https://doi.org/10.1007/978-1-0716-2966-6_8.
- Folch, Jordi, M. Lees, et G. H. Sloane Stanley. 1957. « A SIMPLE METHOD FOR THE ISOLATION AND PURIFICATION OF TOTAL LIPIDES FROM ANIMAL TISSUES ». *Journal of Biological Chemistry* 226 (1): 497-509. [https://doi.org/10.1016/S0021-9258\(18\)64849-5](https://doi.org/10.1016/S0021-9258(18)64849-5).
- Forsythe, Jay G., Anton S. Petrov, Chelsea A. Walker, Samuel J. Allen, Jarrod S. Pellissier, Matthew F. Bush, Nicholas V. Hud, et Facundo M. Fernández. 2015. « Collision Cross Section Calibrants for Negative Ion Mode Traveling Wave Ion Mobility-Mass Spectrometry ». *The Analyst* 140 (20): 6853-61. <https://doi.org/10.1039/C5AN00946D>.
- Fowble, Kristen L., Kanae Teramoto, Robert B. Cody, David Edwards, Donna Guarrera, et Rabi A. Musah. 2017. « Development of “Laser Ablation Direct Analysis in Real Time Imaging” Mass Spectrometry: Application to Spatial Distribution Mapping of Metabolites Along the Biosynthetic Cascade Leading to Synthesis of Atropine and Scopolamine in Plant Tissue ». *Analytical Chemistry* 89 (6): 3421-29. <https://doi.org/10.1021/acs.analchem.6b04137>.
- Franck, J, et R Pohl. 1908. « A method for the determination of the ionic mobility in small gas volumes ». *Ber. Phys. Ges* 9: 69-74.
- Fuhrer, Tobias, et Nicola Zamboni. 2015. « High-throughput discovery metabolomics ». *Current Opinion in Biotechnology, Analytical Biotechnology*, 31 (février): 73-78. <https://doi.org/10.1016/j.copbio.2014.08.006>.
- Futerman, Anthony H. 2021. « Chapter 9 - Sphingolipids ». In *Biochemistry of Lipids, Lipoproteins and Membranes (Seventh Edition)*, édité par Neale D. Ridgway et Roger S. McLeod, 281-316. Elsevier. <https://doi.org/10.1016/B978-0-12-824048-9.00009-2>.
- Gabelica, Valérie. 2021. « Ion Mobility -Mass Spectrometry: An Overview ». In *Ion Mobility-Mass Spectrometry:: Fundamentals and Applications*, édité par Frank Sobott et Alison Ashcroft, 1-25. New Developments in Mass Spectrometry. Royal Society of Chemistry. <https://doi.org/10.1039/9781839162886-00001>.
- Gabelica, Valérie, Carlos Afonso, Perdita Barran, Justin L P Benesch, Mansfield Road, Matthew F Bush, Iain D G Campuzano, Tim Causon, Brian H Clowers, et Colin S Creaser. 2019. « Recommendations for Reporting Ion Mobility Mass Spectrometry Measurements ». *Mass Spectrometry Reviews*, 59. <https://doi.org/10.1002/mas.21585>.
- Gabelica, Valérie, et Erik Marklund. 2018. « Fundamentals of Ion Mobility Spectrometry ». *Current Opinion in Chemical Biology* 42 (février): 51-59. <https://doi.org/10.1016/j.cbpa.2017.10.022>.
- Gao, Si-Qi, Jin-Hui Zhao, Yue Guan, Ying-Shu Tang, Ying Li, et Li-Yan Liu. 2023. « Mass Spectrometry Imaging Technology in Metabolomics: A Systematic Review ». *Biomedical Chromatography* 37 (7): e5494. <https://doi.org/10.1002/bmc.5494>.
- Gelb, Abby S., Rebecca E. Jarratt, Yuting Huang, et Eric D. Dodds. 2014. « A Study of Calibrant Selection in Measurement of Carbohydrate and Peptide Ion-Neutral Collision Cross Sections by Traveling Wave Ion Mobility Spectrometry ». *Analytical Chemistry* 86 (22): 11396-402. <https://doi.org/10.1021/ac503379e>.
- George, Anaïs C., Isabelle Schmitz-Afonso, Vincent Marie, Benoit Colsch, François Fenaille, Carlos Afonso, et Corinne Loutelier-Bourhis. 2022. « A Re-Calibration Procedure for Interoperable Lipid Collision Cross Section Values Measured by Traveling Wave Ion Mobility Spectrometry ». *Analytica Chimica Acta*, août, 340236. <https://doi.org/10.1016/j.aca.2022.340236>.
- Giacomini, Franck, Gildas Le Corguillé, Misharl Monsoor, Marion Landi, Pierre Pericard, Mélanie Pétéra, Christophe Duperier, et al. 2015. « Workflow4Metabolomics: a collaborative research

- infrastructure for computational metabolomics ». *Bioinformatics* 31 (9): 1493-95. <https://doi.org/10.1093/bioinformatics/btu813>.
- Gibson, Katherine, Dale A. Cooper-Shepherd, Edward Pallister, Sophie E. Inman, Sophie E. Jackson, et Viv Lindo. 2022. « Toward Rapid Aspartic Acid Isomer Localization in Therapeutic Peptides Using Cyclic Ion Mobility Mass Spectrometry ». *Journal of the American Society for Mass Spectrometry*, mai. <https://doi.org/10.1021/jasms.2c00053>.
- Giles, Kevin, Steven D. Pringle, Kenneth R. Worthington, David Little, Jason L. Wildgoose, et Robert H. Bateman. 2004. « Applications of a Travelling Wave-Based Radio-Frequency-Only Stacked Ring Ion Guide ». *Rapid Communications in Mass Spectrometry* 18 (20): 2401-14. <https://doi.org/10.1002/rcm.1641>.
- Giles, Kevin, Jakub Ujma, Jason Wildgoose, Steven Pringle, Keith Richardson, David Langridge, et Martin Green. 2019. « A Cyclic Ion Mobility-Mass Spectrometry System ». *Analytical Chemistry* 91 (13): 8564-73. <https://doi.org/10.1021/acs.analchem.9b01838>.
- Gil-Solsona, Rubén, Montse Raro, Carlos Sales, Leticia Lacalle, Ramon Díaz, María Ibáñez, Joaquim Beltran, Juan Vicente Sancho, et Felix J. Hernández. 2016. « Metabolomic Approach for Extra Virgin Olive Oil Origin Discrimination Making Use of Ultra-High Performance Liquid Chromatography – Quadrupole Time-of-Flight Mass Spectrometry ». *Food Control* 70 (décembre): 350-59. <https://doi.org/10.1016/j.foodcont.2016.06.008>.
- Godzien, Joanna, Michal Ciborowski, Luke Whiley, Cristina Legido-Quigley, Francisco J. Ruperez, et Coral Barbas. 2013. « In-Vial Dual Extraction Liquid Chromatography Coupled to Mass Spectrometry Applied to Streptozotocin-Treated Diabetic Rats. Tips and Pitfalls of the Method ». *Journal of Chromatography A* 1304 (août): 52-60. <https://doi.org/10.1016/j.chroma.2013.07.029>.
- Gong, Xinying, Shu Lin, Xiaoyu Huang, Sheng Peng, Minhui Shen, Sai Ouyang, Juan Zheng, Jianqiao Xu, et Gangfeng Ouyang. 2022. « Applications of in Vivo SPME Based on Mass Spectrometry for Environmental Pollutants Analysis and Non-Target Metabolomics: A Review ». *Green Analytical Chemistry* 1 (avril): 100004. <https://doi.org/10.1016/j.greeac.2022.100004>.
- Gonzales, Gerard Bryan, Guy Smagghe, Sofie Coelus, Dieter Adriaenssens, Karel De Winter, Tom Desmet, Katleen Raes, et John Van Camp. 2016. « Collision Cross Section Prediction of Deprotonated Phenolics in a Travelling-Wave Ion Mobility Spectrometer Using Molecular Descriptors and Chemometrics ». *Analytica Chimica Acta* 924 (juin): 68-76. <https://doi.org/10.1016/j.aca.2016.04.020>.
- González-Domínguez, Raúl, Tamara García-Barrera, et José Luis Gómez-Ariza. 2015. « Application of a Novel Metabolomic Approach Based on Atmospheric Pressure Photoionization Mass Spectrometry Using Flow Injection Analysis for the Study of Alzheimer's Disease ». *Talanta* 131 (janvier): 480-89. <https://doi.org/10.1016/j.talanta.2014.07.075>.
- González-Domínguez, Raúl, Álvaro González-Domínguez, Ana Sayago, et Ángeles Fernández-Recamales. 2020. « Recommendations and Best Practices for Standardizing the Pre-Analytical Processing of Blood and Urine Samples in Metabolomics ». *Metabolites* 10 (6): 229. <https://doi.org/10.3390/metabo10060229>.
- González-Domínguez, Raúl, Ana Sayago, et Ángeles Fernández-Recamales. 2017. « Direct infusion mass spectrometry for metabolomic phenotyping of diseases ». *Bioanalysis* 9 (1): 131-48. <https://doi.org/10.4155/bio-2016-0202>.
- Gordillo, Ruth. 2021. « Supercritical Fluid Chromatography Hyphenated to Mass Spectrometry for Metabolomics Applications ». *Journal of Separation Science* 44 (1): 448-63. <https://doi.org/10.1002/jssc.202000805>.
- Gosciny, Séverine, Michael McCullagh, Johann Far, Edwin De Pauw, et Gauthier Eppe. 2019. « Towards the Use of Ion Mobility Mass Spectrometry Derived Collision Cross Section as a Screening Approach for Unambiguous Identification of Targeted Pesticides in Food ». *Rapid Communications in Mass Spectrometry* 33 (S2): 34-48. <https://doi.org/10.1002/rcm.8395>.
- Gruending, Till, Volker Sauerland, César Barahona, Corinna Herz, et Ute Nitsch. 2016. « Polyalanine – a Practical Polypeptide Mass Calibration Standard for Matrix-Assisted Laser

- Desorption/Ionization Mass Spectrometry and Tandem Mass Spectrometry in Positive and Negative Mode ». *Rapid Communications in Mass Spectrometry* 30 (6): 681-83.
<https://doi.org/10.1002/rcm.7492>.
- Guasch-Ferré, Marta, Shilpa N Bhupathiraju, et Frank B Hu. 2018. « Use of Metabolomics in Improving Assessment of Dietary Intake ». *Clinical Chemistry* 64 (1): 82-98.
<https://doi.org/10.1373/clinchem.2017.272344>.
- Guevremont, Roger. 2004. « High-field asymmetric waveform ion mobility spectrometry: A new tool for mass spectrometry ». *Journal of Chromatography A, Mass Spectrometry: Innovation and Application. Part III*, 1058 (1): 3-19. <https://doi.org/10.1016/j.chroma.2004.08.119>.
- Guijas, Carlos, J. Rafael Montenegro-Burke, Benedikt Warth, Mary E. Spilker, et Gary Siuzdak. 2018. « Metabolomics Activity Screening for Identifying Metabolites That Modulate Phenotype ». *Nature Biotechnology* 36 (4): 316-20. <https://doi.org/10.1038/nbt.4101>.
- Habchi, Baninia, Sandra Alves, Alain Paris, Douglas N. Rutledge, et Estelle Rathahao-Paris. 2016. « How to Really Perform High Throughput Metabolomic Analyses Efficiently? » *TrAC Trends in Analytical Chemistry* 85 (décembre): 128-39. <https://doi.org/10.1016/j.trac.2016.09.005>.
- Haler, Jean R. N., Christopher Kune, Philippe Massonnet, Clothilde Comby-Zerbino, Jan Jordens, Maarten Honing, Ynze Mengerink, Johann Far, et Edwin De Pauw. 2017. « Comprehensive Ion Mobility Calibration: Poly(Ethylene Oxide) Polymer Calibrants and General Strategies ». *Analytical Chemistry* 89 (22): 12076-86. <https://doi.org/10.1021/acs.analchem.7b02564>.
- Han, Xianlin, et Richard W. Gross. 2005. « Shotgun Lipidomics: Electrospray Ionization Mass Spectrometric Analysis and Quantitation of Cellular Lipidomes Directly from Crude Extracts of Biological Samples ». *Mass Spectrometry Reviews* 24 (3): 367-412.
<https://doi.org/10.1002/mas.20023>.
- Hankin, Joseph A, Robert M Barkley, Karin Zemski-Berry, Yiming Deng, et Robert C Murphy. 2016. « Mass Spectrometric Collisional Activation and Product Ion Mobility of Human Serum Neutral Lipid Extracts ». *Analytical Chemistry* 88 (12): 6274-82.
<https://doi.org/10.1021/acs.analchem.6b00292>.
- Harrison, Julian A., Adam Pruška, Philipp Bittner, Alexander Muck, Dale A. Cooper-Shepherd, et Renato Zenobi. 2022. « Advancing Cyclic Ion Mobility Mass Spectrometry Methods for Studying Biomolecules: Toward the Conformational Dynamics of Mega Dalton Protein Aggregates ». *Analytical Chemistry*, septembre.
<https://doi.org/10.1021/acs.analchem.2c02406>.
- Hartler, Jürgen. 2015. « LipidHome ». In *Encyclopedia of Lipidomics*, édité par Markus R. Wenk, 1-3. Dordrecht: Springer Netherlands. https://doi.org/10.1007/978-94-007-7864-1_13-1.
- Harvey, David J., Max Crispin, Camille Bonomelli, et Jim H. Scrivens. 2015. « Ion Mobility Mass Spectrometry for Ion Recovery and Clean-Up of MS and MS/MS Spectra Obtained from Low Abundance Viral Samples ». *Journal of the American Society for Mass Spectrometry* 26 (10): 1754-67. <https://doi.org/10.1007/s13361-015-1163-5>.
- Harvey, David J., Yasunori Watanabe, Joel D. Allen, Pauline Rudd, Kevin Pagel, Max Crispin, et Weston B. Struwe. 2018. « Collision Cross Sections and Ion Mobility Separation of Fragment Ions from Complex N-Glycans ». *Journal of the American Society for Mass Spectrometry* 29 (6): 1250-61.
<https://doi.org/10.1007/s13361-018-1930-1>.
- He, Michelle Junyi, Wenjun Pu, Xi Wang, Wei Zhang, Donge Tang, et Yong Dai. 2022. « Comparing DESI-MSI and MALDI-MSI Mediated Spatial Metabolomics and Their Applications in Cancer Studies ». *Frontiers in Oncology* 12.
<https://www.frontiersin.org/articles/10.3389/fonc.2022.891018>.
- Hemmer, Selina, Sascha K. Manier, Svenja Fischmann, Folker Westphal, Lea Wagmann, et Markus R. Meyer. 2020. « Comparison of Three Untargeted Data Processing Workflows for Evaluating LC-HRMS Metabolomics Data ». *Metabolites* 10 (9): 378.
<https://doi.org/10.3390/metabo10090378>.
- Hernández-Mesa, Maykel, Valentina D'Atri, Gitte Barknowitz, Mathieu Fanuel, Julian Pezzatti, Nicola Dreolin, David Ropartz, et al. 2020. « Interlaboratory and Interplatform Study of Steroids

- Collision Cross Section by Traveling Wave Ion Mobility Spectrometry ». *Analytical Chemistry* 92 (7): 5013-22. <https://doi.org/10.1021/acs.analchem.9b05247>.
- Hernández-Mesa, Maykel, Fabrice Monteau, Bruno Le Bizec, et Gaud Dervilly-Pinel. 2019. « Potential of Ion Mobility-Mass Spectrometry for Both Targeted and Non-Targeted Analysis of Phase II Steroid Metabolites in Urine ». *Analytica Chimica Acta: X* 1 (mars): 100006. <https://doi.org/10.1016/j.acax.2019.100006>.
- Hernández-Mesa, Maykel, David Ropartz, Ana M. García-Campaña, Hélène Rogniaux, Gaud Dervilly-Pinel, et Bruno Le Bizec. 2019. « Ion Mobility Spectrometry in Food Analysis: Principles, Current Applications and Future Trends ». *Molecules* 24 (15): 2706. <https://doi.org/10.3390/molecules24152706>.
- Higgins Keppler, Emily A., Carrie L. Jenkins, Trenton J. Davis, et Heather D. Bean. 2018. « Advances in the Application of Comprehensive Two-Dimensional Gas Chromatography in Metabolomics ». *TrAC Trends in Analytical Chemistry* 109 (décembre): 275-86. <https://doi.org/10.1016/j.trac.2018.10.015>.
- Hines, Kelly M., Josi Herron, et Libin Xu. 2017. « Assessment of Altered Lipid Homeostasis by HILIC-Ion Mobility-Mass Spectrometry-Based Lipidomics ». *Journal of Lipid Research* 58 (4): 809-19. <https://doi.org/10.1194/jlr.D074724>.
- Hines, Kelly M., Jody C. May, John A. McLean, et Libin Xu. 2016. « Evaluation of Collision Cross Section Calibrants for Structural Analysis of Lipids by Traveling Wave Ion Mobility-Mass Spectrometry ». *Analytical Chemistry* 88 (14): 7329-36. <https://doi.org/10.1021/acs.analchem.6b01728>.
- Hinnenkamp, Vanessa, Julia Klein, Sven W. Meckelmann, Peter Balsaa, Torsten C. Schmidt, et Oliver J. Schmitz. 2018. « Comparison of CCS Values Determined by Traveling Wave Ion Mobility Mass Spectrometry and Drift Tube Ion Mobility Mass Spectrometry ». *Analytical Chemistry* 90 (20): 12042-50. <https://doi.org/10.1021/acs.analchem.8b02711>.
- Hofmann, J., H. S. Hahm, P. H. Seeberger, et K. Pagel. 2015. « Identification of Carbohydrate Anomers Using Ion Mobility–Mass Spectrometry ». *Nature* 526 (7572): 241-44. <https://doi.org/10.1038/nature15388>.
- Hofmann, Johanna, et Kevin Pagel. 2017. « Glycan Analysis by Ion Mobility–Mass Spectrometry ». *Angewandte Chemie International Edition* 56 (29): 8342-49. <https://doi.org/10.1002/anie.201701309>.
- Hofmann, Johanna, Weston B. Struwe, Charlotte A. Scarff, James H. Scrivens, David J. Harvey, et Kevin Pagel. 2014. « Estimating Collision Cross Sections of Negatively Charged *N*- Glycans Using Traveling Wave Ion Mobility-Mass Spectrometry ». *Analytical Chemistry* 86 (21): 10789-95. <https://doi.org/10.1021/ac5028353>.
- Hofmann, Johanna, Alexandra Stuckmann, Max Crispin, David J. Harvey, Kevin Pagel, et Weston B. Struwe. 2017. « Identification of Lewis and Blood Group Carbohydrate Epitopes by Ion Mobility-Tandem-Mass Spectrometry Fingerprinting ». *Analytical Chemistry* 89 (4): 2318-25. <https://doi.org/10.1021/acs.analchem.6b03853>.
- Hogan, Christopher J. Jr., Brandon T. Ruotolo, Carol V. Robinson, et Juan Fernandez de la Mora. 2011. « Tandem Differential Mobility Analysis-Mass Spectrometry Reveals Partial Gas-Phase Collapse of the GroEL Complex ». *The Journal of Physical Chemistry B* 115 (13): 3614-21. <https://doi.org/10.1021/jp109172k>.
- Hollerbach, Adam L., Yehia M. Ibrahim, Vanessa Meras, Randolph V. Norheim, Adam P. Huntley, Gordon A. Anderson, Thomas O. Metz, Robert G. Ewing, et Richard D. Smith. 2023. « A Dual-Gated Structures for Lossless Ion Manipulations-Ion Mobility Orbitrap Mass Spectrometry Platform for Combined Ultra-High-Resolution Molecular Analysis ». *Analytical Chemistry*, juin, [acs.analchem.3c00881](https://doi.org/10.1021/acs.analchem.3c00881). <https://doi.org/10.1021/acs.analchem.3c00881>.
- Hollerbach, Adam L., Ailin Li, Aneesh Prabhakaran, Gabe Nagy, Christopher P. Harrilal, Christopher R. Conant, Randolph V. Norheim, et al. 2020. « Ultra-High-Resolution Ion Mobility Separations Over Extended Path Lengths and Mobility Ranges Achieved using a Multilevel Structures for

- Lossless Ion Manipulations Module ». *Analytical Chemistry* 92 (11): 7972-79. <https://doi.org/10.1021/acs.analchem.0c01397>.
- Holm, Niels Bjerre, Maria Deryabina, Carsten Boye Knudsen, et Christian Janfelt. 2022. « Tissue Distribution and Metabolic Profiling of Cyclosporine (CsA) in Mouse and Rat Investigated by DESI and MALDI Mass Spectrometry Imaging (MSI) of Whole-Body and Single Organ Cryo-Sections ». *Analytical and Bioanalytical Chemistry* 414 (24): 7167-77. <https://doi.org/10.1007/s00216-022-04269-z>.
- Holman, Stephen W., Lynn McLean, et Claire E. Eyers. 2016. « RePLiCal: A QconCAT Protein for Retention Time Standardization in Proteomics Studies ». *Journal of Proteome Research* 15 (3): 1090-1102. <https://doi.org/10.1021/acs.jproteome.5b00988>.
- Holmes, Elaine, Ruey Leng Loo, Olivier Cloarec, Muireann Coen, Huiru Tang, Elaine Maibaum, Stephen Bruce, et al. 2007. « Detection of Urinary Drug Metabolite (Xenometabolome) Signatures in Molecular Epidemiology Studies via Statistical Total Correlation (NMR) Spectroscopy ». *Analytical chemistry* 79 (7): 2629-40. <https://doi.org/10.1021/ac062305n>.
- Horai, Hisayuki, Masanori Arita, Shigehiko Kanaya, Yoshito Nihei, Tasuku Ikeda, Kazuhiro Suwa, Yuya Ojima, et al. 2010. « MassBank: A Public Repository for Sharing Mass Spectral Data for Life Sciences ». *Journal of Mass Spectrometry* 45 (7): 703-14. <https://doi.org/10.1002/jms.1777>.
- Huang, Yuting, et Eric D. Dodds. 2015. « Discrimination of Isomeric Carbohydrates as the Electron Transfer Products of Group II Cation Adducts by Ion Mobility Spectrometry and Tandem Mass Spectrometry ». *Analytical Chemistry* 87 (11): 5664-68. <https://doi.org/10.1021/acs.analchem.5b00759>.
- Hupin, Sébastien, Hélène Lavanant, Séverine Renaudineau, Anna Proust, Guillaume Izzet, Michael Groessl, et Carlos Afonso. 2018. « A Calibration Framework for the Determination of Accurate Collision Cross Sections of Polyanions Using Polyoxometalate Standards ». *Rapid Communications in Mass Spectrometry* 32 (19): 1703-10. <https://doi.org/10.1002/rcm.8230>.
- Ibrahim, Yehia M., Erin S. Baker, William F. Danielson, Randolph V. Norheim, David C. Prior, Gordon A. Anderson, Mikhail E. Belov, et Richard D. Smith. 2015. « Development of a new ion mobility time-of-flight mass spectrometer ». *International Journal of Mass Spectrometry, Special Issue: MS 1960 to Now*, 377 (février): 655-62. <https://doi.org/10.1016/j.ijms.2014.07.034>.
- Ibrahim, Yehia M., Sandilya V. B. Garimella, Spencer A. Prost, Roza Wojcik, Randolph V. Norheim, Erin S. Baker, Ivan Rusyn, et Richard D. Smith. 2016. « Development of an Ion Mobility Spectrometry-Orbitrap Mass Spectrometer Platform ». *Analytical Chemistry* 88 (24): 12152-60. <https://doi.org/10.1021/acs.analchem.6b03027>.
- Jackson, Shelley N., Hay-Yan J. Wang, Amina S. Woods, Michael Ugarov, Thomas Egan, et J. Albert Schultz. 2005. « Direct tissue analysis of phospholipids in rat brain using MALDI-TOFMS and MALDI-ion mobility-TOFMS ». *Journal of the American Society for Mass Spectrometry* 16 (2): 133-38. <https://doi.org/10.1016/j.jasms.2004.10.002>.
- Jacob, Minnie, Andreas L. Lopata, Majed Dasouki, et Anas M. Abdel Rahman. 2019. « Metabolomics toward Personalized Medicine ». *Mass Spectrometry Reviews* 38 (3): 221-38. <https://doi.org/10.1002/mas.21548>.
- Jariyasopit, Narumol, Suphitcha Limjiasahapong, Alongkorn Kurilung, Sitanan Sartyoungkul, Pattipong Wisanpitayakorn, Narong Nuntasaeen, Chutima Kuhakarn, et al. 2022. « Traveling Wave Ion Mobility-Derived Collision Cross Section Database for Plant Specialized Metabolites: An Application to Ventilago harmandiana Pierre ». *Journal of Proteome Research* 21 (10): 2481-92. <https://doi.org/10.1021/acs.jproteome.2c00413>.
- Javahery, Gholamreza, et Bruce Thomson. 1997. « A Segmented Radiofrequency-Only Quadrupole Collision Cell for Measurements of Ion Collision Cross Section on a Triple Quadrupole Mass Spectrometer ». *Journal of the American Society for Mass Spectrometry* 8 (7): 697-702. [https://doi.org/10.1016/S1044-0305\(97\)00027-5](https://doi.org/10.1016/S1044-0305(97)00027-5).
- Jeanne Dit Fouque, Kevin, Cesar E. Ramirez, Russell L. Lewis, Jeremy P. Koelmel, Timothy J. Garrett, Richard A. Yost, et Francisco Fernandez-Lima. 2019. « Effective Liquid Chromatography–

- Trapped Ion Mobility Spectrometry–Mass Spectrometry Separation of Isomeric Lipid Species ». *Analytical Chemistry* 91 (8): 5021-27. <https://doi.org/10.1021/acs.analchem.8b04979>.
- Johnson, Caroline H., Julijana Ivanisevic, et Gary Siuzdak. 2016. « Metabolomics: Beyond Biomarkers and towards Mechanisms ». *Nature Reviews Molecular Cell Biology* 17 (7): 451-59. <https://doi.org/10.1038/nrm.2016.25>.
- Junot, Christophe, François Fenaille, Benoit Colsch, et François Bécher. 2014. « High Resolution Mass Spectrometry Based Techniques at the Crossroads of Metabolic Pathways: HIGH RESOLUTION MASS SPECTROMETRY FOR METABOLOMICS ». *Mass Spectrometry Reviews* 33 (6): 471-500. <https://doi.org/10.1002/mas.21401>.
- Kahsay, Getu, Huiying Song, Ann Van Schepdael, Deirdre Cabooter, et Erwin Adams. 2014. « Hydrophilic Interaction Chromatography (HILIC) in the Analysis of Antibiotics ». *Journal of Pharmaceutical and Biomedical Analysis, Review Papers on Pharmaceutical and Biomedical Analysis* 2013, 87 (janvier): 142-54. <https://doi.org/10.1016/j.jpba.2013.04.015>.
- Kailemia, Muchena J., Melvin Park, Desmond A. Kaplan, Andre Venot, Geert-Jan Boons, Lingyun Li, Robert J. Linhardt, et I. Jonathan Amster. 2014. « High-Field Asymmetric-Waveform Ion Mobility Spectrometry and Electron Detachment Dissociation of Isobaric Mixtures of Glycosaminoglycans ». *Journal of the American Society for Mass Spectrometry* 25 (2): 258-68. <https://doi.org/10.1007/s13361-013-0771-1>.
- Kartowikromo, Kimberly Y., Orobola E. Olajide, et Ahmed M. Hamid. 2023. « Collision Cross Section Measurement and Prediction Methods in Omics ». *Journal of Mass Spectrometry*, août, e4973. <https://doi.org/10.1002/jms.4973>.
- Kaszycki, Julia L., Aurelio La Rotta, Benoit Colsch, François Fenaille, Claire Dauly, Anas Kamleh, et Ching Wu. 2019. « Separation of Biologically Relevant Isomers on an Orbitrap Mass Spectrometer Using High-resolution Drift Tube Ion Mobility and Varied Drift Gas Mixtures ». *Rapid Communications in Mass Spectrometry* 33 (S2): 3-10. <https://doi.org/10.1002/rcm.8414>.
- Kaur-Atwal, Gushinder, Gavin O'Connor, Alexander A. Aksenov, Victor Bocos-Bintintan, C. L. Paul Thomas, et Colin S. Creaser. 2009. « Chemical Standards for Ion Mobility Spectrometry: A Review ». *International Journal for Ion Mobility Spectrometry* 12 (1): 1-14. <https://doi.org/10.1007/s12127-009-0021-1>.
- Keelor, Joel D., Stephen Zambrzycki, Anyin Li, Brian H. Clowers, et Facundo M. Fernández. 2017. « Atmospheric Pressure Drift Tube Ion Mobility–Orbitrap Mass Spectrometry: Initial Performance Characterization ». *Analytical Chemistry* 89 (21): 11301-9. <https://doi.org/10.1021/acs.analchem.7b01866>.
- Kell, Douglas B., et Stephen G. Oliver. 2004. « Here Is the Evidence, Now What Is the Hypothesis? The Complementary Roles of Inductive and Hypothesis-Driven Science in the Post-Genomic Era ». *BioEssays* 26 (1): 99-105. <https://doi.org/10.1002/bies.10385>.
- Kemperman, Robin H.J., Christopher D. Chouinard, et Richard A. Yost. 2023. « Characterization of Bile Acid Isomers and the Implementation of High-Resolution Demultiplexing with Ion Mobility-Mass Spectrometry ». *Journal of the American Society for Mass Spectrometry*, juin. <https://doi.org/10.1021/jasms.3c00143>.
- Kind, Tobias, et Oliver Fiehn. 2010. « Advances in structure elucidation of small molecules using mass spectrometry ». *Bioanalytical Reviews* 2 (1): 23-60. <https://doi.org/10.1007/s12566-010-0015-9>.
- Kind, Tobias, Kwang-Hyeon Liu, Do Yup Lee, Brian DeFelice, John K. Meissen, et Oliver Fiehn. 2013. « LipidBlast in Silico Tandem Mass Spectrometry Database for Lipid Identification ». *Nature Methods* 10 (8): 755-58. <https://doi.org/10.1038/nmeth.2551>.
- Kirkwood, Kaylie I., Brian S. Pratt, Nicholas Shulman, Kaipo Tamura, Michael J. MacCoss, Brendan X. MacLean, et Erin S. Baker. 2022. « Utilizing Skyline to Analyze Lipidomics Data Containing Liquid Chromatography, Ion Mobility Spectrometry and Mass Spectrometry Dimensions ». *Nature Protocols* 17 (11): 2415-30. <https://doi.org/10.1038/s41596-022-00714-6>.

- Knapman, Tom W., Joshua T. Berryman, Iain Campuzano, Sarah A. Harris, et Alison E. Ashcroft. 2010. « Considerations in Experimental and Theoretical Collision Cross-Section Measurements of Small Molecules Using Travelling Wave Ion Mobility Spectrometry-Mass Spectrometry ». *International Journal of Mass Spectrometry* 298 (1-3): 17-23. <https://doi.org/10.1016/j.ijms.2009.09.011>.
- Knittelfelder, Oskar L., Bernd P. Weberhofer, Thomas O. Eichmann, Sepp D. Kohlwein, et Gerald N. Rechberger. 2014. « A versatile ultra-high performance LC-MS method for lipid profiling ». *Journal of Chromatography. B, Analytical Technologies in the Biomedical and Life Sciences* 951-952 (mars): 119-28. <https://doi.org/10.1016/j.jchromb.2014.01.011>.
- Knorr, F. J., R. L. Eatherton, W. F. Siems, et H. H. Hill. 1985. « Fourier Transform Ion Mobility Spectrometry ». *Analytical Chemistry* 57 (2): 402-6. <https://doi.org/10.1021/ac50001a018>.
- Kodra, Dritan, Petros Pousinis, Panagiotis A. Vorkas, Katerina Kademoglou, Theodoros Liapikos, Alexandros Pechlivanis, Christina Virgiliou, Ian D. Wilson, Helen Gika, et Georgios Theodoridis. 2022. « Is Current Practice Adhering to Guidelines Proposed for Metabolite Identification in LC-MS Untargeted Metabolomics? A Meta-Analysis of the Literature ». *Journal of Proteome Research* 21 (3): 590-98. <https://doi.org/10.1021/acs.jproteome.1c00841>.
- Koeniger, Stormy L., Samuel I. Merenbloom, Stephen J. Valentine, Martin F. Jarrold, Harold R. Udseth, Richard D. Smith, et David E. Clemmer. 2006. « An IMS-IMS Analogue of MS-MS ». *Analytical Chemistry* 78 (12): 4161-74. <https://doi.org/10.1021/ac051060w>.
- Kontunen, Anton, Markus Karjalainen, Anna Anttalainen, Osmo Anttalainen, Mikko Koskenranta, Antti Vehkaoja, Niku Oksala, et Antti Roine. 2021. « Real Time Tissue Identification From Diathermy Smoke by Differential Mobility Spectrometry ». *IEEE Sensors Journal* 21 (1): 717-24. <https://doi.org/10.1109/JSEN.2020.3012965>.
- Kozole, Joseph, Jason R. Stairs, Inho Cho, Jason D. Harper, Stefan R. Lukow, Richard T. Lareau, Reno DeBono, et Frank Kuja. 2011. « Interfacing an Ion Mobility Spectrometry Based Explosive Trace Detector to a Triple Quadrupole Mass Spectrometer ». *Analytical Chemistry* 83 (22): 8596-8603. <https://doi.org/10.1021/ac201999a>.
- Krasny, Lukas, et Paul H. Huang. 2021. « Data-Independent Acquisition Mass Spectrometry (DIA-MS) for Proteomic Applications in Oncology ». *Molecular Omics* 17 (1): 29-42. <https://doi.org/10.1039/D0MO00072H>.
- Krylov, E. V. 2003. « Comparison of the planar and coaxial field asymmetrical waveform ion mobility spectrometer (FAIMS) ». *International Journal of Mass Spectrometry* 225 (1): 39-51. [https://doi.org/10.1016/S1387-3806\(02\)01037-0](https://doi.org/10.1016/S1387-3806(02)01037-0).
- Kurulugama, Ruwan T., Ed Darland, Frank Kuhlmann, George Stafford, et John Fjeldsted. 2015. « Evaluation of Drift Gas Selection in Complex Sample Analyses Using a High Performance Drift Tube Ion Mobility-QTOF Mass Spectrometer ». *Analyst* 140 (20): 6834-44. <https://doi.org/10.1039/C5AN00991J>.
- Labine, Lisa M., et Myrna J. Simpson. 2020. « The Use of Nuclear Magnetic Resonance (NMR) and Mass Spectrometry (MS)-Based Metabolomics in Environmental Exposure Assessment ». *Current Opinion in Environmental Science & Health, Environmental Toxicology: Exposomics: analytical challenges and emerging exposures*, 15 (juin): 7-15. <https://doi.org/10.1016/j.coesh.2020.01.008>.
- Laparre, Jérôme, Zied Kaabia, Mark Mooney, Tom Buckley, Mark Sherry, Bruno Le Bizec, et Gaud Dervilly-Pinel. 2017. « Impact of Storage Conditions on the Urinary Metabolomics Fingerprint ». *Analytica Chimica Acta* 951 (janvier): 99-107. <https://doi.org/10.1016/j.aca.2016.11.055>.
- Larriba, Carlos, et Christopher J. Hogan. 2013. « Free molecular collision cross section calculation methods for nanoparticles and complex ions with energy accommodation ». *Journal of Computational Physics* 251 (octobre): 344-63. <https://doi.org/10.1016/j.jcp.2013.05.038>.
- Larriba-Andaluz, Carlos, Juan Fernández-García, Michael A. Ewing, Christopher J. Hogan, et David E. Clemmer. 2015. « Gas Molecule Scattering & Ion Mobility Measurements for Organic Macro-

- Ions in He versus N₂ Environments ». *Physical Chemistry Chemical Physics* 17 (22): 15019-29. <https://doi.org/10.1039/C5CP01017A>.
- Leao, Tiago F., Chase M. Clark, Anelize Bauermeister, Emmanuel O. Elijah, Emily C. Gentry, Makhai Husband, Michelli F. Oliveira, Nuno Bandeira, Mingxun Wang, et Pieter C. Dorrestein. 2021. « Quick-Start Infrastructure for Untargeted Metabolomics Analysis in GNPS ». *Nature Metabolism* 3 (7): 880-82. <https://doi.org/10.1038/s42255-021-00429-0>.
- Leaprot, Katrina L., Jody C. May, James N. Dodds, et John A. McLean. 2019. « Ion Mobility Conformational Lipid Atlas for High Confidence Lipidomics ». *Nature Communications* 10 (1): 985. <https://doi.org/10.1038/s41467-019-08897-5>.
- Leggett, Abigail, Cheng Wang, Da-Wei Li, Arpad Somogyi, Lei Bruschweiler-Li, et Rafael Bruschweiler. 2019. « Chapter Eleven - Identification of Unknown Metabolomics Mixture Compounds by Combining NMR, MS, and Cheminformatics ». In *Methods in Enzymology*, édité par A. Joshua Wand, 615:407-22. Biological NMR Part B. Academic Press. <https://doi.org/10.1016/bs.mie.2018.09.003>.
- Lelli, Veronica, Antonio Belardo, Anna Maria Timperio, Veronica Lelli, Antonio Belardo, et Anna Maria Timperio. 2021. « From Targeted Quantification to Untargeted Metabolomics ». In *Metabolomics - Methodology and Applications in Medical Sciences and Life Sciences*. IntechOpen. <https://doi.org/10.5772/intechopen.96852>.
- Leng, Jiapeng, Qing Guan, Tuanqi Sun, Haoyang Wang, Jianlan Cui, Qinghao Liu, Zhixu Zhang, Manyu Zhang, et Yinlong Guo. 2015. « Direct infusion electrospray ionization–ion mobility–mass spectrometry for comparative profiling of fatty acids based on stable isotope labeling ». *Analytica Chimica Acta* 887 (août): 148-54. <https://doi.org/10.1016/j.aca.2015.06.029>.
- Lesur, Antoine, et Gunnar Dittmar. 2021. « The clinical potential of prm-PASEF mass spectrometry ». *Expert Review of Proteomics* 18 (2): 75-82. <https://doi.org/10.1080/14789450.2021.1908895>.
- Letertre, Marine P. M., Gaud Dervilly, et Patrick Giraudeau. 2021. « Combined Nuclear Magnetic Resonance Spectroscopy and Mass Spectrometry Approaches for Metabolomics ». *Analytical Chemistry* 93 (1): 500-518. <https://doi.org/10.1021/acs.analchem.0c04371>.
- Letertre, Marine P. M., Patrick Giraudeau, et Pascal de Tullio. 2021. « Nuclear Magnetic Resonance Spectroscopy in Clinical Metabolomics and Personalized Medicine: Current Challenges and Perspectives ». *Frontiers in Molecular Biosciences* 8. <https://www.frontiersin.org/articles/10.3389/fmolb.2021.698337>.
- Letunic, Ivica, Takuji Yamada, Minoru Kanehisa, et Peer Bork. 2008. « iPath: Interactive Exploration of Biochemical Pathways and Networks ». *Trends in Biochemical Sciences* 33 (3): 101-3. <https://doi.org/10.1016/j.tibs.2008.01.001>.
- Li, Ailin, Christopher R. Conant, Xueyun Zheng, Kent J. Bloodsworth, Daniel J. Orton, Sandilya V.B. Garimella, Isaac K. Attah, Gabe Nagy, Richard D. Smith, et Yehia M. Ibrahim. 2020. « Assessing Collision Cross Section Calibration Strategies for Traveling Wave-Based Ion Mobility Separations in Structures for Lossless Ion Manipulations ». *Analytical Chemistry* 92 (22): 14976-82. <https://doi.org/10.1021/acs.analchem.0c02829>.
- Li, Ailin, Gabe Nagy, Christopher R. Conant, Randolph V. Norheim, Joon Yong Lee, Cameron Giberson, Adam L. Hollerbach, et al. 2020. « Ion Mobility Spectrometry with High Ion Utilization Efficiency Using Traveling Wave-Based Structures for Lossless Ion Manipulations ». *Analytical Chemistry* 92 (22): 14930-38. <https://doi.org/10.1021/acs.analchem.0c02100>.
- Li, Amy, Kelly M. Hines, et Libin Xu. 2020. « Lipidomics by HILIC-Ion Mobility-Mass Spectrometry ». In *Ion Mobility-Mass Spectrometry : Methods and Protocols*, édité par Giuseppe Paglia et Giuseppe Astarita, 119-32. Methods in Molecular Biology. New York, NY: Springer US. https://doi.org/10.1007/978-1-0716-0030-6_7.
- Li, Bin, Junyue Ge, Wei Liu, Dejun Hu, et Ping Li. 2021. « Unveiling Spatial Metabolome of Paeonia Suffruticosa and Paeonia Lactiflora Roots Using MALDI MS Imaging ». *New Phytologist* 231 (2): 892-902. <https://doi.org/10.1111/nph.17393>.
- Li, Li, Kristin R. McKenna, Zhao Li, Mahipal Yadav, Ramanarayanan Krishnamurthy, Charles L. Liotta, et Facundo M. Fernández. 2018. « Rapid Resolution of Carbohydrate Isomers via Multi-Site

- Derivatization Ion Mobility-Mass Spectrometry ». *Analyst* 143 (4): 949-55.
<https://doi.org/10.1039/C7AN01796K>.
- Li, Shubo, Yufeng Tian, Pingyingzi Jiang, Ying Lin, Xiaoling Liu, et Hongshun Yang. 2021. « Recent advances in the application of metabolomics for food safety control and food quality analyses ». *Critical Reviews in Food Science and Nutrition* 61 (9): 1448-69.
<https://doi.org/10.1080/10408398.2020.1761287>.
- Li, Xiaohang, Hongda Wang, Meiting Jiang, Mengxiang Ding, Xiaoyan Xu, Bei Xu, Yadan Zou, Yuetong Yu, et Wenzhi Yang. 2023. « Collision Cross Section Prediction Based on Machine Learning ». *Molecules* 28 (10): 4050. <https://doi.org/10.3390/molecules28104050>.
- Liebisch, Gerhard, Eoin Fahy, Junken Aoki, Edward A. Dennis, Thierry Durand, Christer S. Ejsing, Maria Fedorova, et al. 2020. « Update on LIPID MAPS Classification, Nomenclature, and Shorthand Notation for MS-Derived Lipid Structures ». *Journal of Lipid Research* 61 (12): 1539-55.
<https://doi.org/10.1194/jlr.S120001025>.
- Lin, Yanping, Gary W. Caldwell, Ying Li, Wensheng Lang, et John Masucci. 2020. « Inter-Laboratory Reproducibility of an Untargeted Metabolomics GC–MS Assay for Analysis of Human Plasma ». *Scientific Reports* 10 (1): 10918. <https://doi.org/10.1038/s41598-020-67939-x>.
- Lísa, Miroslav, Eva Cífková, Maria Khalikova, Magdaléna Ovčáčíková, et Michal Holčápek. 2017. « Lipidomic Analysis of Biological Samples: Comparison of Liquid Chromatography, Supercritical Fluid Chromatography and Direct Infusion Mass Spectrometry Methods ». *Journal of Chromatography A* 1525 (novembre): 96-108.
<https://doi.org/10.1016/j.chroma.2017.10.022>.
- Liu, Fanny C., Samuel R. Kirk, Kirsten A. Caldwell, Thais Pedrete, Florian Meier, et Christian Bleiholder. 2022. « Tandem Trapped Ion Mobility Spectrometry/Mass Spectrometry (tTIMS/MS) Reveals Sequence-Specific Determinants of Top-Down Protein Fragment Ion Cross Sections ». *Analytical Chemistry* 94 (23): 8146-55. <https://doi.org/10.1021/acs.analchem.1c05171>.
- Liu, Fanny C., Mark E. Ridgeway, Melvin A. Park, et Christian Bleiholder. 2018. « Tandem Trapped Ion Mobility Spectrometry ». *The Analyst* 143 (10): 2249-58.
<https://doi.org/10.1039/C7AN02054F>.
- . 2022. « Tandem-Trapped Ion Mobility Spectrometry/Mass Spectrometry (t TIMS/MS): A Promising Analytical Method for Investigating Heterogenous Samples ». *The Analyst*, 10.1039.D2AN00335J. <https://doi.org/10.1039/D2AN00335J>.
- Liu, Rui, Jing Chou, Shaoying Hou, Xiaowei Liu, Jiaying Yu, Xinshu Zhao, Ying Li, Liyan Liu, et Changhao Sun. 2018. « Evaluation of Two-Step Liquid-Liquid Extraction Protocol for Untargeted Metabolic Profiling of Serum Samples to Achieve Broader Metabolome Coverage by UPLC-Q-TOF-MS ». *Analytica Chimica Acta* 1035 (décembre): 96-107.
<https://doi.org/10.1016/j.aca.2018.07.034>.
- Liu, Xinyu, Miriam Hoene, Xiaolin Wang, Peiyuan Yin, Hans-Ulrich Häring, Guowang Xu, et Rainer Lehmann. 2018. « Serum or Plasma, What Is the Difference? Investigations to Facilitate the Sample Material Selection Decision Making Process for Metabolomics Studies and Beyond ». *Analytica Chimica Acta, Analytical Metabolomics*, 1037 (décembre): 293-300.
<https://doi.org/10.1016/j.aca.2018.03.009>.
- Llorach, Rafael, Ignacio Garrido, María Monagas, Mireia Urpi-Sarda, Sara Tulipani, Begoña Bartolome, et Cristina Andres-Lacueva. 2010. « Metabolomics Study of Human Urinary Metabolome Modifications After Intake of Almond (*Prunus dulcis* (Mill.) D.A. Webb) Skin Polyphenols ». *Journal of Proteome Research* 9 (11): 5859-67. <https://doi.org/10.1021/pr100639v>.
- López-Bascón, M. A., F. Priego-Capote, A. Peralbo-Molina, M. Calderón-Santiago, et M. D. Luque de Castro. 2016. « Influence of the Collection Tube on Metabolomic Changes in Serum and Plasma ». *Talanta* 150 (avril): 681-89. <https://doi.org/10.1016/j.talanta.2015.12.079>.
- López-Hernández, Yamilé, Joel Monárrez-Espino, Ana-Sofía Herrera-van Oostdam, Julio Enrique Castañeda Delgado, Lun Zhang, Jiamin Zheng, Juan José Oropeza Valdez, et al. 2021. « Targeted Metabolomics Identifies High Performing Diagnostic and Prognostic Biomarkers

- for COVID-19 ». *Scientific Reports* 11 (1): 14732. <https://doi.org/10.1038/s41598-021-94171-y>.
- Ma, Xin, et Facundo M. Fernández. 2022. « Advances in Mass Spectrometry Imaging for Spatial Cancer Metabolomics ». *Mass Spectrometry Reviews* n/a (n/a): e21804. <https://doi.org/10.1002/mas.21804>.
- MacLean, Brendan X., Brian S. Pratt, Jarrett D. Egertson, Michael J. MacCoss, Richard D. Smith, et Erin S. Baker. 2018. « Using Skyline to Analyze Data-Containing Liquid Chromatography, Ion Mobility Spectrometry, and Mass Spectrometry Dimensions ». *Journal of The American Society for Mass Spectrometry* 29 (11): 2182-88. <https://doi.org/10.1007/s13361-018-2028-5>.
- MacNeil, Amber, Xiaolei Li, Roshanak Amiri, Derek C. G. Muir, Andre Simpson, Myrna J. Simpson, Frank L. Dorman, et Karl J. Jobst. 2022. « Gas Chromatography-(Cyclic) Ion Mobility Mass Spectrometry: A Novel Platform for the Discovery of Unknown Per-/Polyfluoroalkyl Substances ». *Analytical Chemistry* 94 (31): 11096-103. <https://doi.org/10.1021/acs.analchem.2c02325>.
- Maillard, Julien F., Johann Le Maître, Christopher P. Rüger, Mark Ridgeway, Christopher J. Thompson, Benoit Paupy, Marie Hubert-Roux, Melvin Park, Carlos Afonso, et Pierre Giusti. 2021. « Structural Analysis of Petroporphyrins from Asphaltene by Trapped Ion Mobility Coupled with Fourier Transform Ion Cyclotron Resonance Mass Spectrometry ». *Analyst* 146 (13): 4161-71. <https://doi.org/10.1039/D1AN00140J>.
- Maillard, Julien, Sébastien Hupin, Nathalie Carrasco, Isabelle Schmitz-Afonso, Thomas Gautier, et Carlos Afonso. 2020. « Structural Elucidation of Soluble Organic Matter: Application to Titan's Haze ». *Icarus* 340 (avril): 113627. <https://doi.org/10.1016/j.icarus.2020.113627>.
- Manz, Christian, Michael Götze, Clemens Frank, Andreas Zappe, et Kevin Pagel. 2022. « Dextran as Internal Calibrant for N-Glycan Analysis by Liquid Chromatography Coupled to Ion Mobility-Mass Spectrometry ». *Analytical and Bioanalytical Chemistry*, mai. <https://doi.org/10.1007/s00216-022-04133-0>.
- Manz, Christian, et Kevin Pagel. 2018. « Glycan analysis by ion mobility-mass spectrometry and gas-phase spectroscopy ». *Current Opinion in Chemical Biology, Omics*, 42 (février): 16-24. <https://doi.org/10.1016/j.cbpa.2017.10.021>.
- Margaryan, Tigran, Mariam Sargsyan, Arpine Gevorgyan, Hasmik Zakaryan, Armine Aleksanyan, Armen Harutyunyan, Yeghig Armoudjian, et Astghik Mikayelyan. 2020. « High-Throughput Protein Precipitation Method with 96-Well Plate for Determination of Doxepin and Nordoxepin in Human Plasma Using LC-MS/MS ». *Biomedical Chromatography* 34 (8): e4844. <https://doi.org/10.1002/bmc.4844>.
- Masike, Keabetswe, Maria A. Stander, et André de Villiers. 2021. « Recent Applications of Ion Mobility Spectrometry in Natural Product Research ». *Journal of Pharmaceutical and Biomedical Analysis* 195 (février): 113846. <https://doi.org/10.1016/j.jpba.2020.113846>.
- Mason, E. A. ; Shamp Jr. 1958. « Mobility of gaseous ions in weak electric fields ». *Annals of physics*, 4, 233-270.
- Matyash, Vitali, Gerhard Liebisch, Teymuraz V. Kurzchalia, Andrej Shevchenko, et Dominik Schwudke. 2008. « Lipid Extraction by Methyl-Tert-Butyl Ether for High-Throughput Lipidomics[†] ». *Journal of Lipid Research* 49 (5): 1137-46. <https://doi.org/10.1194/jlr.D700041-JLR200>.
- May, Jody C., Cody R. Goodwin, Nichole M. Lareau, Katrina L. Leaptrot, Caleb B. Morris, Ruwan T. Kurulugama, Alex Mordehai, et al. 2014. « Conformational Ordering of Biomolecules in the Gas Phase: Nitrogen Collision Cross Sections Measured on a Prototype High Resolution Drift Tube Ion Mobility-Mass Spectrometer ». *Analytical Chemistry* 86 (4): 2107-16. <https://doi.org/10.1021/ac4038448>.
- May, Jody C., Richard Knochenmuss, John C. Fjeldsted, et John A. McLean. 2020. « Resolution of Isomeric Mixtures in Ion Mobility Using a Combined Demultiplexing and Peak Deconvolution Technique ». *Analytical Chemistry* 92 (14): 9482-92. <https://doi.org/10.1021/acs.analchem.9b05718>.

- May, Jody C., et John A. McLean. 2013. « The Influence of Drift Gas Composition on the Separation Mechanism in Traveling Wave Ion Mobility Spectrometry: Insight from Electrodynamics Simulations ». *International Journal for Ion Mobility Spectrometry* 16 (2): 85-94. <https://doi.org/10.1007/s12127-013-0123-7>.
- . 2015. « Ion Mobility-Mass Spectrometry: Time-Dispersive Instrumentation ». *Analytical Chemistry* 87 (3): 1422-36. <https://doi.org/10.1021/ac504720m>.
- . 2016. « Advanced Multidimensional Separations in Mass Spectrometry: Navigating the Big Data Deluge ». *Annual Review of Analytical Chemistry* 9 (1): 387-409. <https://doi.org/10.1146/annurev-anchem-071015-041734>.
- . 2022. « Integrating Ion Mobility into Comprehensive Multidimensional Metabolomics Workflows: Critical Considerations ». *Metabolomics* 18 (12): 104. <https://doi.org/10.1007/s11306-022-01961-0>.
- May, Jody C., Caleb B. Morris, et John A. McLean. 2017. « Ion Mobility Collision Cross Section Compendium ». *Analytical Chemistry* 89 (2): 1032-44. <https://doi.org/10.1021/acs.analchem.6b04905>.
- Meckelmann, Sven, Pia Wittenhofer, Kristina Tötsch, et Oliver Schmitz. 2022. « Supercritical Fluid Chromatography Coupled with Drift Time Ion Mobility Quadrupole Time-of-Flight Mass Spectrometry as a Tool for Lipid Characterization of HepG2 Cells ». *LCGC Europe*, June 2022, 35 (6): 207-12.
- Meier, Florian, Scarlet Beck, Niklas Grassl, Markus Lubeck, Melvin A. Park, Oliver Raether, et Matthias Mann. 2015. « Parallel Accumulation–Serial Fragmentation (PASEF): Multiplying Sequencing Speed and Sensitivity by Synchronized Scans in a Trapped Ion Mobility Device ». *Journal of Proteome Research* 14 (12): 5378-87. <https://doi.org/10.1021/acs.jproteome.5b00932>.
- Meier, Florian, Andreas-David Brunner, Max Frank, Annie Ha, Isabell Bludau, Eugenia Voytik, Stephanie Kaspar-Schoenefeld, et al. 2020. « diaPASEF: Parallel Accumulation–Serial Fragmentation Combined with Data-Independent Acquisition ». *Nature Methods* 17 (12): 1229-36. <https://doi.org/10.1038/s41592-020-00998-0>.
- Mendes Siqueira, Anna Luiza, Mathieu Beaumesnil, Marie Hubert-Roux, Corinne Loutelier-Bourhis, Carlos Afonso, Yang Bai, Marion Courtiade, et Amandine Racaud. 2018. « Atmospheric Solid Analysis Probe Coupled to Ion Mobility Spectrometry-Mass Spectrometry, a Fast and Simple Method for Polyalphaolefin Characterization ». *Journal of the American Society for Mass Spectrometry* 29 (8): 1678-87. <https://doi.org/10.1007/s13361-018-1991-1>.
- Merenbloom, Samuel I., Rebecca S. Glaskin, Zachary B. Henson, et David E. Clemmer. 2009. « High-Resolution Ion Cyclotron Mobility Spectrometry ». *Analytical chemistry* 81 (4): 1482-87. <https://doi.org/10.1021/ac801880a>.
- Merenbloom, Samuel I., Stormy L. Koeniger, Brian C. Bohrer, Stephen J. Valentine, et David E. Clemmer. 2008. « Improving the Efficiency of IMS–IMS by a Combing Technique ». *Analytical Chemistry* 80 (6): 1918-27. <https://doi.org/10.1021/ac7018602>.
- Mesleh, M. F., J. M. Hunter, A. A. Shvartsburg, G. C. Schatz, et M. F. Jarrold. 1996. « Structural Information from Ion Mobility Measurements: Effects of the Long-Range Potential ». *The Journal of Physical Chemistry* 100 (40): 16082-86. <https://doi.org/10.1021/jp961623v>.
- Michelmann, Karsten, Joshua A. Silveira, Mark E. Ridgeway, et Melvin A. Park. 2015. « Fundamentals of Trapped Ion Mobility Spectrometry ». *Journal of the American Society for Mass Spectrometry* 26 (1): 14-24. <https://doi.org/10.1007/s13361-014-0999-4>.
- Michopoulos, Filippou, Antony M. Edge, Georgios Theodoridis, et Ian D. Wilson. 2010. « Application of Turbulent Flow Chromatography to the Metabonomic Analysis of Human Plasma: Comparison with Protein Precipitation ». *Journal of Separation Science* 33 (10): 1472-79. <https://doi.org/10.1002/jssc.200900789>.
- Millar, Joshua, Ema Ozaki, Susan Campbell, Catherine Duckett, Sarah Doyle, et Laura M. Cole. 2022. « Multiomic Mass Spectrometry Imaging to Advance Future Pathological Understanding of Ocular Disease ». *Metabolites* 12 (12): 1239. <https://doi.org/10.3390/metabo12121239>.

- Miller, Rebecca L., Scott E. Guimond, Ralf Schwörer, Olga V. Zubkova, Peter C. Tyler, Yongmei Xu, Jian Liu, et al. 2020. « Shotgun Ion Mobility Mass Spectrometry Sequencing of Heparan Sulfate Saccharides ». *Nature Communications* 11 (1): 1481. <https://doi.org/10.1038/s41467-020-15284-y>.
- Misra, Biswapriya B. 2021. « New Software Tools, Databases, and Resources in Metabolomics: Updates from 2020 ». *Metabolomics* 17 (5): 49. <https://doi.org/10.1007/s11306-021-01796-1>.
- Misra, Biswapriya B, et Michael Olivier. 2020. « High Resolution GC-Orbitrap-MS Metabolomics Using Both Electron Ionization and Chemical Ionization for Analysis of Human Plasma ». *J. Proteome Res.*, 15.
- M. Kolakowski, Beata, et Zoltán Mester. 2007. « Review of Applications of High-Field Asymmetric Waveform Ion Mobility Spectrometry (FAIMS) and Differential Mobility Spectrometry (DMS) ». *Analyst* 132 (9): 842-64. <https://doi.org/10.1039/B706039D>.
- Moco, Sofia. 2022. « Studying Metabolism by NMR-Based Metabolomics ». *Frontiers in Molecular Biosciences* 9. <https://www.frontiersin.org/articles/10.3389/fmolb.2022.882487>.
- Morris, Caleb B., Jody C. May, Katrina L. Leaptrot, et John A. McLean. 2019. « Evaluating Separation Selectivity and Collision Cross Section Measurement Reproducibility in Helium, Nitrogen, Argon, and Carbon Dioxide Drift Gases for Drift Tube Ion Mobility–Mass Spectrometry ». *Journal of the American Society for Mass Spectrometry* 30 (6): 1059-68. <https://doi.org/10.1007/s13361-019-02151-4>.
- Morrison, Kelsey A., William F. Siems, et Brian H. Clowers. 2016. « Augmenting Ion Trap Mass Spectrometers Using a Frequency Modulated Drift Tube Ion Mobility Spectrometer ». *Analytical Chemistry* 88 (6): 3121-29. <https://doi.org/10.1021/acs.analchem.5b04223>.
- Mortensen, Daniel N., Anna C. Susa, et Evan R. Williams. 2017. « Collisional Cross-Sections with T-Wave Ion Mobility Spectrometry without Experimental Calibration ». *Journal of The American Society for Mass Spectrometry* 28 (7): 1282-92. <https://doi.org/10.1007/s13361-017-1669-0>.
- Morze, Jakub, Clemens Wittenbecher, Lukas Schwingshackl, Anna Danielewicz, Andrzej Rynkiewicz, Frank B. Hu, et Marta Guasch-Ferré. 2022. « Metabolomics and Type 2 Diabetes Risk: An Updated Systematic Review and Meta-analysis of Prospective Cohort Studies ». *Diabetes Care* 45 (4): 1013-24. <https://doi.org/10.2337/dc21-1705>.
- Mun, Dong-Gi, Rohit Budhreja, Firdous A. Bhat, Roman M. Zenka, Kenneth L. Johnson, Abhay Moghekar, et Akhilesh Pandey. 2022. « Four-Dimensional Proteomics Analysis of Human Cerebrospinal Fluid with Trapped Ion Mobility Spectrometry Using PASEF ». *PROTEOMICS* n/a (n/a): 2200507. <https://doi.org/10.1002/pmic.202200507>.
- Mushtaq, Mian Yahya, Young Hae Choi, Robert Verpoorte, et Erica G. Wilson. 2014. « Extraction for Metabolomics: Access to The Metabolome ». *Phytochemical Analysis* 25 (4): 291-306. <https://doi.org/10.1002/pca.2505>.
- Nakayasu, Ernesto S., Carrie D. Nicora, Amy C. Sims, Kristin E. Burnum-Johnson, Young-Mo Kim, Jennifer E. Kyle, Melissa M. Matzke, et al. 2016. « MPLEx: A Robust and Universal Protocol for Single-Sample Integrative Proteomic, Metabolomic, and Lipidomic Analyses ». *mSystems* 1 (3): e00043-16. <https://doi.org/10.1128/mSystems.00043-16>.
- Nam, Seo Lin, Kieran Tarazona Carrillo, A. Paulina de la Mata, Olle M. de Bruin, Evgueni Doukhanine, et James Harynuk. 2022. « Evaluation of Fresh, Frozen, and Lyophilized Fecal Samples by SPME and Derivatization Methods Using GC×GC-TOFMS ». *Metabolomics* 18 (4): 25. <https://doi.org/10.1007/s11306-022-01881-z>.
- Naznin, Marufa, Md Badrul Alam, Rafiqul Alam, Syful Islam, Sultonov Rakhmat, Sang-Han Lee, et Sunghwan Kim. 2023. « Metabolite Profiling of *Nymphaea Rubra* (Burm. f.) Flower Extracts Using Cyclic Ion Mobility–Mass Spectrometry and Their Associated Biological Activities ». *Food Chemistry* 404 (mars): 134544. <https://doi.org/10.1016/j.foodchem.2022.134544>.
- Neumann, Elizabeth K., Lukasz G. Migas, Jamie L. Allen, Richard M. Caprioli, Raf Van de Plas, et Jeffrey M. Spraggins. 2020. « Spatial Metabolomics of the Human Kidney using MALDI Trapped Ion

- Mobility Imaging Mass Spectrometry ». *Analytical Chemistry* 92 (19): 13084-91. <https://doi.org/10.1021/acs.analchem.0c02051>.
- Nichols, Charles M., James N. Dodds, Bailey S. Rose, Jaqueline A. Picache, Caleb B. Morris, Simona G. Codreanu, Jody C. May, Stacy D. Sherrod, et John A. McLean. 2018. « Untargeted Molecular Discovery in Primary Metabolism: Collision Cross Section as a Molecular Descriptor in Ion Mobility-Mass Spectrometry ». *Analytical Chemistry* 90 (24): 14484-92. <https://doi.org/10.1021/acs.analchem.8b04322>.
- Nikolaichuk, Hanna, Kacper Przykaza, Anna Kozub, Magdalena Montowska, Grażyna Wójcicka, Jolanta Tomaszewska-Gras, et Emilia Fornal. 2022. « Shotgun Lipidomic Analysis for Differentiation of Niche Cold Pressed Oils ». *Molecules* 27 (6): 1848. <https://doi.org/10.3390/molecules27061848>.
- Nordberg, Gunnar F. 2010. « Biomarkers of Exposure, Effects and Susceptibility in Humans and Their Application in Studies of Interactions among Metals in China ». *Toxicology Letters*, ISBM-7: Biological Monitoring in a Globalized World, 192 (1): 45-49. <https://doi.org/10.1016/j.toxlet.2009.06.859>.
- Nordström, Anders, Elizabeth Want, Trent Northen, Janne Lehtiö, et Gary Siuzdak. 2008. « Multiple Ionization Mass Spectrometry Strategy Used To Reveal the Complexity of Metabolomics ». *Analytical Chemistry* 80 (2): 421-29. <https://doi.org/10.1021/ac701982e>.
- Nye, Leanne C., Jonathan P. Williams, Nyasha C. Munjoma, Marine P.M. Letertre, Muireann Coen, Robbin Bouwmeester, Lennart Martens, et al. 2019. « A Comparison of Collision Cross Section Values Obtained via Travelling Wave Ion Mobility-Mass Spectrometry and Ultra High Performance Liquid Chromatography-Ion Mobility-Mass Spectrometry: Application to the Characterisation of Metabolites in Rat Urine ». *Journal of Chromatography A* 1602 (septembre): 386-96. <https://doi.org/10.1016/j.chroma.2019.06.056>.
- Odenkirk, Melanie T., et Erin S. Baker. 2020. « Utilizing Drift Tube Ion Mobility Spectrometry for the Evaluation of Metabolites and Xenobiotics ». *Methods in Molecular Biology (Clifton, N.J.)* 2084: 35-54. https://doi.org/10.1007/978-1-0716-0030-6_2.
- Oliinyk, Denys, et Florian Meier. 2023. « Ion Mobility-Resolved Phosphoproteomics with Dia-PASEF and Short Gradients ». *PROTEOMICS* 23 (7-8): 2200032. <https://doi.org/10.1002/pmic.202200032>.
- Oliver, Stephen G., Michael K. Winson, Douglas B. Kell, et Frank Baganz. 1998. « Systematic Functional Analysis of the Yeast Genome ». *Trends in Biotechnology* 16 (9): 373-78. [https://doi.org/10.1016/S0167-7799\(98\)01214-1](https://doi.org/10.1016/S0167-7799(98)01214-1).
- Ollivier, Simon, Mathieu Fanuel, Hélène Rogniaux, et David Ropartz. 2021. « Molecular Networking of High-Resolution Tandem Ion Mobility Spectra: A Structurally Relevant Way of Organizing Data in Glycomics? ». *Analytical Chemistry* 93 (31): 10871-78. <https://doi.org/10.1021/acs.analchem.1c01244>.
- . 2022. « Using a Cyclic Ion Mobility Spectrometer for Tandem Ion Mobility Experiments ». *Journal of Visualized Experiments: JoVE*, n° 179 (janvier). <https://doi.org/10.3791/63451>.
- Ouyang, Hui, Carlos Larriba-Andaluz, Derek R. Oberreit, et Christopher J. Hogan. 2013. « The Collision Cross Sections of Iodide Salt Cluster Ions in Air via Differential Mobility Analysis-Mass Spectrometry ». *Journal of the American Society for Mass Spectrometry* 24 (12): 1833-47. <https://doi.org/10.1007/s13361-013-0724-8>.
- Pacini, Tommaso, Weiqi Fu, Steinn Gudmundsson, A. Eugenio Chiaravalle, Sigurdur Brynjolfson, Bernhard O. Palsson, Giuseppe Astarita, et Giuseppe Paglia. 2015. « Multidimensional Analytical Approach Based on UHPLC-UV-Ion Mobility-MS for the Screening of Natural Pigments ». *Analytical Chemistry* 87 (5): 2593-99. <https://doi.org/10.1021/ac504707n>.
- Pagel, Kevin, et David J. Harvey. 2013. « Ion Mobility–Mass Spectrometry of Complex Carbohydrates: Collision Cross Sections of Sodiated N-linked Glycans ». *Analytical Chemistry* 85 (10): 5138-45. <https://doi.org/10.1021/ac400403d>.
- Paglia, Giuseppe, Pegggi Angel, Jonathan P. Williams, Keith Richardson, Hernando J. Olivos, J. Will Thompson, Lochana Menikarachchi, et al. 2015. « Ion Mobility-Derived Collision Cross

- Section As an Additional Measure for Lipid Fingerprinting and Identification ». *Analytical Chemistry* 87 (2): 1137-44. <https://doi.org/10.1021/ac503715v>.
- Paglia, Giuseppe, et Giuseppe Astarita. 2017. « Metabolomics and Lipidomics Using Traveling-Wave Ion Mobility Mass Spectrometry ». *Nature Protocols* 12 (4): 797-813. <https://doi.org/10.1038/nprot.2017.013>.
- Paglia, Giuseppe, Andrew J. Smith, et Giuseppe Astarita. 2021. « Ion Mobility Mass Spectrometry in the Omics Era: Challenges and Opportunities for Metabolomics and Lipidomics ». *Mass Spectrometry Reviews*. <https://doi.org/10.1002/mas.21686>.
- Paglia, Giuseppe, Jonathan P. Williams, Lochana Menikarachchi, J. Will Thompson, Richard Tyldesley-Worster, Skarphédinn Halldórsson, Ottar Rolfsson, et al. 2014. « Ion Mobility Derived Collision Cross Sections to Support Metabolomics Applications ». *Analytical Chemistry* 86 (8): 3985-93. <https://doi.org/10.1021/ac500405x>.
- Paizs, Béla. 2015. « A divide-and-conquer approach to compute collision cross sections in the projection approximation method ». *International Journal of Mass Spectrometry, SI: Bierbaum 65th Birthday*, 378 (février): 360-63. <https://doi.org/10.1016/j.ijms.2014.10.005>.
- Pang, Huanhuan, et Zeping Hu. 2023. « Metabolomics in Drug Research and Development: The Recent Advances in Technologies and Applications ». *Acta Pharmaceutica Sinica B*, mai. <https://doi.org/10.1016/j.apsb.2023.05.021>.
- Pareek, Vidhi, Hua Tian, Nicholas Winograd, et Stephen J. Benkovic. 2020. « Metabolomics and mass spectrometry imaging reveal channeled de novo purine synthesis in cells ». *Science (New York, N.Y.)* 368 (6488): 283-90. <https://doi.org/10.1126/science.aaz6465>.
- Parrot, Delphine, Stefano Papazian, Daniel Foil, et Deniz Tasdemir. 2018. « Imaging the Unimaginable: Desorption Electrospray Ionization – Imaging Mass Spectrometry (DESI-IMS) in Natural Product Research ». *Planta Medica* 84 (9/10): 584-93. <https://doi.org/10.1055/s-0044-100188>.
- Perez De Souza, Leonardo, Saleh Alseekh, Yariv Brotman, et Alisdair R Fernie. 2020. « Network-based strategies in metabolomics data analysis and interpretation: from molecular networking to biological interpretation ». *Expert Review of Proteomics* 17 (4): 243-55. <https://doi.org/10.1080/14789450.2020.1766975>.
- Pezzatti, Julian, Víctor González-Ruiz, Julien Boccard, Davy Guillarme, et Serge Rudaz. 2020. « Evaluation of Different Tandem MS Acquisition Modes to Support Metabolite Annotation in Human Plasma Using Ultra High-Performance Liquid Chromatography High-Resolution Mass Spectrometry for Untargeted Metabolomics ». *Metabolites* 10 (11): 464. <https://doi.org/10.3390/metabo10110464>.
- Pham, Huong T., Alan T. Maccarone, Michael C. Thomas, J. Larry Campbell, Todd W. Mitchell, et Stephen J. Blanksby. 2013. « Structural Characterization of Glycerophospholipids by Combinations of Ozone- and Collision-Induced Dissociation Mass Spectrometry: The next Step towards “Top-down” Lipidomics ». *Analyst* 139 (1): 204-14. <https://doi.org/10.1039/C3AN01712E>.
- Pičmanová, Martina, Tessa Moses, Joan Cortada-Garcia, Georgina Barrett, Hannah Florance, Sufyan Pandor, et Karl Burgess. 2022. « Rapid HILIC-Z Ion Mobility Mass Spectrometry (RHIMMS) Method for Untargeted Metabolomics of Complex Biological Samples ». *Metabolomics* 18 (3): 16. <https://doi.org/10.1007/s11306-022-01871-1>.
- Plante, P. L., E. Francovic-Fontaine, J. C. May, J. A. McLean, E. S. Baker, F. Laviolette, M. Marchand, et J. Corbeil. 2019. « Predicting Ion Mobility Collision Cross-Sections Using a Deep Neural Network: DeepCCS ». *Anal Chem* 91 (8): 5191-99. <https://doi.org/10.1021/acs.analchem.8b05821>.
- Poad, Berwyck, Lachlan Jekimovs, Reuben Young, Puttandon Wongsomboon, David Marshall, Felicia Hansen, Therese Fulloon, et al. 2023. « Revolutions in Lipid Isomer Resolution: Application of Ultra-High Resolution Ion Mobility to Reveal Lipid Diversity ». Preprint. Chemistry. <https://doi.org/10.26434/chemrxiv-2023-20nmh>.

- Poad, Berwyck L. J., Xueyun Zheng, Todd W. Mitchell, Richard D. Smith, Erin S. Baker, et Stephen J. Blanksby. 2018. « Online Ozonolysis Combined with Ion Mobility-Mass Spectrometry Provides a New Platform for Lipid Isomer Analyses ». *Analytical Chemistry* 90 (2): 1292-1300. <https://doi.org/10.1021/acs.analchem.7b04091>.
- Pringle, Steven D., Kevin Giles, Jason L. Wildgoose, Jonathan P. Williams, Susan E. Slade, Konstantinos Thalassinos, Robert H. Bateman, Michael T. Bowers, et James H. Scrivens. 2007. « An Investigation of the Mobility Separation of Some Peptide and Protein Ions Using a New Hybrid Quadrupole/Travelling Wave IMS/Oa-ToF Instrument ». *International Journal of Mass Spectrometry* 261 (1): 1-12. <https://doi.org/10.1016/j.ijms.2006.07.021>.
- Psychogios, Nikolaos, David D. Hau, Jun Peng, An Chi Guo, Rupasri Mandal, Souhaila Bouatra, Igor Sinelnikov, et al. 2011. « The Human Serum Metabolome ». *PLoS One* 6 (2): e16957. <https://doi.org/10.1371/journal.pone.0016957>.
- Purves, Randy W., et Roger Guevremont. 1999. « Electrospray Ionization High-Field Asymmetric Waveform Ion Mobility Spectrometry–Mass Spectrometry ». *Analytical Chemistry* 71 (13): 2346-57. <https://doi.org/10.1021/ac981380y>.
- Qi, Keke, Liutian Wu, Chengyuan Liu, et Yang Pan. 2021. « Recent Advances of Ambient Mass Spectrometry Imaging and Its Applications in Lipid and Metabolite Analysis ». *Metabolites* 11 (11): 780. <https://doi.org/10.3390/metabo11110780>.
- Raetz, Michel, Ron Bonner, et Gérard Hopfgartner. 2020. « SWATH-MS for Metabolomics and Lipidomics: Critical Aspects of Qualitative and Quantitative Analysis ». *Metabolomics* 16 (6): 71. <https://doi.org/10.1007/s11306-020-01692-0>.
- Rainey, Markace A., Chandler A. Watson, Carter K. Asef, Makayla R. Foster, Erin S. Baker, et Facundo M. Fernández. 2022. « CCS Predictor 2.0: An Open-Source Jupyter Notebook Tool for Filtering Out False Positives in Metabolomics ». *Analytical Chemistry* 94 (50): 17456-66. <https://doi.org/10.1021/acs.analchem.2c03491>.
- Ramautar, Rawi, Ayla Demirci, et Gerhardus J. de Jong. 2006. « Capillary Electrophoresis in Metabolomics ». *TrAC Trends in Analytical Chemistry* 25 (5): 455-66. <https://doi.org/10.1016/j.trac.2006.02.004>.
- Ramsden, Jeremy J. 2009. « Metabolomics and Metabonomics ». In *Bioinformatics: An Introduction*, édité par Jeremy Ramsden, 1-6. Computational Biology. London: Springer. https://doi.org/10.1007/978-1-84800-257-9_16.
- Rathahao-Paris, Estelle, Sandra Alves, Christophe Junot, et Jean-Claude Tabet. 2015. « High Resolution Mass Spectrometry for Structural Identification of Metabolites in Metabolomics ». *Metabolomics* 12 (1): 10. <https://doi.org/10.1007/s11306-015-0882-8>.
- Rathahao-Paris, Estelle, Sandra Alves, et Alain Paris. 2021. « High-Throughput Metabolomics Using Flow Injection Analysis and Fourier Transform Ion Cyclotron Resonance Mass Spectrometry ». In *Metabolomics*, édité par Paul L. Wood, 9-23. Neuromethods. New York, NY: Springer US. https://doi.org/10.1007/978-1-0716-0864-7_2.
- Ratiu, Ileana Andreea, Victor Bocos-Bintintan, Adrian Patrut, Victor Hugo Moll, Matthew Turner, et C. L. Paul Thomas. 2017. « Discrimination of bacteria by rapid sensing their metabolic volatiles using an aspiration-type ion mobility spectrometer (a-IMS) and gas chromatography-mass spectrometry GC-MS ». *Analytica Chimica Acta* 982 (août): 209-17. <https://doi.org/10.1016/j.aca.2017.06.031>.
- Rawat, Vivek K., Guillermo Vidal-de-Miguel, et Christopher J. Hogan. 2015. « Modeling Vapor Uptake Induced Mobility Shifts in Peptide Ions Observed with Transversal Modulation Ion Mobility Spectrometry-Mass Spectrometry ». *Analyst* 140 (20): 6945-54. <https://doi.org/10.1039/C5AN00753D>.
- Regueiro, Jorge, Noelia Negreira, et Marc H. G. Berntssen. 2016. « Ion-Mobility-Derived Collision Cross Section as an Additional Identification Point for Multiresidue Screening of Pesticides in Fish Feed ». Research-article. ACS Publications. American Chemical Society. World. 4 novembre 2016. <https://doi.org/10.1021/acs.analchem.6b03381>.

- Reis, Ana, Alisa Rudnitskaya, Gavin J. Blackburn, Norsyahida Mohd Fauzi, Andrew R. Pitt, et Corinne M. Spickett. 2013. « A Comparison of Five Lipid Extraction Solvent Systems for Lipidomic Studies of Human LDL ». *Journal of Lipid Research* 54 (7): 1812-24. <https://doi.org/10.1194/jlr.M034330>.
- Reischl, G. P. 1991. « Measurement of Ambient Aerosols by the Differential Mobility Analyzer Method: Concepts and Realization Criteria for the Size Range Between 2 and 500 nm ». *Aerosol Science and Technology* 14 (1): 5-24. <https://doi.org/10.1080/02786829108959467>.
- Revercomb, H. E., et E. A. Mason. 1975. « Theory of plasma chromatography/gaseous electrophoresis. Review ». *Analytical Chemistry* 47 (7): 970-83. <https://doi.org/10.1021/ac60357a043>.
- Richardson, K., D. Langridge, S. M. Dixit, et B. T. Ruotolo. 2021. « An Improved Calibration Approach for Traveling Wave Ion Mobility Spectrometry: Robust, High-Precision Collision Cross Sections ». *Analytical Chemistry* 93 (7): 3542-50. <https://doi.org/10.1021/acs.analchem.0c04948>.
- Richardson, K., D. Langridge, et K. Giles. 2018. « Fundamentals of travelling wave ion mobility revisited: I. Smoothly moving waves ». *International Journal of Mass Spectrometry* 428 (mai): 71-80. <https://doi.org/10.1016/j.ijms.2018.03.007>.
- Ridenour, Whitney. B., Michal Kliman, John A. McLean, et Richard M. Caprioli. 2010. « Structural Characterization of Phospholipids and Peptides Directly from Tissue Sections by MALDI Traveling-Wave Ion Mobility-Mass Spectrometry ». *Analytical chemistry* 82 (5): 1881-89. <https://doi.org/10.1021/ac9026115>.
- Ridgeway, Mark E., Christian Bleiholder, Matthias Mann, et Melvin A. Park. 2019. « Trends in trapped ion mobility – Mass spectrometry instrumentation ». *TrAC Trends in Analytical Chemistry* 116: 324-31. <https://doi.org/10.1016/j.trac.2019.03.030>.
- Ridgeway, Mark E., Markus Lubeck, Jan Jordens, Mattias Mann, et Melvin A. Park. 2018. « Trapped Ion Mobility Spectrometry: A Short Review ». *International Journal of Mass Spectrometry* 425 (février): 22-35. <https://doi.org/10.1016/j.ijms.2018.01.006>.
- Righetti, Laura, Nicola Dreolin, Alberto Celma, Mike McCullagh, Gitte Barknowitz, Juan V. Sancho, et Chiara Dall'Asta. 2020. « Travelling Wave Ion Mobility-Derived Collision Cross Section for Mycotoxins: Investigating Interlaboratory and Interplatform Reproducibility ». *Journal of Agricultural and Food Chemistry* 68 (39): 10937-43. <https://doi.org/10.1021/acs.jafc.0c04498>.
- Rister, Alana L., et Eric D. Dodds. 2020. « Steroid Analysis by Ion Mobility Spectrometry ». *Steroids* 153 (janvier): 108531. <https://doi.org/10.1016/j.steroids.2019.108531>.
- Rister, Alana L., Tiana L. Martin, et Eric D. Dodds. 2019. « Application of Group I Metal Adduction to the Separation of Steroids by Traveling Wave Ion Mobility Spectrometry ». *Journal of the American Society for Mass Spectrometry* 30 (2): 248-55. <https://doi.org/10.1007/s13361-018-2085-9>.
- Rivera, Emilio S., Katerina V. Djambazova, Elizabeth K. Neumann, Richard M. Caprioli, et Jeffrey M. Spraggins. 2020. « Integrating Ion Mobility and Imaging Mass Spectrometry for Comprehensive Analysis of Biological Tissues: A Brief Review and Perspective ». *Journal of Mass Spectrometry* n/a (n/a): e4614. <https://doi.org/10.1002/jms.4614>.
- Robinson, Errol W., David E. Garcia, Ryan D. Leib, et Evan R. Williams. 2006. « Enhanced Mixture Analysis of Poly(ethylene glycol) Using High-Field Asymmetric Waveform Ion Mobility Spectrometry Combined with Fourier Transform Ion Cyclotron Resonance Mass Spectrometry ». *Analytical Chemistry* 78 (7): 2190-98. <https://doi.org/10.1021/ac051709x>.
- Roca, Marta, Maria Isabel Alcoriza, Juan Carlos Garcia-Cañaveras, et Agustín Lahoz. 2021. « Reviewing the Metabolome Coverage Provided by LC-MS: Focus on Sample Preparation and Chromatography-A Tutorial ». *Analytica Chimica Acta* 1147 (février): 38-55. <https://doi.org/10.1016/j.aca.2020.12.025>.
- Rokushika, Souji, Hiroyuki Hatano, et Herbert H Hill. 1987. « Ion Mobility Spectrometry after Supercritical Fluid Chromatography ».

- Ropartz, David, Mathieu Fanuel, Simon Ollivier, Adrien Lissarrague, Mounir Benkoulouche, Laurence A. Mulard, Isabelle André, David Guieysse, et Hélène Rogniaux. 2022. « Combination of High-Resolution Multistage Ion Mobility and Tandem MS with High Energy of Activation to Resolve the Structure of Complex Chemoenzymatically Synthesized Glycans ». *Analytical Chemistry* 94 (4): 2279-87. <https://doi.org/10.1021/acs.analchem.1c04982>.
- Rose, Bailey S., Katrina L. Leaptrot, Rachel A. Harris, Stacy D. Sherrod, Jody C. May, et John A. McLean. 2021. « High Confidence Shotgun Lipidomics Using Structurally Selective Ion Mobility-Mass Spectrometry ». In *Mass Spectrometry-Based Lipidomics: Methods and Protocols*, édité par Fong-Fu Hsu, 11-37. Methods in Molecular Biology. New York, NY: Springer US. https://doi.org/10.1007/978-1-0716-1410-5_2.
- Rose, Bailey S., Jody C. May, Allison R. Reardon, et John A. McLean. 2022. « Collision Cross-Section Calibration Strategy for Lipid Measurements in SLIM-Based High-Resolution Ion Mobility ». *Journal of the American Society for Mass Spectrometry*, juin. <https://doi.org/10.1021/jasms.2c00067>.
- Ross, Dylan H., Jang Ho Cho, et Libin Xu. 2020. « Breaking Down Structural Diversity for Comprehensive Prediction of Ion-Neutral Collision Cross Sections ». *Analytical Chemistry* 92 (6): 4548-57. <https://doi.org/10.1021/acs.analchem.9b05772>.
- Ross, Dylan H., Jang Ho Cho, Rutan Zhang, Kelly M. Hines, et Libin Xu. 2020. « LiPydomics: A Python Package for Comprehensive Prediction of Lipid Collision Cross Sections and Retention Times and Analysis of Ion Mobility-Mass Spectrometry-Based Lipidomics Data ». *Analytical Chemistry* 92 (22): 14967-75. <https://doi.org/10.1021/acs.analchem.0c02560>.
- Ross, Dylan H., Jian Guo, Aivett Bilbao, Tao Huan, Richard D. Smith, et Xueyun Zheng. 2023. « Evaluating Software Tools for Lipid Identification from Ion Mobility Spectrometry–Mass Spectrometry Lipidomics Data ». *Molecules* 28 (8): 3483. <https://doi.org/10.3390/molecules28083483>.
- Ross, Dylan H., Ryan P. Seguin, Allison M. Krinsky, et Libin Xu. 2022. « High-Throughput Measurement and Machine Learning-Based Prediction of Collision Cross Sections for Drugs and Drug Metabolites ». *Journal of the American Society for Mass Spectrometry* 33 (6): 1061-72. <https://doi.org/10.1021/jasms.2c00111>.
- Rudt, E., M. Feldhaus, C. G. Margraf, S. Schlehuber, A. Schubert, S. Heuckeroth, U. Karst, et al. 2023. « Comparison of Data-Dependent Acquisition, Data-Independent Acquisition, and Parallel Reaction Monitoring in Trapped Ion Mobility Spectrometry–Time-of-Flight Tandem Mass Spectrometry-Based Lipidomics ». *Analytical Chemistry*, juin. <https://doi.org/10.1021/acs.analchem.3c00440>.
- Ruotolo, Brandon T, Justin L P Benesch, Alan M Sandercock, Suk-Joon Hyung, et Carol V Robinson. 2008. « Ion Mobility–Mass Spectrometry Analysis of Large Protein Complexes ». *Nature Protocols* 3 (7): 1139-52. <https://doi.org/10.1038/nprot.2008.78>.
- Ruskic, David, Frank Klont, et Gérard Hopfgartner. 2021. « Clustering and Nonclustering Modifier Mixtures in Differential Mobility Spectrometry for Multidimensional Liquid Chromatography Ion Mobility–Mass Spectrometry Analysis ». *Analytical Chemistry* 93 (17): 6638-45. <https://doi.org/10.1021/acs.analchem.0c04889>.
- Rutherford, E. 1897. « LIV. The velocity and rate of recombination of the ions of gases exposed to Röntgen radiation ». *The London, Edinburgh, and Dublin Philosophical Magazine and Journal of Science* 44 (270): 422-40. <https://doi.org/10.1080/14786449708621085>.
- Ryan, Danielle, et Kevin Robards. 2006. « Metabolomics: The Greatest Omics of Them All? ». *Analytical Chemistry* 78 (23): 7954-58. <https://doi.org/10.1021/ac0614341>.
- Saba, Julian, Eric Bonneil, Christelle Pomiès, Kevin Eng, et Pierre Thibault. 2009. « Enhanced Sensitivity in Proteomics Experiments Using FAIMS Coupled with a Hybrid Linear Ion Trap/Orbitrap Mass Spectrometer ». *Journal of Proteome Research* 8 (7): 3355-66. <https://doi.org/10.1021/pr801106a>.
- Šala, Martin, Miroslav Lísa, J. Larry Campbell, et Michal Holčápek. 2016. « Determination of Triacylglycerol Regioisomers Using Differential Mobility Spectrometry ». *Rapid*

- Communications in Mass Spectrometry: RCM* 30 (2): 256-64.
<https://doi.org/10.1002/rcm.7430>.
- Salek, Reza M, Christoph Steinbeck, Mark R Viant, Royston Goodacre, et Warwick B Dunn. 2013. « The role of reporting standards for metabolite annotation and identification in metabolomic studies ». *GigaScience* 2 (1): 2047-217X-2-13. <https://doi.org/10.1186/2047-217X-2-13>.
- Salviati, Emanuela, Eduardo Sommella, et Pietro Campiglia. 2022. « Chapter 15 - MALDI–Mass Spectrometry Imaging: The Metabolomic Visualization ». In *Metabolomics Perspectives*, édité par Jacopo Troisi, 535-51. Academic Press. <https://doi.org/10.1016/B978-0-323-85062-9.00015-5>.
- Samaraweera, Milinda A., Dennis W. Hill, et David F. Grant. 2020. « MolFind2: A Protocol for Acquiring and Integrating MS3 Data to Improve In Silico Chemical Structure Elucidation for Metabolomics ». In *Ion Mobility-Mass Spectrometry : Methods and Protocols*, édité par Giuseppe Paglia et Giuseppe Astarita, 283-95. Methods in Molecular Biology. New York, NY: Springer US. https://doi.org/10.1007/978-1-0716-0030-6_18.
- San-Martin, Breno Sena De, Vinicius Guimarães Ferreira, Mariana Rechia Bitencourt, Paulo Cesar Gonçalves Pereira, Emanuel Carrilho, Nilson Antônio de Assunção, et Luciani Renata Silveira de Carvalho. 2020. « Metabolomics as a Potential Tool for the Diagnosis of Growth Hormone Deficiency (GHD): A Review ». *Archives of Endocrinology and Metabolism* 64 (octobre): 654-63. <https://doi.org/10.20945/2359-3997000000300>.
- Schmid, Robin, Steffen Heuckeroth, Ansgar Korf, Aleksandr Smirnov, Owen Myers, Thomas S. Dyrland, Roman Bushuiev, et al. 2023. « Integrative Analysis of Multimodal Mass Spectrometry Data in MZmine 3 ». *Nature Biotechnology* 41 (4): 447-49. <https://doi.org/10.1038/s41587-023-01690-2>.
- Schmid, Robin, Daniel Petras, Louis-Félix Nothias, Mingxun Wang, Allegra T. Aron, Annika Jagels, Hiroshi Tsugawa, et al. 2021. « Ion Identity Molecular Networking for Mass Spectrometry-Based Metabolomics in the GNPS Environment ». *Nature Communications* 12 (1): 3832. <https://doi.org/10.1038/s41467-021-23953-9>.
- Schomakers, Bauke V., Jill Hermans, Yorrick R. J. Jaspers, Gajja Salomons, Frédéric M. Vaz, Michel van Weeghel, et Riekelt H. Houtkooper. 2022. « Polar Metabolomics in Human Muscle Biopsies Using a Liquid-Liquid Extraction and Full-Scan LC-MS ». *STAR Protocols* 3 (2): 101302. <https://doi.org/10.1016/j.xpro.2022.101302>.
- Schrimpe-Rutledge, Alexandra C., Simona G. Codreanu, Stacy D. Sherrod, et John A. McLean. 2016. « Untargeted Metabolomics Strategies—Challenges and Emerging Directions ». *Journal of The American Society for Mass Spectrometry* 27 (12): 1897-1905. <https://doi.org/10.1007/s13361-016-1469-y>.
- Schroeder, Mark, Sven W. Meyer, Heino M. Heyman, Aiko Barsch, et Lloyd W. Sumner. 2020. « Generation of a Collision Cross Section Library for Multi-Dimensional Plant Metabolomics Using UHPLC-Trapped Ion Mobility-MS/MS ». *Metabolites* 10 (1): 13. <https://doi.org/10.3390/metabo10010013>.
- Selamat, Jinap, Nur Amalyn Alyaa Rozani, et Suganya Murugesu. 2021. « Application of the Metabolomics Approach in Food Authentication ». *Molecules* 26 (24): 7565. <https://doi.org/10.3390/molecules26247565>.
- Seo, Youjin, Matthew R. Schenauer, et Julie A. Leary. 2011. « Biologically relevant metal-cation binding induces conformational changes in heparin oligosaccharides as measured by ion mobility mass spectrometry ». *International Journal of Mass Spectrometry* 303 (2): 191-98. <https://doi.org/10.1016/j.ijms.2011.02.003>.
- Shamim, Arshiya, Tarique Mahmood, Farogh Ahsan, Arun Kumar, et Paramdeep Bagga. 2018. « Lipids: An Insight into the Neurodegenerative Disorders ». *Clinical Nutrition Experimental* 20 (août): 1-19. <https://doi.org/10.1016/j.yclnex.2018.05.001>.
- Sharma, Ajay, Saurabh Sharma, Anil Kumar, Vinod Kumar, et Anil Kumar Sharma. 2022. « Plant Secondary Metabolites: An Introduction of Their Chemistry and Biological Significance with

- Physicochemical Aspect ». In *Plant Secondary Metabolites: Physico-Chemical Properties and Therapeutic Applications*, édité par Anil Kumar Sharma et Ajay Sharma, 1-45. Singapore: Springer Nature. https://doi.org/10.1007/978-981-16-4779-6_1.
- Shen, Liming, Huajie Zhang, Jing Lin, Yan Gao, Margy Chen, Naseer Ullah Khan, Xiaoxiao Tang, et al. 2022. « A Combined Proteomics and Metabolomics Profiling to Investigate the Genetic Heterogeneity of Autistic Children ». *Molecular Neurobiology* 59 (6): 3529-45. <https://doi.org/10.1007/s12035-022-02801-x>.
- Shulaev, Vladimir, et Giorgis Isaac. 2018. « Supercritical Fluid Chromatography Coupled to Mass Spectrometry – A Metabolomics Perspective ». *Journal of Chromatography B* 1092 (août): 499-505. <https://doi.org/10.1016/j.jchromb.2018.06.021>.
- Shvartsburg, Alexandre A., et Richard D. Smith. 2008. « Fundamentals of Traveling Wave Ion Mobility Spectrometry ». *Analytical chemistry* 80 (24): 9689-99. <https://doi.org/10.1021/ac8016295>.
- Silveira, Joshua A., Karsten Michelmann, Mark E. Ridgeway, et Melvin A. Park. 2016. « Fundamentals of Trapped Ion Mobility Spectrometry Part II: Fluid Dynamics ». *Journal of the American Society for Mass Spectrometry* 27 (4): 585-95. <https://doi.org/10.1007/s13361-015-1310-z>.
- Simón-Manso, Yamil. 2023. « Ion-Neutral Collision Cross Section as a Function of the Static Dipole Polarizability and the Ionization Energy of the Ion ». *The Journal of Physical Chemistry A* 127 (15): 3274-80. <https://doi.org/10.1021/acs.jpca.2c07157>.
- Singh, Randolph R., Yann Aminot, Karine Héas-Moisan, Hugues Preud'homme, et Catherine Munsch. 2023. « Cracked and shucked: GC-APCI-IMS-HRMS facilitates identification of unknown halogenated organic chemicals in French marine bivalves ». *Environment International* 178 (août): 108094. <https://doi.org/10.1016/j.envint.2023.108094>.
- Sitnikov, Dmitri G., Cian S. Monnin, et Dajana Vuckovic. 2016. « Systematic Assessment of Seven Solvent and Solid-Phase Extraction Methods for Metabolomics Analysis of Human Plasma by LC-MS ». *Scientific Reports* 6 (1): 38885. <https://doi.org/10.1038/srep38885>.
- Skowronek, Patricia, et Florian Meier. 2022. « High-Throughput Mass Spectrometry-Based Proteomics with Dia-PASEF ». In *Proteomics in Systems Biology: Methods and Protocols*, édité par Jennifer Geddes-McAlister, 15-27. Methods in Molecular Biology. New York, NY: Springer US. https://doi.org/10.1007/978-1-0716-2124-0_2.
- Smith, Colin A., Grace O' Maille, Elizabeth J. Want, Chuan Qin, Sunia A. Trauger, Theodore R. Brandon, Darlene E. Custodio, Ruben Abagyan, et Gary Siuzdak. 2005. « METLIN: A Metabolite Mass Spectral Database ». *Therapeutic Drug Monitoring* 27 (6): 747. <https://doi.org/10.1097/01.ftd.0000179845.53213.39>.
- Smith, Colin A., Elizabeth J. Want, Grace O' Maille, Ruben Abagyan, et Gary Siuzdak. 2006. « XCMS: Processing Mass Spectrometry Data for Metabolite Profiling Using Nonlinear Peak Alignment, Matching, and Identification ». *Analytical Chemistry* 78 (3): 779-87. <https://doi.org/10.1021/ac051437y>.
- Smith, David P., Tom W. Knapman, Iain Campuzano, Richard W. Malham, Joshua T. Berryman, Sheena E. Radford, et Alison E. Ashcroft. 2009. « Deciphering Drift Time Measurements from Travelling Wave Ion Mobility Spectrometry-Mass Spectrometry Studies ». *European Journal of Mass Spectrometry* 15 (2): 113-30. <https://doi.org/10.1255/ejms.947>.
- Snyder, Dalton T., Benjamin J. Jones, Yu-Fu Lin, Dale A. Cooper-Shepherd, Darren Hewitt, Jason Wildgoose, Jeffery M. Brown, James I. Langridge, et Vicki H. Wysocki. 2021. « Surface-Induced Dissociation of Protein Complexes on a Cyclic Ion Mobility Spectrometer ». *Analyst* 146 (22): 6861-73. <https://doi.org/10.1039/D1AN01407B>.
- Soek Sin, Teh. 2016. « EFFECTS OF FATTY ACIDS AT DIFFERENT POSITIONS IN THE TRIGLYCERIDES ON CHOLESTEROL LEVELS ». *Journal of Palm Oil Research* 28 (2): 211-21. <https://doi.org/10.21894/jopr.2016.2802.09>.
- Sokol, Elena, Reinaldo Almeida, Hans Kristian Hannibal-Bach, Dorota Kotowska, Johannes Vogt, Jan Baumgart, Karsten Kristiansen, Robert Nitsch, Jens Knudsen, et Christer S. Ejsing. 2013. « Profiling of Lipid Species by Normal-Phase Liquid Chromatography, Nanoelectrospray

- Ionization, and Ion Trap–Orbitrap Mass Spectrometry ». *Analytical Biochemistry* 443 (1): 88-96. <https://doi.org/10.1016/j.ab.2013.08.020>.
- Song, Yuelin, Qingqing Song, Wenjing Liu, Jun Li, et Pengfei Tu. 2023. « High-confidence structural identification of metabolites relying on tandem mass spectrometry through isomeric identification: A tutorial ». *TrAC Trends in Analytical Chemistry* 160 (mars): 116982. <https://doi.org/10.1016/j.trac.2023.116982>.
- Sotelo-Orozco, Jennie, Shin-Yu Chen, Irva Hertz-Picciotto, et Carolyn M. Slupsky. 2021. « A Comparison of Serum and Plasma Blood Collection Tubes for the Integration of Epidemiological and Metabolomics Data ». *Frontiers in Molecular Biosciences* 8. <https://www.frontiersin.org/articles/10.3389/fmolb.2021.682134>.
- Sreekumar, Arun, Laila M. Poisson, Thekkelnaycke M. Rajendiran, Amjad P. Khan, Qi Cao, Jindan Yu, Bharathi Laxman, et al. 2009. « Metabolomic Profiles Delineate Potential Role for Sarcosine in Prostate Cancer Progression ». *Nature* 457 (7231): 910-14. <https://doi.org/10.1038/nature07762>.
- St. Louis, Robert H., Herbert H. Hill, et Gary Alan Eiceman. 1990. « Ion Mobility Spectrometry in Analytical Chemistry ». *Critical Reviews in Analytical Chemistry* 21 (5): 321-55. <https://doi.org/10.1080/10408349008050848>.
- Steppert, Isabel, Jessy Schönfelder, Carolyn Schultz, et Dirk Kuhlmeier. 2021. « Rapid in Vitro Differentiation of Bacteria by Ion Mobility Spectrometry ». *Applied Microbiology and Biotechnology* 105 (10): 4297-4307. <https://doi.org/10.1007/s00253-021-11315-w>.
- Steuer, Andrea E., Lana Brockbals, et Thomas Kraemer. 2019. « Metabolomic Strategies in Biomarker Research—New Approach for Indirect Identification of Drug Consumption and Sample Manipulation in Clinical and Forensic Toxicology? ». *Frontiers in Chemistry* 7 (mai): 319. <https://doi.org/10.3389/fchem.2019.00319>.
- Stopka, Sylwia A., et Akos Vertes. 2020. « Metabolomic Profiling of Adherent Mammalian Cells In Situ by LAESI-MS with Ion Mobility Separation ». In *Ion Mobility-Mass Spectrometry : Methods and Protocols*, édité par Giuseppe Paglia et Giuseppe Astarita, 235-44. *Methods in Molecular Biology*. New York, NY: Springer US. https://doi.org/10.1007/978-1-0716-0030-6_15.
- Stow, Sarah M., Tim J. Causon, Xueyun Zheng, Ruwan T. Kurulugama, Teresa Mairinger, Jody C. May, Emma E. Rennie, et al. 2017. « An Interlaboratory Evaluation of Drift Tube Ion Mobility–Mass Spectrometry Collision Cross Section Measurements ». *Analytical Chemistry* 89 (17): 9048-55. <https://doi.org/10.1021/acs.analchem.7b01729>.
- Stow, Sarah Markley. 2015. « STRATEGIES FOR SELECTING COMPUTATIONAL PROTOCOLS IN SUPPORT OF SMALL MOLECULE STRUCTURAL ANALYSIS BY ION MOBILITY-MASS SPECTROMETRY ». Dissertation in chemistry, Vanderbilt University.
- Sud, Manish, Eoin Fahy, Dawn Cotter, Alex Brown, Edward A. Dennis, Christopher K. Glass, Alfred H. Merrill Jr, et al. 2007. « LMSD: LIPID MAPS structure database ». *Nucleic Acids Research* 35 (suppl_1): D527-32. <https://doi.org/10.1093/nar/gkl838>.
- Sueur, Maxime, Julien F. Maillard, Oscar Lacroix-Andrivet, Christopher Paul Rüger, Pierre Giusti, Hélène Lavanant, et Carlos Afonso. 2022. « PyC2MC: An Open-Source Software Solution for Visualization and Treatment of High-Resolution Mass Spectrometry Data ». Preprint. *Chemistry*. <https://doi.org/10.26434/chemrxiv-2022-cmnk3>.
- Sugimoto, Masahiro. 2021. « Capillary Electrophoresis–Mass Spectrometry of Hydrophilic Metabolomics ». In *Metabolomics*, édité par Paul L. Wood, 113-20. *Neuromethods*. New York, NY: Springer US. https://doi.org/10.1007/978-1-0716-0864-7_10.
- Sun, Jiachen, Runcheng Fang, Hua Wang, De-Xiang Xu, Jing Yang, Xiaochen Huang, Daniel Cozzolino, Mingliang Fang, et Yichao Huang. 2022. « A Review of Environmental Metabolism Disrupting Chemicals and Effect Biomarkers Associating Disease Risks: Where Exposomics Meets Metabolomics ». *Environment International* 158 (janvier): 106941. <https://doi.org/10.1016/j.envint.2021.106941>.
- Szyrwił, Lukasz, Christoph Gille, Michael Müller, Vadim Demichev, et Markus Ralser. 2023. « Speedy-PASEF: Analytical Flow Rate Chromatography and Trapped Ion Mobility for Deep

- High-Throughput Proteomics ». Preprint. *Biochemistry*.
<https://doi.org/10.1101/2023.02.17.528968>.
- Tang, Keqi, Fumin Li, Alexandre A. Shvartsburg, Eric F. Strittmatter, et Richard D. Smith. 2005. « Two-Dimensional Gas-Phase Separations Coupled to Mass Spectrometry for Analysis of Complex Mixtures ». *Analytical Chemistry* 77 (19): 6381-88. <https://doi.org/10.1021/ac050871x>.
- Tebani, Abdellah, Isabelle Schmitz-Afonso, Douglas N. Rutledge, Bruno J. Gonzalez, Soumeya Bekri, et Carlos Afonso. 2016. « Optimization of a Liquid Chromatography Ion Mobility-Mass Spectrometry Method for Untargeted Metabolomics Using Experimental Design and Multivariate Data Analysis ». *Analytica Chimica Acta* 913 (mars): 55-62.
<https://doi.org/10.1016/j.aca.2016.02.011>.
- Theodoridis, Georgios, Helen Gika, Daniel Raftery, Royston Goodacre, Robert S. Plumb, et Ian D. Wilson. 2023. « Ensuring Fact-Based Metabolite Identification in Liquid Chromatography–Mass Spectrometry-Based Metabolomics ». *Analytical Chemistry* 95 (8): 3909-16.
<https://doi.org/10.1021/acs.analchem.2c05192>.
- Tian, He, Jinfa Bai, Zhuoling An, Yanhua Chen, Ruiping Zhang, Jiuming He, Xiaofeng Bi, Yongmei Song, et Zeper Abliz. 2013. « Plasma Metabolome Analysis by Integrated Ionization Rapid-Resolution Liquid Chromatography/Tandem Mass Spectrometry ». *Rapid Communications in Mass Spectrometry* 27 (18): 2071-80. <https://doi.org/10.1002/rcm.6666>.
- Tiziani, Stefano, Abdul-Hamid Emwas, Alessia Lodi, Christian Ludwig, Christopher M. Bunce, Mark R. Viant, et Ulrich L. Günther. 2008. « Optimized Metabolite Extraction from Blood Serum for 1H Nuclear Magnetic Resonance Spectroscopy ». *Analytical Biochemistry* 377 (1): 16-23.
<https://doi.org/10.1016/j.ab.2008.01.037>.
- Tolmachev, Aleksey V., Ian K. Webb, Yehia M. Ibrahim, Sandilya V.B. Garimella, Xinyu Zhang, Gordon A. Anderson, et Richard D. Smith. 2014. « Characterization of Ion Dynamics in Structures for Lossless Ion Manipulations ». *Analytical Chemistry* 86 (18): 9162-68.
<https://doi.org/10.1021/ac502054p>.
- Tonoyan, Narine M., Vitaliy V. Chagovets, Natalia L. Starodubtseva, Alisa O. Tokareva, Konstantin Chingin, Irena F. Kozachenko, Leyla V. Adamyan, et Vladimir E. Frankevich. 2021. « Alterations in lipid profile upon uterine fibroids and its recurrence ». *Scientific Reports* 11 (juin): 11447. <https://doi.org/10.1038/s41598-021-89859-0>.
- Tsugawa, Hiroshi, Kazutaka Ikeda, Mikiko Takahashi, Aya Satoh, Yoshifumi Mori, Haruki Uchino, Nobuyuki Okahashi, et al. 2020a. « MS-DIAL 4: accelerating lipidomics using an MS/MS, CCS, and retention time atlas ».
- . 2020b. « A Lipidome Atlas in MS-DIAL 4 ». *Nature Biotechnology* 38 (10): 1159-63.
<https://doi.org/10.1038/s41587-020-0531-2>.
- Tu, Jia, Zhiwei Zhou, Tongzhou Li, et Zheng-Jiang Zhu. 2019. « The Emerging Role of Ion Mobility-Mass Spectrometry in Lipidomics to Facilitate Lipid Separation and Identification ». *TrAC Trends in Analytical Chemistry* 116 (juillet): 332-39.
<https://doi.org/10.1016/j.trac.2019.03.017>.
- Tumanov, Sergey, et Jurre J Kamphorst. 2017. « Recent Advances in Expanding the Coverage of the Lipidome ». *Current Opinion in Biotechnology*, Analytical biotechnology, 43 (février): 127-33.
<https://doi.org/10.1016/j.copbio.2016.11.008>.
- Turner, R. B., et J. L. Brokenshire. 1994. « Hand-held ion mobility spectrometers ». *TrAC Trends in Analytical Chemistry* 13 (7): 275-80. [https://doi.org/10.1016/0165-9936\(94\)87064-0](https://doi.org/10.1016/0165-9936(94)87064-0).
- Turzo, SM Bargeen, Justin Seffernick, Sergey Lyskov, et Steffen Lindert. 2023. « Predicting Ion Mobility Collision Cross Sections Using Projection Approximation with ROSIE-PARCS Webserver ». ChemRxiv. <https://doi.org/10.26434/chemrxiv-2023-4j9gl>.
- Ujma, Jakub, David Ropartz, Kevin Giles, Keith Richardson, David Langridge, Jason Wildgoose, Martin Green, et Steven Pringle. 2019. « Cyclic Ion Mobility Mass Spectrometry Distinguishes Anomers and Open-Ring Forms of Pentasaccharides ». *Journal of The American Society for Mass Spectrometry* 30 (6): 1028-37. <https://doi.org/10.1007/s13361-019-02168-9>.

- Ulmer, Candice Z., Christina M. Jones, Richard A. Yost, Timothy J. Garrett, et John A. Bowden. 2018. « Optimization of Folch, Bligh-Dyer, and Matyash Sample-to-Extraction Solvent Ratios for Human Plasma-Based Lipidomics Studies ». *Analytica Chimica Acta* 1037 (décembre): 351-57. <https://doi.org/10.1016/j.aca.2018.08.004>.
- Valentine, Stephen J., Ruwan T. Kurulugama, Brian C. Bohrer, Samuel I. Merenbloom, Renã A. Sowell, Yehia Mechref, et David E. Clemmer. 2009. « Developing IMS–IMS–MS for rapid characterization of abundant proteins in human plasma ». *International Journal of Mass Spectrometry, A Collection of Invited Papers Dedicated to Michael T. Bowers on the Occasion of his 70th Birthday*, 283 (1): 149-60. <https://doi.org/10.1016/j.ijms.2009.02.030>.
- Valmori, Marie, Vincent Marie, François Fenaille, Benoit Colsch, et David Touboul. 2023. « Recent Methodological Developments in Data-Dependent Analysis and Data-Independent Analysis Workflows for Exhaustive Lipidome Coverage ». *Frontiers in Analytical Science* 3 (février): 1118742. <https://doi.org/10.3389/frans.2023.1118742>.
- Vasilopoulou, Catherine G., Karolina Sulek, Andreas-David Brunner, Ningombam Sanjib Meitei, Ulrike Schweiger-Hufnagel, Sven W. Meyer, Aiko Barsch, Matthias Mann, et Florian Meier. 2020. « Trapped Ion Mobility Spectrometry and PASEF Enable In-Depth Lipidomics from Minimal Sample Amounts ». *Nature Communications* 11 (1): 331. <https://doi.org/10.1038/s41467-019-14044-x>.
- Velde, Bas van de, Davy Guillarme, et Isabelle Kohler. 2020. « Supercritical Fluid Chromatography – Mass Spectrometry in Metabolomics: Past, Present, and Future Perspectives ». *Journal of Chromatography B* 1161 (décembre): 122444. <https://doi.org/10.1016/j.jchromb.2020.122444>.
- Velosa, Diana C., Andrew J. Dunham, Marcus E. Rivera, Shon P. Neal, et Christopher D. Chouinard. 2022. « Improved Ion Mobility Separation and Structural Characterization of Steroids using Derivatization Methods ». *Journal of the American Society for Mass Spectrometry* 33 (9): 1761-71. <https://doi.org/10.1021/jasms.2c00164>.
- Vidal-de-Miguel, G., M. Macía, C. Barrios, et J. Cuevas. 2015. « Transversal Modulation Ion Mobility Spectrometry (IMS) Coupled with Mass Spectrometry (MS): Exploring the IMS-IMS-MS Possibilities of the Instrument ». *Analytical Chemistry* 87 (3): 1925-32. <https://doi.org/10.1021/ac504178n>.
- Vidal-de-Miguel, G., M. Macía, et J. Cuevas. 2012. « Transversal Modulation Ion Mobility Spectrometry (TM-IMS), A New Mobility Filter Overcoming Turbulence Related Limitations ». *Analytical Chemistry* 84 (18): 7831-37. <https://doi.org/10.1021/ac301127u>.
- Vignoli, Alessia, Leonardo Tenori, Cristina Morsiani, Paola Turano, Miriam Capri, et Claudio Luchinat. 2022. « Serum or Plasma (and Which Plasma), That Is the Question ». *Journal of Proteome Research* 21 (4): 1061-72. <https://doi.org/10.1021/acs.jproteome.1c00935>.
- Vineis, P., M. Chadeau-Hyam, H. Gmuender, J. Gulliver, Z. Herceg, J. Kleinjans, M. Kogevinas, et al. 2017. « The Exposome in Practice: Design of the EXPOsOMICS Project ». *International Journal of Hygiene and Environmental Health, Special Issue: Human Biomonitoring 2016*, 220 (2, Part A): 142-51. <https://doi.org/10.1016/j.ijheh.2016.08.001>.
- Vuckovic, Dajana, et Janusz Pawliszyn. 2011. « Systematic Evaluation of Solid-Phase Microextraction Coatings for Untargeted Metabolomic Profiling of Biological Fluids by Liquid Chromatography-Mass Spectrometry ». *Analytical Chemistry* 83 (6): 1944-54. <https://doi.org/10.1021/ac102614v>.
- Wang, Jianing, Chunyan Wang, et Xianlin Han. 2019. « Tutorial on Lipidomics ». *Analytica Chimica Acta* 1061 (juillet): 28-41. <https://doi.org/10.1016/j.aca.2019.01.043>.
- . 2021. « Mass Spectrometry-Based Shotgun Lipidomics for Cancer Research ». In *Cancer Metabolomics: Methods and Applications*, édité par Shen Hu, 39-55. Advances in Experimental Medicine and Biology. Cham: Springer International Publishing. https://doi.org/10.1007/978-3-030-51652-9_3.
- Wang, Yang, Shuying Liu, Yuanjia Hu, Peng Li, et Jian-Bo Wan. 2015. « Current State of the Art of Mass Spectrometry-Based Metabolomics Studies – a Review Focusing on Wide Coverage,

- High Throughput and Easy Identification ». *RSC Advances* 5 (96): 78728-37.
<https://doi.org/10.1039/C5RA14058G>.
- Want, Elizabeth J., Grace O'Maille, Colin A. Smith, Theodore R. Brandon, Wilasinee Uritboonthai, Chuan Qin, Sunia A. Trauger, et Gary Siuzdak. 2006. « Solvent-Dependent Metabolite Distribution, Clustering, and Protein Extraction for Serum Profiling with Mass Spectrometry ». *Analytical Chemistry* 78 (3): 743-52. <https://doi.org/10.1021/ac051312t>.
- Waraksa, Emilia, Urszula Perycz, Jacek Namieśnik, Mika Sillanpää, Tomasz Dymerski, Marzena Wójtowicz, et Jarosław Puton. 2016. « Dopants and gas modifiers in ion mobility spectrometry ». *TrAC Trends in Analytical Chemistry* 82 (septembre): 237-49.
<https://doi.org/10.1016/j.trac.2016.06.009>.
- Wawrzyniak, Renata, Anna Kosnowska, Szymon Macioszek, Rafał Bartoszewski, et Michał Jan Markuszewski. 2018. « New plasma preparation approach to enrich metabolome coverage in untargeted metabolomics: plasma protein bound hydrophobic metabolite release with proteinase K ». *Scientific Reports* 8 (juin): 9541. <https://doi.org/10.1038/s41598-018-27983-0>.
- Webb, Ian K., Sandilya V. B. Garimella, Aleksey V. Tolmachev, Tsung-Chi Chen, Xinyu Zhang, Randolph V. Norheim, Spencer A. Prost, et al. 2014. « Experimental Evaluation and Optimization of Structures for Lossless Ion Manipulations for Ion Mobility Spectrometry with Time-of-Flight Mass Spectrometry ». *Analytical Chemistry* 86 (18): 9169-76.
<https://doi.org/10.1021/ac502055e>.
- Weidt, Stefan, Jennifer Haggarty, Ryan Kean, Cristian I. Cojocariu, Paul J. Silcock, Ranjith Rajendran, Gordon Ramage, et Karl E. V. Burgess. 2016. « A Novel Targeted/Untargeted GC-Orbitrap Metabolomics Methodology Applied to *Candida Albicans* and *Staphylococcus Aureus* Biofilms ». *Metabolomics* 12 (12): 189. <https://doi.org/10.1007/s11306-016-1134-2>.
- Wellmann, Johannes, Conny Tränkner, Nicolas Dostert, Esther-Corinna Schwarze, Silke Hillebrand, Jakob P. Ley, et Peter Winterhalter. 2022. « Comprehensive Metabolite Profiling of *Hydrangea macrophylla* ssp. *serrata* Extracts Using Liquid Chromatography Coupled with Electrospray Ionization Ion Mobility Quadrupole Time-of-Flight Mass Spectrometry ». *Journal of Agricultural and Food Chemistry* 70 (37): 11823-31.
<https://doi.org/10.1021/acs.jafc.2c04351>.
- Wen, Shan-Shan, Hong-Shan Zhou, Chuan-Sheng Zhu, Ping Li, et Wen Gao. 2022. « Direct infusion electrospray ionization-ion mobility-mass spectrometry for rapid metabolite marker discovery of medicinal *Phellodendron Bark* ». *Journal of Pharmaceutical and Biomedical Analysis* 219 (septembre): 114939. <https://doi.org/10.1016/j.jpba.2022.114939>.
- Werres, Tobias, Juri Leonhardt, Martin Jäger, et Thorsten Teutenberg. 2019. « Critical Comparison of Liquid Chromatography Coupled to Mass Spectrometry and Three Different Ion Mobility Spectrometry Systems on Their Separation Capability for Small Isomeric Compounds ». *Chromatographia* 82 (1): 251-60. <https://doi.org/10.1007/s10337-018-3640-z>.
- Westhoff, Michael, Maren Friedrich, et Jörg I. Baumbach. 2022. « Simultaneous Measurement of Inhaled Air and Exhaled Breath by Double Multicapillary Column Ion-Mobility Spectrometry, a New Method for Breath Analysis: Results of a Feasibility Study ». *ERJ Open Research* 8 (1): 00493-02021. <https://doi.org/10.1183/23120541.00493-2021>.
- Whiley, Luke, Joanna Godzien, Francisco J Ruperez, Cristina Legido-Quigley, et Coral Barbas. 2012. « In-Vial Dual Extraction for Direct LC-MS Analysis of Plasma for Comprehensive and Highly Reproducible Metabolic Fingerprinting. » *Analytical Chemistry* 84 (14): 5992-99.
<https://doi.org/10.1021/ac300716u>.
- Wilks, Ashley, Matthew Hart, Andrew Koehl, John Somerville, Billy Boyle, et David Ruiz-Alonso. 2012. « Characterization of a Miniature, Ultra-High-Field, Ion Mobility Spectrometer ». *International Journal for Ion Mobility Spectrometry* 15 (3): 199-222.
<https://doi.org/10.1007/s12127-012-0109-x>.

- Wishart, David S. 2016. « Emerging Applications of Metabolomics in Drug Discovery and Precision Medicine ». *Nature Reviews Drug Discovery* 15 (7): 473-84. <https://doi.org/10.1038/nrd.2016.32>.
- Wishart, David S., Leo L. Cheng, Valérie Copié, Arthur S. Edison, Hamid R. Eghbalnia, Jeffrey C. Hoch, Goncalo J. Gouveia, et al. 2022. « NMR and Metabolomics—A Roadmap for the Future ». *Metabolites* 12 (8): 678. <https://doi.org/10.3390/metabo12080678>.
- Wishart, David S., AnChi Guo, Eponine Oler, Fei Wang, Afia Anjum, Harrison Peters, Raynard Dizon, et al. 2022. « HMDB 5.0: The Human Metabolome Database for 2022 ». *Nucleic Acids Research* 50 (D1): D622-31. <https://doi.org/10.1093/nar/gkab1062>.
- Wishart, David S., Timothy Jewison, An Chi Guo, Michael Wilson, Craig Knox, Yifeng Liu, Yannick Djoumbou, et al. 2013. « HMDB 3.0—The Human Metabolome Database in 2013 ». *Nucleic Acids Research* 41 (Database issue): D801-807. <https://doi.org/10.1093/nar/gks1065>.
- Witting, Michael, et Sebastian Böcker. 2020. « Current Status of Retention Time Prediction in Metabolite Identification ». *Journal of Separation Science* 43 (9-10): 1746-54. <https://doi.org/10.1002/jssc.202000060>.
- Woods, Amina S., Michael Ugarov, Tom Egan, John Koomen, Kent J. Gillig, Katrin Fuhrer, Marc Gonin, et J. Albert Schultz. 2004. « Lipid/Peptide/Nucleotide Separation with MALDI-Ion Mobility-TOF MS ». *Analytical Chemistry* 76 (8): 2187-95. <https://doi.org/10.1021/ac035376k>.
- Wormwood Moser, Kelly L., Gregory Van Aken, Daniel DeBord, Nathan Galen Hatcher, Laura Maxon, Melissa Sherman, Lihang Yao, et Kim Ekroos. 2021. « High-Defined Quantitative Snapshots of the Ganglioside Lipidome Using High Resolution Ion Mobility SLIM Assisted Shotgun Lipidomics ». *Analytica Chimica Acta* 1146 (février): 77-87. <https://doi.org/10.1016/j.aca.2020.12.022>.
- Wu, I-Lin, Sherri B. Turnipseed, Joseph M. Storey, Wendy C. Andersen, et Mark R. Madson. 2020. « Comparison of data acquisition modes with Orbitrap high-resolution mass spectrometry for targeted and non-targeted residue screening in aquacultured eel ». *Rapid communications in mass spectrometry : RCM* 34 (7): e8642. <https://doi.org/10.1002/rcm.8642>.
- Wu, Jianqiang, et Youhe Gao. 2015. « Physiological conditions can be reflected in human urine proteome and metabolome ». *Expert Review of Proteomics* 12 (6): 623-36. <https://doi.org/10.1586/14789450.2015.1094380>.
- Wu, Qian, Jian-Ying Wang, Dong-Qi Han, et Zhong-Ping Yao. 2020. « Recent Advances in Differentiation of Isomers by Ion Mobility Mass Spectrometry ». *TrAC Trends in Analytical Chemistry* 124 (mars): 115801. <https://doi.org/10.1016/j.trac.2019.115801>.
- Xia, Jianguo, Nick Psychogios, Nelson Young, et David S. Wishart. 2009. « MetaboAnalyst: a web server for metabolomic data analysis and interpretation ». *Nucleic Acids Research* 37 (Web Server issue): W652-60. <https://doi.org/10.1093/nar/gkp356>.
- Xia, Tian, Ming Yuan, Yongwei Xu, Feng Zhou, Kate Yu, et Yu Xia. 2021. « Deep Structural Annotation of Glycerolipids by the Charge-Tagging Paterno–Büchi Reaction and Supercritical Fluid Chromatography–Ion Mobility Mass Spectrometry ». *Analytical Chemistry* 93 (23): 8345-53. <https://doi.org/10.1021/acs.analchem.1c01379>.
- Xie, Chengyi, Yanyan Chen, Xiaoxiao Wang, Yuanyuan Song, Yuting Shen, Xin Diao, Lin Zhu, Jianing Wang, et Zongwei Cai. 2022. « Chiral Derivatization-Enabled Discrimination and on-Tissue Detection of Proteinogenic Amino Acids by Ion Mobility Mass Spectrometry ». *Chemical Science* 13 (47): 14114-23. <https://doi.org/10.1039/D2SC03604E>.
- Ye, Li-Hong, Xin Dong, et Jun Cao. 2023. « A Highly Sensitive Method (Supercritical Fluid Chromatography Coupled with Ion Mobility Mass Spectrometry) for Determination of Multiple Compounds in Radix Curcumae ». *Biomedical Chromatography* 37 (1): e5514. <https://doi.org/10.1002/bmc.5514>.
- Yu, Zhonghao, Gabi Kastenmüller, Ying He, Petra Belcredi, Gabriele Möller, Cornelia Prehn, Joaquim Mendes, et al. 2011. « Differences between Human Plasma and Serum Metabolite Profiles ». *PLoS ONE* 6 (7): e21230. <https://doi.org/10.1371/journal.pone.0021230>.

- Zhang, Haixia, Randy W. Purves, Thomas D. Warkentin, et Albert Vandenberg. 2023. « Validated approach for vicine, convicine and levodopa quantification from faba bean seeds by flow injection analysis high-field asymmetric waveform ion mobility mass spectrometry ». *Food Chemistry* 405 (mars): 134857. <https://doi.org/10.1016/j.foodchem.2022.134857>.
- Zhang, Lingzhi, Yinghao Wang, Fang Zheng, Di Zhu, Yongmei Liang, et Quan Shi. 2022. « Influence Exerted by the Solvent Effect on the Mobility Peak of 1,8-Naphthalic Anhydride in Ion Mobility Spectrometry ». *Journal of the American Society for Mass Spectrometry*, janvier. <https://doi.org/10.1021/jasms.1c00299>.
- Zhang, Wei, Thomas Hankemeier, et Rawi Ramautar. 2017. « Next-Generation Capillary Electrophoresis–Mass Spectrometry Approaches in Metabolomics ». *Current Opinion in Biotechnology*, Analytical biotechnology, 43 (février): 1-7. <https://doi.org/10.1016/j.copbio.2016.07.002>.
- Zhang, Xing, Yehia M. Ibrahim, Tsung-Chi Chen, Jennifer E. Kyle, Randolph V. Norheim, Matthew E. Monroe, Richard D. Smith, et Erin S. Baker. 2015. « Enhancing Biological Analyses with Three Dimensional Field Asymmetric Ion Mobility, Low Field Drift Tube Ion Mobility and Mass Spectrometry (μ FAIMS/IMS-MS) Separations ». *Analyst* 140 (20): 6955-63. <https://doi.org/10.1039/C5AN00897B>.
- Zhang, Xing, Michelle Romm, Xueyun Zheng, Erika M Zink, Young-Mo Kim, Kristin E Burnum-Johnson, Daniel J Orton, et al. 2016. « SPE-IMS-MS: An Automated Platform for Sub-Sixty Second Surveillance of Endogenous Metabolites and Xenobiotics in Biofluids ». *Clinical Mass Spectrometry (Del Mar, Calif.)* 2 (décembre): 1-10. <https://doi.org/10.1016/j.clinms.2016.11.002>.
- Zheng, Xueyun, Noor A. Aly, Yuxuan Zhou, Kevin T. Dupuis, Aivett Bilbao, Vanessa L. Paurus, Daniel J. Orton, et al. 2017. « A Structural Examination and Collision Cross Section Database for over 500 Metabolites and Xenobiotics Using Drift Tube Ion Mobility Spectrometry ». *Chem. Sci.* 8 (11): 7724-36. <https://doi.org/10.1039/C7SC03464D>.
- Zheng, Xueyun, Kevin T. Dupuis, Noor A. Aly, Yuxuan Zhou, Francesca B. Smith, Keqi Tang, Richard D. Smith, et Erin S. Baker. 2018. « Utilizing ion mobility spectrometry and mass spectrometry for the analysis of polycyclic aromatic hydrocarbons, polychlorinated biphenyls, polybrominated diphenyl ethers and their metabolites ». *Analytica Chimica Acta*, Analytical Metabolomics, 1037 (décembre): 265-73. <https://doi.org/10.1016/j.aca.2018.02.054>.
- Zheng, Xueyun, Richard D Smith, et Erin S Baker. 2018. « Recent advances in lipid separations and structural elucidation using mass spectrometry combined with ion mobility spectrometry, ion-molecule reactions and fragmentation approaches ». *Current Opinion in Chemical Biology*, Omics, 42 (février): 111-18. <https://doi.org/10.1016/j.cbpa.2017.11.009>.
- Zheng, Xueyun, Roza Wojcik, Xing Zhang, Yehia Ibrahim, Kristin Burnum-Johnson, Daniel Orton, Matthew Monroe, Ronald Moore, Richard Smith, et Erin Baker. 2017. « Coupling Front-End Separations, Ion Mobility Spectrometry, and Mass Spectrometry For Enhanced Multidimensional Biological and Environmental Analyses ». *Annual review of analytical chemistry (Palo Alto, Calif.)* 10 (février). <https://doi.org/10.1146/annurev-anchem-061516-045212>.
- Zheng, Xueyun, Xing Zhang, Nathaniel S Schocker, Ryan S Renslow, Daniel J Orton, Jamal Khamsi, Roger A Ashmus, et al. 2017. « Enhancing Glycan Isomer Separations with Metal Ions and Positive and Negative Polarity Ion Mobility Spectrometry-Mass Spectrometry Analyses ». *Analytical and Bioanalytical Chemistry* 409 (2): 467-76. <https://doi.org/10.1007/s00216-016-9866-4>.
- Zhou, Z., X. Shen, X. Chen, J. Tu, X. Xiong, et Z. J. Zhu. 2019. « LipidIMMS Analyzer: integrating multi-dimensional information to support lipid identification in ion mobility-mass spectrometry based lipidomics ». *Bioinformatics* 35 (4): 698-700. <https://doi.org/10.1093/bioinformatics/bty661>.
- Zhou, Zhiwei, Mingdu Luo, Xi Chen, Yandong Yin, Xin Xiong, Ruohong Wang, et Zheng-Jiang Zhu. 2020. « Ion Mobility Collision Cross-Section Atlas for Known and Unknown Metabolite

- Annotation in Untargeted Metabolomics ». *Nature Communications* 11 (1): 4334. <https://doi.org/10.1038/s41467-020-18171-8>.
- Zhou, Zhiwei, Jia Tu, Xin Xiong, Xiaotao Shen, et Zheng-Jiang Zhu. 2017. « LipidCCS: Prediction of Collision Cross-Section Values for Lipids with High Precision To Support Ion Mobility–Mass Spectrometry-Based Lipidomics ». *Analytical Chemistry* 89 (17): 9559-66. <https://doi.org/10.1021/acs.analchem.7b02625>.
- Zhou, Zhiwei, Xin Xiong, et Zheng-Jiang Zhu. 2017. « MetCCS Predictor: A Web Server for Predicting Collision Cross-Section Values of Metabolites in Ion Mobility-Mass Spectrometry Based Metabolomics ». Édité par Oliver Stegle. *Bioinformatics* 33 (14): 2235-37. <https://doi.org/10.1093/bioinformatics/btx140>.
- Zietek, Barbara M., Ynze Mengerink, Jan Jordens, Govert W. Somsen, Jeroen Kool, et Maarten Honing. 2018. « Adduct-ion formation in trapped ion mobility spectrometry as a potential tool for studying molecular structures and conformations ». *International Journal for Ion Mobility Spectrometry* 21 (1-2): 19-32. <https://doi.org/10.1007/s12127-017-0227-6>.
- Zivkovic, Angela M., Michelle M. Wiest, Uyen Thao Nguyen, Ryan Davis, Steven M. Watkins, et J. Bruce German. 2009. « Effects of Sample Handling and Storage on Quantitative Lipid Analysis in Human Serum ». *Metabolomics* 5 (4): 507-16. <https://doi.org/10.1007/s11306-009-0174-2>.
- Züllig, Thomas, et Harald C. Köfeler. 2021. « High Resolution Mass Spectrometry in Lipidomics ». *Mass Spectrometry Reviews* 40 (3): 162-76. <https://doi.org/10.1002/mas.21627>.
- Züllig, Thomas, Martin Trötz Müller, et Harald C. Köfeler. 2020. « Lipidomics from Sample Preparation to Data Analysis: A Primer ». *Analytical and Bioanalytical Chemistry* 412 (10): 2191-2209. <https://doi.org/10.1007/s00216-019-02241-y>.

Titre : Spectrométrie de mobilité ionique pour la lipidomique du plasma humain : vers la mesure standardisée de sections efficaces de collision

Résumé : La métabolomique consiste en l'étude des petites molécules d'un organisme vivant, pour permettre une meilleure compréhension des systèmes biologiques. L'identification des molécules d'intérêt au sein d'extraits biologiques complexes reste un défi majeur. C'est dans ce cadre que de nouvelles avancées sont réalisées pour développer des méthodes d'identification plus fiables et performantes. La spectrométrie de mobilité ionique peut être facilement couplée à la spectrométrie de masse ajoutant ainsi une capacité de séparation et un descripteur supplémentaire, la section efficace de collision ou CCS, prenant en compte la structure tridimensionnelle de l'ion.

Différentes technologies IMS sont disponibles et différentes méthodes de détermination des CCS (primaire, sans étalonnage et secondaire, avec procédure d'étalonnage) ont été décrites. Des études sont nécessaires pour vérifier la reproductibilité et la robustesse des mesures de CCS dans ces différentes conditions. Mes travaux de recherche portent sur cette problématique. Dans un premier temps, toutes les sources de déviations affectant la détermination des CCS de lipides ont été étudiées et évaluées. Ainsi, il a été vérifié que les paramètres de source et de mobilité ionique ont un impact négligeable devant la précision actuellement admise de 2%. Dans un deuxième temps, divers étalons commerciaux actuellement utilisés pour la détermination des CCS à l'aide de méthodes secondaires ont ensuite été étudiés. Enfin, la comparabilité des CCS de lipides de plasma humain obtenues à l'aide de trois technologies distinctes, Travelling wave IMS (TWIMS), Drift Tube IMS (DTIMS) and Trapped IMS (TIMS) a été évaluée. Un bon accord a pu être obtenu entre les valeurs de CCS obtenues à l'aide de trois technologies IMS différentes en utilisant le même étalon. Il a été démontré que la constitution de bibliothèques de CCS interopérables est clairement réalisable si des conditions standardisées tant du côté analytique que du côté du traitement des données sont définies et utilisées.

Cette étude est donc un pas vers la généralisation de l'utilisation de ce descripteur, ce qui ouvre la voie à de nombreuses autres applications de la mobilité ionique dans des domaines tels que la santé, la nutrition, l'environnement.

Mots clés : Mobilité ionique, Section efficace de collision, Spectrométrie de masse, Métabolomique, Lipidomique, Etalonnage en mobilité ionique, TWIMS, TIMS, DTIMS

Title: Ion mobility spectrometry for human plasma lipidomics: towards standardized collision cross sections

Abstract: Metabolomics is the study of the whole set of small molecules in living organisms and it can provide a better understanding of biological systems. Identifying molecules of biological interest remains a major analytical challenge. It is in this context that new advances are made to find more reliable and efficient identification methods. Ion mobility spectrometry (IMS) can be easily coupled to high resolution mass spectrometry to provide an additional separation dimension and an additional descriptor, the collision cross section or CCS, which reflects the three-dimensional structure of an ion in a buffer gas.

Different IMS technologies are currently available and different methods for CCS determination (primary method without calibration and secondary methods including a calibration procedure) have been described and investigations are required to evaluate the reproducibility and robustness of CCS measurements. My research project addressed this aspect. First, all sources of deviations that could affect lipid CCS determination were investigated and evaluated. We have checked that changes in source and ion mobility parameters had negligible impact on CCS determination. Then, various commercial calibrants currently utilized for CCS determination using secondary methods were evaluated. Finally, the comparability of human plasma lipid CCS retrieved from three distinct technologies, Travelling wave IMS (TWIMS), Drift Tube IMS (DTIMS) and Trapped IMS (TIMS) was assessed. Good agreement was achieved between CCS values from three different IMS technologies using the same calibrant. My results have also showed that the constitution of interoperable CCS libraries is clearly achievable if standardized conditions and procedures are defined and applied for both data acquisition and processing.

This study thus represents a first step towards the widespread use of this descriptor, and potentially the opening up to many other applications of ion mobility in various fields such as health, nutrition and environment.

Key words: Ion mobility spectrometry, Collision cross section, High-resolution mass spectrometry, Metabolomics, Lipidomics, Ion mobility calibration, TWIMS, TIMS, DTIMS